ISBN : 978-602-53531-8-5

FoITIC
Faculty of Industrial Technology International Congress

itenas
Institut Teknologi Nasional

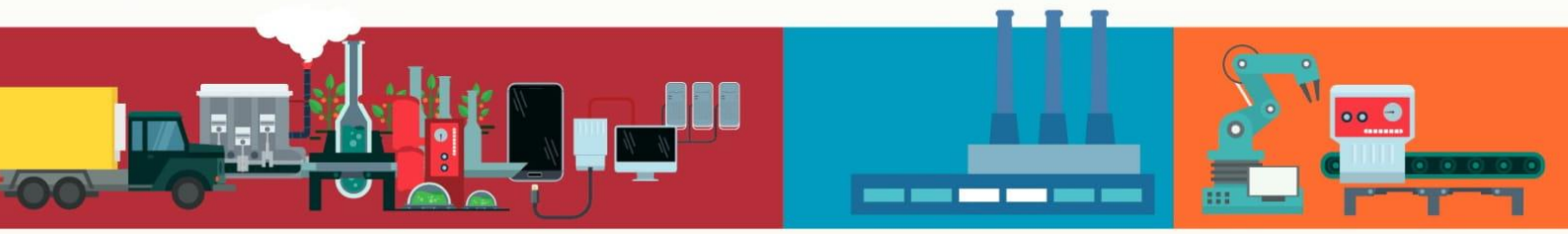

Organized by:
Faculty of Industrial Technology, Institut Teknologi Nasional (Itenas) Bandung, West Java Indonesia.

Supported by:
Institut Teknologi Nasional (Itenas) Bandung, West Java Indonesia.

Conference Proceedings

The 1st Faculty of Industrial Technology International Congress 2017

International Conference

Towards Reliable Renewable and Sustainable Energy Systems: Challenges and Opportunities

October 9 - 11, 2017
Faculty Building, 3rd floor
Campus of Itenas Bandung – Indonesia

Co-organized:
The ISR
Indonesian Society for Reliability
IEEE SSIT Society on Social Implications of Technology

University Partner:
Universiti Malaysia PAHANG

FACULTY OF INDUSTRIAL TECHNOLOGY INTERNATIONAL CONGRESS

(FoITIC)

PROCEEDINGS

The 1st FoITIC 2017

International Conference

ISBN 978-602-53531-8-5

Campus of Institut Teknologi Nasional Bandung

West Java – Indonesia

October 9 – 11, 2017

Organized

Co-organized

University Partner

Proceedings of FoITIC 2017 – International Conference

Reviewer:

Dr. Ing. M. Alexin Putra	Mechanical Engineering	Itenas – Indonesia
Dr. Dani Rusirawan	Mechanical Engineering	Itenas – Indonesia
Dr. Dyah Setyo Pertiwi	Chemical Engineering	Itenas – Indonesia
Dr. Jono Suhartono	Chemical Engineering	Itenas – Indonesia
Dr. Marisa Widyastuti P	Electrical Engineering	Telkom University – Indonesia
Dr. Fahmi Arif	Industrial Engineering	Itenas – Indonesia
Dr. Achmad Ghazali	School of Business and Management	ITB – Indonesia
Dr. Winarno Sugeng	Informatics Engineering	Itenas – Indonesia

Edited by:

Dr. Dani Rusirawan
Dr. Dyah Setyo Pertiwi
Dr. Fahmi Arif
Mr. Liman Hartawan
Ms. Dina Budhi Utami
Mr. Muktiadi Akhmad Januar

Conference Organizer:
Faculty of Industrial Technology, Institut Teknologi Nasional Bandung - Indonesia
Jl. PKHH. Mustapa No. 23 Bandung 40124, West Java - INDONESIA
Phone: +62-22- 7272215, Fax: +62-22 – 7202892
Email: foitic@itenas.ac.id,
Website: http://foitic.itenas.ac.id.
www.itenas.ac.id

ISBN 978-602-53531-8-5

Cover Design: Aldrian Agusta, S.Sn.,M.Ds.

Produced by: Penerbit Itenas

penerbit itenas

5 4 3 2

COMMITTEE

Organizing Committee:

Chairman	: Dr. Dani Rusirawan	Itenas – Indonesia
Co-chairman	: Dr. Ahmad Taufik Joenoes	Indonesian Society for Reliability
Members	: Dr. Dyah Setyo Pertiwi	Itenas – Indonesia
	Dr. Fahmi Arif	Itenas – Indonesia
	Mr. Liman Hartawan	Itenas – Indonesia
	Ms. Dina Budhi Utami	Itenas – Indonesia
	Mr. Aldrian Augusta	Itenas – Indonesia

Steering Committee:

Dr. Imam Aschuri	Itenas Bandung – Indonesia
Prof. Dr. Meilinda Nurbanasari	Itenas Bandung – Indonesia
Ms. Yuniar	Itenas Bandung – Indonesia
Dr. Dewi Kania Sari	Itenas Bandung – Indonesia
Prof. Dr. Soegijardjo Soegijoko	Itenas Bandung – Indonesia
	IEEE Indonesia SSIT Chapter
Dr. Kusmaningrum Soemadi	Itenas Bandung – Indonesia
Prof. Dr. Isa Setiasah Toha	ITB – Indonesia
Dr. Iwan Inrawan Wiratmadja	ITB – Indonesia

Scientific Committee:

Dr. Hendi H. Rachmat	Electrical Engineering	Itenas – Indonesia
Dr. Waluyo	Electrical Engineering	Itenas – Indonesia
Dr. Marisa Widyastuti P.	Electrical Engineering	Telkom University – Indonesia
Dr. T. Kristyadi	Mechanical Engineering	Itenas – Indonesia
Dr. Agus Hermanto	Mechanical Engineering	Itenas – Indonesia
Dr. Ing. M. Alexin Putra	Mechanical Engineering	Itenas – Indonesia
Dr. Arif Imran	Industrial Engineering	Itenas – Indonesia
Dr. Chandra Ade Irawan	Industrial Engineering	Itenas – Indonesia
Dr. Caecilia S. Wahyuning	Industrial Engineering	Itenas – Indonesia
Dr. Jono Suhartono	Chemical Engineering	Itenas – Indonesia
Dr. Maya Ramadianti M.	Chemical Engineering	Itenas – Indonesia
Dr. rer. Nat. Riny Y. Parapat	Chemical Engineering	Itenas – Indonesia
Dr. Winarno Sugeng	Informatics Engineering	Itenas – Indonesia
Dr. Achmad Ghazali	SBM	ITB – Indonesia

International Scientific Committee:

Prof. Dr. Istvan Farkas	Szent Istvan University – Hungary
Prof. Dr. Istvan Szabo	Szent Istvan University – Hungary
Prof. DSc. Józef Horabik	Polish of Academy of Sciences – Poland
Prof. Ing. CSc. Martin Libra	Czech University of Life Sciences Prague – Czech Republic
Prof. RNDr. Ing. Jiri Blahovec, DrSc.	Czech University of Life Sciences Prague – Czech Republic
Prof. Dr. Henrik Lund	Aalborg University – Denmark
Prof. Dr.-Ing. Klaus Günter Gottschalk	Leibniz Institute for Agricultural Engineering and Bioeconomy- Germany
Prof. R. Schomaecker	Technical University Berlin – Germany
Prof. M. Schwarze	Technical University Berlin – Germany
Prof. Colin Webb	The University of Manchester – UK
Prof. Paul Sharratt	Institute of Chemical and Engineering Sciences – Singapore
Dr. Istvan Seres	Szent Istvan University – Hungary
Doc. Ing. Jan Banout, Ph.D.	Czech University of Life Sciences Prague – Czech Republic
Doc. RNDr. Zuzana Hlaváčová, CSc.	Slovak University of Agriculture in Nitra – Slovak Republic
Doc. RNDr. Vlasta Vozárová, PhD.	Slovak University of Agriculture in Nitra – Slovak Republic
Dr. Agus Saptoro	Curtin University – Malaysia
Dr. Martino Luis	University Utara – Malaysia

PREFACE
WELCOME FROM THE RECTOR
INSTITUT TEKNOLOGI NASIONAL BANDUNG

Dear speakers and participants,

Welcome to Bandung and welcome to Itenas campus!

It is great pleasure for me to welcome you in campus of Itenas Bandung at the 1st Faculty of Industrial Technology International Congress (FoITIC) 2017.

The theme for the 1st FoITIC 2017 “Toward Reliability Renewable and Sustainable Energy Systems: Challenges and Opportunities”, is very relevant with the current hot issues about climate change, growing populations and limited fossil fuel resources.

We believe that scientists and researchers will hand in hand with industrial experts, to create and develop new renewable and sustainable technologies that enable human to make products and services more efficient, protect environment and keep people healthier.

I am deeply grateful appreciative to the Faculty of Industrial Technology Itenas, Indonesian Society Reliability, Institute of Electrical & Electronics Engineers Indonesia Society on Social Implication of Technology Chapter, IEEE CAS Hyderabad, delegates, organizing committee and many others who have contributed to the success of this conference.

I am confident that this event will serve to promote much valuable communication and information exchange among scientist – researcher and industrial expert.

May we have a successful, stimulating, fruitful and rewarding the conference.

Thank you.

Dr. Iman Aschuri

Rector
Institut Teknologi Nasional Bandung

PREFACE

WELCOME FROM THE DEAN OF FACULTY OF INDUSTRIAL TECHNOLOGY, INSTITUT TEKNOLOGI NASIONAL BANDUNG

Dear distinguished Guest, Ladies and Gentlemen,

Welcome to the 1st Faculty of Industrial Technology International Congress (FoITIC) 2017, which is organized by Faculty of Industrial Technology, Institut Teknologi Nasional (Itenas) Bandung, in conjunction with Indonesian Society for Reliability (ISR) and Institute of Electrical & Electronics Engineers Indonesia Society on Social Implication of Technology Chapter (IEEE Indonesia SSIT Chapter). In our Faculty, we have agreed that FoITIC event will be held every two years (biennial program).

The main theme for the 1st congress is "Towards Reliable Renewable and Sustainable Energy Systems: Challenges and Opportunities". The congress will divide into 2 (two) main programs i.e. International Conference and international workshop.

The aim of the International Conference is invites academics, researchers, engineers, government officers, company delegates and students from the field of energy and other discipline to gather, present and share the results of their research and/or work, and discuss strategies for the future utilization of renewable and sustainable energy system.

Taking this opportunity, I would like to convey my sincere thanks and appreciations to our keynote speakers and invited speakers from Szent Istvan University Hungary, IEEE Indonesia SSIT Chapter, Indonesian Society for Reliability, University Malaysia Pahang and Indonesian Wind Energy Society, workshop facilitators i.e. IEEE Circuits and Systems (IEEE CAS) Hyderabad – India) and national and international scientific committee for their support of this important event. I would also like to invite all participants in expressing our appreciation to all members of the FoITIC 2017 organizing committee for their hard work in making this conference success.

Finally, we wish you all fruitful networking during conference and workshop, and we do hope that you will reap the most benefit of it.

Do enjoy your stay in Bandung, and thank you very much!

Dr. Dani Rusirawan

Dean Faculty of Industrial Technology – Institut Teknologi Nasional Bandung
Chairman of FoITIC 2017

ACKNOWLEDGEMENT

The completion of this undertaking could not have been possible without the participation and assistance of so many people whose names may not all be enumerated. The contributions are sincerely appreciated and gratefully acknowledged. The 1st International Conference on FoITIC (Faculty of Industrial Technology Congress) Organizing Committee wishes to express its gratitude and deep appreciation to the following:

1. Dr. Imam Aschuri, Rector of Institut Teknologi Nasional Bandung;
2. All keynote and invited speakers, moderators, conference speakers, all participants and others who have in one way or another contributed for their valuable participation;
3. Institute of Electrical & Electronics Engineers Indonesia Society on Social Implication of Technology Chapter (IEEE Indonesia SSIT Chapter);
4. Institute of Electrical & Electronics Engineers Circuits and Systems (IEEE CAS), Hyderabad India;
5. Indonesian Society for Reliability (ISR);
6. Universiti Malaysia Pahang;
7. Indonesian Wind Energy Society (IWES).

KEYNOTE AND INVITED SPEAKERS INTERNATIONAL CONFERENCE

Prof. Dr. Istvan Farkas (Szent Istvan University)

Prof. Dr. Istvan Farkas is Director of Institute for Environmental Engineering System, Szent Istvan University (SZIU), Godollo – Hungary. He is also Head of Department Physics and Process Control and head of Engineering Doctoral School, at SZIU. He got Doctoral Degree from Technical University Budapest (1985). Presently, a lot of his activities devotes on International professional societies such as: International Solar Energy Societies (ISES), International Federation of Automatic Control (IFAC), European Federation of Chemical Engineering (EFChE), European Thematic Network on Education and Research in Biosystems Engineering, European Network on Photovoltaic Technologies, FAO Regional Working Group on Greenhouse Crops in the SEE Countries, Solar Energy Journal Associate Editor, Drying Technology Journal Editorial Board, etc. He was a visiting Professor in several universities: Solar Energy Applications Laboratory, Colorado University State University, Fort Collins - USA; Department of Energy, Helsinki University of Technology, Espoo - Finland; Institut for Meteorology and Physics, University of Agricultures Sciencies, Vienna - Austria; Laboratory of Bioprocess Engineering, The University of Tokyo - Japan.

Ahmad Taufik, M.Eng., Ph.D (Indonesian Society for Reliability)

Ahmad Taufik, M.Eng, Ph.D (Graduated from Georgia Institute of Technology, USA – 1996) is a lecturer and a professional trainer and consultant. He is member of American Society for Metals (ASM) and American Society for Mechanical Engineer (ASME). He performs research in fatigue and fracture mechanics of oil and gas pipeline. Dr. Ahmad Taufik highly experienced in providing industrial training and consulting work more than 20 projects related to Pipelines Failure Analysis, Risk and Reliability Assessment, Repair Design, Pipeline Corrosion Protection in Oil and Gas Industries. Dr. Ahmad Taufik has been chairman and speakers for many Oil and Gas International Conferences in Indonesia, (INDOPIPE, MAPREC), Malaysia (ASCOPE), Singapore and China (IPTEC) for the last five years. He is founder of Indonesian Society Reliability (ISR) and presently he is a chairman of the ISR. Since 2006, he was work as part time lecturer at Dept. of Mechanical Engineering, Itenas.

Prof. Dr. Soegijardjo Soegijoko (Institut Teknologi Nasional Bandung)

Soegijardjo Soegijoko (born in Yogyakarta, 1942) earned his Engineer Degree in Telecommunication Engineering from the Department of Electrical Engineering, Institut Teknologi Bandung (ITB), Indonesia, in 1964. His Doctor Degree (*Docteur Ingenieur*) was obtained from USTL (*Universite des Sciences et Techniques du Languedoc, Montpellier, France*) in 1980. Additionally, he has also completed a number of non-degree or post-doctoral programs, such as: tertiary education (UNSW, Australia, 1970), VLSI Design (Stanford University – 1986; UNSW- 1991; Tokyo Institute of Technology-1984, 1985, 1990).

Since 1966, he joined ITB as a teaching staff at the Department of Electrical Engineering, (currently School of Electrical Engineering & Informatics) ITB, and appointed as a Professor on Biomedical Engineering in 1998. During his academic services at ITB (from 1966 – 2007), he has actively involved in the developments and operations of various units, e.g.: Electronics Laboratory, Master Program on Microelectronics, Inter University Center on Microelectronics, Biomedical Engineering Program (Undergraduate, Master & Doctorate programs), and Biomedical Engineering Laboratory. Although he has been officially retired in 2007, he has appointed as an adjunct Professor at ITB for some years. At present (August 2017), he is an adjunct Professor at the Department of Electrical Engineering, Institut Teknologi Nasional (ITENAS) Bandung (Indonesia). His current research interests include: Biomedical Engineering Instrumentation, e-Health &Telemedicine Systems, and Biomedical Engineering Education.

He has published more than 100 international papers in the above-mentioned research interests. Moreover, he (and his colleagues) have also authored five different book chapter titles (on biomedical engineering, ehealth & telemedicine) published by Jimoondang (Korea, 2008), Springer (Singapore, 2014), CRC Press – Taylor Francis (2016), and Springer (2017).

Currently, he actively involves in various societies within the IEEE that include: EMBS, SSIT, CASS, Computer, and Education, as well as SIGHT (Special Interest Group on Humanitarian Activities). He is currently the IEEE Indonesia SSIT Chapter Chair, EMBS Chapter Chair and actively involves in the Indonesian eHealth & Telemedicine Society (IeHTS) as well as the Indonesian Biomedical Engineering Society (IBES).

Prof. Dr. Ir. Soegijardjo Soegijoko is a *Life Senior Member* of the IEEE, and can be reached through: soegi@ieee.org

Prof. Dr. Rizalman Mamat (Universiti Malaysia Pahang)

Prof. Dr. Rizalman Mamat presently is Dean of Faculty Mechanical Engineering, Universiti Malaysia Pahang, Malaysia. He got Doctoral degree from University of Birmingham, United Kingdom in fuel and energy. Previously, he obtained his BSc and MSc from University Teknologi Malaysia (UTM). His field research interest is Heat transfer, Combustion, Internal Combustion Engine, Alternative Energy, Computational Fluid Dynamics, Propulsion System. Prof. Dr. Rizalman Mamat was visiting Professor at Karlsruhe University of Applied Science Germany (2017), Faculty of Engineering Universitas Abulyatama Aceh, Indonesia (2017), Faculty of Engineering Universitas Gajah Putih Aceh, Indonesia (2017), Department of Mechanical Manufacture & Automation Ningxia University, Yinchuan, China (2016), Department of Mechanical Manufacture & Automation Ningxia University, Yinchuan, China (2015).

Mr. Soeripno Martosaputro (Indonesia Wind Energy Society)

Soeripno Martosaputro, graduated from Universitas Sebelas Maret (Bachelor) and University of Pancasila (MSc.). Presently, he is worked at PT UPC Renewables. Moreover, he is Chairman of Indonesia Wind Energy Society (IWES) and Chairman of Expert Board of Indonesia Wind Energy Association (IWEA). Previously he worked as a researcher at the National Institute of Aeronautics and Space (LAPAN), Aerospace Technology Center, particularly in the field of technology development and engineering of the Wind Energy Conversion Systems. He is active in the field of science and technology utilization in particular wind energy technology as speakers and resource persons in seminars nationally and internationally. He is member of the Asia Pacific Wind Energy Forum (APWEF), Indonesia National Committee World Energy Congress (KNI-WEC), Indonesia Renewable Energy Society (METI), and National Research Council (DRN). In 2012 – 2016, he was act as National Project Manager of WHYPGEN (Wind Hybrid Power Generation market initiatives Project) – UNDP Project.

LIST OF CONTENTS

ISBN 978-602-53531-8-5

A. Renewable Energy Resources Assessment; Producing and storing renewable electricity; Off-grid & rural energy access; Renewable energy grid integration & distribution: utilities of the future

Proceedings of the 1st Faculty of Industrial Technology International Congress International Conference
Bandung, Indonesia, October 9-11, 2017
ISBN 978-602-53531-8-5

New trends in solar thermal and photovoltaic applications

István Farkas
Department of Physics and Process Control, Szent István University, Gödöllő - HUNGARY
Corresponding author e-mail: Farkas.Istvan@gek.szie.hu

Abstract

This paper deals with the overview of worldwide position and new application possibilities of solar thermal and photovoltaic (PV) technologies.

The worldwide situation is analysed based on the recent development shown intensively at the Solar World Congresses organized by the International Solar Energy Society and also by the ISES-Europe Unit. Moreover, the most recently published books in this topic served also a basic source to the overview statements.

The main area of solar thermal energy use covers the solar domestic hot water systems, the combined systems, the large-scale systems, the swimming pool collectors, the solar district heating systems, the process heat and the solar thermal assisted cooling systems.

The most important standpoints of the PV manufacturing and applications are as: increasing trend in energy mix, decreasing cell and module prices, cell efficiency does not increase fast, competition between different technologies, multi-Gigawatts applications, widening feed-in tariff system. Due to the growing market demand of solar photovoltaic applications, several new issues came to the light, as colouring, transparency and extra size of modules, application of thin film technologies and new fixation systems.

Examples are shown for both solar thermal and photovoltaic application possibilities.

Keywords: New technologies, environmental issues, thermal energy use, third generation PV, passive solar

1. Introduction

Generally saying, within the use of solar energy the solar thermal field identified at a lower innovation potential however their application shows large varieties. Especially the production of electricity from solar thermal is a preferred solution.

In spite of the recent economic situation all over the world a significant yearly increase of photovoltaic module production and their installation were performed in last couple of year period. However, it can be observed sensitivity of the market change on the photovoltaic industry, the PV technologies still show increasingly high priority.

The worldwide situation is analyzed based on the recent development shown intensively at the Solar World Congress events. The recent one will be organized by the International Solar Energy Society in Abu Dhabi, UAE during October 29 - November 2, 2017. The motto of the Congress is "Innovation for the 100% renewable energy transformation". Within the congress beside the technical-scientific topics several forums are organized to talk on local, national and international problems of energy politics which are responsible for the wider dissemination such technologies.

The main thematic questions are as follows:

1. SHC systems and components
   - Solar thermal collectors
   - Low to medium temperature thermal storage
   - Other innovative components and systems
   - Performance measurement, durability and reliability
   - Solar and heat pump systems
   - PVT systems

- Testing, standards, and certification for solar thermal technologies
- Solar ponds

2. SHC applications
   - Domestic solar water heating
   - Solar space heating and hybrid applications
   - District heating
   - Solar heat for industrial and agricultural processes
   - Solar refrigeration and solar air conditioning

3. Producing and storing renewable electricity
   - Photovoltaics: Cells, materials and components; advanced materials and concepts; design, operation and performance of PV systems; balance of system components; codes and standards; testing and certification; concentrating PV
   - Concentrating solar power technologies: solar concentration fundamentals and optical engineering, heat transfer, materials and components; solar thermal electricity systems; co-generation; solar thermochemical production of fuels and chemicals
   - Wind energy, ocean energy, hydro and other direct conversion renewables
   - Biomass energy, geothermal and other thermal renewables
   - Electrical storage technologies at Grid or utility-scale
   - Medium/high temperature thermal storage for electricity production with CSP systems

4. Renewable energy grid integration & distribution: Utilities of the future
   - Grid integration of variable renewable and energy storage systems
   - Active demand-side management
   - Smart Grids strategies including smart metering

5. Off-grid & rural energy access
   - Off-grid energy supply
   - Community micro power and hybrid systems
   - Solar cooking and clean cook stoves

6. Solar architecture and building integration
   - Integrating renewable technologies into buildings
   - Sustainable building materials and components
   - Net zero energy buildings
   - Daylighting
   - Energy storage in buildings

7. Renewable cities and community power programs
   - Urban and regional planning to maximize renewable energy
   - Policies and financial mechanisms
   - Clean transportation technologies and strategies

8. Solar resource assessment and energy meteorology
   - Renewable resource assessment and applications
   - Resource forecasting
   - Resource measurement and instrumentation

9. From laboratory to the real world: Solar energy markets, policies and initiatives that enable commercialization
   - Strategies, policies and case studies for renewable heat and electricity
   - Education and workforce development

10. Water, food, and energy nexus
    - Solar thermal desalination technology
    - Solar electrical desalination technology
    - Solar detoxification of water
    - Integrating desalination with thermal and electrical systems
    - Solar supported agriculture in desert regions

Additionally, the most recently published books serve also a basic source to the overview statements and the future vision, which are listed in the reference list.

2. Solar thermal

There are several attempts in order to improve the solar thermal technologies. Accordingly, a great number of books, publications and conference proceeding are presented to share all the available information in the field (Renewables 2015 – Global Status Report, Rethinking Energy 2015, Solar Heat Worldwide – 2015, Farkas, 2011).

The rate of development of the solar thermal applications in a long-time horizon is shown in Fig. 1 (based on Seyboth et al. 2008).

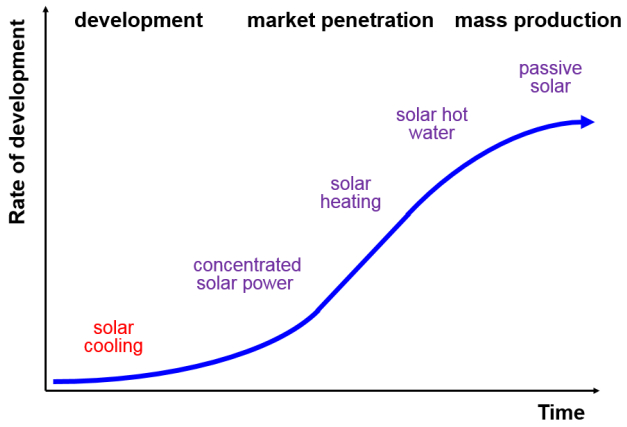

Fig. 1: Development of solar thermal applications in a long-term time horizon

Focusing the solar heat energy worldwide several comments can be drawn. The most important ones are as follows:

In the share of the total installed capacity in operation (including the glazed and unglazed water and air collectors) China is taking leading position with 71%, following by Europe with about 11% and USA/Canada with about 4% as shown in Fig. 2 (Weiss et al., 2017).

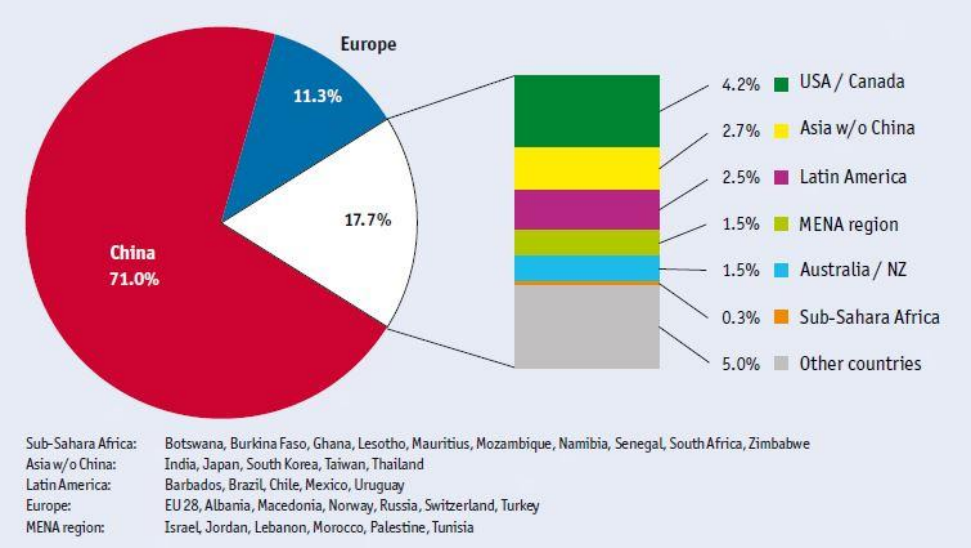

Fig. 2: Share of the solar thermal capacity by the end of 2015

In the period of 2000-2016 the global solar thermal capacity of glazed and unglazed water collectors in operation grew from 62 GWth (89 million m2) to 456 GWth (652 million m^2) in 2016. The corresponding annual solar thermal energy yields amounted from 51 TWh to 375 TWh as can be seen in Fig. 3 (Weiss et al., 2017).

Fig. 3: Global solar thermal capacity in operation and energy yield for the period of 2000-2016

The main issues of the use of solar thermal energy especially in Europe can be summarized along with the statements as:

- mainly solar domestic hot water systems are in use,
- growing share of combined systems,
- growing number of collective (large) systems,
- plastic absorber for swimming pool collectors,
- several solar district heating systems,
- some pilot plants for process heat,
- about 200 pilot plants for solar thermal assisted cooling system.

3. Solar architecture

In the coming period several trials are to be performed to increase significantly the building oriented solar applications, so lowering the energy consumption in buildings and/or find new solutions for providing energy resources from renewable energies.

The solar thermal vision for 2030 in Europe, especially to the building industry, is projected by European Renewable Heating and Cooling Technology Platform (RHC-ETP):

New buildings:

100% solar heated buildings will be the standard.

Existing buildings:

50% solar heated will be the most effective way to refurbish the building stock,

The new building components will be:

- the entire roof is covered by solar collectors and solar photovoltaic modules,
- the faced is used to harvest solar energy,
- seasonal heat storage,
- active heating system,
- compact units for solar heating and cooling,
- very well insulated.

The existing building components will be:

- renovation with multi-function modules for roof and facade,
- insulation and solar collector,
- seasonal heat storage,
- solar assisted cooling,
- around 70% heat demand is covered by solar thermal energy,
- remaining heat demand will be covered with other type of renewables.

Thus, nowadays it is strongly focusing to the development and design aspects of building integrated solar collectors. The literature review confirms that solar collectors appreciated not only by their thermal efficiency and the entire energetic performance, but also according to their aesthetic considerations. In Fig. 4 a new type of shell-structured solar collector is shown, which is a proper combination of the traditional and new type of construction materials. During the investigation the temperature distribution on the collector surface was validated by an infrared camera recording (Farkas, Fekete, 2017; Kendrick, 2009).

Fig. 4: The layout of a shell-structured solar collector

Concerning to the passive solar applications, it can be stated that:

- several trials are to be performed to increase significantly the building oriented solar applications,
- especially in Europe 100% solar heated buildings will be the standard by 2030.

4. Solar photovoltaic

In spite of the recent economic situation all over the world a significant yearly increase of photovoltaic module production and their installation were performed in last couple of year period. However, it can be observed sensitivity of the market change on the photovoltaic industry, the PV technologies still show increasingly high priority.

The solar photovoltaic global capacity (reaching 303 GW_{pv} in 2016) and the annual additions worldwide are indicated in Fig. 5 for the period 2006-2016 (Renewables 2017). In 2016, the increased amount of 75 GW_{pv} is equivalent to the production of 31,000 modules every hour.

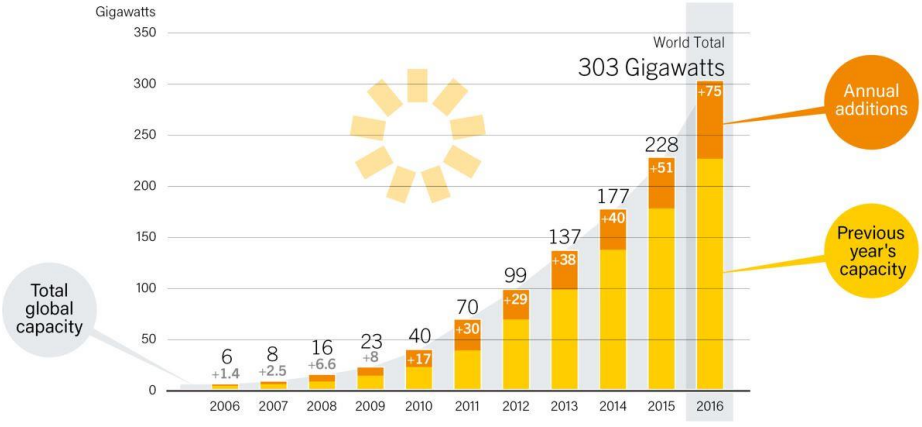

Fig. 5: The solar PV global capacity and the annual additions for the period 2006-2016

Just making a comparison of the different total renewable energy capacities in operation and their produced energy in 2016 is shown in Fig. 6, along with their the growth rate of for the period of 2010-2016 (Fig. 7). From the referred figures it can be easily justified the increasing importance of the solar photovoltaic technology (Weiss et al., 2017).

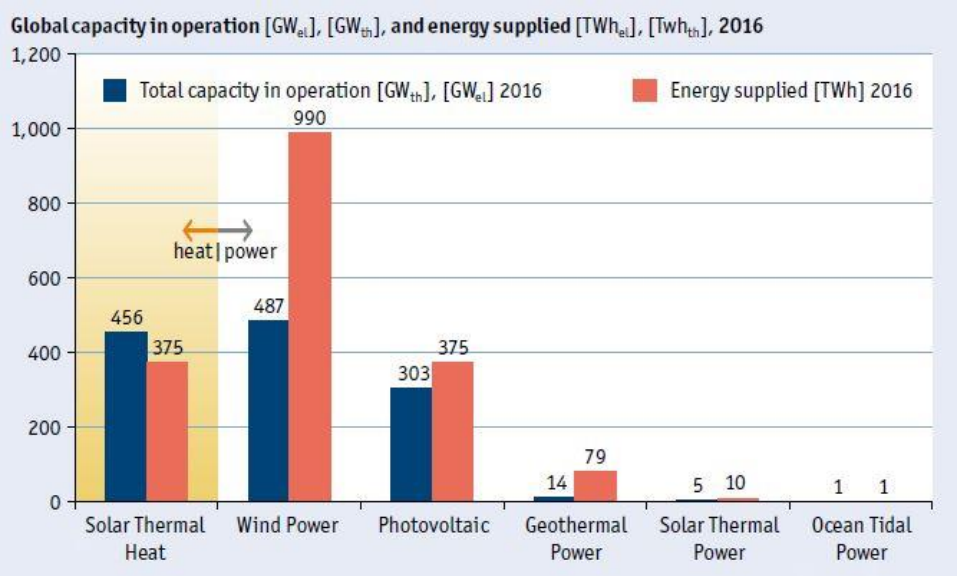

Fig. 6: The total renewable capacity and energy produced in 2016

Fig. 7: The growth rate of different renewables for the period of 2010-2016

The most important standpoints, which are characterising and influencing the PV manufacturing and applications industry could be summarized as follows:

- 20-30% of the part of renewables in the energy mix,
- at around 30-40% yearly decrease of the PV cell and module prises,
- the cell efficiency in market products does not increase in a great extent as expected,
- strong competition between the crystalline and the thin film technologies,
- multi-Gigawatts applications are getting into the practice,
- widening the feed-in tariff system in several countries in worldwide,
- presence of the Chinese PV products in worldwide and especially in the European Union market.

Due to the growing market demand of the solar photovoltaic applications several new specific issues came to the light. These factors include new type of modules along with their colouring and extra size, wide range application of thin film technologies, colouring of the modules, transparency of the modules, extra size of modules and new type of fixation systems.

3.1. Transparent PV applications

The attractiveness of the applications is increased with the use of the different colours of modules. A possible colour of the planned semi-shade cells (Suntech, 2015) can be seen in Fig. 8. The main features of the Suntech modules are the standard framed unit with a tempered front glass and the durable clear polymer substrate. The module has got 50% transparency, so it can be used to increase natural light behind the module along with providing energy production and surely some shading.

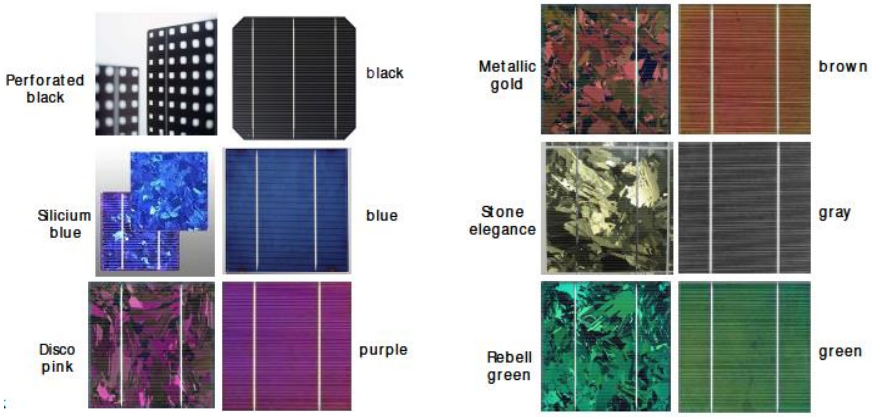

Fig. 8: Suntech glass PV colours

The most recently installed transparent PV applications is shown in Fig. 9. The system consists of 2x10 modules along with the total nominal power of 3,3 kWp.

Fig. 9: Suntech glass PV colours

3.2. New type of fixation system

Several cases when the roof of an existing building covered with a special plastic cover in order to keep it water tight. In cause some difficulty in the fixation of the support for the modules. For such a purpose, for example, it can be used the solution of Tectum flat roof system (Fig. 10.a), which has a feature of quick installation, lightweight (~12 kg/m^2) and high yields. It provides an intelligent, well-engineered, easy installation and simple maintenance solution (Tectum, 2015).

In Fig. 10 b. another type of fast fixation system is shown which provide a very fast installation procedure. Such solution allows a tilt angel at around 10-15 degrees.

Fig. 10.a. Tectum flat roof PV system

Fig. 10.b. Flat fixation of PV module installation, NVS (2014)

5. Conclusion

This paper gives an overview of the solar energy application fields worldwide. It discusses the solar thermal and the solar photovoltaic issues along with an attention to solar architectural questions. The new trends and technologies are also analysed and providing information on the solutions methods and approaches. Several examples are also given.

6. Acknowledgements

This work was supported by the Erasmus fund at Szent István University, Gödöllő, Hungary.

7. References

Farkas I., 2011. Solar energy applications, in Hungarian Renewable Energy Handbook 2011, /ed. by Kovács R./, Poppy Seed Bt, pp. 32-34.

Fekete I., Farkas I., 2017. Application possibilities of building integrated solar tile collectors, Proceedings of First International Conference on Building Integrated Renewable Energy Systems, BRIES 2017, March 6-9, 2017, Paper No 11, pp 1-8.

Kendrick, C., 2009. Metal roofing on residential buildings in Europe: A dynamic thermal simulation study, Report 090903ECC, Oxford, September 2009.

Weiss, W., Spörk-Dür, M. Mauthner, F., 2017. Solar heat worldwide, Global market developments and trends in 2016, SHC - Solar Heating and Cooling Programme, International Energy Agency.

Renewables 2017 - Global Status Report, REN 21, Renewable Energy Policy Network for the 21th Century.

REthinking energy, 2015. Renewable energy and climate change, IRENA

Seyboth, K., Beurskens, L., Langniss, O., Sims. R.E.H., 2008. Recognising the potential for renewable energy heating and cooling, Energy policy, Vol. 36 Issue 7, pp 2460-2463.

Reference to web page:

Soltecture, Tectum flat roof system, www.soltecture.com/uploads/media/Datasheet_TECTUM_EN_REV2.3_02.pdf, accessed on 28.04.2015

Suntech, Semi-shade modules, www.suntech-power.com, 28.04.2015

Photovoltaic Geographical Information System - Interactive Maps, http://re.jrc.ec.europa.eu/pvgis/apps4/pvest.php#, 28.04.2015

Proceedings of the 1st Faculty of Industrial Technology International Congress
International Conference
Bandung, Indonesia, October 9-11, 2017
ISBN 978-602-53531-8-5

Distribution of Direct and Diffuse Radiation on Bawean Island, East Java Indonesia

Yusuf Suryo Utomo
Research Center for Electrical Power and Mechatronics, Indonesian Institute of Sciences, Bandung - INDONESIA
Corresponding author e-mail: yustomo@gmail.com

Abstract

A study of the availability of solar energy is an interesting topic. By knowing the amount of solar energy available at a location, it can be determined how much power can be generated by a solar energy equipment and what utilization system should be used (whether solar electric or solar thermal systems). Solar radiation that falls on the earth's surface is a total radiation consisting of direct radiation components and diffuse radiation components. In their use, direct radiation is more effective for photovoltaic solar cell applications to generate electricity and solar concentrators in high temperature thermal applications, whereas total radiation and diffuse radiation will be more effective for solar collector fittings for thermal applications with relatively low to moderate temperatures. This paper discusses the distribution of both radiation components, especially in Bawean Island. Based on observational data from Sangkapura Meteorology Station, Bawean for 15 years (1994-2010) obtained an illustration of direct radiation distribution is more dominant than the diffuse radiation. This indicates that Bawean Island is suitable for solar photovoltaic applications as well as solar concentrator for electricity generation purposes. This can help local people to overcome the problem of limited electricity supply from state owned electricity (PLN) on the island.

Keywords: Bawean Island, direct radiation, diffuse radiation, solar electric, solar thermal

1. Introduction

In the 2016 national energy mix, the new EBT portion is 7.7% or fails to reach the target of 10.4%. Though Indonesia can be said to be rich in EBT, such as sun, geothermal, water, until the wind. To achieve the 23% EBT target in the national energy mix by 2025, it is impossible to do with the usual things but it needs breakthrough and accelerated EBT development. The government needs to boost the installation of solar panels in buildings and factories so that renewable energy can be increased, as well as shifting sources of fossil energy such as petroleum, gas, coal. In addition, the mandatory 20% biodiesel program (B20) to reduce diesel oil consumption should also continue (finance.detik.com, 2017).

Basic data for the development of electricity in a region is the need for electricity. Electricity needs are two kinds of electricity needs for household and industrial electricity needs and public facilities. The needs of households and public facilities can be estimated based on population. Electricity can also be produced from Solar Power Systems. The corresponding solar radiation location data is needed to activate the Solar Power Plant. Solar radiation data are crucial to the active solar energy facilities (Li et al., 2012) and passive energy-efficient building design (Li et al., 2013). However, solar radiation readings vary with geographic latitude, season and time of day, due to the various positions of the sun under unpredictable weather conditions (Li et al., 2010). Long-term data measurement is the most effective and accurate way of setting up such databases. In many parts of the world, however, the basic solar radiation data for the surfaces of interest are not always readily available (Munner, 2004). Accurate prediction of solar energy resources over the potential location is very important for proper siting, sizing and life-cycle cost analysis of solar power plant (Charabi et al, 2016).

Bawean Island as one of the sub districts in Gresik Regency, East Java is a sub district with a very rapid growth.

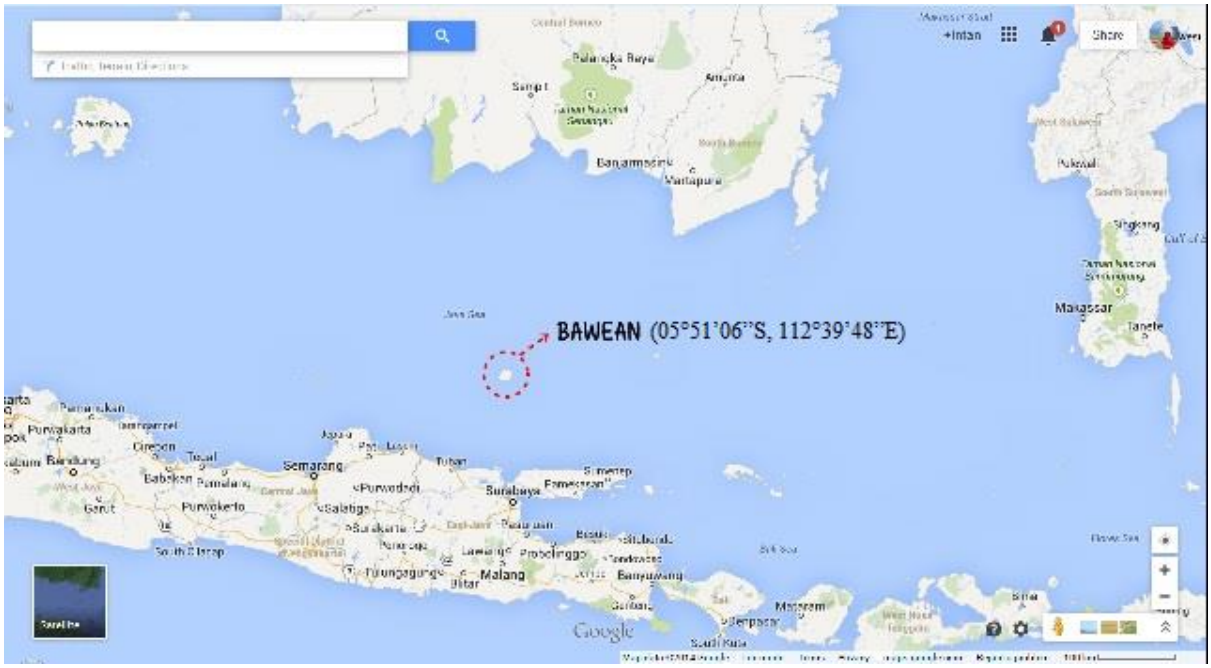

Fig. 1: Bawean Island Location

Figure 1 shows the location of Bawean Island located 150 km north of Gresik regency, East Java, with an area of 190 km^2. There are two sub districts on Bawean Island, namely Sangkapura and Tambak sub districts as shown in Figure 2. Based on the book Gresik in Figures 2010 the population in both sub districts can be detailed as can be seen in Table 1 (Statistics Gresik, 2010).

Table 1: Population Data on Bawean Island in 2009

Sub District	Population (person)
Sangkapura	70.372
Tambak	39.495
Jumlah	**109.867**

Fig. 2: Map of Bawean Island

The total population of 109,867 people consists of 18,436 households with details, number of families in Sangkapura sub district is 11,607 families and Tambak sub district 6.829 households. The electricity system in Bawean Island is currently supplied by PLTD through JTM (*Jaringan Tegangan Menengah*, JTM) Medium Voltage Network of 20 kV with 1750 kW power capacity and 5230 kW installed capacity. The highest peak load ever achieved is 2555 kW at the time of sufficient supply, and then dropped due to the decreased power capable of diesel. While the lowest load of 1893 kW. The load factor of the electricity system in Bawean Island is about 67%.

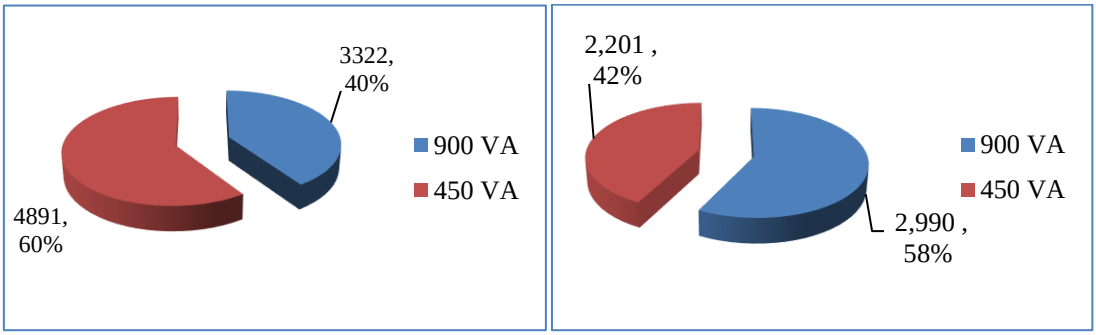

Fig. 3: Number of Prospective Customers of Household & Business Sector (a)
Demand for Electricity Bawean Island Household & Business Sector (kVA) (b)

Bawean island residents have not all enjoyed electricity, because only about 10% (10,964 customers until September 2010) who have become State-owned Electricity Company (*Perusahaan Listrik Negara*, PLN) electricity customers. Meanwhile, in September 2010, about 8,213 potential customers were on the waiting list with 4,891 potential customers (60%) of R1 / 450 VA and 3,322 prospects (40%) R2 / 900 VA as presented in Figure 3. Thus, the total demand for power by the local community is 5,191 kVA. Taking into account the waiting list of 8,213 prospects, the projection of total peak load that will occur in the electricity system in Bawean Island is 6756 kW with the same load pattern assumption. Thus, the base load of Bawean Island's electrical system is 3 MW. The increasing electricity demand from year to year must be balanced with the increase of power capacity that can be generated by local PLN. To meet these needs can be met by utilizing the potential of local energy resources, such as solar energy. Nevertheless, it is necessary to study the potential of solar energy to ensure the fulfillment of local electrical energy needs. By knowing the amount of solar energy available at a location, it can be determined how much power can be generated by a solar energy equipment and what utilization system should be used (whether solar electric or solar thermal systems). Solar radiation that falls on the earth's surface is a total radiation consisting of direct radiation components and diffuse radiation components. In their use, direct radiation is more effective for solar photovoltaic applications to generate electricity and solar concentrators in high temperature thermal applications, whereas total radiation and diffuse radiation will be more effective for solar collector fittings for thermal applications with relatively low to moderate temperatures. This paper discusses the distribution of both radiation components, especially in Bawean Island.

2. Datasets and Methodology

In Bawean Island, the data used to analysis are sunshine duration measured in the meteorological stations of Sangkapura (05°51'06"S, 112°39'48"E, 3.3m asl). This sunshine duration data is used in the framework of Feasibility Study of Electricity Addition in Bawean Island using local energy resources by PLN East Java in 2011. Thus, in this paper sunshine data used is data collection for the last 15 years, 1994-2010 periods. Sunshine duration measurements were performed using Campbell Stokes belonging to the local Meteorological Station. The data collected is the duration of sun exposure in percent. In order to reflect the amount of energy, the data needs to be converted in units of energy power.

First, the sunshine duration data is converted into global radiation data using Angstrom correlation (Utomo et al, 2005a and Utomo et al, 2005b). Furthermore, global radiation data is broken down into two components, namely the diffuse radiation component and direct radiation components using a model that has been developed previously (Hoesin, 2005). Starting from the standard atmospheric model used to estimate the intensity of solar radiation, the mathematical model of standard atmospheric solar radiation (H_c), Hoesin (1983) and Utomo et al (2004) developed the form of mathematical model H_c as follows:

$$H_c = C_1 + C_2\,cos(t) + C_3\,cos(2t) + C_4\cos(3t) + C_5\sin(t) + C_6\sin(2t) + C_7\sin(3t) \quad (1)$$

$$t = \frac{365(h_n - 80)}{360} \quad (2)$$

The mathematical model is formulated based on standard atmospheric model, sunshine duration data, day length and global radiation data on the surface of the earth. The mathematical model which expresses the relation of global radiation (H_{g0k}) to sunshine duration (n_{0k}) is in the form of non-linear regression:

$$\frac{H_{g0k}}{H_{c0k}} = f\left(\frac{n_{0k}}{N_k}\right) \quad (3)$$

The sunshine duration data obtained from the meteorology / climatology station consists of two forms of Time Period, ie 1) 12 hours of sunshine duration, between 6:00 am to 6:00 pm or 2) 8 hours of sunshine duration, between 8:00 am to 4:00 pm. For the purposes of equation 1, sunshine duration (n) Meteorology/Climatology Station needs to be converted into sunshine duration based on length of day N. The sunshine duration relationship with the day length N is as follows:

$$n_{0k} = \left\{\frac{(W\ x\ n)+r}{N}\right\} \quad (4)$$

n_0 is sunshine duration after correction, W = 8 or 12, Time Period of sunshine period and should be determined in accordance with calculations performed by the climatological station. While n is sunshine duration (observer station), N is day length and r is correction factor for sunshine duration data. Value of r is in range $0 \leq r \leq 2.5$. The determination of r value is determined by sunshine duration data pattern. While the mathematical model which states the sunshine duration relationship between Meteorological Station (measuring sunsine duration only) with Climatology Station (measuring global radiation and sunsine duration) is in the form of linear regression:

$$\frac{n_{0k}}{N_k} = f\left(\frac{n_{0l}}{N_l}\right) \quad (5)$$

Both models (equations 3 and 5) are used to calculate solar radiation in locations where there is sunshine duration data. The day length (N) is calculated by the formula:

$$N = 0.133\ arc\cos\left(\frac{\omega_s}{360}\right) \quad (6)$$

$$\omega_s = -\tan\varphi\ x\tan\delta \quad (7)$$

Declination (δ) is calculated by the formula:

$$\delta = 23.45\sin\left\{360\ \left[\frac{284+h_n}{365}\right]\right\} \quad (8)$$

3. Result and Discussion

3.1. Global Radiation

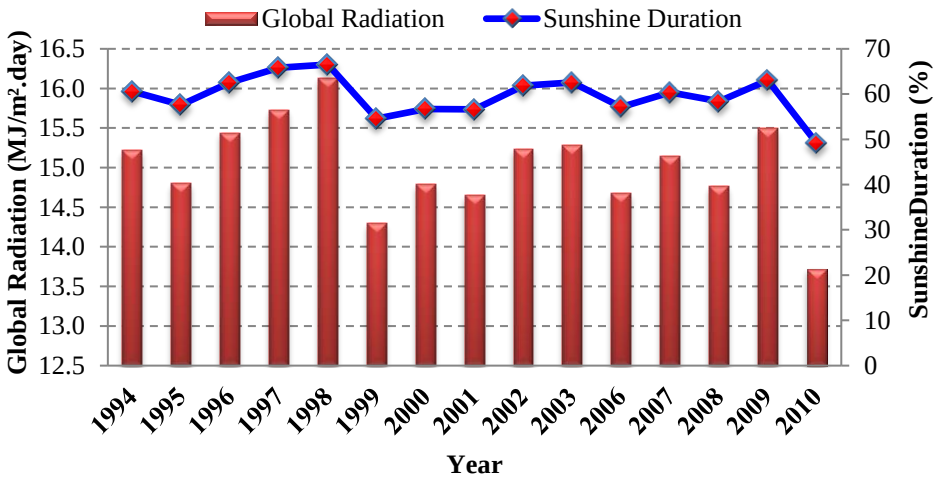

Fig. 4: Yearly Global Radiation and Sunshine Duration in Bawean Island.

Figure 4 shows the yearly-average-daily sunshine duration (%) data that has been converted to global radiation (MJ/m². day). It can be seen that Bawean Island receives quite a lot of solar energy, ranging from 13.72 MJ/m². day in 2010 to 16.14 MJ/m². day in 1998. Daily global radiation data are useful for evaluating the performance of solar electric or solar thermal systems. For further analysis purposes, global radiation is broken down into two components, namely the diffuse radiation component and direct radiation components.

3.2. Diffuse and Direct Radiations

Solar radiation that falls on the earth's surface is a total radiation consisting of direct radiation components and diffuse radiation components.

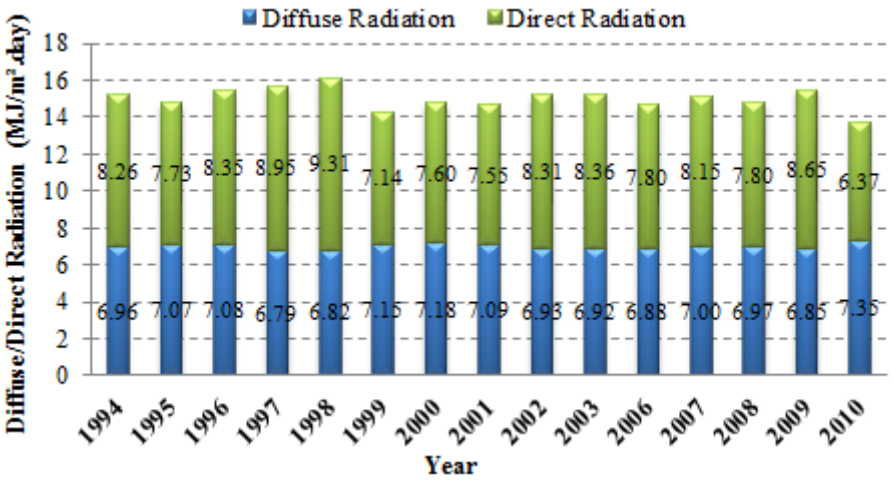

Fig. 5: Yearly Diffuse and Direct Radiation in Bawean Island

Figure 5 shows the global radiation after broken down into its two components, namely the diffuse and direct radiation. In their use, direct radiation is more effective for photovoltaic solar cell applications to generate electricity and solar concentrators in high temperature thermal applications, whereas total radiation and diffuse radiation will be more effective for solar collector fittings for thermal applications with relatively low to moderate temperatures.

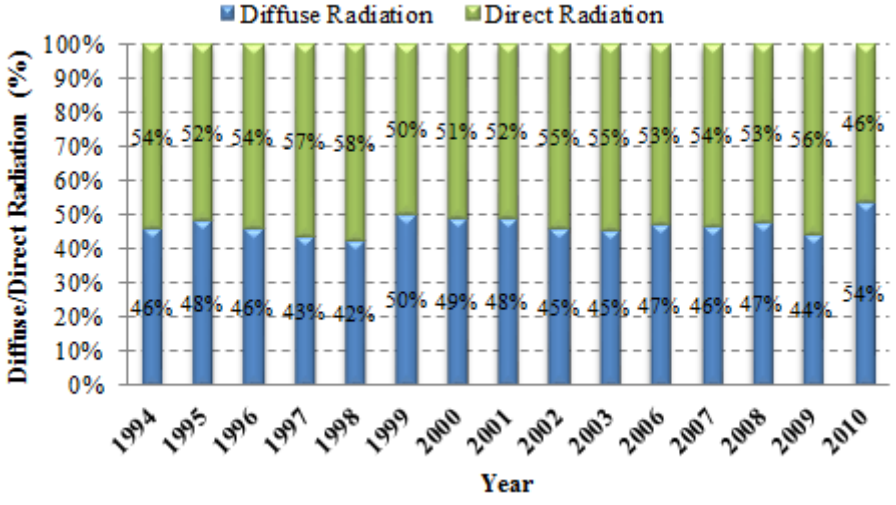

Fig. 6: Percentage Diffuse and Direct Radiation in Bawean Island

Figure 6 shows that the direct radiation distribution is more dominant than the diffuse radiation. It can be seen direct radiation dominates over 50%, except in 2010 only 46%. This indicates that Bawean Island is suitable for photovoltaic solar energy applications as well as solar concentrator for electricity generation purposes. It is expected to help local communities to overcome the problem of limited electricity supply from state owned electricity (PLN) on the island.

4. Conclusion

This paper assesses the distribution of diffuse radiation and direct radiation components in Bawean Island which growth very rapid and a lot of potential customers were on the waiting list. Based on observational data from Sangkapura Meteorology Station, Bawean for 15 years (1994-2010) obtained an illustration of direct radiation distribution is more dominant than the diffuse radiation. This indicates that Bawean Island is suitable for photovoltaic solar energy applications as well as solar concentrator for electricity generation purposes. This can help local people to overcome the problem of limited electricity supply from state owned electricity (PLN) on the island. Therefore, the availability of potential solar energy data in a potential location becomes very important, especially for proper siting, sizing and life-cycle cost analysis of solar power plant.

5. Nomenclature

$C_{1..}C_7$ harmonic constants

H_c	standard atmospheric solar radiation	$cal.cm^{-2}.day$
H_g	global radiation	$cal.cm^{-2}.day$
h_n	the n^{th} day in one year	1, January 1st to 365
n_0	sunshine duration after correction	hour
n	sunshine duration	%
N	day length	hour
r	correction factor for sunshine duration data	in the range $0 \leq r \leq 2.5$
W	Time Period for sunshine duration data	8 or 12

Greek letters

δ	declination	^{o}
ϕ	Location latitude	^{o}
ω_s	sun hour angle	rad

Subscripts

k	climatology station
l	meteorological station
n	n^{th} day

6. Acknowledgements

The author gratefully acknowledgment the support of the Research Center for Electrical Power and Mechatronics, Indonesian Institute of Science (LIPI) for funded and has given encouragement and opportunity to work in the field of conversion and conservation energy research.

7. References

https://finance.detik.com/energi/3586204/ri-kaya-energi-terbarukan-tapi-penggunaan-minim accessed on August 4, 2017.

Li, D.H.W., Cheung, K.L., Lam, T.N.T., Chan, W.W.T.H., 2012. A study of grid-connected photovoltaic system in Hongkong. ***Applied Energy 90(1)***, 122-127.

Li, D.H.W., Yang, L., Lam, J.C., 2013. Zero energy buildings and sustainable development implications – A review. ***Energy 54***, 1-10.

Li, D.H.W., Tang, H.L., Lee, E.W.M., Munner, T., 2010. Classification of CIE standard skies using probability

neural network. ***Int. J. Climatol 20***, 205-315.

Munner, T., 2004. Solar radiation and daylight models. Elsevier Oxford.

Charabi, Y., Gastli, A., Al-Yahyai, S., 2016. Production of solar radiation bankable datasets from high-resolution solar irrradiance derived with dynamical downscaling Numerical Weather Prediction model. ***Energy Report 2 (2016)***, 67-73.

Statistic Gresik, East Java, 2010. Gresik in Figures 2010.

Utomo, Y.S., Haen, I., Hoesin, H., 2005a. Conversion Analysis of Sunshine Duration Data for Making Solar Radiation Map. Proceeding of National Seminar of Research Development in the Field of Industry, cooperation between Center for Engineering Science and Engineering Department of Chemistry and Mechanical Engineering Faculty of Engineering Gadjah Mada University Yogyakarta, Indonesia, KP 36-41 ISBN: 979-99266-1-0 (in Bahasa Indonesia).

Utomo, Y.S., Haen, I., Hoesin, H., 2005b. Analysis and Compilation of Solar Radiation Intensity Data for Making Solar Radiation Map. Proceeding of National Seminar of Research Development in the Field of Industry, cooperation between Center for Engineering Science and Engineering Department of Chemistry and Mechanical Engineering Faculty of Engineering Gadjah Mada University, Yogyakarta, Indonesia, KP 31-35 ISBN: 979-99266-1-0 (in Bahasa Indonesia).

Utomo, Y.S., Haen, I., Hoesin, H., 2004. Mathematical Modeling for Solar Radiation Analysis on Earth's Equatorial Terrain (15° S - 15° N). Proceeding Seminar on Chemical Engineering and Process 2004, Chemical Engineering Department Faculty of Engineering Diponegoro University, Semarang, Indonesia, 35-41. ISSN: 1411-4216.

Hoesin, H., Utomo, Y.S., Haen, I., 2005. Mathematical Model of Solar Radiation Estimation at Sunshine Duration Measurement Station, Proceedings of National Seminar on Chemical Engineering and Process 2005, Department of Chemical Engineering Diponegoro University, Semarang, Indonesia A-4/1-6 ISSN: 1411 – 4216 (in Bahasa Indonesia).

Proceedings of the 1st Faculty of Industrial Technology International Congress
International Conference
Bandung, Indonesia, October 9-11, 2017
ISBN 978-602-53531-8-5

Comparison Study of Solar Flat Plate Collector with Two Different Absorber Materials

Amrizal*, Amrul, Ahmad Yonanda, Zulfa
Department of Mechanical Engineering, Universitas Lampung (Unila), Bandar Lampung - INDONESIA
* Corresponding author e-mail: amrizal@eng.unila.ac.id

Abstract

The major component of a flat plate solar collector consists of an absorber which is basically made of several narrow metal strip and pipe. They act as a conductive material that absorb heat from the incoming solar energy and then transfer it to the circulating fluid in the pipe to increase the temperature of the working fluid. The thermal performance of the collector is usually depending on the types of absorber material. The aim of this study is to determine the effect of different types of material absorber on the thermal performance of solar collector. The use of the same tube diameter size for risers and header were considered in the present study. The two types of absorber materials used in the current work are copper and aluminum. Both materials have thermal conductivity values of 386 W/mK for copper and 201 W/mK for aluminum respectively. The thermal performance characterization was performed under steady state condition according to the European Standard EN 12975. Collected data was processed by least square method (*Multiple Linear Regression*) to get collector performance parameters such as collector efficiency and heat losses. The test results show that there is no a significant difference of the collector thermal performance values in the use of the copper and aluminum material as an absorber. Furthermore, aluminum material provides an advantage in terms of thermal performance and production costs due to the higher thermal conductivity value and the lower material price and lower material density.

Keywords: solar collector, absorber plate, thermal performance

1. Introduction

Flat-plate collectors are the most common type of solar hot fluid panels. They are useful in meeting hot fluid needs for residential water, space heating, industrial application, etc. In principle, flat-plate collectors are more simple design, low maintenance and easy to operate. This type collector consists of an absorber, a transparent cover, a heat transport fluid and a heat insulating material.

Regarding the absorber, this material is a major component of the flat plate solar collectors, which play an important role in heat transfer between the absorber and the transport medium. Correspondingly, materials of high thermal conductivity are widely used in heat sink applications. The absorber acts as a conductive material that absorb heat from the incoming solar energy and then the heat is transferred to the transport medium in the fluid conduit. Copper, aluminum, brass and steel are the common material used in the absorber due to their high thermal conductivity.

Several studies have been reported regarding the performance of flat-plate collectors. Ekramian et al. (2015) simulated the use of the different absorber plates of copper, aluminum and steel with various thermal conductivities. The result showed that by increasing the absorber conductivity, the collector efficiency increases. The large difference value in the thermal efficiency between copper and steel (35 %) and slight difference between copper and aluminum (3.4%) was reported, respectively. The results were validated using those obtained by Cruz et al. (2014).

Nahar (2002) also investigated the effect of different absorber material by replacing copper in combination with aluminum and galvanized steel material. Furthermore, copper tube material replaces with galvanized steel tube and copper plate with aluminum plate. The result reported that there is no significant difference of thermal efficiency from the use of these kind of materials. While the price of the materials are large difference each other's.

In general, based on the tubing configuration there are two types of flat-plate collectors namely parallel tube collectors and serpentine tube collectors. The parallel tube collectors are most common type of flat-plate collectors available on the market and this collector has small parallel tubes connected to a larger main carrier pipes. These small parallel tubes are called riser tubes, while the larger ones are header tubes and so that the diameter size of both risers and header are different. Majority of studies reported here investigated the use of conventional collectors (parallel flat-plate collectors) in which the diameter dimension between riser tubes and header tubes are not the same. Facao (2012) also investigated the thermal efficiency of flat-plate collector based on the diameter of header and riser tubes. The result concluded that the outlet header should have a higher diameter compared to the diameter of the inlet header.

Most of the flat plate thermal collectors as in the market have risers and header of tubes with different diameter size. Unfortunately, in practice, this kind of flat plate thermal collector with different tubes geometry need a special design and much effort to attach it underneath of a surface of Photovoltaic/Thermal (PV/T) collectors. In this case, the flat plate thermal collectors will act as a heat exchanger for PV/T collector system. Meanwhile, the PV/T collectors are combination between a photovoltaic module and a solar thermal collector, forming a single device that converts solar energy into electricity and heat at the same time. In order to improve the electrical performance of PV modules, the heat from the PV can be removed and converted into useful thermal energy. It is well known that PV/T systems enhance the PV efficiency through a cooling effect.

The aim of this work is to study the effect of using different material as an absorber on the thermal efficiency of flat plate solar collectors. The use of the same tube diameter size for risers and header were considered in the present study. There is a lack information on the literature available on the use of different material as absorber associated with geometry of riser and header tubes. Therefore, it was necessary to carry out an experimental study on a flat plate solar collector and investigate on improvement of thermal efficiency.

2. Parallel Tube Collector Design

The tested of solar collectors with the two types of absorber materials, that is, copper and aluminum were designed and made in the current work. While the copper material almost provide the value of thermal conductivity 2 times higher than aluminum material as given in the characteristic of the solar collector. The configuration of the parallel tubes collector with aluminum as absorber was identical to that of the copper material. Both solar collectors were built under the same tube diameter size of riser and header. The tested solar collector used in this study has the characteristic:

- The number of risers is 7 tubes
- The diameter of header and risers is 0.00953 m
- Tube spacing is 0.08 m
- Absorber plate materials are copper (k = 386 W/m^{o}C) and aluminum (k = 201 W/m^{o}C)
- Area of absorber plate is 0,8 m^2
- Thickness of absorber plate is 0.003 m

Fig. 1: The tested solar collectors with (a) aluminum absorber plate (b) copper absorber plate

3. Experimental Procedure

The two different absorber material types of the collectors as presented in Figure 1 were tested indoors using a solar simulator based on European Standard EN 12975 (2006). According to this standard for indoors testing, the collector must be tested under incident radiation more than 700 W/m^2. Data collection were made for inlet and outlet fluid temperatures, ambient temperature and incident radiation, respectively. Then, all the temperature data and radiation data were measured using K-type Thermocouples with TM 947SD Thermometer and a Solar Power Meter SPM 1116SD, respectively. The mass flow rate of the working fluid was regulated by using a valve at a constant flow rate of 0.02 kg/m^{2}s (EN 12975). The mass flow rate was applied constant for all the measurement tests performed in the current work. To vary inlet fluid temperatures during the test, electrical heaters were used. All measurement data were recorded every 10 seconds.

In the current work a simple model based on the energy balance for the useful heat power is presented in the Equation (1), Dufie et al. (2006):

$$Q_u = A_{abs}(\tau\alpha)K_\theta(\theta)R_s - A_{abs}U_L(T_{pm} - T_a) \quad (1)$$

The mean temperature of the absorber plate (T_{pm}) as shown in the Equation 1 is difficult to calculate since this temperature is a function of the collector design, the entering fluid conditions and the incident radiation. Furthermore, it is convenient to relate the performance of the solar collector to the temperature of the heat transfer fluid, as the plate temperature is usually not known.

In view of simplification purpose, the whole mass (the tube, absorber plate, cover and insulation of the collectors) can be represented by a single temperature that refers to the mean temperature of the working fluid (T_m). By rearrangging Equation 1, an efficiency factors of the collector F' is introduced to allow the use of the mean inlet fluid temperature (T_m) as presented in Equation 2:

$$Q_u = A_{abs}F'(\tau\alpha)_e K_\theta(\theta)R_s - A_{abs}F'U_L(T_m - T_a) \quad (2)$$

Since the tested solar collectors are performed perpendicular to solar simulator radiation, furthermore the function of $K_\theta(\theta)$ incident angle modifier can be eliminated and then Equation 2 can be rewritten as presented in the Equation 3:

$$Q_u = A_{abs}F'(\tau\alpha)_e R_s - A_{abs}F'U_L(T_m - T_a) \quad (3)$$

From the above equation, the Q_u as the useful heat power is determined by the following equation:

$$Q_u = \dot{m}\, c_p(T_m - T_a) \quad (4)$$

As stated in EN 12975, curve fitting and least square method can be implemented in order to calculate the performance of solar thermal collector. A number of such tests should be carried out for at least four different values of the fluid inlet temperature T_i and led to the collection of 16 experimental points. Computations were applied using Multiple Linear Regresion (MLR) method to further identify the collector parameters as reported by Amrizal et al. (2010,2012,2013).

4. Results and Discussion

Several thermal performance tests were conducted associated with different absorber materials and the same diameter of riser and header tubes. The solar thermal parameters as shown in Table 1 are zero loss efficiency $F'(\tau\alpha)_e$ and heat loss $F'U_L$ respectively.

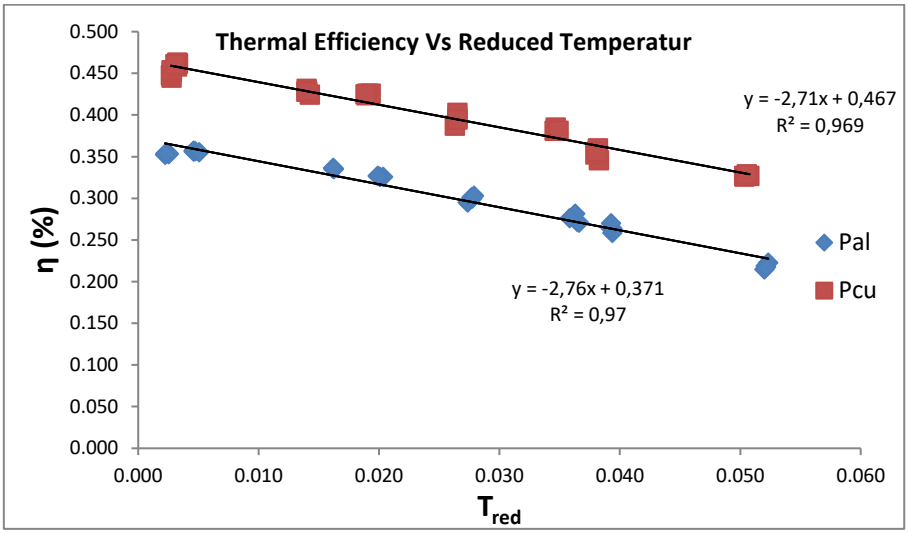

Fig. 2: The efficiency of the flat plate solar collector with different absorber materials

Table 1. Comparison between the two materials for price and thermal performance

Absorber Materials	Price per m2 (IDR)*	Zero Loss Efficiency $F'(\tau\alpha)_e$ (%)	Heat Loss ($F'U_L$) (W/m2 K)
Cu	750.000,00	46,7	2.71
Al	55.000,00	37,1	2.76

*Price of materials based on the market in Bandar Lampung (Indonesian Currency-IDR)

Figure 2 presents variation of thermal efficiency against reduced temperature parameter ($T_{red} = \frac{(T_m - T_a)}{R_s}$) for different absorber materials. From Figure 2, it describes the effect of two absorber materials on thermal efficiency of solar collector. As shown in the Figure 2, it presents that at zero reduced temperature, the thermal efficiency levels of the solar collector is 46.7% for copper and 37.1 % for aluminum, respectively. Therefore, the copper as an absorber material has better thermal performance than the aluminum material. However, increasing the value of zero loss efficiency $F'(\tau\alpha)_e$ for copper is only 9.6 % compared to that of the aluminum material. This means that the copper material does not significantly increase the thermal efficiency of the solar collector in comparison with its thermal conductivity value. Meanwhile, heat losses $F'U_L$ parameters of the two materials are nearly the same as given in the Table 1.

Meanwhile, the experimental results were compared with those obtained by Ekremian et al. (2015) associated with conventional solar collector. There is a significant different between the thermal efficiency obtained from the two results. The zero loss efficiency (at zero reduced temperature) of the conventional solar collector is 80 % for copper material which is 33% higher than that of the present study. This may be affected by using the same diameter of header and risers, therefore the dwell time of the fluid circulation will be shorter than that of the conventional collector. Consequently, the working fluid also absorb the heat shorter than that of the conventional collector with the bigger header tubes.

Table 1 presents comparison between the two materials based on price and thermal performance of the solar collector. Concerning the absorber material, the price of copper is higher 14 times than the price of aluminum material. While, the difference of the thermal performance between the two material is only 10 %. Again, the price of materials is not proportional to increasing the thermal performance of the collectors. For this reason, the use of aluminum material as an absorber for solar thermal collector should decrease the material cost.

5. Conclusion

The different materials used as an absorber affect thermal efficiency of solar collectors. Comparing to the thermal performance of two absorber materials (between copper and aluminum) give different values of 10 % for zero loss efficiency and 0.05 W/m^{2}K for heat loss, respectively. These values are not proportional to the price difference between the two materials as shown in Table 2. While the price of copper is 14 times higher than the

price of aluminum. Since the price of the two materials is large differences each others and it can be recommended the use of aluminum material is more suitable in terms of thermal performance and material cost. Regarding the use of the same geometry implemented in the present study, thermal performance decrease significantly compared to that of the conventional collector. This may be dwell time of the fluid circulation shorter than the dwell time of the conventional collector. The zero loss efficiency (at zero reduced temperature) of the present study is 33% lower than that of the conventional solar collector.

6. Acknowledgements

The author is grateful to have financial support from Research Grant (PPs-BLU), University of Lampung.

7. Nomenclature

F'	collector efficiency factor	-
R	radiation	W/m^2
T	temperature	C
$\dot{m}$	mass flow rate	kg/s
Q	energy gain	W
k	thermal conductivity	W/mK
c	heat specific of fluid	kJ/kgK
U	overall heat loss coefficient	W/m^2K
A	area	m^2
Greek letter		
τ	transmissivity	-
α	absorptivity	-
θ	incident angle	deg
Subscript		
e	efficiency	
s	solar	
i	inlet	
o	outlet	
m	mean	
a	ambient	
u	useful	
p	pressure	
L	losses	
abs	absorber	

8. References

Amrizal Nalis, Daniel Chemisana, J. I. Rosell, 2010. The Use of Filtering for the Dynamic Characterization of PV/T Flat-Plate Collectors. International Conference on Solar Heating,Cooling and Buildings EuroSun, Graz University, Austria.

E. Ekramian, S, Gh. Etemad, M Haghesnasfard, 2015. Numerical Analysis of Heat Transfer Performance of Flat-plate Solar Collectors. Journal of Fluid Flow, Heat and Mass Transfer Vol I 38-42.

European Standard EN 12975-2:2006. CEN (European Committee for Standardisation).

F. Cruz-Peragona, J.M. Palomara, P.J. Casanovab, M.P. Doradoc, F. Manzano-Agugliarod, 2012. Characterization of solar flat plate collectors. Renewable and Sustainable Energy Reviews (16) 1709– 1720

Jorge Facao, 2015. Optimization of flow distribution in flat plate solar thermal collectors with riser and header arrangements. Solar Energy (120) 104 –112.

John A. Dufie, William A. Beckman. 1991. Solar Engineering of Thermal Processes, John Wiley & Sons, Inc.

N.M. Nahar, 2002. Capital cost and economic viability of thermosyphonic solar water heaters manufactured from alternate materials in India. Renewable Energy (26) 623–635.

N.Amrizal, D. Chemisana, J.I. Rosell, J.Barrau, 2012. A dynamic model based on the piston flow concept for the thermal characterization of solar collectors. Applied Energy, 94, 244-250.

N.Amrizal, D. Chemisana, and J. I. Rosell, 2013. Hybrid Photovoltaic-Thermal Solar Collector Dynamic Modelling. Applied Energy, 101, 797-807.

Proceedings of the 1st Faculty of Industrial Technology International Congress
International Conference
Bandung, Indonesia, October 9-11, 2017
ISBN 978-602-53531-8-5

Hybrid System Solution for Off-Grid and Rural Energy Access in Indonesia

Soeripno Martosaputro*, Eduardus Jonathan*
Indonesia Wind Energy Society (IWES), Jakarta - INDONESIA
*Corresponding author e-mail: eduardus.jonathan@gmail.com, ripnoms@gmail.com

Abstract

Based on a recent study in 2016, there are still 12.659 underdeveloped villages or 16% of the total number of villages in Indonesia are still lacking in electric power from PT PLN (persero). To fulfill the electricity target in these villages, the government has issued the Program Indonesia Terang (PIT/Electrification Program). This program consists of efforts to extend the grid (for villages where PT PLN is present), install mini grid/off grid/hybrid systems, and implement solar home systems. It is hoped that this program will contribute to the penetration of renewable energy into the national energy mix to reach 25% in 2025. Regulation No. 38/2016 published by the Ministry of Energy and Mineral Resources (ESDM) titled ACCELERATION of ELECTRIFICATION IN UNDERDEVELOPED, SOLITARY, BORDER RURAL AREAS, AND INHABITED SMALL ISLAND THROUGH the BUSINESS OF PROVIDING A SMALL-SCALE POWER, outlines how to structure rural electrification projects.

In order to support these programs, an off-grid hybrid power system is a viable option, depending on the available resource at the project location. Whether a mix of one or more renewables with one or more non-renewable generators, a hybrid system is considered when it can achieve a higher cost-benefit compared with just using one generation independently. Existing hybrid power systems in Indonesia, including the Baron Technopark_Gunung Kidul Regency and Pantai Baru_ Bantul Regency are good examples of how an off-grid hybrid power plant can be constructed. Overall, this paper will assess the current trends in hybrid and off-grid electricity generation and determine why an off-grid hybrid system could be a better option compared to a single generation method.

Keywords: off grid, hybrid system, renewable energy, energy mix, rural energy

1. Introduction

1.1 Background Information on Electrification Ratio in Indonesia

Indonesia, a nation with more than 17,000 islands spanning 5,000 km is no stranger to issues in electrification. Having a coastline of more than 80,000 km, rural development in remote areas are impeded due to the degree of difficulty of interconnecting all the islands in the country into major electrical grids. Although smaller diesel powered systems are common in remote areas in the country, increasing oil price, along with major logistical problems are hindering villages to have full and reliable access to electricity. Solely responsible for providing electricity, including for customers in remote areas, is state-owned utility PT Perusahaan Listrik Negara (Persero)/ (PT PLN) along with ongoing support from the Ministry of Energy and Mineral Resources (MEMR).

According to data provided by the Directorate General of Electricity of the MEMR in the Book of Electricity Statistics No. 29/2016 (Directorate General of Electricity, 2016), the total electrification ratio in Indonesia is approximately 88%. The remaining 12% non-electrified households account for approximately 12,659 villages. Fortunately, over the past few years, electrification of remote areas in the country has been a key focus of the national electrical utility company, PLN, and the Ministry of Energy and Mineral Resources. The following figure below, taken from the Directorate General of Electricity of the MEMR, shows the increase in electrification in Indonesia, following the efforts by PLN and MEMR.

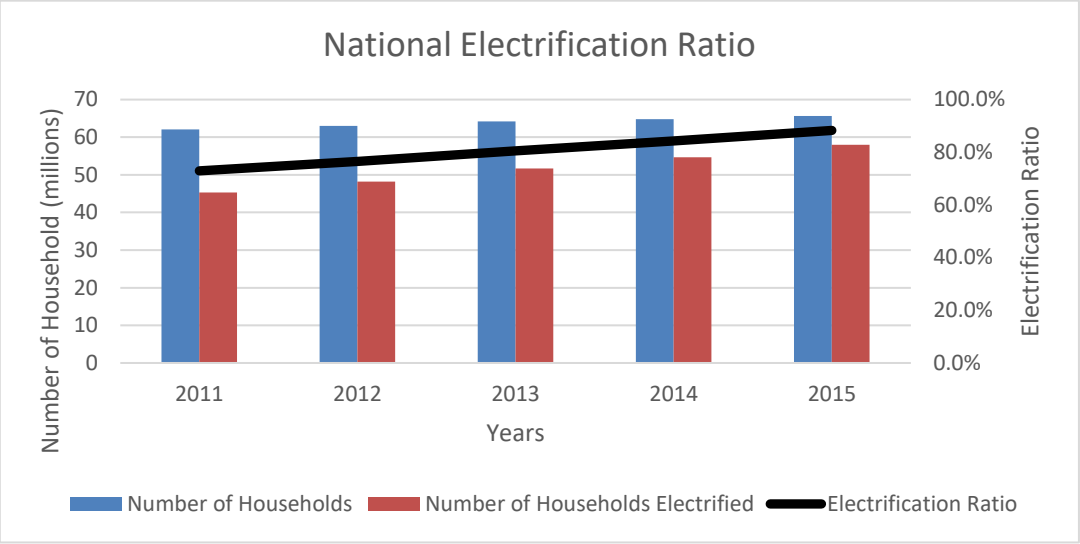

Fig. 1: National Electrification Ratio Graph (Source: Directorate General of Electricity, MEMR, 2016)

As seen from Figure 1 above, there is significant effort from PLN and MEMR to drive remote electrification programs. Recently, due to the difficulty of providing non-renewable electricity in remote regions, PLN and MEMR has turned their attention towards more sustainable and renewable energy solutions. Due to the rapid maturity of renewable energy technology, along with the steep decrease in costs, programs conducted by both PLN and the MEMR have provided facilities for stakeholders to go hand-in-hand to develop a cheaper, cleaner energy access for the country.

1.2. Existing Policy Support for Rural Electrification

As a sign of commitment to provide electricity to rural areas of the country, and to integrate more renewable energy into the electricity system, the MEMR launched a rural electrification program in April 2016, targeted specifically to eastern Indonesian regions where electricity access is usually much more difficult to find. Formally titled the Electrification Program (Program Indonesia Terang, PIT), is a part of the country's ambitious 35,000 MW program to fulfill the rapidly growing electricity demand in the country. This program has the vision of increasing the national electrification ratio from 88% in 2015 to 97% in 2019 via off-grid or mini-grid solar and micro-hydro power plants with a total capacity of approximately 9.4 MW to electrify 12,659 villages untouched by PT PLN, (Ministry of Energy and Mineral resources, 2016).

The following Table 1 below outlines the six provinces in Eastern Indonesia which are considered to be the main targets of this program, along with their expected total installed capacity and the budget the MEMR has allocated for each region.

Table 1: Provinces targeted by the PIT (Source: MEMR, 2016)

Province	Total Capacity (MW)	Budget (Rp Milllion)
Papua	5,4	198,9
West Papua	3,3	91,8
Maluku	0,3	42,8
North Maluku	0,1	11,1
East Nusa Tenggara	1,1	77,2
West Nusa Tenggara	0,3	19,2

Furthermore, in support of providing clean electricity for remote areas, in 2016, the MEMR has recently released a Minister Regulation (Peraturan Menteri) ESDM No. 38 year 2016, titled Acceleration of Electrification in Underdeveloped, Solitary, Border Rural Areas, And Inhabited Small Island through the Business of Providing a Small-Scale Power Plant, which outlines how to structure rural electrification projects.

Governing projects of up to 50MW for underdeveloped villages to small islands, MEMR Minister Regulation No. 38/2016 states that for rural electrification projects, whether developed by a regional government body, a private entity, or a local union, must first prioritize local and readily available renewable energy resources ahead of non-renewable fuels. Upon getting approval from the Minister of Energy and Mineral Resources, the project owner might also be eligible for subsidy on the electricity price. The following equation outlines the amount of subsidy that can be provided by the government.

$$S = -\big(TTL - BPP(1 + M)\big) \times V \quad (1)$$

Where:

- S = Subsidy (Rp)
- TTL = PLN Electricity tariff for households rated at 450VA (Rp/kWh)
- BPP = Cost of electricity generation locally (Rp/kWh)
- M = Margin (%)
- V = Volume of electrical energy usage per connection per month (kWh/month). This is limited to a maximum of 84 kWh per connection per month.

On the other hand, projects which are not eligible for subsidies will have the electricity selling price determined by the Minister or the local governor, in accordance with the prevailing laws.

2. Hybrid System and its Applications

A hybrid power system is defined by PLN as a system with two or more power generation sources, either renewable or non-renewable sources or a combination of both. A system with only one generation source and a storage is not considered a hybrid. There are various ways of configuring a hybrid power system, depending on a lot of external factors that are usually making the project more feasible by going hybrid, such as: cost considerations, geographical considerations, fuel or resource availability, etc. A hybrid system can consist of a combination of solar, wind or hydro power in conjunction with diesel and even may or may not be coupled with energy storage systems, such as batteries. Figure 2 below is an example of a wind-PV-diesel hybrid configuration.

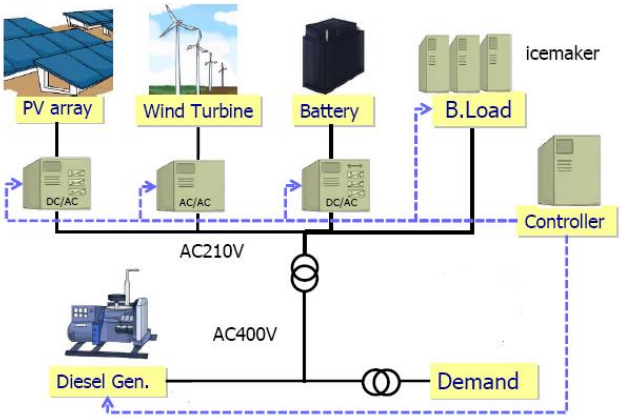

Fig. 2: Simple wind-PV-Diesel Hybrid Configuration diagram

Benefits of a Hybrid System

A hybrid system is usually implemented to reduce the weakness of its individual power source which is being offset by the other power sources. For example, an intermittent but renewable power source (e.g. solar PV) can have its intermittency offset by a stable but non-renewable power source (e.g. diesel). The high and fluctuating cost of diesel, especially in remote locations, can be compensated on certain periods of time using readily available sunlight through solar PV technology. However, for periods that solar PV are unable to operate, such as at night or when there is minimum sunlight, the diesel can take over and provide reliable electricity to the demand.

For illustration purposes, the following Figure 3 shows an example of a 4 kWh/day household's electricity demand being met by a hybrid system consisting of a solar PV system and a diesel generator. During the night, where the peak load is reached, the solar PV is not operational so the diesel will provide all the electricity needed for the

house. In this example, a 130Wp PV system can reduce approximately 22% of the electricity consumed from a 300W diesel system during the day when the sun is shining. This 22% of electricity generation from diesel reduced is linearly correlated to the price of electricity that is charged to the house, hence when the price of diesel increase, the benefit in using a hybrid system with the solar PV will be much more apparent.

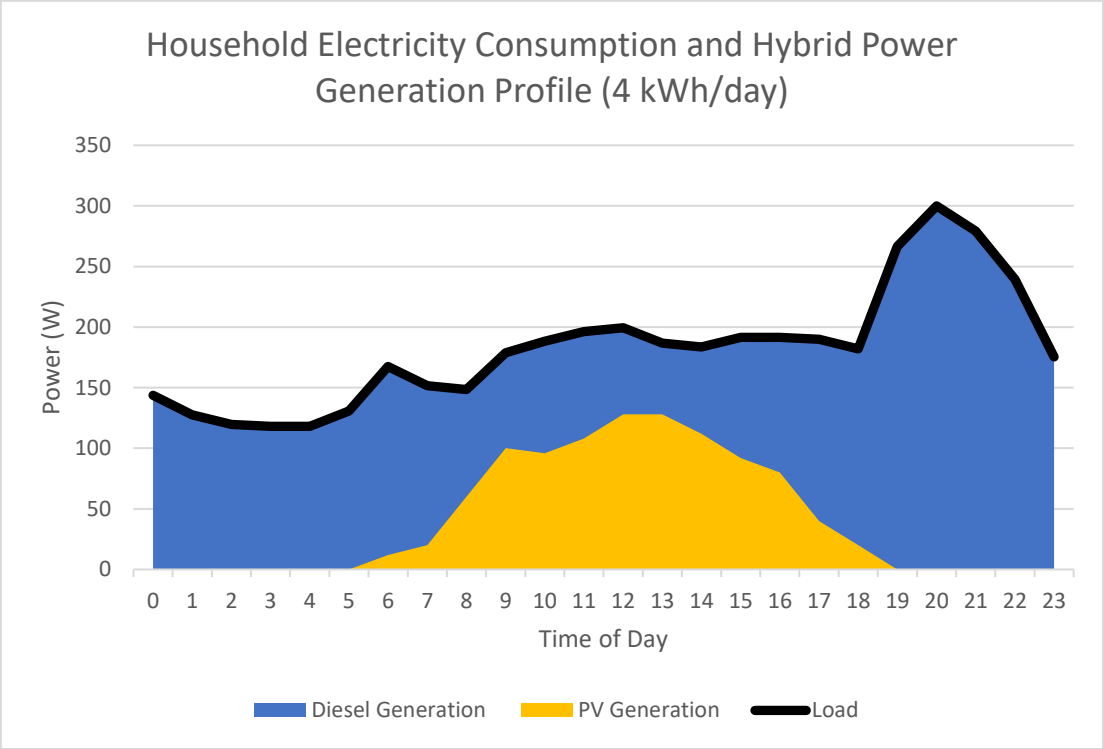

Fig. 3: 4kWh/day Household Electricity Consumption and Hybrid Power Generation (example)

Off-Grid Hybrid System

Due to the reliability and accessibility of hybrid power systems, it is usually more suitable for off-grid remote electrification systems without electricity access from PLN compared to its individual components separately. For an off-grid system, a base load power source is usually very much needed. An already relatively stable renewable energy source, like a hydro or geothermal powered system, which can be turned on and off as needed, is typically sufficient to provide electricity for an off-grid load, depending on resource. However, for systems like hydro and geothermal, resources are much more location dependent, unlike intermittent but more readily-available solar or wind, which may be inaccessible for remote villages.

To determine the most suitable mix for an off-grid hybrid system, it is important to also perform an economic analysis of the model by comparing the cost of each technology on per kWh generated basis. The Levelized Cost of Electricity (LCOE) is a common term of assessing the cost-benefit of different generation sources and their combinations. According to a study conducted in 2013 (Blum et al, 2013), a hybrid system for an Indonesian village grid is a more cost-efficient system compared with a solar PV coupled with a battery system, or a stand-alone conventional diesel system. The study assesses two scenarios; Scenario A, is a basic scenario, whereby electricity is demanded only at night time and zero electricity is needed during the day, therefore making PV obsolete. Scenario B, is a more advanced scenario where power generation is smoother during the day due to small commercial activities and the system never reduces to an idle state, although higher demand from the household sector is still the peak during night time. The following Figure 4 shows the LCOE for the different system configurations for both scenarios.

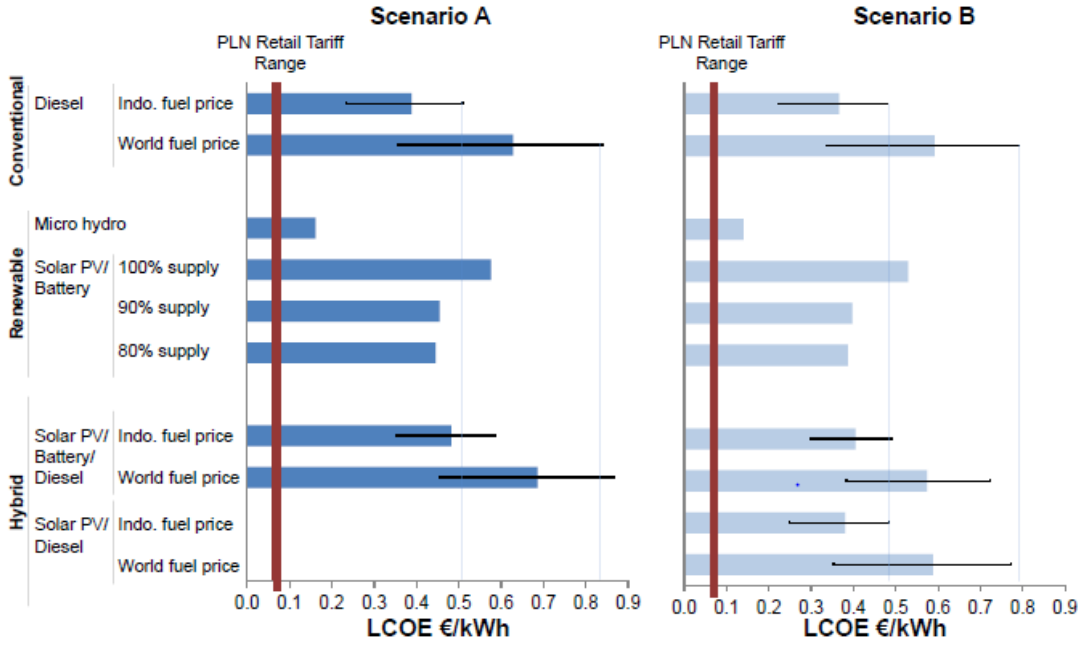

Fig. 4: LCOE of different renewable energy technologies (Source: Blum et al, 2013)

Hybrid Resource Maps in Indonesia

As mentioned in the previous section, determining the available renewable energy resource at the proximity of the location is critical in determining the viability of possible combinations of hybrid systems. In spirit of MEMR Minister Regulation No. 38/2016 above, assessment of the available renewable energy resource in a specific location must first be done. For renewable energy sources, such as wind and solar, there are already maps available publicly online based on satellite measurements, which can be used for preliminary project prospecting. For wind power generation, the MEMR has worked together with the Danish aid agency Danida to create an online portal for available wind data throughout the country on a 3x3 grid. This can be accessed through the following link: http://indonesia.windprospecting.com/. There are also various solar resource maps available online for free which covers Indonesia. Companies, such as SolarGIS (https://solargis.info/) provides high resolution solar data on their online global atlas. The International Renewable Energy Agency (IRENA) has also published an online wind and solar atlas for Indonesia, which can be accessed from the following link; https://irena.masdar.ac.ae/gallery/. During project prospecting phase, it is critical to identify the available resources at the specific site and whether access to harness these sources is possible.

3. Existing Hybrid Power Plants in Indonesia

Hybrid System in Baron Technopark – Gunung Kidul Regency

Indonesia has established a number of pilot off-grid small-scale hybrid power plants in Indonesia. Mostly developed, constructed and operated by the Agency for Assessment and Application of Technology (Badan Pengkajian dan Penerapan Teknologi, BPPT) and its extensions, the hybrid power plants (Pembangkit Listrik Tenaga Hibrid, PLTH) are scattered throughout the country, both in remote areas and in places where there is enough resources.

One project that was successfully developed by BPPT and is still operational up to today is the Baron Technopark Hybrid Power Plant located on Baron beach in Jogjakarta. Originally constructed in 2010 together with the Norwegian Agency for Development Cooperation (NORAD), Baron Technopark has been a long-standing showcase on the implementation of hybrid power plants in Indonesia. The power plant generates electricity using a combination of 36 kWp mono-crystalline PV modules produced by PT LEN Industri and 2 wind turbines, rated at 10 kW and 5 kW. These two intermittent sources are then used to power the loads in the vicinity of the power plant along with a battery bank with a total capacity of 1000Ah that can supply 240 kWh/day and a 25kVA diesel generator (Badan Pengkajian dan Penerapan Teknologi. BPPT, 2010). The following diagram in Figure 5 dan Figure 6 shows the single line diagram and photograph for this hybrid power plant and the flow of energy through its components.

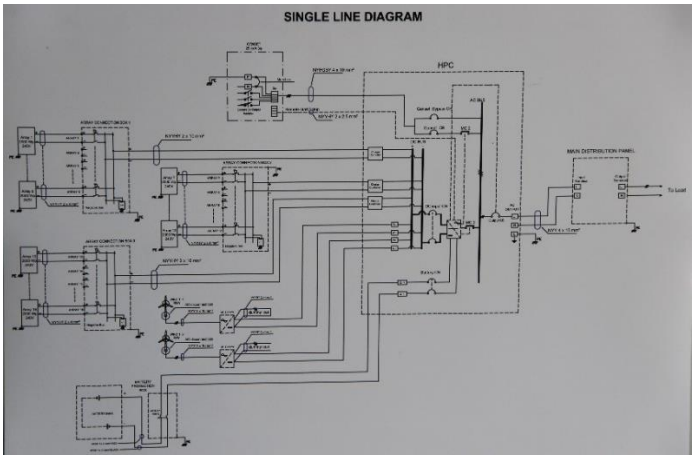

Fig. 5: Single line diagram for Baron Technopark (Source: BPPT, 2013)

Fig. 6: Baron Technopark, wind-PV-Diesel (Source: Soeripno)

Hybrid System in Pantai Baru Bantul Regency

A wind-PV-battery hybrid system in Pantai Baru – Pandansimo, Bantul was constructed by the Ministry of Research and Technology (Kementrian Riset dan Teknologi) of Indonesia supported by the Indonesian National Institute of Aeronautics and Space (Lembaga Penerbangan dan Antariksa Nasional, LAPAN), BPPT, the Ministry of Marine Affairs and Fisheries (Kementrian Kelautan dan Perikanan Indonesia) and the local Bantul government. The project was initiated in an effort to utilize the energy resource available in the region to increase the livelihood of the local community and as a hybrid power plant showcase for coastal areas. The Pantai Baru hybrid power plant supplies electricity to local farmers and fishermen also to a nearby icemaking plant, which supplies ice to local fishermen, eateries, and irrigation for farms and fisheries.

The hybrid power plant is a combination of two renewable power generation sources, wind power and solar power, totaling a rated capacity of 77.5 kW. The electricity produced by the hybrid power plant is used to operate the ice making machine, water pumps, blowers, street lighting, electronic equipment, etc. Aside from the availability of both the wind and solar resource at the site, the hybrid power plant, the hybrid power plant is equipped with an energy storage system and a hybrid control system. The wind turbine used in the wind farm consists of several types of small wind turbines: 21 x 1 kW, 6 x 2,5 kW dan 2x 10 kW, The solar part of the plant consists of 100 Wp solar panels with a total capacity of 15 kWp. Figure 7 shown the part of hybrid system plant in Pantai Baru

Fig. 7: Pantai Baru hybrid system of Wind-PV-Diesel for ice making (Source: Soeripno)

4. Challenges and Opportunities in Hybrid Power Development

The Baron Technopark pilot project, among other hybrid projects in Indonesia are meant to be a guideline for all stakeholders involved in the power generation industry. However, many of these pilot projects are not performing for as long as it was initially thought to be. There are various learning points from the operations of these hybrid plants over the past few years. These include:

- Operation and maintenance is critical to ensure the longevity of hybrid power plants. Since most off-grid hybrid power plants are projects done by international aid organizations, there are budgetary issues for keeping the plants running
- Capacity building. Due to the remote locations of these power plants and the complexity of combining different types of power generation, local expertise is scarce.
- Spare parts for replacement. Hybrid power plants, especially those utilizing batteries need parts replacement every several years. Shortage of spare parts in rural areas are becoming a hindrance to the operation of hybrid power plants

Nonetheless, there is still room for growth for hybrid power plants in Indonesia, especially with the recent regulations and government programs which incentivizes the development of off-grid hybrid power plants in Indonesia for rural electrification. From an economic point of view, hybrid systems are becoming much more attractive now with the rapid reduction in costs of generating renewable energy and energy storage in the past few years. From a technical point of view, with all the available resource maps and existing hybrid power plants that are operational, it is now easier than ever to develop off-grid hybrid power plants for remote electrification.

5. Conclusion

Off-grid hybrid power plants are now very viable options due to recent techno-economic trends in the renewable energy industry in Indonesia. Along with regulatory support from the Government, off-grid hybrid power plants are expected to penetrate regions untouched by PLN in order to push development in remote regions. However, it is recommended that operation and maintenance of these power plants are to be performed rigorously to prevent unwanted breakdowns.

Usually, off-grid hybrid power plants are located in remote areas with difficult access and low electricity load demand. Due to these challenges, hybrid systems are typically not economically viable as a venture and can be constructed together with support from the Government together with ministries such as the Ministry of Villages, Disadvantaged Regions and Transmigration (Kementrian Desa, Pembangunan Daerah Tertinggal dan Transmigrasi), or the Ministry of Marine Affairs and Fisheries. Without support from the Government, off-grid hybrid power systems will have difficulties in penetrating the commercial market.

6. References

Directorate General of Electricity, Ministry of Energy and Mineral Resources. 2016. The Book of Electricity Number 29 -2016. 25.

Program Indonesia Terang Dicanangkan, available at: http://ebtke.esdm.go.id/post/2016/04/21/1194/program.indonesia.terang.dicanangkan, accessed on August 31 2017

Blum, N. U., Wakeling, R. S., & Schmidt, T. S. 2013. Rural electrification through village grids—Assessing the cost competitiveness of isolated renewable energy technologies in Indonesia. Renewable and Sustainable Energy Reviews, 22, 482-496.

Badan Pengkajian dan Penerapan Teknologi (BPPT). 2010. Technical Document 1: Desain Pembangkit Listrik Tenaga Hibrida di Kawasan Baron Technopark, Gunung Kidul, DI Yogyakarta.

Hasil Program Listrik Pedesaan, available at: http://www.iesr.or.id/Hasril_Program Listrik Perdesaan.pdf, accessed on August 2017

Proceedings of the 1st Faculty of Industrial Technology International Congress
International Conference
Bandung, Indonesia, October 9-11, 2017
ISBN 978-602-53531-8-5

An Experimental Model Piezoelectric Cantilever Beam for Energy Harvesting

Aditya Sukma Nugraha* and Sapdo Utomo
Research Center for Electric Power and Mechatronics
Indonesian Institute of Sciences, Kompleks LIPI - Jl Sangkuriang, Bandung, West Java, 40135, Indonesia
* Corresponding e-mail: aditngrh@gmail.com

Abstract

Research of energy harvesting is increasing rapidly over last decade. In this study has effort in laboratory scale of energy harvesting with a piezoelectric cantilever beam. The harvester is placed in the middle of the cantilever beam to simulate. This paper is intended to investigate piezoelectric energy harvesting from vibration induced by vertical loads. The design of Cantilever beam configuration piezoelectric is analyzed by finite element method (FEM) to get the first mode of the system. The prediction result by finite element software for the first mode is 91,24 Hz. The effect of displacement, velocity, acceleration with Piezoelectric moving load function on the produced power also investigated in this paper. The experimental result shows the studied mode shape variable can be effected on the energy harvesting result. Lastly, the research results prove that the theory of vibration is the highest voltage is located in the natural frequency of the system.

Keywords: Piezoelectric, cantilever, beam, mode-shape, vibration, voltage.

1. Introduction

The utilization of structure vibration is used for capturing energy from vibration environment is a solution to increase the energy source in the rural area. Among different approach to collect vibration component moving to power energy such as vibration from rotary equipment [1][2], railroad application [3] and structural health monitoring [4]. The most popular research about vibration energy harvesting is piezoelectric with environments component.

Piezoelectric research is mostly done to increase the power output of a particular vibration source. Improper piezo design will cause low the efficiency of the energy harvested [5]. Theoretically, in mechanical vibrations, a system that resonates at a frequency that coincides with the natural frequency of the system will produce maximum electrical power. One thing that needs to be proved in this paper is the opinion from Liu that results in a solution that the output power will drop when the excitation frequency shifts away from the natural frequency of the mechanical system[6]. Many studies use adaptive adjustments to conform to the natural frequency of the piezo system, as did by Clark using the shunt method to adjust the resonator frequency of the piezo system [7]. The study also studied in this paper is the evaluation of structural responses, in this case, is the material and geometry functions of the cantilever beam to external excitation functions, some studies also do the same regarding checking the diversity of materials and geometry associated with the excitation function with statistical approach[8][9].

Typically modeling in piezoelectric for energy harvesting used the simplification of single degree of freedom (SDOF)[10]. SDOF modeling done in this paper using Finite Element Method (FEM) approach. Initial modeling will illustrate the characteristics of the cantilever beam used, such as the vibration mode occurring in some natural frequencies of the cantilever beam system. In this study present distributed parameter solution from cantilever beam with a connection to piezoelectric. The steady state voltage response is measured in such a way that measurements of the vibration mode predicted by the finite element method (FEM) using ANSYS software. Validation through experiment aims to know the role of vibration mode at the natural frequency of the system against the amount of voltage generated.

2. Governing Equation and Theory

There are basically has two types of piezoelectric materials: piezoceramics such as Lead Zirconate Titanate (PZT) and piezopolymers such as Polyvinylidene Fluoride (PVDF)[11]. The workings of the piezoelectric depend on how the material undergoes a bending process. The mechanical and electrical functions of piezo electric can be described in the following equation:

$$S = S^E \cdot T + d^t \cdot E \quad (1)$$

$$D = d \cdot T + \varepsilon^T \cdot E \quad (2)$$

The most useful mode of vibration in piezoelectric is mode one because this mode occurs in the first natural frequency of beam cantilever system. A cantilever beam subjected to free vibration, and the system is considered as a continuous system in which the beam mass is considered as distributed along with the stiffness of the shaft, the equation of motion can be written as:

$$\frac{d^2}{dx^2}\left\{EI(x)\frac{d^2Y(x)}{dx^2}\right\} = \omega^2 m(x)Y(x) \quad (3)$$

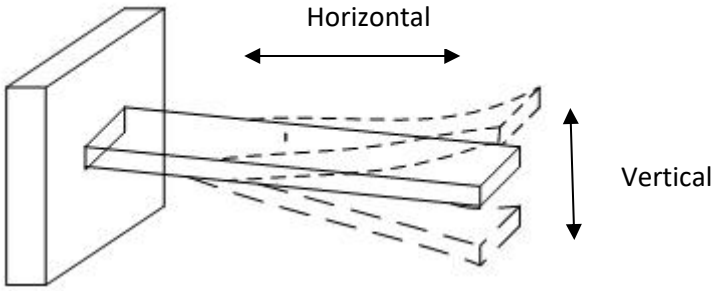

Fig. 1: The beam free vibration

Based on fig.1 boundary conditions for a cantilever beam

$$at\ x = 0, Y(x) = 0, \frac{dY(x)}{dx} = 0 \quad (4)$$

$$at\ x = l, \frac{d^2Y(x)}{dx^2} = 0, \frac{d^3Y(x)}{dx^3} = 0 \quad (5)$$

for beam cantilever under free vibration get :

$$\frac{d^4Y(x)}{dx^4} - \beta^4 Y(x) = 0 \quad (6)$$

with ,

$$\beta^4 = \frac{\omega^2 m}{EI} \quad (7)$$

The mode shape for a continuous cantilever beam can be written as [11]:

$$f_n = \frac{{V_n}^2}{2\pi}\sqrt{\frac{EI}{12AL^4}} \quad (8)$$

3. Cantilever Beam FEM Result

Modeling a cantilever beam using three-dimensional model. Piezoelectric is placed in the middle of the cantilever beam as shown in Figure 2. As shown in Figure 2, the meshing and modal analysis model are simulated using ANSYS software with FEM approach. With Modal analysis simulation it is known that the first mode in the cantilever beam system is 91 Hz with a single moving vertical direction. The design of the Mode shape for cantilever beam is shown below:

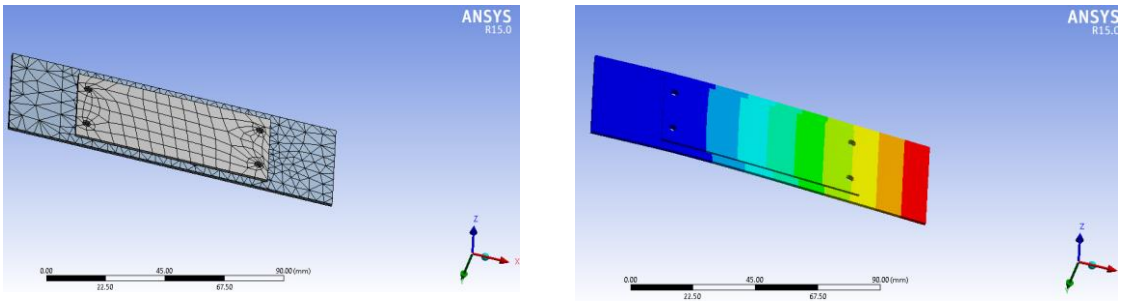

(a) Meshed model **(b) Frist mode at 91 Hz**

Fig. 2: The Cantilever beam FEM simulation

The experiment was carried out using mini shaker as a tool to excite cantilever beam system with a peak to peak force produced by a mini shaker is 20 N, so that graph of response function to amplitude displacement, velocity, and acceleration, according to figures 3, 4 and 5, respectively.

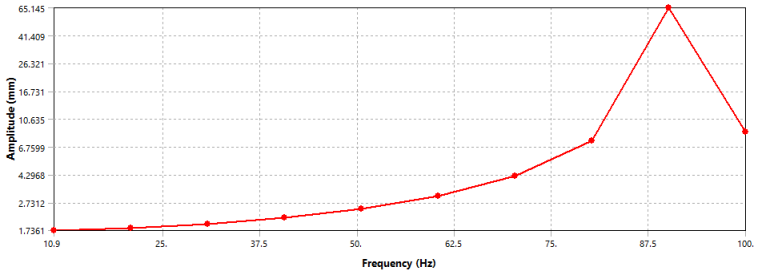

Fig. 3: Function response to amplitude displacement

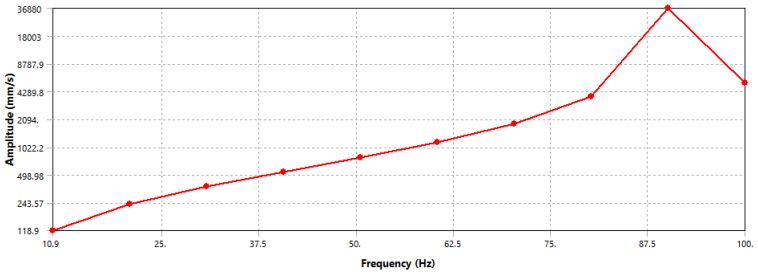

Fig. 4: Function response to amplitude velocity

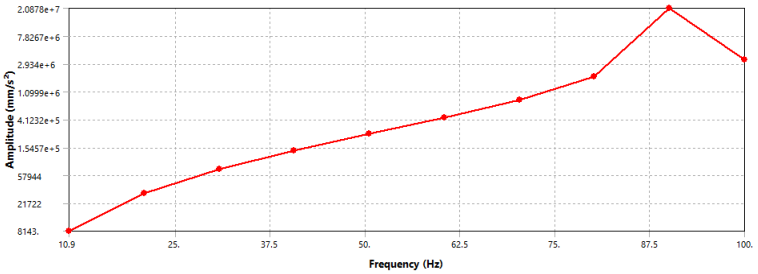

Fig. 5: Function response to amplitude acceleration

4. Experimental result and discussion

3.1. Experimental setup

Cantilever beam energy harvester is connected to a fixed support. The piezoelectric coupled with cantilever beam attached used the bolt in a location in the middle of the beam. In figure 6 and 7 are shown the side view of experimental setup and the scheme of experimental setup.

Fig. 6: the side view of experimental setup

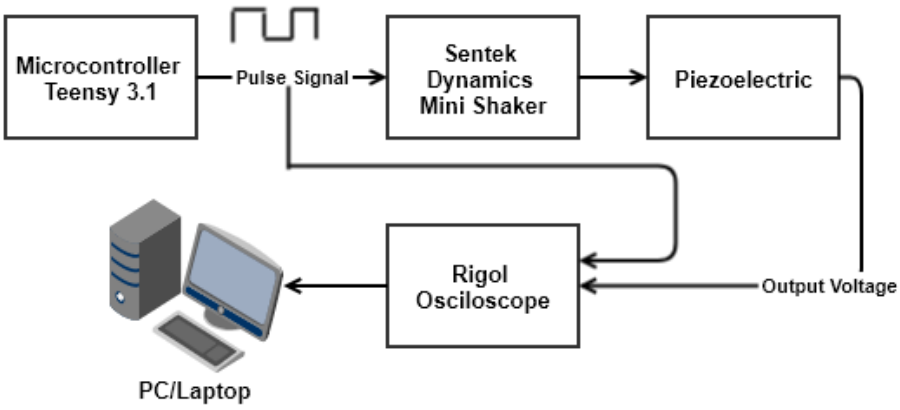

Fig. 7: Experimental setup for piezoelectric data acquisition

In this research, the experimental setup shown in Figure 7. Teensy 3.1 Microcontroller is used to generate pulses (square wave signal as an input signal) in Frequency of 30 Hz , and 91.24 Hz. These pulses will trigger the mini shaker to generate the vibration, the frequency of vibration depends on the frequency of the pulse. The vibration from the mini shaker is coupled to the piezoelectric, so the piezoelectric will produce the electrical energy (output signal in voltage). Input signal from Teensy 3.1 and output signal from piezoelectric are measured using oscilloscope, and then the data from oscilloscope are recorded to the PC/laptop.

3.2. Result and discussion

In the test used 2 different case study there are 30 Hz and 91 Hz. Fig 8 Shown the result of output voltage characteristic from piezoelectric with the 91.24 Hz input pulse vibration. According to the result, the characteristic of output voltage has identical cycle in every two cycle of input pulse (two periode of input pulse). The highest postive voltage is 45.3 V and the highest negative voltage is -53.1 V. The detail of one cycle of piezoelectric output voltage is shown in Fig 9

Fig 8. Data Capturing from Oscilloscope with The Input Pulse 91.24 Hz

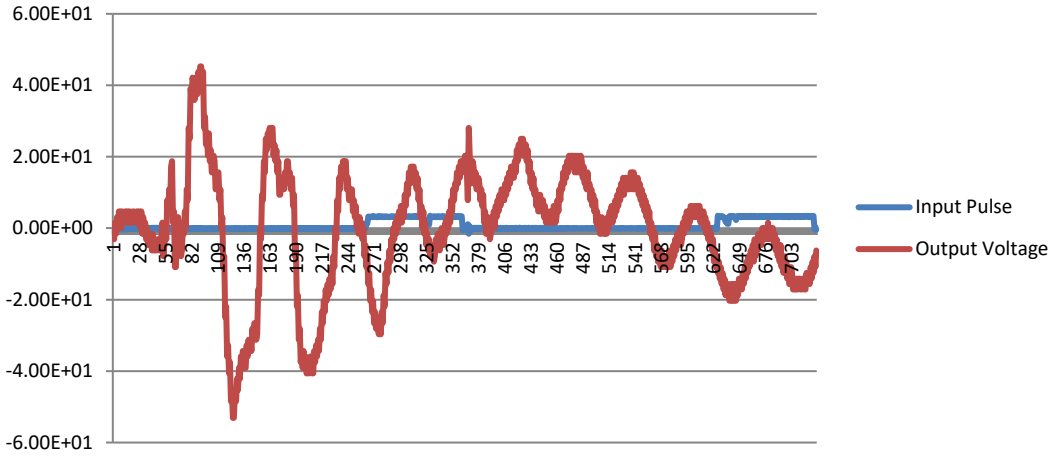

Fig 9. One Cycle of Piezoelectric Output Voltage at 91.24 Hz Vibration

Because of the output voltage has a negative value, we have to create the filter if we want to use the piezoelectric as a source of electrical energy. The simple way to filter the output by using bridge rectifier. After using the bridge rectifier as a filter, the output voltage that has a negative value will be converted to become a positive value, then the output voltage will looks like in the Fig 10. With this filter the highest positive voltage is 53.1V and the average voltage is 12.493 V.

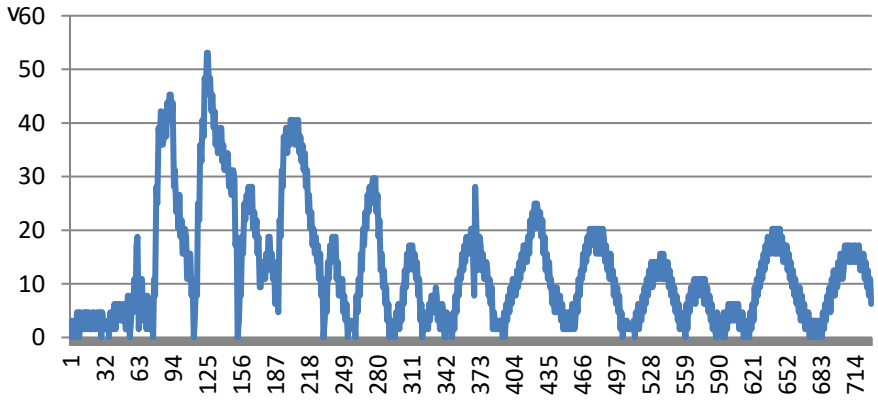

Fig 10. Output Voltage from Piezoelectric at 91.24 Hz Vibration with Bridge Rectifier Filter

Fig 11. Shown the result of output voltage characteristic from piezoelectric with the 30 Hz input pulse vibration. From the measurement results, it was found that at 30 Hz vibration obtained the output voltage is smaller than the previous measurements.The detail of one cycle of piezoelectric output voltage at 30 Hz is shown in Fig 12. The highest of positive voltage is 26.6 V and the highest negative voltage is 34,4 V.

Fig. 11: Data Capturing from Oscilloscope with The Input Pulse 30 Hz

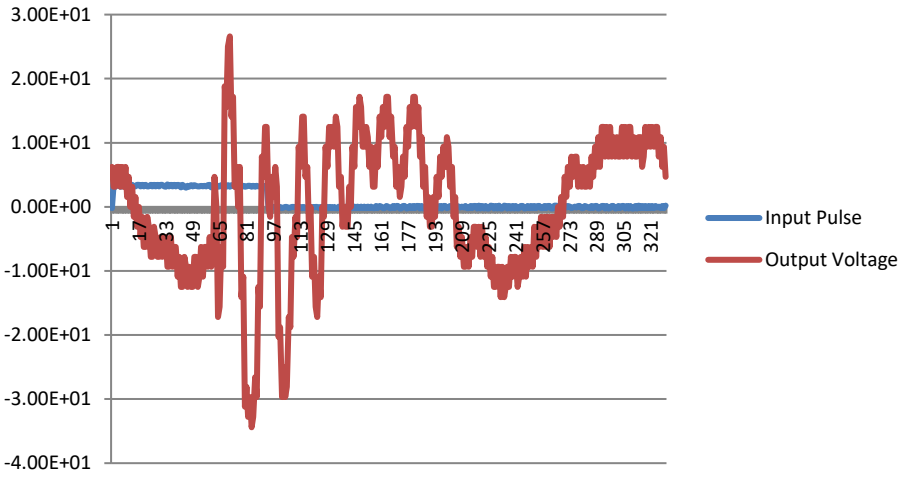

Fig. 12: One Cycle of Piezoelectric Output Voltage at 30 Hz Vibration

Fig 13 Show the result of output voltage with bridge rectifier. At 30 Hz vibratrion, the voltage average of piezoelectric is 8.623 V.

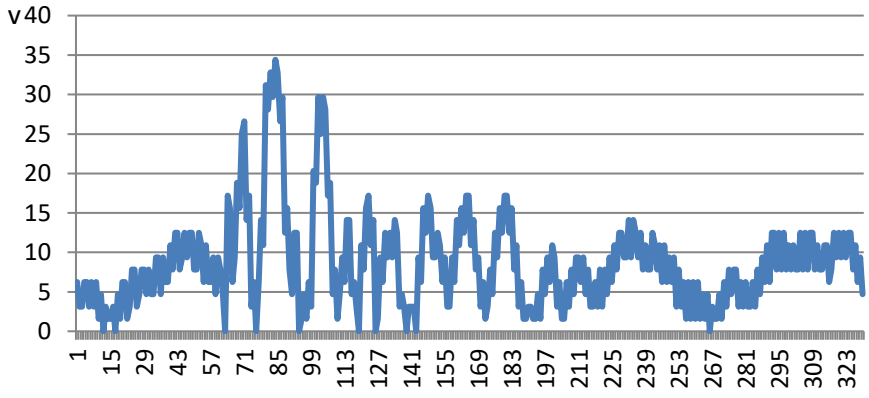

Fig. 13: Output Voltage from Piezoelectric at 30 Hz Vibration with Bridge Rectifier Filter

5. Conclusion

Cantilever beam energy harvester are the most popular devices found in the literature, there are still much more to learn. The research results prove that the theory of vibration is the highest voltage is located in the natural frequency of the system. From this research note that piezoelectric is able to produce the largest output voltage at frequency 91,24 Hz. This is particularly interesting to be studied more deeply especially for research related to the design of appropriate energy storage systems for piezoelectric energy harvesting.

6. Nomenclature

S = Mechanical strain
D = Electrical Displacement
T = Mechanical stress
E = A simply Hooke's law relating strain and stress
S^E= Matrix of elasticity under condition of constant electric field
d and d^t = the matrices for the direct and the reverse piezoelectric effect where the superscript t means the transposed matrix
ε^T = dielectric permittivity under a zero or constant stress
I = The moment inertia of the beam cross section
Y(x) = Displacement in vertical direction (see figure 1)
x = Distance in horizontal measured from fixed end.
ω = Natural frequency
m = mass per unit length
f_n = Natural frequency
A = Area
L = Cantilever beam length
v_n = 1,875 for fundamental mode (first mode).

7. Acknowledgements

The author would like to thank to the officials of Research Centre of Electrical Power and Mechatronics for the support and assistance that have been given in this research.

8. References

J. Li *et al.*, "Sensors and Actuators A : Physical A piezoelectric-driven rotary actuator by means of inchworm motion," vol. 194, pp. 269–276, 2013.

D. Maˇ, "Sensors and Actuators A : Physical An inertial piezoelectric plate type rotary motor," vol. 263, pp. 131–139, 2017.

X. Zhang, H. Pan, L. Qi, Z. Zhang, Y. Yuan, and Y. Liu, "A renewable energy harvesting system using a mechanical vibration rectifier (MVR) for railroads," *Appl. Energy*, 2017.

M. Quyen *et al.*, "Progress in Aerospace Sciences Review on energy harvesting for structural health monitoring in aeronautical applications," *Prog. Aerosp. Sci.*, vol. 79, pp. 147–157, 2015.

K. Shin, Z. Shakir, O. Zhi, Y. Huang, and C. Wen, "Structural dynamics effect on voltage generation from dual coupled cantilever based piezoelectric vibration energy harvester system," *Measurement*, vol. 107, pp. 41–52, 2017.

J. Liu, H. Fang, Z. Xu, X. Mao, and X. Shen, "A MEMS-based piezoelectric power generator array for vibration energy harvesting," vol. 39, pp. 802–806, 2008.

M. G. Muriuki and W. W. Clark, "Analysis of a technique for tuning a cantilever beam resonator using shunt switching," vol. 1527.

T. Chang and H. Chang, "Stochastic dynamic finite element analysis of a nonuniform beam," *Int. J. Solids Struct.*, vol. 31, no. 5, pp. 587–597, 1994.

M. Asme and M. Asme, "Finite Element Method for Stochastic Beams Based on Variational Principles," vol. 64, no. September, pp. 664–669, 1997.

A. Erturk and D. J. Inman, "An experimentally validated bimorph cantilever model for piezoelectric energy harvesting from base excitations," vol. 18, 2009.

M. Bhanusri, "Design and Simulation of Unimorph Piezoelectric E nergy H arvesting S ystem," pp. 1–6, 2013.

Proceedings of the 1st Faculty of Industrial Technology International Congress
International Conference
Bandung, Indonesia, October 9-11, 2017
ISBN 978-602-53531-8-5

DESIGN AND OPTIMIZATION OF HYBRID POWER PLANT IN HOUSEHOLD SCALES USING HOMER MODELS

Ibrahim[1,*] and Dani Rusirawan[2]

[1]Graduate Student of Mechanical Engineering, Itenas, Bandung – INDONESIA

[2]Dept. of Mechanical Engineering, Itenas Bandung – INDONESIA

[*] Corresponding author e-mail: ibrahimst@live.com

Abstract

The hybrid system is used in power plants by using more than one of system. Presently, utilization of the hybrid system growth and can be used in order to optimize the potential renewable energy resources at each locality. Generally, a home stay (household) is designed to utilize some of the potential of renewable energy in parallel, as energy saving measures. For the purpose study, simulation and optimization of hybrid system with the output target: estimate system capacity, lifecycle cost and green house gas (GHG) emissions are performed using Homer model software (Homer version 3.7.6). The hybrid system applied consisted of PLN grid, biogas generator, photovoltaic (PV), fuel cell (FC), wind turbine (WT), Li Bat, converters, controller, electrolysis and hydrogen storage tank. The simulation results showed that the most optimal system is hybrid system without a Li-Bat. The hybrid system components capacity are 7 kW of Biogas generator, 1 kWp of PV, 1 kW of FC, 1KW of WT, 5 kW of converter, 1 kW of Electrolysis, and 1 kg of H-Tank. Techno-economic parameters consist of Initial Capital ($ 13.100) were the highest of any other combination. COE ($ 0151), NPC ($ 86.197) and Operating Cost ($ 5.654) are lower than the other combinations. The IRR Value about 42.2% and the Renewable Fraction value about 61%.

Keywords: Household Scale, Hybrid Power Plant, Sustainable Energy, HOMER, Simulation

1. Introduction

The term of hybrid power generation system used at power plants that contain more than one generator, usually a combination of conventional generators (diesel or gas) and renewable energy (solar power, Wind Power, thermal power station or Microhydro). Hybrid system has grown and has been operating in many countries to take advantage of the local potential of each, from small scale till big scale (Sandia National Laboratories, 2009). Several advantages HYBRID system (Sukarman and Othman 2005), are: (1) improve the reliability of the system in fulfilling the load, (2) reducing emissions and pollution, (3) provide continuous electrical power supply, (4) increasing the age of the system, and (5) reduce costs and improve the efficiency of electrical energy use. PT PLN is currently implementing the cooperation of buying and selling electricity to households, especially for homeowners who installed solar cell roof of their house. In order to be buying and selling of electricity between PLN with homeowners, kWh meter used is also different, namely kWh of electricity meters 'import-export'. KWh meter for 'export - import' the electricity may be split between the electricity generated from the solar cell or photovoltaic with electricity from the grid.

This paper discusses the use HOMER model to design Hybrid system in a household in Bandung, West Java Province, utilizing new and renewable energy resources available in the local, such as, sun, wind and kitchen organic waste, for electricity supply which is interconnected with the grid power 2200 VA.

The purpose adding Hybrid system is to optimize the utilization of renewable energy as an effort to save electricity payments. Hybrid system has a variety of configurations that can be selected for their designated purpose, among other things: (1) series hybrid system, (2) switched hybrid system, and (3) parallel hybrid system (Nayar et.al 1993).

The simulation used a configuration parallel hybrid system, where, PLN grid, biogas generator and battery bank together in parallel to supply the load. Parallel hybrid inverter system uses two-way (bi-directional) that can serve as inverters (convert dc power into ac) and as a charger and regulator (convert ac power into dc). The pattern of charged or discharged of the Hybrid system using HOMER Control, wherein, when the load is lower than battery

bank power, the load is supplied by the battery through the bi-directional inverter (which functions as an inverter) whereas biogas generator and PLN Grid conditioned in the OFF position. At the time of intermediate load exceeds the capacity of the battery, Biogas generator is turned on to supply the load and charge the batteries together with FC, WT and PV (bi-directional inverter and charger functions as a regulator). At peak load, turning biogas generator and bi-directional inverter and PLN Grid together in parallel to supply the load.

2. Research Methods

The method used in this simulation includes three main stages, namely the calculation of daily electrical load in the home, the determination of potential energy sources and technologies are available that can be applied, and the system design. Figure 2 shows a diagram of research methods.

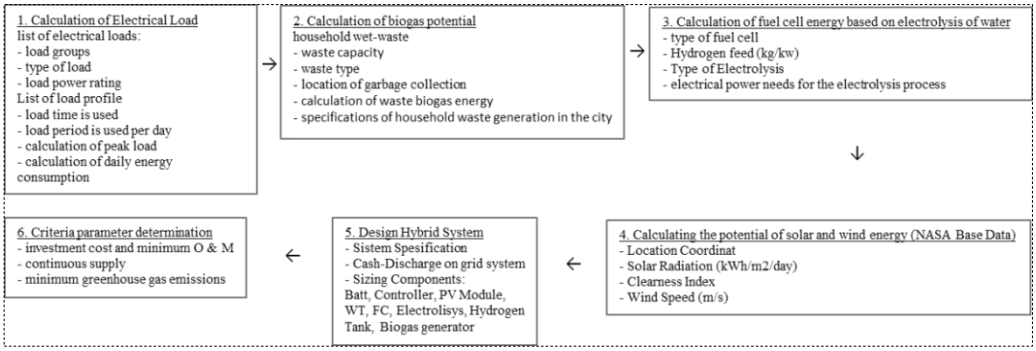

Fig. 1: Method Research

3. Homer System Description

HOMER is an acronym for Hybrid Optimization Model for Electric Renewables, one of the popular tools to design Hybrid system using renewable energy. HOMER simulates and optimizes power generation systems both stand-alone and grid-connected which may consist of a combination of wind turbines, photovoltaic, micro hydro, biomass generators (diesel / petrol), micro turbine, fuel-cell, battery and hydrogen storage, servicing burden electrical or thermal (Lambert, Gilman, and Lilienthal 2006). Figure 1 shows a flow simulation and optimization of HOMER Program.

HOMER simulates the operation of the system by providing energy balance calculations for every 8.760 hours a year. If the system is interconnected with the grid (ON GRID) and using the battery and the ICE generator, HOMER can also specify the run and off the generator as well as determine whether the battery is charged or discharged. Furthermore, HOMER determine the best configuration of the system and then estimate the cost of installing and operating the system during the period of operation (life time costs) as the initial cost, the cost of replacement of components, the cost of O & M, fuel costs, and others. When performing the simulation, HOMER determine all possible system configurations, then displayed sequentially by presents net costs-NPC (also called life cycle costs). If a sensitivity analysis is required, HOMER will repeat the simulation process for each variable sensitivity set. Relative error of about 3% yearly and monthly relative error of about 10% (Sheriff and Ross 2003).

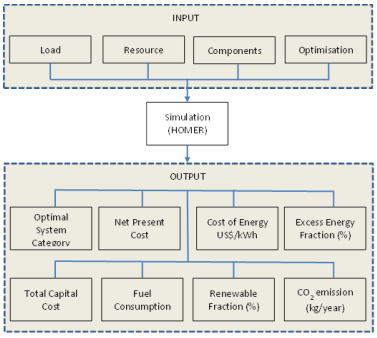

Fig. 2: Simulation and Optimization HOMER

4. Results and Discussions

4.1. Location

Figure 3 and Table 1 shown general information about household used in this study.

Fig. 3: House hold Location

Table 1: General Information

Location[1]	06°56'46.24"S 107°38'35.40"E
Electricity rates	R1/TR
Power limit	2200 VA
Tariff	IDR. 1457.72 per kWh.

1) Source: HOMER

4.2. Load

The types of power tools used in the simulation, as follows; lamp; irons; cooking ware; washing machines; water pump; air conditioning; dispenser; water heater; electrical apparatus for entertainment; communications equipment; computer hardware; storage and cooling food.

The various types of the equipment above, there are tools that continuously operates for 24 hours and 7 days per week, 41% (900 watts) of maximum power (= 2200 watt). Assumptions in the simulation expressed electricity consumption is constant throughout the year. The type of electricity consumption in use can be shown in Figure 4.

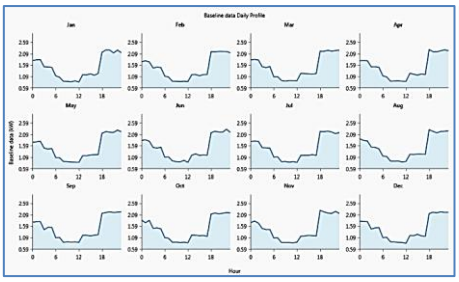

Fig. 4: Baseline Data Daily

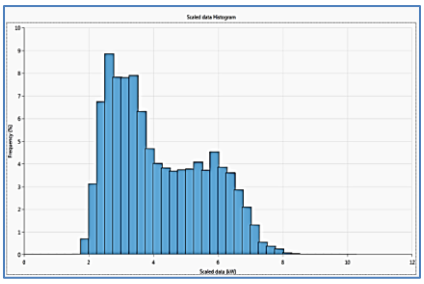

Fig. 5: Electricity Consumption

Figure 4 shows the load profiles are being simulated with 2.2 kW peak load that occurs from 18:00 until 23:00. In this simulation assumed that the peak load occurs because all the residents conducting activities within the house after work with all the facilities available. While most low load power consumption occurred at 09.00 am to 12.00 noon. Assumptions carried in this simulation states that the main occupants in the home at this time to go to work and do all activities outside the home. The frequency for the electrical load that occurs can be shown in Figure 5. The greatest frequency is 8.84% at a scale of 2.8 kW

4.3. Potential of New and Renewable Energy Systems

4.3.1. Household Waste for Biogas

The digits of waste in Indonesia are between 2-3 liters / person / day with a density of 200-300 kg / m^3 and composition of organic waste 70-80%. This goes along with calculation methods according to ISO 19- 964-1994. Housing is the largest source of the waste. The composition of wet waste or organic waste by 73-78% and the total of wet waste up to 85% are junk leftovers. Characteristics of waste can be grouped according to its properties, such as:

- Physics Characteristics: The most important is the density, moisture content, volatile content, ash content, calorific value, the size distribution.
- Chemical Characteristics: particularly that describes the chemical make-up of the waste consisting of the elements C, N, O, P, H, S, etc.

Table 2: Characteristics of Waste in Bandung City

Parameters	Value
Humidity (% kg-wet)	64.27
pH	6.27
Organic Content (% kg-wet)	44.70
Carbon (% kg-dry)	44.70
Nitrogen (% kg-dry)	1.57
Phosphor (% kg-dry)	241
Ash Content (% kg-dry)	23.09
Heating Value (kcal/kg)	1197

In this simulation, the specified conversion process waste into biogas through anaerobic fermentation process using a digester. This is determined by the availability of raw material composition of household waste with wet waste or organic waste by 73-78% dominant from food. Availability of the amount of daily waste that can be collected in trash receptacle housing is a maximum of 250 kg per day. Therefore, the design of the size of the digester biogas created has to feed daily volume amounted to 240 kg of organic waste per day with a stay of feed made as optimal as possible under the terms of the design of the biogas digester. Based on the daily amount of feed can be determined that the biogas produced enough to operate the generator with capacity up to 10 kWh of electricity for 8 hours per day.

4.3.2. Fuel Cell, Electrolysis and Hydrogen Storage Tank

For Fuel Cell, the selected equipment types of hydrogen feeds. Because the price is still expensive so the determination of the FC power capacity is limited to only 1 kW. The hydrogen and oxygen as the feed will be supplied using a powerful 1 kW water electrolysis to meet the hydrogen needs. Electricity for electrolysis will be supplied at the time of low load only from 09.00 am to 12.00 pm, every day. Hydrogen product obtained is stored in Hydrogen-tank with 1 kg of hydrogen capacity.

4.3.3. Solar Cell (Photovoltaic) and Wind Turbine (WT)

a) Solar Cell

Data Surface meteorology and solar energy (SMSE) of the National Aeronautics and Space Administration (NASA) has been used as a source of information on the analysis location. SSMSE NASA database derived from the meteorological parameters and solar energy were recorded for 22 years (1983-2005) by more than 200 satellites. Data Accuracy is 6 - 12% (NASA 2010). For this simulation only parameter the intensity of solar radiation on a horizontal surface and the clearness index is used. Data sun's daily average was obtained for 4.81 kWh / m2 / day. Such information can be shown in Figure 6. In designing this simulation, the power capacity for PV types Flat Plate is 1 kWp for reasons prices are still high.

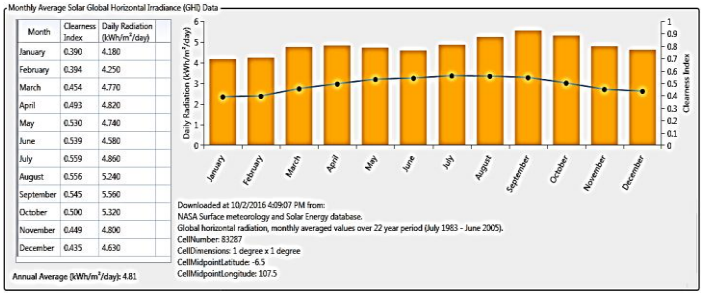

Fig. 6: Monthly Average Solar GHI Data (Source: HOMER Pro 3.7.6)

b) Wind Turbine (WT)

For the wind potential at the location of the research and simulation can know the data as shown in Figure 7. Sources of data obtained from Homer Pro 3.7.6 as the data potential of the sun. From these data it is known that the daily wind speed average of 3.81 m / s. The data obtained in anemometer height of 50 m above the ground on the altitude 1450 m asl. In designing this simulation, the power capacity is designed only for WT 1 kWp who has overall loss factor of 4.9% for reasons of prices are still high.

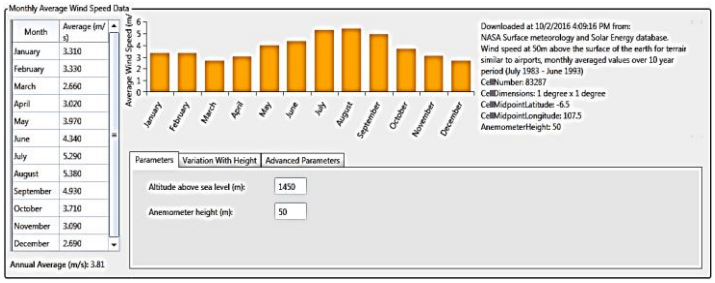

Fig. 7: Monthly Average Wind Speed Data (Source: HOMER Pro 3.7.6)

4.4. System Design

In the simulation, set a few options available components based on source, such as; The primary load in the form of electrical load, biogas generators, PV (photovoltaic), WT (wind turbines), FC (Fuel Cell), converters, controllers and battery bank. Figure 8 shows the design of the selection of components in HOMER.

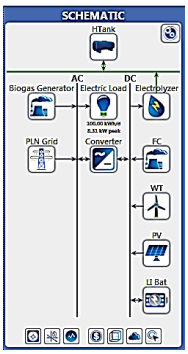

Fig. 8: Design Hybrid Systems on HOMER Pro 3.7.6

There are some parameters that are determined in advance by the designer as inserted into HOMER simulation program to achieve the objectives. Some parameters can be specified as shown in Table 3.

Table 3: Input Parameters

No	Input Parameters	Note
1	PLN Grid	Simple Rate
		Grid Power Price 0.2 $/kWh
		Grid Sellback Price 0.25 $/kWh
2	Biogas Generator	Biomass Resource 240 kg/day ($10/ton)
		System Price 500 $/kW
3	H-tank	Price 500 $/kg
4	Electrolyser	Price 500 $/kW
5	FC	Fuel: Storage Hydrogen
		Price 1500 $/kW
6	Converter	Parallel With Generator
		Price 100 $/kW
7	Controller	HOMER Cycle Charging
		Price 100 $
8	Li-Bat	Price 250 $/kWh
9	PV	Price 1500 $/kWp; Flat Plate PV; No Tracking; eff. 13%.
10	WT	Price 1500 $/kWp
11	Financial	Discount rate 8%
		Inflation Rate 2%
		Project Life Time 25 Years

4.5. Design Results

The HOMER program simulation results can be shown in Table 4. Hybrid system most optimal combination is achieved by PV (1 kW); WT (1 kW); Biogas Generator (7 kW); FC (1 kW); Li-Bat (none); Electrolyzer (1 kW); H-tank (1 kg) and the converter (5 kW).

Table 4: The Results of HOMER Simulation

Architecture																Cost			
							PV (kW)	WT	Biogas Generator (kW)	FC (kW)	LI Bat	PLN Grid (kW)	Electrolyzer (kW)	HTank (kg)	Converter (kW)	Efficiency1	Dispatch	COE ($)	NPC ($)	Operating cost ($)	Initial capital ($)
							1.00	1	7.00	1.00		999,999	1.00	1.00	5.00		CC	$0.151	$86,197	$5,654	$13,100
								1	7.00	1.00		999,999	1.00	1.00	5.00		CC	$0.158	$88,612	$5,957	$11,600
							1.00	1	8.00	1.00	1	999,999	1.00	1.00	5.00		CC	$0.171	$97,330	$6,419	$14,350
								1	8.00	1.00	1	999,999	1.00	1.00	5.00		CC	$0.178	$99,879	$6,732	$12,850
							1.00	1		1.00	1	999,999	1.00	1.00	5.00		CC	$0.254	$119,924	$8,785	$6,350
								1		1.00	1	999,999	1.00	1.00	5.00		CC	$0.259	$122,211	$9,078	$4,850

System	Biogas Generator					FC					PV		WT			
Ren Frac (%)	Hours	Production (kWh)	Fuel (kg)	O&M Cost ($)	Fuel Cost ($)	Hours	Production (kWh)	Fuel (kg)	O&M Cost ($)	Fuel Cost ($)	Capital Cost ($)	Production (kWh)	Quantity	Capital Cost ($)	Production (kWh)	O&M Cost ($)
61	4,380	29,127	88	3,066	876	1,216	391	82	12	0	1,500	1,286	1	1,500	570	1
59	4,380	29,127	88	3,066	876	1,216	391	82	12	0			1	1,500	570	1
60	4,380	28,908	88	3,504	876	1,184	381	80	12	0	1,500	1,286	1	1,500	570	1
58	4,380	28,908	88	3,504	876	1,191	382	80	12	0			1	1,500	570	1
0.0						899	899	189	9	0	1,500	1,286	1	1,500	570	1
0.0						899	899	189	9	0			1	1,500	570	1

LI Bat					Converter		PLN Grid			
Quantity	Electrolyte	CellStacks	Autonomy (hr)	Annual Throughput (kWh)	Rectifier Mean Output (kW)	Inverter Mean Output (kW)	Capacity	MonthlyCapacity	Energy Purchased (kWh)	Energy Sold (kWh)
					0.3	0.1	999,999		17,155	7,566
					0.4	0.07	999,999		17,737	6,816
1	0	0	0.17	2,094	0.4	0.2	999,999		17,653	7,539
1	0	0	0.17	2,121	0.5	0.1	999,999		18,326	6,826
1	0	0	0.17	0.8	0.7	0.02	999,999		43,624	0
1	0	0	0.17	0.8	0.8	0.006	999,999		45,094	0

4.6. Economic Analysis

Hybrid systems require Cost of Energy (COE) and Net Present Cost (NPC) is the lowest and the benefits are saving electricity payment every month. This is shown also in Table 4, Energy Purchased the least 17.155 kWh and provide Energy Sold 7.566 kWh is highest among the other Hybrid system combination.

Table 5: Economy Comparison

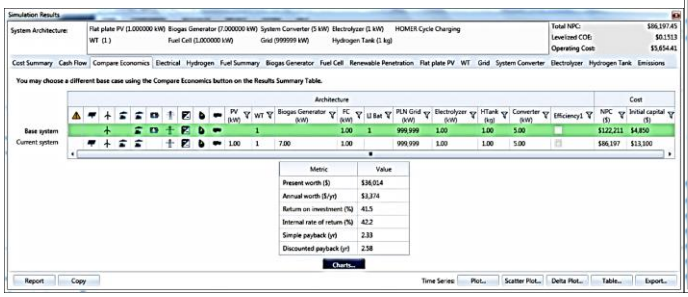

Table 6: Cost Summary

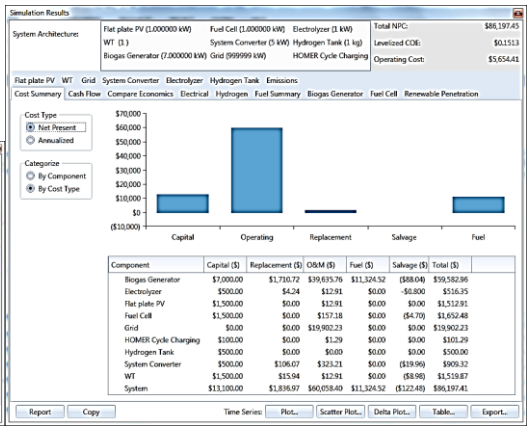

Table 5 shows the combination of selected hybrid system (Base System HOMER plus PV and Biogas Generator without Li Bat) requires a value Initial Capital's most expensive compared with the Base System HOMER (grid, FC, PV, Li Bat, converters, electrolysis and hydrogen storage tanks). The selected combination of hybrid systems provide NPV (Net Present Cost) most low and also provide value IRR 42.2% the highest of the other. In Table 6 demonstrated that the combination of hybrid systems, biogas generator is a component of the most high O & M costs, but also is a component that provides the greatest energy supply Renewable Fraction among others.

4.7. Analysis of Electricity

From Table 7 obtained information that the largest power supply is obtained from biogas generator (> 60%) of the total supply of the required load current carrying AC electricity. 35.35% electricity obtained from GRID PLN, 2.65% is obtained from PV, 1:17% of WT and only 0.81% is obtained from FC.

Total electricity consumption amounted to 47.881 kWh / year and 15.80% of the total are the results obtained from the hybrid system. This condition is based on the assumption of no excess electricity, unmet electricity load and capacity shortage.

Table 7: Electrical

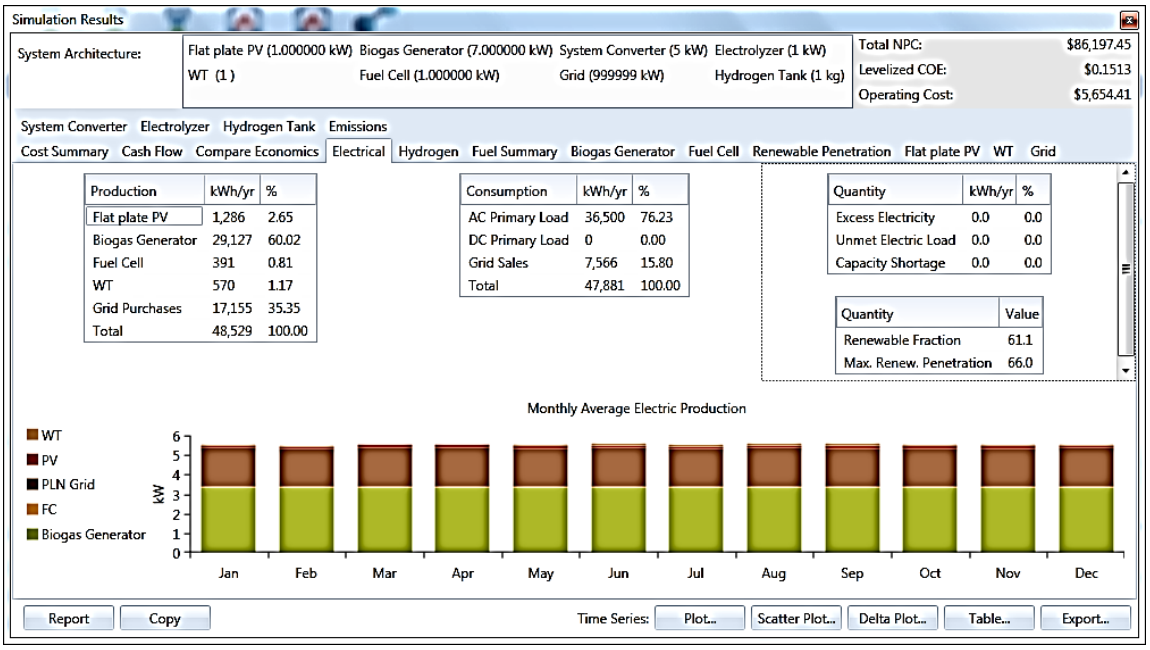

4.8. Greenhouse Emissions Analysis

This hybrid system produces emissions of carbon dioxide (CO2) 6,076.03 tons / year and nearly all generated by Grid PLN. Becouse the net CO2 emissions from biogas generator, DC, PV and WT is zero (= 0).Untuk kasus ini Grid PLN menghasilkan emisi CO2 sebesar 632.00 g/kWh.

Table 8: Emissions

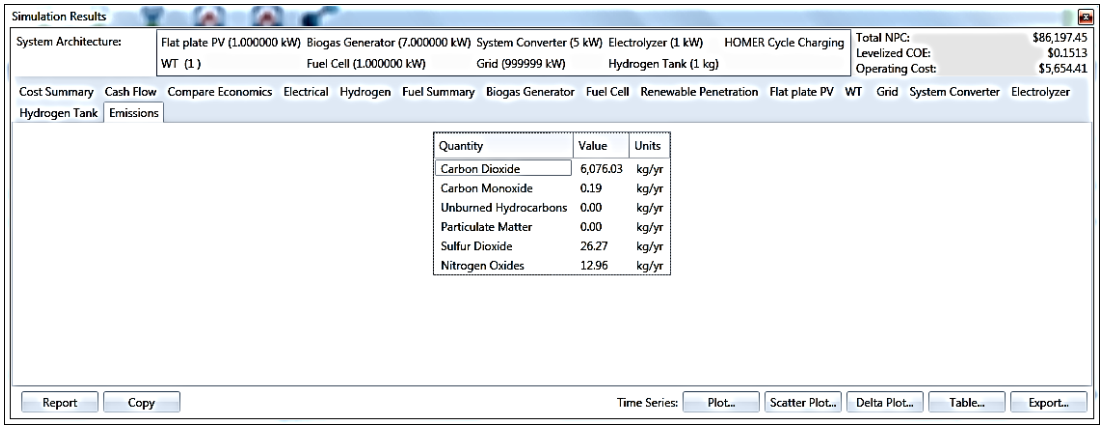

4.9. Renewable Penetration Analysis

Table 9 shows the Renewable Fraction of the hybrid system was chosen by 61%, and ultimately provide a significant contribution to the economic and greenhouse emissions. the condition of the hybrid system can be used as a model for carbon credit project (Carbon Emission Reduction-CER) in a larger scale.

Table 9: Renewable Penetration

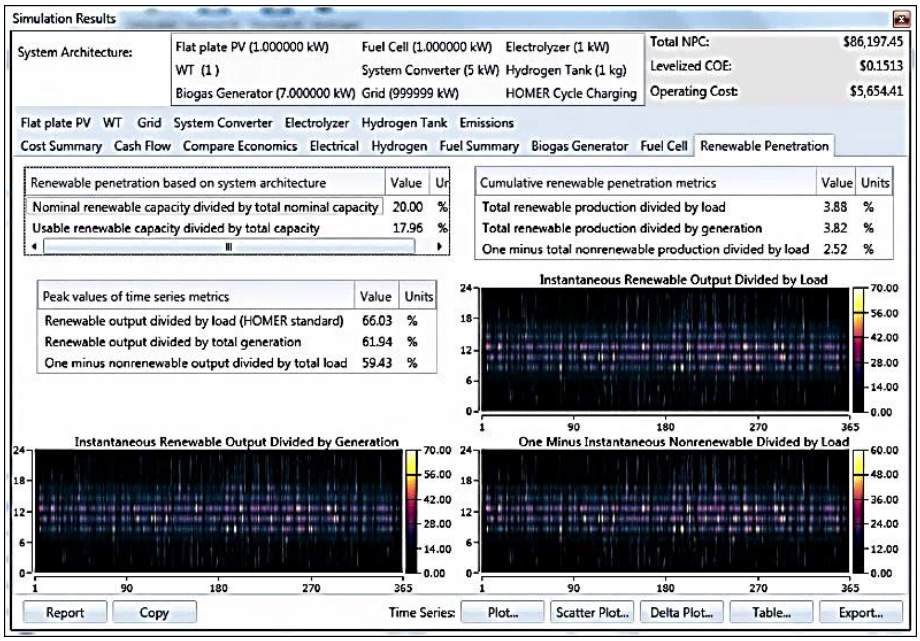

5. Conclusion

In this simulation obtained full information to conduct techno-economic assessment of the hybrid system is designed. The parameters of the techno-economics can be concluded as follows;

1. Base system HOMER Pro version 3.7.6 in this case consists of components; grid, WT, FC, Li Bat, converters, electrolysis and hydrogen storage tank is comparative economics of the hybrid system is the most optimal.
2. Hybrid System the most optimal is selected Base System + PV and biogas without Li Bat.
3. The combination of selected hybrid system requires Initial Capital ($13.100) highest compared with other combinations.
4. The combination of selected hybrid systems requires COE ($ 0151), NPC ($ 86.197) and Operating Cost ($ 5.654) is the lowest compared with other combinations.
5. The combination of selected hybrid systems requires O & M (= $ 60,058.40) and over 50% (=$ 39,635.76) is the cost of O & M Biogas Generator.
6. The combination of selected hybrid system provides IRR 42.2% the highest of the other.
7. 60.02% Electric Supply is supplied by Biogas Generator from the total electricity supply.
8. Biogas Generator is a hybrid system component that require O & M highest.
9. CO2 emissions produced from PLN Grid.
10. Renewable Fraction hybrid system was chosen by 61%.

6. References

Fung, C. C., W. Rattanongphisat dan C. Nayar, 2002, A Simulation Study on the Economic Aspects of Hybrid Energy Systems for Remote Islands in Thailand, Proceedings of 2002 IEEE Region 10 Conference on Computers, Communications, Control and Power Engineering 3(3):1966-1969.

Homer Energy, 2016, Homer Help Manual, Boulder CO 80301 USA

Kunaifi, 2009, Options for the Electrification of Rural Villages in the Province of Riau - Indonesia, Master Thesis in Renewable Energy, Perth: Murdoch University.

Lambert, T., P. Gilman, dan P. Lilienthal, 2006, Micropower System Modelling With HOMER, dalam Integration of Alternative Sources of Energy, ed. Felix A. Farret dan M. Godoy Simoes, John Wiley & Sons, Inc.

Odax Ugirimbabazi, 2015, Analysis of Power System Options for Rural Electrification in Rwanda, Master Thesis in Spring, Faculty of Engineering and Science University of Agder, Grimstad.

Proceedings of the 1st Faculty of Industrial Technology International Congress
International Conference
Bandung, Indonesia, October 9-11, 2017
ISBN 978-602-53531-8-5

Battery-Integrated Hybrid Renewable Energy Optimization to Reduce Intermittency in Weak Grids by Supplying Baseload-Like Generation Profile

Bimo Adi Kusumo
Jakarta - INDONESIA
Corresponding author: bimoadikusumo@gmail.com

Abstract

Being non-dispatchable and intermittent, wind and solar energy is least favorable in the eyes of grid operator. One of the solution to RE's intermittency is Battery Energy Storage System (BESS) which can store energy and dispatch them as necessary. Major drawback of BESS is high upfront cost; hence the utilization of BESS should be optimized to achieve competitive Cost of Energy (COE) while providing stable electricity. This paper presents a study on best combination of intermittent renewable sources coupled with BESS and diesel generator to provide stable and baseload-like constant power daily. Taking case from Sumba Island in East Nusa Tenggara which represent small-to-medium sized island with abundance renewable energy source but minimum grid support system, the hybrid renewable is configured using HOMER software to analyze net present cost, cost of energy, BESS operational pattern and allocation. The research found out that combining BESS+PV+wind yield the lowest cost of energy and net present cost. Most of the time BESS recover its state of charge at noon where PV panels yield is biggest. Inclusion of diesel in the system reduce the net present cost & cost of energy owing to the smaller capacity of BESS needed to provide base-load like. Full renewable energy system is able to provide baseload-like yield to reduce intermittency with some limitations taking into accounts.

Keywords: Battery, Weak Grids, Hybrid, Non-dispatchable Renewable Energy Integration

1. Introduction

Indonesia as one of the largest energy producer & consumer in Southeast Asia has a crucial part in reducing carbon emission in the region. Indonesia produce 240.3 Terra Watt Hour (TWh) energy in 2014 and only 29.9 TWh sourced from renewable energy (IRENA & ACE, 2016). Since 2011, Indonesian government has set a roadmap to increase renewable energy portion in the energy to 23% by 2025 (Presiden Republik Indonesia, 2011). Latest report from Indonesian Agency for The Assessment and Application of Technology (BPPT) states that in 2025, new & renewable energy portion sits at 12.5% which is far less than previously aimed by the government (Agency for The Assessment and Application of Technology (BPPT), 2016). Renewable energy generation in Indonesia dominated by hydropower and biofuels, meanwhile as of 2016 there is only 0.3 MW operating wind farm and 12.94 MW of solar farm (PT PLN (Persero), 2017).

Solar energy is considered as intermittent renewable energy as the output of the solar panel fluctuate depending on solar radiation, cloud cover and other relevant factors (Ela, Diakov, Ibanez, & Heaney, 2013). Meanwhile wind energy is considered as a variable renewable because as a collection of wind turbines in a wind farm, the output of wind turbines doesn't drop significantly over a short period of time owing to the distributed turbines among large areas and kinetic inertia stored in its blades (Muyeen, 2012; Palchak et al., 2017). Utilizing intermittent and variable electricity generation facility in the grid increase the risk of operational failure and/or plant-level economic issues (Deutch, 2011). Power instability might occur when there is a sudden loss of load or generation which caused frequency oscillation that might trigger system blackout in weak grids. Owing to this fact that there is a challenge in developing wind and solar power for electricity production. Other electricity generations that can produce a stable electricity are needed to act as a base load in the grid system for the integration of wind & solar PV plants in weak grids.

The implementation of wind and solar renewable energy is naturally challenging in Indonesia. Geographically Indonesia builds from various island size, from large islands of Java, Sumatra & Kalimantan to smaller island in Nusa Tenggara & Maluku. The larger island is the home of Indonesia's largest electricity grid which consist of large coal and gas powerplant, whereas the smaller island usually consists of small systems that rely on distributed diesel generator. According to Ministerial Decree number 12 year 2017 and Ministerial Decree number 50 year 2017, states that the sale & purchase of electricity from renewable energy is only allowed if the grid can accept the renewable energy. which means that most likely weak grids won't be able to accept a large amount of variable renewable energy electricity (Ministry of Energy and Mineral Resources Indonesia, 2017). But based on

measurement conducted by National Institute of Aeronautics & Space (LAPAN) and various government agencies, the smaller islands in eastern Indonesia possess high potential of wind and solar radiation. For example, in Oelbubuk, East Nusa Tenggara Province the wind can reach up to 6.1 m/s (30m measurement height) and in Sumba Island Nusa Tenggara Timur the wind can reach up to 8.2 m/s at 30m above sea level (Martosaputro & Murti, 2014; Setiawan & Wu, 2016). The case to build more electricity infrastructure in the areas is strengthen by the low electrification ratio. Electrification ratio in East Nusa Tenggara Province as reported by PT. PLN (Persero) is at 52.47% (PT PLN (Persero), 2017).

Battery Energy Storage System (BESS) application is considered as an alternative to integrate intermittent & variable renewable energy to the grid. BESS can be implemented as a spinning reserve, voltage support and ramping support. Ramping rate support reduce the fluctuation of renewable energy output to prevent frequency fluctuation and compliance with existing grid code (Görtz, 2015). BESS can used to prevent excess power flow from solar farm that can cause voltage rise on distribution feeder (Khadkikar, Varma, & Seethapathy, 2009). Utilizing BESS as spinning reserve allows the plant to store energy and release it as scheduled. Spinning reserve in intermittent renewable will increase penetration of renewable energy sources by reducing the amount of fossil-fuel spinning reserve needed to maintain grid integrity which is threaten by fluctuation output of intermittent & variable renewable (Dolara, Grimaccia, Magistrati, & Marchegiani, 2017).

Battery remain one of the most component in hybrid renewable energy system. In a hybrid wind & solar desalination plant, battery contribute 35% of the total cost which followed by wind generators at 31% (Koutroulis & Kolokotsa, 2010). Nookuea et al. combine wind, solar PV and BESS to provide reliable power for shrimp cultivation which implies that percentage of reliability is increased with the increase of life cycle cost (Nookuea, Campana, & Yan, 2016). Techno-economic analysis has been done by Khan et al. to supply a stable electricity up for telecommunication Base Transceiver Station (BTS) using combination of Wind, Solar, Diesel & Battery. the research conclude that PV-wind-diesel-battery hybrid can provide stable power up to 50 kW with the least Cost of Energy (COE) (Khan, Yadav, & Mathew, 2017).

In this study, various scenario of hybrid renewable energy system will be simulated to provide constant power to the system of east Sumba island in Indonesia. due to lack of automation and control on the existing generator, The Hybrid Renewable Energy System (HRES) should be able to provide constant power throughout the day and night similar to a base load generator. HOMER Software is used for sizing the equipment of the HRES to satisfy the baseload operational constraint. The economics of the electricity generated is calculated in terms of Levelized cost of electricity as one HRES with various generation sources and sizing based on HOMER simulation. Software version used is HOMER Pro version 3.8.7. HOMER has been used extensively to model micro grid and renewable energy integration around the globe (Ajlan, Tan, & Abdilahi, 2016; Halabi, Mekhilef, Olatomiwa, & Hazelton, 2017; Hiendro, Kurnianto, Rajagukguk, Simanjuntak, & Junaidi, 2013; Kalinci, Hepbasli, & Dincer, 2015; Khan et al., 2017; Shaahid, Al-Hadhrami, & Rahman, 2013).

2 Methodology

2.1 Case Study

Sumba Island in East Nusa Tenggara province is selected as the case study for the implementation of HRES with BESS due to their abundance of renewable energy and critical electricity infrastructure condition. Sumba Island has been chosen as the Iconic Island of 100% Renewable Energy based on a study conducted by Hivos in 2010 together with Winrock International, a non-profit organization based on the abundance of renewable energy resource and low electrification ratio across the island. As of 2016 the electrification ratio in Sumba is at 42.5 % where 10 % is generated by renewable energy (Hivos, 2016).

Sumba Island electrical grid consist of 2 small grids, East Sumba grid and West Sumba Grid. Both systems are not interconnected to one another. East Sumba grid consist of overall diesel power plant with installed capacity of 8.698 MW. Due to the age of these diesel generator generally the diesel generator can only work at 70 % of their nameplate capacity. In 2016 the average hourly peak load in East Sumba Grid is 5.67 MW and average hourly load is 4.19 MW. The amount of able generation capacity is matched with the load in a critical manner which means that if one of the power plant is under maintenance there will be rolling blackout across East Sumba grid as happened in September 2016 (Kompas, 2016). The control of the power plant is maintained using radio between 3 power plant centrals hence no grid automation is in place. The system is connected via a 20 kV medium voltage transmission line.

Based on studies conducted by Hivos and their partners, Sumba has 4 renewable energy resource that can be utilized. Hivos studied that Sumba has a good wind and solar resource which can be developed to a 10 MW Wind farm and 10 MW Solar Farm in Hambapraing, East Sumba. Micro-Hydro source is also being looked as one of the alternative with potency up to 10.2 MW in 300 Mini-grid locations. Sumba also claimed to have a potency for 8.5 MW hydro storage dams in Memboro river and Kadahang River (Sumba Iconic Island, 2016). For this simulation only wind & Solar PV renewable sources is used due to their location adjacent to existing grid.

2.2 Wind Speed

Wind speed data in East Sumba gathered from Modern Era Retrospective-Analysis for Research and Applications-2 (MERRA-2) released by National Aeronautic & Space Administration or NASA (Rienecker et al., 2011). MERRA-2 data has a resolution of a 0.5° in latitude (± 55 Km, close to equator) and 0.625° (± 69 Km, close to equator) in longitude. The hourly wind data is retrodicted since 1 January 1980 up to 1 July 2017. The closest data point located in -9.5° latitude and 120° Longitude which is 20 km from the site.

Based on MERRA, average wind speed in case area is 6.05 m/s at 100m height. The peak of the wind speed is in June, July & August with monthly mean up to 7.941 m/s as can be seen on **Error! Reference source not found.**a. There is no large diurnal pattern in East Sumba's Wind speed where in hourly average the wind speed is varies between 5.966 m/s between 03:00 to 04:00 and 6.164 m/s at 11:00 to 12:00 as can be seen on Fig. 1b.

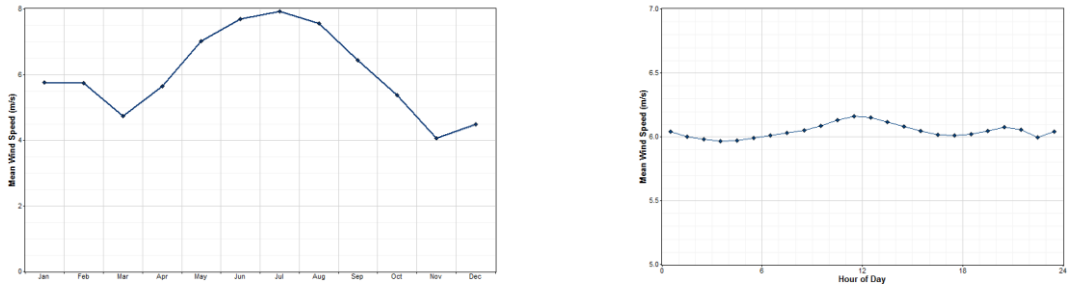

(a) (b)

Fig. 1: Monthly average wind speed (a) and diurnal wind speed profile (b) in East Sumba based on MERRA-2 data

2.3 Solar Irradiation

Solar global horizontal Irradiation (GHI) data in East Sumba gathered from NASA's Surface Meteorology and Solar Energy version 6 or SSE-6 (Stackhouse et al., 2016). SSE-6 data has a resolution of a 1° in latitude and longitude (± 111 Km, close to equator). The hourly wind data is modelled since July 1983 to June 2005. The closest data point located in -9.5° latitude and 120.5° Longitude which is 35 km from the site.

Based on SSE-6, annual average of daily radiation is 5.54 kWh/m^2/day with a average clearness index of 0.562. Based on data from local meteorological station, the sun is shining throughout the year 12-13 hour daily. The peak of the GHI is in September, October & November with monthly mean up to 6.65 kWh/m^2/day as can be seen on Fig. 2a. Clearness index in East Sumba ranging from 0.477 in February to 0.632 in September as can be seen on Fig. 2b. The higher index indicates there is large portion of the time the sky is cloudless.

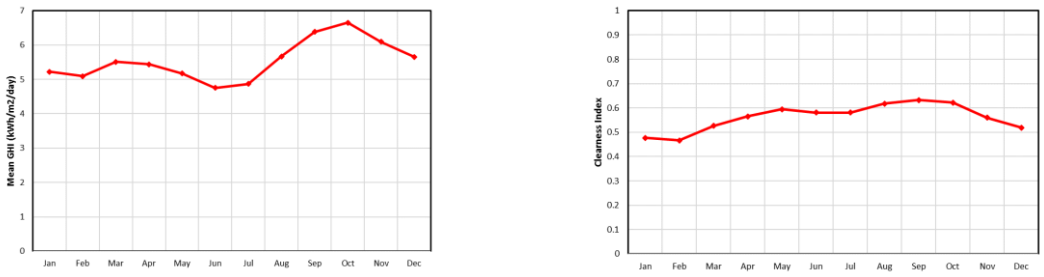

(a) (b)

Fig. 2: Monthly Average GHI (a) and clearness index (b) in East Sumba based on SSE-6 data

2.4 Load Scenarios

Fig. 3 shows the hourly load average of East Sumba in 2016. Electricity peak load starts from 18:00 to midnight which peaked at 19:30 around 5000 kW. The non-peak load hover around 4000 kW for the rest of the day. The small load showed indicates that there is a blackout on some of the area and/or observational error of the grid operator due to manual data collection.

In this research, the author aware of the grid limitation on integrating HRES to East Sumba grid, hence the output of the HRES is limited to provide constant power for 24/7 utilizing BESS. With this operational pattern, the grid operator can always rely on HRES as a baseload for their system. Referring to load pattern of 2016 in East Sumba, the author creates 2 baseload scenarios and 1 load following scenario. Load scenario A represent a base load of 25% from non-peak load which is set around 1000 kW. Load scenario B further simulate a larger portion of renewable in the electricity mix with 50% of non-peak load supplied by baseload HRES. Load-following scenario C is the baseline where actual historic grid load is simulated assuming that the HRES maintain 25% portion in the electricity generation composition. Load scenario C is modelled as a comparison between baseload scenarios and the load following HRES integration. Scenario C is expected to have lower cost and spill compare to the base load scenarios.

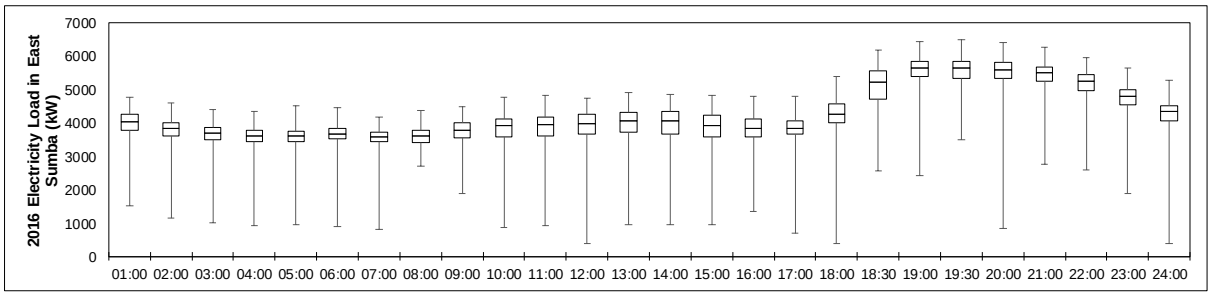

Fig. 3*:* East Sumba Electricity Load in 2016

2.5 Hybrid Renewable Energy System (HRES) Scenarios

Hybrid Renewable Energy System with Battery Energy Storage System (HRES+BESS) scenario simulated is listed in Table 2a. Scenario 4 to 6 is simulated with a diesel to assess the impact of introducing diesel generator to HRES+BESS in terms of cost and excess. HRES specification data and assumption listed in Table 2b.

Table 2*:* HRES combination scenarios (a) and HRES specification data & assumption (b)

(a)

Scenario	HRES Component			
	BESS	Solar PV	Wind	Diesel
1	•	•		
2	•		•	
3	•	•	•	
4	•	•		•
5	•		•	•
6	•	•	•	•

(b)

Description	Details
Type of Solar PV Module	Polycrystalline
PV System Lifetime	25 years
Cost of PV Module	US$ 1.0/W
Module Efficiency	0.1639
Temperature Correction Factor	0.41 %/°C
Inverter Efficiency	0.95
Cost of Inverter	US$ 0.04/W
Inverter Lifetime	15 years

Description	Details
Type of Wind Turbine	2500 kW - 121m rotor dia.
Cost of Wind Turbine	US$ 4.0/W
Life time of Wind Turbine	25 years
Hub Height	100 Meter
Type of Battery System	Lithium ion
Battery nominal capacity	210 kWh/string
Cost of BESS	US$ 0.5/Wh
Type of Diesel Generator	50 kW HSD
Cost of Diesel Generator	US$ 0.5/W
Diesel Generator Fuel Cost	US$ 0.74/Litre

Boundary and limitations is applied to increase the accuracy of HRES optimizations. Configuration wise, The Wind turbine & Diesel generator are connected to the AC. PV panels and BESS are connected with DC bus. The installed diesel in scenario 4 to 6 is limited to 50 % of the aimed base load which is 500 kW (load scenario A) and 1000 kW (load scenario B). limitation of installed diesel is to prevent HOMER to rely mainly on diesel to generate electricity when the cost of energy (COE) is cheaper when running on diesel.

3 Results and Discussion

The scenarios in the result is shown as combination of both load scenario and HRES scenario. For example, simulation for load scenario A with HRES scenario 3 is displayed A3. The nomenclature goes thru load scenario A to C and HRES scenario 1 to 6. Designation HRES-1 to HRES-6 referring to scenarios involving all load simulation for each HRES component scenario 1 to 6.

3.1 HRES Component Optimization

Optimizing all possible scenarios resulting to HRES components with the feasible solution with the lowest Net Present Cost (NPC) can be seen on Table 3. As seen on scenario 1,2 & 3, hybrid combination of both wind & solar PV reduces the amount of BESS needed to provide baseload. Having wind turbine in AC bus also reduce the capacity of inverter/rectifier needed to satisfy the required baseload. Massive amounts of battery & Wind turbines are allocated on HRES-2 & HRES-5 scenarios are caused by period when the wind is not blowing hence BESS is needed to store excess wind generated.

Table 3: HOMER Optimized HRES Components

Load Scenario	A						B						C					
HRES Scenario	1	2	3	4	5	6	1	2	3	4	5	6	1	2	3	4	5	6
BESS (kWh)	23,100	38,850	14,910	11,130	18,270	13,230	48,510	204,750	31,290	20,790	34,650	27,720	26,880	34,230	16,800	12,810	32,550	30,450
Solar PV (kW)	10,592		5,312	5,875		4,601	20,509		13,209	12,509		10,993	10,469		6,289	6,727		12,702
Wind (kW)		22,500	2,500		17,500	2,500		25,000	2,500		20,000	2,500		25,000	2,500		25,000	2,500
Inverter (kW)	5,231	1,439	3,277	1,719	2,500	1,884	4,805	7,188	2,450	6,647	4,060	7,202	1,920	1,459	1,657	1,483	1,493	4,940
Diesel (kW)				450	500	500				900	1,000	950				450	400	50

3.2 BESS Operational Pattern

Fig. 4 display the State of Charge (SOC) pattern of BESS for all non-diesel scenarios. For HRES scenario 1 & 3 where solar PV exist, the BESS is being used throughout the night extensively and charged during the day by the Solar PV. HRES-3 have a higher SOC level than HRES-1 owing to wind turbine that generate electricity but the pattern remains similar with HRES-1. HRES-2 shows a very different SOC profile with the rest of the scenarios. BESS's SOC in HRES-2 is constantly stays above 90%. This SOC pattern concludes that on average every hour of the day wind produces electricity and BESS provide smoothing facility to stabilize the total output of the system.

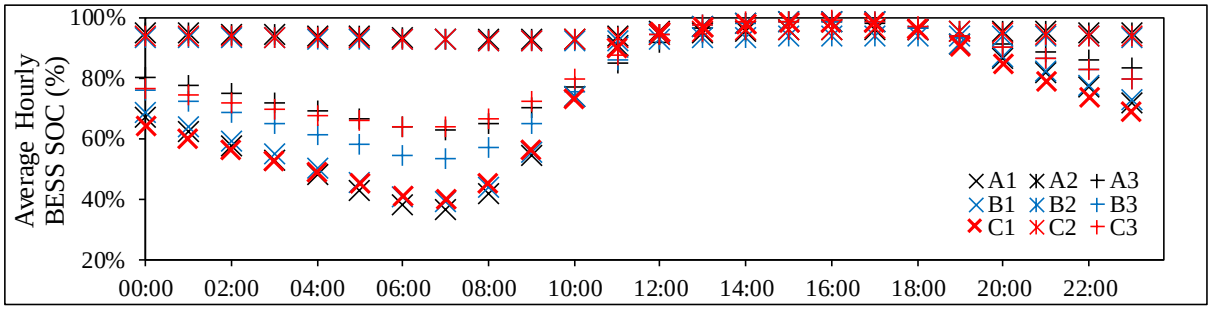

Fig. 4: BESS's SOC diurnal profile

3.3 HRES Yield & Spilled Energy

Key to optimizing HRES is harnessing BESS to store energy to service required load and minimize spill. Fig. 5a show the yield of HRES in non-diesel component. Other scenario's yield is dwarfed by the yield of the wind turbine in HRES-2 scenario. But as can be seen on Fig. 5b, more than 80% of the yield in HRES-2 is spilled. The spill is considerably less in load scenario B compare to load scenario A & C. the spill in the HRES is caused because after the BESS is fully charged, the total output of the wind and/or solar PV generation exceed the required load. HRES-1 has lower spill compared to HRES-3, but the size of the BESS installed in HRES-3 is far less compare to HRES-1 as can be seen on the bar charts in Fig. 5b.

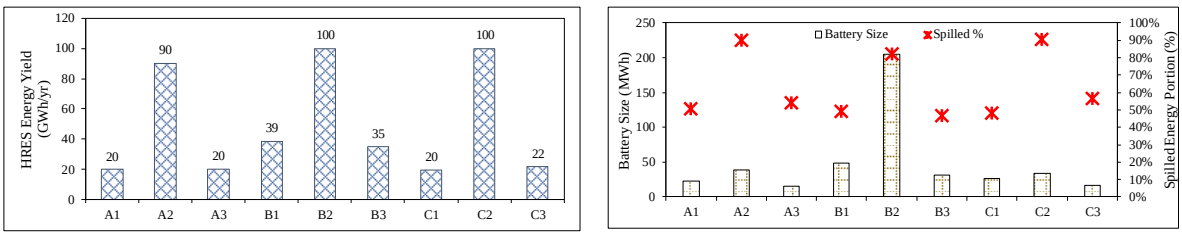

Fig. 5: HRES energy yield (a) and HRES Spilled energy compared with its BESS capacity (b)

3.4 Cost of Energy & Net Present Cost

Bar chart in Fig. 6 shows the Cost of Energy (COE) in US$/kWh of HRES for non-diesel scenarios. The crosses in Fig. 6 represent their respective Net Present Cost (NPC) to construct HRES. Highest COE & NPC is calculated for HRES-2 which render the scenarios to be infeasible economically to provide a relatively small baseload. COE-wise & NPC-wise, HRES-3 provide the most efficient costing compare with HRES-1 & HRES-2 on all load scenarios. COE to provide 1 MW baseload (Scenario A) and 2 MW baseload (Scenario B) is very similar and there is a linear up-trend on the NPC provide evidence that these baseload-like scenarios are scalable. As a comparison, the local Sumba average generation cost (grid's COE) as of 2016 is at US$ 0.142 hence none of the scenarios can compete with the existing average generation cost.

Comparing baseload operational pattern (A & B) and load following operational pattern (C), showed that it shows similar cost with load scenario A as the average 25 % of East Sumba load being followed is on average close to 1 MW. The notable shift of the load pattern is the capacity of inverter/rectifier installed on load scenario C is

significantly less than scenario A & B, although lower inverter/rectifier is countered with higher PV/wind capacity in scenario C.

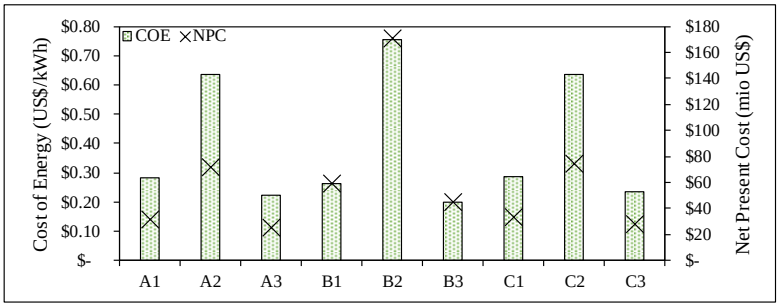

Fig. 6 HRES COE & NPC for non-diesel scenarios

3.5 Inclusion of Diesel in HRES

On hypotheses, adding diesel to the HRE system could potentially reduce the amount of BESS needed and therefore reduce the COE of the system. In this study, simulation HRES-3 to HRES-6 on multiple load scenarios are conducted to prove the hypothesis. Fig. 7 shows the COE, NPC & yield for HRES+diesel scenarios which shows similar result with the non-diesel counterpart except for scenario C6 which require 12 MWp of Solar PV (compare to 6 MWp in C3) to service 25 % of actual load in East Sumba. Fig. 8b shows the renewable penetration of the HRES+diesel scenarios. HRES-4 constantly shows lowest renewable penetration indicating that the diesel will run when to support the battery when the SOC is low. Fig. 9 shows the SOC diurnal pattern of the HRES+diesel which is similar pattern to the non-diesel counterpart especially the part where PV+BESS scenario (HRES-4) is the one with the lowest SOC at the end of the night. The dependency of HRES-4 towards it's diesel generator is strengthen by the average diesel generator load diurnal pattern shown in Fig. 10. At night, there is almost certainty that diesel generator run at full power (450 kW) to support the discharge of BESS to the grid. HRES-5 & HRES-6 diesel generator load on average are working less than 30% most of the times especially during the day when Solar PV is producing electricity.

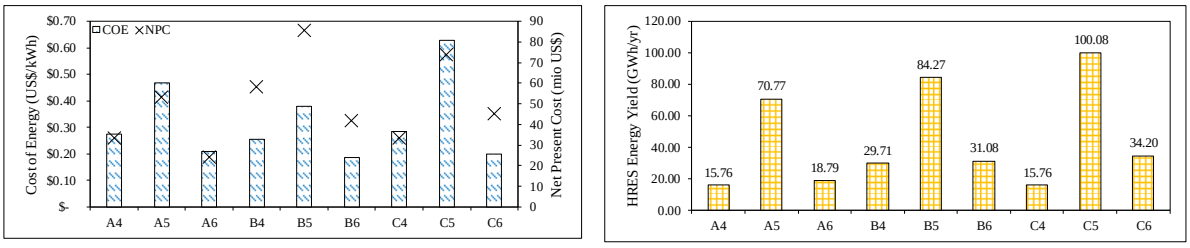

(a) **(b)**

Fig. 7: HRES+Diesel scenarios COE & NPC (a) and Energy yield (b)

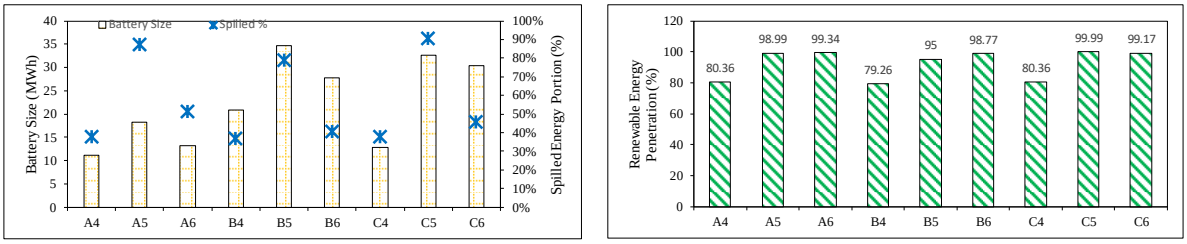

(a) **(b)**

Fig. 8: HRES+Diesel scenarios BESS size, spilled ratio (a) & renewable energy penetration (b)

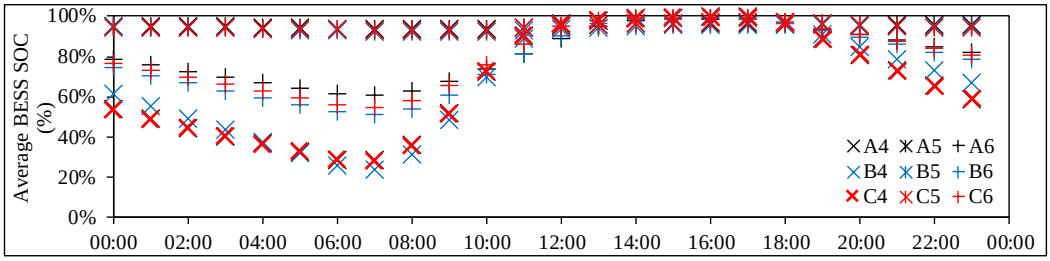

Fig. 9: HRES+Diesel scenarios BESS SOC diurnal pattern

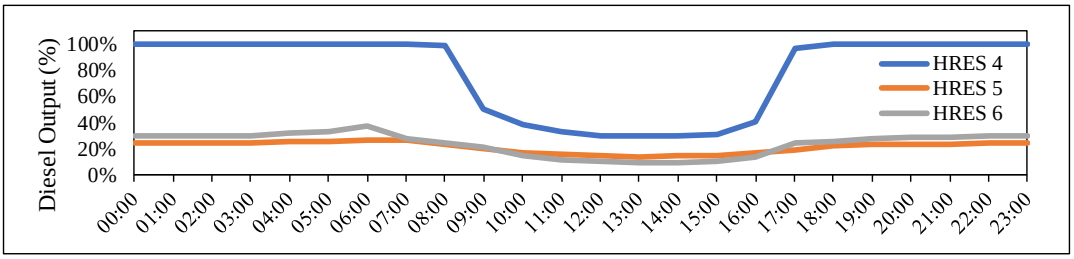

Fig. 10: Diesel generator load percentage for HRES+Diesel scenarios

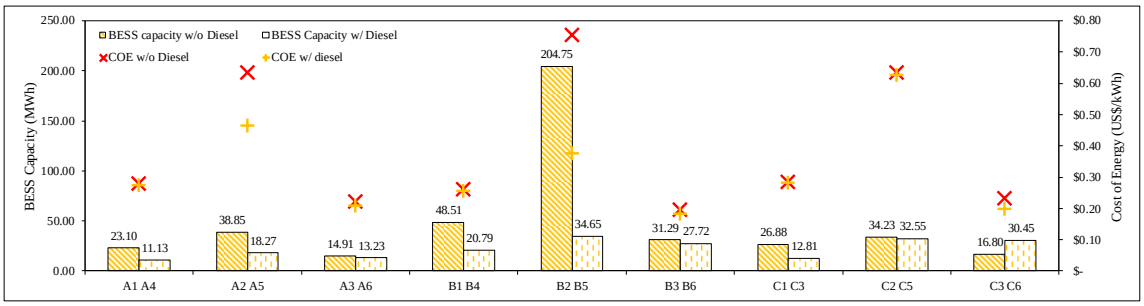

Fig. 11: BESS capacity & COE Comparison between diesel and non-diesel HRES

Table 4: Annual pollutant emission from HRES+diesel scenarios

Pollutant	Scenarios								
	A4	A5	A6	B4	B5	B6	C4	C5	C6
Carbon Dioxide (Kg/yr)	2,552,847.84	575,121.37	98,957.48	5,083,825.60	3,768,542.80	306,312.49	2,552,847.84	11,743.99	241,032.40
Carbon Monoxide (Kg/yr)	15,934.17	3,589.75	617.67	31,731.84	23,522.21	1,911.92	15,934.17	73.3	1,504.46
Unburned Hydrocarbons (Kg/yr)	702.12	158.18	27.22	1,398.22	1,036.47	84.25	702.12	3.23	66.29
Particulate Matter (Kg/yr)	95.57	21.53	3.7	190.31	141.08	11.47	95.57	0.44	9.02
Sulfur Dioxide (Kg/yr)	5,156.84	1,161.77	199.9	10,269.51	7,612.59	618.76	5,156.84	23.72	486.89
Nitrogen Oxides (Kg/yr)	14,977.54	3,374.23	580.58	29,826.76	22,110.01	1,797.13	14,977.54	68.9	1,414.14

Fig. 11 shows the comparison of BESS capacity & COE between HRES without diesel & HRES with diesel. In general, the capacity of BESS for each scenario is decreased with the introduction of diesel in the system except for scenario C6. However, throughout scenarios the COE is decreasing with the combination of diesel generator. The introduction of diesel generator resurfaces another problem needs to be considered which is emission. Table 4 list the emission per year of the HRES+diesel scenarios. Unfortunately, there is no standard economic valuation of emission in Indonesia which can affect the COE of HRES+diesel and shift the downward trend when comparing to non-diesel HRES.

4 Conclusions

This study is aimed to prove the capability of Hybrid Renewable Energy System (HRES) with Battery Energy Storage System (BESS) to provide a baseload-like output for weak grids with minimum system automation. The study concludes that having Solar PV, wind and BESS in one system can provide baseload-like power output with lowest Cost of Energy (COE) and Net Present Cost (NPC). Study also found that wind+BESS system is not practical and infeasible due to high percentage of spills and massive amount of battery to provide power when the wind is not blowing. PV+wind+BESS scenario reduces the amount of BESS needed to service the flat load when compared to PV+BESS only. Introducing diesel to HRES system does reduce the amount of BESS needed even further which in turn will reduce the NPC & COE. The drawbacks of this inclusion are the emission of pollutants from the system. Diesel used mostly during the night to support the dwindling State of Charge of the BESS.

5 References

Agency for The Assessment and Application of Technology (BPPT). (2016). *Indonesia Energy Outlook 2016*. (A. Sugiyono, Anindhita, L. Wahid, & Adiarso, Eds.).

Ajlan, A., Tan, C. W., & Abdilahi, A. M. (2016). Assessment of environmental and economic perspectives for renewable-based hybrid power system in Yemen. *Renewable and Sustainable Energy Reviews*, (November), 1–12. https://doi.org/10.1016/j.rser.2016.11.024

Deutch, J. (2011). *Managing Large-Scale Penetration of Intermittent Renewables*. *MITEI Associates Program/Symposium Series*. Massachusetts Institute of Technology.

Dolara, A., Grimaccia, F., Magistrati, G., & Marchegiani, G. (2017). Optimization Models for Islanded Micro-Grids: A Comparative Analysis between Linear Programming and Mixed Integer Programming. *Energies*, *10*(2), 241. https://doi.org/10.3390/en10020241

Ela, E., Diakov, V., Ibanez, E., & Heaney, M. (2013). *Impacts of Variability and Uncertainty in Solar Photovoltaic Generation at Multiple Timescales*.

Görtz, S. (2015). Battery energy storage for intermittent renewable electricity production : A review and demonstration of energy storage applications permitting higher penetration of renewables. Retrieved from http://www.diva-portal.org.proxy.library.adelaide.edu.au/smash/record.jsf?pid=diva2%3A818683&dswid=4584

Halabi, L. M., Mekhilef, S., Olatomiwa, L., & Hazelton, J. (2017). Performance analysis of hybrid PV/diesel/battery system using HOMER: A case study Sabah, Malaysia. *Energy Conversion and Management*, *144*, 322–339. https://doi.org/10.1016/j.enconman.2017.04.070

Hiendro, A., Kurnianto, R., Rajagukguk, M., Simanjuntak, Y. M., & Junaidi. (2013). Techno-economic analysis of photovoltaic/wind hybrid system for onshore/remote area in Indonesia. *Energy*, *59*, 652–657. https://doi.org/10.1016/j.energy.2013.06.005

Hivos. (2016). Brightening The Classrooms in East Sumba. Retrieved August 31, 2017, from https://hivos.org/news/brightening-classrooms-east-sumba

IRENA, & ACE. (2016). *Renewable Energy Outlook for ASEAN*. Abu Dhabi & Jakarta.

Kalinci, Y., Hepbasli, A., & Dincer, I. (2015). Techno-economic analysis of a stand-alone hybrid renewable energy system with hydrogen production and storage options. *International Journal of Hydrogen Energy*, *40*(24), 7652–7664. https://doi.org/10.1016/j.ijhydene.2014.10.147

Khadkikar, V., Varma, R. K., & Seethapathy, R. (2009). Grid voltage regulation utilizing storage batteries in PV solar — Wind plant based distributed generation system. *2009 IEEE Electrical Power Energy Conference EPEC*, 1–6. https://doi.org/10.1109/EPEC.2009.5420966

Khan, M. J., Yadav, A. K., & Mathew, L. (2017). Techno economic feasibility analysis of different combinations of PV-Wind-Diesel-Battery hybrid system for telecommunication applications in different cities of Punjab, India. *Renewable and Sustainable Energy Reviews*, *76*(January), 577–607. https://doi.org/10.1016/j.rser.2017.03.076

Kompas. (2016, September 19). Sumba Timur Selalu Gelap 12 Jam per Hari, p. 21. Waingapu. Retrieved from http://regional.kompas.com/read/2016/09/19/15020071/sumba.timur.selalu.gelap.12.jam.per.hari

Koutroulis, E., & Kolokotsa, D. (2010). Design optimization of desalination systems power-supplied by PV and W/G energy sources. *Desalination*, *258*(1–3), 171–181. https://doi.org/10.1016/j.desal.2010.03.018

Martosaputro, S., & Murti, N. (2014). Blowing the Wind Energy in Indonesia. *Energy Procedia*, *47*, 273–282. https://doi.org/10.1016/j.egypro.2014.01.225

Ministry of Energy and Mineral Resources Indonesia. Peraturan Menteri Energi dan Sumber Daya Mineral Republik Indonesia Nomor 12 Tahun 2017 Tentang Pemanfaatan Sumber Energi Terbarukan Untuk Penyediaan Tenaga Listrik (2017). Jakarta.

Muyeen, S. M. (2012). *Wind Energy Conversion Systems : Technology and Trends*. London: Springer. https://doi.org/10.2174/97816080528511060101

Nookuea, W., Campana, P. E., & Yan, J. (2016). Evaluation of solar PV and wind alternatives for self renewable energy supply: Case study of shrimp cultivation. *Energy Procedia*, *88*(0), 462–469. https://doi.org/10.1016/j.egypro.2016.06.026

Palchak, D., Cochran, J., Ehlen, A., McBennett, B., Milligan, M., Chernyakhovskiy, I., … Sreedharan, P. (2017). *GREENING THE GRID : Pathways to Integrate 175 Gigawatts of Renewable Energy into India's Electric Grid, Vol.I-National Study* (Vol. I).

Presiden Republik Indonesia. (2011). Peraturan Presiden Republik Indonesia Nomor 61 Tahun 2011 Tentang Rencana Aksi Nasional Penurunan Emisi Gas Rumah Kaca. Jakarta. Retrieved from http://www.bappenas.go.id/files/6413/5228/2167/perpres-indonesia-ok__20111116110726__5.pdf

PT PLN (Persero). (2017). *Statistik PLN 2016*. Jakarta: Sekretariat Perusahaan PT PLN (Persero).

Rienecker, M., Suarez, M. J., Gelaro, R., Todling, R., Bacmeister, J., Liu, E., … Woollen, J. (2011). MERRA : NASA ' s Modern-Era Retrospective Analysis for Research and Applications. *Journal of Climate*, *24*, 3624–3648. https://doi.org/10.1175/JCLI-D-11-00015.1

Setiawan, D., & Wu, J.-C. (2016). Assessing Solar and Wind Energy Technical Potential using GIS Approach: A case study in Sumba Island, Indonesia. In *The Asian Conference on Sustainability, Energy & the Environment 2016*. iafor.

Shaahid, S. M., Al-Hadhrami, L. M., & Rahman, M. K. (2013). Economic feasibility of development of wind power plants in coastal locations of Saudi Arabia – A review. *Renewable and Sustainable Energy Reviews*, *19*, 589–597. https://doi.org/10.1016/j.rser.2012.11.058

Stackhouse, P. W., Chandler, W. S., Zhang, T., Westberg, D., Barnett, A. J., & Hoell, J. M. (2016). *Surface meteorology and Solar Energy (SSE) Release 6.0 Methodology Version 3.2.0*. Norfolk. Retrieved from https://power.larc.nasa.gov/documents/SSE_Methodology.pdf

Sumba Iconic Island. (2016). Pulau Sumba Punya Empat Potensi EBT. Retrieved July 31, 2017, from http://sumbaiconicisland.org/pulau-sumba-punya-empat-potensi-ebt/

Proceedings of the 1st Faculty of Industrial Technology International Congress
International Conference
Bandung, Indonesia, October 9-11, 2017
ISBN 978-602-53531-8-5

Characteristic of Taperless Blade Wind Turbine

Muhammad Haekal* and Dani Rusirawan
Department of Mechanical Engineering, Institut Teknologi Nasional (Itenas), Bandung - INDONESIA
* Corresponding author e-mail: mhaekalt@gmail.com

Abstract

Presently, source of energy in Indone sia is still predominated by fossil energy. Since fossil energy is limited and not environmentally friendly, alternative of energy should be considered to be implemented. As consequences, research in renewable energy field has developed due to a bove reason. One of renewable energy source is wind energy. The potential of wind energy in Indone sia is estimate d 9.290 MWe, and presently, the installed capacity of wind energy conversion system (WECS) approxima tely is 1.1 MWe. Nevertheless, there is problem in development of utilize of WECS in Indonesia , due to most of the WECS, which available in market, are not designed for Indonesia wind condition. Based on this fact, it is reasonable if the WECS whic h operated in Indone sia not working properly (in performance point of view). Blades in a WECS are the main components, which have major influenced on the performance of WECS. In this research, design of blades will be carried out based on predetermined power capacity, using wind velocity condition in Indonesia. As an outcome this research, concept of blade based on aerodynamic design have been proposed and ready to be implemented.

Keywords: Renewable energy, wind velocity, wind energy conversion system (WECS), aerodynamic design, WECS performance.,

1. Introduction

The concept on renewable enery is known since 1970's, as efforts to balance the use of nuclear and fossil fuels. The common definition of that is that energy resources that can be naturally renewed, and the process is sustainable. By this definition, fossil and nuclear are not categorized as renewable energy resources. Hence, research and development of water, geothermal, biomass, solar, and wind need to be done.

Indonesia is a country with wind potential that can be used to produce electricity. Indonesia wind energy potential is predicted arount 9,290 MWe if it is converted to electricity, and the utilization of it untill the date is about 11 MWe (BPPT, 2014:17).

Most of Wind Energy Convertion System (WECS) that available in markets are producted not from Indonesia which the design is adjusted with the wind condition of where this WECS is produced or designed. It is reasonable to design the blades of Wind Energy Convertion System (WECS) the meet the condition of Indonesia wind.

2. Research Methodology

Overall, method that I have used to design the blades of wind turbine is studying literature, choosing airfoil, optimizing dimension, simulating and documenting the concept of wind turbine blades that ready to be produced.

3. Rotor / Blade

Base on the shape of the blades from the hub to tip, Blades of WECS are divided into 3 type which are taper, taperless, and inverse-taper, as can be seen in Figure 1. In this research, writer choosed taper blade with assumption it will suit for low wind velocity.

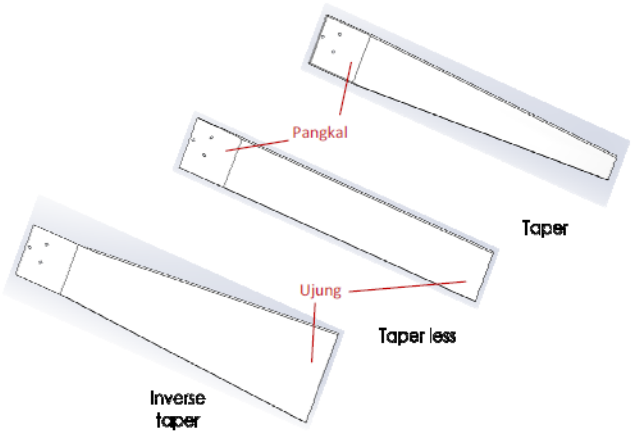

Fig. 1: Types of Blade Based on Its shape (Lentera Angin Nusantara, 2014)

4. Coefficient of Performance

Overall, method that I have used to design the blades of wind turbine is studying literature, choosing airfoil, optimizing dimension, simulating and documenting the concept of wind turbine blades that ready to be produced.

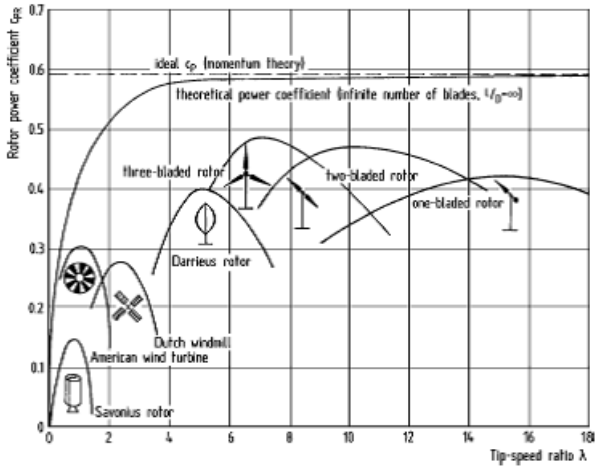

Fig. 2: Characteristic of different types of wind turbines (Wind Turbine Technology, 2014)

5. Dimension Optimization

Dimension optimization of blades of WECS in this research is using predetermined of maximum power at 500 Watt.

5.1. Rotor radius calculation

In order to determine the chord of the blades, these equations that Cancelli used in his thesis, Aerodynamic Optimization of A Small-Scale Wind Turbine Blade for Low Windspeed Conditions, are used.

$$W_{wind} = \frac{W_{design}}{\eta_{sys}} \quad (1)$$

$$A = \frac{2 \times W_{wind}}{v_{max}{}^3} \quad (2)$$

$$R = \sqrt{\frac{A}{\pi}} \quad (3)$$

Table 1: Calculations results of rotor radius

Power Capacity (Watt)	Efficiency (%)				Wind Power (W_{angin})	V_{max} (m/s)
	Blades	Generator	*Controller*	System		
500	0.3	0.8	0.8	0.192	2604.166667	12
	0.4			0.256	1953.125	

Cross-Sectional Area (A)	Radius	Average Radius	Used Radius
2.460474931	0.8849822	0.825699634	0.80
1.845356198	0.76641707		

After getting the "used radius" for the rotor/blades, dividing the blades into 10 section is done in order to get the accuracy in this design. In this design, dimension of the hub section is already determined by 0.14 m, which is suited to the supporting component for testing process. The calculation is using equation 4 and the result is shown in Table 2.

$$r = 0.14 + \left[\frac{R-0.14}{n}\right] \times (element) \quad (4)$$

Table 2: Calculation result of radius section

Segmen	r (m)
0	0.14
1	0.21
2	0.27
3	0.34
4	0.40
5	0.47
6	0.54
7	0.60
8	0.67
9	0.73
10	0.80

5.1. Airfoil selection

Airfoil is chosen based on Cl max in Cl vs α graph, and Cl/Cd max in Cl/Cd vs α graph. Also, I choose the airfoil that the gap is not steep. Hence, the change of α will not have big impact to Cl. Below, is the list of airfoils that is categorized as "common use" for wind turbine in low wind velocity.

1. SD7034
2. SD7032-099-88
3. S4180-098-84
4. Rhode St. Genese 30
5. NACA 4412, NACA 4415, NACA 2410, NACA 4418, NACA 6412, NACA 25112
6. Goe 225, Goe 426, Goe 621, Goe 795
7. MH 102, MH 110.

From the graph Cl vs α and Cl/Cd vs α, also from the shape of the graph that declivous, It can be decide to used SD7032-099-88, as the shape can be seen in Figure 3.

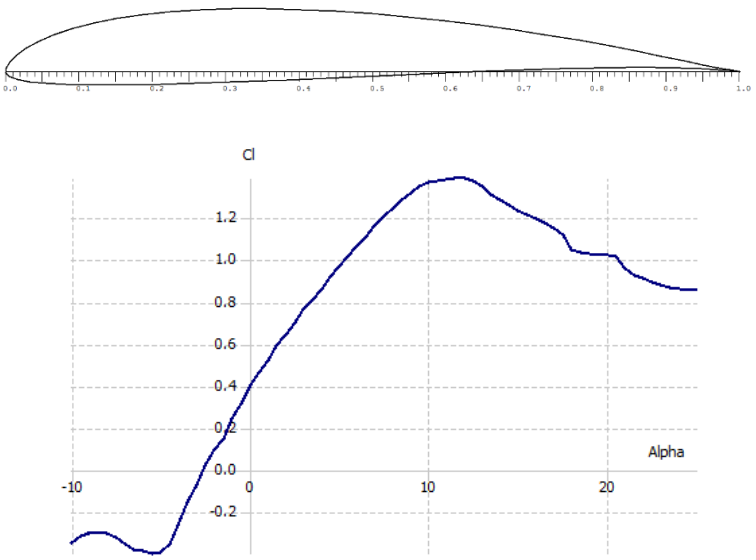

Fig. 3: Airfoil Profile, Graph Cl vs α, and Graph Cl/Cd vs α of SD7032-099-88

3.1. Chord calculation

In order to determine the chord of the blades, these equations that Cancelli used in his thesis, Aerodynamic Optimization of A Small-Scale Wind Turbine Blade for Low Windspeed Conditions, are used. And safety factor for the blades for an uncertain condition are predetermined, 1.25.

$$Dynamic\ Pressure\ (qs) = \frac{1}{2}\rho v^2 \quad (6)$$

$$Axial\ Load\ (P) = qs.\ ct.\ c \quad (7)$$

$$Momen: \frac{P}{2}(R^2 - r^2) \quad (8)$$

$$Tegangan\ (\sigma) = \frac{Md}{Iyy} \quad (9)$$

$$Dynamic\ Pressure\ (qs) = \frac{1}{2}\rho v^2 \quad (10)$$

$$Tegangan\ izin\ (\sigma) = 36000\ Pa \text{ (Properties of Wood)} \quad (11)$$

$$Sf = 1.25 = \frac{Allowable\ Stress\ (\sigma)}{Actual\ Stress\ (\sigma)} \quad (12)$$

An approach in Airfoil profile is needed to get Iyy and d, as can be seen in Figure 4 and its result in Table 3.

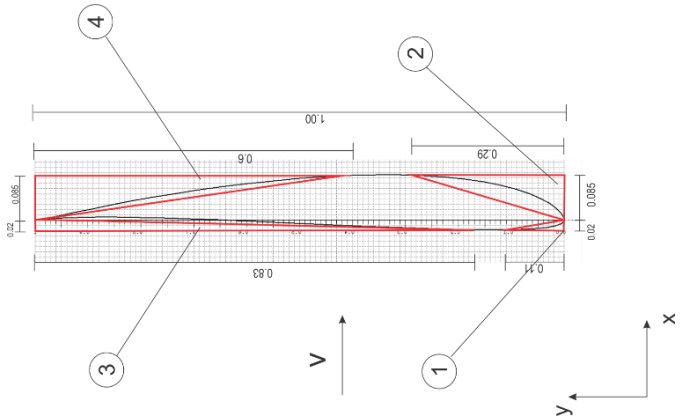

Fig. 4: An approach to airfoil profile (SD7032-099-88)

Table 3: Calculation Result of Iyy dan d

Geometry	Plane	Xbar (m)	Ybar (m)	Iyy (c^4) (m^4)	d (c) (m)	c (m)
Triangle	1	0.044135	0.430369	0.000171	0.044135	0.126172
Triangle	2			0.00143		
Triangle	3			0.00103		
Triangle	4			0.003994		
Rectangular	All			0.009259		
Iyy Airfoil				0.002634		

3.1. Twist at the blades

Other needed dimension for simulation is twis. Initialy, TSR partial is calculated then followed by Cl, α (angle of attack) and ϕ (flow angle).

$$\lambda_r = \frac{r}{R} \times \lambda_R \quad (10)$$

$$C_l = \frac{16\pi \times R \times \frac{R}{r}}{9\lambda_R \times B \times C_r} \quad (11)$$

$$\phi = \frac{2}{3} tan^{-1} \frac{1}{\lambda_r} \quad (12)$$

$$\beta = \phi - \alpha \quad (13)$$

From the twist, a graph are made and a linearisation from section 7 to 8 are done. This is to simplify the design and to make it easy to be produced without reduce its performance. This linearisation can be seen in Figure 5. Dotted line (blue line) show the twist of each section after linearisation.

Table 4: Calculation Result of Twist

Section	r (m)	TSR Parsial	Cl	α (°)	ϕ (°)	β (°)
0	0.14	1.225	1.34	9.5	26.15	16.65
1	0.21	1.8025	0.91	4.5	19.35	14.85
2	0.27	2.38	0.69	2.4	15.19	12.79
3	0.34	2.9575	0.55	1.2	12.45	11.25
4	0.40	3.535	0.46	0.5	10.53	10.03
5	0.47	4.1125	0.40	-0.05	9.11	9.16
6	0.54	4.69	0.35	-0.3	8.02	8.32
7	0.60	5.2675	0.31	-0.55	7.17	7.72
8	0.67	5.845	0.28	-0.75	6.47	7.22
9	0.73	6.4225	0.25	-1	5.90	6.90
10	0.80	7	0.23	-1.1	5.42	6.52

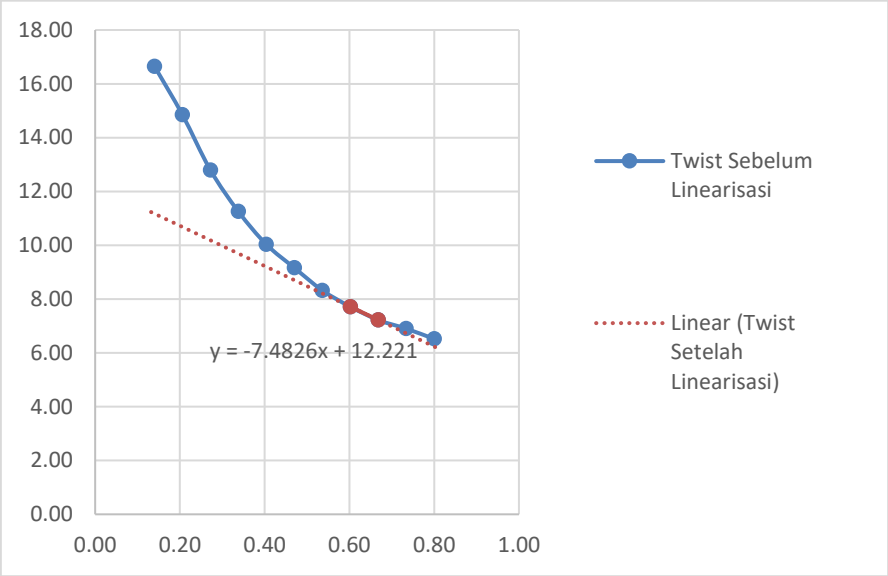

Fig. 5: Graph of twist angle vs r (section radius) dan linearization of the twist

Table 4: Twist that already linear (β')

β (°)	β' (°)
11.17	11.00
10.68	Linear
10.19	
9.69	
9.20	
8.70	
8.21	
7.72	
7.22	
6.73	
6.23	6.00

6. Simulation

Simulation are done using software, Qblade, by putting data as an input such as airfoil types, chord, and twist of the blades.

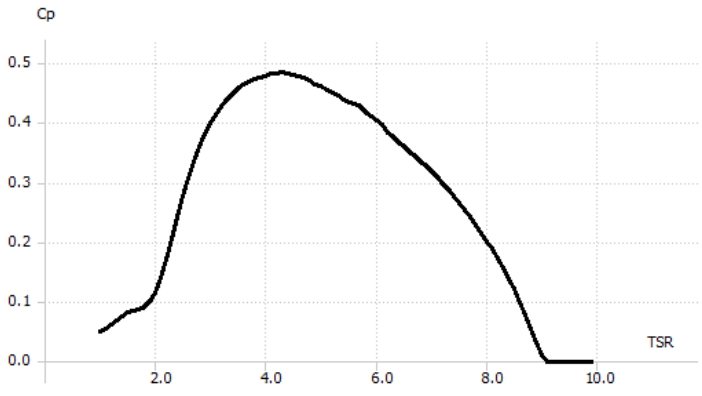

Fig. 6: Result of simulation, Cp vs TSR

7. Conclusion

An important conclusion from designing this blades of horizontal axis wind turbine, 500 Watt as maximum power, is that the dimension of the blade are obtained. In addition, from the result, the 3D visualization of the blades are made and ready to be produced.

8. Nomenclature

A	Wind cross-sectional area of the blade	m2
R	Rotor radius	m
R	Radius, to n element	m
W	Power	Watt
I	Inertia moment in y axis	m4
d	the outer distance from the center of mass from the load come	m
M	Momen	Nm
ct	Coefficient trust	
cl	Coefficient lift	
c	Chord	m

Greek letters

α	angle of attack	^{o}
ϕ	flow angle	^{o}
β	twist angle	^{o}
ρ	residence time	kg/m^3

Subscripts

yy	in Y axis
sys	system

9. References

Cancelli, Nicolette Arnalda. 2006. Aerodynamic Optimisation of a Small-Scale Wind Turbine Blade for Low Windspeed Conditions.

Piggott, Hugh. 2000. Windpower Workshop Building Your Own Wind Turbine. UK: British Wind Energy Association

Sugiyono, Agus, Anindhita, M. Sidik Boedoyo, Adiarso. Outlook Energi Indonesia 2014. Jakarta: BPPT.

Tim LAN. 2014. Pengenalan Teknologi Pemanfaatan Energi Angin. Tasikmalaya: 2014

Wind Energy How It Work. tersedia di: http://www.renewableuk.com/en/renewable-energy/wind-energy/how-it-works.cfm, diakses tanggal 15 September 2015.

Wind Turbine Technology. Tersedia di: https://energypedia.info/wiki/Wind_Turbine_ Technology, diakses pada 12 Januari 2016.

Shaun. Mechen. Tersedia di: http://www.shaunmechen.com/Props/Props.html, diakses pada 12 Januari 2016.

Proceedings of the 1st Faculty of Industrial Technology International Congress
International Conference
Bandung, Indonesia, October 9-11, 2017
ISBN 978-602-53531-8-5

Off-grid Renewable Energy Program for Sustainable Rural Electrification in Indonesia

Ilyas Taufiqurrohman
Energy Change Institute, The Australian National University (ANU), Canberra - AUSTRALIA
Corresponding author e-mail: u6295529@anu.edu.au

Abstract

There are many rural areas in Indonesia without electricity, especially in remote islands. It is challenging to provide electricity to remote areas through the electrical grid from existing power plants. One of the solutions for rural electrification is providing diesel generators, but it has an issue with the fuel shortage and negative impact on the environment. To overcome the issue related to the lack of rural electrification and dependence on fossil fuel, the off-grid renewable energy system can be the appropriate solution. There is an enormous potential of renewable energy resources, such as solar energy, micro-hydro, and wind energy. These resources are available as local energy resources in remote areas and can be utilized for generating electricity. However, there is another issue related to the sustainability of rural electrification program. For example, many infrastructures that have been built for rural electrification are not able to operate for long term period. This paper analyses factors that hamper the implementation of sustainable rural electrification based on renewable energy and discusses how to involve local community participation to ensure a sustainable program. The application of rural electrification based on renewable energy not only just to provide the electricity and increase rural electrification rate, but it also needs to provide the program that can be used by the local community to support their productive activities.

Keywords: off-grid system, renewable energy utilization, sustainable rural electrification, local community participation, community empowerment

1. Introduction

There is a significant gap in the electrification rate between urban and rural areas in Indonesia. It has been reported that Indonesia's national electrification rate is 81% with the ratio of urban electrification is 94%, but the ratio of rural electrification is only 66 % (World Energy Outlook, 2015). There are many rural areas without electricity because they are in remote areas which are challenging to access. It is challenging to bring electricity to rural areas through the electrical grid from existing power plants. Most of the existing power plants in Indonesia are still generated from fossil fuel, such as coal and oil (Tharakan, 2015). Extending electrical grids to transmit electricity from those existing power plants to remote areas can be very expensive and inefficient. Electrical grids from existing power plants, which have high electric capacity transmission, are not efficient for rural electrification because low electricity demand in the rural areas. A suitable solution for the problems related to rural electrification would be to utilize local renewable energy resources by implementing the off-grid system in the remote areas.

Indonesia has a huge local potential in relation to renewable energy resources that can be used for generating electricity. For instance, Indonesia has potential of hydropower about 75,000 MW, and potential of wind energy about 970 MW, potential of solar energy about 4.8 kWh/m²/day, potential of biomass about 32,654 MWe, and potential of geothermal about 12,386 MWe (Agency for the Assessment and Application of Technology, 2016, p. 18). However, the utilization of renewable energy resources for generating electricity is still low. In 2016, only 2% of electricity was generated from the total potential of all available renewable energy resources in Indonesia (Agency for the Assessment and Application of Technology, 2016). Rural areas without access to existing electrical grids can utilize the renewable energy resources that available in their areas. These resources can be categorized as their domestic energy resources which mean accessible and non-vulnerable to supply.

This paper discusses how the implementation of off-grid renewable energy program can provide the sustainable rural electrification. The following section, Section 2 introduces the objectives of this paper to provide the off-grid renewable energy program as the appropriate solution to rural areas which do not have access to existing electrical grids and to discuss the active participation of local community as the key factor to achieve the sustainable off-grid renewable energy. Section 3 provides the methods that are used in this paper. Then, Section 4 discusses and analyses in terms of issues of previous off-grid renewable energy projects for rural electrification, the application of off-grid renewable energy program, and how to understand the local community needs and involve their active participation in the off-grid renewable energy program. The last section, Section 5 is the conclusion of the discussion.

2. Objectives

The paper has following objectives:

- Provides that the application of off-grid renewable energy can be the appropriate solution for rural electrification to remote areas which are difficult to access.
- Discusses how to involve local community participation to ensure a sustainable program for rural electrification based on renewable energy.

3. Methods

We use literature-based to collect information and analyse it to address the objectives in Section 2. There are procedures that we do before we get the results and conclude it.

- Analyses factors that hamper the application of sustainable rural electrification based on off-grid renewable energy.
- Identifies factors that are important in the implementation of off-grid renewable energy program in rural areas.
- Identifies the needs of the local community in rural areas to empower the society through off-grid renewable energy program.

4. Analysis

4.1. Issues of Off-Grid Renewable Energy for Rural Electrification

Providing electricity to remote areas in Indonesia is a very challenging task. Blum et al. (2013) suggest that because of the challenging geographical nature of Indonesia, a decentralized off-grid is the appropriate technology for rural electrification, especially for remote and rural areas in mountainous areas or on isolated islands. This off-grid systems can be supplied by fossil fuel or renewable energy. Most of off-grid systems for rural electrification are still supplied by diesel generators (Blum et al., 2013). Diesel generators are mostly used in rural areas because of their long track-record for generating electricity and the communities are more familiar with this technology, it makes diesel generators as a standard for rural electrification solution (Schmidt et al., 2013). However, this solution cannot be used as the sustainable solution for rural electrification because fossil fuel is depletable resource and fossil fuel not only generates electricity, but also produces greenhouse gas emissions. Therefore, by shifting diesel generator to the renewable energy system, it can increase the rural electrification rate and at the same time not produce the greenhouse gas emissions.

However, there are some issues from previous rural electrification projects for the application of the off-grid renewable energy. Rural electrification programs by the utilization of renewable energy resource tend to be characterised by scattered low-income consumers, and high initial capital costs (Urmee et al., 2008). These are the reasons why most of the utilization of renewable energy for rural electrification to be funded by either the government or donor organisations. Over dependence on donors and the limited availability of financing can be the factors that hamper the implementation of sustainable rural electrification based on the off-grid renewable energy. Institutional weaknesses are also identified as factors that affect the off-grid renewable energy program (Urmee et al., 2008). If local institutions that has the responsibility to manage the off-grid system have no management capacity to administrate the services and no ability to handle technical issues, it will be a big problem (Feron, 2016). All these factors are the reasons why many off-grid renewable energy infrastructures that have been built for rural electrification are not able to operate for long term period. To provide sustainable rural electrification through the off-grid renewable energy, we have to address these issues.

4.2. The Implementation of Off-Grid Renewable Energy Program

The provision of electricity in Indonesia is handled by Perusahaan Listrik Negara (PLN), State Electricity Company. PLN is a state-owned company which has a monopoly to responsible on electricity distribution across Indonesia. The Ministry of Energy and Mineral Resources has the responsibility as the policy making body and regulator for PLN and other ministries are also stakeholders in the electricity sector (Schmidt et al., 2013). Since 2009, Indonesia has opened the market of power generation for competition (Schmidt et al., 2013). This policy is taken by the government to increase the capacity of electricity generation and to fulfil the growth of annual energy demand, so small scale Independent Power Producers (IPPs) can produce electricity, but they are still required to sell the electricity to PLN for distribution, only rural electricity cooperatives can generate and distribute electricity independently (Schmidt et al., 2013). Figure 1 shows a schematic diagram of government and industrial stakeholders in the Indonesian electricity sector. To encourage the implementation of off-grid system and involve the participation of local community in rural areas, this system can be done in cooperatives.

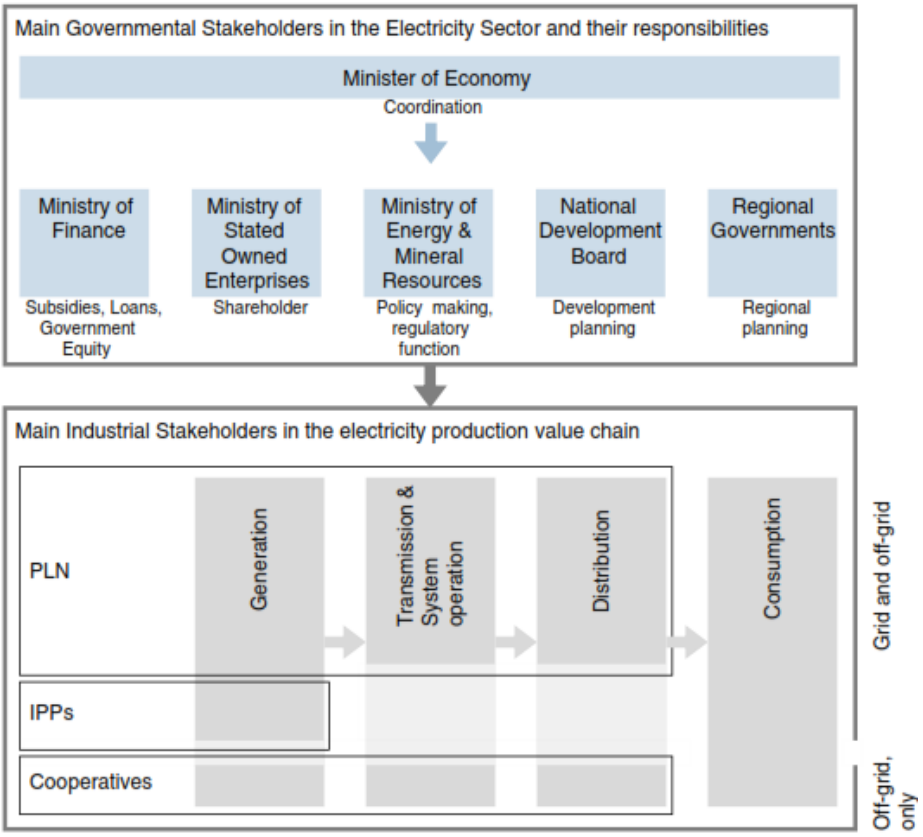

Fig. 12: Governmental and industrial stakeholders in Electricity Sector. (Schmidt et al., 2013)

Off-grid renewable energy program needs to consider the potential local energy resources in the specific areas. It means that the government cannot generalize to implement the rural electrification by only using single solution, such as providing the photovoltaic system to all rural areas. For example, if there is a potential of micro-hydro in that areas, it should generate electricity by implementing micro-hydro power plants. Micro-hydro power plants are already the proven technologies which are more reliable and require less maintenance rather than other renewable energy resources, such as solar energy or wind energy (Veldhuis and Reinders, 2015). However, micro-hydro is only available in the mountainous areas or area that has stable water flow with different elevation. For the areas without the potential of micro-hydro, photovoltaic system can be the solution because there is a huge potential of solar energy across Indonesia. Regarding the implementation of off-grid PV system, Table 1 describes the indicators for the sustainability of off-grid PV system (Feron, 2016). These indicators can be used to qualitatively evaluate the sustainability of the program. Therefore, the renewable energy program can be implemented by considering the availability of local renewable energy resources in rural areas.

Table 5: Indicators for the sustainability of off-grid PV system (Feron, 2016)

Institutional	Economic	Environmental	Socio-Cultural
Stability (durability) and long-term vision	Cost effectiveness	Environmental awareness	Accessibility (disparity, equity)
Regulation, standards and enforcement	Reliability	Environmental impact	Social acceptance
Decentralization and openness to participation	Funding (initial investment; operation and maintenance)		Accuracy
Adaptability (ability to meet future needs)	Contribution to the income of users		Cultural justice
Expert know-how			

There is an issue related to the technology of off-grid renewable energy system that can be identified as unfamiliar technology to rural inhabitants. Most rural inhabitants usually use a generator based on diesel fuel. The technology which is used in the off-grid renewable energy system is totally different from a diesel generator. If local communities in rural areas are not ready to use this technology, utilization of renewable energy cannot be a sustainable solution for rural electrification. In order to overcome this problem, an adequate training and support system need to be provided to rural inhabitants. A good example of implementing the program for the utilization of renewable energy is demonstrated by Cinta Mekar Village, Subang, West Java. Cinta Mekar Microhydro Power Plant Project has been in operation since 2005 and it became the prototype for providing rural electrification based on renewable energy because the project, which was initiated by IBEKA, a Jakarta-based NGO, has successfully involved the local community in the maintenance of micro hydro power plant (Utomo, 2015). IBEKA also provides rural electrification based on renewable energy not only to fulfil household electricity, but also encourage the local community to use electricity for supporting their productive activities, such as small enterprises and domestic industries. By eliciting active participation of rural inhabitants in the implementation of renewable energy, it can make them become more aware and expand their knowledge and responsibility in maintaining the operation of the infrastructure over long periods of time. This can be achieved by educating rural inhabitants in terms of understanding the technology used for renewable energy power plants before building the infrastructure, and then providing them with knowledge about how to operate and maintain this system. Therefore, the technology of renewable energy system can be implemented appropriately in rural areas.

A further issue that should be considered relates to the cost of the renewable energy infrastructure. Renewable energy power plants require a higher investment cost rather than fossil fuel power plants (U.S. Energy Information Administration, 2016). For example, photovoltaics system has a high investment cost with a low conversion rate from solar energy to electrics, and the system still requires battery units for saving energy (Sandhu and Thakur, 2014). More solar panels and batteries need to be implemented in solar power plants to make the system robust, but this infrastructure also requires more funding. However, there is a trend in the photovoltaics systems which have progressively low cost and the investment cost of solar PV can be more affordable (Pauser et al., 2015). Another solution that is provided by the government for rural electrification is diesel generator. However, local communities still need to buy diesel fuel to produce electricity for their daily use and consequently, the diesel generator has a high operational cost (Blum et al., 2013). There are also several issues in relation to fuel shortage and the higher price of fuel because the fuel comes from outside of the rural areas. As a result, operational problems may arise depending on the availability of stocks of diesel fuel in rural areas. In contrast, renewable energy, such as solar energy is the local resource that are available in rural areas. There is no needed to import fuel to operate a renewable energy system, but local communities in rural areas still have a responsibility to pay a fee for maintaining the infrastructure. The utilization of renewable energy, such off-grid photovoltaic system is more competitive than diesel generator in economic terms (Blum et al., 2013). Hence, the off-grid renewable energy system has a lower operational cost than a diesel generator.

4.3. Local Community Needs and Their Active Participation

To achieve sustainable rural electrification based on renewable energy resources not only depend on affordable cost, the implementation of appropriate technology, and understanding the technology, but also requires more attention to social, cultural and political issues in the rural areas. Every community has their own characteristics, included different social and cultural attitudes, failure to appropriately address these socio-cultural and policy dimensions can also cause failure in the implementation of rural electrification based on renewable energy which means wastage of resources and time (Urmee and Anisuzzaman, 2016). It is very important to understanding the community in the rural areas as the subject of the rural electrification, not only as the object of the program. Therefore, policies and programs related to the implementation of rural electrification should fulfil local community needs as a main target and involve their active participation in the programs.

Figure 2 shows the framework for integration of social, cultural, and policy issues regarding the off-grid renewable energy program for rural electrification. This framework also considers some aspect regarding technology and institutional, but more focus on social, cultural, and policies dimension to provide the sustainable rural electrification program (Urmee and Anisuzzaman, 2016).

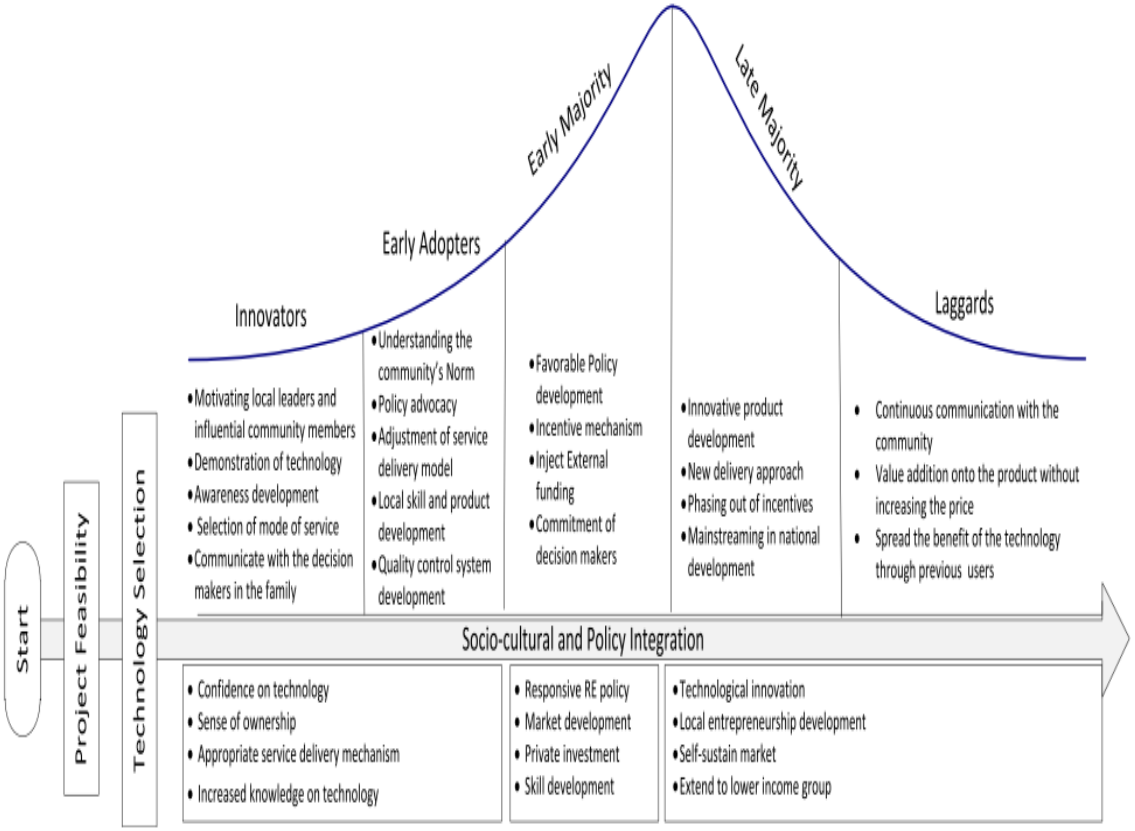

Fig. 13: Framework for integration of social, cultural and policy issues in an off-grid rural energy delivery program (Urmee and Anisuzzaman, 2016)

The implementation of rural electrification not only to provide the electricity in rural areas and increase the rural electrification rate, but it also needs to provide the program that can be used by local community to support their needs, especially for the productive activities. Understanding the community needs is the main point to encourage active community participation. For development projects, such as rural electrification programs, active community participation is the key process where advantages not only receive the benefits directly of the project, but also has an impact on the direction and execution of the project (Urmee and Anisuzzaman, 2016).

Access to the electricity is the important factor in the economic and social development. The off-grid renewable energy program for rural electrification is not only used to provide electricity for the household needs, but also provide electricity to support their economic activities. Therefore, off-grid PV system can be used to support their productive activities and increase their welfare.

5. Conclusion

The off-grid renewable energy program can be the sustainable solution for rural electrification in Indonesia. There are many rural areas without access to electricity due to the challenging geographical nature of Indonesia. Indonesia has a huge potential of renewable energy resources, such as micro-hydro and solar energy are available as the local energy resources. The off-grid renewable energy system can be implemented appropriately in rural areas by analysing the potential renewable energy resources in the regions. By eliciting active participation of rural inhabitants in the off-grid renewable energy program, it can make them become more aware and expand their knowledge and responsibility in maintaining the operation of the infrastructure over long periods of time. It can be achieved by educating rural inhabitants in terms of understanding the technology and assisting them with management capability to handle the infrastructure. Another key factor is providing the empowerment program to the local community that can encourage and assist them to use electricity for supporting their productive activities, such as domestic industries. Therefore, the sustainable rural electrification not only just provides electricity to fulfil the household need and increase national electrification rate, but also has to support their social and economic life, then increase their welfare.

6. References

Agency for the Assessment and Application of Technology, 2016. Indonesia Energy Outlook 2016, available at: http://repositori.bppt.go.id/index.php?action=download&dir=_data%2FDownload%2FOUTLOOK+ENERGI+2016&item=BPPT+-+Outlook+Energi+Indonesia+2016.pdf&order=name&srt=yes&lang=en, accessed on April 15, 2017.

Blum, N. U., Sryantoro, W. R., Schmidt, T. S., 2013. Rural Electrification through Village Grids—Assessing the Cost Competitiveness of Isolated Renewable Energy Technologies in Indonesia. Renewable and Sustainable Energy Reviews, 22, 482-496. doi:10.1016/j.rser.2013.01.049.

Feron, S., 2016. Sustainability of Off-grid Photovoltaic Systems for Rural Electrification in Developing Countries: A Review. Sustainability, 8(12).

Pauser, D., Fuente, K., Djerma, M., 2015. Sustainable Rural Electrifcation. State University of New York College of Environmental Science and Forestry.

Sandhu, M., Thakur, T., 2014. Issues, Challenges, Causes, Impacts, and Utilization of Renewable Energy Sources - Grid Integration. International Journal of Engineering Research and Applications 4 (3), pp. 636-643.

Schmidt, T. S., Blum, N. U., Sryantoro, W. R., 2013. Attracting Private Investments into Rural Electrification — A Case Study on Renewable Energy Based Village Grids in Indonesia. Energy for Sustainable Development, 17(6), 581-595. doi:10.1016/j.esd.2013.10.001.

Tharakan, P., 2015. Summary of Indonesia's Energy Sector Assessment. Asian Development Bank, available at: https://www.adb.org/sites/default/files/publication/178039/ino-paper-09-2015.pdf, access on April 15, 2017.

Urmee, T., Harries, D., Schlapfer, A., 2008. Issues related to rural electrification using renewable energy in developing countries of Asia and Pacific. Renewable Energy, vol. 34, no. 2, pp. 354-357.

Urmee, T., Anisuzzaman, Md., 2016. Social, cultural and political dimensions of off-grid renewable energy programs in developing countries. Renewable Energy, vol. 93, pp. 159-167.

U.S. Energy Information Administration, 2016. Annual Energy Outlook 2016 with Projections to 2040, available at: https://www.eia.gov/outlooks/aeo/pdf/0383(2016).pdf, accessed on July 10, 2017.

Utomo, S., 2015. Improving Rural Electrification in Eastern Indonesia through Institutional Capacity Development. International Institute of Social Studies.

Veldhuis, A. J., & Reinders, A. H. M. E., 2013. Reviewing the Potential and Cost-Effectiveness of Grid-Connected Solar PV in Indonesia on a Provincial Level. Renewable & Sustainable Energy Reviews, 27, 315-324. doi:10.1016/j.rser.2013.06.010.

World Energy Outlook, 2015. Electricity Access Database, available at: www.worldenergyoutlook.org/media/weowebsite/2015/WEO2015Electricityaccessdatabase.xlsx, access on April 15, 2017.

Proceedings of the 1st Faculty of Industrial Technology International Congress
International Conference
Bandung, Indonesia, October 9-11, 2017
ISBN 978-602-53531-8-5

Study of Hybrid "Photovoltaic and Wind Turbine" System Using Homer Program for Regional Cidahu Central – District Kuningan

Agus Adi Nursalim[1,*] and Dani Rusirawan[2]
[1]Graduate Student of Mechanical Engineering, Itenas, Bandung – INDONESIA
[2]Dept. of Mechanical Engineering, Itenas Bandung – INDONESIA
*Corresponding author e-mail: adi_nursalim@yahoo.com

Abstract

Electricity supply for East Kuningan Regency especially for Cidahu sub-district is experiencing constraints due to frequent power outages caused by natural and other factors. The area is very potential to be a small and medium-sized industrial area that is environmentally friendly due to a lot of unproductive land, sand excavation. The potential of renewable energy in the form of solar energy and wind energy can be built into a hybrid photovoltaic and wind turbine power plant technology so that it does not rely on electricity supply from the Perusahaan Listrik Negara (PLN). Weather conditions in the region produce an average of year is 25.57°C of Temperature Air, 3.44 m/s Wind Speed , 81% Humidity and 5,08 kWh/m²/day of Sun Radiation. The load requirement for the area is 80 kWh/d 8.22 kW peak using renewable energy is Photovoltaics, Wind Turbine, Converter and Battery. This Hybrid Technology study using the Homer program, obtained the highest COE value 1.75 $/kWh, the lowest 1.73 $/kWh and the highest NPC value of 659,703 $ and the lowest 654,139 $.

Keywords : renewable energy, hybrid, photovoltaic, wind turbin, homer,

1. Introduction

The location of astronomical district of Kuningan is at 6 ° 47'-7 ° 12 'South Latitude and 108 ° 23'-108 ° 47' East Longitude. Viewed from the geographical position, Kuningan Regency is located in the eastern part of West Java on a regional road that connects the City of Cirebon with East Priangan region and Central Java Province. Boundaries as follows: North side with Cirebon regency of West Java Province, East side with Brebes Regency Central Java Province, South side with Ciamis Regency West Java Province and Cilacap Regency Central Java Province, West side with Majalengka Regency of West Java Province.

Currently, Kuningan Regency is planning the development of industrial estate in 6 districts of Cidahu district, Kalimanggis district, Ciawigebang district, Luragung district, Japara district and Pancalang district. The development of industrial estate in Kuningan Regency is one of the means for the development of environmentally friendly industry / warehousing. Industrial Estate can act as the driving of regional economy, give the economic effect of multiplier very big for the increase of Original Regional Revenue (PAD), the absorption of labor, the emergence of new entrepreneurs, the purchasing power of the community will rise, the development of markets, financial institutions,

To establish an industrial estate, the accuracy of location, local government policy that is able to attract investors is to provide ease of providing ready-made industrial sites, the availability of facilities and infrastructure needed (electricity network), ease of licensing on the condition of environmentally friendly industrial areas. The type of industry that can be developed consists of various industries that process forest and agricultural resources such as wood, rattan, bamboo and non-metallic minerals, small industries such as food or beverages and tobacco industries, clothing such as leather and textiles, and building materials such as paper, printing, publishing, rubber and plastic goods and metals industries such as machinery, electricity, science tools. To activate the industrial estate, the necessary electricity infrastructure.

In accordance with the government's energy-efficient program, the availability of electrical energy is exploited to utilize as optimally as possible local renewable energy sources such as solar energy and wind energy. So it is necessary to study first for the operation of Wind Energy (PLT Angin) and Solar Energy (PLTS). Overall integration of the two kinds of power plants is called Hydride Power Generation (PLTH). The output of this study is the performance or capability of PLTH, namely the integration between PLTS and PLT Angin based on renewable energy, in the form of total power of PLTH, the excess of electrical energy generated, and the cost of electricity generation. Data processing using HOMER software.

HOMER (Hybrid Optimization Model for Energy Renewable).

HOMER is a software used to help modeling of a power system by using a variety of renewable resources options. With HOMER, the most optimal specification of energy sources can be obtained - a possible source of energy. We must include load data, solar resource data, wind resources from areas where we will build industrial estates (loads), economic data, data constraints, system control inputs, emissions data and solar price data. Energy sources that may be used are diesel generators, solar cells (PV), wind turbines and so on.

HOMER simulates the operating system of a system based on the calculation of each energy for 8,760 hours in 1 year. The HOMER compares the electrical and thermal loads within an hour for the energy that the system can supply at that time. If the system meets the load throughout the year,

HOMER estimates the lifecycle cost of the system, calculates capital costs, replacement, operation and maintenance, fuel and interest. The hourly energy flow can be seen in each component, as well as annual costs and performance summaries.

After simulating all possible system configurations, HOMER displays a list of system feasibility, which is sorted by lifecycle cost. The lowest cost system is at the top of the list so it can easily be found as well as a list of other eligible systems eligibility.

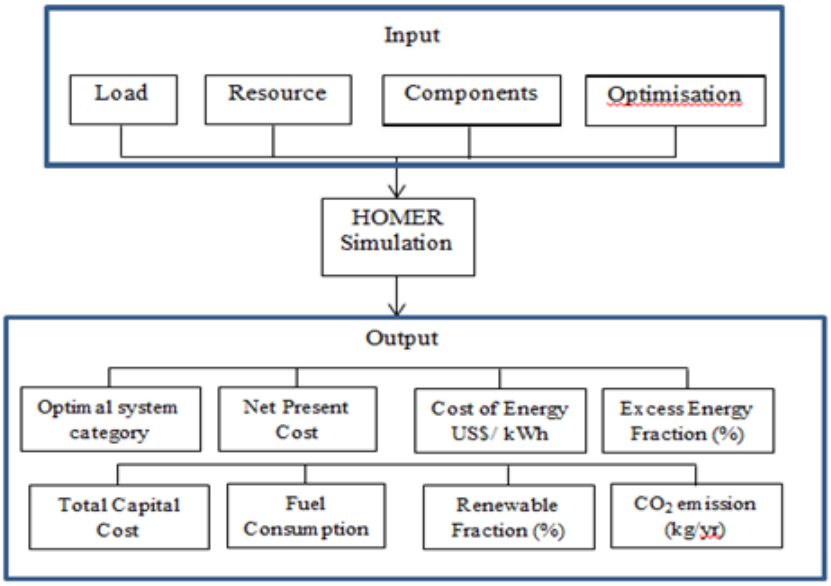

Fig. 1: HOMER Simulation and Optimization System

To know the optimum design of renewable energy, especially wind energy and solar energy. The output of this study is a configuration between PLT Angin and PLTS based on renewable energy in the form of total power of PLT Angin, PLTS, excess electricity generated, electricity generation cost and emission output.

The problems that will be discussed in this paper are as follows:

1. How is the potential of renewable energy in Cidahu District, Kuningan Regency, West Java in this case wind energy, solar energy
2. Why in need optimumisasi using software HOMER.
3. Optimization study of PLT Angin and PLTS development in Cidahu District, Kuningan Regency West Java using Homer software.
4. Evaluation of capacity optimization of PLT Angin and PLTS development using Homer software.
5. Environmental impacts that occur from the development of PLT Angin and PLTS to the community local, in terms of the amount of emissions generated.

Hybrid Power Generation System

Renewable energy sources have great potential when used to generate electrical energy, which can be used in isolated areas using hybrid generating systems. Hybrid generating systems are designed to produce electrical energy. The system consists of several generating units such as PV, wind turbines, micro hydro, and generators. The size of a hybrid generating system varies, from systems that have the capacity to supply one or more homes,

to systems with very large capacity to supply power grids in remote areas. The hybrid generation system is one way to provide electrical energy to remote areas in different parts of the world where the cost of developing large-scale power lines is too high and diesel fuel transportation costs are also very high. The use of hybrid generation systems reduces the use of expensive fuels, enabling clean and environmentally friendly electricity production and improving living standards of people living in remote areas.

2. Research Methodology

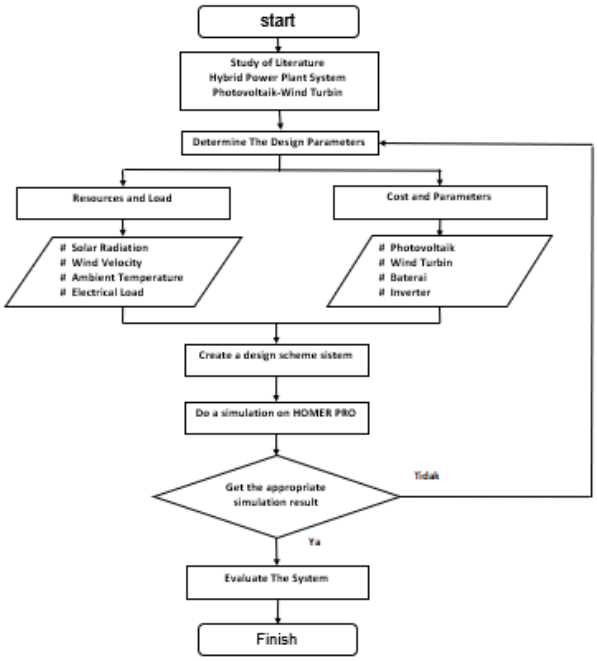

Fig 2: Flow Diagram of Research

Study of literature

Learn the working principles, characteristics and configurations of photovoltaic hybrid power generation systems, wind turbines and generators.

Define Design Parameters

The choice of location for this study is Cidahu District, Kuningan Regency, West Java, by obtaining design parameters such as solar radiation, wind speed and temperature of BMKG, and other conditions that can affect hybrid system performance, as well as component cost and technical specifications of the manufacturer.

Create a System Schema

Schematic design of hybrid power plant system with 20 kW design capacity and component specifications made using HOMER software.

Conducting Simulation

The simulation is done by using HOMER software to get some optimization results from the design of hybrid photovoltaic power system-wind turbine generator, so that can be selected combination of expected system based on capacity and cost.

Evaluating the System

To evaluate macro (economic and technical) to the simulation result by conducting sensitivity analysis to see the effect of a variable on the simulation result, in this case to the selection of system combination viewed from the cost factor of photovoltaic capital, wind turbine and generator, and the performance of any component if the design of this system is operating later.

3. Research Result and Discussion

3.1. Research Sites

Research location for industrial area / factory is in Cieurih Village Cidahu District Kuningan Regency West Java. (6 ° 57.8 'South Latitude, 108 ° 39.5' East Longitude).

Fig.3: Research Site

3.2. Environmental Data Conditions

Data of environmental weather conditions that occurred in the research location of Cidahu sub-district from HOMER average in 1 year are as follows:

- Temperature = 27.28 ° C
- Wind Speed = 6.81 m/s
- Moisture = 81%
- Solar Radiation = 5.04 kWh/m^2/day

Fig 4: Temperature Data and Graph at the research location

Potential Wind

Based on data obtained average wind speed in District Cidahu Kuningan measured with a height of 10 meters from the surface of the soil and altitude of 1450 m above sea level is 6.810 m / s. Wind speed data of Cidahu sub-district of Kuningan District for one year can be seen in Fig 6.

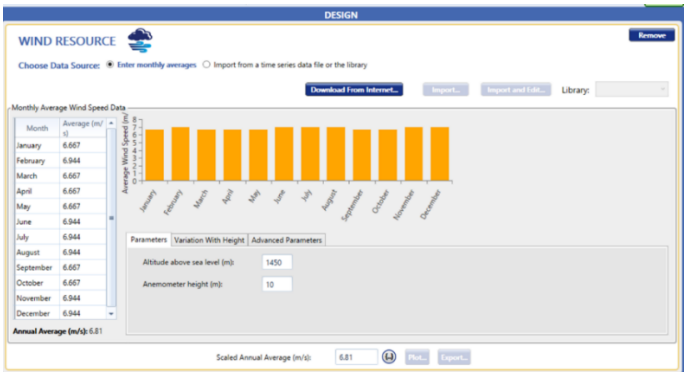

Fig. 5: Wind Speed Data and Graph at the study site

The Potential of Solar Radiation

HOMER required data to perform optimization of power plant system is clearness index and daily radiation (kWh/m^2/day) for one year in District of Cidahu Regency of Kuningan. Clearness Index and Solar Radiation data are the global average of solar radiation on a horizontal surface, expressed in kWh/m^2, for every day of the year. Clearness Index averaged 0,509 and average daily radiation for Cidahu District of Kuningan Regency is 5.040

kWh/m^2 /day. Data sources are obtained through HOMER assistance that will connect to NASA satellite via internet connection by providing latitude and longitude of research location.

Fig. 7 is data clearness index and daily radiation.

Fig. 6: Sunlight radiation data and graphs at the study sites

3.3. Schematic Configuration Systems

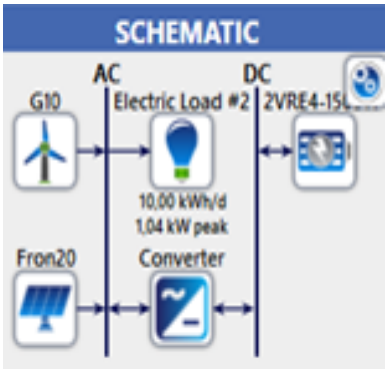

Fig 7: PLTH design using HOMER program

3.4. Electrical Expenses

Electrical system in Cidahu District Kuningan Regency to condition or supply a small and medium industry is isolated system. Electrical needs are supplied by PLT Angin and PLTS with a capacity of 10 kWh/day 18.36 kW peak. The main load here is the burden for small and medium business activities with a daily average load of 7.38 kW and 177 kWh/d and for peak loads of 10 kW occurs at 5:30 to 21:30 pm, with a load factor of 0.4.

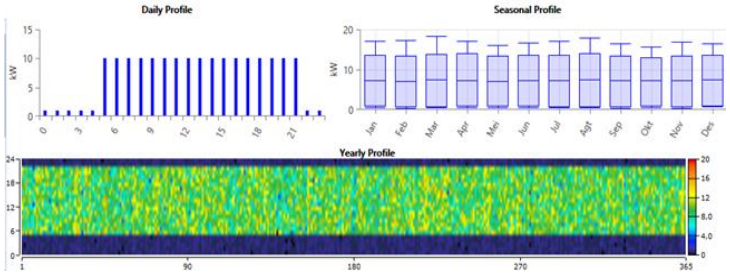

Fig 8: Graphs and daily load curves at the research site

3.5. Photovoltaik

The Photovoltaics module used in this study is

Table 1: Technical details and Photovoltaics costs

PV SYSTEM	
Model name	Fronius Symo 20.0-3-M with generic PV
Rate capacity	1 kW

Derating factor	96 %
Panel type	Flate plate
Ground reflection	20 %
Operating temperature	45°C
Efficiency	17,30 %
Capital cost	$ 3.000
Replacement cost	$ 2.250
O & M cost	$ 10 / year
Life time	25 years

3.6. Wind Turbine

The wind turbine used is

Table 2: Technical details and cost of Wind Turbine

WIND TURBINE	
Model name	G10 Generic 10 kW
Rate power	10 kW
Hub height	24 m
Capital cost	$ 4.500
Replacement cost	$ 3.000
O & M cost	$ 50 / year
Life time	20 years

3.7. Battery

Battery used is

Table 3: Technical details and Battery cost

BATTERY	
Model name	Discover 2VRE24-1500TF
Nominal capacity	1,48 kWh
Nominal voltage	2 Volt
Roundtrip efficiency	85 %
Min. State of charge	40 %
Float life	18 years
Max. Charge life	1 A/Ah
Max. Charge current	158,7 A
Capital cost	$ 300
Replacement cost	$ 275
O & M cost	$ 10 / year
Life time	1.750 kWh , 15 years

3.8. Converter

The costs and the technical details of the power converters

Table 4: Technical details and Converter costs

CONVERTER	
Rated power	1 kW
Capital cost	$ 800
Replacement cost	$ 600
O & M cost	$ 5 / year
Efficiency	95 %
Life time	15 years

3.9. Cost On PLTH System (PLT Angin - PLTS)

The overall costs of the Hybrid Power Plant generated by the combined system of the Wind Power Generator (PLT Angin) and the Solar Power Plant (PLTS) are the initial Investment Capital ($ 3,000), the Operating Cost of $ 497,81 per year, Net Present Cost (NPC) of $ 659,703, Electricity Cost (COE) of $ 1.75/kWh.

3.10. Results Of Design

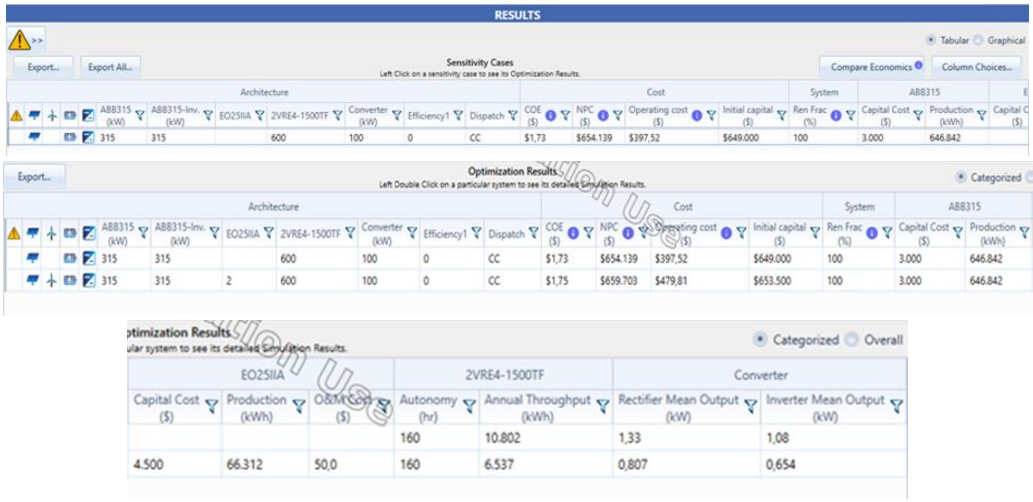

Fig 9: Results of HOMER program optimization of PV system, Wind Turbine, Battery and Converter

The cost of the initial capital of a component (capital cost) is the total component installation cost at the beginning of the project. At the time of zero of the project periods for all components; diesel generators, wind turbines, power converters, batteries and PV arrangements. The replacement cost is the cost of replacing the components and includes the cost of disposal of waste at the end of its useful life. In the 25th year of project age for PV systems, 20th year for wind turbines, in the 15th year for batteries and in 15 years for converters. The component O & M cost is the cost associated with operating and maintaining that component.

4. Analysis and Conclusion

4.1. Analysis

According to the optimization results shown in Figure 9, obtained from HOMER software, it can be noted that the optimal configuration is a hybrid system (PV / wind turbine / converter / battery), consisting of 315 kW PV, 0 kW wind turbine, 100 kW converter power and 600 batteries. The leveled COE (Cost Of Energy) of this hybrid system is $ 1.73 / kWh; it is the cheapest COE compared to other configuration systems (wind / PV $ 1.75 / kWh).

The total NPC (Net Present Cost) of a system is the present value of all costs incurred during the process, minus the value of all revenue it earns during the process. Costs include; cost of capital, replacement cost at the cost of waste disposal, operation with maintenance cost and fuel cost. This NPC system is $ 654,139, which is the cheapest NPC in comparison with other system configurations. Renewable fraction of the energy of the optimum system is 100%, ie the energy fraction is sent to the load coming from renewable resources.

4.2. Conclusion

Based on the analysis presented in this paper, it can be concluded that the PV / wind turbine / converter / battery hybrid system is a practical and cost-effective solution to meet the electrical energy needs for environmentally friendly small and medium enterprises in Cidahu district, Kuningan Regency. According to the simulation results, using Home software, a hybrid system consisting of PV, wind turbines, power converters, and batteries, each found an optimal hybrid system configuration in accordance with NPC (Net Present Cost) and COE (Cost Of Energy).

In the results of the HOMER program analysis the cheapest NPC is the NPC of the optimum configuration system ($ 654,139) (PV / converter / battery) compared to other NPC system configurations ($ 659,703) (PV / Wind Turbine / converter / battery); The resulting COE is also small $ 1.73 / kWh.

In the techno-economic studies of the designed PLTH system. These techno-economic parameters can be summarized as follows;

1. The most selected PLTH system is Base System without Wind Turbine added with PV, Converter and Battery.
2. The combination of selected PLTH systems requires Initial Capital ($ 649,000).
3. The combination of selected PLTH systems requires COE ($ 1.73 / kWh), NPC ($ 654,139) and Operating Cost ($ 397,52) the lowest compared with other combinations.
5. Renewable Fraction of selected PLTH system of 100%.

5. References

Fahd Diab, Hai Lan, Lijun Zhang dan Salwa Ali, 2016, An environmentally friendly factory in Egypt based on hybrid photovoltaic/wind/diesel/battery system, College of Automation, Harbin Engineering University, Harbin 150001, China, Communications, Electrical Engineering Department, Assiut University, Assiut 71516, Egypt.

D.Saheb-Koussa , M.Koussa, M.Belhamel dan M.Haddadi, 2011, Economic and environmental analysis for grid-connected hybrid photovoltaic-wind power system in the arid region, Centre de Développment des Energies Renouvelable Route de l'observatoire, BP.62 Bouzareah, Alger, Algérie, Laboratoire de Dispositif de Communication et de Conversion Photovoltaïque E. N. P, 10 Avenue Hassen Badi, El Harrach, Alger, Algérie.

Homer Help Manual, 2016, Homer Energy, Boulder CO 80301 USA

Arif Febriansyah Juwito, Sasongko Pramonohadi, T. Haryono, 2012, Optimalisasi Energi Terbarukan pada Pembangkit Tenaga Listrik dalam Menghadapi Desa Mandiri Energi di Margajaya, Jurnal Ilmiah Semesta Teknika, Vol. 15, No. 1, 22-34, Mei 2012.

Maula Sukmawidjaja, dan IlhamAkbar, 2013, Simulasi Optimasi Sistem PLTH Menggunakan Software HOMER Untuk Menghemat Pemakaian BBM Di Pulau Penyengat Tanjung Pinang Kepulauan Riau, Dosen Jurusan Teknik Elektro, FTI Universitas Trisakti, Alumni Jurusan Teknik Elektro, FTI Universitas Trisakti, JETri, Volume 11, Nomor 1, Agustus 2013, Halaman 17 - 42, ISSN 1412-037

Proceedings of the 1st Faculty of Industrial Technology International Congress
International Conference
Bandung, Indonesia, October 9-11, 2017
ISBN 978-602-53531-8-5

SIMULATION OF WATER FLOW DISTRIBUTION ON LOW-HEAD PICOHYDRO CAPACITY 2 kW

Agung M. Werdhana[1,*], Agus Hermanto[2]
[1]Graduate Student of Mechanical Engineering, Itenas, Bandung – INDONESIA
[2]Dept. of Mechanical Engineering, Itenas Bandung – INDONESIA
[*] Corresponding author e-mail: agungmukti@gmail.com

Abstract

The amount of potential water energy in irrigation channels in Indonesia has not been optimally utilized because it has a small flow and low head. This study will simulate a low-head picohydro plant with a net head of 1.5 m whice is easily applied without altering the civil structure of the irrigation canal. The phenomenon of water flow pattern in headtank and horizontal axial turbine intake have an effect on the potential energy of water flow. Potential energy of flow at 0.22 m3/s discharge and 1.86 m head will be simulated using CFD (Computational Fluid Dynamic). The CFD results show that the reverse flow occurs at several positions in the headtank affecting the uniformity of the flow pattern and reducing the potential for utilization of electric water. The simulation results show that the flow power potential for a low-head picohydro generating system is 3190.2 Watt with a fluid velocity passing through a turbine runner of 2.28 m/s.

Keywords: Design, Picohydro, Low Head, Flow Pattern, and CFD Simulation.

1. Introduction

The uneven distribution of electrical energy occurs in rural areas due to inaccessibility of the power grid to the countryside, it takes electricity procurement effort to fulfill rural energy necessity. One way to fulfill this necessity in order to cover the lack of distribution is utilizing the existing energy sources, water energy in irrigation channels having energy from flowing water and low head water. Unfortunately, no one has developed and applied a low head picohidro power plant system, therefore a design that can exploit the potential energy of water in the irrigation canals is absolutely needed. Generally the use of irrigation channels is limited to irrigating rice fields and plantations.

The picohidro power plant system is designed with capacity of 2 kW, net head of 1.5 m. It uses horizontal axial flow turbine utilizing irrigation channel without altering the existing civil structure, verificated with potential energy generated and recognizing the flow pattern on the generating system without involving the turbine blade used dynamic fluid flow computation software (CFD).

The working principle of picohidro generating system by utilizing irrigation channel is similar to hydro power in general, the difference is in the intake channel and head race directly using the irrigation channel. Thus it does not require lead or steering dam. The water flow in the irrigation channel will be accommodated in the head tank firstly, the collected water has a height difference between the upper and lower water levels it's called name head as the water comes out from the accommodated water turbine, channeled through a conductor channel which consist of nozzles and a small pipe in which the turbine will be placed properly so that it can rotate well. The turbine rotation generates torque and the torque is connected with spinning velocity, it will produce power that will be transmitted through the shaft, pulley and v-belt for rotating the generator that serveing as a power plan.

2. Design of Picohydro

The potential energy of water available for energy generation can be calculated based on the equation below:

$$P = \rho \times g \times Q \times H_n \times \eta \quad (1)$$

Designing a 2 kW picohidro generating system requires several design criteria for design calculating design serving as limitations in the design, the required criteria are provided in table 1.

Table 1: Design criteria

Information	Design Criteria
Generated power	2 000 Watt
Net head	1.5 m
Turbin efficiency	75%
Generator efficiency	85%
System transmission efficiency	95%

The power that must be provided by the irrigation channel to generate 2 kW generation power using equation 1 is 3.3 kW and turbine output power of 2.48 kW with the requirement water discharge of 0.22 m^3/s.

Specific speed is an important parameter in designing a turbine used in a generating system such as to determine the type of turbine to be used, the turbine rotational speed during operation and determining the geometry of the turbine especially the diameter of the turbine. The specific speed equations used are as follows:

$$n_{QE} = \frac{n\sqrt{Q}}{E^{3}/_{4}} \quad (2)$$

The specific speed of the propeller turbine has a limit value that has been developed, used and made as a reference for the designing of turbine propellers. Limitations of the specific velocity value using the ESHA (2004) reference is $0.19 \leq n_{qe} \leq 1.55$ with using equation 2 obtained turbine rotational speed at the time of operation has a minimum of 180.8 rpm and a maximum of 1474.9 rpm. The turbine turn speed of design to be used in this design is 500 rpm, this value is based on the design use of a generator having specification of operating speed on 1500 rpm simplifiying the designing transmission system to be used.

The dimensions of turbine diameter can be obtained using the equation of ESHA as follows:

$$\mathrm{D} = 84{,}5\left[0{,}79 + \left(1{,}602 \times \mathrm{n_{QE}}\right)\right]\frac{\sqrt{\mathrm{H_n}}}{60 \times \mathrm{n}} \quad (3)$$

Dimension of turbine diameter base on from calculating using equation 3 is obtained 0.34 m. It is used as reference to the dimension of pipe diameter for delivering water to the turbine.

The position of the turbine set on the generating system affects the cavitation phenomena during the turbine operation. The cavitation will occur when the dynamic hydro pressure in the flow stream falls below the vapor pressure of the water properties there will be the formation of the vapor phase. This phenomenon will result in the form of small bubbles that occur in the area of low pressure by the flow and when the bubble burst it will produce a high pressure. If it happens, it produces a noisy sound which will cause damage to the turbine such as pitting will occur on the runner causing the effects of vibration while turbine operates. Cavitation is a characteristic marked with the value of the cavitation coefficient called the thoma number (Celso Pence, 2004), defined by the following equation:

$$\sigma = \frac{NPSE}{gH_n} \quad (4)$$

in order to avoid the cavitation phenomenon it requires minimum pressure during the turbine to operate so it takes the ideal placement distance for the turbine that is the vertical distance from the bottom water surface level to the center of the turbine is also called a turbine suction head (Celso Pence, 2004), The turbine suction head can be calculated by the following equation:

$$NPSE = \frac{p_{atm} - P_v}{\rho} + \frac{V^2}{2} - gH_s \quad (5)$$

In order to obtain thoma numbers, the following empirical equation can be used :

$$\sigma = 1{,}5241\ x\ n_{QE}^{1{,}46} + \frac{V^2}{2\ x\ g\ x\ H_n} \quad (6)$$

Placement of the turbine to avoid cavitation, from the calculation results obtained thoma number of 0.92 with head suction of 8.2 m. The value of the head suction is positive knowned, position of the turbine can be placed at above the water surface with a maximum limit of 8.2 m from the water surface to the turbine center.

Total head loss (overall energy losses) is the value of major head loss and minor head loss (Fox, R. w., McDonald, A. T., 1998)head loss major in pipe is where the position of turbine is located and minor head loss is in accessories which is used in channel of delivery that is entrance between outside head tank with nozzle (gradual contraction), nozzle and diffuser (gradual enlargement) or called draft tube. The inlet channel on the inlet side to be used has a diameter of 0.7 m with a length of 0.3 m, using pipe diameter of 0.35 m with a length of 0.25 m and a diffuser with 0.7 m diameter outlet side with a length of 0.3 m, water velocity 2.42 m s. The flow of water in the pipeline undergoes turbulent flow, based on the reynold number of 947427.3, thus the major head loss experienced by the pipe is 0.0007 m, while the minor head loss is 0.36 m, the total head loss at system amount 0.3607 m. The required gross head of the picohidro generating system is 1.86 m.

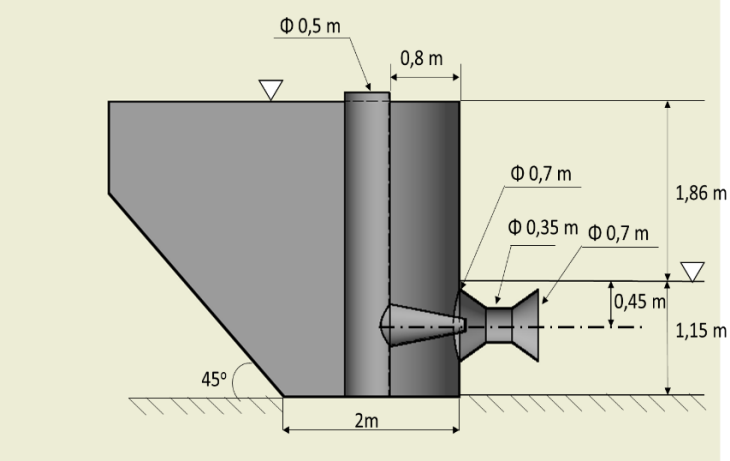

Fig. 1: Generating system design

Site surveys are conducted to record data and find to locate potential energy available according to the design criteria, data to be extracted from selected locations in the form of water debit, channel dimension and upper lower water level. The characteristics of irrigation channels has a constant flow rate and typical civil construction. One of the irrigation channel locations shown in figure 3, it is has the potential power generated amount 5022.7 Watt and average debit of 0.256 m^3/s. The generating system to be developed in this plan is based on the results of obeservation and the initial calculation is given as shown in figure 2.

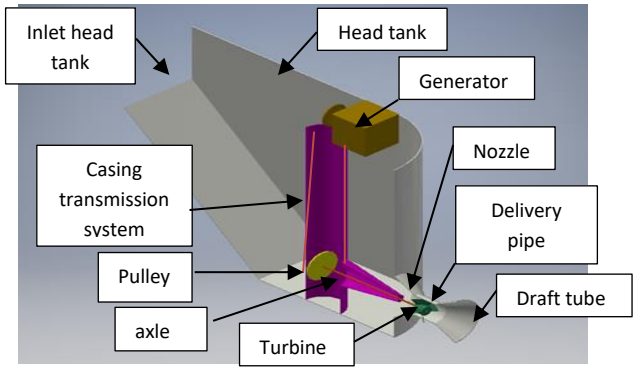

Fig. 2: Generator system design

Fig. 3: Location photos

3. CFD Simulation

This simulation is intended to verify the calculation result and to recognize the phenomenon of water flow pattern occuring in the picohidro generating system without involving the turbine blades, the simulation used with dynamic fluid flow computation method using software from ansys. the simulation process must go through three steps: preprocessing, solving and post processing (Tuakia.F, 2008). Preprocessing is the step in modeling or geometry in 3D as shown in figure 4.

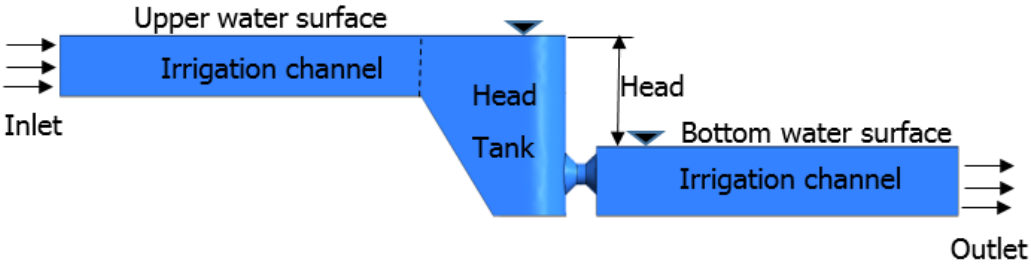

Fig. 4: Head tank model

The model is made based on the head tank geometry design created previously, the next step is making meshing, the field or volume of the model filled with the fluid divided into small volume cells, meshing process is made because in the simulation process uses calculation based on finite volume. In the meshing process applies the naming of boundary conditions on the model as shown in figure 4. The next step of the process of solving is the simulation process by entering the boundary conditions required during the calculation, conditions applied to the fluid flow model in laminar state with steady and gravity conditions. The boundary condition at the inlet side is rated of 220 kg/s on the type of mass flow with the type of water fluid, after all the data needed to perform the simulation process has been fed, the next step is calculating.

4. Simulation Results

After the calculations performed by the fluent software, the next step is postprocessing. It is the result of the simulation performed by fluent in the desired area and interpreting both in the form of vector images and contours with a variation pattern of certain color.

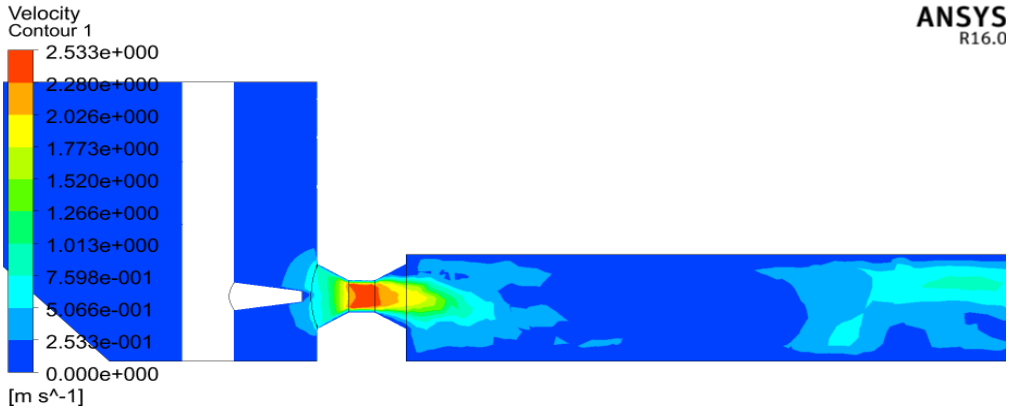

Fig. 5: Velocity Contour

In Figure 6 the high fluid velocity occurs in the area where the turbine will be placed that is in the pipe section, performed in red colour, the average velocity in the area is 2.28 m/s with a mass flow of 216.86 kg/s, by knowing data of speed and mass from simulation result hence the power potential using equation 1 from picohidro generating system is equal to 3190.2 Watt.

From the simulation results can know the pattern of water flow that occurs in the picohidro generating system by looking at the velocity velocity shown clearly in Figure 6, the figure can be interpreted in certain areas.

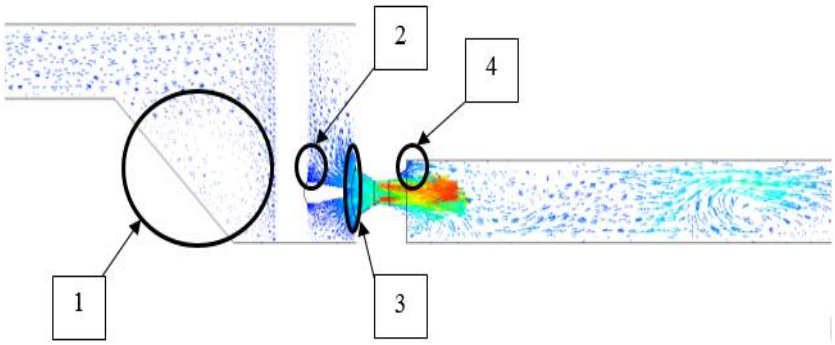

Fig. 6: Vector velocity on the generating system

In figure 7 the water flow is swirling in the sloping surface area close to the inlet from the irrigation canal to the head tank. It is due to the flow of water coming into the head tank can not go directly to the inlet to the turbine conductor as a result the flow of water coming from the inlet head tank stuck by the previous water and reverses direction causing a rotating flow in the area.

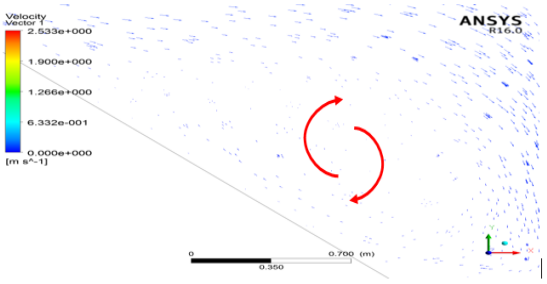

Fig. 7: Detail 1 vector velocity on generating system

In Figure 8 shows a swirling in an area having this angle caused by the moving water can not follow the angled path so the water hits the wall and the water flow split into two cousing swirling in the corner area, This swirling becomes a resistance to the moving flow.

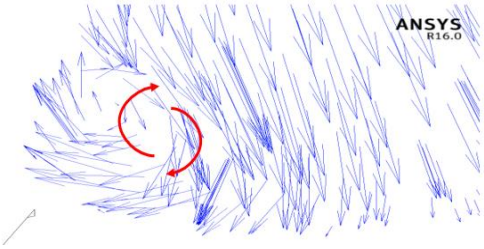

Fig. 8: Detail 2 vector velocity on generating system

In figure 9 shows at the inlet area of the nozzle, the water flow moves at the same time to enter the nozzle. It can be seen clearly from the intensity of vector in the area, caused by the water flowing from all directions try to enter the nozzle.

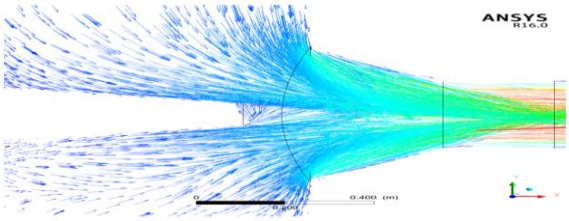

Fig. 9: Detail 3 vector velocity on generating system

In figure 10 shows a backflow in the draft tube region especially near the wall area cause the draft tube angle is too large this is due to the flow of water coming out of the draft tube is not fully developed resulting in the suction between the empty space with the flow of water on the outer side and this may cause resistance to the flow of water coming out of the turbine.

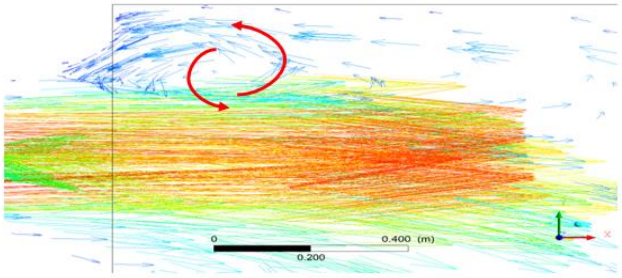

Fig. 10: Detail 4 vector velocity on generating system

Figure 11 shows the flow of water that swirling on the water surface due to the flow of water that is fast enough to hit the head tank wall and the flow back. It is crashed into a new stream from inlet the head tank caused to from swirling pattern.

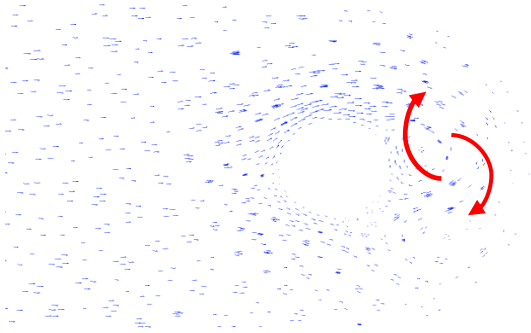

Figure 11: vector velocity on surface water generating system

5. Conclusions

The conclusions can be drawn from the calculation, simulation and analysis that has been done then can be conclude as follows

- Design and simulation results have identical tendency
- Backflow occurs at several positions within the generating system affecting the uniformity of the flow patterns in the system and reduces the potential power flow of the fluid that can be utilized
- Potential power flow simulation results for Pico hydro generating system is 3190.2 Watt with fluid velocity passing the turbine runner position of 2.28 m/s
- Centerline positioning of the turbine can be placed at above a the water level without experiencing cavitation phenomena as the turbine suction head is positive 8.2 m

The continuation and refinement of this research need some system geometry improvements with larger radius to maintain flow uniformity and minimize loss of fluid flow power.

6. Acknowledgment

This research is part of PUPT research funded by Direktorat Riset dan Pengabdian Masyarakat Kementrian Riset, Teknologi dan Pendidikan Tinggi Tahun Anggaran 2017.

7. Nomenclature

D	Diameter	m
g	Gravity	m/s^2
H_n	Head netm	
H_s	Head suction	m
N	Rotating velocity	rpm
N_{QE}	Specific velocity	
P	Power	Watt
P_{atm}	Atmospheric pressure	Pa
P_v	Water vapor pressure	Pa
Q	Water discharge	m^3/s
V	Water flow velocity	m/s

Greek letters

ρ	water density specific	kg/m^3
σ	Thoma number	
η	Efficiency	

8. References

C.C.Warnick, Howard A.Mayo, J., Carson, J. L., & H, L. (1984). Hydro Power Engineering. New Jersey: Prentice-Hall,Inc.

EM20, E. M. (1976). Selecting Hydraulic Reaction Turbine. Washington: U.S.Goverment Printing Office.

Data Rasio Elektrifikasi Jawa Barat, available at: www.esdm.jabarprov.go.id, accessed on june, 2016.

European Small Hydropower Association, Celso Pence. (2004). The Guide on How to Develop a Small Hydropower Plant. European: European Renewable Energy Council.

F.Dietzel, Sriyono, D. (1990). Turbin Pompa dan Kompresor. Jakarta: Erlangga.

Fox, R. w., McDonald, A. T. (1998). Introduction to Fluid Mechanics. Singapore: John Wiley & sons.

Indian Institute of Technology Roorkee. (1990). Standard/Manuals/Guidelines fo Selection of Turbine and Governing System for SHP. India: Ministry of New and Renewable energy Govt. of India.

JICA. (2009). Manuals and Guidelines for Micro-Hydropower Development in Rural Electrification. Japan: Energy Utilization Management Bureau.

Mott, R. L. (1994). Apllied Fluid Mechanics. United State of America: Prentice Hall.

Rencana Usaha Pengadaan Tenaga Listrik (RUPTL). available at: www.listrik.org, accessed on June, 2016.

Priyono Sutikno, I. K. (2011). Design, Simulation and Experimental of The Very Low Head Turbine with Minimum Pressure and Free Vortex Criterations. International Jurnal of Mechanical & Mechatronics Engineering IJMEE-IJENS, 8.

Sayers, A. T. (1992). Hydraulic and Compressible Flow Turbomachines. Singapore: MCGraw-Hill Book.

Susatyo, A., Subekti, R. A. (2016). Rancang Bangun Turbin Arus Sungai/ Head Sangat Rendah. LIPI, 8.

Tuakia, F. (2008). Dasar-dasar CFD Menggunakan Fluent. Bandung: Informatika.

Proceedings of the 1st Faculty of Industrial Technology International Congress
International Conference
Bandung, Indonesia, October 9-11, 2017
ISBN 978-602-53531-8-5

Effect of combustion saturated and unsaturated fatty acids pure vegetable oil for noise

Dony Perdana*, Eddy Gunawan
Department of Mechanical Engineering, Universitas Maarif Hasyim Latif (Umaha), Sidoarjo - INDONESIA
* Corresponding author e-mail: dony_perdana@yahoo.co.id

Abstract:

The steady increase in fossil fuel prices and the dependence on oil from producing countries to searched fuel alternatives to combustion engines. Vegetable oil is one of the renewable sources of energy that can be used. Vegetable oils also have the advantage of containing little to nitrogen. Radiated noise from diesel engines can be broken down into mechanical noise and combustion noise. The sound of combustion is distinguished into direct combustion noise and indirect combustion noise. The purpose of this researched is to know the effect of the chemical composition of variated pure vegetable oils to the noise generated in the combustion process. The study was conducted in an open tray which is heated by a heating element, which is filled with vegetable oil and then burned and given airflow variatiated velocity 39, 49 and 55 cm/s, the combustion is recorded using a softwere steinberg wavelab 6 (spectrum analyzer). Combustion of pure vegetable oil (jatropha curcas lin, ceiba petandra, catton seed, coconut) produced the highest noise level is on jatropha oil (-81 dB) followed ceiba petandra oil (-90 dB), catton oil seed oil (-99 dB) and Coconut oil (-108 dB). The study concluded that the content of unsaturated fatty acids one double bond (monounsaturated fatty acids) in the hydrocarbon chain thus facilitate reacted with oxygen and flammable.

Keywords: vegetable oil, saturated, noise, combustion, open tray

1. Introduction

The consumption of energy has ever increasing trend due to two reasons, mainly: (1) a change in the lifestyle and (2) the significant growth of population. Two of the main contributors are the transportation and the basic industry sectors. This increase of energy demand has been supplied using fossil resources (crude oil, natural gas and coal, principally), which have caused serious environmental impacts as global warming, acidification, deforestation, ozone depletion, eutrophication and photochemical smog, among others as demonstrated (Korbitz W, 1999). The world is facing two major problems, namely energy and environment. Another issue which is closely linked with the above is economy. So, energy, economy and environment are bonded by three dimensional relation-ships with bidirectional causal relationship among them as demonstrated (Omri,A.,2013). Ong,H.C et al. (2011) have recently shown the world energy consumption is likely to grow faster than the increase in the population. The Kyoto Protocol was a significant step for reduction of carbon dioxide and five other greenhouse gases as it set a legal binding on quantitative emanation for industrialized nations. It indirectly introduced the concept of ‘‘carbon neutral fuel’’. There are many emission standards, which focus on regulating pollutants released by automobiles and other powered vehicles, which generally specify certain limiting value of the emissions of nitrogen oxides (NOx), particulate matter (PM) or soot, carbon monoxide (CO), or volatile hydrocarbons. Traffic noise is the second environmental burden on health after air pollution according to the World Health Organization. These finite reserves are highly concentrated in certain regions of the world. Therefore, those countries not having these resources are facing energy/foreign exchange crisis, mainly due to the import of crude petroleum. Hence, it is necessary to look for alternative fuels which can be produced from resources available locally within the country such as alcohol, biodiesel, vegetable oils etc. as demonstrated (Agarwal AK., 2007).

Noise emissions are a major concern for both aircraft and engine manufacturers. This is mainly caused by increasing restrictions and regulations regarding the global noise generated by aircraft during take-off and landing. At the same time, aircraft operators are concerned with passenger comfort and therefore demand a quieter cabin. Noise has become another pollutant source due to engines and airframe, which must be controlled both outside

and inside aircraft and helicopters. For these reasons, the reduction of acoustic emissions is now a major field of research both for industry and research groups. There are various studies to clarify the mechanism of noise and vibration in diesel engines and classified various sources and their contribution to the total engine noise. Pruvost L et.al. (2009), Tousignant T et.al. (2009), Redel-Macı ´as MD et.al. (2012) have recently shown internal combustion engine radiated noise can be divided into mechanical noise, combustion noise and noise resulting from the accessories. Furthermore, combustion-related noise is divided into direct and indirect combustion noise as well as flow noise. The combustion noise is purely a load dependent phenomenon. Russell MF et.al. (1985), Rust A and Pflueger M (2000), Albarbar A et.al. (2010) have recently shown the conventional combustion process in diesel engines is considered as the most important source of noise. Payri F et.al. (2002) have recently shown efforts are mainly concentrated on the overall level reduction of the combustion noise and improvement of sound quality, mainly oriented to customer satisfaction. Generally, the radiated noise from diesel engines can be broken down into mechanical noise and combustion noise, as shown in Fig. 1. Pruvost L et.al. (2009), Tousignant T et.al. (2009) have recently shown combustion noise is separated into direct combustion noise (directly proportional to the combustion gas pressure) and indirect combustion noise. When combustion takes place, a sudden pressure rise is produced causing the vibration of the engine block, which in turn radiates air-borne noise. The block vibration is caused by pressure forces exerted directly by the gas and the mechanical forces associated with piston slap, bearing clearances and friction. Redel-Macı ´as MD et.al. (2012) have recently shown a combined analysis of exhaust and noise emissions of an three-cylinder direct injection diesel engine running on palm oil methyl esters (PME) and olive pomace oil methyl esters (OPME), both blended with diesel fuel in different proportions, is proposed to evaluate their suitability as partial substitute to fossil fuels. A strong correlation the saturation degree of the raw materials used to produce biodiesel seems to have a positive influence over air and noise emissions was found.

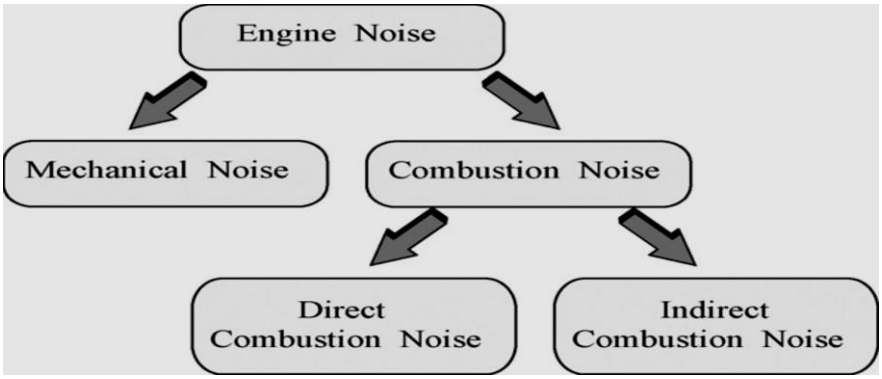

Fig. 1: Engine noise contributions

In this paper, to evaluate the effect of saturated fatty acids and unsaturated fatty acids degree of pure vegetable oils, an analysis of noise emissions of a combustion open tray fueled with jatropha curcas oil, ceiba petandra oil, catton seed oil and coconut oil is proposed.

2. Experimental procedure

2.1 Experimental set up

The experiments were conducted using the experimental Equipment shown schematically in Figure 2. A blower to exhale the air velocity is placed parallel with a stainless steel tray 184 x 25 x 15 mm (LxWxH) pure vegetable oil filled above the heated tray of combustion with heating element, with the highness of oil above the tray is 14 mm. Softwere steinberg wavelab 6 associated with microphone placed on the tray is burning drained by blowing air from the blower

2.2 Measuring technique

Pure vegetable oil was heated using a tray above the heating element until it evaporated and then switched thus formed the flame. At the time of the flame formed heating element is switched off then followed with a switch on the blower with the velocity of air flow being varied in varied amount 39, 49, and 55 cm/s. The sound waves from burning flames recorded microphone connected to softwere steinberg wavelab 6 over 100 seconds, these steps are performed until the until the flame is extinguished. The recordings of sound waves of flame be cut by

using a photo software free video to jpg converter. Photos of the results of free video to jpg converter in the form of an image spectrum analyzer.

2.3 Fuel in test

The types of pure vegetable oils to be tested include jatropha curcas lin oil, ceiba petandra, cotton seed oil and coconut oil. All vegetable oils that are obtained as a result of oil presses from the seeds that are available commercially. Physical properties of pure vegetable oils are presented in Table 1.

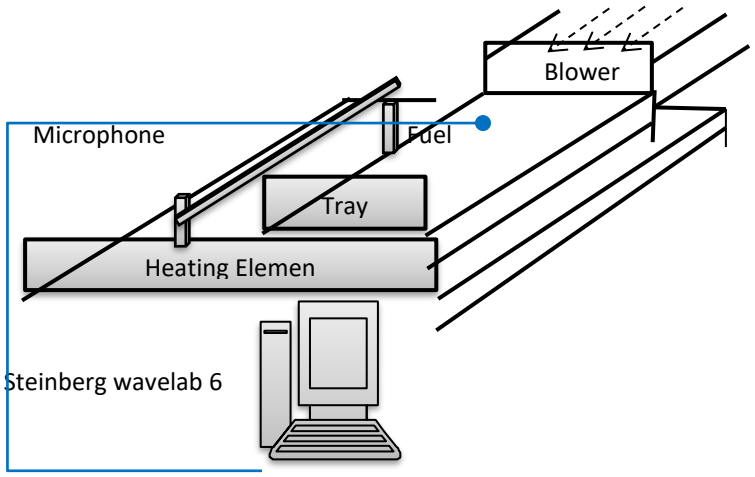

Fig. 2: Equipment used for the experiments.

Tabel 1: Physical properties of pure vegetable oils

Property	ASTM methode	Instrument	Model	Value				
				Ceiba petandra oil	Jatropha curcas lin oil	Catton seed oil	Coconut oil	Palm kernel oil
Density at 40^{0}C (kg/m^3)	D1298	Hydrometer	Nikky, Japan	974	921	955	936	940
Kinematic vizcosity at 40^{0}C (cSt)	D445	Kinematic viscometer	Leybold Didactic, Germany	45,55	35,48	41,65	55,55	52,65
Flash point (^{0}C)	D93	Pensky-Martens closed cup tester	Leybold Didactic, Germany	260	240	250	265	270
pH	D6423	pHep tester	UAS HANNA Instrument UAS	5,0	4,5	4,0	6,0	6,0

Tabel 2: The chemical composition of pure vegetable oil fatty acids

Pure Vegetable oil	Fatty acid									
	Saturated fatty acid						Unsaturated fatty acid			
	C6:0 - C10:0	C12:0	C14:0	C16:0	C18:0	C20:0	C18:2	C18:3	C16:1	C18:1
		Laurat	Miristat	Palmitat	Stearat	Arachidat	Linoleat	Linolenat	Palmitoleat	Oleat
Coconut oil	10,123	46,256	20,508	10,706	3,711	0,051	0,060	0,107	0,018	8,413
Catton seed oil	-	-	1,4	24,70	2,60	1,30	51,10	0,70	0,60	17,60
Ceiba petandra oil	-	-	0,25	16,10	3,55	0,10	56,22	1,00	0,40	21,88
Jatropha curcas lin oil	-	-	0,05	14,0	3,70	0,05	37,55	0,30	0,10	44,05

3. Result and discussion

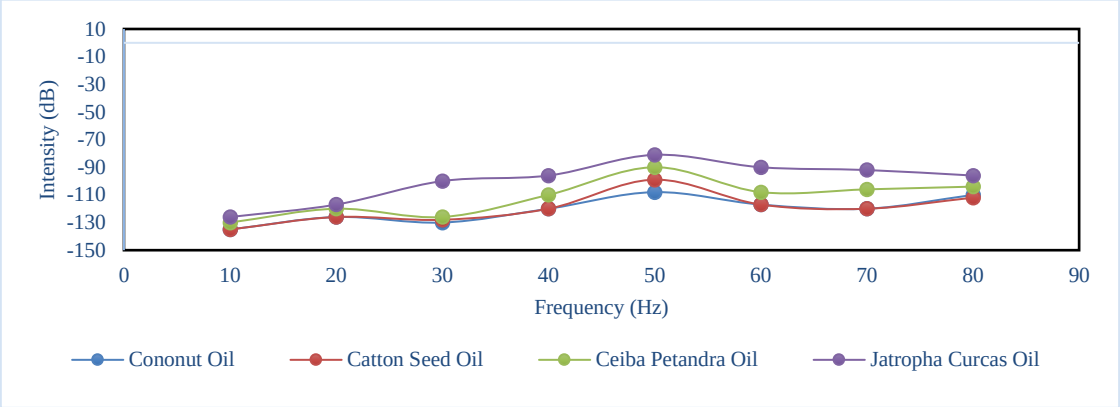

Fig. 3: Spectrum analyzer pure vegetable oil (v = 39 cm/s)

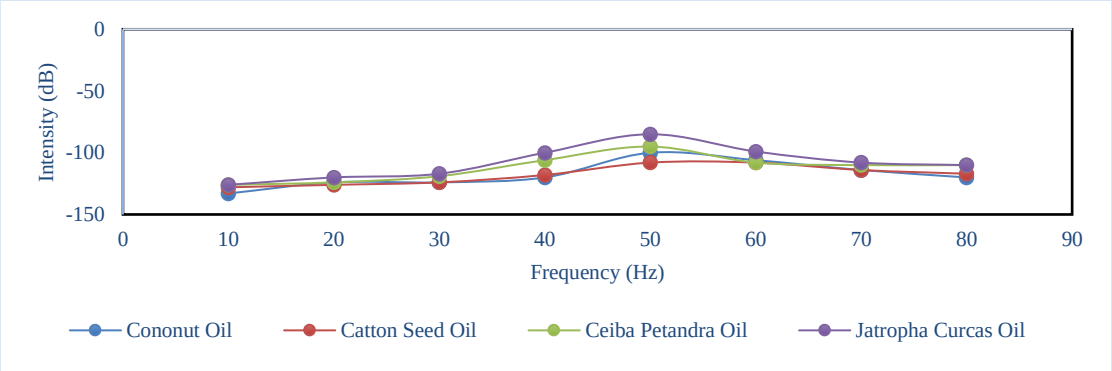

Fig. 4: Spectrum analyzer pure vegetable oil (v = 49 cm/s)

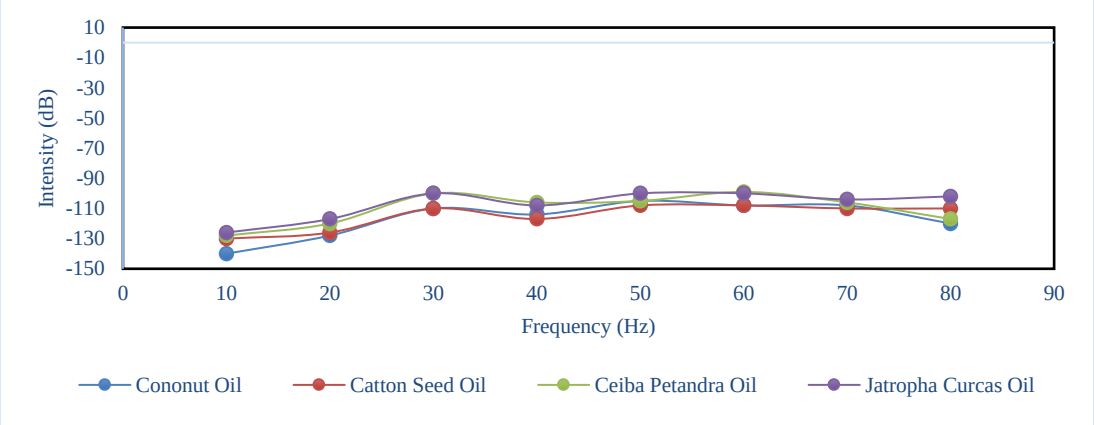

Fig. 5: Spectrum analyzer pure vegetable oil (v = 55 cm/s)

Figs 3-5 showed the spectrum analyzer of combustion of pure jatropha curcas lin oil, ceiba petandra oil, catton seed oil and coconut oil with the speed of air flow being varied in varied amount 39, 49, and 55 cm/s. Each combustion process of into four pure vegetable oil had different characteristic spectrum analyzer with air generated from the blower velocity varied. Figs 3 (39 cm/s) showed the noise that occurs on the jatropha curcas lin oil range -80 dB at frequency range of 50 Hz, as well as in figs 4 (49 cm / s) noise occurred at 50 Hz with range of -85 dB as well as on the figs 5 (55 cm/s) that is equal to -100 dB. This was due to the fact that pure jatropha curcas lin oil consisted of trglyceride molecules containing glycerol with three carbon chains and three fatty acid branches. Whereas, saturated fatty acid (table 2) contains single bond on its hydrocarbon chains enabling them to bind. As a result, the tensile strength of vander waals among its molecules became very strong. There fore more energy was needed to separates its molecules. When the oil was heated, three reactions were occur. The first reaction was the hydrolysis of trglyceride molecules to be fatty acid and glycerol by the water cointained in the oil. The second reaction was the combustion of unsaturated fatty acid (table 2) due to its lower flash point (table 1). At hight temperature, unsaturated fatty acid was highly flammable due to its volatile and highly reactive characteristic. In addition it has faster. It was also highly flammable when heated.

4. Conclusions

The experiment findings on the combustion of pure jatropha curcas lin oil, ceiba petandra oil, catton seed oil and coconut oil which were recorded by wavelab 6 (spectrum analyzer) can be conclude as follows:

The combustion of pure jatropha curcas lin oil, ceiba petandra oil, catton seed oil and coconut oil occurred noise pollution is highest in jatropha curcas lin oil followed by ceiba petandra oil, catton seed oil and coconut oil with each noise value of -81 dB, -90 dB, -99 dB and -108 dB. Due to the combustion of unsaturated fatty acid, its lower flash point, unsaturated fatty acid was highly flammable, its volatile and highly reactive.

5. Nomenclature

L	length	cm
W	width	cm
H	high	cm
V	velocity	cm/s
I	intencity	dB
F	frequency	Hz
T	temperature	^{0}C
Greek letters		
ρ	density	kg/m^3
U	Kinematic viscosity	cSt

6. Acknowledgements

Authors are thankful to Maarif Hasyim Latif University (UMAHA), Sidoarjo, East Java, Indonesia for granting funds for carrying out the research work for ermitting to carry out extensive trials in the combustion laboratory.

7. References

Agarwal AK (2007). Biofuels (alcohols and biodiesel) applications as fuels for internal Combustion engines. Progress in Energy and Combustion 33, 233–71.

Albarbar A, Gu F, Ball AD (2010). Diesel engine fuel injection monitoring using acoustic measurements and independent component analysis. Measurement 43, 1376–86.

Korbitz W (1999). Biodiesel production in Europe and North America, an encouraging prospect. Renewable Energy 16, 1078–83

Omri,A (2013). CO_2 Emissions, Energy Consumption and Economic Growth Nexus in MENA Countries: Evidence from Simultaneous Equations Models.Energy Economics 40, 657-664.

Ong,H.C.,Mahlia,T.M.I. and Masjuki,H.H.(2011). A Review on Energy Scenario and Sustainable Energy in Malaysia.Renewable and Sustainable Energy Reviews 15, 639-647.

Payri F, Torregrosa AJ, Broatch A, Marant V, Beauge Y (2002). Methodologie d'etude de la qualite du bruit de combustion d'un moteur Diesel automobile a partir de l'analyse de sa pression en cylindre. Acoustics and Technology 30, 25–9

Pruvost L, Leclere Q, Parizet E (2009). Diesel engine combustion and mechanical noise separation using an improved spectrofilter. Mechanical Systems and Signal Processing 23, 2072–87.

Redel-Macı ´as MD, Pinzi S, Ruz MF, Cubero-Atienza AJ, Dorado MP (2012). Biodiesel from saturated and monounsaturated fatty acid methyl esters and their influence over noise and air pollution. Fuel 97, 751–6.

Russell MF, Haworth R (1985). Combustion noise from high speed direct injection Diesel engines. SAE technical paper 850973.

Rust A, Pflueger M (2000). Future demands for Diesel engine acoustics. Proc Int SIA Congress ''What challenges for the Diesel engine of the year 2000 and beyond'' Lyon, France.

Tousignant T, Wellmann T, Govindswamy K (2009). Application of combustion sound level (CSL) analysis for powertrain NVH development and benchmarking. SAE technical paper 01-2168.

ISBN 978-602-53531-8-5

B. From laboratory to the real world renewable energy system

Proceedings of the 1st Faculty of Industrial Technology International Congress
International Conference
Bandung, Indonesia, October 9-11, 2017
ISBN 978-602-53531-8-5

Experimental investigation on combustion and emission of CI engine fueled with gasoline-biodiesel blends in early injection HCCI mode

Yanuandri Putrasari [1,2] and Ocktaeck Lim [3,*]

[1] Graduate School of Mechanical Engineering, University of Ulsan, Ulsan, 44610, South Korea

[2] Research Centre for Electrical Power and Mechatronics-Indonesian Institute of Sciences, Jl. Cisitu 154D/21, Bandung 40135, Indonesia

[3] School of Mechanical Engineering, University of Ulsan, 44610, South Korea

[*] Corresponding author e-mail: otlim@ulsan.ac.kr

Abstract

The experimental investigation of combustion and emission of CI engines fueled with gasoline and biodiesel blends was conducted in this study. The study was conducted using a single-cylinder direct-injection diesel engine fueled with 5% biodiesel proportion in gasoline fuel blends compared with 100% neat diesel fuel. A HCCI with early direct injection was applied in this study. Some initial control parameters such as intake temperature, EGR rate and intake pressure were also adjusted to investigate their influences on combustion and emissions of this CI engine. It is found that gasoline-biodiesel blends with HCCI combustion mode and initial engine parameters especially intake boosting rate takes effect on the improvement of combustion characteristics which is closely tied to HC, CO and NOx emissions, respectively.

Keywords: HCCI, Emission, Gasoline, Biodiesel, EGR

1. Introduction

Compression ignition (CI) engines have higher thermal efficiency compared to SI engines. One of the advantages of CI engines over SI engines is that CI engine do not suffer from knocking at high loads. Therefore, CI engines can have higher ratios compared to spark ignition (SI) engine. In CI engines only air is compressed, rather than a mixture of fuel and air, which brings the performance closer to the ideal cycle efficiency. However, CI engines fueled with diesel engine usually produce high emissions, especially nitrogen oxide (NOx) and soot/smoke/particulate matter, which are difficult to control through subsequent treatments.

The higher interest on CI engines than SI engines due to its higher efficiency lead to the unbalance supply and demand between diesel and gasoline fuel in several countries. Furthermore, the more strict limitations of vehicle emission regulation especially for CI engines with diesel fuel stimulate many researchers to explore the utilization of low volatile fuels, such as gasoline and alternative biofuels for CI engines which can obtain high efficiency, but produce lower emissions or so called low temperature combustion (LTC).

Recently, several studies have shown that gasoline and some other fuels with low cetane number and higher volatility are potentially advantages for low temperature combustion(Kalghatgi 2014)(Kalghatgi et al. 2006). Blending gasoline fuel with certain percent of biodiesel is the one way to obtain the good combustion and emissions results. Biodiesel, which is made from various renewable resources, is known to be very suitable as a sustainable alternative fuel for CI engines(Bae & Kim 2017)(Tesfa et al. 2013). Furthermore, biodiesel has proven to have high advantages in reducing engine soot emissions(Cordiner et al. 2016)(Rakopoulos et al. 2008), because the presence of oxygen in the biodiesel plays a significant role in reducing soot formation during combustion(Wang et al. 2016).

Previous studies have presented detailed analysis and discussion of the combustion and emission characteristics fueled with gasoline biodiesel blends using direct injection gasoline compression ignition (GCI) concept(Putrasari & Lim 2017)(Adams et al. 2013). However, the combustion and emission characteristics of CI engines are also influenced by various other factors, such as fuel injection strategy and its combustion modes. The HCCI engine

mode is promising method to obtain an appropriate technology with its own characteristics of the low emissions of the SI engine and the high efficiency of the CI engine (Yao et al. 2009). The HCCI engine is one of methods that potentially to achieve an advanced LTC, which possible to produce low particulate matter (PM) and nitrogen oxides (NOx) emissions to replace conventional diesel engine combustion(Krishnan et al. 2016).

The objective of this study was to determine the effects of early injection HCCI mode on the combustion and emissions of a CI engine fueled with gasoline-biodiesel blends. The analysis of the combustion characteristics of cylinder pressure and emission characteristics are discussed in this study.

2. Methodology

A single-cylinder, water-cooled, naturally aspirated, 4-stroke diesel engine with 498 cm^3 of displacement and 4-valve SOHC was used to carry out the engine tests. The engine specification data is given in Table 1. The engine was coupled with a 57 kW Dynamometer Elin AVL Puma engine test system (MCA325MO2. An Autonics E40S8-1800-3-T-24 encoder and Kistler 6056A pressure transducer combined with a Kistler 5018 amplifier were installed on the engine and connected to a Dewetron DEWE-800-CA combustion analyzer. A Bosch 7-hole injector was used to deliver the fuel into the engine combustion chamber. The injector was controlled using a Zenobalti multi-stage injection engine controller (ZB-8035) combined with a common rail solenoid injector peak and hold driver (ZB-5100) and encoder interfacing box (ZB-100) to adjust the injection timing and duration. A schematic diagram of the test engine and measurement setup is presented in Figure 1.

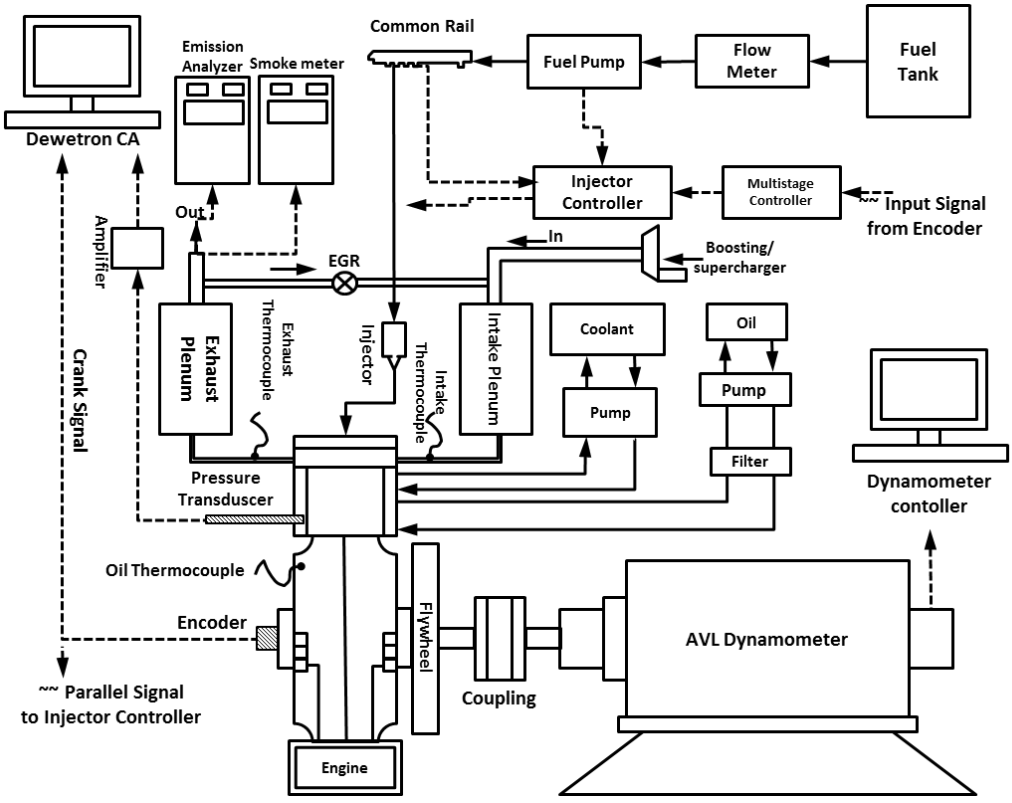

Fig. 1: Schematic diagram of test engine

The fuels utilized in this study were commercial gasoline (GB00) and diesel (D100) and pure soya bean biodiesel (B100). Biodiesel and gasoline were then mixed to make a gasoline-biodiesel blend. The concentration of biodiesel in the blend was 5% by volume, and the blend was referred to as GB05. The gasoline-biodiesel blend was prepared through a mixing/shaking process for approximately 2 to 10 minutes to obtain homogeneity. The fuel blending process in this study was performed immediately before the experiment was conducted to minimize the fuel separation stratification phenomenon. The physical properties of gasoline, diesel, biodiesel, and GB05 from laboratory tests based on international standards are presented in Table 2[30].

Table 1: Engine specification

Engine Parameters	Value
Displacement	498 cm3
Bore	83 mm
Stroke	92 mm
Compression Ratio	19.5
Con. Rod Length	145.8 mm
Crank Radius	43.74 mm
Valve System	SOHC 4 valve
Fuel System	Electronic Common Rail

Table 2: Physical properties of fuels

Test item	Unit	Test method	Gasoline	GB05	B100	Diesel
Heating value	MJ/kg	ASTM D240:2009	45.86	45.32	39.79	45.93
Kinematic Viscosity (40 °C)	mm^2/s	ISO 3104:2008	0.735	-	4.229	2.798
Lubricity	mm	ISO 12156-1:2012	548	290	189	238
Cloud Point	°C	ISO 3015:2008	-57	-37	3	-5
Pour Point	°C	ASTM D6749:2002	-57	-57	1	-9
Density (15 °C)	kg/m^3	ISO 12185:2003	712.7	722.3	882.3	826.3

The engine was operated at 1200 rpm, with an injection pressure of 70 MPa and multiple injections, comprised of the pilot injection at 100 °C A BTDC for approximately 500 μs, followed by the main injection at 20 °C A BTDC for approximately 500 μs. The initial parameters of intake temperature, oil temperature, and coolant temperature were maintained at 85 °C, 75 °C, and 65 °C, respectively. Hot EGR was applied in this study from 0% to 50% of flow rate. Boosting pressure 0.1 MPa and 0.12 MPa were also applied in the intake manifold. The engine operating parameters and injection strategies are presented in Table 3. The in-cylinder pressure data was recorded for 100 engine cycles. The emissions of unburned total hydrocarbon, carbon monoxide, and NOx were measured using a Horiba MEXA-7100DEGR.

Table 3: Engine operating parameters

Operating Parameters	D100	GB05
Speed (rpm)	1200	1200
Inj. Pressure (MPa)	70	70
Inj. Timing (°CA BTDC)	110 and 40	110 and 40
Inj. Duration (μs)	500 and 500	500 and 500
Total Inj. Quantity (mg)	10.28	14.72
T in (°C)	85	85
T oil (°C)	75	75
T coolant (°C)	65	65
EGR (%)	0, 20 and 50	0, 20 and 50
Intake pressure (MPa)	0.1 and 0.12	0.1 and 0.12

3. Results and discussion

In this study, some parameters are kept constant. The engine speed is 1200rpm and the compression ratio is 19.5. The inlet air temperature, oil temperature and coolant temperature were kept at 85 ºC, 75 ºC and 65 ºC, respectively. Pilot injection timing was set at 110 ºCA with 500 µs duration and main injection at 20 ºCA with same duration 500 µs. Variable parameters are D100 and GB05, EGR rate and boosting pressures. Commonly these variable parameters affect to the combustion and emission of HCCI engines.

a. Effects of fuels properties on engine combustion and emissions

Figure 2 shows the in-cylinder pressure of HCCI engine fueled with D100 and GB05. The same injection timing and duration between D100 and GB05 not guaranteed that the injection amount of fuel will be the same. The injection amount of D100 is 10.28 mg/cycle and GB05 is 14.72 mg/cycle. The higher injection amount of GB05 due to the lower density approximately 722.3 kg/m^3 compared to D100 approximately 826.3 kg/m^3. The higher amount of injected fuel leads to the higher in-cylinder pressure caused by the nearly similar value of heating value (LHV) of D100 and GB05 approximately 45 MJ/kg.

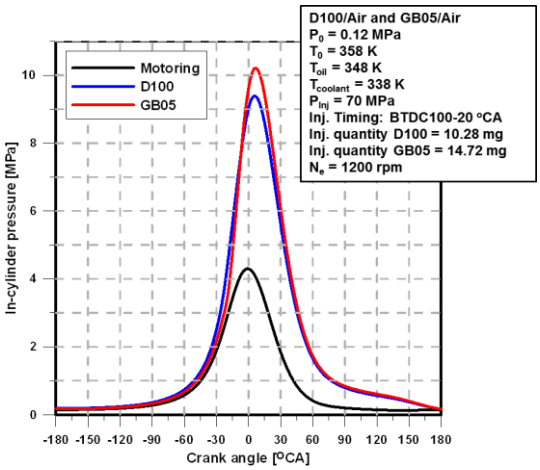

Fig. 2: Effects of fuel properties on in-cylinder pressure of HCCI engine

Figure 3 shows the THC, CO and NOx emissions of HCCI engine fueled with D100 and GB05. Meanwhile, Figure 4 shows the smoke emission of HCCI engine fueled with D100 and GB05. The lower density of GB05 leads to the higher amount of injected fuel then finally the higher emissions of THC, CO, NOx and smoke. The THC and CO emission is related to the quality of combustion inside the chamber. The higher THC and CO emission indicated the higher inefficiency of combustion. The NOx emission is related to the temperature trace of combustion inside the chamber. The NOx emission will be higher when the in-cylinder temperature more than 1800 K. However, the oxygenated fuel such as biodiesel which is contained in GB05 usually produce higher NOx emission compared to the conventional fossil fuel. The trend of smoke emission normally, is contrary to NOx emission. When the NOx emission higher the smoke emission will be lower. However, as already mentioned that the containing of higher oxygen in the fuel lead to the higher NOx and the incomplete combustion lead to the higher smoke emission. The early pilot injection timing method expected to promote the homogeneity of mixing process the resulted the improvement of complete combustion of GB05. However, D100 indicated better combustion results by lower THC, CO and NOx even smoke emission.

b. Effects of EGR rate and GB05 on engine combustion and emissions

Figure 5 shows the in-cylinder pressure of HCCI engine fueled with GB05 running with various EGR rate from 0% to 50%. The EGR20 resulted highest in-cylinder pressure. The higher EGR rate for heavy EGR rate condition (50%) the engine is almost stall indicated by the lower in-cylinder pressure which is almost similar with motoring in-cylinder pressure trace. Figure 6 shows the effects of EGR rate and GB05 on THC, CO and NOx emissions of HCCI engine. Meanwhile, Figure 7 shows the effects of EGR rate and GB05 on smoke emissions of HCCI engine. The increasing of EGR rate does not effect to the amount of THC and CO emission. However, the higher EGR rate the lower NOx emission. Contrary, the higher EGR rate the higher smoke emission.

c. Effects of intake boosting rate and GB05 on engine combustion and emissions

Figure 8 shows the in-cylinder pressure of HCCI engine fueled with GB05 running with various intakes boosting rate. The intake boosting 0.12 MPa resulted higher in-cylinder pressure. The higher boosting rate leads to the higher in-cylinder pressure. Figure 9 shows the effects of boosting rate and GB05 on THC, CO and NOx emissions

of HCCI engine. Meanwhile, Figure 10 shows the effects of boosting rate and GB05 on smoke emissions of HCCI engine. The increasing of boosting rate does not effect to the amount of THC and CO emission. However, small amount of NOx reduction happened when the higher boosting rate was applied. The higher boosting rate also affected to the lower smoke emission.

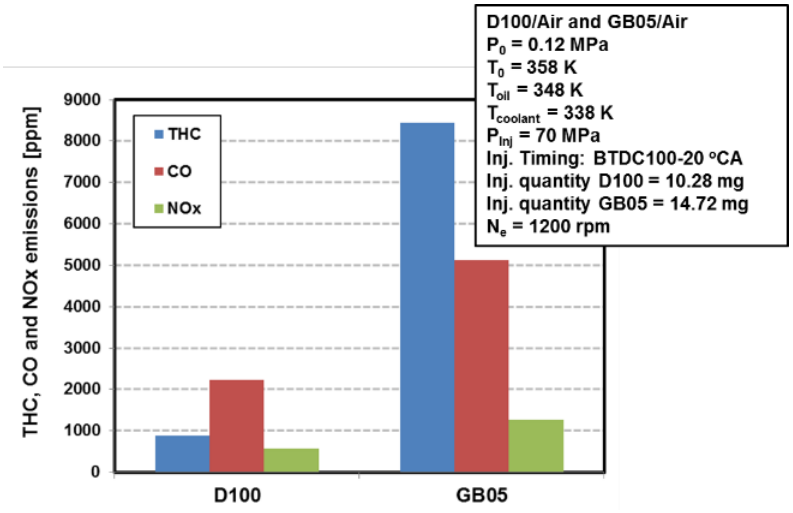

Fig. 3: Effects of fuel properties on THC, CO and NOx emissions of HCCI engine

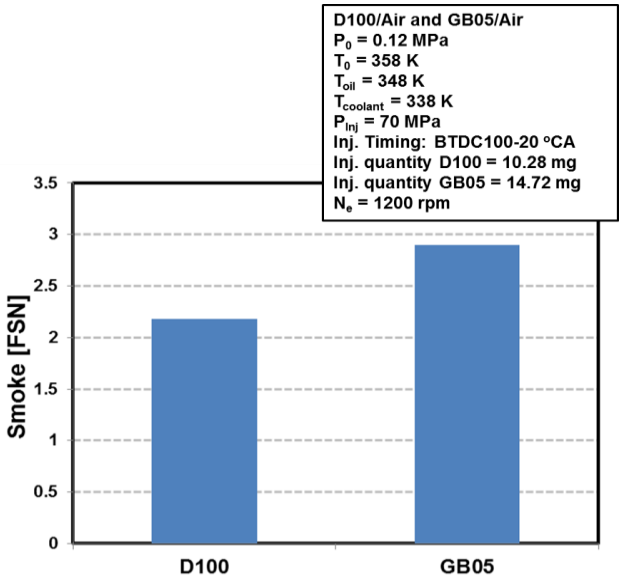

Fig. 4: Effects of fuel properties on smoke emissions of HCCI engine

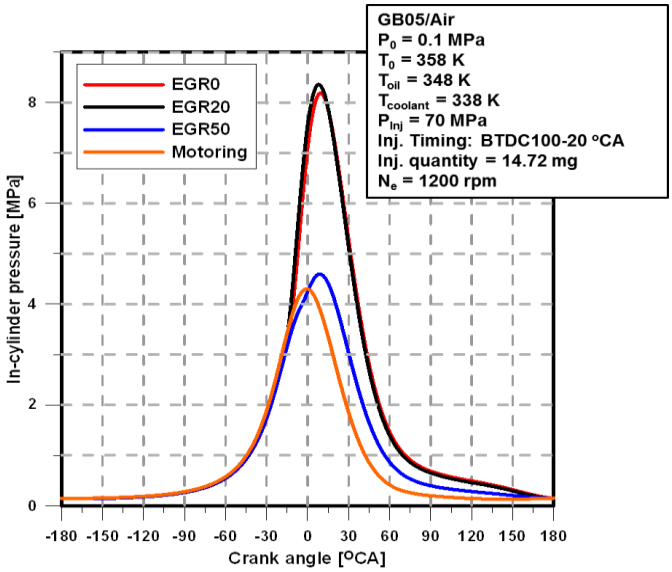

Fig. 5: In-cylinder pressure of GB05 HCCI engine running on various EGR rate

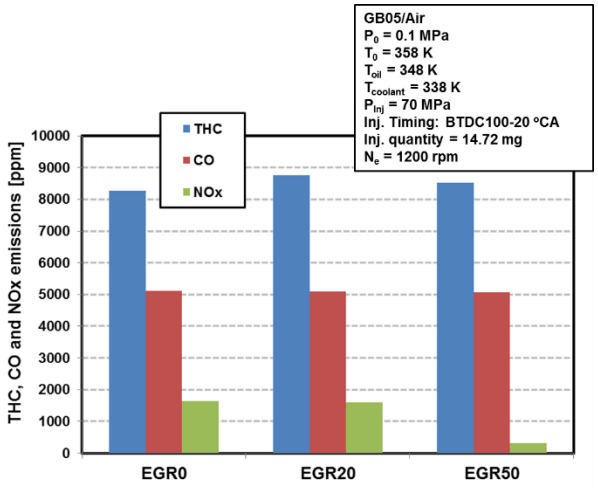

Fig. 6: Effects of EGR rate and GB05 on THC, CO and NOx emissions of HCCI engine

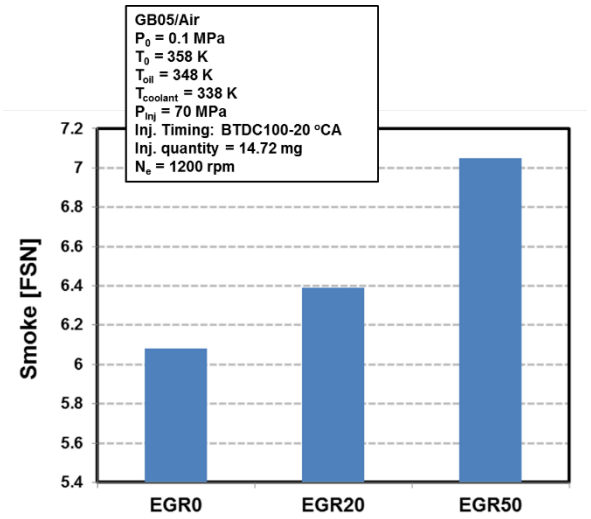

Fig. 7: Effects of EGR rate and GB05 on smoke emissions of HCCI engine

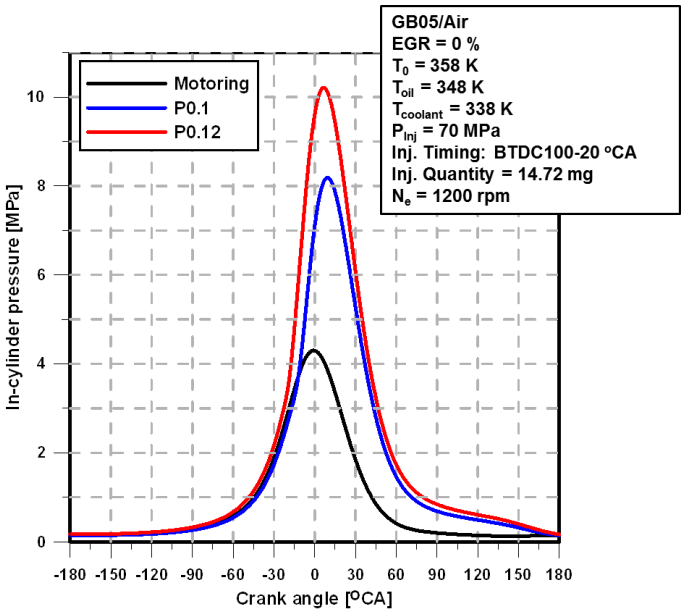

Fig. 8: In-cylinder pressure of GB05 HCCI engine running on various intakes boosting rate

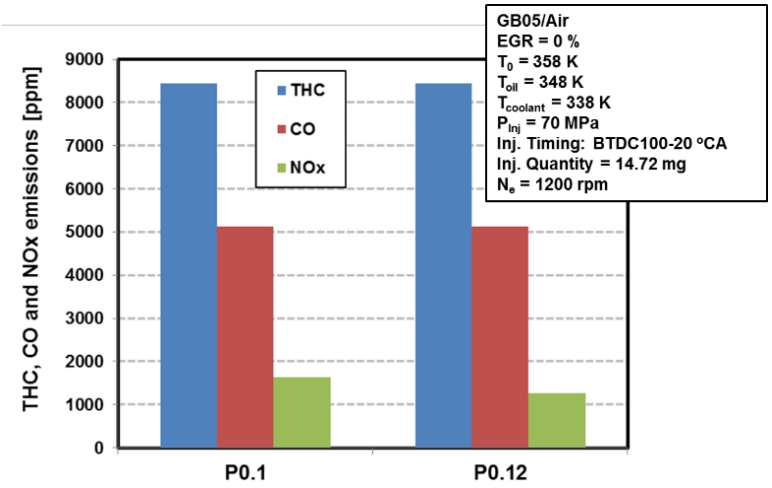

Fig. 9: Effects of intake boosting rate and GB05 on THC, CO and NOx emissions of HCCI engine

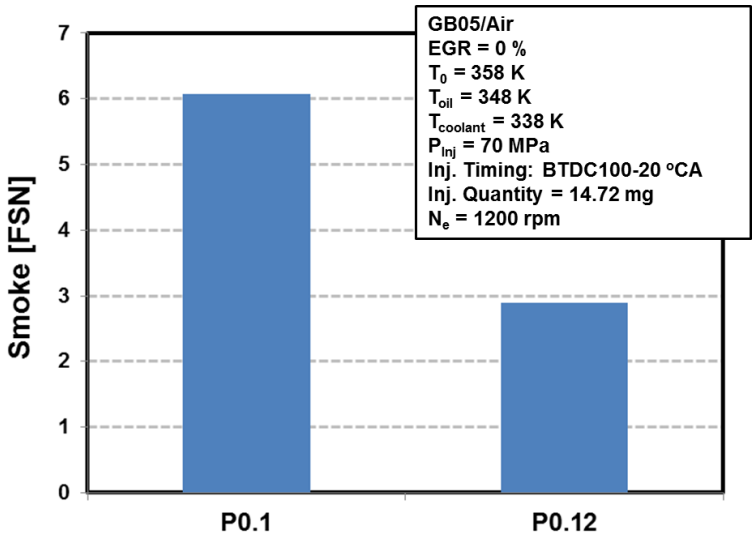

Fig. 10: Effects of intake boosting rate and GB05 on smoke emissions of HCCI engine

4. Conclusion

A study was conducted to investigate of combustion and emission of CI engines fueled with gasoline and biodiesel blends in early injection HCCI mode. Based on the results, the following general conclusions can be drawn:

- The GB05 has higher in-cylinder pressure due to the higher amount of injected fuel, which is nearly similar value of heating value (LHV) of GB05 and D100 approximately 45 MJ/kg. The trend of smoke emission normally, is contrary to NOx emission. When the NOx emission higher the smoke emission will be lower. However, as already mentioned that the containing of higher oxygen in the GB05 lead to the higher NOx and the incomplete combustion lead to the higher smoke emission.
- Heavy EGR rate condition (50%) the engine is almost stalling. The increasing of EGR rate does not effect to the amount of THC and CO emission. However, the higher EGR rate the lower NOx emission and higher smoke emission.
- Higher boosting rate leads to the higher in-cylinder pressure The increasing of boosting rate does not effect to the amount of THC and CO emission. However, small amount of NOx reduction happened when the higher boosting rate was applied. The higher boosting rate also affected to the lower smoke emission.

5. Nomenclature

B	Biodiesel
B100	100% biodiesel
BTDC	Before top dead center
CA	Crank angle

CI	Compression ignition
D100	100% diesel
EGR	Exhaust gas recirculation
G	Gasoline
GB	Gasoline-biodiesel
GB00	100% gasoline
GB05	Blend of 95% gasoline and 5% biodiesel
HCCI	Homogeneous charge compression ignition
LTC	Low temperature combustion
MPa	Mega Pascal
Ne	Engine speed
NOx	Nitrogen oxides
TDC	Top dead center
THC	Total hydrocarbons

6. Acknowledgements

This research was financially supported by CEFV (Centre for Environmentally Friendly Vehicle) as Global Top Project of KMOE (2016002070009, Development of Engine System and Adapting Vehicle for Model 110 cc and 300 cc Correspond to EURO-5 Emission). This research was supported by The Leading Human Resource Training Program of Regional Neo industry through the National Research Foundation of Korea (NRF) funded by The Ministry of Science, ICT and Future Planning (2016H1D5A1908826). This research was also supported by the Industrial Strategic technology development program (10053151, Development of the 800 kPa Fuel System of a High Pressure Precision Control for NGV) funded by the Ministry of Trade, Industry & Energy (MI, Korea).

7. References

Adams, C.A. et al., 2013. Effects of biodiesel-gasoline blends on gasoline direct-injection compression ignition (GCI) combustion. *Fuel*, 111, pp.784–790.

Bae, C. & Kim, J., 2017. Alternative fuels for internal combustion engines. *Proceedings of the Combustion Institute*, 36(3), pp.3389–3413. Available at: http://dx.doi.org/10.1016/j.proci.2016.09.009.

Cordiner, S. et al., 2016. Impact of biodiesel fuel on engine emissions and Aftertreatment System operation. *Applied Energy*, 164, pp.972–983. Available at: http://dx.doi.org/10.1016/j.apenergy.2015.07.001.

Kalghatgi, G.T., 2014. *Fuel/engine interactions*, Warrendale, Pennsylvania : SAE International.

Kalghatgi, G.T., Risberg, P. & Ångström, H., 2006. Advantages of Fuels with High Resistance to Auto-ignition in Late-injection, Low-temperature, Compression Ignition Combustion. *SAE Int.*, (724), p.SAE 2006-01-3385.

Krishnan, S.R., Srinivasan, K.K. & Raihan, M.S., 2016. The effect of injection parameters and boost pressure on diesel-propane dual fuel low temperature combustion in a single-cylinder research engine. *Fuel*, 184, pp.490–502. Available at: http://dx.doi.org/10.1016/j.fuel.2016.07.042.

Putrasari, Y. & Lim, O., 2017. A study on combustion and emission of GCI engines fueled with gasoline-biodiesel blends. *Fuel*, 189, pp.141–154. Available at: http://dx.doi.org/10.1016/j.fuel.2016.10.076.

Rakopoulos, C.D. et al., 2008. Performance and emissions of bus engine using blends of diesel fuel with bio-diesel of sunflower or cottonseed oils derived from Greek feedstock. *Fuel*, 87(2), pp.147–157.

Tesfa, B. et al., 2013. Combustion and performance characteristics of CI (compression ignition) engine running with biodiesel. *Energy*, 51, pp.101–115.

Wang, Z. et al., 2016. Effect of biodiesel saturation on soot formation in diesel engines. *Fuel*, 175, pp.240–248.

Yao, M., Zheng, Z. & Liu, H., 2009. Progress and recent trends in homogeneous charge compression ignition (HCCI) engines. *Progress in Energy and Combustion Science*, 35(5), pp.398–437.

Proceedings of the 1st Faculty of Industrial Technology International Congress
International Conference
Bandung, Indonesia, October 9-11, 2017
ISBN 978-602-53531-8-5

Stress and Displacement Analysis on Communal Horizontal Composter 40 Kg Capacity Using Solidwork

Noviyanti Nugraha*, M. Aziz Mahardika*, Alfie Juli Pratama
Department of Mechanical Engineering, Institut Teknologi Nasional (Itenas), Bandung - INDONESIA
* Corresponding author e-mail: noviyanti.nugraha.itenas@gmail.com; m.azis.mahardika@gmail.com

Abstract

Organic waste can be processed become the compost. One of the most important to support the composting process is the composter. It has been designed a 40kg communal horizontal composter machine used to accelerate the composting process. This machine is powered by an electric motor and spins horizontally. On the machine there is an agitator that serves to stir, mix, and flatten the waste. Agitators should be able to lift the load on the waste in the composting process. The maximum ability of the horizontal agitator in lifting the waste load cannot be seen visually, but it can be known by analysis using Solidwork. The purpose of this research is to analyze the stress and displacement that occurs in composer. There are two types of agitator, namely agitator horizontal which amounted to 3 pieces and agitator end of which given the corner of 30º which amounted to 6 pieces. Different types of agitators affect the function of each agitator, which is to flatten the stirring, and some are enabled to break up the waste blob. Analyzes were performed at various position positions i.e. 0º, 45º, 90º, 135º and 180º. The analysis is performed on static state. The result shows that the maximum stress of the agitator at the position of 180˚ is 65N/mm², and the maximum displacement is 0.9mm for the angular position 180˚. While the results of agitator analysis that has a position of 30º, maximum stress of 47 N/mm² and maximum displacement of 0.7 mm. The results of the analysis show that the stress that occurs is still below the allowable stress of 344.7 N/mm².

Keywords: stress analysis, composter machine, agitator, Solidwork, organic waste

1. Introduction

Organic waste can cause environmental pollution and disease sources. One of the efforts of organic waste processing is by processing it into a compost fertilizer. Basically compost raw materials can be obtained from all organic materials in nature such as leaves, agricultural waste, household organic waste, animal waste, etc. [Tahir, 2008]

Processing of organic waste in Indonesia is commonly done in rural areas, by making a hole in a piece of land. Waste treatment by throwing the waste into the hole and left to rot along with time. The disadvantage of this method when applied in urban areas is the cost of making a relatively expensive soil hole and view of waste that is not good to see, and the compost produced takes a long time. To overcome the problem is needed composter in organic waste processing.

Composting is a process in which organic substances are reduced from large volumes of rapidly decomposable materials to small volumes of materials which continue to decompose slowly. In this process, the ratio of carbon to other elements is brought into balance, thus avoiding temporary immobilization of nutrients. One of the many benefits of adding compost to the soil is that the nutrients in it are slowly released to the soil and are then available for use by plants. [Robert D. Raabe]

Composting is the controlled aerobic biological decomposition of organic matter into stable, humus like product called compost. It is essentially the same process as natural decomposition except that it is enhanced and accelerated by mixing organic waste with other ingredients to optimize microbial growth [Robert E. Graves, 2000]

Composter is one of determinant factor in composting process and compost quality. Composter is designed with attention to perfect aeration system by considering the sufficiency of air circulation to supply oxygen demand for microorganisms in the process of decomposition of compostable organic material. [Mudiatun, 2008]

Composter communal household is a composter to process kitchen waste into compost. Based on the capacity of the composter is divided into two types, namely individual composter and communal composter. Individual composter is a composter for one family head. Communal composter for some families.

In previous research has designed a rotary type communal composter machine. In addition to functioning to overcome the problem of organic waste, this composter helps the composting process becomes faster. Composter can be moved rotary with the agitator on the inside of the composter. Agitators work to stir, mix, and flatten waste with activators to shorten the composting process.

The schematic drawings and components of the designed communal composter are shown in Figure 1 and 2 below.

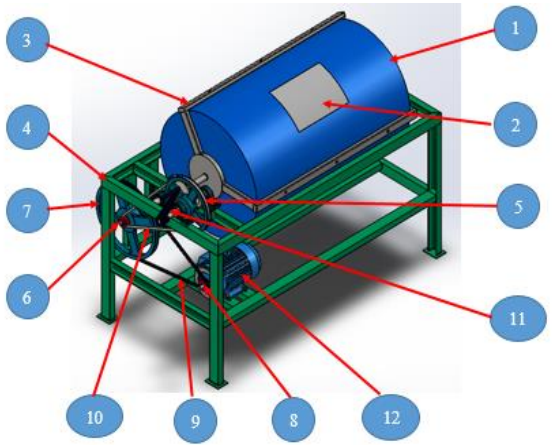

Fig. 1: outer component and communal composter scheme

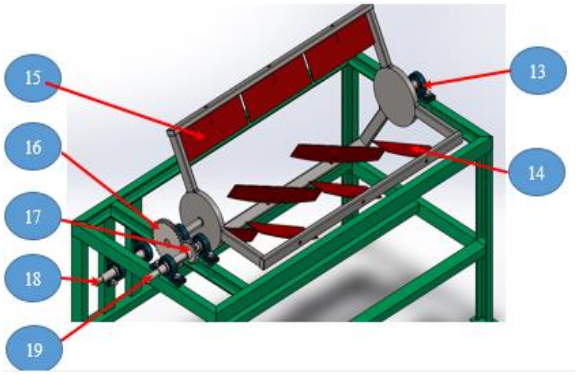

Fig. 2: Internal communal composter scheme

The name and function of the composter component, shown in table 1

Table 1. Composter machine components

No	Component name	Keterangan
1	HDPE Drum	to accommodate organic waste to be processed
2	Drum door	to cover the drum so that the waste inside does not spill during stirring. as a hole for waste and composting
3	Drum holder frame	As a drum support
4	Main Frame	As a support / holder of all machine components
5	*Driven pulley R1*	Pulley is driven at the first reduction to drive the gear, with a size of 10 inc
6	*Driver pulley R2*	Pulley that drives the pulley at the first reduction, with a size of 2 inches
7	*Driven pulley R1*	Pulley is driven at the second reduction to drive the first reduction, with a size of 14 inches

8	*Driver pulley R2*	Pulley that drives the pulley on the second reduction and attaches to the motor, with a size of 2 inches
9	Belt R2	Belt used for the second reduction, with size No.65 type A
10	Belt R1	Belt used for first reduction, with size No. 57 type A
11	Crank	To ratate drums manually
12	Electric Motor	As a driving force to rotate drums with electric automatically
13	*Pillow block*	As a bearing a component in the form of rotary axis
14	Agitator 30^o	Agitator with a 30^o slope to the agitator holder frame
15	Agitator horizontal	Agitator
16	*Driven gear*	The reduction which is output with Module 4, z (36)
17	*Driver gear*	The reduction which is the input with Module 4, z (18)
18	Poros *gear*	Axis that serves as the successor style of the motor or hand to the gears
19	Poros *pulley*	A shaft that serves as a holder of a pulley

Agitators should be able to lift the load on the waste in the composting process. The maximum ability of the horizontal agitator in lifting the waste load can not be seen visually, but it can be known by the analysis using Solidwork.
The purpose of this research is to analyze the loading of rotary horizontal communal composter machine using Solidworks.

2. Methodology

The stirring process is horizontally spaced with a drum spin inside which there is an agitator as the main component of stirring. The agitator attaches itself to a certain slope of the drum. There are two types of agitators, horizontal agitator and agitator whose end is formed angle 30^o. In determining the angle, through the simulation process. Figure 3 shows an agitators mounted on the frame

Fig. 3: shows an agitators mounted on the frame

Assuming one agitator line sustains a maximum load of 200N or 1/2 maximum load of waste, in one line has 3 agitators, then the working force is 33.3 N. The 3 horizontal agitators are mounted on one side of the agitator frame. Installed in series. The horizontal agitator dimensions are as follows; length of agitator (l) = 296 mm, width of agitator (b) = 100 mm, thickness of agitator (h) = 2 mm, cross section, A_h = 0.0296 m^2, material used is AISI 1030 with σ_y = 34.5 kg /mm^2. As for the agitator which has its 30^o dimension is as follows; length of agitator (b) = 330 mm, agitator thickness (b) = 100 mm, radius agitator (r) = 690 mm, min width of agitator (b2) = 75 mm, slope = 30^o from right side and left side, cross section area A_{30} = 0.029904 m^2. Working force F = 66.67 N, Number of 6 pieces agitator, paired on two sides of the agitator frame, each side mounted 3 pieces in series. The material used is AISI 1030 with σ_y = 34.5 kg / mm^2. The horizontal agitator and agitator 30^o, schematic drawing is shown in Figure 4a and 4b below.

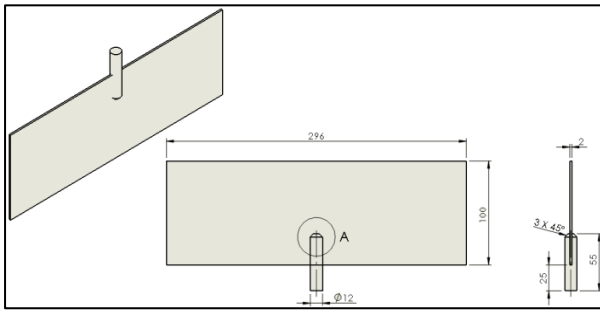

Fig. 4a: Horizontal Agitator Scheme

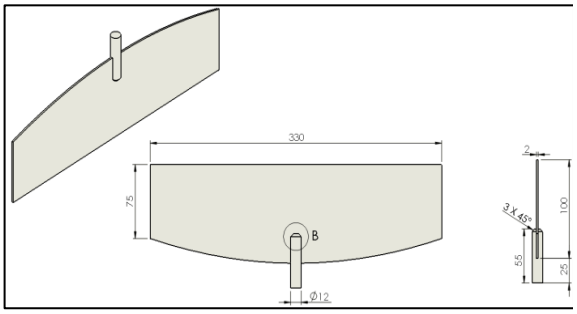

Fig. 4b: Agitator 30º Scheme

Before performing the load analysis using Solidwork, please note the loads that occur on the compound in the analysis by using the Load Free Diagram (DBB). The load given to the agitator is a distributed load, while on the agitator handle to the agitator frame, is a centralized load. Figure 5 shows the DBB on the horizontal agitator, the 30 ag agitator, and the agitator frame.

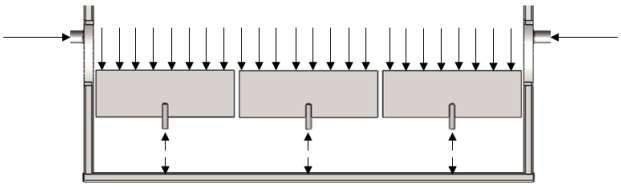

Fig. 5: DBB on the horizontal agitator, the 30 ag agitator, and the agitator frame.

In this study the analysis is only done on the agitator only, while the analysis on the framework agitator will be done in subsequent research. The analysis is performed on static state, for some position of agitator on drum. The position 0˚ is the starting position for stirring where the agitator has not received the load from the waste because the waste is still under the agitator. The 45˚ position is a stirring position with a slope of 45˚ The 90˚ position is the position when the load is above the agitator with a small cross-sectional area. The 135˚ position is positioned with the same load as in position 45˚. The position 180˚ is the position when lifting the load, the position with the largest loading compared to other positions. The agitator position scheme is shown in Figure 6.

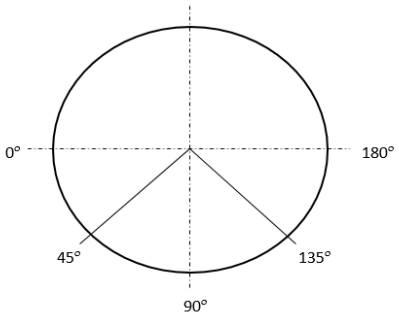

Fig. 6: Load position on agitator

In this publication only an example of analysis is shown in position 180o. The analysis on the other positions is the same as the example in position 180º with the force and load it in adjust. This position is the position when lifting the waste / load in which the position of the agitator is straight and the load from the waste is 66.67 N, as illustrated in figure 7.

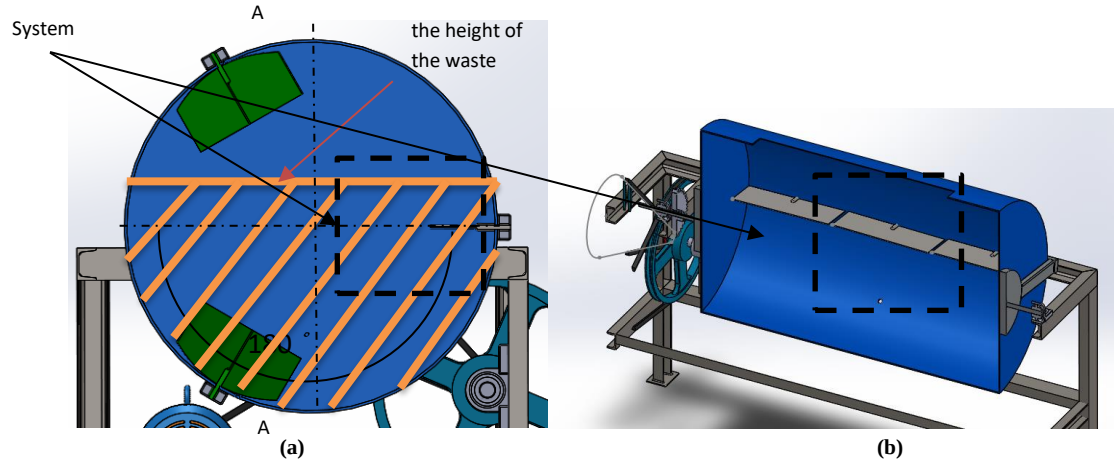

Fig. 7: horizontal agitator at position 180º (a) front view (b) side view with A-A

The load distribution on the position agitator 180º (a) front view (b) appears side-to-side with A-A pieces, as described in Fig. 8.

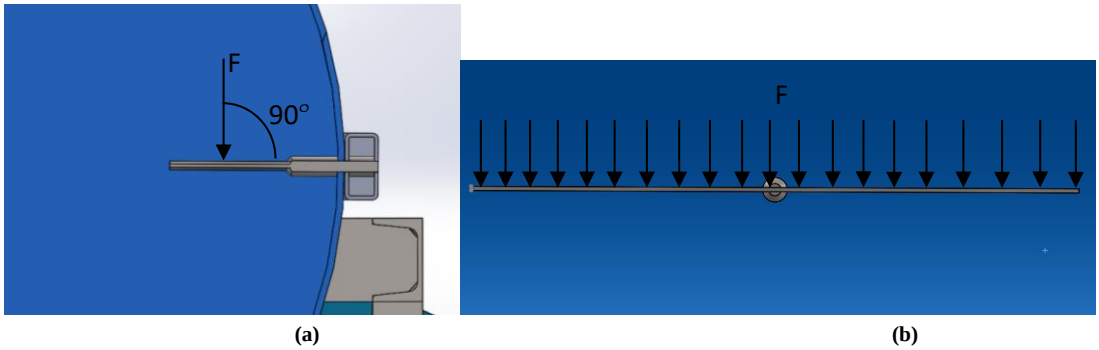

Fig. 8: The load distribution on the position agitator 180º (a) front view (b) appears side-to-side with A-A pieces

The force distribution at 180º is described in Fig. 9.

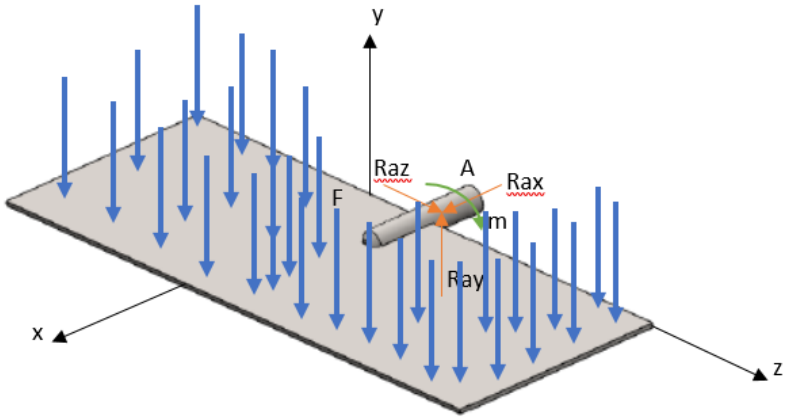

Fig. 9: Force distribution at 180º

For agitator 30˚ does not analyses its position because the working principle of this agitator only stirs / flattens the waste so that the waste is evenly distributed, the image and the shape of the agitator can be seen in Figure 10.

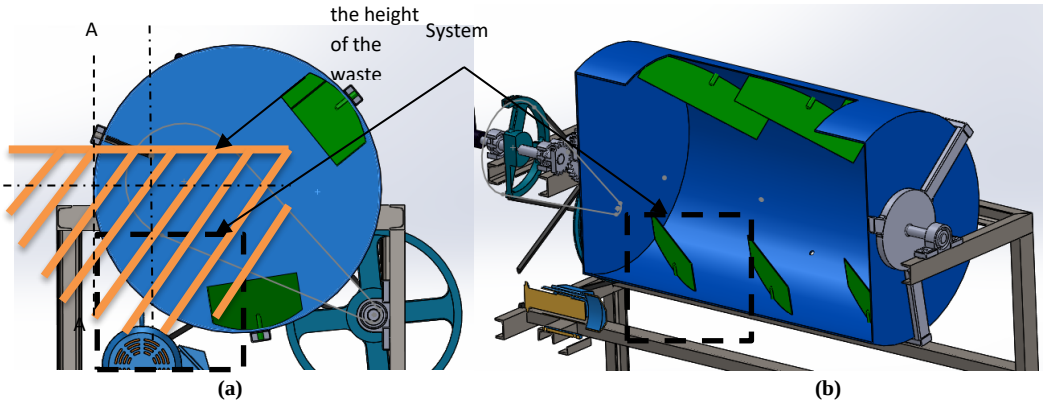

Fig. 10: load distribution of agitator 30º (a) front view (b) side view with A-A

Agitator 30 ˚ is different from the horizontal agitator because the position of this agitator in pairs is not horizontal, so the angle of this agitator is 30˚ which serves to stir the waste originally on the edge to be in the middle. The total force is 66.67 N, then the force in the direction is Fy = 66.66 N (sin 30 º), Fy = 33.33 N. The force on the agitator with an angle of 30º is shown in fig. 11.

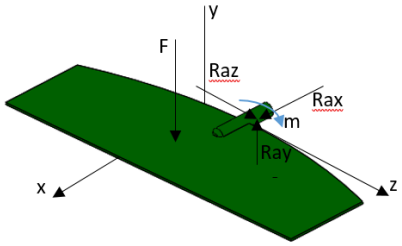

Fig. 11: Load distribution of agitator 30º

3. Analysis Result

The results consist of stress analysis and Displacement. Stress is a collection of force on a surface of an object. The results of stress analysis shown below. If the force constant, the narrower the surface area make the stress is greater. Maximum stress is shown on the dark red color, the minimum stress shown on dark blue, while the others with medium stress are shown on light yellow-green-blue color. Maximum stress that occurs on Horizontal Agitator with angular position 0º is 19 N/mm^2 with red color. These result can be explained in Figure 12. The largest stress that occurs at Horizontal Agitator with angular position 45º is 32 N/mm^2 shown in red color. These result can be explained in Figure 13 below.

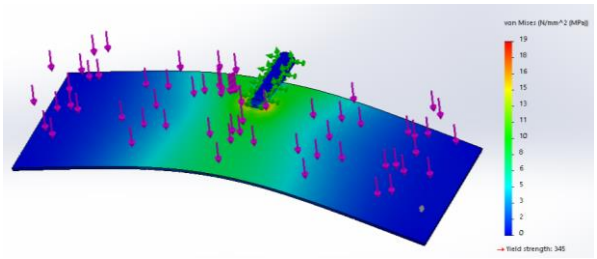

Fig. 12: Horizontal agitator stress at angular position 0˚

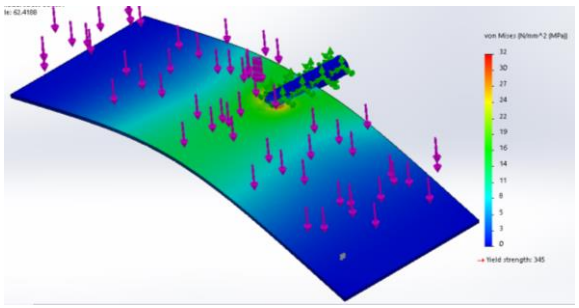

Fig. 13: Horizontal agitator stress at angular position 45 ˚

The largest stress that occurs at Horizontal Agitator with angular position 90º is 1 N/mm^2 .These result can be explained in Figure 14. The largest stress that occurs at Horizontal Agitator with angular position 135º is 46 N/mm^2 shown in red color. These result can be explained in Figure 15.

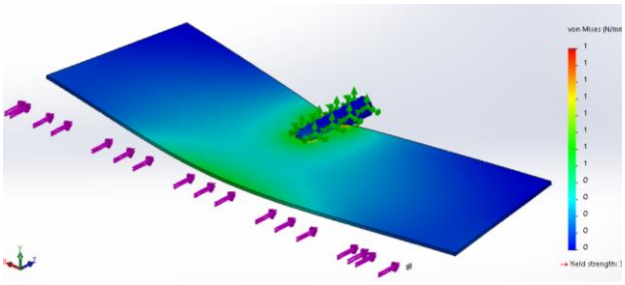

Fig. 14: Horizontal agitator stress at angular position 90˚

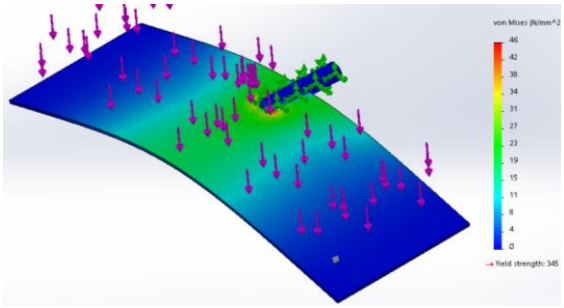

Fig. 15: Horizontal agitator stress at angular position 135 ˚

The largest stress that occurs at Horizontal Agitator with angular position 180º is 65 N/mm^2 shown in red color. These result can be explained in Figure 16. The largest stress that occurs at Horizontal Agitator with angular position 30º is 47 N/mm^2 shown in red color. These result can be explained in Figure 17.

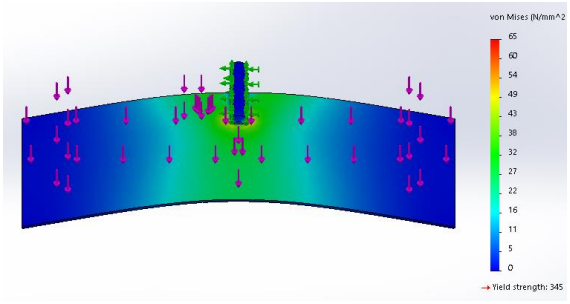

Fig. 16: Horizontal agitator stress at angular position 180˚

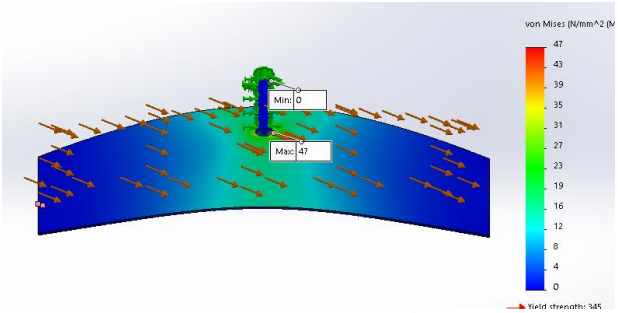

Fig. 17: Horizontal agitator 30 ˚ stress

Object subjected with force will deform (displacement), in this case curved.

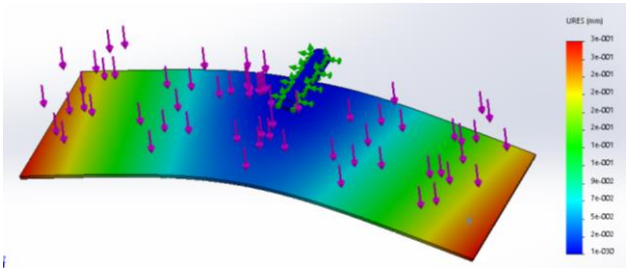

Fig. 18: Horizontal agitator displacement at position 0˚

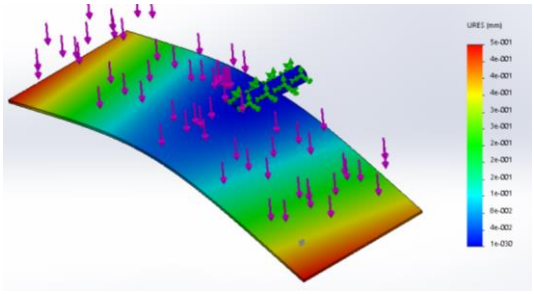

Fig. 19: Horizontal agitator displacement at position 45˚

The largest displacement occurs at horizontal agitator with angular position 0º is 0.043 mm shown in red color. these result explained in Figure 18. The largest displacement occurs at horizontal agitator with angular position 45º is 0.5 mm shown in red color. These result explained in Figure 19 above.

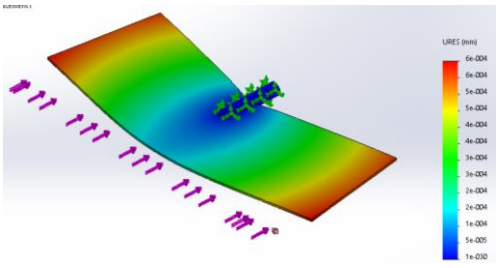

Fig. 20: Horizontal agitator displacement at position 90˚

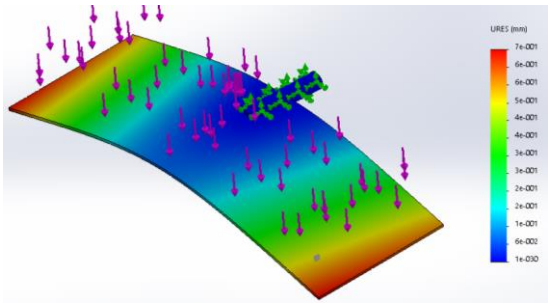

Fig. 21: Horizontal agitator displacement at position 135˚

The largest displacement occurs at horizontal agitator with angular position 90º is 0.0004 mm shown in red color, these result explained in Figure 20 above. The largest displacement occurs at horizontal agitator with angular position 135º is 0.07 mm shown in red color, these result explained in Figure 21 above.

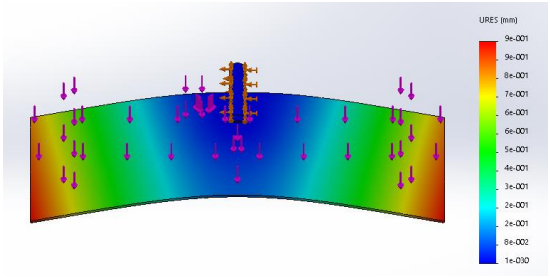

Fig. 22: Horizontal agitator displacement at position 180˚

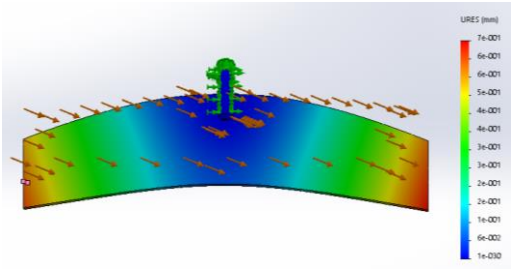

Fig. 21: displacement at agitator 30˚

The largest displacement occurs at horizontal agitator with angular position 180^o is 0.9 mm shown in red color, these result explained in Figure 22. At 30^o position, the largest displacement is not much different with horizontal agitator where the largest displacement is 0.7 mm, as shown in figure 21.

4. Conclusion

1. The maximum horizontal agitator loading occurs at 0^o position, the maximum stress is 65 N/mm^2, the maximum displacement is 0.9 mm, while the permit stress of AISI 1030 is 344.7 N/mm^2 , then the component is safe to use
2. Loading at agitator 30^o, The maximum stress is 47 N/mm^2, the maximum displacement is 0.7 mm, while the permit stress of AISI 1030 is 344.7 N/ mm^2, then the component is safe to use.

5. Nomenclature

A	Surface area	m^2
r	radius	m
b	Thickness	m

Greek letters

σ	stress	N/mm^2,

Subscripts

30	30^o
y	length co-ordinate

6. References

Abdurohim, O., 2008. Pengaruh Kompos Terhadap Ketersediaan Hara dan Produksi Tanaman Caisin (lang: Indonesia). Bogor Agricultural Institute.

Damanhuri, Padmi., 2010, Environmental Engineering Lecture- Bandung Institute of Technology

Tahir, I., 2008. Pembuatan Kompos (lang: Indonesia) . Lecture of Universitas Gadjah Mada

Mutaqin, Totok Heru TM., 2010. Pengelolaan sampah limbah rumah tangga dengan komposter elektrik berbasis komunitas (lang: Indonesia). Litbang Sekda DIY Biro Adm Pembang Journal.. V0l. II, No.2

Nurjazuli, A. Awiyatul, C. Juliana, K. D. Pertiwi, K. Samosir, P. Prasetyawati, S. Pertiwi., 2016. Teknologi Pengolahan Sampah Organik Menjadi Kompos Cair (lang: Indonesia). National Seminar on Science and Environmental Technology II

Robert E. Graves., 2000 Environmental Engineering National Engineering Handbook, Chapter 2 Composting, Natural Resources Conservation Service-United States Department of Agriculture.

Robert D., Raabe., The Rapid Composting Method. Vegetable Research and Information Center-University Of California.

Sudarmanto., 2010. Penerapan teknologi pengolahan sampah dan pemanfaatan nya (Lang: Indonesia). Proceedings of National Seminar on Science and Technology Faculty of Engineering, University of Wahid Hasyim Semarang.

Proceedings of the 1st Faculty of Industrial Technology International Congress
International Conference
Bandung, Indonesia, October 9-11, 2017
ISBN 978-602-53531-8-5

A Study on the Spray Characteristics of an 800kPa CNG Port Injector

Sakda Thongchai[1] and Ocktaeck Lim[2, *]

[1] Graduate School of Mechanical Engineering, University of Ulsan, Ulsan, 44610, South Korea

[2] School of Mechanical Engineering, University of Ulsan, Ulsan, 44610, South Korea

[*] Corresponding author e-mail: otlim@ulsan.ac.kr

Abstract

This paper investigated the spray characteristics of an 800 kPa compress natural gas (CNG) port injector which was developed in the domestic Korea. The CNG port injector with multi-holes, employed in this experiment, was designed to inject CNG in manifold at high pressure of 800 kPa. The spray macroscopic visualization test was carried out via Schlieren photography to study fuel-air mixing process. The fundamental spray characteristics, such as spray penetration, spray cone angle and spray velocity, were evaluated in the constant volume combustion chamber (CVCC) with varying the constant back pressure in CVCC from 0 to 1.8 bar. For the safety reason, nitrogen (N_2) and an acetone tracer were utilized as a surrogate gas fuel instead of CNG. The surrogate gas fuel pressures were controlled at 3, 5.5 and 8 bar, respectively. Injection durations were set at 5 ms throughout the experiment. The simulating events of the low engine speed were arranged at 1,000 rpm. The spray images were recorded by using a high-speed camera with a frame rate of 10,000 f/s at 512 x 256 pixels. The spray characteristics were analyzed by using the image processing (Matlab). The results showed the significant difference that higher injection pressure had more effect on the spray shape than the lower injection pressure. When the injection pressure was increased, the longer pray penetration occurred. Moreover, the linear relation between speed and time are dependent on the injection pressure as well.

Keywords: Spray characteristics, Spray penetration and cone angle, CNG port injector

1. Introduction

Due to concerning energy crisis and the air pollution and exhaust emission control, natural gas is the one of the most important alternative fuel and also consider as the cleanest fossil fuel. The abundance of natural gas has become a attracting factor for the wider usage of the fuel in the internal combustion engine (Bae & Kim 2017). Therefore, many engine scientists are interested to research on the natural gas engine. However, there are a few studies focusing on the mixture formation of gas jet.

This paper studied the spray characteristics in CVCC by varying the injection pressure of an 800 kPa CNG port injector developed in the domestic Korea. To understand the spray behaviours, macroscopic spray visualization was investigated via Schlieren photography technic (G.S.Settles 2001; Mazumdar 2011). The spray penetration and cone angle, and speed of spray were analysed for studying the fuel-air mixing process.

2. Methodology

2.1 Experimental setup

The 800 kPa CNG port injector as shown in Figure 1 was a solenoid injector. The general specification showed in Table 1. The diameter of nozzle exit is 6 mm. and its maximum injection pressure was 8 bar. It was mounted on the constant volume combustion chamber (CVCC) to evaluate the spray characteristics as well as injection mass flow rate with mass flow meter. For the safety reason, nitrogen (N2) mixed with acetone tracer was utilized as a surrogate gas instead of CNG (Yu, Hillamo, et al. 2013; Yu et al. 2012b; Yu, Vuorinen, et al. 2013; Yu et al. 2012a).

The injection pressure was set at 3, 5.5 and 8 bar. The back pressure in CVCC was varied with 1.0, 1.4 and 1.8 bar. The injection duration was controlled by supplying electrical on 5 ms. throughout the experiment. The spray cone angle and penetration, and speed of spray were assessed by using image processing (Barriga-Rivera & Suaning 2011; Mathworks 2014).

2.2 spray visualization

The Schlieren photography technic arranging in z-type as shown in Figure 2 was employed in the whole experiment. The spray images were recorded by using a high-speed camera, Photron model S3, with a frame rate of 10,000 f/s. The resolution was selected at 512 x 256 pixels. All of The spray images were saved in a personal computer via Protron FASTCAM Viewer (PFV) software. The spray characteristics were analyzed by using the image processing (Matlab)

Fig. 1: The 800 kPa CNG port injector.

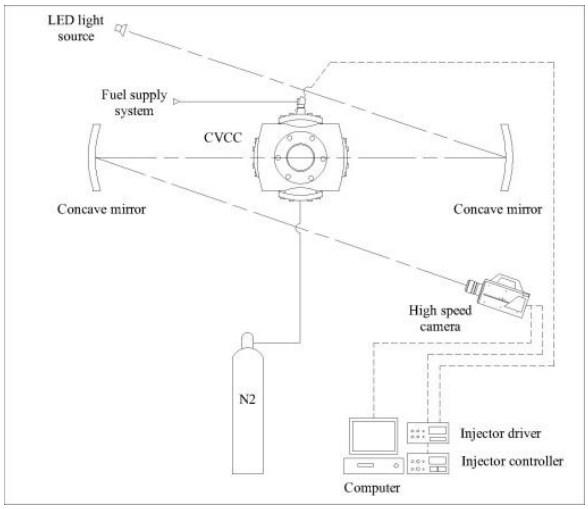

Fig. 2. The spray visualization setup with the Schlieren photography technic (Z-type).

Table 1: General data of 800kPa port injector.

Description	Value
Model	800 kPa (Prototype)
Type	Solenoid injector
Number of hole	4 holes
Tip diameter	6 mm.
Max. operating pressure	8 bar
Input voltage	10-14 V.

3. Results and Discussions

The definitions of spray cone angle and penetration length as shown in Figure 3 were declared as following (Liu et al. 2013); spray cone angle (θ) was measured the angle from the end of nozzle edge and following along the edge of spray penetration length and spray penetration length (L) was measured the distance from the end of nozzle tip to the end of spray tip where the last pixel is located. Figure 4 showed mass flow rate of the 800 kPa injector that the higher injection pressure increases, the higher mass flow rate increases. The maximum mass flow rate at 8 bar was 36 slpm approximately. The spray developed patterns of injection pressure of 8 bar as shown in Figure 5 exhibited that mixing process of the gas jet was significantly different when the back pressure was changed. Figure 6 showed the spray cone angle with a variation of injection pressure and back pressure. The results showed that the spray cone angle was reduced by 24-27° approximately. In addition, the higher injection pressure led to convert the spray cone angle to narrow angle.

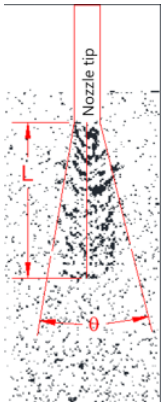

Fig. 3: The definition of spray cone angle and penetration length.

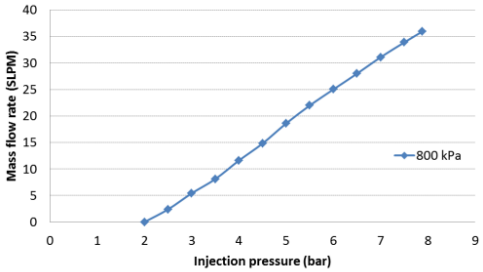

Fig. 4: The injection mass flow rate with N2 at the variation injection pressure.

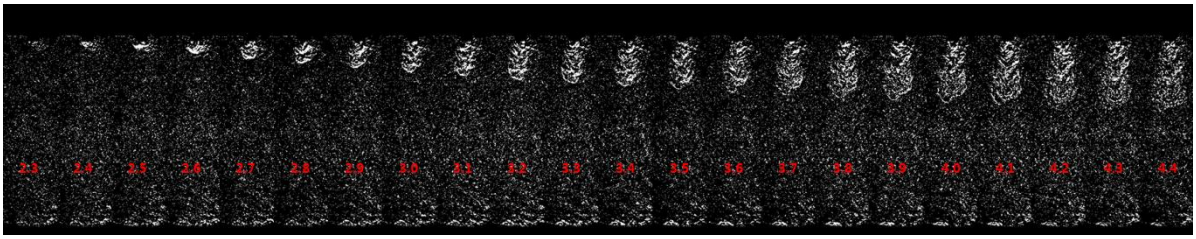

(a)

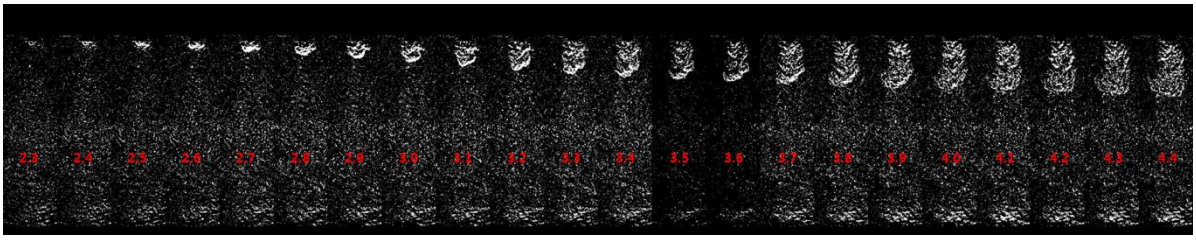

(b)

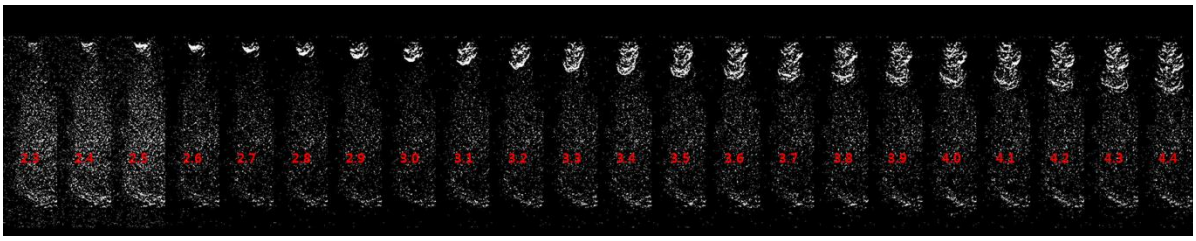

(c)

Fig. 5: The spray developed patterns of (a) injection pressure 8 bar and back pressure 1.0 bar, (b) Injection pressure 8 bar, back pressure 1.4 bar and Injection pressure 8 bar, back pressure 1.8 bar

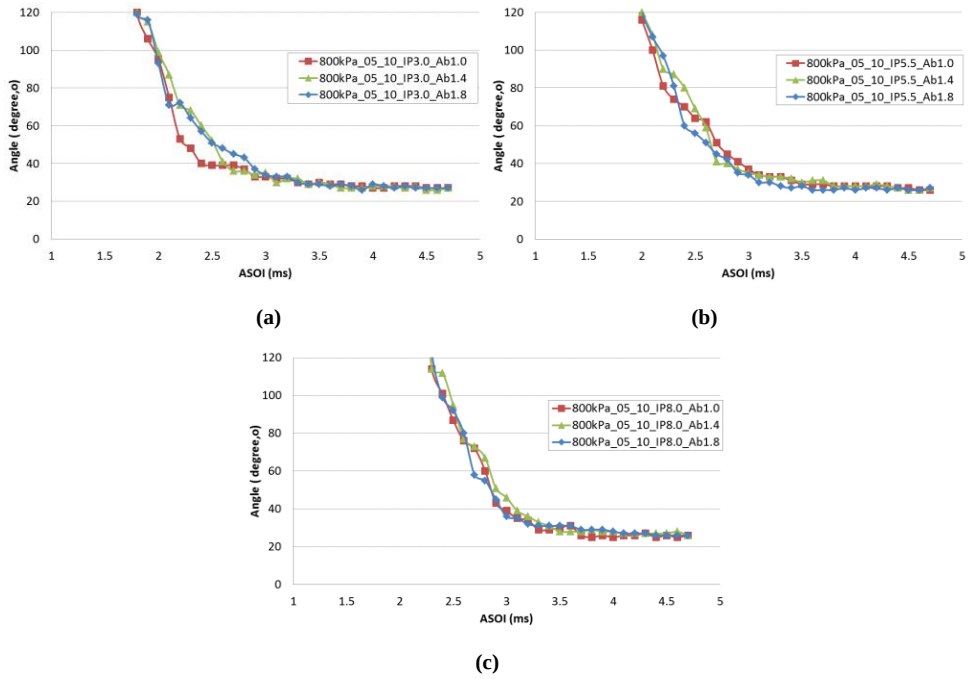

Fig. 6: The spray developed patterns of (a) injection pressure 8 bar and back pressure 1.0 bar, (b) Injection pressure 8 bar, back pressure 1.4 bar and Injection pressure 8 bar, back pressure 1.8 bar.

Figure 7 illustrated the spray penetration with the variation of injection pressures and back pressure. The results showed that the back pressures of 1.4 and 1.8 bar effect the spray penetration length which was shorter than the back pressure of 1.0 bar and their penetration length not too much different with each other. Moreover, at high injections, it also affected on the injection delay.

Figure 8 showed the speed of gas jet that at the low back pressure, the speed of gas jet was faster than high back pressure due to low ambient density. In addition, the speed of gas jet was sharply increased after injection a few milliseconds.

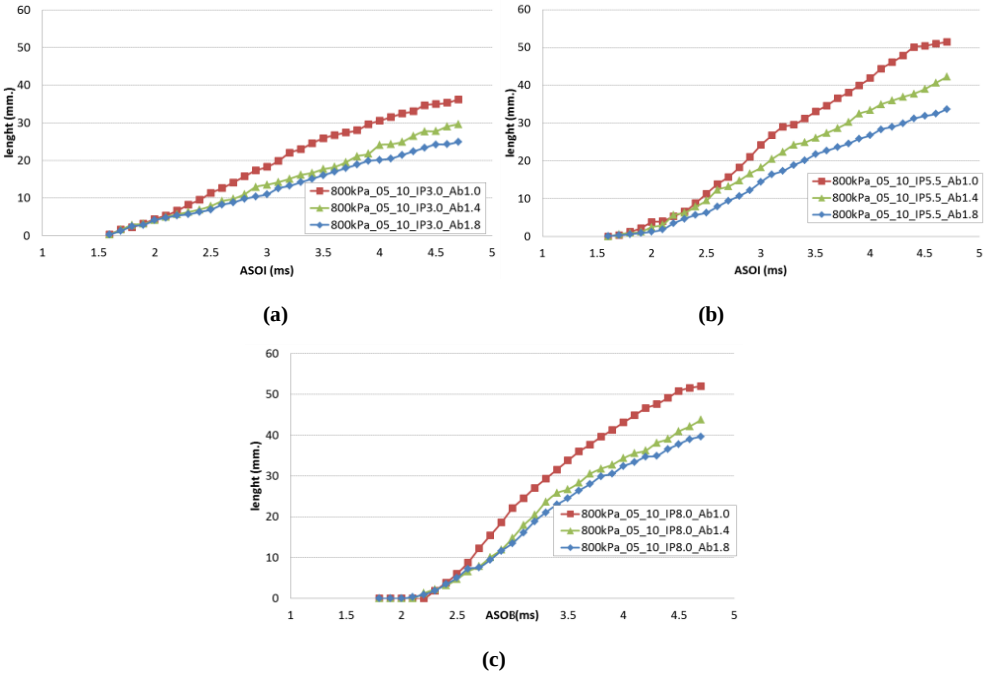

Fig. 7: Effect of the injection pressure on the spray penetrations at (a) 3, (b) 5.5, and (c) 8 bar with the variations of the back pressure.

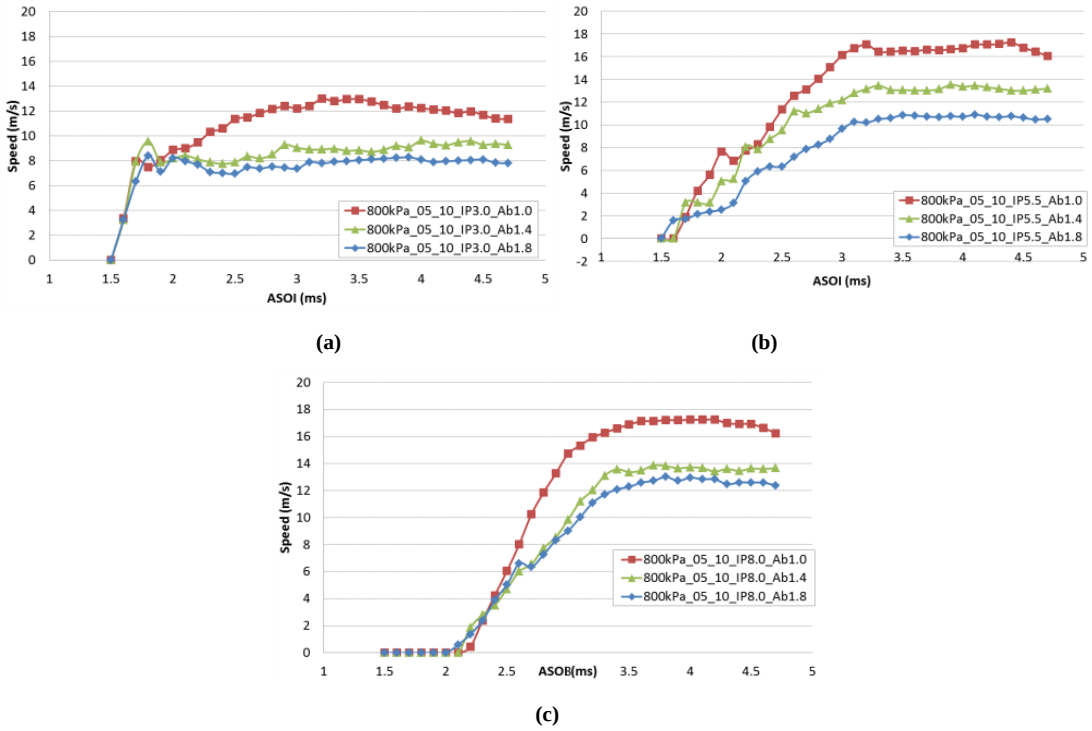

Fig. 8: Effect of the injection pressure on the spray speed at (a) 3, (b) 5.5, and (c) 8 bar with the variations of the back pressure

4. Conclusion

This paper focused on the spray characteristics of the 800kPa CNG port injector. The mass flow rate, the spray cone angle and penetration length, and the speed of gas jet are investigated. To analysis the spray behaviours, Schlieren photography technic and image processing are employed throughout the experiment. The results are compared with each other. The important conclusions are summarized as follows:

1). The higher injection pressure increases, the higher mass injection flow increases.

2). The higher injection pressure had more effect on the spray shape than the lower injection pressure. When the injection pressure is increased, the longer spray penetration occurs.

3). The higher back pressure has also effect on the spray form. However, at the back pressure of 1.4 and 1.8 bar, the spray characteristics are quite similar.

4). The linear relation between speed gas jet and time are dependent on the injection pressure as well.

5. Nomenclature

CNG Compress natural gas

CVCC Constant volume combustion chamber

IP Injection pressure

Ab Ambient pressure

N2 Nitrogen

PFV Protron FASTCAM Viewer

L Spray penetration

θ Spray cone angle

6. Acknowledgements

This research was supported by the Industrial Strategic technology development program (10053151, Development of the 800 kPa Fuel System of a High-Pressure Precision Control for NGV) funded by the Ministry of Trade, Industry & Energy (MI, Korea).

7. References

Bae, C. & Kim, J., 2017. Alternative fuels for internal combustion engines. Proceedings of the Combustion Institute, 36(3), pp.3389–3413. Available at: http://dx.doi.org/10.1016/j.proci.2016.09.009.

Barriga-Rivera, A. & Suaning, G.J., 2011. Digital Image Processing using Matlab, Available at: http://www.ncbi.nlm.nih.gov/pubmed/22255427.

G.S.Settles, 2001. Schlieren and shadowgraph Techniques 1st editio., Springer.

Liu, Y., Yeom, J. & Chung, S., 2013. A study of spray development and combustion propagation processes of spark-ignited direct injection (SIDI) compressed natural gas (CNG). Mathematical and Computer Modelling, 57(1–2), pp.228–244. Available at: http://dx.doi.org/10.1016/j.mcm.2011.06.035.

Mathworks, 2014. Image Processing Toolbox ™ User ' s Guide R2014b. , p.664.

Mazumdar, A., 2011. Principles and Techniques of Schlieren Imaging. Columbia University, pp.1–16. Available at: http://hdl.handle.net/10022/AC:P:20839.

Yu, J. et al., 2012a. An experimental investigation on the flow structure and mixture formation of low pressure ratio wall-impinging jets by a natural gas injector. Journal of Natural Gas Science and Engineering, 9, pp.1–10. Available at: http://dx.doi.org/10.1016/j.jngse.2012.05.003.

Yu, J. et al., 2012b. An Experimental Study on High Pressure Pulsed Jets for DI Gas Engine Using Planar Laser-Induced Fluorescence. SAE Technical Paper 2012-01-1655, c, pp.1–13.

Yu, J., Hillamo, H., et al., 2013. Experimental Study on Structure and Mixing of Low-Pressure Gas Jet Using Tracer-Based PLIF Technique. SAE Technical Paper 2011-24-0039, (Di).

Yu, J., Vuorinen, V., et al., 2013. Visualization and analysis of the characteristics of transitional underexpanded jets. International Journal of Heat and Fluid Flow, 44(x), pp.140–154. Available at: http://dx.doi.org/10.1016/j.ijheatfluidflow.2013.05.015.

Proceedings of the 1st Faculty of Industrial Technology International Congress
International Conference
Bandung, Indonesia, October 9-11, 2017
ISBN 978-602-53531-8-5

Investigation of Flow Field Modeling on Gasoline Engine of Motor Cycles

Bambang Wahono[1,2], Yanuandri Putrasari[1,2], and Ocktaeck Lim[3,*]

[1] Graduate School of Mechanical Engineering, University of Ulsan, Ulsan, 44610, South Korea

[2] Research Center for Electrical Power and Mechatronics, Indonesian Institute of Sciences (LIPI), Jl. Cisitu No 21/154 D, Gd.20, Bandung 40135, Indonesia

[3]School of Mechanical Engineering, University of Ulsan, Ulsan, 44610, South Korea

*Corresponding author e-mail: otlim@ulsan.ac.kr

Abstract

Internal combustion engine is the best available source of power for transportation sectors. The big issue appears at the efficiency of these engines. Every effort made to improve these engines to obtain the maximum efficiency. The gasoline engine performance is improved by the proper design of inlet manifold, combustion chamber, exhaust manifold, etc. The goal of this study is to investigate the in-cylinder flow characteristic of gasoline engine of motor cycles using Computational Fluid Dynamics (CFD) at three different speed (1500 rpm, 2000 rpm and 2500 rpm) like tumble, swirl, turbulence during cold start condition. The model of the intake port was analyzed by using Converge. The mesh was generated using the polyhedral scheme which includes primarily of tetrahedral mesh elements. The pressure boundary conditions were used to define the fluid pressure at the inlet and outlet of port. The tumble is decreased two folds between the speeds 1500 and 2000 rpm, and down one time in tumble between 2000 and 2500 rpm. The swirl in negative axis is increased two folds between the speeds 1500 and 2000 rpm, and increased a half time between 2000 and 2500 rpm. The results indicate that the CFD model can be used as a tool to investigate deeply the effect of various parts of port for optimization like manifold, spray, film, mixture formation and combustion. Finally, this study gives an effect to reduce the number of experiments to be carried out for arriving at the final optimized system.

Keywords: Gasoline Engine, In-Cylinder, CFD, Speed, Converge

1. Introduction

In the last decades, internal combustion engine is the best available reliable power source for many sectors and applications especially in transportation sector. The big issue arises at the internal combustion engine is engine efficiency performance and low emission. Every effort made to improve the internal combustion engines tends to get the maximum efficiency performance and low emission. This is demanded to protect the environment and energy conservation. The performances of the internal combustion engines are obtained by proper design of intake manifold, exhaust manifold, combustion chamber, piston etc. In other side, to achieve the maximum efficiency performance and low emission, it is important to improve the combustion characteristics, that means it reduces the pollutant or unburned elements in exhaust gas by achieving a homogeneous mixture with controlled in-cylinder flow like swirl and tumble flow (Li et al., 2001; Nonaka et al., 2004).

The Swirl flow is defined as a rotation of the charge about the cylinder axis and the tumble flow is defined as a rotation orthogonal to the cylinder axis (Lumley, 1999). These two flows occur simultaneously inside the cylinder. It should be noted that there is a range of ideal levels of swirl, tumble, flow speed and turbulent kinetic energy (TKE). Small levels of these variables lead to slow flame propagation, poor mixture formation resulting in reduced efficiency. But very high levels of those can lead to increased heat transfer to walls, reduced volumetric efficiency and even flame quenching and incomplete burning (Li et al., 2001; Hill and Zhang, 1994; Aita et al., 1991; Wheeler et al., 2013). The flow field model inside an engine especially in cylinder can be visualized by several ways such as using experimental techniques like Laser Doppler Anemometry (LDA) (Li et al., 2001; Le Coz et al., 1990; Fansler and French, 1988) and Particle image velocimetry (PIV) (Li et al., 2001; Rouland et al., 1997; Choi et al., 1999; Reuss et al., 2000). These techniques are good but expensive (Kurniawan et al., 2007). Other choice to visualize the flow field model is using numerical techniques such as CFD. It can lead to very accurate results, which can help detecting problems in the engine design and accelerate the project phase.

A CFD analysis is based on the continuity, Navier-Stokes and energy equations along with some modelling for turbulence. The turbulence models most used industrially are based on the Reynolds Averaged Navier Stokes (RANS) approach, and among those the most widely validated belong to the k-ε family (Versteeg and Malalasekera, 2007).

As we know that the engine cycle of typical internal combustion engines consists of four consecutive processes i.e. intake process, compression process, expansion process and exhaust process. Of these four processes, the intake and compression stroke process are two of the most important processes which influences the pattern of air flow structure coming inside cylinder during intake stroke and generates the condition needed for the fuel injection during the compression stroke. Especially for intake manifold, a deep knowledge of the intake processes and compression stroke process are basic science to design and optimize modern internal combustion engines efficiently.

The objective of this research is analysis of flow field model especially in cylinder engine by numerical simulations that performed in a four stroke of gasoline engine of motor cycle under cold flow conditions at three different speeds (1500 rpm, 2000 rpm and 2500 rpm) to investigate the flow characteristics like swirl, tumble, turbulence during cold start condition.

2. Methodology

2.1 Simulation Setup

The internal combustion engine is a heat engine that converts chemical energy in a fuel into mechanical energy, usually made available on a rotating output shaft. The wide range of internal combustion engines is classified and they have its own advantages and disadvantages. According to the type of the fuel used the engine is classified as follows: gasoline engine, diesel engine and gas engine. The gasoline engine used in this research. The detailed specification of the gasoline engine selected for the simulation is given in Table 1. By the CFD Numerical simulation, the gasoline engine 249 cc used in this study. In the beginning research, the important and the main component of this research is engine.

In this study, the CFD analysis is carried out using Converge, a commercial CFD package. The Converge uses a fully automatic structured grid generation technique for meshing a geometry during run time (Converge, 2017). The grid independence study is carried out for the engine under consideration (Krishna and Mallikarjuna, 2015). The flow turbulence is analyzed using the renormalized group (RNG) k-e model (Krishna, et al., 2013; Yakhot et al., 1994). The finite volume-based implicit discretization procedure is used to solve the discretized Navier–Stokes' equations on a Cartesian grid. The in-cylinder flow is modeled by solving mass, momentum and energy conservation equations along with the equations for species, turbulent kinetic energy (TKE) and turbulent dissipation rate at each cell and at each time step. The ''pressure implicit for splitting of operator" (PISO) algorithm is used to solve the pressure-velocity coupling.

Table 1: Specification of gasoline engine

Parameter	Value
Type air / Urethane	DOHC 8 valve 75 °V type
Number of cylinder	2
Displacement	249cc
Bore	57 mm
Stroke	48.8 mm
Compression ratio	10.2: 1
Maximum output	25.5 ps / 9000 rpm
Maximum torque	2.21kg-m / 7000 rpm
Fuel injection	Electric Port Fuel Injection

2.2 The CAD Model

The engine model was scanned by three-coordinate measuring machine to gain its clouding points figure. Then the figure was putted into the Solid Work or other CAD software to be modified. Finally, three-dimensional CAD model of the engine was obtained. It is showed in figure 1. Then this CAD model was modified to become a simulation calculation model. The fluid volume is extracted in one step and the inlet and outlet boundaries are created by renaming the surfaces. Converge uses a fully automatic structured grid generation technique for meshing the geometry during run time. However, the grid size and total number of cells can be controlled by the user through the base grid size, adaptive mesh refinement and grid embedding controls.

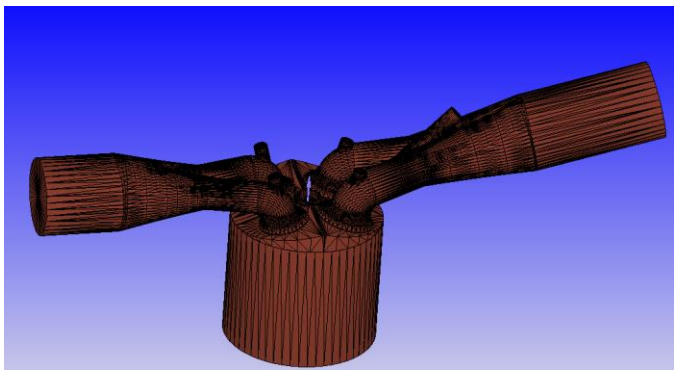

Fig. 1: The CAD model of gasoline engine

2.3 Boundary Condition

In this study, the piston and valves are defined as moving boundaries. The domain is divided into three regions i.e. cylinder, intake and exhaust. All the three regions are connected based on events described by the valve closing and opening. The inlet and outlet pressure, and temperature are defined at 1 bar and 300 K respectively. An initial turbulence level of 10% is specified at the inlet (Sagayaraj et al., 2013). The summary of boundary conditions is given in Table 2.

Table 2: Boundary conditions

Parameter	Value
Inlet	Pressure inlet at 1 bar 300K
Outlet	Pressure outlet at 1bar 300K
Piston and valves	Moving walls
Cylinder, intake and exhaust ports	Stationary walls

In this study, the global transport number are prandtl number with 0.9 and Schmidt number with 0.78. A length scale of 10% of the port diameter at the inlet plane were presented to estimate the inlet boundary condition on turbulent kinetic energy (Tke) and its dissipation rate. The choice of differencing scheme will affect the convergence rate and accuracy of the final computational solution. Lower order schemes tend to be more stable but introduce numerical viscosity into the solution, while higher order schemes are more accurate but require more computer time to solve and are less stable. Present study makes use of first order scheme, which is stated to be far more robust and stable. Currently the most popular turbulence model, which is used in a practical setting, is the two-equation k-ε model. This model employs two additional transport equations one for turbulence kinetic energy and another one for the turbulent dissipation rate (Tdr). Near wall treatment is handled through generalized wall functions. In this study, the flow turbulence is renormalized group (RNG) k-e, the in-cylinder flow is modeled by solving mass, momentum and energy conservation, turbulent kinetic energy (TKE) and turbulent dissipation rate at each cell and at each time step and the pressure implicit for splitting of operator (PISO) algorithm is used to solve the pressure-velocity coupling. This model is well established and the most widely validated turbulence model.

3. Result and Discussions

3.1. In-cylinder Tumble ratio

The gasoline engines are normally designed to be tumble oriented. The pent roof combustion chamber and the orientation of the intake port geometry helps in the generation of tumbling motion inside the engine cylinder. Tumble flow has been studied by using the numerical simulation method. The change in tumble flow of in-cylinder according to the crank angle (around both X-axis and Y-axis) is shown in Fig. 2. Fig. 2 shows the temporal variation of tumble flow for the three speeds 1500, 2000 and 2500 rpm. The rotation of vortices about the axis Y (T_{ry}) is called as normal tumble about y coordinate and the tumbling vortices about the axis X is denoted as cross tumble (T_{rx}). This tumble ratio is the average from T_{rx} and T_{ry}. Tumble motion inside the engine cylinder can be divided into three phases as generation, stabilization and destruction. Generation phase occurs usually during the intake stroke which proceeds from 360 up to 420° CA. The stabilization and spin up phase occur due to the upward moving piston. Because of the moving piston the spin up phase enhances the tumble motion again up to 300 degrees. The tumble destruction phase results in increased turbulence. This can be confirmed with reference to Fig 2 where there is increase in the turbulence level starting from 200°CA and lasts up to 330°CA. Regarding the effect of speed, the tumble is decreased two folds between the speeds 1500 and 2000 rpm, whereas down one time in tumble between 2000 and 2500 rpm. This may be attributed to the poor strength of the intake generated tumbling vortices which are not sustained during the stabilization and spin up phase.

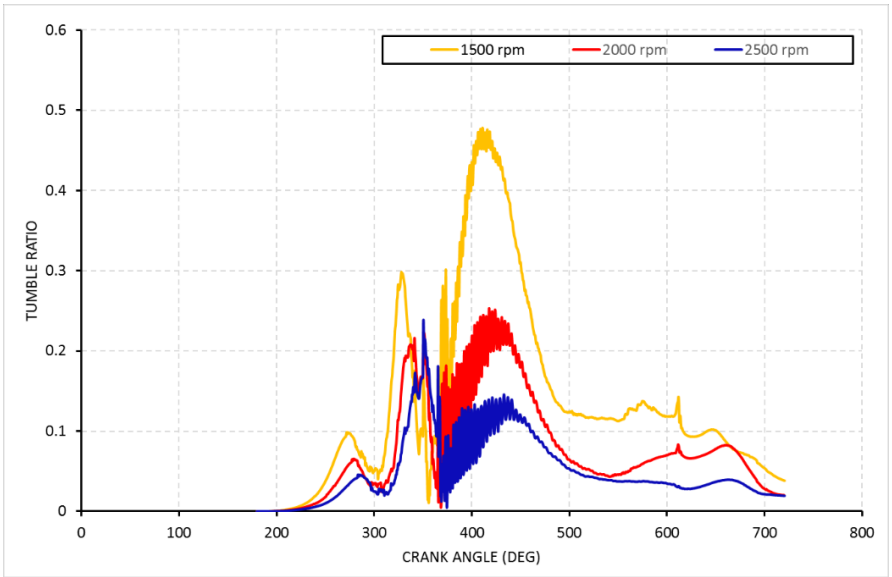

Fig 2: In-cylinder tumble ratio in variation speed

3.2. In-cylinder Swirl ratio

Swirl is created by bringing the intake flow into the cylinder with an initial angular momentum and the interaction of the intake jet/cylinder wall/piston face. While many other flow structures generated during the intake process decay very quickly, swirl can survive throughout the compression process, and even into combustion and expansion processes. The swirl flow has been studied by using the numerical simulation method. The change in swirl flow of in-cylinder according to the crank angle is shown in Fig. 3. Swirl flow is generated even with the standard condition of in-cylinder flow at full throttle. Fig. 3 shows the temporal variation of swirl flow for the three speeds 1500, 2000 and 2500 rpm. Fig. 3 shows the predicted swirl ratio versus crank angle during the exhaust, intake and compression strokes. It isn't appeared in the exhaust process and begin appeared and formed during the induction process. The swirl ratio is greatest at the middle of the intake stroke (approximately 350° CA) and has a slight drop after that point as angular momentum is dissipated owing to friction at the walls and turbulent dissipation within the fluid. However, the swirl is fairly stable and the swirl ratio remains almost constant during the early phase of the compression stroke. The swirl ratio increases during the late compression stroke. This phenomenon is expected as the tangential velocity of the swirling air flow is increased owing to the compact bowl-in-piston/combustion chamber interaction. Regarding the effect of speed, the swirl in negative axis is increased two folds between the speeds 1500 and 2000 rpm, and increased a half time between 2000 and 2500 rpm. This may be attributed to the poor strength of the intake generated swirling vortices which are not sustained during the stabilization and spin up phase.

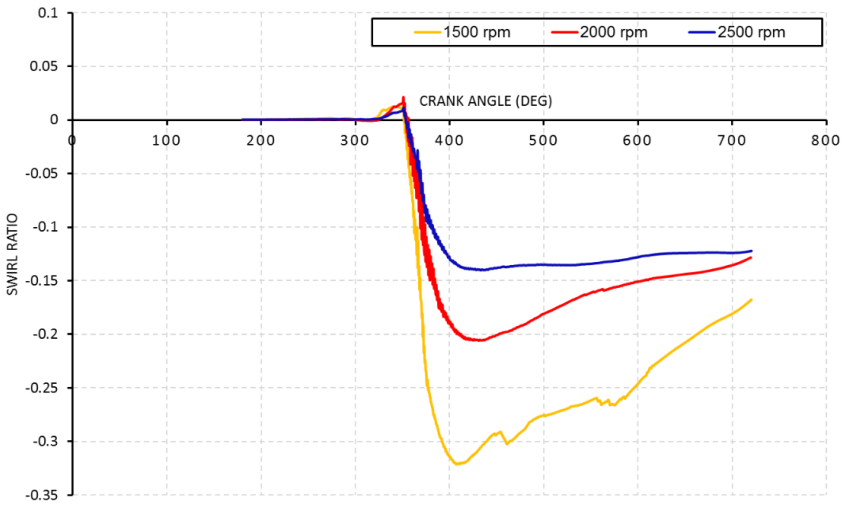

Fig 3: In-cylinder Swirl ratio in variation speed

3.3. In-cylinder Turbulent Kinetic Energy (TKE)

Turbulent Kinetic Energy is the mean kinetic energy per unit mass associated with eddies in turbulent flow. Physically, the turbulence kinetic energy is characterized by measured root-mean-square (RMS) velocity fluctuations. The turbulent kinetic energy (Tke) is an important parameter to determine the turbulent viscosity. Figure 4 shows the Turbulent Kinetic Energy (Tke) versus crank angle. There are two peaks in turbulent kinetic energy seen in Fig. 4. The first peak appears during the intake stroke despite a slight decline and a rebound, and is related to turbulence generated as the air flows through the intake valve curtain area. It is observed that this configuration affects the turbulence of the fluid inside the cylinder. The second peak appears lower than the first peak and occur in compression stroke process. It reaches the peak value during the maximum valve open condition (400°CA) and converge from 700 °CA. The effect of the speed is the higher the speed the lower the value tke. The variation of Tke is probably due to different level of air induced through the inlet manifold.

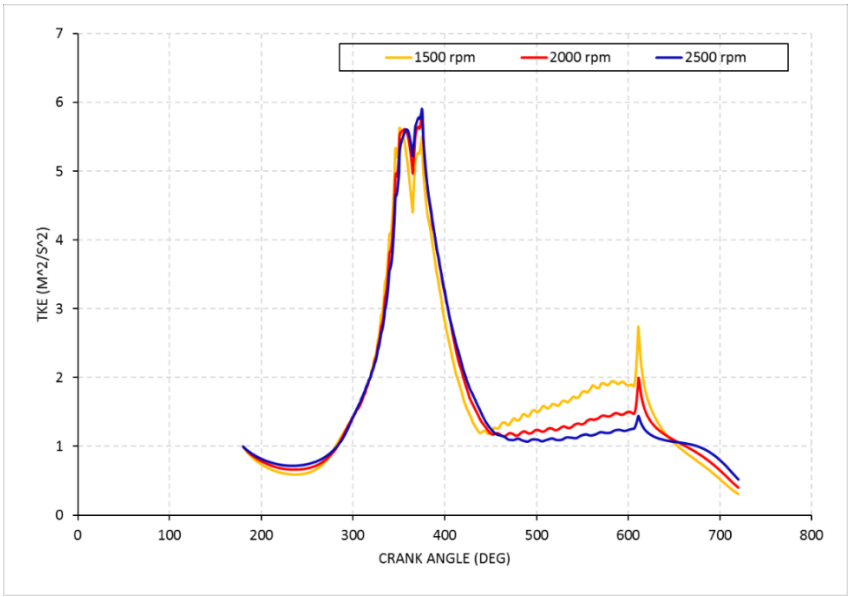

Fig 4: In-cylinder TKE in variation speed

3.3. In-cylinder Turbulent Dissipation rate (TDR)

Figure 4 shows the Turbulent Dissipation rate (TDR) versus crank angle. This figure similar with the turbulent kinetic energy. There are two peaks in turbulent dissipation rate seen in Fig. 4. The first peak appears during the intake stroke despite a slight decline and a rebound, and is related to turbulence generated as the air flows through the intake valve curtain area. It is observed that this configuration affects the turbulence of the fluid inside the cylinder. The second peak appears lower than the first peak and occur in compression stroke process. The effect of the speed is the higher the speed the lower the value tke. The variation of Tke is probably due to different level of air induced through the inlet manifold.

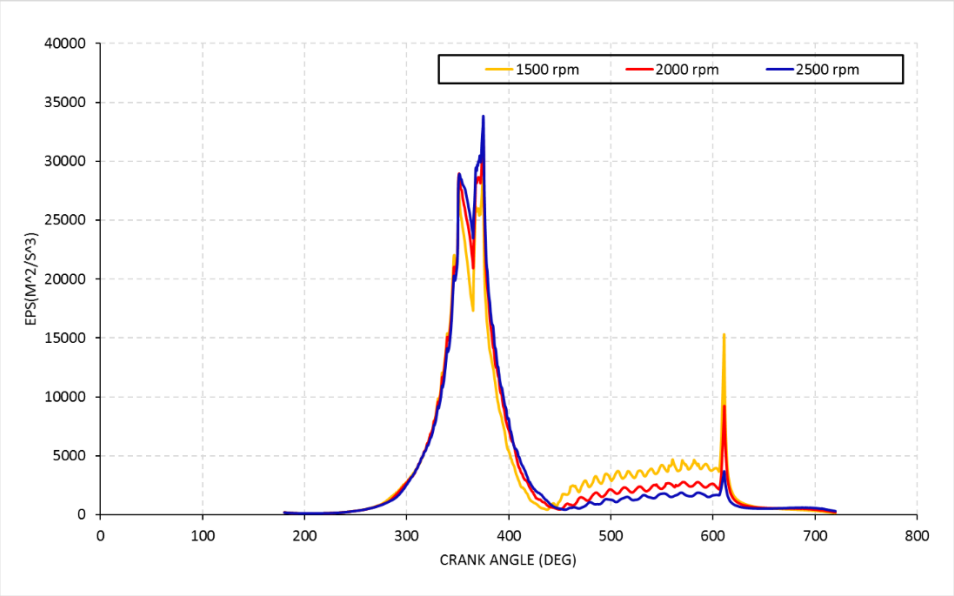

Fig 4: In-cylinder TDR in variation speed

4. Conclusion

A three-dimensional unsteady turbulent compressible Navier–Stokes solver, Converge, was utilized in the present study to investigate the in-cylinder flow field of a four-valve gasoline direct injection engine of motor cycle. The following conclusions were found.

1. The tumble flow is formed during the late intake stroke and then compressed during the compression stroke. It is broken down at the end of the compression stroke, which results in enhanced turbulence kinetic energy. Such flow phenomena will be important to improve atomization distribution of the fuel spray in the engine operation.
2. Swirl flow can survive through the compression stroke. The swirl ratio even increases with crank angle at the end of the compression stroke.
3. The results indicate that the CFD model can be used as a tool to investigate deeply the effect of various parts of port for optimization like manifold, spray, film, mixture formation and combustion. Finally, this study gives an effect to reduce the number of experiments to be carried out for arriving at the final optimized system.

5. Nomenclature

CFD: Computational Fluid Mechanic

PFI: Port Fuel Injection

TKE: Turbulent Kinetic Energy

TDR: Turbulent Dissipation Rate

RMS: root-mean-square

6. Acknowledgments

This research was financially supported by CEFV (Centre for Environmentally Friendly Vehicle) as Global Top Project of KMOE (2016002070009, Development of Engine System and Adapting Vehicle for Model 110 cc and 300 cc Correspond to EURO-5 Emission). This research was supported by The Leading Human Resource Training Program of Regional Neo industry through the National Research Foundation of Korea (NRF) funded by The Ministry of Science, ICT and Future Planning (2016H1D5A1908826). This research was also supported by the Industrial Strategic technology development program (10053151, Development of the 800 kPa Fuel System of a High Pressure Precision Control for NGV) funded by the Ministry of Trade, Industry & Energy (MI, Korea).

7. References

Li, Y., Zhao, H., Peng, Z., and Ladommatos, N., "Analysis of Tumble and Swirl Motions in a Four-Valve SI Engine," SAE Technical Paper 2001-01-3555, 2001, doi: 10.4271/2001-01- 3555.

Nonaka, Y., Horikawa, A., Nonaka, Y., Hirokawa, M. et al., "Gas Flow Simulation and Visualization in Cylinder of Motor-Cycle Engine," SAE Technical Paper 2004-32-0004, 2004, https://doi.org/10.4271/2004-32-0004.

Lumley, L. J., "Engines, an Introduction," Cambridge University Press, Cambridge, 1999.

Hill, P. G.; Zhang, D., "The effect of swirl and tumble on combustion in spark ignition engines", Progress in Energy and Combustion Science, 20(5):373-429, 1994, doi: 10.1016/0360-1285(94)90010-8.

Aita, S., Tabbal, A., Munck, G., Montmayeur, N. et al.,"Numerical Simulation of Swirling Port-Valve-Cylinder Flow in Diesel Engines," SAE Technical Paper 910263, 1991, doi:10.4271/910263.

Wheeler, J., Polovina, D., Ramanathan, S., Roth, K. et al., "Increasing EGR Tolerance using High Tumble in a Modern GTDI Engine for Improved Low-Speed Performance," SAE Technical Paper 2013-01-1123, 2013, doi: 10.4271/2013-01-1123.

Le Coz, J., Henriot, S., and Pinchon, P., "An Experimental and Computational Analysis of the Flow Field in a Four-Valve Spark Ignition Engine-Focus on Cycle-Resolved Turbulence," SAE Technical Paper 900056, 1990, doi: 10.4271/900056.

Fansler, T. and French, D., "Cycle-Resolved Laser-Velocimetry Measurements in a Reentrant-Bowl-in-Piston Engine," SAE Technical Paper 880377, 1988, doi: 10.4271/880377.

Rouland, E., Trinité, M., Dionnet, F., Floch, A. et al., "Particle Image Velocimetry Measurements in a High Tumble Engine for In-Cylinder Flow Structure Analysis," SAE Technical Paper 972831, 1997, doi: 10.4271/972831.

Choi, K., Park, J., Lee, N., Yu, C. et al., "A Research on Fuel Spray and Air Flow Fields for Spark-Ignited Direct Injection using Laser Measurement Technology," SAE Technical Paper 1999-01-0503, 1999, doi: 10.4271/1999-01-0503.

Reuss, D., "Cyclic Variability of Large-Scale Turbulent Structures in Directed and Undirected IC Engine Flows," SAE Technical Paper 2000-01-0246, 2000, doi: 10.4271/2000-01-0246.

Kurniawan, W. H.; Abdullah, S.; Shamsudeen, A., "A computational fluid dynamics study of cold-flow analysis for mixture preparation in a motored four-stroke direct injection engine". Journal of applied sciences 7(19):2007-2724, 2007.

Versteeg, H.; Malalasekera, W. "An Introduction to Computational Fluid Dynamics: The Finite Volume Method". 2a edition. Prentice Hall, 2007. 520p.

CONVERGE v2.3.21, Theory Manual, Convergent Science Inc, 2017.

A.S. Krishna, J.M. Mallikarjuna, Effect of fuel injector location on the equivalence ratio near the spark plug in a GDI engine – a CFD analysis, in: 24th National Conference on Internal Combustion Engines and Combustion, Oct 30th –Nov 1st, Dehradun India, 2015.

A.S. Krishna, J.M. Mallikarjuna, K. Davinder, Y.R. Babu, Incylinder flow analysis in a two-stroke engine – a comparison of different turbulence models using CFD, SAE paper no. 2013-01-1085, 2013.

V. Yakhot, S.A. Orszag, S. Thangam, T.B. Gatski, C.G. Speziale, Development of turbulence models for shear flows by a double expansion technique, Phys. Fluids A4 (7) (1994).

Sagayaraj, A. G., J. M. Mallikarjuna, V. Ganesan. Energy efficient piston configuration for effective air motion – A CFD study, Applied Energy, Volume 102, February 2013, Pages 347-354.

Proceedings of the 1st Faculty of Industrial Technology International Congress
International Conference
Bandung, Indonesia, October 9-11, 2017
ISBN 978-602-53531-8-5

INFLUENCE OF CONFIGURATION STEAM JET EJECTOR - LRVP ON GEOTHERMAL POWER PLANT 55 MW CAPACITY

Fajri Jayakelana[1,*], Agus Hermanto[2]

[1]Graduate Student of Mechanical Engineering, Itenas, Bandung – INDONESIA

[2]Dept. of Mechanical Engineering, Itenas Bandung – INDONESIA

[*] Corresponding author e-mail: Fajri.fjk@gmail.com

Abstract

The stability performance of geothermal power plants is maintained by the use of a gas exhaust system (*GRS)* to remove non-*condensable* gas (*NCG)* which is a natural element of steam. *NCG* will cause an increase in pressure in the condenser and affect the turbine power. Equipment commonly used in *GRS* is steam jet ejectors (*SJE)* and or liquid ring vacuum pump (*LRVP)*. The *GRS* stage variation and the *SJE-LRVP* configuration affected the ability of the *GRS* to handle *NCG* content variations. The first stage will be using *SJE* with 30%, 40%, and 60% capacity and the second stage will be used *SJE* 130% or *LRVP* 2x65% capacity. The simulation results using the Cycle Tempo 5.0 software showed the increase in *NCG* caused an increase in condenser pressure and caused a decrease power on the *GPP* system. The use of 2x65% *LRVP* on stage two generally shows the smaller influence on *GPP* power (or larger *GPP* output power) compared to 130% *SJE* usage except for *NCG* content values smaller or equal to 0.5%.

Keywords: Configuration, Gas Removal System, Steam Jet ejector, Liquid ring vacuum pump, Geothermal power plant.

1. Introduction

Overall the total geothermal potential for Indonesia reached 27,189 MW or equivalent to 11 billion barrels of oil. The amount of potential Indonesia is 40% of the total potential for the world. Geothermal potential for West Java is very large, equal to 5311 MW or 20% of the total potential of Indonesia. Mean that 8% of the world's geothermal potential is in West Java. The purpose of this research is to obtain the effect of SJE and LRVP performance on the main condenser pressure variations and their effect on the increase or decrease of the performance of the generating system using Cycle Tempo 5.0 from a GPP.

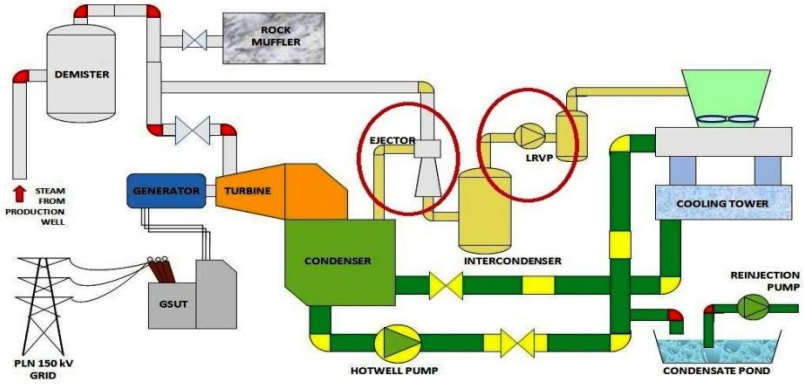

Fig. 1: Schematic GPP capacity 55 MW (Geodipa, 2015)

GRS is a tool used to trap non-condensable gas (NCG), any geothermal power plant uses a gas removal system (GRS) because it has the presence of NCG in the condenser that causes the rise of condenser pressure. To deal with this case used two main equipment, namely: steam jet ejectors (SJE) and liquid ring vacuum pump (LRVP). Both of these tools are commonly used in GPP, both of which can be used single or hybrid depending on the NCG concentration on the GPP and used on stage 1, stage 2 or stage 3.

2. NCG Flow pattern Configuration Scheme

With this two stage System design *GRS*, there are 14 configurations can be operated to depend on the % *NCG* at source of the steam. Configuration K (Configuration-1) and Configuration L (Configuration-2) will be simulated and compared the influence to the *GPP* Net Power Produced.

Table 1: GRS Configuration Pattern on GPP 55 MW

No	Configuration	*Stage* 1	*Stage* 2
1	A	SJE 30%	SJE 130%
2	B	SJE 30%	1 LRVP 65%
3	C	SJE 40%	SJE 130%
4	D	SJE 40%	1 LRVP 65%
5	E	SJE 60%	SJE 130%
6	F	SJE 60%	1 LRVP 65%
7	G	SJE 30% + 40%	SJE 130%
8	H	SJE 30% + 40%	1 LRVP 65%
9	I	SJE 30% + 60%	SJE 130%
10	J	SJE 30% + 60%	2 LRVP 65%
11	K	SJE 40% +60%	SJE 130%
12	L	SJE 40% +60%	2 LRVP 65%
13	M	SJE 30%+40%+60%	SJE 130%
14	N	SJE 30%+40%+60%	2 LRVP 65%

For concentrations of NCG below 3% the configuration that allows use is configuration A, B, C, D, E, F, G, H and for concentrations on 3% the configuration that allows use is configuration I, J, K, L, M, N. The reason for using *SJE* at stage-1 is *SJE* stable performance, low cost component criteria, easy to operate, long life component, almost maintenance free, despite the consequences of vapor discharging. At stage-1 it does not use *LRVP* due to large in-house power considerations of *LRVP* on *GPP* and expensive component price, short component life.

3. SJE - LRVP Configuration

The variables studied include: NCG concentration in Steam content, NCG removal rate based on GRS configuration, mass vapor flow rate delivered to SJE, Power on LRVP, increased pressure caused by NCG concentration, and recent simulation of it and view its impact on the increase or decrease in performance at 55 MW GPP system capacity by using Cycle Tempo 5.0. With concentration of 3% NCG and 0.0973 bar condenser pressure. Two stages GRS will be evaluated. Stage-1 uses 40% and 60% SJE capacity. Stage 2 becomes Configuration 1 using LRVP 2x65% and Configuration 2 uses SJE 130%.

.

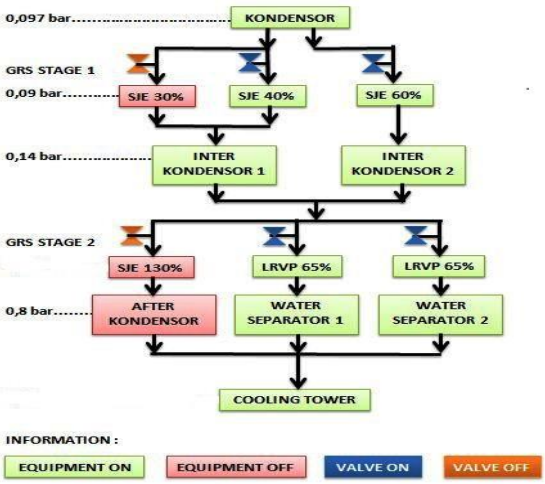

Fig. 2: NCG Flow Pattern Configuration 1

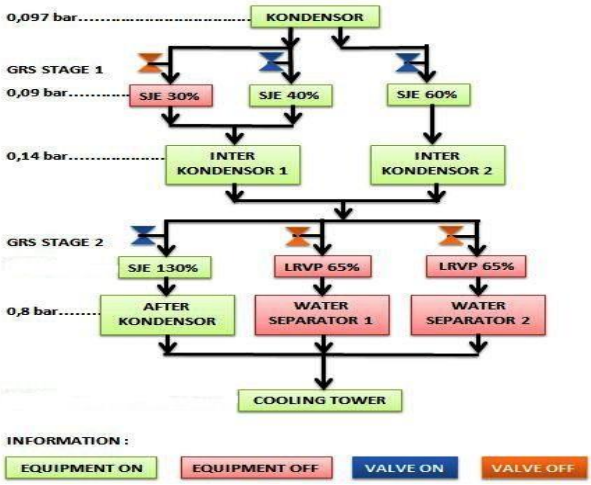

Fig. 3: NCG Flow Pattern Configuration 2

In Figure 2 showing at stage 1, the SJE will be at 0.09 bar suction pressure and 0.14 bar discharge pressure. After NCG and Steam mixed it will flow to Inter-condenser 1 and Inter-condenser 2. NCG will be sucked again by GRS stage 2 using 2x 65% LRVP capacity, and flowed to Separator Air 1 and Water Separator 2 at pressure of 0.8 bar for further flow to Cooling Tower. In Figure 3 shows the NCG 2 Flow Pattern Configurations, the phase 2 GRS will use a 130% SJE capacity with 0.14 bar suction pressure and will be discharged at a pressure of 0.8 bar in the after-condenser for subsequent flow to the Cooling Tower.

4. Calculation of SJE steam consumption.

The gas in this case NCG can be captured by an SJE, with a very varying capacity. Relate to NCG to be handled. The Heat Exchanger Institute (HEI), sponsored a test to predict the NCG handling capacity of the suction pressure and discharge pressure handling capacity. The results of the test were published in 1951 and incorporated into the HEI Standard for SJE as entrainment ratio curves.

The HEI procedure for using curves does not simplify and standardize load calculations for SJE. This procedure can have several disadvantages such as the absence of NCG-specific heat and the specific heat ratio of the correlation, as well as the neglect of the SJE dimension. But this weakness is compensated by the simplicity of the method. To model some also different conditions.

The determination of the NCG massed to flow rate and the suction and exhaust pressure on the SJE is the most flexible procedure for determining the amount of vapor required to operate the SJE. This curve can change the NCG at any temperature in DAE (dry air entrainment) which is the main parameter to determine the steam consumption of the steam release stage. DAE means the constituent composition of a substance, which in this case DAE consists of steam H2O and NCG in a particular composition.

If the NCG to be extracted from the SJE system is a mixture of steam and other gases, This should be done separately and then added to get the DAE value, then the first step is to calculate the vapor equivalent value, the NCG equivalent value and Finally the DAE is the sum of the two values.

The first step is to convert the vapor extracted from the condenser to an equivalent of 70°F. This is done by using correction factors of the weight ratio of entrainment molecules and temperature.

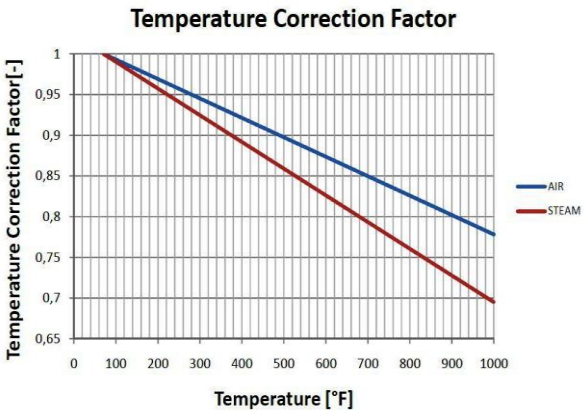

Fig. 4: ***Temperature correction Factor*** **(HEI, 2000)**

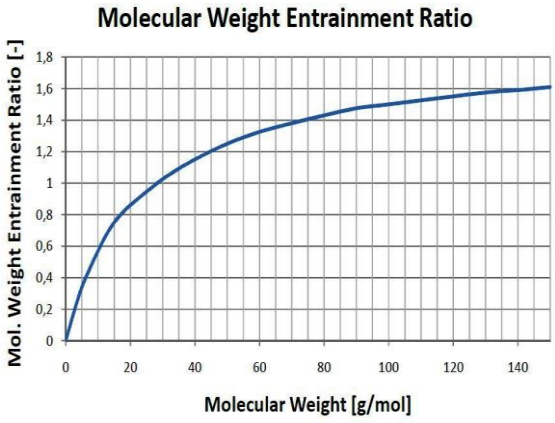

Fig. 5: ***Molecular Weight Entrainment Ratio*** **(HEI, 2000)**

For temperature correction it is necessary to compare the temperature of the entrainment to determine the equivalent air flow. This can be done using the Figure of, entering the graph with a steam temperature at °F and cutting the steam line to obtain the correction factor value of the y-axis. Correcting after the temperature values it is necessary to calculate the weight entrainment ratio value of the figure of, using the molecular weight of water (vapor) 18.02, and entering the graph from x-axis to curve, is performed to read the entrainment weight. The value of the y-axis.

Then the steam into the equivalent air is calculated by:

$$\mathrm{DAE}_{\mathrm{h20}} = \frac{\acute{m}_{\mathrm{h20}}}{\mathrm{TCF}_{\mathrm{h20}} * \mathrm{WER}_{\mathrm{h20}}} \quad (1)$$

The non-condensable gases in this case the NCG is assumed to consist of 100% CO2 in fact the CO2 content of the measurement data is about 98%. For then the NCG equivalent calculation, the procedure according to HEI is similar to the vapor equivalent calculation, Only in this which case is necessary first to fix the weight of CO2 into the NCG equivalent using Figure molecular weigh entrainment ratio and then fix the temperature of NCG using °F equivalent by using the temperature correction factor of the Image temperature correction factor.
Then the CO2 airs equivalent is calculated by:

$$\mathrm{DAE}_{\mathrm{CO2}} = \frac{\acute{m}_{\mathrm{CO2}}}{\mathrm{TCF}_{\mathrm{CO2}} * \mathrm{WER}_{\mathrm{CO2}}} \quad (2)$$

Finally the total steam equivalent is the addition of DAE steam and DAE NCG values.

$$DAE = DAE_{CO2} + DAE_{H20} \quad (3)$$

Once DAE is determined, it is necessary to calculate the amount of vapor required to suck NCG from the condenser, this is done by using the ratio of air to vapor, which determines the amount of vapor required to remove a certain amount of NCG. Under certain pressure conditions. This pressure condition is related to the steam mass flow rate entering the SJE, the SJE NCG suction pressure and the SJE release pressure.

The ratio of NCG to steam is obtained from the graph shown in the figure of air to steam ratio, the input data is the compression ratio (CR), and the expansion ratio (ER) defined as:

$$CR = \frac{P_{dis}}{P_{suc}} \quad (4)$$

$$ER = \frac{P_{ms}}{P_{suc}} \quad (5)$$

For this case it is important to note that in the event of pressure velocity mass flow rate entering the *SJE, SJE NCG* suction pressure and *SJE* release pressure. Each then stage has the same compression ratio, and the expansion ratio is the same as well.

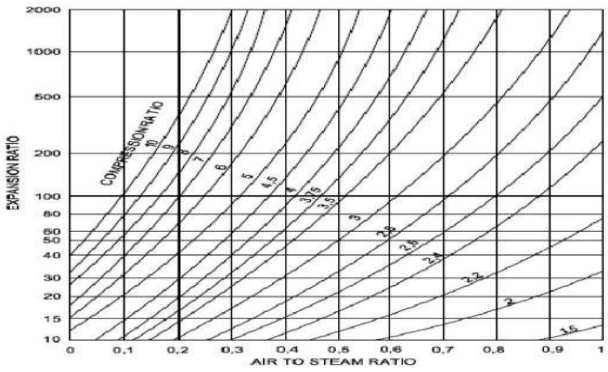

Fig. 6: ***Air to Steam Ratio*** **(HEI, 2000)**

Eventually the consumption of steam (SC) for each stage in SJE is defined as

$$SC = \frac{DAE}{AS} \quad (6)$$

Pressure into SJE (motive steam) and condenser will affect the compression and expansion ratio, thus modifying the ratio of air to vapor and steam consumption. These parameters can greatly affect the amount of vapor consumed at each stage of the SJE system.

When non-condensable gases are removed from the condenser, some vapors are also carried out along with the NCG, as they are mixed in the condenser. The suction pressure on the SJE is at least 0.01 bars lower than the condenser pressure assuming a constant pressure drop between the condenser and the GRS system. (Pálsson, 2010). The design parameters are:

- The steam mass flow rate entering the turbine is 101,44 kg/s.
- Percentage of NCG at 3%.
- SJE or Psuc suction pressure of 0.09 bar.
- SJE or Pdis out pressure of 0.14 bar.

Temperature interconnected 38°C.In determining the required power an LRVP can work required some design parameters in suction pressure, discharge pressure, mixed mass flow rate, inter-condensor temperature and NCG concentration. To calculate the electrical energy requirements required to turn on one LRVP the following formula is used (Siregar, 2004):

$$W_{lrvp} = \left[\frac{\gamma}{\gamma-1}\right] * \frac{\acute{m}_{mix} * R * T_{mix}}{\eta_{lrvp} * M_{mix}} * \left[\left(\frac{P_{dis}}{P_{suc}}\right)^{1-\frac{1}{\gamma}} - 1\right] \quad (7)$$

5. SIMULATION

The simulation is done in two configurations with the help of software cycle tempo 5.0. After obtaining a manual calculation of the concentration of NCG, and steam consumption wasted in SJE and then incorporated into the simulation. Configuration 1 modeled the stage 1 GRS (SJE 40% and SJE 60%). On stage 2 uses LRVP 2x65% Capacity.

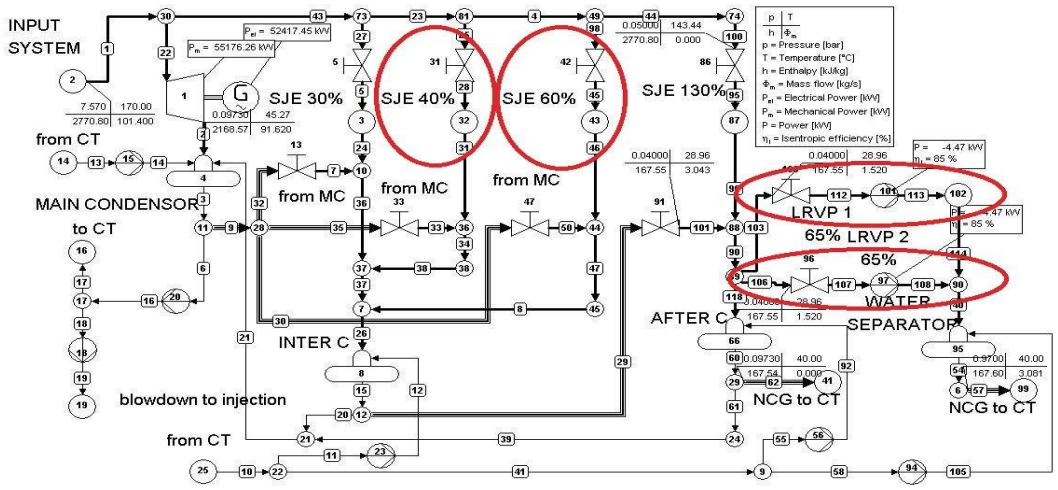

Fig. 7: Simulation results at NCG 3% in configuration 1

Configuration-2 modeled the stage 1 GRS (SJE 40% and SJE 60%). On stage 2 using (SJE 130%) everything is on.

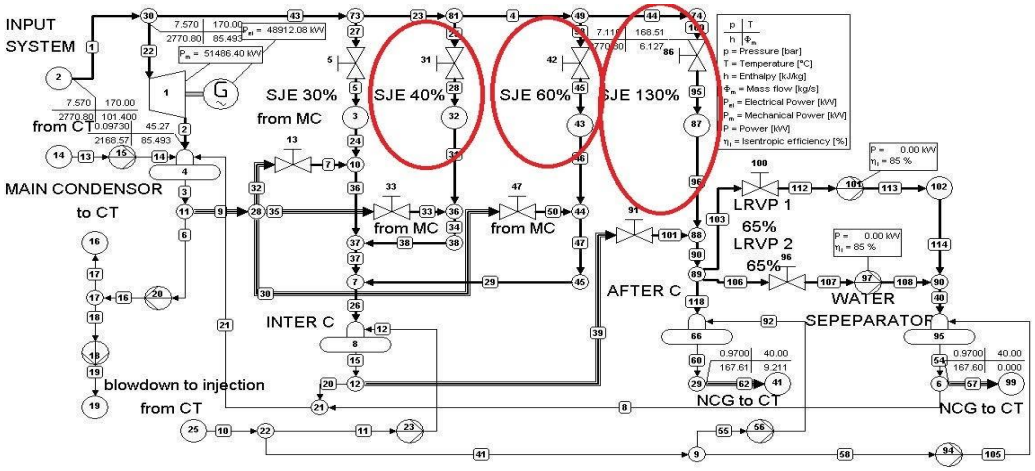

Fig. 8: Simulation results at NCG 3% in configuration 2

The simulation result shows at table 2.

Table 2: Simulation results for Configuration 1 and Configuration 2.

No	NCG (%)	M Uap	M NCG	P In (bar)	ΔP condensor (bar)	P condensor (bar)	Power System (MW)	
							LRVP ON SJE OFF	SJE ON LRVP OF
1	0,0	1,000	0,000	7,570	0,0000	0,0945	58,305	58,305
2	0,5	0,995	0,005	7,570	0,0005	0,0950	57,317	56,721
3	1,0	0,990	0,010	7,570	0,0009	0,0954	56,332	55,146
4	1,5	0,985	0,015	7,570	0,0014	0,0959	55,343	53,570
5	2,0	0,980	0,020	7,570	0,0018	0,0963	54,369	52,013
6	2,5	0,975	0,025	7,570	0,0023	0,0968	53,390	50,458
7	3,0	0,970	0,030	7,570	0,0028	0,0973	52,417	48,912
8	3,5	0,965	0,035	7,570	0,0032	0,0977	51,458	47,384
9	4,0	0,960	0,040	7,570	0,0037	0,0982	50,495	45,858
10	4,5	0,955	0,045	7,570	0,0041	0,0986	49,548	44,349
11	5,0	0,950	0,050	7,570	0,0046	0,0991	48,596	42,842
12	5,5	0,945	0,055	7,570	0,0051	0,0996	47,648	41,345
13	6,0	0,940	0,060	7,570	0,0055	0,1000	46,715	39,864

6. ANALYSIS

After performing manual calculations for the NCG mass to flow rate, and mass to flow rate of steam-driving consumption of the SJE, then from the calculation, after collecting all the calculation results from the increase of each NCG 0,5% from NCG 0% to NCG 6%.

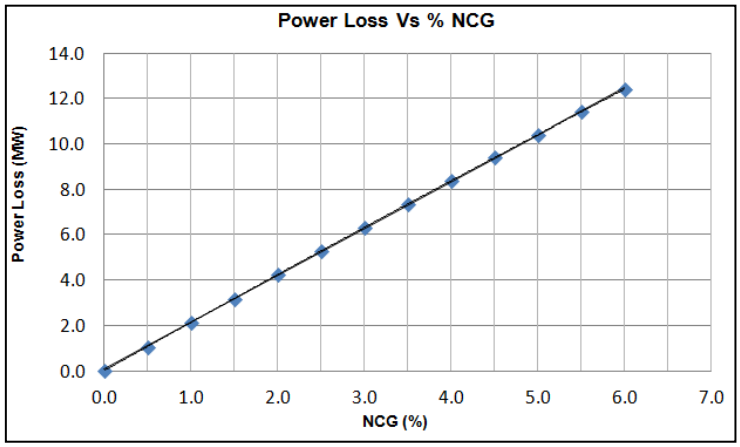

Fig. 9: The power loss to the increased of NCG

% NCG has very significantly influence on the system power loss. From the results obtained from Figure 9 shows the loss of power in the GPP system due to losses caused by GRS stage 2 installed capacity of SJE 130%, at the opening of GRS stage 1 (SJE 40% and SJE 60%) up to 12.617 MW maximal at concentration increases to 6%. With NCG 3 %, the system will be 6.423 MW reduced power. The power loss is approximately 2 MW per 1% increased NCG.

Figure 10 shows the influence of % NCG to the Power of GPP System

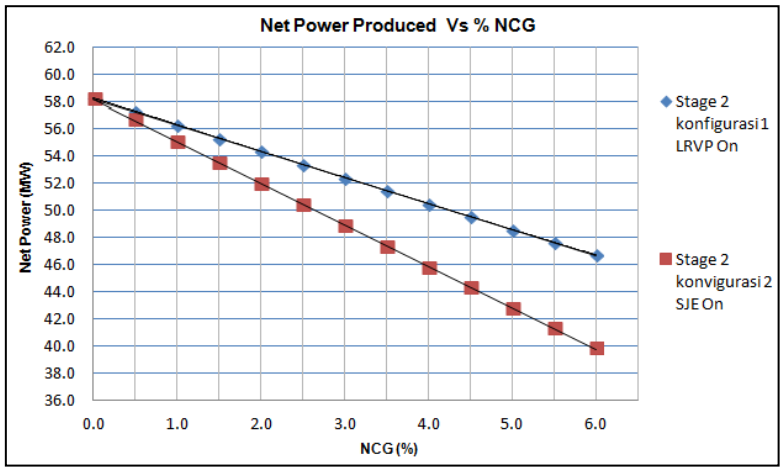

Fig. 10: Net Power Produced to the increase in NCG

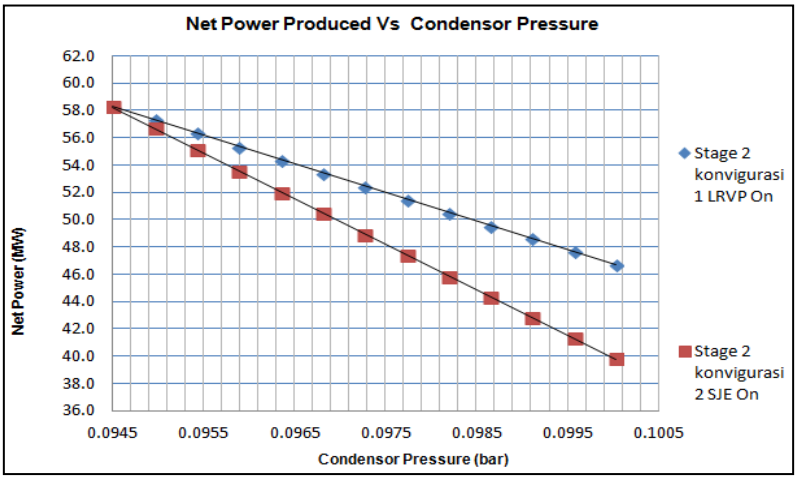

Fig. 11: Net Power Produced to the increase in NCG

With a mixed mass vapor flow rate of 104,4 kg/s and 1 % NCG, Configuration-1 can generate power of 56.332 MW and Configuration-2 produces 55.146 MW of power. Configuration-1 is better at saving power in the in-house power of GPP using LRVP 2x65% capacity of discharging consequences, This can be seen when the concentration of NCG increases to 6% system power produces 46,715 MW. Configuration-2 is worse in saving

power in the in-house power of GPP, because it uses SJE 130% with the consequence of discharging the steam to suck the NCG present in the condenser. This can be seen when the concentration of NCG increased to 6% system power output 39.864 MW. When the concentration of NCG above 0.5%, then the use of LRVP is better compared to SJE.

7. CONCLUSION

1. GPP system modeling can be simulated using software cycle tempo 5.0 by adjusting the input parameters that exist on the technical specifications of existing equipment in software cycle tempo 5.0.
2. The simulation of Configuration 1 and Configuration 2, configuration 1 is better at saving power for GPP systems capacity of 55 MW in the face of 3% NCG concentration.
3. For NCG less than 0.5% using Configuration 1 on stage 2 is better in system performance than using configuration 2 on stage 2.
4. For NCG concentrations greater than 0.5% using configuration-1 on stage 2 save more powers than using configuration 2 on stage 2.
5. For every 0.5% NCG concentration increase using configuration-1 is better in performance of GPP system than configuration 2.
6. For NCG concentrations of 0.5%-6%, the use of LRVP in stage 2 is better in system performance compared to using SJE.

8. NOMENCLATURE

DAE_{h2o} : Dry air constituents from H_2O [kg/s]
DAE_{co2} : Dry air constituents from CO_2 [kg/s]
h. : Entalpi [kJ/kg]
$\acute{m}_{co2}$: Mass flow rate of CO_2 [kg/s]
$\acute{m}_{h2o}$: Mass flow rate of steam [kg/s]
$\acute{m}_{ncg}$: Mass flow rate of NCG [kg/s]
$\acute{m}_{mix}$: Mass flow rate of NCG and steam [kg/s]
M_{ncg} : Mole mass NCG [kg/kmol]
M_{h2o} : Mole mass steam [kg/kmol]
M_{mix} : Mole mass NCG and steam [kg/kmol]
P_{cond} : Condenser pressure [bar]
P_{IC} : Inter condenser pressure [bar]
P_{ms} : Push Pressure of steam jet ejector [bar]
P_{suc} : Inside Pressure of steam jet ejector [bar]
P_{dis} : Outside Pressure of steam jet ejector [bar]
R : The ideal gas constants [J/mol K]

S : Entropi [kJ/kg.K]
T_{co2} : Temperature [°F]
T_{h2o} : Temperature [°F]
T_{mix} : Mix temperature of interkondensor [°K]
TCF_{h2o} : Temperature correction factor of steam [-]
TCF_{co2} : Temperature correction factor of NCG [-]
WER_{co2} : The carrying mass ratio in CO_2 [-]
WER_{h2o} : The carrying mass ratio in H_{2O} [-]
W_{Pompa} : Power pump [kW]
W_{Turbin} : Power steam turbin [MW]
W_{Sistem} : Power system [MW]
η : efisiensi [%]
γ : Gamma: Cpgas/Cvgas [-]
GPP : Geothermal Power Plant.
SPP : Solar Power Plant.
WPG : Wind Power Generation.

9. REFERENCES

Moran., N. Shapiro., 2006. Fundamental of Engineering Thermodynamc. Fifth edition. Jhon Wiley & son.

Cengel, Y., Boles, M., 2006. Thermodynamics and engineering approach. Fifth edition. McGraw Hill.

Saptadji., Miryani N., 2012. Teknik panas bumi. ITB. Bandung.

PT. Geodipa energi., 2015. Dokumentasi. Pembangkit Listrik Tenaga Panas Bumi PATUHA unit 1. Jakarta.

PT. Indonesia Power., 2014. File Presentasi. Pembangkit Listrik Tenaga Panas Bumi Darajat. UBP Garut.

Perry, R.. 2008. Chemical engineering handbook. Eighth edition. McGraw Hill.

Heat Exchange Institute., 2000. HEI standards for steam jet vacuum systems. Fifth edition. Heat exchange institute Inc.

Siregar, P., 2004. Optimization of electrical power production process for the Sibayak geothermal field, Indonesia. Geothermal training programme reports. UNU-GTP.

Cycle Tempo 5.0., 2010. Simulation Heat Mass balance. Delft university of Tecnology (TU Delft)

Pálsson, H., 2010. Utilization of geothermal energy for power productions. Geothermal power development lecture notes. Iceland University. Iceland.

DiPippo, R., 2008. Geothermal power plants, principles, applications, cases studies and environmental impact. Second edition. Elsevier science.

Proceedings of the 1st Faculty of Industrial Technology International Congress
International Conference
Bandung, Indonesia, October 9-11, 2017
ISBN 978-602-53531-8-5

The Development of Investment Casting Technology for the Manufacture of Import Substitution Casting Products by Using of Local Raw Materials

Hafid[1,*], T. Taryaman[2], S.B. Pratomo[3]
[1,3] Metal Industies Development Centre (MIDC) - Ministry of Industry Indonesia
Jl. Sangkuriang No. 12 Bandung 40135
[2] Foundry Engineer and Consultant Foundy
Corresponding author e-mail : hafidochan@yahoo.com

Abstract

The development of investment casting technology for the manufacture of import substitution casting products by using of local raw materials has been done. Compared to the conventional casting process, investment casting has the advantage of being able to create a complex casting product and produce a product that is near net shape so that it is no need machining process. The objective is as an effort to find an alternative method of making a quality casting product, has high added value with the utilization of local raw materials available in Indonesia so as to reduce the cost of production and dependence on imports of industrial raw materials which are very expensive in the investment casting process. The method of making casting products with investment casting process, including: pattern making, mould making, dewaxing, melting, pouring, finishing and testing. Investment casting technology has been successfully applied to the manufacture of rocker arm, impeller pump and turbine blade with the utilization of local raw materials ie: epoxy resin as a substitute for metal pattern, mixture wax of paraffin and celo resin for the pattern of wax and zircon sand of Bangka as coating slurry for ceramic mould. The discussion of this paper is expected to be a case of developing other casting products needed by Indonesia for industry: medical equipment, agricultural equipment, textile equipment, gun and small armaments, electronics, automotive and electrical components etc.

Keywords: investment casting, epoxy resin, wax pattern, zircon sand, ceramic mould

1. Introduction

Investment casting (Soemardi T.P, et al. 2016; D.L. Datta, 2014) is one type of precision casting technology that has advantages, namely: (1) can produce a casting product with complex geometry specification (Bemblage and Benny, 2011) and almost does not require machining process as conventional casting process, (2) compared to the forging process (Hafid, et al, 2002) can make the product complex and high surface smoothness, can also save the cost of dies making process because to make one product requires five to six times the forging process, (3) casting products produced generally using materials that have high hardness resulting in good product quality, increase productivity and has high added value.

The weakness of the investment casting process is a maximum casting product size of about 5 kg, investment and high production costs, compared to other processes, cost of dies making for expensive patterns, there are some complicated process steps and need to be automatic, foundry cost should be proportional to machining cost when done with other casting process (Parkinar, S.K, 2014; MIDC, 2007).

Investment casting process is one of the oldest metal forming techniques. Its origin can be traced back to 5000 years and was first used in China and Egypt. This manufacturing technique is also know as the lost wax process (Chalekar et al, 2015). Traces its roots to the Sang Dynasty in China from 1776 B.C. to 112 B.C. The method was brought into modern industrial use when American manufacturers applied investment casting to make high quality military parts during World War II. It was found practical for many wartime needs - and during the postwar period it expanded into many non-aircraft applications. Today, investment casting is recognized and used worldwide as a technique for producing close-tolerance metal parts at highly competitive costs (www.spmb.com, 2017).

Casting products that can be produced by investment casting are needed by Indonesia and widely used in various industries, such as automotive, oil and gas, agriculture, textile, electronics, electrical components, weapons/military, health/orthopedies, ornament and jewelery/silver) (Parkinar, 2014), construction, aircraft components, steam turbines and so on (Hafid,2013). More details can be shown in Fig. 1 (Rita, 2012; www.spmb.com, 2017).

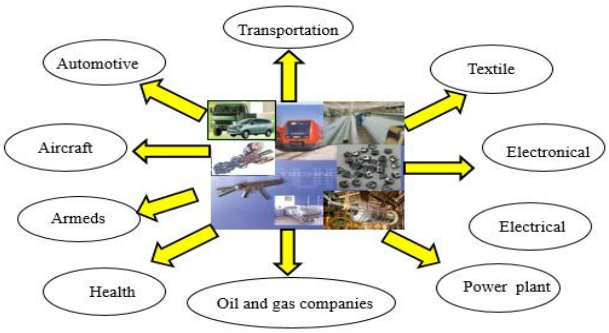

Fig. 1: The application of investment casting products

But in conducting investment casting process technology, foundry industry is still very large dependence on imported raw materials. This causes the selling price of casting products to be high so that the technology is considered expensive. This can be seen from the at least national foundry industry engaged in the field.

Indonesia is a country with abundant natural resources (Adid et al, 2015) which is contained in it is controlled by the state and used for the greatest prosperity of the people and improve the welfare for all the people of Indonesia as stated in the mandate by article 22 of the 1945 Constitution (Anonymous, 2012). Potential natural resources that are likely to be utilized as local raw materials in the investment casting process in order to reduce the cost of production economically is the use of local wax and sand for wax patterns and ceramic molds and epoxy resin material as a substitute for metal patterns.

There is an assumption that the investment casting process is a foundry process using high technology that is very expensive, it can be broken because after being studied the technology can be simplified by MIDC which is an R & D institution owned by the Ministry of Industry of Indonesia. Imported raw materials that are still imported can be substituted with raw materials made in Indonesia. In fact, machines and equipment can also be transferred to home-made products.

As an effort to reduce the dependence on the need of imported and hard-made components (spare parts) by conventional casting process, MIDC has conducted R & D in the investment casting field, its tasks and roles must be able to translate, transfered and socialize the investment casting process loaded with new technology to industry small and medium enterprises casting to improve competitiveness to meet the needs of domestic precision casting products (Anonymous, 2012).

The breakthrough to overcome the dependence of the national foundry industries on imported raw materials, this research was conducted in order to create high quality casting products with high added value with the utilization of local raw materials available in Indonesia. It is expected that with the dissemination of investment casting technology that can use local raw materials to SMEs, the foundry will reduce the dependence of various industrial sectors as mentioned above from the invasion of imported casting products.

2. Methodology

The research methodology was conducted through the following steps:

1. Materials and Equipment

The materials used for the investment casting process are as follows: (a) metal material for casting products, (b) epoxy resin FMSC 935, (c) imported wax (filler NF 411 and non filler NC 586) and local wax (mix of paraffin RRT and resin cello), (d) sand zircon import (20 mesh, 70 mesh, 150 mesh) and local zircon sand (350 mesh and 200 mesh), (e) other auxiliary materials: wetting agent, surface active agent, defoamer, acetone, silicone spray.

The machines and equipment used are: (a) wax injection machine, (b) slurry mixer, (c) slurry tank, (d) fluidized bed, (e) de wax vessel, (f) compressor (g) induction furnace capacity 250 kg, (h) burning furnace, (i) impact testing tool (charpy testing machine), (j) zahn cup.

2. The working stages

The working stages in the investment casting process include (Chalekar et al, 2015; DL Datta, 2014; Parkinar, SK 2014; www.trieka.co.id; Hafid, et al., 2010, 2012; www.turbo-cast; www.investment-casting):

a. Dies making from duralumin metal to save the cost of used epoxy resin material.
b. Preparing tools and raw materials for wax molds and ceramic molds

c. Making a wax pattern with wax injection machine.
d. Cleaning the wax pattern with acetone for slurry (zircon sand material and other auxiliary materials) can be attached to the pattern.
e. Assembly a wax pattern into a cluster.
f. Making primary slurry and secondary slurry
g. Dipping the cluster that has been assembled into the slurry continued sanding to be a ceramic mold with a thickness of ± 1 cm.
h. Remove the wax from the ceramic mold by heating at ± 100ºC.
i. Burning ceramic molds followed by preheat process on ceramic mold.
j. Prepare material for melting as per casting product specification to be made.
k. Melting metal material reaches the melting point of the metal used.
l. Pouring the molten metal from the induction kitchen into the ladle.
m. Pouring the metal liquid from the ladle into the mold
n. To knock out and clean the ceramic molds continued cutting into casting products.
o. Visually inspect casting products for defective/defective casting products re-incorporated into the fuser as raw material of liquid metal.
p. Testing: chemical composition, hardness and metallography.
q. Analyze and discuss the research results
r. Conclusing and making suggestions.

To get a clearer picture of the investment casting process steps shown in Fig. 2.

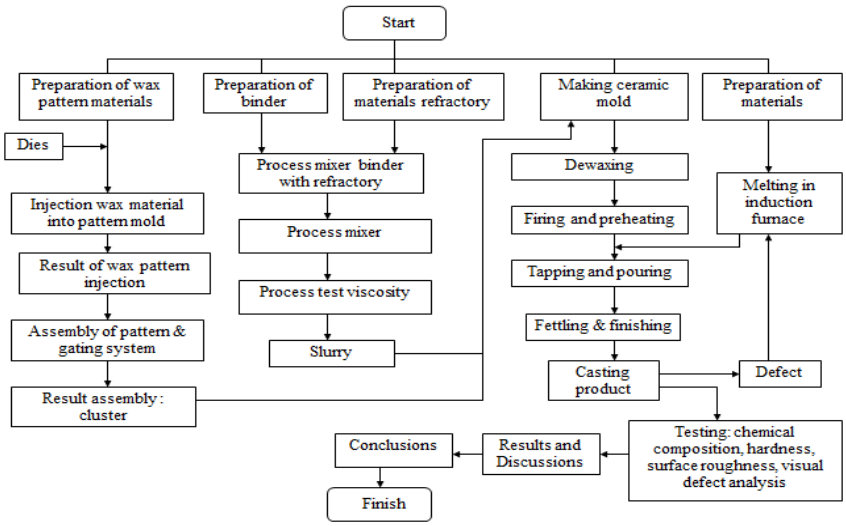

Fig. 2: Flow chart of metodologies research

3. Result and Discussion

3.1. Investment Casting Tehnology

In this research, there are several important steps in investment process:

1. *Dies* Making

Pattern dies used is made of aluminum metal machining process. However, in this study used epoxy resin FMSC 935 with consideration:

a. Molds making of FMSC 935 epoxy resin material requires a relatively faster machining time compared to using metal materials.
b. The required cost is cheaper than the mold of aluminum metal (Al)
c. The process of making the mold is relatively cheaper.

2. *Pattern Making*

The material used for pattern making is wax because the wax characteristics have a liquid temperature and a low viscosity of liquid (Hafid et al, 2009). This condition allows the wax to be mixed, injected, assembled and melted out of ceramic mold. The wax used in this study is imported wax (filler 411 and NC 586) and local wax (beeswax, resin wax, carnauba wax, paraffin wax) (A. Wahid et al, 2000; Bemblage and Benny, 2011; Parkinar, SK 2014). Fig. 3 shows the wax pattern of the injection results.

The process of injection of wax into pattern mold (dies pattern) using injection wax machine capacity of 5 ton grant from National Institute of Advanced Industrial Science and Technology (AIST) Chubu Japan. The best parameters to be controlled during wax injection time into the pattern mold are wax temperature (± 64°C), nozzle

temperature (± 30°C), injection pressure (1.75 Mpa) and injection time (15 seconds) (Hafid, 2013). To get the best pattern, then when the first injection first need heated dies.

3. Making of ceramic mold

In this research, the utilization of local sand zircon from P. Bangka as one of the alternative raw material of imported sand zircon. Ceramic mold making process is done by coating the cluster with slurry. After being drained for a while, clusters that have been coated with slurry are immediately scattered with zircon sand until the entire cluster is covered by a zircon (Fig. 4). After drying process at room temperature, this process is repeated several times until the desired ceramic thickness (between 0,25 to 0,5 inch) is obtained.

In the manufacture of ceramic mold used 2 types of slurry, the primary slurry and secondary slurry. Stages of manufacture are as follows:

a. Primary *slurry*:

Zircon sand material from P. Bangka the 325 mesh pound that has been ground into a slurry container. Add colloidal silica, surface active agent and defoamer into the container and then stir with a continuous mixer until homogeneous. Calculate the slurry viscosity by means of zahn cup no 4 with a viscosity time of 43 seconds (standard time of 40 second viscosity). The result is the primary slurry solution can be attached well to the cluster of wax patterns then drained a few moments and directly scattered sand zircon P. Bangka 200 mesh. The coating process with primary slurry is only done once. Cluster is dried at room temperature minimum 12 hours.

b. Secondary *slurry*:

Making it the same as primary slurry just does not use surface active agent and defoamer. Calculate the viscosity of about 10-12 seconds. Then cluster wax pattern coated/immersed into secondary slurry, after drained a few moments immediately scattered sand zircon Bangka 200 mesh. After drying between 5 - 7 hours then repeated the same process again. Furthermore the secondary slurry process is repeated again as much as 4x up to 7x again with the sand dissipated are: 200 mesh, 150 mesh, 70 mesh, and 20 mesh. Drying process at each process for at least 5 hours. Finally after the above process is done, before the dewaxing process the whole cluster first coated once again with secondary slurry and dry at least 1 day.

Fig. 3: Wax pattern of the injection results

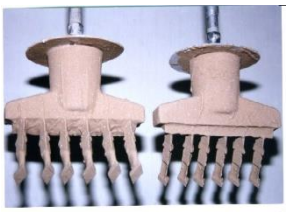

Fig. 4: Ceramic slurry made of domestic zircon sand

4. Dewaxing

Eliminating the wax pattern from ceramic mold is called dewaxing, its processing through 2 stages, namely: (a) warming wax pattern by using fire that burns until wax melts and out of gating system, (b) to remove wax which still attached after first stage used de wax vessel. Then the mold is immersed in de wax vessel containing water with a tempetarur around which is set to reach 110^{o}C with the condition of the gating system at the top. Allow a few moments until the remaining wax is lifted entirely to the surface of the water.

5. Firing dan Preheating

Heating ceramic molds at a temperature of 1,000^{o}C for 2 hours in a firing furnace with diesel fuel as preheating before pouring. Firing process is a sintering ceramic mold for increased strength. The thing to note is that the temperature used for firing is adapted to the type of melting material and the amount of casting products as well as the thickness of the ceramic molding wall. This firing process other than as preheating to ceramic mold, as well as the process of removing the remaining wax that is still slightly attached to the ceramic wall.

6. Melting

The melting is done in the induction kitchen of 250 kg capacity to reach the melting point of the metal used. The process of pouring liquid metal from the kitchen into the ladle is then poured into a mold that is still in a hot state until the liquid metal fills the entire mold cavity which is then left to stand still to freeze and cool.

7. Mold removal

After the pouring is finished and the molten metal poured into the ceramic mold frozen then carried out the mold removal and cleaning of casting products. After clean casting of ceramics then cutting casting products. Casting

products results (rocker arm, impeller pump, turbine blade, etc) by using investment casting can be shown in Fig. 5.

8. Testing of casting product

In this research, we have done several tests on the result of casting product: (1) chemical composition, (2) metallographic test done to see microstructure from samples of casting (3) surface hardness test (4) surface roughness test and (5) dimensional checking and (6) visual defect analysis based on casting product observation results.

Fig. 5: Casting product results by using investment casting

3.2. Potential of Local Raw Materials

To realize the independence of technology by increasing the added value of local natural resources, the potential of quartz sand reserves in Indonesia is very abundant in the areas of P. Bangka and Belitung, Rembang (Central Java), Tuban (East Java) and Sintang, Melawi, Pangkalan Bun and Kumai (West and Central Kalimanten). Local Silica fuse can be used in the process of making ceramic molds because the characteristics of silica sand (SiO_2) fulfill the requirements as raw material for the manufacture of silica fuse because it has SiO_2 content above 99,5% and Fe_2O_3 content below 0,05%. The selection of silica fuse instead of zircon flour can reduce the cost of production because it is much cheaper (Hafid, et al. 2012; S.B. Pratomo, et al., 2014).

In order to obtain a good casting product, the zircon sand utilized for casting process should has a ZrO_2 content not less 64%. Testing reveated that ZrO_2 content of Bangka is only 28.29% so that we (the researcher) suggest that Bangka is not good to be used as primary slurry because it will contact directly metal fluid, but it can be used as sand materials during sanding process (Hafid, 2013).

The local wax raw materials that can be used for candlestick patterns are paraffin, damarselo and arpus mixtures, as well as the ratio of paraffin, carnauba and wax (60%; 20%; 20%).

4 Conclusion

The development of investment casting technology for the manufacture of import substitution casting products by using of local raw materials has been done, namely: local silica and zircon sand for ceramic mold, mixture wax of paraffin and cello resin for the pattern of wax, epoxy resin as a substitute for metal pattern (dies). Local fused silica can be used for making ceramic molds because it has SiO_2 content above 99.5% and Fe_2O_3 levels below 0.05%. Bangka zircon sand can be used for sanding process because the testing result has ZrO_2 content of about 28.29% (minimum standard 64%) and can not be recommended for primary slurry material because it will experience direct contact with metal liquid. Mixture wax of paraffin and cello resin can be used for pattern of wax with optimal injection temperature (64^{o}C), nozzle temperature (30^{o}C), injection pressure (1.75 Mpa) and injection time (15 seconds). Need to the development other precision casting products making for industrial needs: medical devices, automotive, oil and gas, textiles, electronics, electrical components, weapons/military, health/orthopedies, ornament and jewelery/silver) and so on.

5. Acknowledgements

The authors would like to thank: (1) The Director, management and MIDC foundry technicians of the Ministry of Industry in particular to A. Wahid PhD, Mr. Mario, Mr. Dedy S., Mr. Rahmat who has provided to give opportunities for research and also his advice and suggestions during the research, (2) expert judgment of: PT. Trieka Aimex (Mr. Gunawan Lukito & Mr. Iyus Yusuf), PT Karya Deli Steelindo (Mr. Roni and Mr. Pander Sitindaon), PT. Pindad (Mr. Rohendi), (3) all those who can not be mentioned one by one who have contributed the successful completion of this research.

6. References

A.A. Chalekar, S.A. Daphal, A.A. Somatkar, S.S. Chinchanikar. 2015. Minimization of investment casting defects by using computer simulation – A Case study. Journal of Mechanical Engineering and Automation 2015, 5(3B): 43-46 DOI: 10.5923/c.jmea.201502.09. India, pp. 43

Adid A. Hermansyah, Kosasih and Hafid. 2015. Research on the manufacturing process of concentrates and ingot of copper from Cu mineralized rock as import substitution. Journal of Industrial Technology Research. Vol.9 No.1 June 2015. ISSN 1978-6891, Industrial Research and Standardization Center of Samarinda. pp. 20.

Abdul Wahid dan Mitsuo Ninomiya, Mitsuo, 2002. Precission casting technology, Joint Research between National Industrial Research Institute of Nagoya (NIRIN) Japan and Institute for Research and Development of Metal and Machinery Industries (IRDMMI) Indonesia, Nagoya, Japan. pp. 6.

Anonymous, 2012. Impact analysis of the prohibition on export policy of raw materials of minerals and minerals, Agency for the Assessment and Development of Trade Policy of the Center for Foreign Trade Policy, Jakarta, pp.4.

Anonymous, 2007. Guidance on waste pollution handling in the foundry industry. Metal Industries Development Center (MIDC), Ministry of Industry Indonesia, Bandung. pp. 16-17.

G.L. Datta. 2014. Reinventing investment casting process for sustainable development, Indian Foundry Journal. Vol.60, No.6 June, 2014. Kolkata India, pp. 22, 23.

Hafid, Sri Bimo Pratomo and Sony H.2014, The development of process technology of track link tank scorpion to countermeasure defects at casting product, Journal of Industrial Research, Vol.8 No.1, April 2014 ISSN:1978-5852, Ministry of Industry Indonesia, Jakarta. Pp. 2,3.

_____,. Tatang Taryaman, A. Wahid and Mitsuo Ninomiya. 2002. Research on the manufacture of rocker arm products for automotive components from austempered ductile iron (ADI) materials by using investment casting technology. Journal of Metal Indonesia. Vol.024/2002. ISSN 0126-3463. Metal Industries Development Center (MIDC), Ministry of Industry Indonesia, Bandung.pp. 9.

_____,. 2013. Research on the manufacturing of steam turbine blade by using investment casting technology. Advanced Materials Research. Vol.789. ISSN: 1022-6680, ISSN/ISO:Adv. Mater.Res. Trans Tech Publications Ltd, Switzerland. pp.330.

_____,. 2013. MIDC Development Mapping: The Vision and Mission toward the Year of 2020, Final Report Government Internal Budget MIDC, the Ministry of Industry, Bandung. pp 1-1.

_____,. 2012. Research on material import substitution for ceramic molds by using investment casting, Proceedings of Scientific Meeting on Science and Technology 2012, ISSN: 1411-2213, BATAN Serpong, pp. 107-108.

_____,. Tatang T. and Abdul Wahid, 2009. Research on manufacturing of impeller pump product from Cu based by using investment casting technology, Journal Metal Indonesia. Vol. 31 No.2 December 2009, ISSN 0126 - 463, Metal Industries Development Center (MIDC), Ministry of Industry Indonesia, Bandung, pp. 76.

_____,. Tatang Taryaman, A. Wahid. 2010. Manufacture of import substitution casting products by using lost wax process. Proceedings of Metallurgical Materials 2010, pp.274-275.

Omkar Bemblage and D. Benny Karunakar. 2011. A Study on the blended wax pattern in investment casting process. Proceeding of the world congress on engineering 2011. Vol. I WEC 2011, July-8, 2011. ISBN: 978-988-18210-6-5, London UK. pp. 1.

Parkinar, S.K. 2014. An Innovation formula for investment casting process. Indian Foundry Journal. Vol.60, No.6 June, 2014. Kolkata India, pp. 28, 29

Rita Normila. 2012. Uji performa gas turbin engine Saturn T 1302 setelah proses overhaul. Journal of Metal Indonesia. Vol.34 No. 1. Juni 2012. ISSN 0126-3463. MIDC, Ministry of Industry Indonesia. pp. 54.

Sri Bimo Pratomo, Martin, Eva, 2014. Using the local zircon sand for ceramic mold of precision casting, Journal of Industrial Research, Vol. 8 No.1 April 2014, ISSN:1978-585, Ministry of Industry Indonesia, Jakarta. pp. 34.

Soemardi TP, Agri Suwandi, Ganjar Kiswanto, Widjajalaksmi Kusumaningsih. 2016. The effect of temperature increase, holding time and number of layers on ceramic shell usung the investment casting process. International Journal of Technology. ISSN 2086-9614, pp.1035.

Triswan Suseno, 2016. Analysis of zircon sand ($ZrSO_4$) processing cost to zircon sand $ZrO_2 \geq 65,5\%$ and micronized zircon, Mineral and Coal Technology Journal Volume 12, No 3, September 2016, TEKMIRA, Bandung, pp. 179 - 180.

Undang-Undang Dasar Republik Indonesia tahun 1945.

www.spvmb.com, accessed on august 29, 2017.

www.trieka.co.id, accessed on august 29, 2017.

www.karyadeli.com, accessed on august 29, 2017.

www.turbocast, accessed on august 29, 2017.

www.investment casting, accessed on august 29, 2017.

Proceedings of the 1st Faculty of Industrial Technology International Congress
International Conference
Bandung, Indonesia, October 9-11, 2017
ISBN 978-602-53531-8-5

Comparative Performance of Several Fixed Bed Dryer Arrangement for Seaweed Product Drying

Salafudin[1,*], Daren Ferreiro[2,*], Ronny Kurniawan[1], Nayl Diab[2]
[1]Department of Chemical Engineering, Faculty of Industrial Engineering,
Institut Teknologi Nasional Bandung
[2)]Student of Bachelor Study Program on Chemical Engineering
Dept. of Chemical Engineering, Faculty of Industrial Engineering, Institut Teknologi Nasional Bandung
[*]Corresponding author: salafudin2004@yahoo.com, daren.ferreiro@gmail.com

Abstract

Eucheuma cottonii is a type of seaweed that is widely available on the coast of Indonesia. Seaweed is processed into carrageenan types of Alkali Treated Cottonii to improve quality and sell higher. Carrageenan types Alkali Treated Cottonii contain water very much, so to obtain a high quality of Alkali Treated Cottonii, it would require the drying process by using the right tools, namely fixed bed dryer. The drying process uses such methods to obtain high energy efficiency tools with high quality carrageenan. This study aimed to compare the energy efficiency from a method of single fixed bed dryer, closed loop fixed bed dryer, and a series of fixed bed dryer. These results indicate that the method of series fixed bed dryer is the most effective method for drying carrageenan types ATC with the energy efficiency of 62.1653%; the rate of energy consumption amounted to 0.0100 kWh / min; the ability to evaporate the water of 26.6368 g / kWh.

Keywords: Drying, Alkali Treated Cottonii, Energy Efficiency, Single Fixed Bed Dryer, Closed Loop Fixed Bed Dryer, Series Fixed Bed Dryer.

1 Introduction

Seaweed in scientific language known as algae. Based on pigment contained, Eucheuma cottonii seaweed is a group Rhndopyceae (red algae) were capable of producing carrageenan was widely used in various industries. One of the popular seaweeds, Eucheuma cottonii, contains carrageenan for starch or fiber sources that can be applied for beverages or gelatin[3]. Carrageenan is used to thickeners, stabilizers, and gelling. Carrageenan is also used in the food industry to improve the appearance of the products, such as ice cream and jelly. The pharmaceutical industry uses carrageenan for the manufacture of drugs, syrups, tablets, toothpaste, shampoo, and so forth.

Carrageenan industry that was growing in Indonesia today is semi-finished carrageenan. One of them is the ATC (Alkali Treated Cottonii). ATC industry has had a complex equipment, especially in the drying process. Drying is arguably one of the most popular methods for preserving fruits, vegetables and other foods[1]. ATC drying process is commonly done today is sun drying and the disadvatages of sun drying is dependent on natural weather[4,5,6]. Because of this, the ATC has a water content of about 90% need to be dried with other drying methods[3]. Adsorption dryer with zeolite can be an option for seaweed drying. In this case, the air as drying medium was contacted with zeolite to remove the water content. With low relative humidity, the driving force for drying can be enhanced[3,4,7,9]. And the effects of air temperature and humidity on the drying time of seaweed have been done[8]. Thus, one of the main methods that can be used appropriately in drying is by appliance a fixed bed dryer[2]. This method was chosen because of the nature of the hydrogel ATC. Additionally, fixed bed dryer operated in single, series, and closed-loop. Therefore, Objective of this study was to compare the energy efficiency between single fixed bed dryer, closed loop fixed bed dryer, and series fixed bed dryer.

2 Methods

Fixed bed dryer in this study was equipped with a column as a place to put the ATC was channeled hot air as drying air. Fixed bed dryer using hot air as the media dryers and the material to be dried was contacted directly. The drying process in this study has the following variables:

1. Material used was carrageenan types of ATC (Alkali Treated Cottonii) of seaweed eucheuma cottonii.
2. ATC (Alkali Treated Cottonii) used by 80% of the height of the drying column.
3. Drying air flow rate was 498.0051 ml / s
4. The drying air temperature was 60ºC.
5. The method used is single fixed bed dryer, double fixed bed dryer, and a closed loop fixed bed dryer.

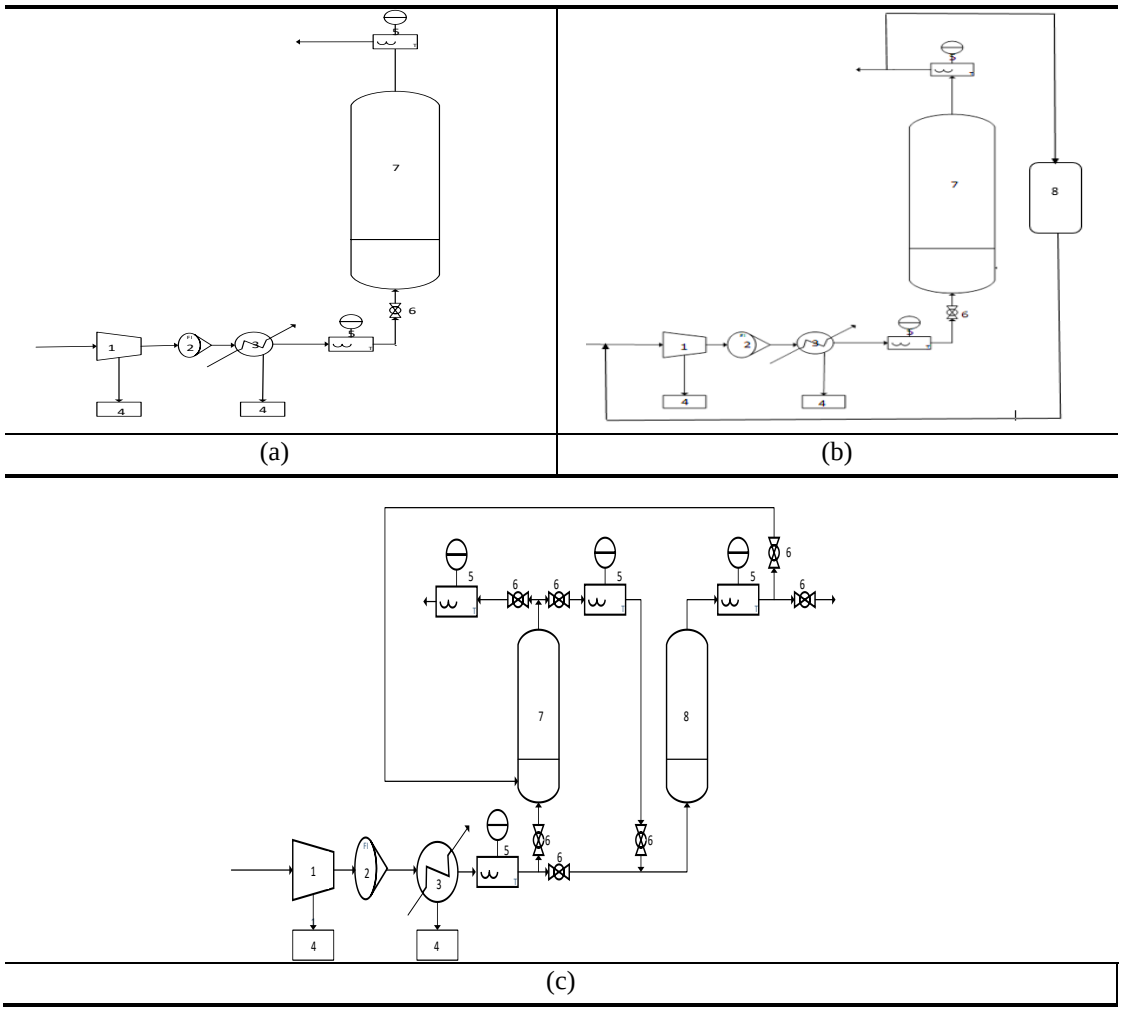

Fig. 1: (a) Schematic tool single fixed bed dryer (b) Schematic tool closed loop fixed bed dryer (c) Schematic tool series fixed bed dryer

There were little difference between a single method, closed loop, and series. The difference between a single and a closed loop that was the method of closed loop air was circulated back into the process after passing through the dehumidifier, while the single method, the air is thrown away. In the series method, the air coming out of the first column is used to dry the ATC in the second column.

3 Result and discussion

3.1 Effect of Drying Method to Decrease Relative Humidity Every Time

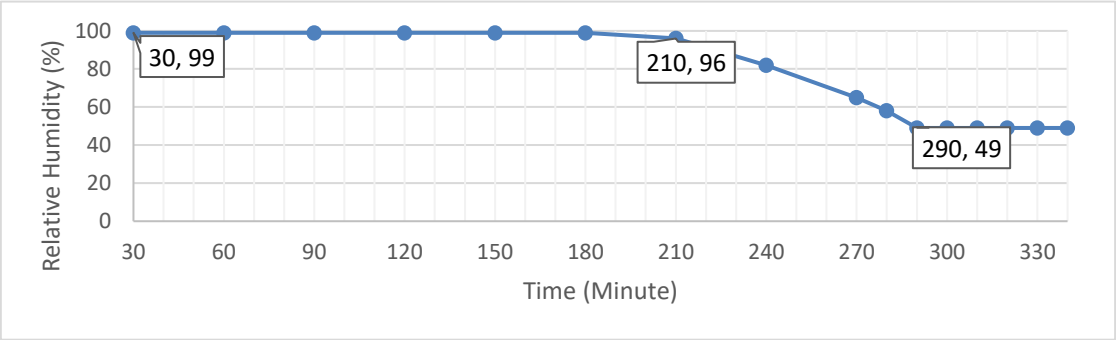

Fig. 2: Relative humidity against time on a single fixed bed dryer

In the Single fixed bed dryer, drying air relative humidity output at the start of the drying was 99% and no change to 180 minutes, because there were many water in ATC can be evaporated by the drying air. Then in 210 minutes, drying air relative humidity output fell to 96%, because the water contained in the surface of the ATC began few in number and difficult to be evaporated by the drying air, so that the water content in the drying air was getting low. Relative humidity of the drying air output continued to fall to 49% in 340 minutes of the drying process. In this method, the air coming out of the drying column still contains fairly low relative humidity and should not be just thrown away and can be used for further drying. Then, we conducted method of series fixed bed dyer.

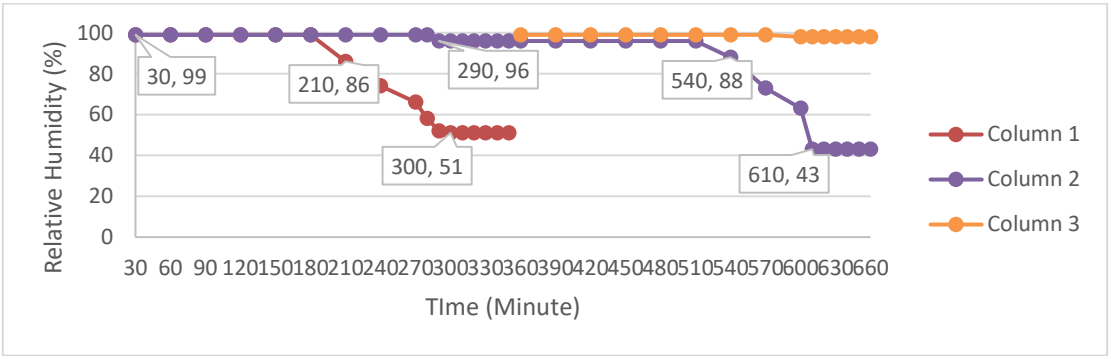

Fig. 3: Relative humidity against time on a series fixed bed dryer

In the method of series fixed bed dryer, drying air was passed in series from the first column to the second column. At the beginning of the process of drying, drying air relative humidity outputs of the first column and the second column was 99%. The process of drying at 30 minutes, only occurs on the first column, whereas, in the second column does not happen the drying process. This was because the relative humidity of the drying air at the output of the first column was worth 99% as a result of the amount of water evaporated from the ATC in the first column, so the ability of the air dryer to evaporate the water from the ATC in the second column was very small. In 210 minutes of drying, drying air relative humidity outputs of first column fell to 86% and the second column remains 99%. That was because water on the surface of the ATC in the first column were few in number and difficult to evaporate, so the drying process started in the second column, because the air drying has the ability to evaporate water from the ATC in the second column, although only slightly. Relative humidity of the drying air in the first column output continued to fall to 51% and was completed in 350 minutes of drying time, while in the second column of the drying air relative humidity at 96% output.

After the drying process in the first column was completed, the drying process was continued with the drying air was passed in series from the second column to the third column. The third column was the first column to be reused after the drying process was complete and filled back with wet ATC. In 360 minutes of drying, drying air relative humidity outputs in the second column was 96% and in the third column was 99%. In these circumstances, the drying process occurs in the second column and the third column, due to the drying air relative humidity outputs second column still has the ability to evaporate water from the surface in the third column. At 540 minutes

of drying time, drying air relative humidity outputs second column dropped to 88% and the third column was 99%. The relative humidity of drying air decreases the output of the second column caused by the water content in the surface of the second column ATC decreased, so the drying air has more ability to evaporate the water surface ATC in the second column. The drying process in the second column was completed in 660 minutes drying time with a relative humidity of the drying air output was 43% and the third column has a relative humidity of 98% with a drying time for 330 minutes.

Seen from Figure 6 that the relative humidity of the drying air discharged after the process contains saturated humidity of around 96-99%. It states that the drying air has been fully utilized, because the air was removed from the process contains saturated moisture and ineffective if used again to dry the ATC.

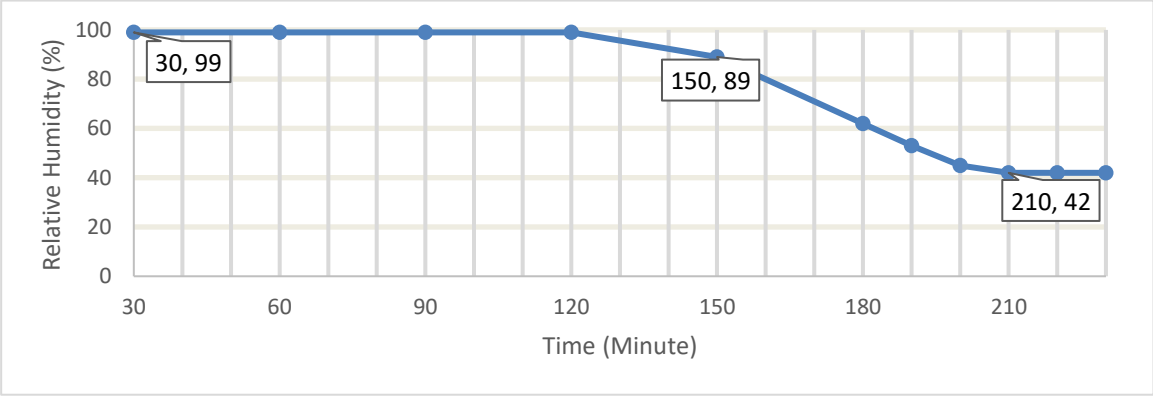

FIG. Fig. 4: Relative humidity against time in closed loop fixed bed dryer

In the picture above, the drying air relative humidity outputs closed loop method of fixed bed dryer was 99% and fell to 96% at 190 minutes. The decline in output drying air relative humidity occur because of water on the surface ATC vaporized into the air dryer becomes less and difficult to evaporate the water bound in the ATC. Relative humidity of the drying air output continued to fall to 49% at 230 minutes drying time at temperatures of 38°C. Method closed loop fixed bed dryer is done with the aim to be able to utilize the energy wasted in the method of single fixed bed dryer ww shown with the temperature, because the drying air is disposed on the method of single fixed bed dryer having a temperature higher than room temperature, so that in the method this, the air output of the drying column inserted back into the process after the dehumidification process. It aims to reduce the heating load carried by the heater.

3.2 Effect of Drying Method to Total Water Evaporated

ATC Drying process carried out at a temperature of 60°C with several methods such as single fixed bed dryer, closed loop fixed bed dryer, and a series of fixed bed dryer. The drying process occurs as a result of mass transfer between the drying air with the water in the ATC. Good mass transfer can be shown by the evaporation of water most of the ATC in a short time.

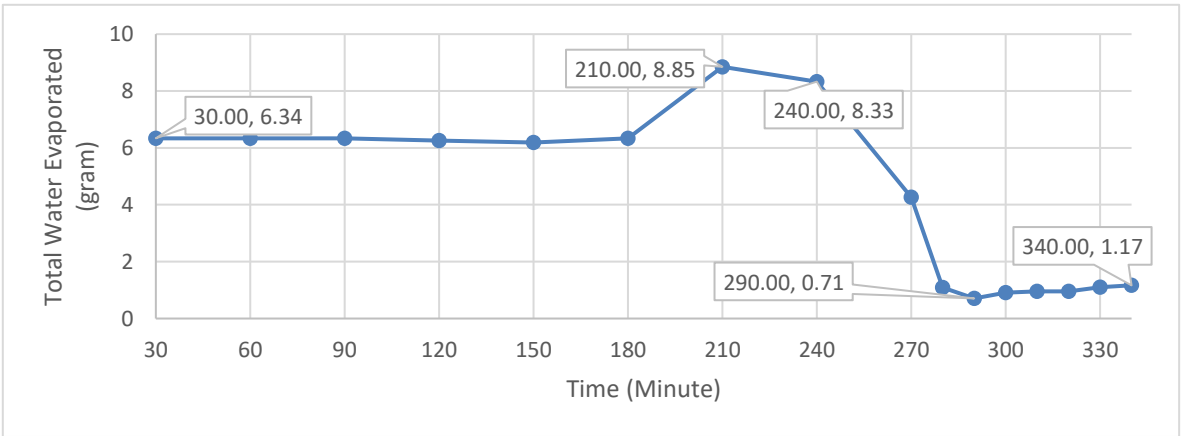

Fig. 5: Water evaporation curve against time in method single fixed bed dryer

In the Single fixed bed dryer, water evaporated within the 30 minutes of the drying process of 6.4 grams and increased to 8.85 grams in 210 minutes due to amount of water moving to the drying air, because of free water on the surface of ATC easy to evaporated by the drying air. Then in 240 minutes, the amount of water evaporated declining due to the amount of water on the surface of the ATC was in decline, it was because of free water on the surface of the ATC have been exhausted and the remaining were bound water contained in ATC and difficult to be evaporated. In the Single fixed bed dryer obtained total evaporated water was 66.1351 grams with drying time was 340 minutes.

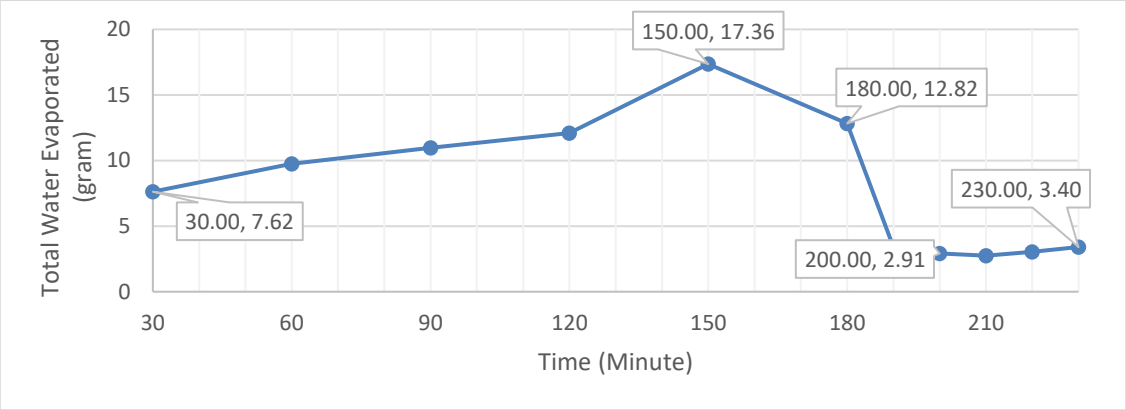

Fig. 6: Water evaporation curve against time in method closed loop fixed bed dryer

In the picture above, it can be seen that using the closed loop fixed bed dryer, water obtained evaporated in 30 minutes drying process that was 7.62 grams and increased to 17.36 grams in 150 minutes. That was because the amount of free water on the surface of ATC easy to be evaporated by the drying air. Then the water is evaporated at 180 minutes to be reduced, due to free water on the surface of the ATC have been exhausted and the remaining are bound water contained in ATC and difficult to be evaporated. In the closed loop method, the total water evaporated totaling 86.0788 grams with drying time for 230 minutes.

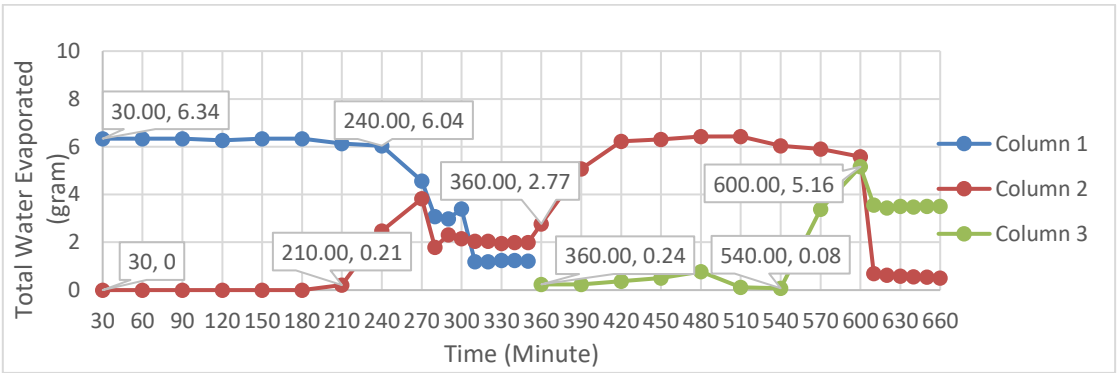

Fig. 7: Water evaporation curve against time in method series fixed bed dryer

For the method of series fixed bed dryer, hot air that flowed in series from the first column to the second column with water that evaporated during the 30 minutes of the drying process in the first column was 6.34 grams and the second column was 0 grams. The drying process does not occur in the second column because the rate of air out of the first column was very low and the moisture content is high, so there was no water in the ATC that move to the drying air. In 210 minutes of drying, the water is evaporated by the first column is reduced to 6 grams, while in the second column of the drying process occurs which is characterized by the evaporation of water as much as 0.2 grams. The cause of the decline of water evaporated in the first column was the water content of ATC the less that can be evaporated because of free water on the surface of the ATC is reduced and the drying process in the second column occurs because the humidity out of the first column is reduced and has the ability to evaporate the water from the ATC in the second column . The drying process in the first column can evaporate the water as much as 63.8951 grams total time of 350 minutes.

After drying in the first column is completed, then the drying process is continued in series in the second column and the third column. At 360 minutes the second column of the drying process, water is evaporated as much as 2.77 grams and the third column of water obtained evaporated as much as 0.24 grams. In the third column of water directly evaporated during the drying process 10 minutes caused by the humidity of air coming out of the second column has been able to evaporate the water in the ATC of the third column, because after the first column was dried, the state of the second column was already half dried and had a low humidity , so that the dry air coming out of the second column had been able to evaporate water from the third column. In 570 minutes of drying, evaporation of water began to decline in the second column as much as 7.42 grams, so that water evaporated from ATC in the third column increased to 3.39 grams. The decrease of water evaporated in the second column because of free water on the surface of the ATC are few in number so that the drying air coming into the third column can evaporate water more than ATC in the third column. By using a series of fixed bed dryer, total evaporative water in the second column was 80.8329 grams for 660 minutes and the total water that can be evaporated from the ATC in the third column was 31.8739 grams by drying for 310 minutes.

TABLE 1: Total evaporation of water and the time needed for each method

Method	T (ºC)	Air Rate (ml/s)	Total Water Evaporated (g/minute)
Single	60	498.0051	0.1945
Closed Loop	60	498.0051	0.3743
	60	498.0051	
Series			0.2676

From the above table, it can be seen that the drying process by using closed loop ATC fixed bed dryer was better than the two other methods that caused the dehumidification process. That was because the air dryer is used in this study was quite humid so require dehumidification process on the drying air, so the inlet air humidity lower and the ability of air to evaporate the water content in the ATC are getting bigger and the faster the drying process is completed. This is evidenced by the total water that evaporated on a closed loop method of fixed bed dryer as much as 0.3743 gram per 1 minute.

3.3 Effect of Drying Method Against Energy Used

The drying process in this research influenced by the needs of the energy used to evaporate water from the ATC. The good drying process can be shown by the evaporation of more water using very little energy.

TABLE 2: Total water evaporated and energy used each method

Method	Total Water Evaporated (g)	Energy Used (kWh)
Closed loop	86.0788	2.35
Single	66.1351	3.31
Series	176.6020	6.63

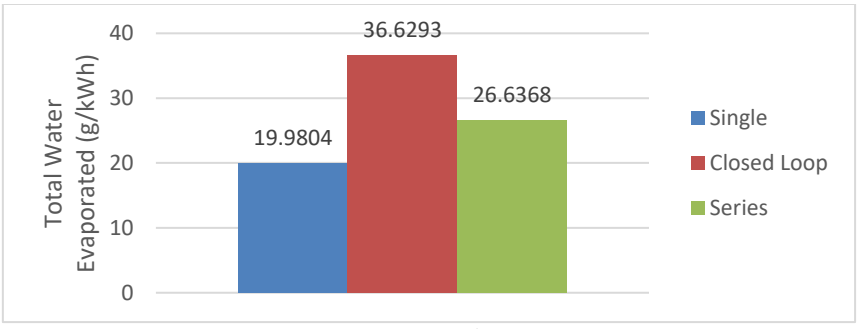

Fig. 8: Graph water evaporation of energy in every method

From the graph above, the drying process which is well demonstrated by the method of closed loop fixed bed dryer, because it was able to evaporate the water more than any other method. This was because the closed loop fixed bed dryer air humidity is lower due to the drying air dehumidification process. Low humidity causes water content in ATC more and faster vaporized. So that the energy used to complete the drying process becomes less

than the two other methods.

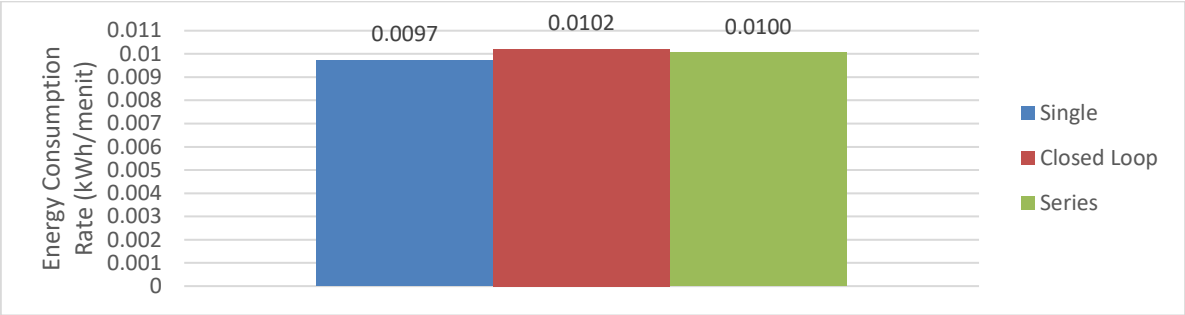

Fig 9: Rate of energy consumption every drying method

Of the three methods, method of closed-loop fixed bed dryer was a method that generate the rate of energy consumption was greater than in the two other methods, because the method of closed loop fixed bed dryer was able to evaporate the water more, in the amount of 34.2286 g / kWh compared with the other method more thus requiring greater energy and also there was just a little difference between the three methods.

3.4 Effect of Drying Method Against Water Content Products

TABLE 3: The water content of the product of each method

Method	Product Water Content (%)
Single	10.1328
Closed loop	7.6987
Series	9.4634

The drying process in this research accomplished with three methods of closed loop fixed bed dryer, single fixed bed dryer, and a series of fixed bed dryer. Products with different water content produced by each method. The good drying process can be shown by the evaporation of more water, which is indicated by the results of a product with a low water content.

From the above table, it can be seen that the products with water content of 10.1328% produced by by the method of single fixed bed dryer, a product with a water content of 7.6987% produced by by the method of closed-loop fixed bed dryer, and a product with a water content of 9.4634% produced by methods series fixed bed dryer. Of the three methods, method of closed-loop fixed bed dryer was a method, which produce products with low water content. That was because the air dryer is used in this study was quite humid, so the process of dehumidification on this method caused the moisture of drying air was getting lower and resulted in the ability of the air dryer to evaporate the water content in the ATC was getting bigger, therefore, products with low water content is equal 7.6987% generated.

3.5 Energy Efficiency of Each Method

At the end of the drying process, the analysis of the efficiency of the drying process is done. The results of the analysis of energy efficiency for the drying of carrageenan are presented in Table 4.

TABLE 4: The energy efficiency of each method

Methods	Number of evaporate water (g)	Energy use (kWH)	Efficiency (%)
Single	66.1350	3.31	18.8691
Closed Loop	80.4371	2.35	26.2101
Series	188.6166	6.63	62.1653

Table 4 shows that the greatest energy efficiency contained in fixed bed dryer series method that was equal to 62.1653%. Although the method of series of fixed bed dryer uses more energy than other methods, but the energy was also vaporize more water. That was because the method of series of fixed bed dryer contained energy utilization, which was the hot air coming out of the first column was used to dry the next column so that the heat energy from the air can be fully utilized and wasted energy was relatively less than in the two other methods.

4 Conclusion

Based on the results of this study, can be concluded that: The energy efficiency of the method of single fixed bed dryer at 18.8691%; the rate of energy consumption amounted to 0.0097 kWh / min; the ability to evaporate the water of 19.9804 g / kWh, energy efficiency of the method of closed loop fixed bed dryer at 26.2101%; the rate of energy consumption amounted to 0.0102 kWh / min; the ability to evaporate the water of 36.6293 g / kWh, and energy efficiency was found in the most excellent method of series fixed bed dryer with energy efficiency of 62.1653%; the rate of energy consumption amounted to 0.0100 kWh / min; the ability to evaporate the water of 26.6368 g / kWh

5 References

Atuonwu, J.C., Jin, X., van Straten, G., van Deventer Antonius, H.C. and Van Boxtel, J.B., 2011. Reducing energy consumption in food drying: Opportunities in desiccant adsorption and other dehumidification strategies. Procedia Food Science, 1, pp.1799-1805.

Balbay, A., Şahin, Ö. and Karabatak, M., 2011. An investigation of drying process of shelled pistachios in a newly designed fixed bed dryer system by using artificial neural network. Drying Technology, 29(14), pp.1685-1696.

Djaeni, M.; Bartels P.V.; Sanders J.P.M.; van Straten, G.; van Boxtel, A.J.B. 2009. Energy efficiency of multistage adsorption drying for low-temperature drying. Journal of Drying Technology, 27(4); 555 – 564

Djaeni, M., & Sari, D. A. 2015. Low Temperature Seaweed Drying Using Dehumidified Air. Procedia Environmental Sciences, 23, 2-10.

Djaeni, M., Sasongko, S. B., Prasetyaningrum, A. A., Jin, X., & van Boxtel, A. J. 2012. Carrageenan drying with dehumidified air: drying characteristics and product quality. International Journal of Food Engineering, 8(3), 2682.

Djaeni, M., Sasongko, S. B., van Boxtel, A. J. B. 2013. Enhancement of energy efficiency and food product quality using adsorption dryer with zeolite. International Journal of Renewable Energy Development, 2(2): 81 –86.

Djaeni, M., van Asselt, C. J., Bartels, P. V., Sanders, J. P. M., van Straten, G., & van Boxtel, A. J. 2011. Low temperature drying with air dehumidified by zeolite for food products: energy efficiency aspect analysis. International Journal of Food Engineering, 7(6), 1-25.

Fudholi, A., Othman, M.Y, Ruslan, M. H., Yahya, M., Zaharim, A., Sopian K. 2011. The effects of drying air temperature and humidity on the drying kinetics of seaweed. Recent Researches in Geography, Geology, Energy, Environment and Biomedicine.

Sosle, V., Raghavan, G. S. V., & Kittler, R. 2003. Low-temperature drying using a versatile heat pump dehumidifier. Drying technology, 21(3), 539-554.

Djaeni, M. (2008). Energy efficient multistage zeolite drying for heat sensitive products. publisher not identified.

ISBN 978-602-53531-8-5

C. Electric power and energy efficiencies; Renewable energy grid integration & distribution: utilities of the future; Automation and measurement technologies

Proceedings of the 1st Faculty of Industrial Technology International Congress
International Conference
Bandung, Indonesia, October 9-11, 2017
ISBN 978-602-53531-8-5

Optimal Scheduling for Dynamic Loads Using Direct Method

Hermagasantos Zein[1,*], Jangkung Raharjo[2] and Yusra Sabri[3]

[1] Depart. of Conversion Energy Eng., State Polytechnic of Bandung (Polban), Bandung - INDONESIA

[2] Candidate Doctor of Institut Teknologi Sepuluh Nopember (ITS), Surabaya – INDONESIA and Department of Electrical Engineering, Telkom University, Bandung - INDONESIA

[3] Electrical Engineering, STEI - Institute Technology of Bandung (ITB), Bandung, INDONESIA

[*] Corresponding author e-mail: hermaga_s@yahoo.co.id

Abstract

The main objective of the dynamic economic dispatch problem is to determine the optimal schedule of output powers of all generating units to meet the load demands and losses at minimum operating cost while satisfying ramp rate and power limits. In addition, the computing time should be as soon as possible because of the scheduling interval in an hour. This paper proposed an application of the direct method with cost functions of the generator units in the quadratic form to solve the problem. In which the proposed method is simplest, applicable and having shortest computing time. To validate the proposed method was done evaluating for 6-generator units in detail and the results compared to the other methods. While to test computing time was done a simulation to the large power system, 47 generator units of Jawa-Bali System. The results state that the proposed method can work efficiently and accurately. These are in line with expectations.

Keywords: accurately, economic dispatch, efficiently, quadratic objective function, ramp rate limits.

1. Introduction

Scheduling of generating units, units, to meet system loads and losses must involve ramp rate limits of each unit because of the unit is not free to raise/down its power. Involving of the ramp rate will guarantee the optimal results for scheduling can be implemented to meet dynamic system loads and losses. A few methods have published in solving an economic dispatch problem, EDP, namely:

- Conventional methods have been published such as iteration lambda method, gradient method, Newton method, linear method and dynamic programming method (A .J. Wood, et al., 1984; Salama, M., M., 1999 and IEEE Committee Report, 1971). These methods work by iteration process so that can take enough large computational time because it must be through iteration process steps. The addition of the computational time will be seen significantly if the economic dispatch problem with large scale. Sometimes these methods cannot converge in the process of iteration.
- Methods based on the artificial intelligent concept such as artificial neural network (J. Nanda, et al. 1997), particle swarm optimization, PSO, (Z. L. Gaing, 2004; J. B. Park, et al., 2005 and D. N. Jeyakumar, et al., 2006) and genetic algorithm, GA, (D. C. Walters, et al., 199; J. Tippayachai, et al. 2003.). The main problem associated with these methods is the need for appropriate control parameters. Sometimes the methods take large computational time due to improper selection of the control parameters.

The methods that were mentioned above are always the completions through iteration process so it can take large computation time. This paper will propose a method without iteration, i.e. the direct method that has been studied by (H. Zein, et al., 2012), so that is expected to reduce the computation time and simpler so easy to be applied. So, this method will be more effective for a dynamic economic dispatch with large scale. But it is limited by cost function of each generator unit in the quadratic form. The formulations have been derived with very clear. Then, the proposed method is verified with doing a test for a system that consists of 6 units through a numerical study. In this study to see the optimal results of the proposed method whether they violate of the ramp rate limit constraints or not. In addition, through this numerical study was conducted also verified the calculation results to the results of the other methods.

2. Research method

2.1. Formulation of a dynamic economic dispatch

The primary objective of an EDP is to minimize the total fuel cost of power plants subjected to the operating constraints of a power system. In general, the EDP can be formulated mathematically as a constrained optimization problem with an objective function of the form:

$$F_T = \sum_{i=1}^{n} F_i(P_i) \tag{1}$$

Where *FT* is the total fuel cost of the system ($/hr), n is the total number of units and *Fi* (*Pi*) is the operating fuel cost of generator unit i ($/hr). Generally, the fuel cost function of the unit is expressed as a quadratic function as given in (2).

$$F_i(P_i) = a_i + b_i P_i + c_i P_i^2 \tag{2}$$

Where *Pi* is the real output power of unit i (MW), *ai* , *bi* and *ci* are the cost coefficients of unit i. The minimization of the EDP problem is subjected to the following constraints:

1. Real Power Balance Constraint: For power balance, an equality constraint should be satisfied. The total generated power should be equal to the total load demand plus the total line losses, system losses. The active power balance is given by:

$$\sum_{i=1}^{n} P_i = P_D + P_L \tag{3}$$

Where P_D is the total load demand (MW), P_L is the system losses (MW). The P_L value will be calculated through (15)

2. Generator Power Limit Constraint: The generation output power of each unit should lie between the minimum and maximum limits. The inequality constraint for each generator can be expressed as:

$$P_{i,\min} \le P_i \le P_{i,\max} \tag{4}$$

Where *Pi*,min and *Pi*,max are the minimum and maximum power outputs of generator i (MW), respectively. The maximum output power of the generator is limited by thermal consideration and minimum power generation is limited by the flame instability of a boiler.

3. Ramp Rate Limit Constraint: The generator constraints due to ramp rate limits of generating units, from [12], is given as:

- As Generation Increases:

$$P_i(t) - P_i(t-1) \le UR_i \tag{5}$$

- As Generation Decreases:

$$P_i(t-1) - P_i(t) \le DR_i \tag{6}$$

Therefore the generator power limit constraints can be modified as:

$$\max(P_{i,\min}, P_i(t-1) - DR_i) \le P_i(t) \le \min(P_{i,\max}, P_i(t-1) + UR_i) \tag{7}$$

From (7), the limits of minimum and maximum output powers of generating units are modified as:

$$P_{i,\min}(t) = \max(P_{i,\min}, P_i(t-1) - DR_i \tag{8}$$

$$P_{i,ma}(t) = \max(P_{i,\max}, P_i(t-1) + UR_i) \tag{9}$$

Where *Pi* (*t*) is the output power of generating unit i (MW) in the time interval (t), *Pi* (*t* −1) is the output power of generating unit i (MW) in the previous time interval (t-1), UR_i is the up ramp limit of generating unit i (MW/time-period) and DR_i is the down ramp limit of generating unit i (MW/time-period).

The ramp rate limits of the generating units with all possible cases are shown in Fig. 1.

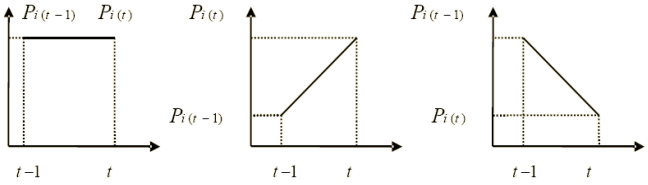

Fig. 1: Ramp rate limits of the generating units

2.2. Dynamic economic dispatch problem

A dynamic economic dispatch problem, DEDP, is to meet ramp rate limits, (5) and (6), in the power change of each unit from t-1 to t. So, the DEDP can be expressed by (10).

$$\text{Objective:} \quad F_T(t) = \sum_{i=1}^{n} F_i(P_i(t))$$

$$\text{Subject to:} \quad \sum_{i=1}^{n} P_i(t) = P_D(t) + P_L(t) \qquad (10)$$

$$P_{i,\min}(t) \le P_i(t) \le P_{i,\max}(t)$$

In this paper is created the research for the objective function in quadratic form and estimated losses, like the problem expressed in the (10). This problem will be solved in two stages. Stage I does optimization without the power limits of units. Stage II evaluates the optimal results of stage I against violent of the power limits for each unit.

For the quadratic objective function (10) and assume P_L(t) constant, then LaGrange multiplier (lambda) at time t is:

$$\lambda(t) = b_i + 2c_i P_i(t) \qquad (11)$$

Or,

$$P_i(t) = \frac{\lambda(t) - b_i}{2c_i} \qquad (12)$$

Where Pi(t) is optimal power for unit-i at time t, λ(τ) is LaGrange multiplier at time t, c_i is price linear parameter for unit-i ($/MWH), bi is price quadratic parameter for unit-i ($/MWH2).

So for n-unit generators are:

$$\sum_{i=1}^{n} P_i(t) = \sum_{i=1}^{n} \frac{\lambda(t) - b_i}{2c_i} \qquad (13)$$

From the last equation, the value of lambda can be obtained directly as expressed by (14) below.

$$\lambda(t) = \frac{P_D(t) + P_L(t) + \sum_{i=1}^{n} \frac{b_i}{2c_i}}{\sum_{i=1}^{n} \frac{1}{2c_i}} \qquad (14)$$

While system losses at time t, $P_L(t)$, in the study are estimated with (15) below.

$$P_L(t) = P_L(t-1)\left(1 + f_c \frac{P_D(t) - P_D(t-1)}{P_D(t)}\right) \qquad (15)$$

Where correction factor, f_c, is dependent on system conditions, like network structure, and load or power plant distributions, which the f_c value lies between 1 and 2.

Equation (14) shows the optimization of completion directly or without through iteration process, so the convergence is always guaranteed. Here needs to be noted that the (14) is valid only for the DEDP with the quadratic objective function. After lambda value has been determined by the (14) and continued to determine optimal power unit with the (12). Then, to be done evaluation against the minimum and maximum power limits to obtain optimal solution, $P_{i,o}(t)$, with the following terms.

$$\text{If } P_{i,o}(t) < P_{i,min}(t), \text{ then } P_{i,o}(t) = P_{i,min}(t) \quad (16)$$

$$\text{If } P_{i,o}(t) > P_{i,max}(t), \text{ then } P_{i,o}(t) = P_{i,max}(t) \quad (17)$$

2.3 Algorithm of the Proposed Method

The following is the steps of completion algorithm for DEDP with the proposed method and it has been described above.

1. Input data
2. Calculate $P_L(t)$ through (15).
3. Remove the unit is not changed and update load by the (18).
4. Update generating power limits through the (8) and (9).
5. Calculate λ through (14)
6. Calculate $P_i(t)$ through (12).
7. If $P_i(t)>P_{i,max}(t)$, then $P_{i,o}(t)=P_{i,max}(t)$, update $P_D(t)=P_D(t)-P_{i,o}(t)$, remove unit i and continue step 4.
8. If $P_i(t)<P_{i,min}(t)$, then $P_{i,o}(t)=P_{i,min}(t)$, update $P_D(t)=P_D(t)-P_{i,o}(t)$, remove unit i and continue step 4.
9. Set $P_{i,o}(t)=P_i(t)$ for not violate the generating power limits.
10. Results.
11. Stop.

From three possibilities of ramp rate, Fig. 1, Fig. 1a is the unit that does not change the power from t-1 to t so that satisfies Pi,o(t-1)=Pi,o(t). Then, this unit is removed in the optimization process and followed with updating system loads

$$P_D(t) = P_D(t) - \sum_{i=1}^{m} P_{i,o}(t) \quad (18)$$

Where m is a number of the generator units that do not experience power change.

3. Numerical study

To verify the effectiveness of the proposed method, a six-unit power generating plant was tested. The Algorithm of the method has been implemented in the program using FORTRAN and laptop Asus core i3. It is applied to 6 generator units with power constraint and ramp rate limits. The fuel cost data and ramp rate limits of the six units were given in Table 1. The load demand for 24 hours is given in Table 2.

Table 1: Fuel cost coefficients and ramp rate limits of six units

Unit	a_i	b_i	c_i	$P_{i,min}$	$P_{i,max}$	UR_i	UD_i
1	240	7	0.007	100	500	80	120
2	200	10	0.0095	50	200	50	90
3	220	8.5	0.009	80	300	65	100
4	200	11	0.009	50	150	50	90
5	220	10.5	0.008	50	200	50	90
6	190	12	0.0075	50	120	50	90

Table 2: Load demand for 24 hours of six Units

Hour	Load (MW)	Hour	Load (MW)	Hour	Load (MW)	Hour	Load (MW)
1	955	7	989	13	1190	19	1159
2	942	8	1023	14	1251	20	1092
3	935	9	1126	15	1263	21	1023
4	930	10	1150	16	1250	22	984
5	935	11	1201	17	1221	23	975
6	965	12	1235	18	1202	24	960

Table 3: Output power, losses and total fuel cost for 24 hours of 6 units

6 Hour	P_1	P_2	P_3	P_4	P_5	P_6	Loss	Fuel Cost
1	382.4	123.9	214.1	75.2	115.9	50.0	6.53	11409.3
2	379.3	121.6	211.7	72.8	113.1	50.0	6.37	11247.0
3	377.6	120.3	210.3	71.4	111.6	50.0	6.28	11159.9
4	376.4	119.4	209.4	70.5	110.6	50.0	6.22	11097.7
5	377.6	120.3	210.3	71.4	111.6	50.0	6.28	11159.9
6	384.4	125.3	215.6	76.7	117.6	50.0	6.62	11509.4
7	390.7	130.0	220.5	81.6	123.1	50.0	6.95	11836.4
8	398.9	136.1	227.0	88.1	130.3	50.0	7.37	12267.7
9	421.6	152.7	244.5	105.7	150.1	60.1	8.71	13598.2
10	426.3	156.2	248.3	109.4	154.3	64.6	9.05	13913.0
11	436.5	163.7	256.1	117.3	163.2	74.0	9.77	14587.4
12	443.2	168.7	261.4	122.5	169.1	80.3	10.27	15041.3
13	434.3	162.1	254.4	115.5	161.2	72.0	9.59	14441.0
14	446.4	171.0	263.9	125.0	171.9	83.3	10.48	15255.8
15	448.8	172.8	265.7	126.8	173.9	85.5	10.66	15417.3
16	446.2	170.9	263.7	124.8	171.7	83.1	10.46	15242.3
17	440.4	166.6	259.2	120.3	166.6	77.7	10.02	14853.5
18	436.7	163.9	256.3	117.4	163.3	74.2	9.74	14600.2
19	428.1	157.6	249.6	110.7	155.8	66.2	9.12	14030.7
20	414.8	147.7	239.3	100.4	144.2	53.8	8.17	13154.1
21	398.9	136.0	226.9	88.0	130.3	50.0	7.24	12266.0
22	389.4	129.1	219.6	80.7	122.0	50.0	6.74	11771.6
23	387.3	127.4	217.9	79.0	120.1	50.0	6.63	11658.3
24	383.6	124.8	215.0	76.1	116.9	50.0	6.45	11470.1
Total							**195.72**	**312988.0**

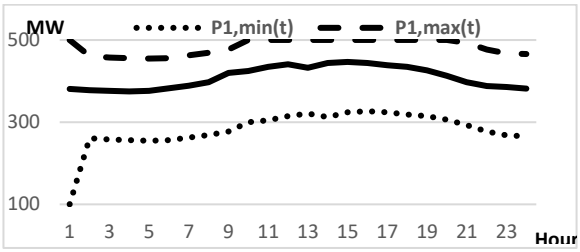

Fig. 2. Power limits and optimal power of unit 1 versus 24 hr

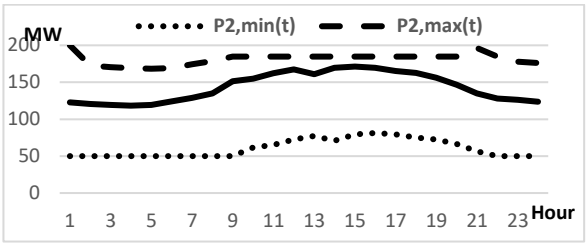

Fig.3. Power limits and optimal power of unit 2 versus 24 hr

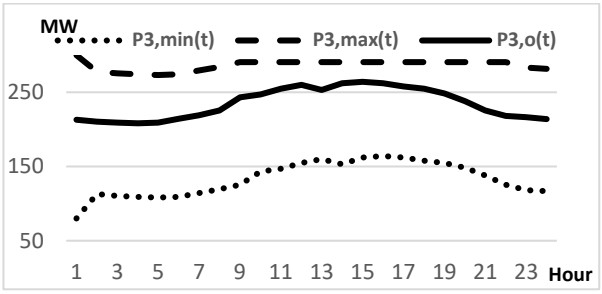

Fig. 4: Power limits and optimal power of unit 3 versus 24 hr

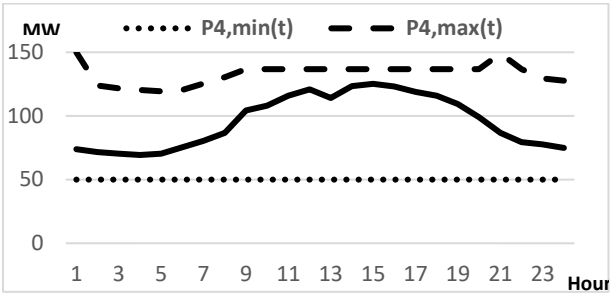

Fig. 5: Power limits and optimal power of unit 4 versus 24 hr

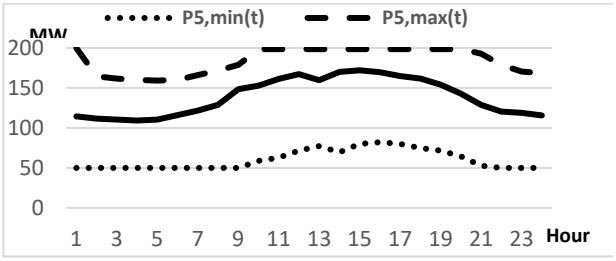

Fig. 6: Power limits and optimal power of unit 5 versus 24 hr

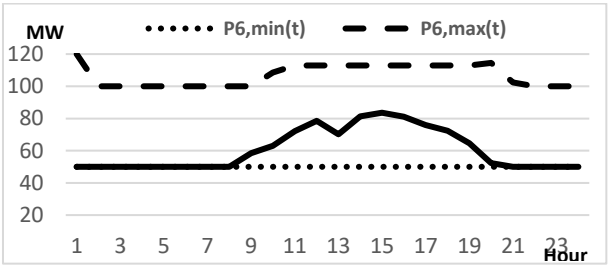

Fig. 7: Power limits and optimal power of unit 6 versus 24 hr

Table 4: Loss and total fuel cost comparison between 4 methods of 6 units

Method	Losses (MW)	Total Fuel Cost ($)
1. Lambda iteration method	-	313045.50
2. Particle Swarm Optimization (PSO)	193.49	313041.40
3. Genetic Algorithm (GA)	194.12	313040.90
4. Proposed Method	195.72	312988.00

While a simulation for the large power system, 47 generator units of Jawa-Bali System, was done successfully and satisfactory. For example, at peak load time,18 o'clock, with system load 13121 MW is obtained computating time of 0.98 seconds and losses of 215 MW. At minimum load time, 4 o'clock with system load 6038 MW is obtained computing time of 87 seconds and losses of 42 MW, The simulation results of 24 hours state that the proposed method can run the program in a very short time, i.e. computing time less than 1 second.

4. Discussion

- A method for calculating an economic dispatch in meeting load demand and losses with ramp rate and power limits has been proposed in this paper. This method is devoted to the dynamic economic dispatch problem with fuel cost function of generating unit in the quadratic form, (2). By using LaGrange optimization is obtained the direct solution of the lambda value, (14). Where the (14) will ensure that the optimization results fall at the point of minimum, but not necessarily optimal because it may violate the ramp rate constraints of generator units. Therefore, it is necessary to evaluate the results through (16) and (17).
- The solving steps of the DEDP have been stated in the algorithm above. The numerical study results for 6 units with system load changes in interval time 24 hours have met satisfy expectation. Optimal scheduling of

the generator units and fuel costs in the 24 hours are loaded in Table III. The results have met the ramp rate limits for every unit, shown in Fig. 2-7. Where the optimal results every hour, $P_{i,o}(t)$, do not violate the minimum and maximum dynamic power limits based on the ramp rate limits, Fig.1. it takes a very short time in the computing process in resolving the optimization problems.

- The contrast thing happened on unit 6, for interval time at 1-8 and 21-24, the optimal results are equal to minimum generating power limit. It is caused by the expensive fuel cost compared to the others so the optimal power less than the minimum generating power limit. Since each generator unit must be operated at least equal to the minimum power limit, then if the optimization results for each generator unit smaller than its minimum power limit will be set equal to the minimum power limit.
- Table IV is a comparison to the other methods, where the calculation results of all methods show the values almost same. From this table is seen that the proposed method produces the larger losses so that the total power generated is also greater than the other three methods. However, this method gives better results due to the total fuel costs are lower when is compared with three other methods.
- From simulation 47 generator of Jawa-Bali System with a minimum load, 6038 MW, at 4 o'clock and peak load, 13121 MW, at 18 o'clock, the proposed method could determine to schedule of the generator units successfully and satisfactory. The simulation results state that the proposed method can work in the short time, where it needs less than 1 second to execute the program. It is shortest compared to the interval time of scheduling, 1 hour.

5. Conclusion

A method for solving the dynamic economic dispatch problem has been proposed in this paper. This method is simpler and without iteration process like the published methods that mention above. It can reduce significantly the computational time. One other advantage is the assurance of completion will always converge. Thus, this proposed method is easy to be implemented and it is expected to work effectively for dynamic economic dispatch problem with large scale. Verification of the method with six generating units and simulation for 47 generator units of Jawa-Bali System has successfully done with satisfactory results. It only took about one second in the computing process of the 47 generator units of Jawa-Bali System. Where the results of the optimization of each unit do not violate the minimum and maximum dynamic constraint as shown in Fig. 2-7. From the comparison of the results with three other methods, Table IV, this method provides convincing results, where the calculation results are very close to the calculation results of three other methods. However, if observed in deeper this method gives better results due to the lower total fuel cost even though the larger system losses.

6. Nomenclature

kV	kilo volt	-
MW	mega Watt	-
n	number of unit	-
$	unit currency	-
hr.	hour	hour
t	time	hour

Greek letters

λ	LaGrange multiplier	$/MW

Subscripts

i	unit number
max	maximum
min	minimum

7. References

A. Bakirtzis, et. al., 1994. Genetic algorithm solution to the economic dispatch problem. IEE Proc. Generation, Transmission and distribution, 141, 4, 377-382.

A .J. Wood and B.F. Wollenberg, 1984. Power generation, operation and control. John Wiley and Sons., New York.

Bhupender S, Shivani S, Ajay N., 2013. Particle Swarm Optimization and Genetic Algorithm based Optimal Power Flow Solutions. International Journal of Application or Innovation in Engineering & Management. 2(7): 307-315.

D. C. Walters and G. B. Sheble, 1993. Genetic algorithm solution of economic dispatch with valve-point loading. IEEE Trans. Power Syst., 8, 1325-1332.

D. N. Jeyakumar, T. Jayabarathi and T. Raghunathan, 2006. Particle swarm optimization for various types of economic dispatch problems. Elec. Power Energy Syst, 28, 36-42.

G. B. Sheble and K. Brittig, 1995. Refined genetic algorithm-economic dispatch example. IEEE Trans. on Power Systems, 10 ,1, 117-124.

H. Zein, Y. Sabri, A. Mashar, 2012. Implementation of Electricity Competition Framework with Economic Dispatch Direct Method, *Telkomnika*.; 10(4): 667-674.

H. Zein, R. Raharjo, 2017. Generator Capability Curve Approaches for Optimal Power Flow, IRACST– Engineering Science and Technology: An International Journal (ESTIJ), ISSN: 2250-3498, 7, 4.

IEEE Committee Report, 1971. Present practices in the economic operation of power systems. IEEE Trans. Power Appa. Syst., PAS-90, 1768-1775.

J. B. Park, K. S. Lee, J. R. Shin and K. Y. Lee, 2005. A particle swarm optimization for economic dispatch with nonsmooth cost functions. IEEE Trans. Power Syst, 20, 34-42.

J. Nanda, A. Sachan, L. Pradhan M.L. Kothari, A. Koteswara Rao, 1997. Application of artificial neural network to economic load dispatch. IEEE Trans. Power Systems, 22.

J. Tippayachai, W. Ongsakul and I. Ngamroo, 2003. Parallel micro genetic algorithm for constrained economic dispatch. IEEE Trans. Power Syst., 17, 790-797.

J. Raharjo, A. Soeprijanto, H. Zein, 2016. Multi Dimension of Coarse to Fine Search Method Development for Solving Economic Dispatch, Indonesian Journal of Electrical Engineering and Computer Science. 3, 1, 1 ~ 9.

Lee KY, El-Sharkawi MA, 2013. Tutorial on Modern Heuristic Optimization Techniques with Applications to Power Systems. *IEEE Power Engineering Society.*

P. H. Chen and H. C. Chang, 1995. Large-scale economic dispatch approach by genetic algorithm. IEEE Trans. on Power Systems, 10, 4, 1918-1926.

Salama, M., M., 1999. Economic control for generations in the thermal power system. Energy Conversion and Management, 40, 669-681.

Shahinzadeh H, Nasr Azadani SM, Amirkabir Jannesari N., 2014. Applications of Particle Swarm Optimization Algorithm to Solving the Economic Load Dispatch of Units in Power Systems with Valve Point Effects. *International Journal of Electrical and Computer Engineering (IJECE)*.; 4(6): 858-867.

Y. H. Song, F, R. Morgen, and D.T.Y. Cheng, 1995. Comparison studies of genetic algorithms in power system economic dispatch. Power System Technology, 19, 3, 28-33.

Z. L. Gaing, 2004. Constrained dynamic economic dispatch solution using particle swarm optimization. IEEE Power Engineering Society General Meeting, 153-158.

W. M. Mansour, et al., 2013. Dynamic Economic Load Dispatch of Thermal Power System Using Genetic Algorithm, IRACST – Engineering Science and Technology: An International Journal (ESTIJ), ISSN: 2250-3498, 3, 2.

Proceedings of the 1st Faculty of Industrial Technology International Congress
International Conference
Bandung, Indonesia, October 9-11, 2017
ISBN 978-602-53531-8-5

Development Control System Of Microgrid During Islanding Condition Using Fuzzy Logic

Hartono Budi Santoso
Department of Energy Conversion Engineering Politeknik Negeri Bandung Indonesia
Corresponding author e-mail: hartono@esi-labs.com

Abstract

In the microgrid each of micro generation (inverter) is connected in parallel with the network or with other micro generation. During on grid conditions, connection with network can be easily done because each generation refers to the parameters of the grid and it will generate energy as much as possible from the potential energy owned, if there is excess power, it will be supplied to the grid. But during off grid conditions, not all micro generation can be connected in parallel directly. Especially on micro generation that are not equipped with power sharing capability.

In this research the control system will be developed to improve the performance of the microgrid. The on-off grid tie inverter (on-off GTI) that cannot be connected in parallel with another inverter during islanding condition will be able to connect in parallel, so that the whole system can improve performance of microgrid. The control system was developed using fuzzy logic to reconfiguration PV circuit, which intended to regulate inter-inverter parallel mechanism by taking into account the amount of radiation and the power state of each inverter. The test results showed an increase in energy absorption from PV up to 26% and increased operation of the battery up to 26.38%.

Keywords: *On-off GTI, microgrid, parallel inverter, fuzzy logic*

1. Introduction

Electrical power problems in the application of renewable energy sources connected to grid can be solved using a distributed generation approach. In this system each power generation is seen as a subsystem of a grid, called microgrids (Lasseter, R.H., 2002; Nikkhajoei, H. and Lasseter, R.H, 2009) (Kroposki B., et al, 2008). Implementation of the free market of electricity and attention to environmental issues related to pollution due to gas emissions as well as efforts to conduct energy efficiency and diversification, encourage the implementation of distributed energy source systems, especially renewable energy sources and small-scale Combined Heat and Power (CHP) plants (European Commission, 2003). In recent years, rapid developments in power electronics and semiconductor technology are driving increased application of power generation uses renewable energy sources using power converter technology. The technology development has improved the transient response faster and neither is the processing time and execution of complex control algorithms can be completed with a faster time (Xiongfei W., et al, 2012). In the solar power plant configuration, solar cells are connected in series and parallel to achieve the desired power and output voltage, according to the DC input voltage required by the power converter. Inverter as power converter will convert DC power to AC to supply load. To obtain optimal power from solar cells, the inverters are equipped with MPPT technology, which will make solar cells operate at maximum power point. Inverter technology also allows the solar power can be connected to the network, so that the electrical energy generated can be supplied to grid, and vice versa grid power will subtitute power to load when power shortage in solar generation due to the sun dim (W. Kramer, et al, 2008).

In the microgrid, each micro generation (inverter) is connected in parallel with the network or with other micro generation. During on grid conditions, connection with network can be done easily because each generation refers to the parameters of the grid and each generation will generate energy as much as possible from the potential energy owned, because if there is excess power, it will be supplied to the grid. But during off grid conditions, not all micro generation can be directly connected in parallel. Especially on micro generation that are not equipped

with power sharing capability. In previous research, the on-off grid tie inverter (on-off GTI) that doesn't have the ability to share power with other inverter, can connected in parallel with other inverters when islanding condition and forming microgrid using master slave network topology and reconfiguration on PV circuit (Hartono BS., et al, 2015).

In this research the control system will be developed to improve the performance of the microgrid. The on-off grid tie inverter (on-off GTI) that can not be connected in parallel with another inverter during islanding condition will be able to connect in parallel, so that the whole system can improve performance of microgrid. The control system was developed using fuzzy logic to reconfiguration PV circuit, which intended to regulate inter-inverter parallel mechanism by taking into account the amount of radiation and the power state of each inverter.

2. Literature Review

2.1 Parallel Inverter

Each energy source in microgrid, either from wind, solar cells and other energy sources, is all converted into electrical energy using suitable power converter circuit and form a distributed power generator network. The inverter circuits operated stand alone or connected in parallel to supply the load at the same time (Chien-Liang, et al, 2010). In grid tie inverter, when tied to grid each inverter can operating in parallel and synchronized by grid power source. In islanding conditions or off grid, where there is no power from grid, it will need a control system that can manage the work of each inverter to be connected, especially in relation to distribution of power that must be supplied by each inverter. Thus each inverters can supply power to other inverter loads that shortage of power to supply the load. Control mechanism that can be use in microgrid during islanding condition can be classified into two types, using communication media and without communication media to coordinate between inverter. Load sharing method with communication media including, centralized control, master slave, average load sharing (ALS), circular chain control (3C) (Josep M. Guerrero, et al, 2008). Equivalent circuit of distributed generator using master-slave control configuration during islanding condition can be seen in Fig. 1. In the circuit below, an inverter works as voltage source that serves as temporary master while other inverters work as a current source that serve as slave.

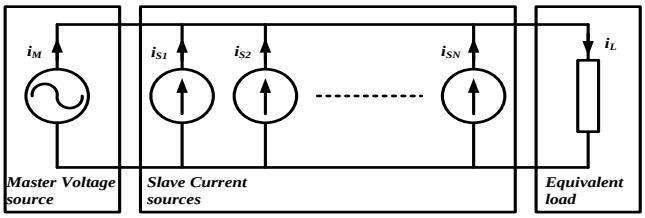

Fig. 1: Equivalent circuit of parallel inverters in distributed generator

The equivalent circuit of two paralleling inverters is shown in Fig. 2. (Hongliang Wang, et al, 2010)

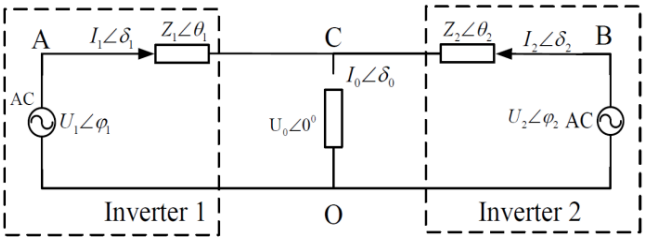

Fig. 2: Equivalent circuits of two paralleling inverters

$$S_1 = \dot{U}_1\dot{I}_1^* = \frac{U_1^2}{Z_1}e^{j\theta_1} - \frac{U_1U_0}{Z_1}e^{(\varphi_1+\varphi_1)} = P_1 + Q_1 \quad (1)$$

$$P_1 = \frac{U_1R_1}{R_1^2+X_1^2}(U_1 - U_0cos\varphi_1) + \frac{U_1U_0X_1}{R_1^2+X_1^2}sin\varphi_1 \quad (2)$$

$$Q_1 = \frac{U_1X_1}{R_1^2+X_1^2}(U_1 - U_0cos\varphi_1) + \frac{U_1U_0R_1}{R_1^2+X_1^2}sin\varphi_1 \quad (3)$$

Where :

- U1 and U2 are output voltages root mean square (RMS) of two inverters.
- φ1 and φ2 are the phase angles.
- U0 is RMS of the load voltage.
- Z and θ are the magnitude and the phase of the output impedance.
- R = Zcosθ, X = Zsinθ

Another thing to be concern when connecting inverters in parallel on a microgrid is the reverse current of the inverter into another inverter. This can be caused by one inverter gives a greater power, while the other inverter has a low load. A reverse current can cause damage to the DC link.

2.2 Fuzzy Logic Control

Fuzzy logic is based on fuzzy relations and fuzzy propositions, the latter being defined on the basis of fuzzy sets (Nikola K. Kasabov, 1998). The fuzzy logic is able to covering the complex system with their uncertainties and inaccuracies that can't solved using classic control theory (Bevrani, H., et al, 2012). Fuzzy Logic is set of multivalued logic that allows intermediate values to be defined between digital logic like true/false or 1/0. Fuzzy logic deal with the concept of partial truth, where the truth value may range between completely true and completely false. Classical logic only permits propositions having a value of truth or falsity.

In the application development of 7-level power inverter, FL controller is used to reduce the rise time and setling time so that the delay time can be reduced. The fuzzy logic controller control the switches present in the boost converter and H-bridge inverter. The six power electronic switches are used only one switch will operate at high frequency at any time (K. S. Gobisha, et al, 2015). Fuzzy logic controller used to control constant load voltage under varying rotor speeds or loads by vary the duty-cycle of the DC-DC converter (Pooja Patel and Jyoti Shrivastava, 2016). An algorithm to determine the optimal scheduling of microgrids is proposed (Juan P. Fossati, et al, 2015). The storage system is controlled by a fuzzy expert system. A genetic algorithm is used to determine the knowledge base of the expert system. The scheduling problem and the building of the knowledge base are jointly tackled. Simulations are performed both for a grid-connected and an islanded microgrid.

2.3 Solar Power Equation

The simplified equivalent circuit of a photovoltaic cell consists of a diode connected in parallel with a current source known as one diode model. In this model current source I_{ph} generated directly proportional to solar radiation (Dorin Petreus, et al, 2008).

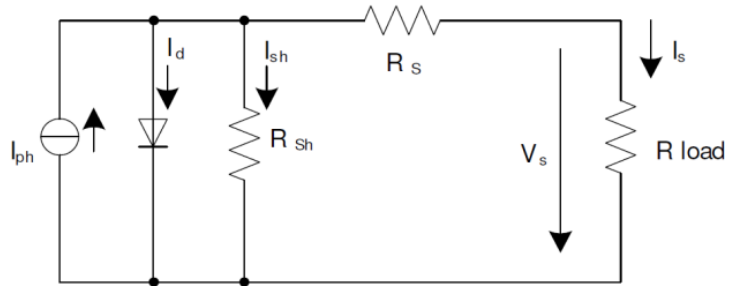

Fig. 3: Equivalent circuit of a photovoltaic cell

With:

- I_{ph} – photo current;
- I_d – diode current;
- I_{sh} – diode reverse saturation current;
- I_S – load current.

The photocurrent I_{ph} is given by the equation:

$$I_{ph} = P_1.F_s[1 + P_2.(F_s - F_o) + P_3.(T_j - T_o)] \quad (4)$$

$$I_d = I_{sat}\left[exp\left(\frac{e_o}{a_f.N_s.k}.\frac{V_s+R_s.I_s}{T_j}\right) - 1\right] \quad (5)$$

$$I_{sh} = \frac{V_s+R_s.I_s}{R_{sh}} \quad (6)$$

$$I_{sat} = P_4.T_j^3.\exp(-\frac{E_g}{k.T_j}) \quad (7)$$

Where

- F_0 = 1000W/m2
- T_0 = 298.15K,
- Tj = junction temperature.

- e_o = 1,60217733.10^{19}[C] is charge of electron
- a_f = "ideally factor", usualy is 1
- Ns = number of cells in series
- k = 1,380658 10 [J/K]$^{-23}$ is Boltzmann's constant
- Rs [Ω] = models the series resistance
- Eg [eV] = The band gap
- P_4 [$\frac{A}{K^3}$] = a correction factor.
- P_1 [Am2 /W], P_2 [m2/W] and P_3 [1/K] are constants, usually given by the producers
- The parameters P_4 [A/K3], R_s [Ω], R_{sh} [Ω] can be obtained from the solar panel's datasheet.

3. Propose Design

Microgrid control system design is based on the results of previous research, that can estimate the amount of power input from solar radiation by looking at the value of the PV voltage and current. While the measurement of the output power of each inverter to the load can determine opportunities for both parallel inverters. By using fuzzy logic rules and conducting a second regulatory mechanism, the inverter can work parallel in a master slave configuration. The control system consists of a controller device that will do the reading input parameters and output actuation devices that will regulate the amount of power input and local load on each inverter. Diagram of development control system as shown in Fig. 4.

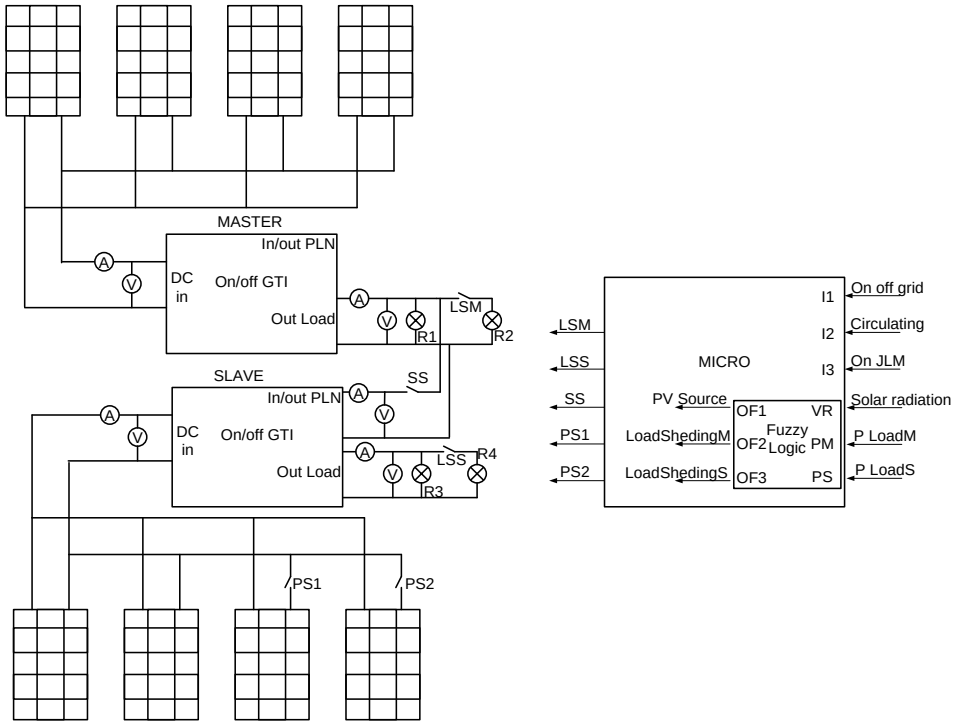

Fig. 4: Control system diagram

Control system design using matlab starts with the setting the parameters control, both for inputs and outputs, to be processed using fuzzy logic. Based on the problems identified,

fuzzy input parameters are:

- Sources of radiation
- Load on inverter master and slave.

As for the fuzzy output parameters are:

- Setting of PV energy sources
- Load shedding on master load
- Load shedding on slave load

Table 1: Mapping of input parameters of fuzzy logic

INPUT	H	M	L
Radiation (RAD)	> 4,5	>3,75	<3,75
Power master (PM)	> 200W	>100	<100
power slave (PS)	> 200W	>100	<100

Table 2: Mapping rules of input and output fuzzy logic

RAD		H	M	L
PS	**PM**	**SPV,LSM,LSS**	**SPV,LSM,LSS**	**SPV,LSM,LSS**
H	H	allon,on,on	allon,on,on	-
H	M	allon,off,on	allon,off,on	-
H	L	allon,off,off	allon,off,on	-
M	H	off1,on,off	allon,on,off	-
M	M	off1,off,off	allon,off,on	-
M	L	off1,off,off	allon,off,off	-
L	H	off1,on,off	allon,off,off	-
L	M	off1,off,off	allon,off,off	-
L	L	off2,off,off	off1,off,off	allon,off,off

Description:

RAD : radiation PM : power master PS: power slave
H : High
M : Medium
L : Low
SPV : PV source
for PV source:

- allon : Relay PS1 and PS2 on
- off1 : Relay PS1 off
- off2 : Relay PS2 and PS2 off

LSM : LoadShedingMaster
LSS : LoadShedingSlave
for LSM and LSS:

- on : perform load shedding relay means open
- off : not perform load sheding relay means close

From output mapping, it appears that the input power settings, from PV is divided into 3 levels:

- allon means, from 4 PV are used, all connected to the inverter while
- Off1 means, there is one unused PV
- Off2 means, there are two unused PV

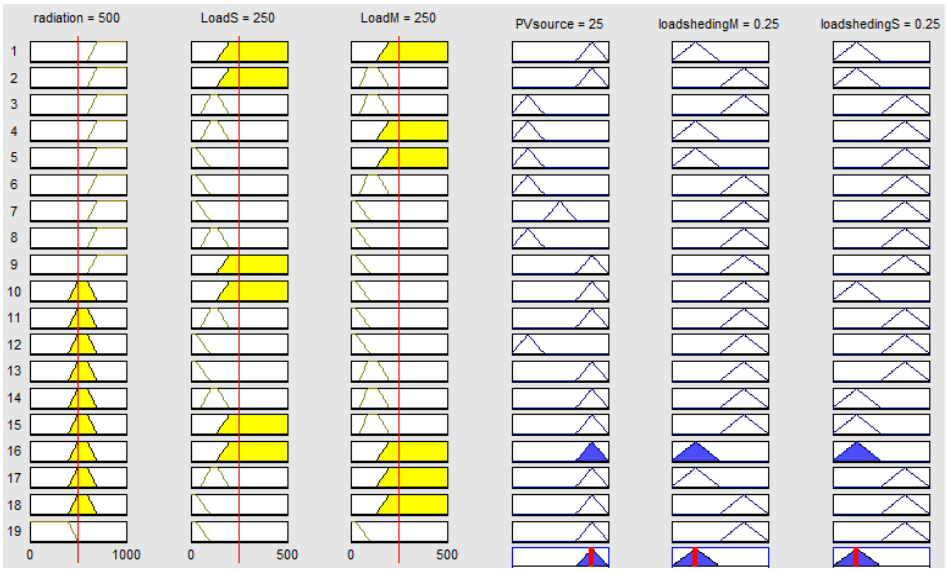

Fig. 5: Rule viewer of fuzzy logic control

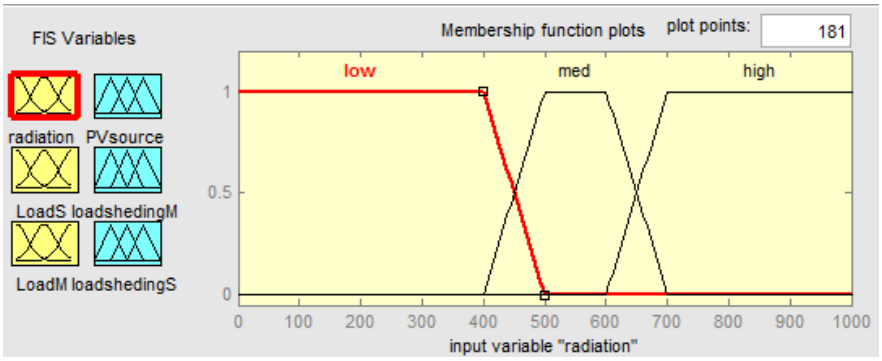

Fig. 6: Membership function plot

Solar radiation will be measured using a radiation measuring circuit, which will convert the amount of radiation into voltage of 0 volts to 5 volts. Based on the measurement results, the amount of radiation is classified into, above 700W/m2 (> 4.5 volts) as high radiation / high (H), above 600W/m2 medium / medium (M) and under 600W/m2 less / low (L). Similarly done to define fuzzy parameters, to power local loads of master and slave, as shown in table above.

Based on the mapping of input and output fuzzy logic, a fuzzy logic control system design using matlab is performed. Design begins with a fuzzy inference system. Starting from the fuzzification of input and output. Proceed with the design of fuzzy rule between inputs and outputs. Designed by using the rule viewer to be seen whether metlab control system works as designed.

4. Result and Discussion

Based on the analysis of the rule viewer, control system design using fuzzy logic has worked corresponds to a mapping of input and output design. In the system controller development, the main operation is having two parallel mechanisms inverter duringthe islanding condition (off grid). during on grid conditions, then microcontroller just read connection status to the grid, without control mechanisms at all. Based on inputs and outputs test on the system microcontroller, it looks that appropriate design program has been running. Program has not been implemented to microgrid system functions as a whole. This is due to limitations of available resources both human resources and testing facilities, but from the representation of the input and output of the I/O microcontroller, it can be concluded that the system has been able to work as designed.

The test results showed that when both paralleled inverters performed without prior arrangement, the instability occurs when both inverter synchronization process failed. This is caused due to excessive power supply of the slave inverter, so that reverse current occurs on master inverter. Protection of the master inverter disconnects both parallel inverters. To balance the power demand on the load, the configuration of solar panels on the slave inverter

is reduced, so that power is supplied to the load is reduced and the condition can occur in both synchronous inverter operated parallel. The measurement results of two synchronous condition inverters operating in parallel as shown in Fig. 7 (Hartono BS., et al, 2015). The test results showed an increase in energy absorption from PV up to 26% and increased operation of the battery up to 26.38%.

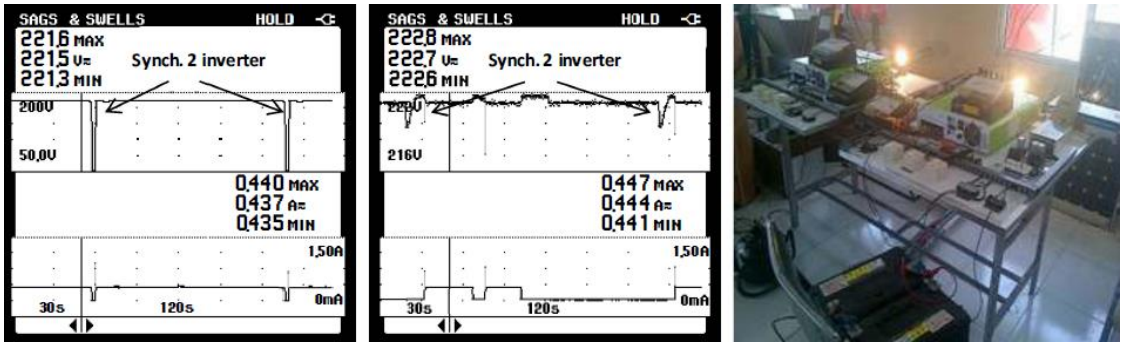

(a) (b) (c)

Fig. 7: (a) unstable condition of parallel 2 inverter (b) Synchronous condition, 2 pieces of inverter stable and stability is achieved due to the setting of fuzzy logic (c) Parallel inverter output voltage

5. Conclusion

Control mechanisms of micro grid systems, consisting of on-off GTI, during islanding conditions, can be done by arranging the PV circuit configuration using the fuzzy control method. The test results showed an increase in energy absorption from PV up to 26% and increased operation of the battery up to 26.38%. The use of on-off GTI in microgrid applications can be performed in a master-slave configuration. In this configuration, one inverter works as reference to other inverter is connected to it.

It should be considered to controlling the operation of two on-off GTI in parallel can be perform by controlling the input energy from PV to the inverter which acts as a slave, does not exceed the power which required by the load so there is no reverse current into the master inverter. Input energy control is done by configuring the number of PV panels connected to slave inverter in order to obtain the appropriate amount of power input, so that both inverters can work as a microgrid.

6. References

Bevrani, H., Habibi, F., Babahajyani, P., Watanabe, M. and Mitani, Y., 2012, Intelligent Frequency Control in an AC Microgrid: Online PSO-Based Fuzzy Tuning Approach, Smart Grid, IEEE Transactions on, Volume: 3 , Issue: 4 2012, pp. 1935 – 1944

Chien-Liang Chen, Yubin Wang, Jih-Sheng (Jason) Lai, Yuang-Shung Lee, and Daniel Martin, 2010, Design of Parallel Inverters for Smooth Mode Transfer Microgrid Applications, IEEE Transactions On Power Electronics, Vol. 25, NO. 1, january 2010

Dorin Petreus, Cristian Farcas, and Ionut Ciocan, 2008, Modelling And Simulation Of Photovoltaic Cells, Acta Technica Napocensis, Electronics and Telecommunications, Volume 49, Number 1, 2008, pp. 42-47

European Commission, 2003, New ERA for electricity in Europe. Distributed Generation: Key Issues, Challenges and Proposed Solutions, EUR 20901, ISBN 92-894-6262-0.

Hartono BS, Rudy Setiabud and Budiyanto, 2015, Development Method for Paralleling Inverters on Microgrid When Islanding Condition Using Reconfiguration of PV Circuit, International Conference on Quality in Research, IEEE, pp. 121-124

Hongliang Wang, Yinyin Xie, Xuejun Pei and Yong Kang, 2010, A New Method of Power Arithmetic for Parallel Inverter, Electronics And Electrical Engineering, No. 10(106), pp. 3-8

Josep M. Guerrero, Lijun Hang, and Javier Uceda, 2008, Control of Distributed Uninterruptible Power Supply Systems, IEEE Transactions On Industrial Electronics, Vol. 55, NO. 8, August 2008

Juan P.Fossati, AinhoaGalarza, AnderMartín-Villate, José M.Echeverría and LuisFontán, 2015, Optimal scheduling of a microgrid with a fuzzy logic controlled storage system, International Journal of Electrical Power & Energy Systems, Volume 68, June 2015, Pages 61-70

K. S. Gobisha, J. S. Monica Shalini, A. Ravi, and Jasper Gnana Chandran, 2015, A Fuzzy Logic Controlled Solar Power Generation with Seven Level Inverter, International Journal of Emerging Technology and Advanced Engineering, Volume 5, Issue 2, February 2015, pp. 285-288

Kroposki B., Lasseter R., Ise T., Morozumi S., Papatlianassiou S. and Hatziargyriou N., 2008, Making microgrids work, Power and Energy Magazine, IEEE, Volume: 6 Issue: 3 2008, pp. 40 – 53

Lasseter, R.H., 2002, MicroGrids, Power Engineering Society Winter Meeting, IEEE, vol.1, pp.305 - 308

Nikkhajoei, H. and Lasseter, R.H., 2009, Distributed Generation Interface to the CERTS Microgrid, IEEE Transactions On Power Delivery, Vol. 24, No. 3, July 2009, Page(s): 1598 – 1608

Nikola K. Kasabov, 1998, Foundations of Neural Networks, Fuzzy Systems, and Knowledge Engineering, AA Bradford Book The MIT Press Cambridge, Massachusetts London, England, ISBN 0-262-11212-4

Pooja Patel and Dr. Jyoti Shrivastava, 2016, Modelling & Performance Analysis of Hybrid Renewable Energy Resources Using Fuzzy Logic Controller, International Journal of Science, Engineering and Technology Research (IJSETR), Volume 5, Issue 5, May 2016, pp. 1421-1428\

W. Kramer, S. Chakraborty, B. Kroposki, and H. Thomas, 2008, Advanced Power Electronic Interfaces for Distributed Energy Systems Part 1: Systems and Topologies, Technical Report NREL/TP-581-42672 March 2008

Xiongfei Wang, Josep M. Guerrero, Frede Blaabjerg, and Zhe Chen, 2012, A Review of Power Electronics Based Microgrids, Journal of Power Electronics, Vol. 12, No. 1, January 2012, page(s): 181-192

Proceedings of the 1st Faculty of Industrial Technology International Congress
International Conference
Bandung, Indonesia, October 9-11, 2017
ISBN 978-602-53531-8-5

Development of a Drowsiness Detector based on the Duration of Eye closure using A Low-Cost EMG

Dian Artanto[1,*], Ign. Deradjad Pranowo[1], M. Prayadi Sulistyanto[2], Ervan Erry Pramesta[2]
[1] Mekatronika, Politeknik Mekatronika Sanata Dharma, Yogyakarta - INDONESIA
[2] Desain Produk Mekatronika, Politeknik Mekatronika Sanata Dharma, Yogyakarta - INDONESIA
*Corresponding author e-mail: dian.artanto@pmsd.ac.id

Abstract

Many traffic accidents are caused by drivers who are less concentrated due to drowsiness. From existing reports, it is known that the loss due to traffic accidents is very large, not only bring bad impact to the victims, also for the family environment, community and country. Seeing the conditions of this traffic problem, a device that can wake the driver while sleepy can be a solution. From several studies on drowsiness, it has been found that there is a connection between the drowsiness with blinking and closing the eyes often and long. This paper proposes a device that can detect the duration and frequency of eye closure using a low-cost EMG. When the accumulated duration of the eye closure exceeds the specified limit, a buzzer will sound to wake the driver. Compared to other detection devices, the low-cost EMG-based drowsy detector is promising, as it can be mounted practically on an eyeglass frame, and does not damage or injure the eyes. The development of this device so that it can be a reliable and economical device becomes an interesting challenge for the author and his team.

Keywords: traffic accidents, a drowsiness detector, an eye closure duration, a low-cost EMG, an eyeglass frame.

1. Introduction

The global status report on road safety that released by the UN WHO in 2015 states that deaths from traffic accidents around the world have reached 1.25 million per year, which means close to 3400 deaths every day. It is also reported that traffic accidents are the leading cause of death globally among people aged 15-29. Without proper effort, deaths from traffic accidents can be around 1.9 million per year by 2030 (WHO, 2015).

Traffic accidents have a terrible impact on individuals, communities and countries. It all causes not only grief and suffering, but also economic losses, productivity losses, reduced quality of life, and other social impacts (Soehodho, 2017; Sugiyanto, 2017).

Traffic accidents are often caused by three different factor types, namely, human error factors, vehicle factors, and external factors (including road conditions). Human error factors are the highest causal to traffic accidents, especially the lack of concentration due to drowsiness (Zuraida et al., 2017; Puspasari et al., 2015).

Drowsy driving is a major contributing factor to a traffic accident. This has been proven by the many studies that found a connection between driver drowsiness and traffic accidents. Preventing the driver from drowsiness will be able to reduce accidents. Physiological measures have frequently been used for drowsiness detection as they can provide a direct and objective measure. Possible measures are EEG (Electro-Encephalo-Graphy), eye movements, eye blinks and eyelid closure (Svensson, 2004).

EEG is an electrophysiological monitoring method to record electrical activity of the brain. EEG has shown to be a reliable indicator of drowsiness. The amount of activity in different frequency bands can be measured to detect the stage of drowsiness. The disadvantage of using EEG are the impractical placement of the device on the driver, and the obtrusive electrodes which make them unsuitable to use in cars, as cabling of the drivers would not achieve any acceptance (Mardi et al., 2011).

Eye movements can be measured using EOG (Electro-Oculo-Graphy). EOG is a technique for measuring the corneo-retinal standing potential that exists between the front and the back of the human eye. However, just like EEG, EOG has a weakness in the impractical placement of the device and the number of electrodes that must be put on the driver (Bandara, 2009).

Eyelid closure can be monitored with the camera very precisely and quickly. However, the use of the camera has a limitation of illumination, as the normal cameras do not work well at night when monitoring is more important. Other concerns for camera-based systems are the high cost and the loss of image when the drivers look in their mirrors outside the view of cameras. In addition, most of the camera-based system need computers, image processing algorithms and feature extraction techniques to extract drowsy symptoms (Garcia et al., 2010).

Instead of the camera, the eyelid closure can be captured using a portable and low-cost device based on IR sensors mounted on an eyeglass, that directing an IR beam to the human eye (Ma'touq et al., 2014). However, strong IR beam in high temperature could be harmful to eyes (Agrawal, 2017).

As an alternative drowsiness detection device, this paper proposes the use of a low-cost EMG (Electro-Myo-Graphy) to monitor the eyelid muscles, and measure the duration of the eyelid closure, then sound a warning when the duration exceed the limit.

2. Methods

2.1. Prototype of the Detector

In this paper, as mentioned earlier, a drowsiness detection device is proposed using a low-cost EMG, which is widely available in the local market under the name Myoware. To be able to measure the muscle electrical activity on skin, that has a very small voltage value (in µV unit), Myoware is equipped with 3 electrodes; 2 of them must be placed on skin in the measured muscle area, and 1 electrode must be placed on skin outside the muscle area, which is used as the ground point. All three electrodes can use any conductor material (Advancer, 2013).

The muscle to open and close the eyelids known as Levator Palpebrae, located at the top of the eye. To measure the tension in the muscle, 2 electrodes must be placed around the muscle, precisely in the upper eyelid, while 1 electrode can be placed outside the muscle, in the area close to the ear. The placement of a pair of EMG electrodes does not need to be pressed, just simply touching the skin. Therefore, the installation of a pair of electrodes can be done with the help of glasses, i.e. by placing it on the frame of the top glasses, such that when the glasses are worn, the pair of electrodes can touch the upper eyelid skin. The following figure is a prototype of drowsiness detection device that involves eyeglasses, electrodes, a Myoware Muscle Sensor, an Arduino Nano, a Potentiometer, a Buzzer and 2 Batteries.

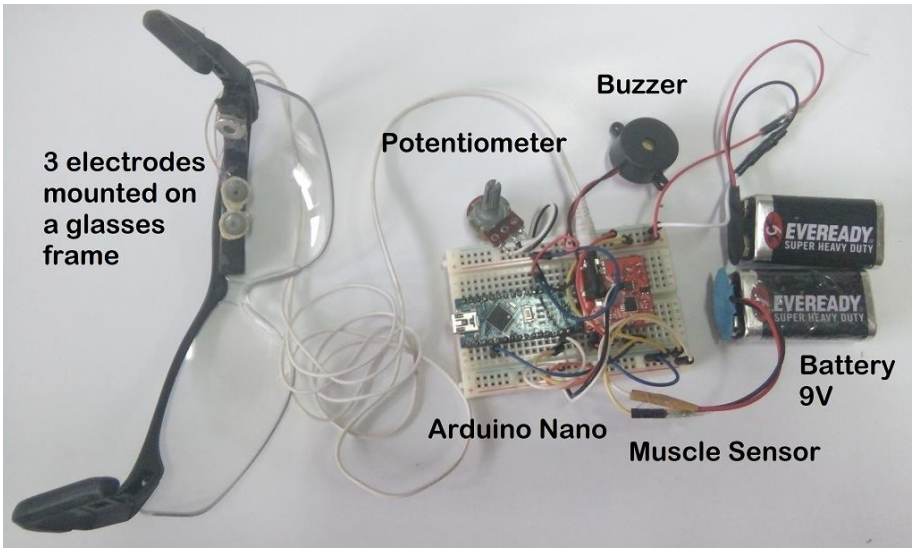

Fig. 1: The hardware prototype of drowsiness detection device

For more details about the circuit schematic of device and the placement of the three electrodes on the frame of eyeglasses, see Fig 2 below.

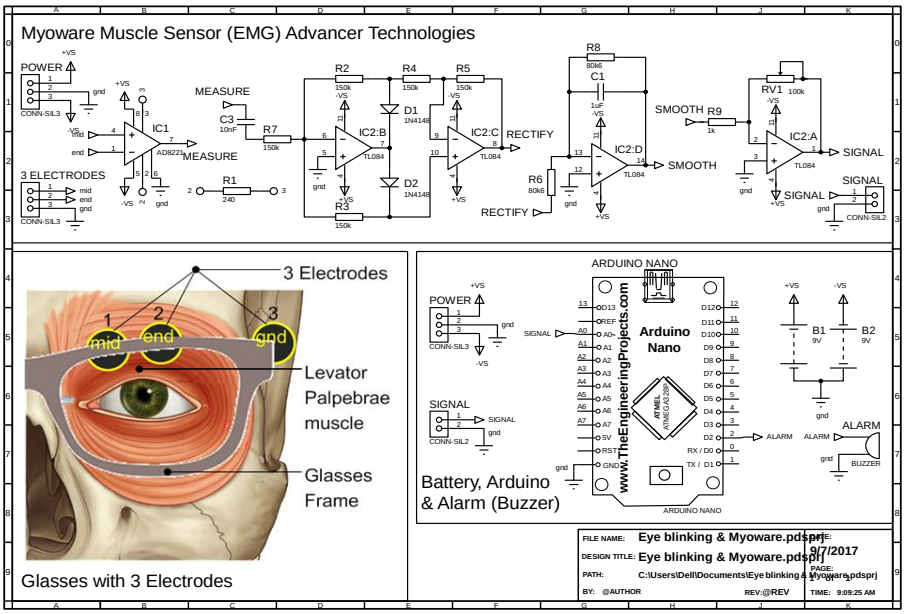

Fig. 2: Circuit Schematic and electrodes placement on eyeglass

Seen from Fig 2 above, a circuit schematic of the drowsiness detection device. The way this circuit works is, starting with an op-amp AD 8221 that measures a very small voltage difference between two electrodes placed in the eye muscle region. The result of the measurement is then rectified, smoothed and then amplified again to get the right value to be read Arduino. Using all the circuit, the Myoware sensor output value when the eyelid is opened is 0, and the output value when the eyelid is closed is greater than 0, and the value will be even greater when the eyelids are closed more tightly.

Fig 3 and 4 below show the graph of the eye muscle sensor output value using Serial Plotter Arduino when the eyelids are closed and when the eyelid are opened. It appears that the value of the graph curve becomes greater than 0 when the eyelid is closed, and is 0 when the eyelid is opened.

Fig 3: The graph when the eyelid is closed

Fig 4: The graph when the eyelid is opened

2.2. Prototype of the Alert System

After the Myoware sensor output value when the eyelid is opened and closed is known, the next step is to add an alert system so that the device can give a warning when a certain limit value is exceeded. To achieve this, a Buzzer and a Potentiometer have been added, as shown in the hardware prototype in Figure 1 above. The Buzzer here is used to generate warning sounds, and the Potentiometer here is used to set the time limit value of closed eyelid duration. Figure 5 below shows the block function diagram of the drowsiness detection system.

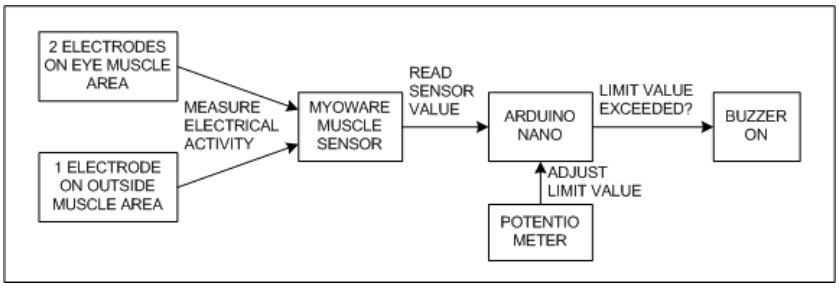

Fig 5: Function Block Diagram of Drowsiness Alert System

To achieve the function of the device following the function block diagram above, here is a more detailed state diagram of the working principle of the drowsiness alert system.

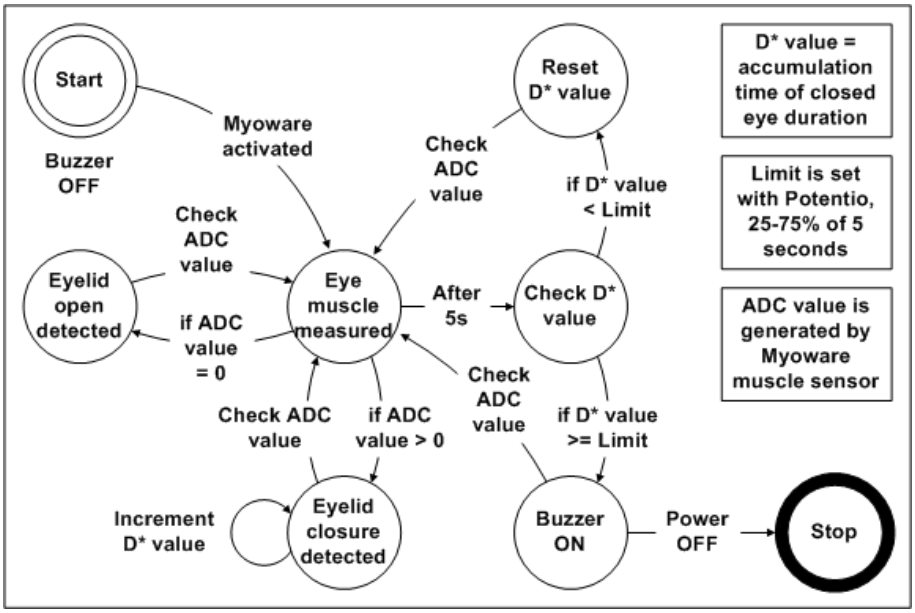

Fig 6: State Diagram of Drowsiness Alert System

Here is an explanation of the State Diagram above. Starting after Myoware is activated. It will get the value of eye muscle electrical activity. When the eye muscle is opened then the sensor value will be 0, and when the eye is closed the sensor value will be greater than 0. When the sensor value is greater than 0, a variable named D, will be incremented by 1. After 5 seconds, the value of D is compared with the time limit set by Potentiometer. If the value of D is greater than the time limit, then Buzzer will be sounded. If the value of D is less than the time limit, the value of D will be reset to 0. After the Buzzer sounds, Buzzer will continue to sound until the power supply to the device is stopped.

3. Results and Discussion

3.1. Results

From the methods of making the drowsiness detection device and the alert system proposed above, it has obtained the results of a portable and easily wearable drowsiness detection device.

Compared to the use of EEG and EOG, the device proposed in this paper is easier to install, because the electrode is installed only 3, so it can be placed on the glasses frame, while in EEG and EOG more than 3, so the use of EEG and EOG is perceived by the driver a little inconvenient, especially for motorcyclists. When compared with the use of cameras to monitor the eyes, the device proposed in this paper is better, because it is not affected lighting, both day and night. When compared to the drowsy detector using an IR beam directed directly to the eye, the device proposed in this paper is better, as it does not injure the eyes.

Another interesting thing, this device is quite economical, because EMG used is a very cheap type of EMG, also Arduino Nano, so the cost of making this device quite affordable. The result of making this tool is quite promising and can be developed to better meet the needs of users.

3.2. Discussion

To be discussed, the time limit setting of the closed eye duration is 25 - 75% of 5 seconds, i.e. 1.25 - 3.75 seconds. The time limit setting is determined by experience and reality on the highway, where for drivers who are driving at high speed, closing the eyes for more than 2 seconds can lead to a traffic accident.

The time limit value is deliberately made to have variations, due to different needs and levels of drowsiness. Some people have a habit of closing the eyes many times even if not sleepy. Some others may have experienced heavy drowsiness but did not close their eyes at all. So, for some cases, closing the eyes is not directly related to drowsiness. It is necessary to observe the habit before wearing this device. However, in general, if a person initially rarely closes and blinks his/her eyes, then after a while becomes frequently closes and blinks it, then this can be a sign that the person is sleepy. So, a change of pattern from closing the eyes suddenly and often can be a sign that there is drowsiness.

4. Conclusion

In this paper, a prototype of drowsiness detection device using cheap and easy-to-wear EMG has been proposed. From the observation results, this device is quite promising because of the following points:

1. The use of closed eye duration indicator has a better chance of detection, because the results are quickly known so that it can give warning more quickly when the driver is sleepy.
2. Use of EMG is better than EEG and EOG, because the number of EMG electrodes is less, so it is not complicated to be mounted on the glasses frame.
3. Use of EMG is better than cameras and IR sensors, because it is not affected by daylight or nighttime light, and does not injure the eyes.

In closing, this proposed device still needs to be developed, because for some people, even if they often close and blink their eyes, it does not mean they're sleepy, but because they're used to such reflexes. But if the person rarely blinks and closes his eyes, then after some time becomes often blinks and closes his/her eyes, then this condition can be a sign of the person is sleepy. These specific conditions need to be considered for the development of this device in the future.

5. References

Advancer Technologies, 2013. Muscle Sensor v3 User's Manual. Available at: http://www.advancertechnologies.com/p/muscle-sensor-v3.html, accessed on September 5, 2017.

Agrawal, D.P., 2017. Embedded Sensor Systems. © Springer Nature Singapore Pte Ltd., ISBN 978-981-10-3037-6. ISBN 978-981-10-3038-3 (eBook) DOI 10.1007/978-981-10-3038-3.

Bandara, I. B., 2009. Driver drowsiness detection based on eye blink", Faculty of Enterprise & Innovation, Buckinghamshire New University, Brunel University, March.

García, I., Bronte, S., Bergasa, L. M., Hernandez, N., Delgado, B., Sevillano, M., 2010. Vision-based drowsiness detector for a Realistic Driving Simulator. Intelligent Transportation Systems (ITSC), 13th International IEEE Conference on.

Ma'touq, J., Al-Nabulsi, J., Al-Kazwini, A., Baniyassien, A., Issa1, G. A., Mohammad, H., 2014. Eye blinking-based method for detecting driver drowsiness. J Med Eng Technology 38(8): 416–419, ©2014 Informa UK Ltd., ISSN: 0309-1902 (print), 1464-522X (electronic).

Mardi, Z., Ashtiani, S.N., Mikaili, M., 2011. EEG-based Drowsiness Detection for Safe Driving Using Chaotic Features and Statistical Tests. J Med Signals Sens. May;1(2):130-7.

Puspasari, M. A., Muslim, E., Moch, B. N., Aristides, A., 2015. Fatigue Measurement in Car Driving activity using Physiological, Cognitive, and Subjective Approaches. International Journal of Technology 6: 971-975, ISSN 2086-9614.

Soehodho, S., 2017. Public Transportation Development and Traffic Accident Prevention in Indonesia. IATSS Research, 40, pp. 76-80.

Sugiyanto, G., 2017. The Cost of Traffic Accident and Equivalent Accident Number in Developing Countries (Case Study In Indonesia). ARPN Journal of Engineering and Applied Sciences, 12(2), pp. 389-397.

Svensson, U., 2004. Blink behaviour based drowsiness detection – method development and validation. Master's thesis project in Applied Physics and Electrical Engineering, Swedish National Road and Transport Research Institute, ISSN 1102-626X.

World Health Organization, 2015. Global Status Report on Road Safety 2015. Available at: http://www.who.int/violence_injury_prevention/ road_safety_status/2015/en/, accessed on September 5, 2017.

Zuraida, R., Iridiastadi, H., Sutalaksan, I. Z., 2017. Indonesian driver's characteristics associated with road accidents. International Journal of Technology 2: 311-319, ISSN 2086-9614.

Proceedings of the 1st Faculty of Industrial Technology International Congress
International Conference
Bandung, Indonesia, October 9-11, 2017
ISBN 978-602-53531-8-5

Effect of Air Gap on Armature Voltage on Axial Flux Permanent-Magnet Generator ac by Using NdFeB 52

Asep Andang*, Nurul Hiron
Department of Electrcial Engineering, Universitas Siliwangi, Tasikmalaya - INDONESIA
* Corresponding author e-mail: andhangs@unsil.ac.id

Abstract

There is an increase in the development of Axial Flux Permanent Magnet Generator (AFPMG) which is proven by numerous types of machine variations which are developed and studied. AFPMG has advantages in terms of lossless and thinner construction and its use in various fields of micro electromechanical system and domestic utilities. In the implementation of this design, we used ANSYS software to design the construction, flux distribution, and the expected voltage. In the design of this AFPMG, we made dual-rotor permanent magnet constructions clamping the stator containing an armature winding with a three-phase AC output voltage with a star winding configuration. The design process also included a simulation of the effect of gap distance differences on the electromotive force generated by the armature winding. The design results were implemented then tested with varying rotation and significant changes in air gap from 2 mm until 6 mm to produce the performance of the machine. Based on the test results, the maximum voltage in the zero-load condition, in which the air gap was at 2 mm, was 10.7. In the loaded test with rpm variation, the voltage regulation was with a range of 32.96% and 43.75% for a 2 mm air gap.

Keywords: Axial Flux Permanent-Magnet Generator, Various Speed, air gap, NdFeB 52

1. Introduction

The development of electricity generation by converting mechanical power continues to grow on a small scale known as the micro-electromechanical system (MEM). MEM with the use of magnetic material as a conversion medium one of which by using axial flux permanent magnet generator (Holmes et al. 2005)

The use of AFPMG is applied to the needs of wind farms(Ashraf & Malik 2017)with 1,200 watts or low power by either using single(Nur et al. 2013) or double savinous turbines (Alqodri et al. 2015). The other uses of AFMG are related to the need for small mechanical motions such as electromagnetic launchers(Sezenoglu & Balikci 2015) also used in vehicles and trains (Gör & Kurt 2015).

The output voltage of the AFPMG is an alternating voltage normally get into the grid but some researches suggest that adding a rectifier generated the DC output used to fill the accumulator(Wijaya et al. 2016). Similarly, continuous developmental construction starts with single-rotor single-stator (Alqodri et al. 2015) single-stator double-rotor (Gör & Kurt 2015) or with TOROS-S Structure (Taran & Ardebili 2014). Various studies suggest that the speed will affect the output voltage as well as the frequency generated which are in accordance with the law of EMF. Therefore, in order to generate AC voltage that can get into the grid, the generator frequency must equal to the frequency of the system.

In line with the high demand of permanent magnets, nowadays, the growth of the permanent magnet industry is becoming a promising industry, especially the NdFeB permanent magnet. Fig 1 shows the growth of permanent magnet production from several country producers. The demand of NdFeB-type magnets is projected to be significantly increased, especially between 2015 and 2020 reaching more than 120 (kt). Currently, China is the largest producer of permanent magnets compared to Japan, Europe and other countries including USA (Fig.1.a). While the world's need for permanent magnets is dominated by the Nd-type permanent magnet (Fig. 1.b).

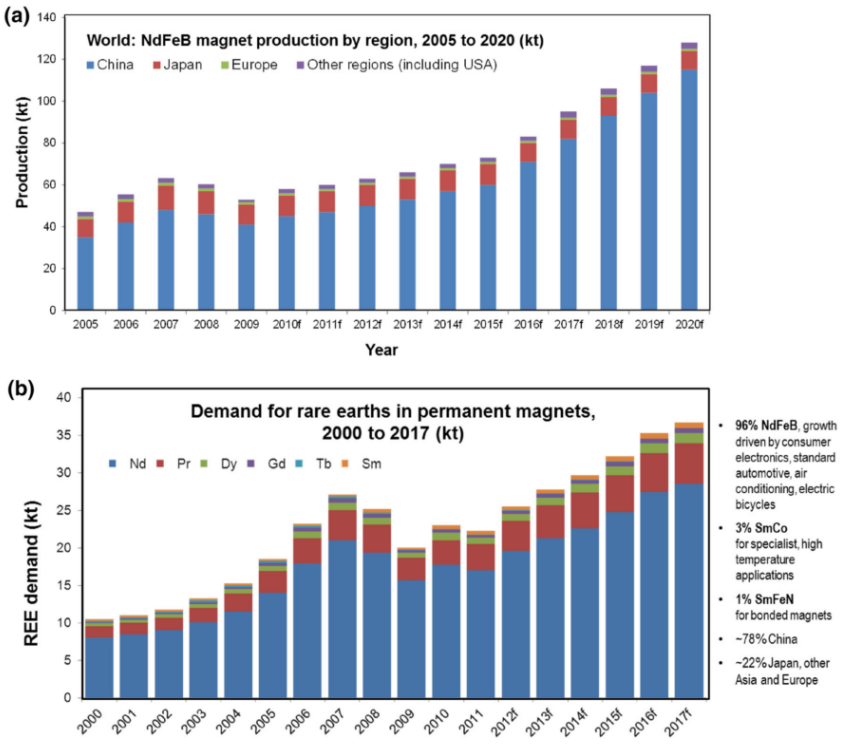

Fig.1: Global production of NdFeB permanent magnets and the demand for the REEs (Shaw S 2012)**,** (Yang et al. 2016)**. (a) Total global NdFeB magnet production and prediction: 2005–2020, (b) Total global REE demands for permanent magnets** (Yang et al. 2016)

This study focuses on preparing simulations for analyzing Air Gap Effect on Armature Voltage on Axial Flux Permanent Magnet AC generator by using NdFeB 52. NdFeB 52 magnets are used because NdFeB 52 magnets have a unique character that is the Maximum Energy Product (Bhmax) is 50 -52 MGOe (398-422 MGO (KJ / m3) (Shaw S 2012)(Yang et al. 2016).

2. Method

The design of Axial Permanent Magnetic Flux Generator was done by using ANSYS in order to find out the finite element distribution and also the magnetic field (Holmes et al. 2005). The use of ANSYS was also carried out to find out the design parameters (Sadeghierad et al. 2008) so that the rotor dimension, big stator winding, and other things are known.

In this design, the dimension of the stator winding that would use was a type of stator that has no iron core on the coil. This is because the type of stator with no iron core was more suitable to the low axial generator. We used 12 coils of armature winding to produce three-phase AC voltage, in other words, in every phase there were 4 coils.

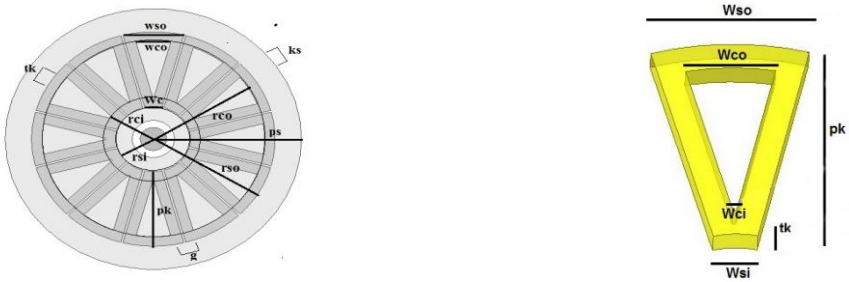

a. The shape of stator disk with 12 coils **b. The shape of stator disk with 1 coil**

Fig. 2: The stator disk with a winding shape

The shape of the armature winding itself is a type of trapezoidal winding with the number of coil windings per phase was 150 winding or 38 winding per coil with non-overlapping windings form. The designed coil was a non-overlapping type aimed at maximizing the induction of the magnetic field on the coil and avoiding the addition of thickness to the stator. We used copper wire with a diameter of 1 mm. As for the dimensions of the stator itself, it can be seen in table 1.

Table 1: The Size of the Stator

No	Description	Size (mm)
1	Stator Diameter	280
2	Stator Length (ps)	140
3	Stator Thickness (ks)	25
4	Distance Between Stator (g)	2
5	Outer Width (wso)	57.5
6	Inner Width (wsi)	16
7	Width of Stator Foot (wc)	2
8	Coil Length (pk)	80
9	Coil Thickness(tk)	10

The type of permanent magnet to be used in the design of the rotor was a Neodynium-Iron-Boron Permanent Magnet (NdFeB). This type of permanent magnet has larger magnetic field value and magnetic flux density than other permanent magnets that is 1.43 tesla. The use of permanent neodynium-iron-boron (NdFeB) permanent magnet (specifically the type of magnet used was N52) aimed at obtaining the maximum magnetic flux value so as to obtain maximum induction voltage.

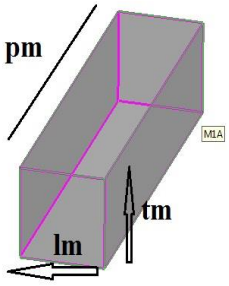

Fig. 3: Dimmension of permanent magnet

The design of the rotor consisted of 8 magnetic poles on each inner side of the rotor. The design of the maximum number of coils and permanent magnets would increase the value of the induced frequency and induced voltage. Installation combinations of magnetic poles were performed in accordance with the N-S type which aimed to increase the magnetic flux density value between the two rotors.

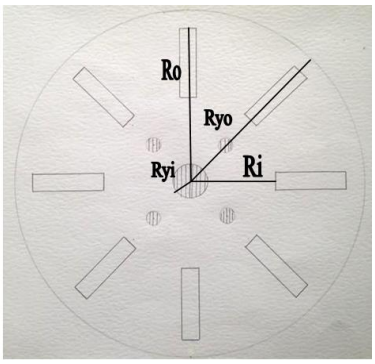

Fig. 4: The distribution of 8 pairs of N-S magnetic poles

As for the stator dimension, it can be seen in the table below:

Table 2: The Size of the Rotor

No	Description	Size (mm)
1	Rotor Diameter (dr)	210 mm
2	Rotor Thickness (kr)	5 mm
3	The outer radius of the rotor (ryo)	110 mm
4	The inner radius of the rotor (ryi)	9.5 mm
5	The outer radius of the magnet (ro)	105 mm
6	The inner radius of the magnet (ri)	65 mm

Then, when the rotor configuration and the three-phase axial stator flux permanent magnet generator with double rotor were set, they were as shown below

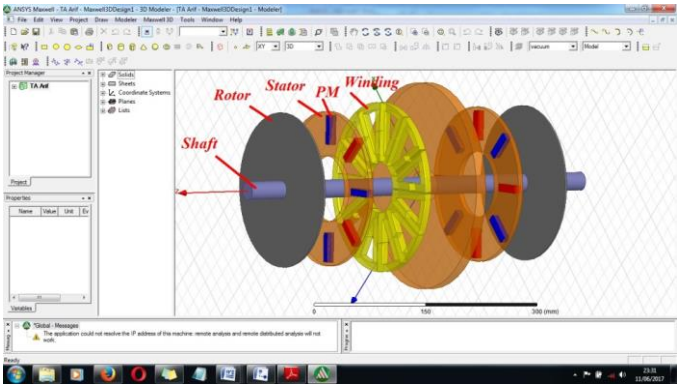

Fig. 5. Double rotor configuration and stator in AFPMG

The flux distribution test was carried out by doing a simulation on ANSYS to understand the spread and magnetization of the armature winding. The spread of this magnetization can be seen in the figure below

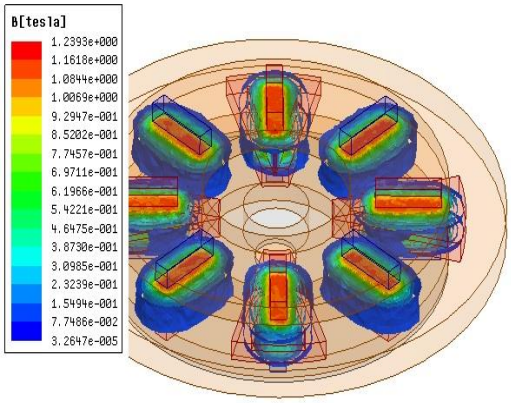

Fig. 6: The simulation of flux distribution by using ANSYS

It produced the flux quantities with the air gap variables with a range of 2 mm and 6 mm from each rotor to the stator as in the table below. There was a non-uniformity of the flux distribution in each winding phase due to the uneven distribution of flux to the position of each winding.

Table 3: The testing of the flux distribution

Phase	The Effect of Air Gap on Flux Distribution				
	2mm	3mm	4mm	5mm	6mm
Phase R	1.239 T	0.993 T	0.860 T	0.764 T	0.698 T
Phase S	1.189 T	0.988 T	0.866 T	0.765 T	0.663 T
Phase T	1.212 T	1.014 T	0.868 T	0.761 T	0.667 T

In the form of a flux distribution graph for the three-phase shown below, it can be seen that the larger the gap the smaller the flux distribution that occured due to the flux became the loss in the air gap, thus the optimum flux distribution was at 2mm. This distribution also did not occur uniformly on each phase windings R, S and T due to the uneven position of the magnetic field toward the winding.

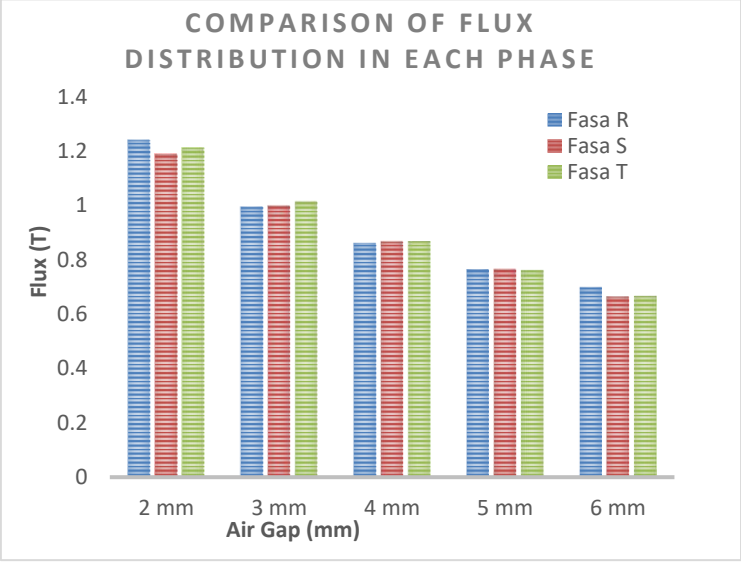

Fig. 7: Flux Distribution

3. Testing and results

The test was carried out by burdening the generator with varying resistance loads with changes in motor speed from 300 to 800 and with a variation of the air gap from 2 mm to 6 mm. This test showed the optimal gap of the generator to produce the greatest power.

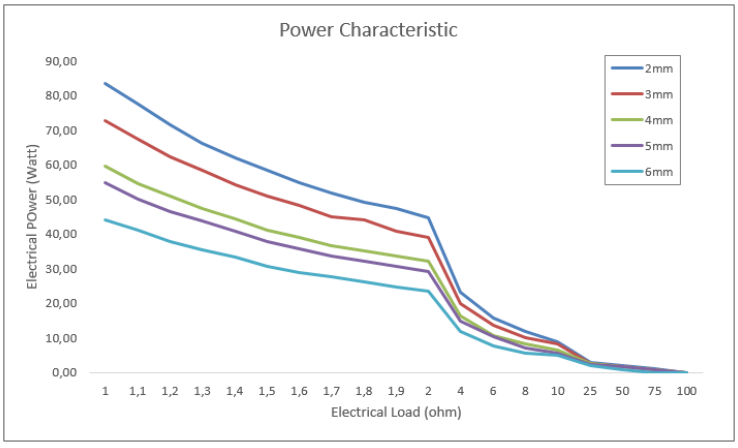

Fig. 7: The testing with variations of air gap with various load quantities

In this test, the rate of decline in electrical power decreases and inversely proportional to the load, as well as the air gap, it was known that the air gap that produced optimal power was at 2 mm. The larger air gap the smaller the power delivered.

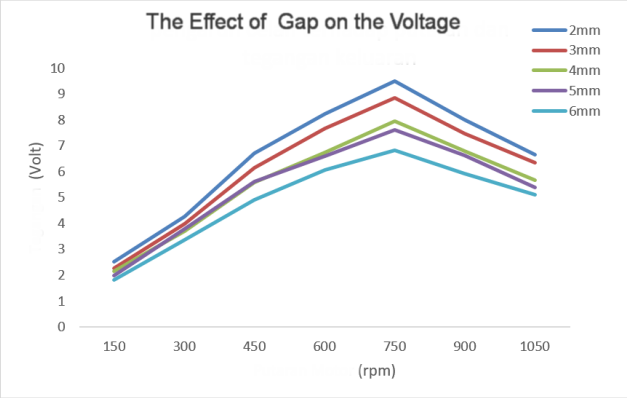

Fig. 8: The effect of air gap on rotation

4. Conclusions

Based on the experiments, it can be seen that optimal air gap was at 2 mm produces flux amounted to an average of 1.2 t. In the test with electrical load load produces the largest electrical power in the gap of 2mm, as well as on testing with variations of motor rotation gap 2 mm The greatest voltage because the air losses are less in comparison with other air gap.

5. References

Alqodri, M.F., Rustana, C.E. & Nasbey, H., 2015. Rancang Bangun Generator Fluks Aksial Putaran Rendah Magnet Permanen Jenis Neodymium (NdFeB) Untuk Turbin Angin Sumbu Vertikal Tipe Double-Stage Savionus. *Seminar Nasional Fisika SNF 2015*, IV, pp.135–142.

Ashraf, M.M. & Malik, T.N., 2017. Design of a three-phase multistage axial flux permanent magnet generator for. *Turkish Journal of Electrical Engineering & Computer Science*, pp.520–538.

Gör, H. & Kurt, E., 2015. Analyses of Losses and Efficiency for a New Three Phase Axial Flux Permanent Magnet Generator. *Electric Power and Energy Conversion Systems (EPECS), 2015 4th International Conference on*.

Holmes, A.S., Hong, G. & Pullen, K.R., 2005. Axial-Flux Permanent Magnet Machines for Micropower Generation. *Journal of Microelectromechanical System*, 14(1), pp.54–62.

Nur, D.F.M., Siregar, R.H. & Syukri, M., 2013. Perancangan Prototype Generator Magnet Permanen Fluks Aksial Pada Pembangkit Listrik Tenaga Angin Untuk Penerangan Lampu Jalan. *Seminar Nasional dan Expo Teknik Elektro 2013*.

Sadeghierad, M. et al., 2008. Design Analysis of High-Speed Axial-Flux Generator. *American J. of Engineering and Applied Sciences*, 1(4), pp.312–317.

Sezenoglu, C. & Balikci, A., 2015. Design of Axial Flux Permanent Magnet Generator for Generator Driven Electromagnetic Launcher. *2015 9th International Conference on Electrical and Electronics Engineering (ELECO)*, pp.595–598.

Shaw S, C.S., 2012. Permanent magnets: the demand for rare earths. In *8th International Rare Earths Conference. 13–15 November 2012*. Hong Kong, p. 2016.

Taran, N. & Ardebili, M., 2014. Efficiency Optimi ization of an Axial Flu ux Permanent Magnet Synchrono ous Generator for Low w Speed Wind. *ICEEE 2014*, (Icee), pp.539–544.

Wijaya, A.A., Syahrial & Waluyo, 2016. Perancangan Generator Magnet Permanen dengan Arah Fluks Aksial untuk Aplikasi Pembangkit Listrik. *Jurnal Reka Elkomika*, 4(2), pp.93–108.

Yang, Y. et al., 2016. REE Recovery from End-of-Life NdFeB Permanent Magnet Scrap: A Critical Review. *Journal of Sustainable Metallurgy*, pp.122–149.

Proceedings of the 1st Faculty of Industrial Technology International Congress
International Conference
Bandung, Indonesia, October 9-11, 2017
ISBN 978-602-53531-8-5

Implementation of Digital Communication System on DSK TMS320C6713

Lita Lidyawati[1,*], Arsyad D. Darlis[1], Dwi Aryanta[1], Lucia Jambola[1] and Feri Kurnia[2]

[1] Department of Electrical Engineering, Institut Teknologi Nasional, Bandung – INDONESIA

[2] Student of Dept. of Electrical Engineering, Institut Teknologi Nasional, Bandung – INDONESIA

[*] Corresponding author e-mail: lita.sunoko@gmail.com

Abstract

Communication system using digital modulation has been used widely on telecommunication system nowadays, including voice communication, video or data. In this research author make a system implementation digital communication using modulation techniques ASK, FSK, BPSK, dan QPSK that passed into AWGN channel (Additive White Gaussian Noise) then added Rayleigh on DSK device (Digital Signal Processing Starter Kit) TMS320C6713 type. Furthermore, the designed system was evaluated. The evaluation of modulator signal output was in accordance with characteristic each modulation, but the received information signal was different from the sent information signal. BER performance that resulted from each system was fluktuatif. Both of these were caused by the AWGN channel and Rayleigh and the system did not use the signal quality improvement techniques of received information. The most efficient system in terms of memory usage on TMS320C6713 DSK is a system with FSK modulation, with a value of 1.15719697%. While most large systems use a memory is ASK communication systems with a value of 1.191666667% efficiency.

Keywords: Digital Modulation, AWGN, Rayleigh, BER, DSK TMS320C6713

Introduction

Telecommunications technology is currently growing very rapidly as a result of the increasing needs of the community in activities or work. Communications technology effectively and efficiently continue to be developed by human to obtain a telecommunication system better than the existing telecommunications system. Therefore, many telecommunications researchers in the world continue to compete until now in order to improve the performance of a telecommunications system.

M-file of the simulation conducted found that the bit error rate (BER) at the BPSK and QPSK are equal in value. This is due to the process of sending data between BPSK (Binary Phase Shift Keying) and QPSK (Quadrature Phase Shift Keying) to within one bit. From these results indicate that the simulator results are in accordance with the theory of BER in digital modulation techniques when passed in AWGN channel (Sa'iyanti, N.P.. Pratiarso, A.,2011; Darlis, A.R, 2015).

Implementation modulation and demodulation on DSK TMS320C6416T to the type of modulation QAM (Quadrature Amplitude Modulation), 16 QAM and 64 QAM is concluded that there worst performance in 64 QAM modulation. This result is due to the BER values obtained worse. When compared with the value of BER of 10-5 BER value, the value of 64 QAM modulation BER is greater than 10-5. As for QAM and 16 QAM modulation BER values that are less than 10-5 (Aryanta, D. et al, (2015); Lidyawati, L. et al, (2015)).

There are several advantages when using TMS320C6713 DSK, which has a very quick process because TMS320C6713 DSK has a larger clock is 225 MHz. TMS320C6713 DSK is a specific application processor is a processor made specifically for certain applications (Nugraha, 2011).

From these studies, the author had the idea to create a digital communications system implementation on the device DSK (Digital Signal Processing Starter Kit) type TMS320C6713. This research will be conducted digital communication system simulation using Matlab software version r2007a and implementation of digital communication systems on the TMS320C6713 DSK. In the simulation and implementation will use a modulation technique ASK, FSK, BPSK and QPSK(Wahyudi, R.A., (2008)). A telecommunications system is always passed on certain tracks or channels that cause noise (interference signal channel). In this study, all modulation will be passed on channel AWGN (Additive White Gaussian Noise) and Rayleigh (Harada dan Prasad, (2002)).

The purpose of this study include the simulated digital communication system that is passed in AWGN channel and Rayleigh using Matlab software version r2007a format m-file, create a simulation of digital communication system that is passed in AWGN channel and Rayleigh using software matlab version r207a using Simulink, implementing on system design software with simulink Matlab version r2007a on TMS320C6713 DSK (Yeh, H.G. et al, (2007); Ghariani, N. et al, (2011)).

2. Methodology

In order for this research is more focused and clear the authors limit the study to be discussed, while the boundary problem is the modulation used modulation techniques ASK, FSK, BPSK and QPSK, the channels used in the system using the AWGN channel and Rayleigh, and do not use the technique improvement of signal quality information received.

Digital communication system is the process of delivering information from the sender to the receiver where the signal information sent or received is digitized, the signals are expressed in the form of bits of data (eg with the numbers 0 and 1). The main part of the digital communication system is the sender, the medium through which the transmitted signal, and a receiver (Emir, H. et al, (2007). With the hope of the received signal is equal to the signal sent by the sender information. Block diagram of a digital transmission system can be seen in Figure 1.

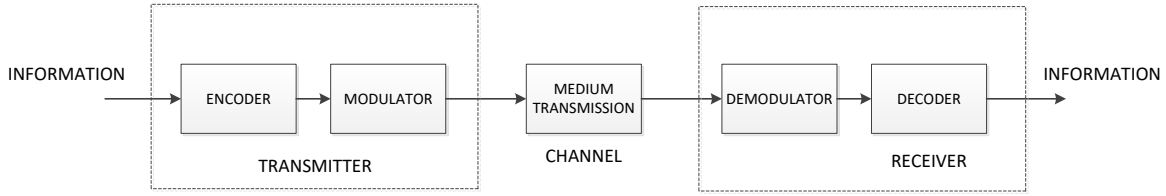

Fig. 1 : Diagram block system Digital Transmission System

If we construct a mathematical model for the received signal at the receiver, the channel through which the signal is assumed to undermine, by white Gaussian noise. When a signal is sent, white Gaussian noise, and received signal is modeled as (t), n (t0, and r (t), then the received signal:

$$r(t) = s(t) + n(t) \tag{1}$$

Where n (t) is a function of the AWGN process with the probability density function (pdf) and the power spectral density, the following equation:

$$\varphi_{nn}(f) = \frac{1}{2} N_0 [\frac{W}{Hz}] \tag{2}$$

Where N_0 is constant and often referred to as the power density noise (noise power density).

In multipath propagation, signal reception sometimes strengthen or weaken. This phenomenon is called multipath fading, and the received signal level change from time to time. Multipath fading increase data errors at the receiver, when the digital radio signal transmitted from the sender through terrestrial channels.

Rayleigh fading is often used as a realistic approach that is good enough for the wireless channel conditions non-LOS (Line Of Sight) and multipath. In the fading Rayleigh happen multiplication distortion h (t) with the transmission signal s (t), with n (t) is the noise, so that the received signal can be approximated by y (t) = [(h (t) • s (t)] + n (t) (Baddour, K. E. et al., (2005); Komninakis, C., (2008); Mathumisaranon, T. et al, (2013)).

Digital Signal Processing (DSP) processor, such as processor family TMS320C6x is a high-speed microprocessor with the type of architecture and instruction set specifically for signal processing. C6x notation indicates that the processor is a member of the Texas Instruments (TI) TMS320C6000 processor family (Texas Instrument. (2001); Kharel, R. et al, (2010); Maji, P. et al, (2012)). Architecture of digital signal processor C6x devoted to numerical calculations are very complex. Based on the architecture very longinstruction - word (VLIW) processor TI C6x considered as the best compared to others. DSP processor is closely related to signal processing in real-time (Ghariani, N. et al, (2011)).

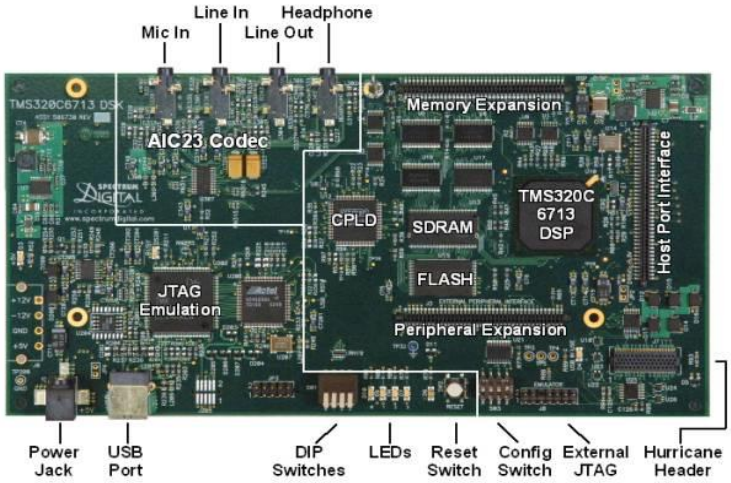

Fig. 3 : DSK TMS320C6713 Board

In this study conducted several stages of the simulation with m-file format, the simulation in Simulink and Simulink implementation of the TMS320C6713 DSK. Figure 4 shows the process flow of the making of this study. In this study will be made of digital communication system with five different types of modulation is ASK, FSK, BPSK and QPSK.

For a channel that is used is the AWGN channel and Rayleigh channel. Specifications of the canal Rayleighyang made are reflected signal to produce a third doppler frequency of 0.01 Hz. The first reflected signal gain of 10 dB and strengthening delay of 1 ms, the second reflected signal gain reinforcement 0:05 dB and 0.05 ms delay, and the third reflected signal gain of 20 dB attenuation and delay of 0.2 ms.

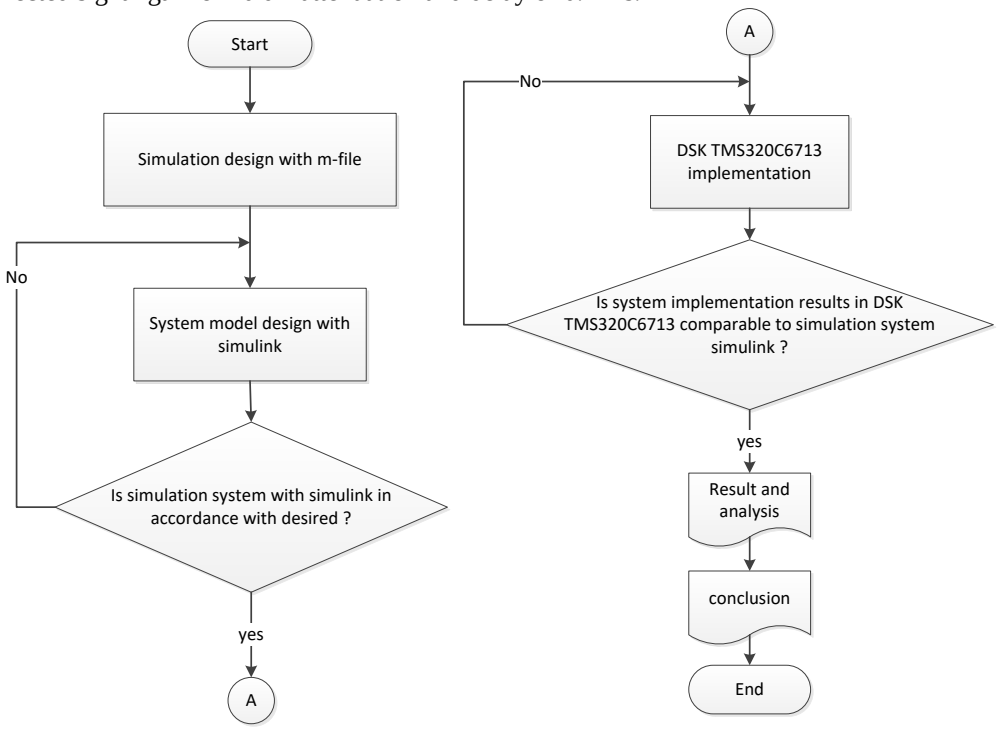

Fig. 4 : System Flowchart Diagram

The digital communication system created is a digital communication system using modulation ASK, FSK, BPSK and QPSK.

Digital communications system modeling with Simulink format created for implementation on TMS320C6713 DSK. But in Simulink modeling simulation can be performed before modeling is implemented on the device. Modelling made a total of five models, namely for systems with modulation ASK, FSK, BPSK and QPSK Of the five systems made, simply modeling made like Figure 5.

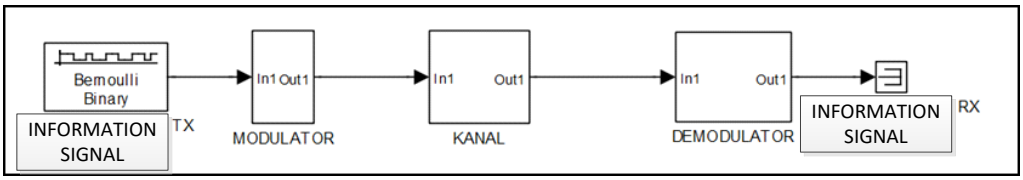

Fig. 5 : Simulink Modeling

3. RESULTS AND DISCUSSION

On systems that have been carefully tested to observe the shape of the signal generated by the system and testing the performance of BER (Bit Error Rate).

The output signal is taken on the simulation ¬m-file and Simulink are signaling information is transmitted, the signal modulator output signal after passing through the canal, and the information signal is received. While the implementation stages, the signal is taken from information transmitted signal, the modulator output signal, and the signal demodulation results. In the test signal generation information used in the form of a digital signal with an infinite amount of data, the value of Eb / N0 (Comparison of Bit Energy to Noise Energy) by 40 dB.

The test signal at the implementation stage done twice integration of the device, the first integration output signal modulator for testing and integration of the two to take the information received after the signal demodulator block. The tools used for image capture signal is 1 oscilloscope, 1 audio generator, one device is a PC (Personal Computer), and the TMS320C6713 DSK. In a system that will be implemented written blocks DSK board, pulse generator, and Block DAC (line out DSK).

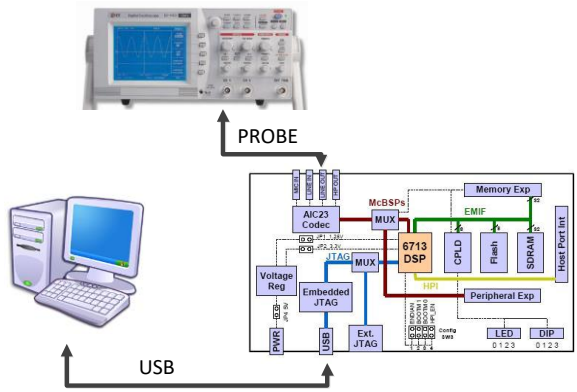

Fig. 6 : The Composition of Signal Testing Tool Implementation at TMS 320C6713 DSK

Block pulse generator is used as an information signal generator. The resulting information signal has an amplitude value of 1 volt, the bit period of 0.02 seconds, and a pulse width of 50% of the width of the signal of the period. The signals generated in the form of data bits 1 and 0 are repeated periodically over 0.01 seconds.

While signaling information used for decision QPSK modulation signal is converted into an information signal predetermined information data bits QPSK signal so that the phase change due to changes in the data bits of information can be observed. Block information signal pulse generator is converted into a block of repeating sequences of stair to generate the desired information signal.

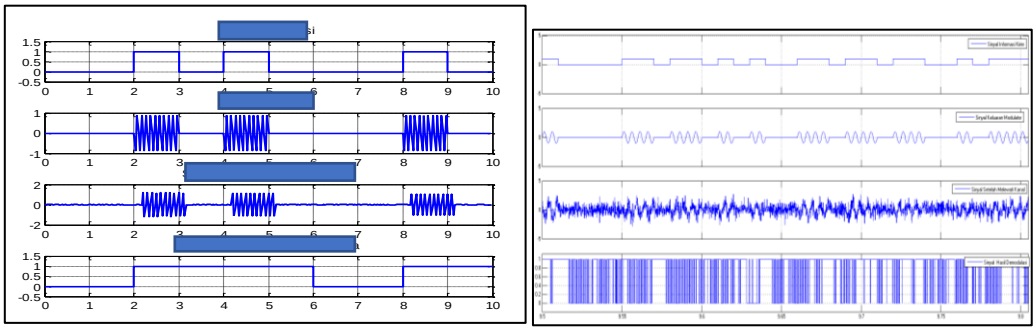

(a) **(b)**

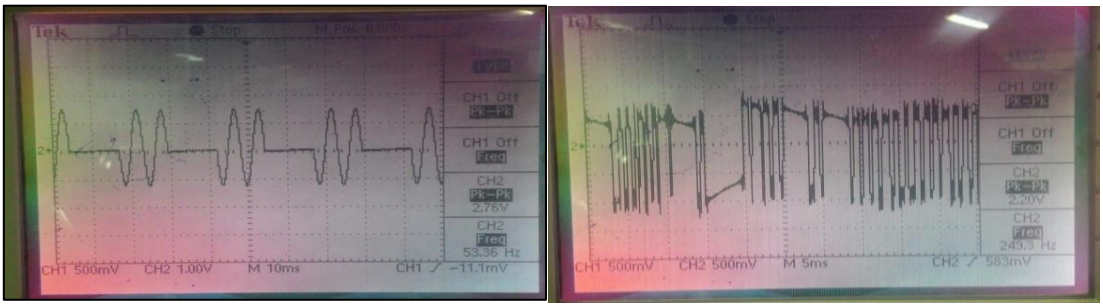

(c) (d)

Fig.7 : Output Signal System ASK (a) *m-file* (b) Simulink (c) Implementation of Modulator output Signal (d) Implementation Signal after Demodulation

Results of testing the output signal m-file shown in Figure 7 (a), Simulink output signal in Figure 7 (b), a modulator output signal implementation results in Figure 7 (c), and implementation of signal demodulation results in Figure 7 (d) . From Figure 7, the signal after passing through the channel on the simulation of m-file get a delay between 0 to 0.3 seconds. The signal after passing through the channel Simulink simulation results have strengthened the amplitude at every second.

Results of testing the output signal m-file shown in Figure 8 (a), Simulink output signal in Figure 8 (b), a modulator output signal implementation results in Figure 8 (c), and implementation of signal demodulation results in Figure 8 (d). From Figure 8 Value amplitude of the signal after passing through the canal on the simulation of m-file damped to 1.6 volts. Signal demodulation results with Simulink simulation opposite to the information signal is sent, the information signal is supposed to be one received data bits are data bits 0 and vice versa continuously. As in 9.54 to 9.56 seconds.

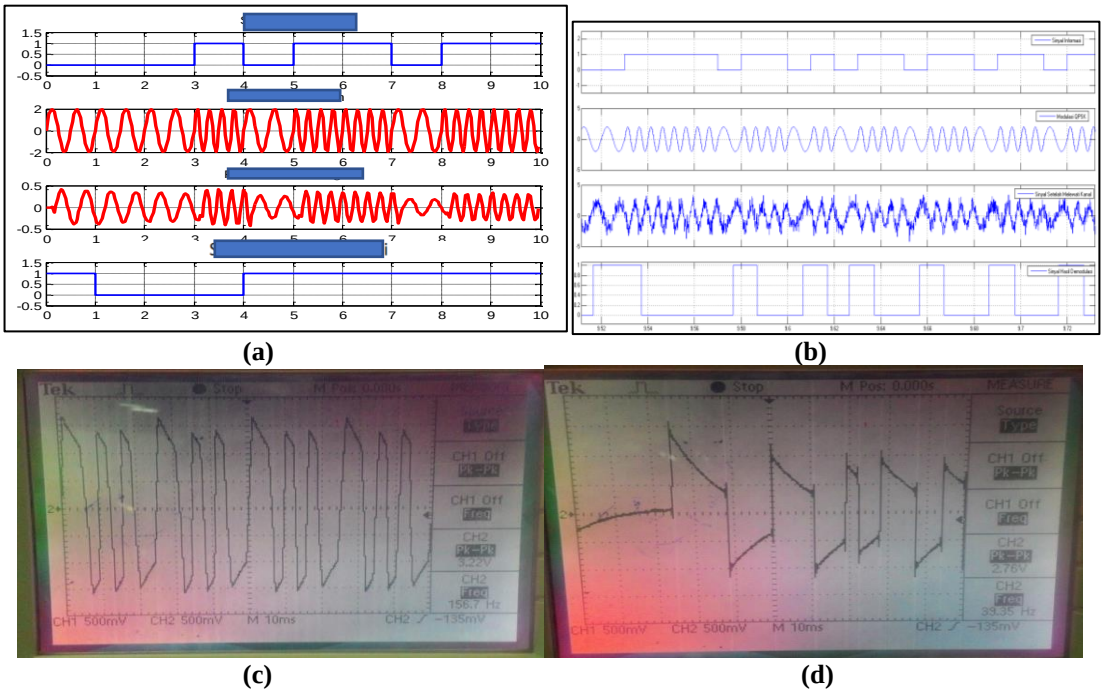

(a) (b)

(c) (d)

Fig. 8 : Output Signal FSK System (a) *m-file* (b) Simulink (c) Implementation of Modulator Output Signal (d) Implementation signal after Demodulation

Results of testing the output signal m-file shown in Figure 9 (a), Simulink output signal in Figure 9 (b), the results of the implementation of a modulator output signal in Figure 9 (c), and implementation of signal demodulation results in Figure 9 (d). From Figure 18, the signal after passing through the canal on the simulation of m-file delayed by 0 to 0.2 seconds and experienced a phase change at 180 °. The signal after passing through the canal Simulink simulation results undergo a phase shift of 180 °.

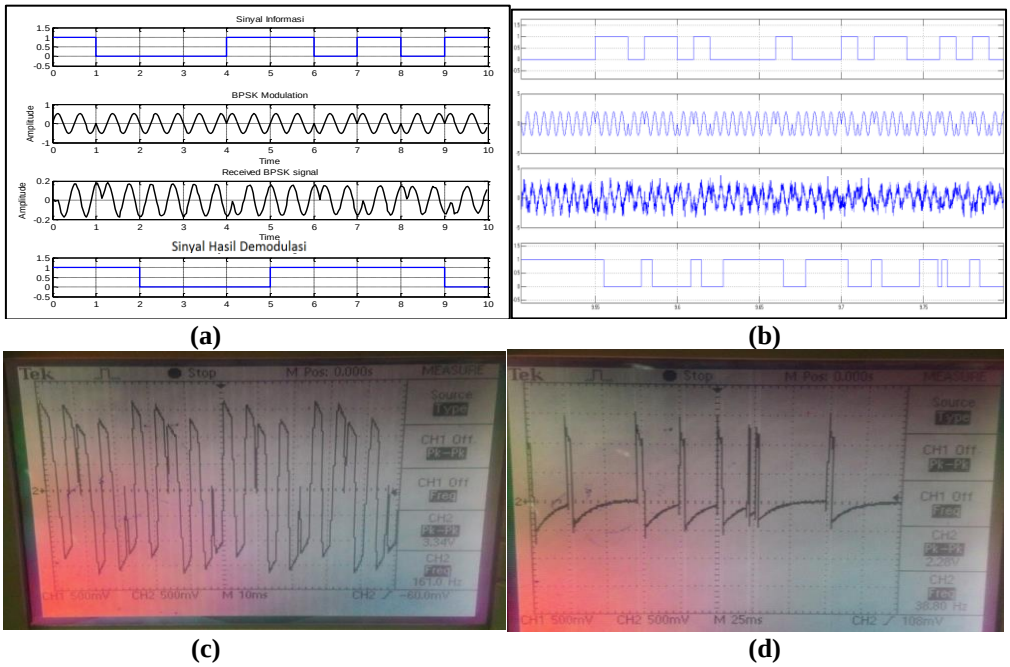

Fig. 9 : Output Signal BPSK Sytem m-file (b) Simulink (c) Implementation of Modulator Output Signal (d) Implementation Signal after Demodulation

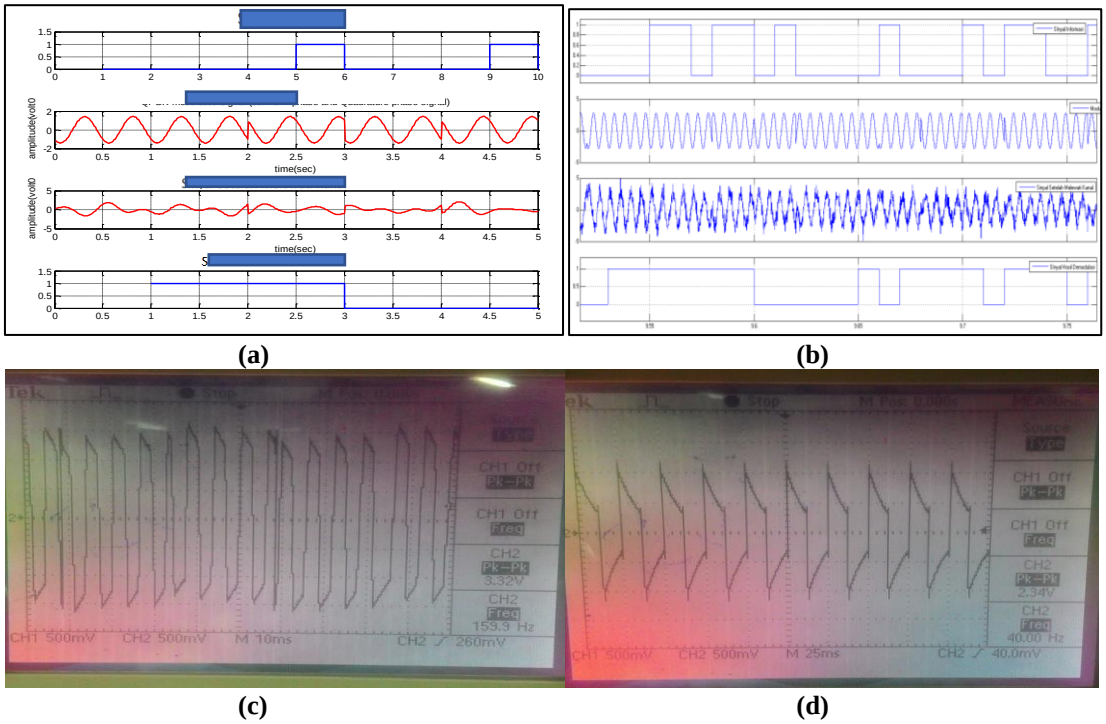

Fig.10 : Output Signal QPSK System(a) *m-file* (b) Simulink (c) Implementation of Modulator Output Signal (d) Implementation Signal after Demodulation

Results of testing the output signal m-file shown in Figure 10 (a), Simulink output signal in Figure 10 (b), a modulator output signal implementation results in Figure 10 (c), and implementation of signal demodulation results in Figure 10 (d). The signal after passing through the canal on the simulation of m-file get every second damping constant and the signal is not worth the experience the phase shift between 150 ° to 180 °. The signal after passing through the canal Simulink simulation results undergo a phase shift between -150 ° to -180 ° and the amplitude value also rose that is not constant, shown in Figure 19.

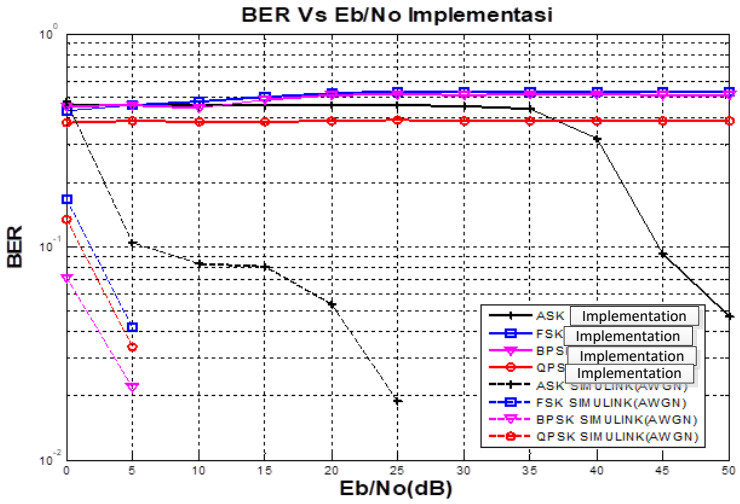

Fig. 11 : BER Curve against Eb/N0 System Implementation Stage ASK, FSK, BPSK, and QPSK

Simulink simulation of BER performance shown in Figure 11 are depicted with dashed lines, while the BER performance results of the implementation depicted without the dotted line. Black curve shows the communication system ASK, FSK communication system in blue, BPSK communication system with the color pink, and communication systems QPSK with red color. Comparison of each system in the implementation phase of the BER performance is shown in Figure 11. Up and down performance occurs when indigo Eb / N0 is increased. At Eb / N0 of 0 dB, in the implementation of the system performance QPSK modulation is better than the other three by a margin of 0.076 against the BER of ASK, BPSK 0.05 on, and 0.073 to BPSK. But when Eb/N0 is increased to 50 dB ASK BER performance is better than the three other modulation by the difference in value of the QPSK BER of 0.342, 0.491 against FSK, BPSK and 0.47 against.

TMS320C6713 DSK device has a data storage capacity of 264 kbytes (TexasInstrument, 2001). Storage capacity constraints become one of the important stages of implementation on the device, so that the efficiency of the system can be observed in terms of data storage capacity.

Observations made by taking the storage capacity of the data memory value of any system that has been implemented (Darlis, 2011). Then calculate the equation 3 for making the comparison value memory used to the total memory capacity of DSK (y) in units of percent

$$y = \frac{used\ memory}{DSK\ total\ memory} \cdot 100\% \qquad (3)$$

Table 5 : Memory used on DSK for each system

Modulation	*Memory (bytes)*	y(%)
ASK	3146	1,191666667
FSK	3055	1,15719697
BPSK	3078	1,165909091
QPSK	3096	1,172727273

Observations memory on implementation, to a communication system with ASK modulation using a memory of 3146 bytes with the y value of 1.191666667%, for communication with FSK modulation system using a memory of 3055 bytes and the y value of 1.15719697%, for communication systems with BPSK modulation using a memory of 3078 bytes and the y value of 1.165909091%, and communications systems with the QPSK modulation using a memory of 3096 bytes and the y value of 1.172727273%.

The result of the four systems were implemented, the most efficient system is a communication system using FSK modulation with a value of 1.15719697%. While most systems use a memory is a communication system using ASK modulation with a value of 1.191666667% efficiency.

From the observation memory used by each system to the implementation stages, if a comparison of each system with the characteristics of the modulation results of observations memory as opposed to BER test results. On the

results of the BER performance, systems with ASK modulation best when Eb / N0 of 40 dB to 50 dB. While the memory used by DSK for system implementation with ASK modulation, using the ASK system memory compared to most other systems, with the unused memory of 3146 bytes.

5. CONCLUSION

From the results of the testing and performance analysis of communication system that has been done, then we got some conclusions, namely:

1. In the communication system with ASK modulation, required Eb / N0 of 50 dB so that BER performance difference between implementations with Simulink simulations that were previously worth 0.21 into 0,014.
2. In communication with FSK modulation system, required EB / N0 35 dB and 50 dB difference in value BER of implementations with Simulink relatively constant at 0.1004.
3. BER performance of a communication system with BPSK modulation at the time of implementation of the BER difference is greater than the average differences Simulink simulation - BER average of 0.08.
4. In communication systems using QPSK modulation BER performance in the implementation of relatively constant with average BER value - average of .387.
5. In the implementation phase on the condition of Eb / N0 0 to 37 dB the best system in terms of BER performance is a communication system with QPSK modulation compared to the three other modulation.
6. In the implementation phase on the condition of Eb / N0 of 50 dB-generating system BER performance is greatest communication system with ASK modulation compared with the three other modulation BER value of 0.047.
7. The most efficient systems in terms of memory usage on TMS320C6713 DSK is a communication system using FSK modulation with a value of 1.15719697%. While most systems use a memory is a communication system using ASK modulation with a value of 1.191666667% efficiency.

6. REFERENCES

Darlis, A.R. (2015). Fractal Communication System Using Digital Signal Processing Starter Kit (Dsk) TMS320C6713. ComTech Jounal Binus University. 6(4).

Baddour, K.E., Beaulieu, N.C., (2005), *Autoregressive modeling for fading channel simulation*, IEEE Trans. Commun.

Wahyudi, R.A. (2008). Rancang Bangun Modulator 16-QAM Pada DSK TMS 320C6713 Dengan Menggunakan Simulink. Dipetik pada 9 Oktober 2014 darihttp://lib.ui.ac.id/file?file=digital/124382-R030890.pdf

Harada. Prasad. (2002). *Simulation and Software Radio for Mobile Communication.* London : Arctech House.

Sa'iyanti, N.P.. Pratiarso, A. (2011). Pembuatan Modul Praktikum Teknik Modulasi Digital FSK, BPSK, dan QPSK Dengan Menggunakan *Software*. Dipetik pada 28 Desember 2014 dari http://repo.eepis-its.edu/336/1/1095.pdf

Nugraha, R.K. (2011). Sistem Keamanan Rumah Berbasis Pengenalan Wicara Menggunakan DSK TMS320C6713 (Hardware). Dipetik pada 9 Oktober 2014 dari http://repo.eepis-its.edu/629/1/841.pdf

Emir, H. Kaya, E. Öztürk, (2015). Design of OFDM on Digital Signal Processors. *23nd Signal Processing and Communications Applications Conference (SIU)*, Malatya, 2015, pp. 300-303. doi: 10.1109/SIU.2015.7129818

Aryanta, D., Darlis, A.R., Mulyadi, Y. (2015). Perancangan dan Implementasi Sistem *Ortogonal Frequency Division Multiplexing* (OFDM) dengan menggunakan DSK TMS320C6713. Jurnal Elektro Telekomunikasi Terapan (JETT). 2(2)

Lidyawati, L., Darlis, A.R., Romadani, S.I. (2015). Implementasi *Filter Infinite Impulse Response* (IIR) dengan *Respons Elliptic* dan *Bessel* menggunakan DSK TMS320C6713. Jurnal Elektro Telekomunikasi Terapan (JETT). 2(2)

ISBN 978-602-53531-8-5

D. Automation and measurement technologies; Computer aided engineering; Computing Technology for Sustainable Industrial System; Supply Chain Management & Logistics

Proceedings of the 1st Faculty of Industrial Technology International Congress
International Conference
Bandung, Indonesia, October 9-11, 2017
ISBN 978-602-53531-8-5

Evaluation of Operational Risks on PT. Global Indo Pangan's Supply Chain Using House of Risk I Method

Edi Susanto[1,*], Nanda Azman[2] and Melati Kurniawati[1]

[1] Department of Industrial Engineering, Institut Teknologi Nasional (Itenas), Bandung - INDONESIA

[2] Student Dept. of Industrial Engineering, Institut Teknologi Nasional (Itenas), Bandung - INDONESIA

[*] Corresponding author e-mail: slitausanto.edi19@gmail.com

Abstract

One of the challenges in managing supply chain is uncertainty. Uncertainty can cause risk which can interfere supply chain activity. In managing their supply chain, PT. Global Indo Pangan meets a lot of uncertainty that can cause risk such as demand uncertainty which makes the company can only rely on forecasting that can lead to miscalculating or even uncertainty from supplier like delivery time or quality of the product. Therefore, supply chain risk management is needed. One of the approaches to manage the risk is house of risk I (HOR I) method. This method will enable company to prioritize risk agents that cause risk events to be treated. Supply Chain Operation Reference (SCOR) model is used to define supply chain activity. First steps is identify risk by doing interview with divition which is related to supply chain. Next, risk is divided into low risk, medium risk, high risk, and very high-risk using risk maps. Risk assessment is performed by calculate aggregate risk potential (ARP) in a way assess severity of risk events, occurance of risk agents, and correlation between risk event and risk agent. The result of HOR 1 shows that there are 8 risk events which is cause by 13 risk agents. 7 risk agents is chosen by pareto analysis to make preventive action against it. There are 6 action plans that can be done to prevent risk agents as the result the severity of risk events can be reduced or even be removed.

Keywords: HOR I, Risk Management, SCOR, ARP, Supply Chain

1. Introduction

Uncertainty is one of the challenges for company in managing supply chain. Supply chain is relationship of companies who working in line on production activity . That companies is included supplier, factory, distributor, store or retail, also company which provides logistics service. Based on the sources, there are three main classifications of uncertainty, that are demand uncertainty, uncertainty from supplier, and uncertainty from internal company (Pujawan I. N., 2010).

PT. Global Indo Pangan is company which produces cocoa powder. There are various uncertainty in implementation of supply chain. One of the uncertainty that happen in company's supply chain is uncertainty from demand which cause company can only forecast the demand. Uncertainty from supplier is that the delivery time is not consistent, also the quantity and quality of material. Internal uncertainty can be formed the machine which the performance is not good or the operator. This uncertainty can cause risk which can disturb the implementation of company's supply chain.

Company needs to assess objectively the supply chain which is done by the company for knowing the risks that can be happened in implementation of supply chain to control the risk. With the assessment, company can identify risks that probably happened and find the cause of the risks.

Assessment of risks from the severity and how frequent the risks happens is done after risk is identified. It is intended to know which risks will become the priority to make proposed ideas for preventing the risks to reduce the severity of the risk or even the occurance of the risks. By doing the preventing action, company can keep the activity of supply chain from various risks that probably appear.

Supply chain's activity has uncertainty in various aspect. Because of that, risk can appear and disturb continuity of supply chain. One of the approaches used is house of risk method. This method using supply chain operation reference model to assess currenct supply chain's activity. By assessing current supply chain's activity, it allows company to know what risks which can probably happen and do preventing actions.

2. Literature

2.1. Supply Chain Management

Supply chain is a network companies which work together to create and deliver a product into the hand of end user (Pujawan I. N., 2010). Supply chain also known as logistic network in this relationship, there are several main cast who has the same importance, supplier, manufacturer, distribution, retail outlets and customers. Three main classification of uncertainty in supply chain are demand uncertainty, supplier uncertainty, dan internal uncertainty.

One of reference model of supply chain is supply chain operation reference which divided supply chain activity into five main process, plan, source, make, deliver, and return (Pujawan I. N., 2010). Chan & Qi quoted from Pujawan (2010) suggest what is called performance of activity (POA). POA is a model to measure activity which is part of supply chain. POA is measured in several dimention, cost, time, capacity, capability, productivity, utility, and outcome.

2.2 Risk Management

Risk management is a set of policy, a compelet procedure which is owned by organization, to manage, monitor, and control organization exposure to risk. Identiciation and assessment risk process continued by risk management which is a main operational activity from risk management. Systematic approach about risk management is divided into three main step (Mulyawan,2015), risk identification, evaluation and risk analysis, and respond or reaction to overcome the risk. To categorize the risk into low, medium, high, and very high, risk map is used. Risk maps that is arranged based on determination level of risk according to joint Australian/ new Zealand standar (2004) can be seen on Table 1.

Table 1: Risk Maps

Likelihood	Impact				
	Insignificant 1	Minor 2	Moderate 3	Major 4	Critical 5
Almost Certain 5	Medium	High	High	Very High	Very High
Likely 4	Medium	Medium	High	High	Very High
Possible 3	Low	Medium	High	High	High
Unlikely 2	Low	Low	Medium	Medium	High
Rare 1	Low	Low	Medium	Medium	High

2.3 House of Risk

House of Risk (HOR) is an FMEA modification and House of Quality (HOQ) Model to prioritize which source of risk is first selected to take the most effective action in order to reduce risk potential from source of risk. Here's the steps in House of Risk I model:

1. Identify risk event that can happened in every business process. It can be done by mapping supply chain (plan, source, make, deliver, and return) and then identify what is lacking in every process.
2. Estimate the severity of the risk event. In this case using 1-10 scale where 10 shows the extreme effects. Severity level of risk event is placed on right column of the table and declared as S_i.
3. Identify the source of risk and assess the probability event for every source of risk. In this case scale 1-10 is set where 1 means that almost never happen. Source of risk (Risk agent) is placed on upper row table and connected with lower row event with O_j.

4. Develop the relationship matrix. Correlation between every source of risk and risk event, $R_{ij}(0,1,3,9)$ where 0 shows that there is no correlation and 1,3,9 consecutive shows low, medium and high correlation.
5. Calculate set of potential risk (Aggregate risk potential of agent j = ARP_j) which is determined as the result from probability event of source of risk j and set of severity from every risk event that caused by source of risk j.
6. Make source of risk ranking based on set of potential risk in descending order.

3. Research Methodology

Research methodology are steps which is done for conducting research to achieve its purpose. Here is the steps of research methodology in Fig. 1.

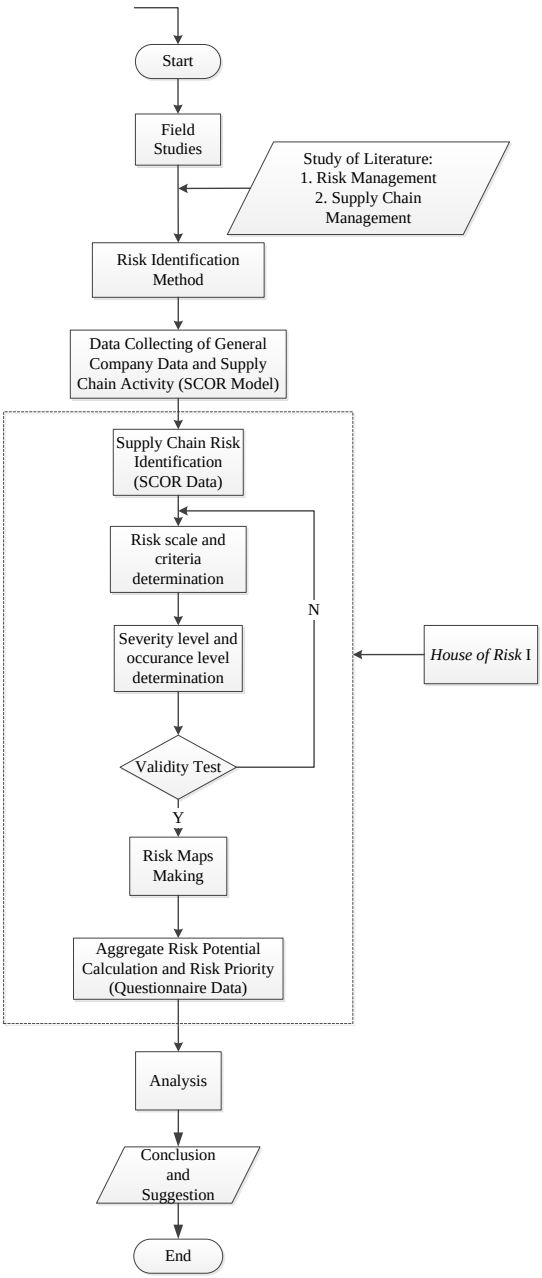

Fig. 1 : Research Methodology

4. Supply Chain Risk Management

4.1 Supply Chain Activity

First steps to identify risks is defining supply chain activity on company used supply chain operation reference (SCOR) model. Supply chain activity on the company can be seen on Table 2.

Table 2: Supply Chain Activity

Business Process	Sub Process	Detail Activity
Plan	Demand Forecasting	Forecast the quantity of demand
	Production Planning	Planning the quantity of raw material
		Planning the quantity of operator
		Planning the quantity of machine
	Inventorty Examine	Quantity of raw material examination
		Quantity of finished good examination
	Production Schedulling	Schedulling for 1 Shift
Source	Comminucate with supplier	Raw material ordering process
	Supplier election	Evaluate Supplier performance
	Procurement Process	Supplier deliver raw material
		Raw material examination
Make	Production Controll	Production capacity in one month
		Maintenance
		Production Layout
	Production Activity	Conducting Production Process
	Quality Examination	Finished Good Quality Filtering
	Packing Process	Packing Finished Goods
Deliver	Determination of modes of transportation	Determination of transportation type
	Order management	Delivering finished good to consumer
		Send bill to consumer
Return	Return of inappropriate product	Return of raw material to supplier
		Handling of product which is returned by consumer

4.2 Risks Identification and Analysis

Risks identification is done based on supply chain activity which is already define before. Risk event severity and the cause of risk event that is risk agent occurance assessment is done by questionnaire. Here are the risks that is possibly to happened and the result of questionnire can be seen on Table 3 and Table 4

Table 3: Severity of Risk Events

Code	Risk Event	Severity
E1	Determination of quantity of demand is less precies	2,2
E2	Raw material come late	2
E3	Raw material which is delivered is not appropriate	3
E4	Sack for packing finished good is damaged	2,2
E5	Finished good does not meet specification	1,6
E6	Finished good become waste	3,4

E7	Changes in production schedule	2,6
E8	Finished good delivery is late	2

Table 4: Occurance of Risk Agents

Kode	Risk Agent	Occurance
A1	There is an error while calculating demand	3,2
A2	There is high demand changing	1,6
A3	There is sudden demand from consumer	2,8
A4	There is problem on distribution path	2,6
A5	Expired of raw material is near	1,8
A6	There is damaged in main raw material packaging	1,4
A7	There is damaged on sack	2,4
A8	There is a mistake from operator while holding sack	3,2
A9	Sack is torn hit by sharp object	1,8
A10	There is a mistake from operator while calculating time in production	1,4
A11	Machine is broken while production	3,6
A12	There is a power outage	3,8
A13	There is re-mixing finished good	2,4

The result of questionnaire is used for making risk maps. The purpose of this maps is to categorize risks into low, medium, high, and very high based on severity/impact and occurance/likelihood. Risk maps can be seen on Table 5.

Table 5: Risk Maps

Likelihood	**Impact**				
	Insignificant 1	**Minor 2**	**Moderate 3**	**Major 4**	**Critical 5**
Almost Certain 5					
Likely 4					
Possible 3	(E5,A12) (E5,A11)	(E7,A12) (E7.A11) (E1,A1) (E4,A8)	(E6,A12) (E6,A11)		
Unlikely 2		(E1,A3) (E4,A7) (E7,A13) (E2,A4) (E8,A4)	(E3,A7)		
Rare 1	(E5,A10)	(E4,A9) (E1,A2)	(E3,A5) (E3,A6)		

Next is calculating aggregate risk potential (ARP) to sort risk from highest to lowest based on ARP value. ARP calculation is done on House of Risk I method. The calculation of ARP value on House of Risk I method can be seen on Table 6.

Table 6: House of Risk I

		Risk Agent (Aj)													
Business Process	Risk Event (Ei)	A1	A2	A3	A4	A5	A6	A7	A8	A9	A10	A11	A12	A13	Severity of Risk Event i (Si)
Plan	E1	9	3	1											2,2
Source	E2				9										2
	E3					9	1	9							3
Make	E4							9	3	9					2,2
	E5										9	3	3		1,6
	E6											1	1		3,4
	E7											3	3	9	2,6
Deliver	E8				3										2
Occurance of agent j		3,2	1,6	2,8	2,6	1,8	1,4	2,4	3,2	1,8	1,4	3,6	3,8	2,4	
Aggregate Risk Potential j		63,36	10,56	6,16	62,4	48,6	4,2	112,3	21,12	35,64	20,16	57,6	60,8	56,16	
Priority rank of agent		4	12	13	1	5	14	2	10	11	8	6	3	7	

Pareto analysis is done after calculating the value of ARP to prioritize risk agent. Then action plan is made to prevent risk is done based on the risk which become priority. The risk priority can be seen on Table 7.

Table 7: Risk Priority

Code	Risk Agent	ARP	Action Plan
A7	There is damaged on sack	112,32	Flexible supply base Coordination
A1	There is an error while calculating demand	63,36	Coordination
A4	There is problem on distribution path	62,4	Mutliple Routes
A12	There is a power outage	60,8	Additional genset and uninterruptible power supply (UPS)
A11	Machine is broken while production	57,6	Schedulling maintenance Additional genset and uninterruptible power supply (UPS)
A13	There is re-mixing finished good	56,16	Schedulling maintenance Additional genset and uninterruptible power supply (UPS)
A5	Expired of raw material is near	48,6	Flexible supply base Coordination

5. Conclusion

Based on the result of this research on PT. Global Indo Pangan's Supply Chain then the following conclusion are obtained:

- There are 8 risk events based on supply chain operation reference model.
- There are 13 risk agents that cause 8 risk events.
- 7 risk agents is choosen from 13 risk agents as risk priority.
- There are 6 action plan to prevent risk priority.

6. Reference

Chan, F. T., Qi, H., Chan, H. K., Lau, H. C., & Ip, R. W. (2003). A Conceptual Model of Performance Measurement For Supply Chains. *Management Decision*, 635-642.

Hanafi, M. M. (2016). *Manajemen Risiko.* Yogyakarta: UPP STIM YKPN.

Haughey, D. (2014). *Pareto Analysis Step by Step*. Retrieved July 11, 2017, from projectsmart.co.uk: https://www.projectsmart.co.uk/pareto-analysis-step-by-step.php

Ishikawa, D. K. (1976). *Guide to Quality Control.* Tokyo: Asian Productivity Organization.

Johnson, P. F., & Flynn, A. E. (2015). *Purchasing and Supply Management.* New York: McGraw-Hill Education.

Larson, E. W., & Gray, C. F. (2011). *Project Management: The Managerial Process (5th ed.).* New York: The McGraw-Hill Companies, Inc.

Merna, T., & Thani, F. A. (2008). *Corporate Risk Management (2nd ed.).* West Sussex: John.

Mulyawan, S. (2015). *Manajemen Risiko.* Bandung: CV Pustaka Setia.

Pujawan, I. N. (2010). *Supply Chain Management.* Surabaya: Guna Widya.

Pujawan, I. N., & Geraldin, L. H. (2009). House of risk, a model for proactive supply chain risk management. *Business Process Management Journal*, 953-967.

Standard, J. A. (2004). *Australian / New Zealand Standard 4360:2004, Risk Management.* Wellington: Australia Internasional Ltd.

Sugiyono, P. D. (2017). *Metode Penelitian Kuantitatif, Kualitatif, dan R&D.* Bandung: ALFABETA,cv.

Tang, C. (2006). robust strategies for mitigating supply chain disruptions. *international journal of logistics: reserach and application*, 33-45.

Warburg, S. (2004). *The Practice of Risk Management.* Euromoney Book.

Water, D. (2007). *Supply Chain Risk Management.* London: Kogan Page Limited.

Proceedings of the 1st Faculty of Industrial Technology International Congress
International Conference
Bandung, Indonesia, October 9-11, 2017
ISBN 978-602-53531-8-5

Making Automatic Unloading Tools on the *Goodway* GV-500 Machine

Suhartinah*, Laeli N. Rohmawati and M. Hidayat
Department of Mechatronics Engineering, Politeknik Manufaktur Astra, Jakarta - INDONESIA
* Corresponding author e-mail: zahrasaina@gmail.com

Abstract

To increase profit, every company must make an improvement or innovation, both in the form of system and machine. Improvement in the machine usually by modifying the machine to be automatic, cycle time faster and revive the unused machine. In this case one form of improvement to do is reduce the handling time operator in line machining, especially in line BD6 which produces brake drum D80N. One of the machines that have a high time handling is Goodway GV – 500 machine which we an OP 4B machine in line BD 6. To reduce handling time operator on the Goodway GV - 500 machine then be made automatic unloading tool or in Japanese is called hanedashi. Hanedashi is a device mounted on the machine and automatically eject the product when the operation of the machine has been completed. Hanedashi operators do not need to carry out the process of unloading the material into the machine. With this instrument of automatic unloading, the operator handling time in Goodway GV – 500 machine has been down to 4 seconds from 12 seconds and increase the productivity of the line BD 6. With increasing line productivity BD 6 makes profit of the company increased.

Keywords: Goodway GV-500 machine, automatic unloading, handling time

1. Introduction

This object research is one of manufacturing companies that produce component/ part of automotive and non automotive. In the production process there is delay in the completion of the brake drum DB06. Line BD 6 is a place to produce this part. In this line is composed of 9 machine with 2 operators on duty to carry out the process of loading unloading material into the machine manually. Each machine has a different handling time. Handling time is the time that the operator needed to carry out the process in accordance with the machine working elements that exist in the standard work table. One of the machines that have a high time handling is Goodway GV – 500 machine that is an OP 4B machine in line BD 6. OP 4B machine is a machine that used to make the process of grooving on the part BD80N. This machine has the operator handling time by 12 seconds. To reduce the handling time operator on the Goodway GV – 500 machine then we made automatic unloading tool or in Japanese is called hanedashi. Hanedashi is a device mounted on the machine and automatically eject the product when the operation of the machine has been completed. Hanedashi operators do not need to carry out the process of unloading the material into the machine. This tool will be installed on the turret of Goodway GV – 500 machine. For the control system utilizes a CNC program by connecting the actuator this device to relay in according with the M Code in the machine. With this tool we expected to decrease handling time operator that exist on the Goodway GV – 500 machine.

2. Goodway GV – 500 Machine

Goodway GV – 500 machine is a type of turning machine that used on OP 4B in line BD 6. This machine is classified as vertical turning CNC machines. As with any other CNC machine Goodway GV - 500 used the code number / Numerical Control (with a mathematical formula) to run or operate.

Below is the position of Goodway GV – 500 machine that is an OP 4B machine in line BD 6.

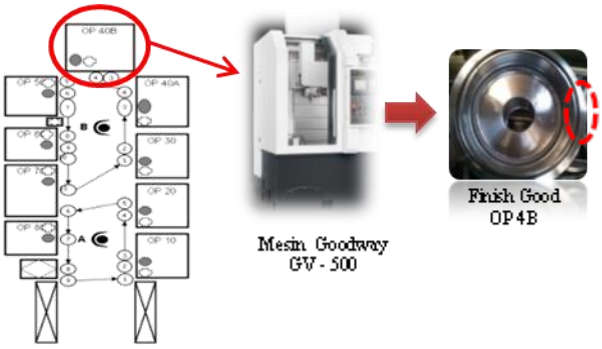

Fig. 1: Location Goodway GV-500 machine

From the picture above we can see that position Goodway GV - 500 machine contained in the OP 4B. Machining process of OP 4B machine is the process of roughing and grooving . Roughing process is performed to reduce the outer diameter of the part BD D80N. While grooving process is a process to form a groove on the part BD D80N. Groove / grooving is shown with a red mark on the image of a good result of OP 4B above. In the process of machining, this machine uses two tools mounted on the turret machine. This turret works as a tool that used in the machining process at the OP 4B and can perform a tool change according to the program. Both of tool that mounted on the turret has a different function, namely for turning and grooving process according to OP 4B machining process that has been described previously. Below is a picture of the turret on the Goodway GV - 500 machine.

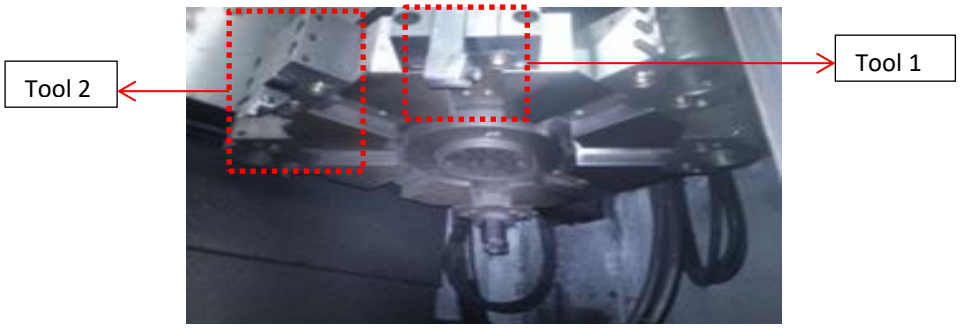

Fig. 2: Position turret in the Goodway GV-500 machine

In the picture above, there are two tools mounted on the turret machine. Tool 1 is doing the process of turning to reduce the outer dimensions BD D80N while tool 2 doing the process grooving for making grooves in the part BD80N.

3. Analysist and design

3.1. Analysis of Concepts in Goodway GV - 500 Machine

After observation of the condition of the Goodway GV 500 machine then there are two concept design for automatic unloading tool that will be installed on the machine. Here are two options automatic unloading tool concepts that will be installed of Goodway GV – 500 machine

Fig. 3: Selection concepts of automatic unloading equipment

Of these two options it was decided to use the second design concept that using the gripper. The concept of the second design have been more effective and efficient than using 3 pistons. In addition to the two concepts do not need to install additional poles for mounting the piston as the gripper can be mounted on a turret, so only need to add the holder and the mounting for the gripper.

3.2. Automatic Unloading Equipment Design

Before starting the process of making the automatic unloading tool, the thing to do is do the design process. The design process is intended to facilitate the execution part and the ordering of goods. All parts are designed using Solidwork for initial design. This drawing concept is the basis in the design dimensions, the suitability of the placement of parts, and mechanical system design further. The design concept for automated unloading apparatus is shown in the following figure.

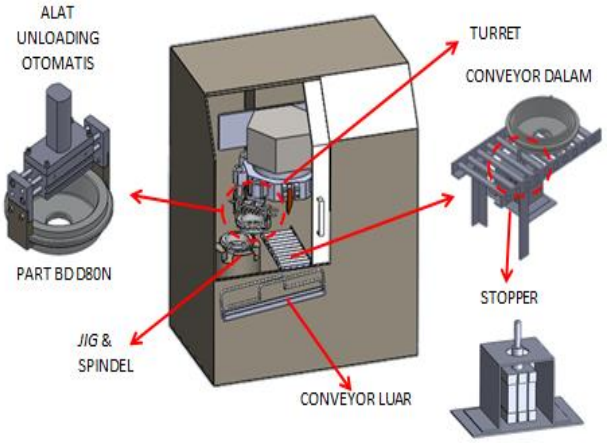

Fig. 4: Concept Design Tool Automatic Unloading

The design concept using the gripper to take part that have been fully processed. The gripper is mounted in the turret so that the movement of the gripper utilize turret movement that can move in two axes, namely X and Z. With this gripper can be closer to spare and after being right in the middle of the spindle gripper can take part and then placed on the conveyor. Before the parts can come out of the machine there is a stopper cylinder under the conveyor. This stopper works to hold the part that came out after the door was opened.

Design of the control system is divided by two: program design and wiring for installation gripper design. In designing the program, the addition of a program for automatic unloading process. Automatic unloading process will use the addition of M20 and M21 code. As for the stopper up and down the reed switch is integrated in the cylinder for auto door. To determine the improvement programs is added automatically unloading the following is a flow chart drawing program of automatic unloading process.

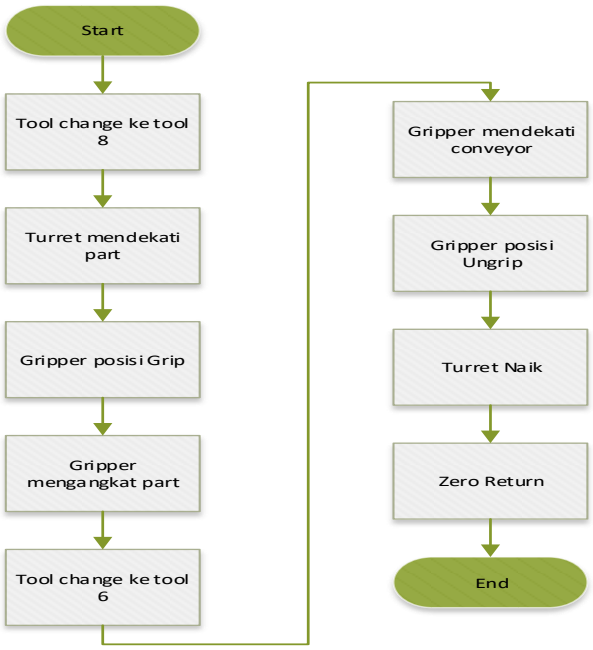

Fig. 5: Concept Design Tool Automatic Unloading

Furthermore, the design of wiring for mounting the gripper on the machine that can be activated using the program. In designing the wiring for the installation gripper done by connecting an external relay on the relay board configured with the program. For more details, here is a picture of the electrical wiring diagram for the installation of an external relay on the relay board and solenoid gripper.

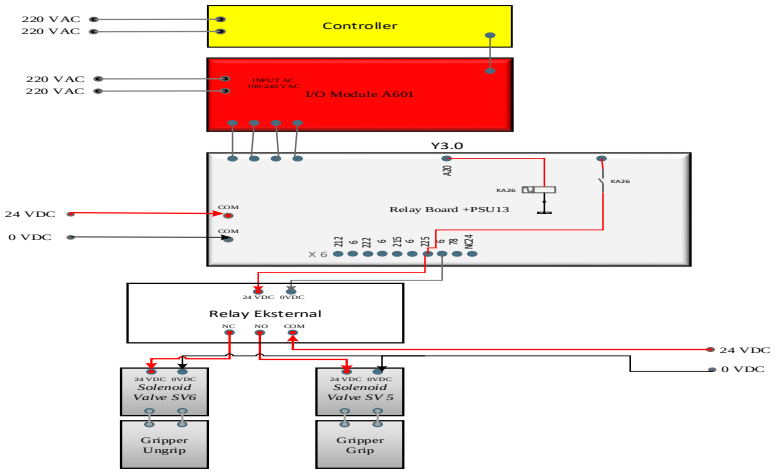

Fig. 6: Wiring diagram of external relays installation

As for the pneumatic circuit can be seen in the picture below.

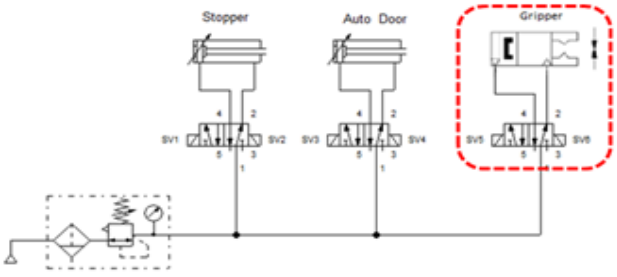

Fig. 7: Pneumatic circuit of Goodway GV -500 achine

4. Making of Control System

The control system of Goodway GV – 500 machine is Fanuc Oi TD. In making the control system is divided into two parts, that is programming and manufacturing of wiring for installation gripper. Making the program means that is making programs for automatic unloading tool is added to the machine. The program for the machining process on the machine does not change. For a detailed explanation of the program described below.

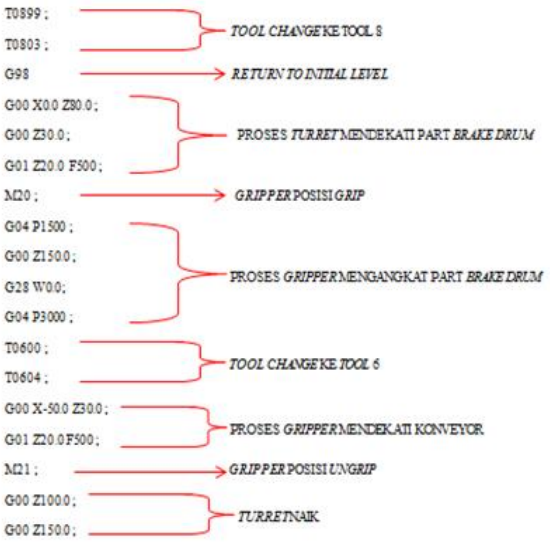

Fig. 8: Example program automatic unloading tools in Fanuc Oi TD

Making of wiring for installation gripper performed on the relay board that exist on the machine. However, before to mounting the gripper on the relay board the installation of an external relay prior to the relay board configured with M20 and M21 program. The socket is connected to an external relay. From the external relay then connected to the gripper solenoid so that the gripper can be activated and deactivated with M20 and M21 program. Actually schematic wiring with the installation of solenoid gripper as shown in the following figure.

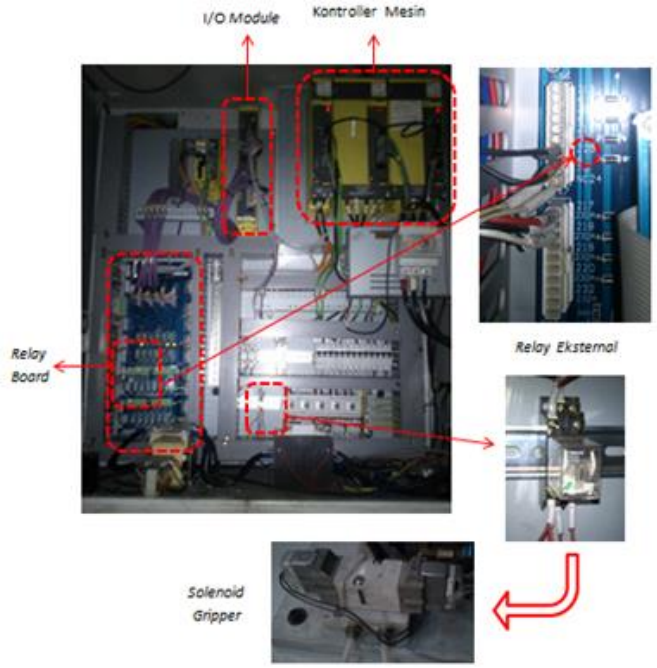

Fig. 9: Installation solenoid gripper to Fanuc Oi TD controller

5. Result of Decreased of Handling Time

The main purpose of the the automatic unloading tool is to reduce the handling time operator on the machine of Goodway GV - 500 according to the improvement plan is 6 seconds. With the automatic unloading tool operator's handling time to 4 seconds with a machining time 86 seconds. Before improvement operator handling time on this machine is 12 seconds with the machining time by 80 seconds. The following chart comparison operator handling time before and after improvement.

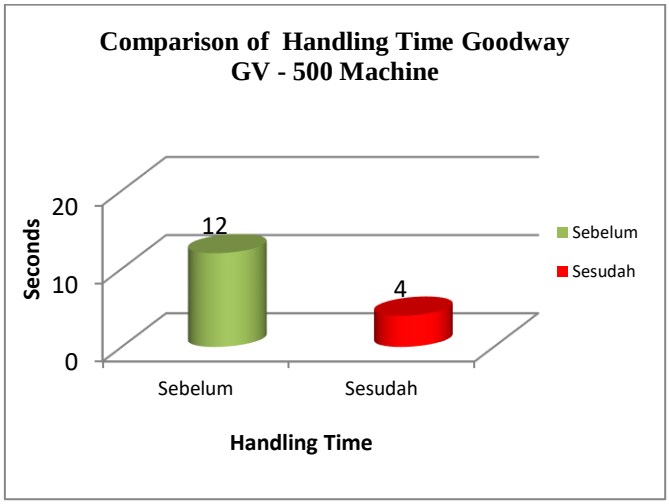

Fig. 10: Comparison of handling time Goodway GV - 500 machine

With reduced handling time of Goodway GV - 500 machine causes the cycle time of Goodway GV – 500 machine to 90 seconds from 92 seconds. The reduced cycle time, causes the number of parts produced increases of 39 pcs / hour to 40 pcs / hour.

6. Conclusion

Based on research conducted it can be concluded that in order to reduce handling time operator on the Goodway GV – 500 machine can be done by removing the elements of the operator is taking part. To eliminate the element of the work carried out improvement by making automatic unloading tool, so that part can come out automatically. The concept of automatic unloading tool is made by adding a gripper in turret machine. With the automatic unloading tool the handling time operator Goodway GV – 500 machine can be reduced from 12 seconds to 4 seconds.

7. References

Amstead B.H, dkk, 1981. Teknologi Mekanik Jilid II. Erlangga – Jakarta

Petruzella, Frank D., 2002. Elektronika Industri. Erlangga – Jakarta

Sigit, Sudarwanto, 2011. Mesin Bubut CNC, Universitas Borobudur – Jakarta

Fanuc, PMC programming manual, http://krcmachinetoolservices.com/downloads/2013/01/0iD_PMC_prog.pdf,

accessed on March 05, 2015.

Velaction Continuous Improvement, Operator Cycle Time, available at : http://www.velaction.com/operator-cycle-time/, accessed on Mei 04, 2015.

Velaction Continuous Improvement, Hanedashi, available at http://www.velaction.com/ hanedashi/ accessed on Mei 04, 2015.

Proceedings of the 1st Faculty of Industrial Technology International Congress
International Conference
Bandung, Indonesia, October 9-11, 2017
ISBN 978-602-53531-8-5

Realization and Key Analysis on Blockchain Bitcoin

Muhammad Lazuardi Wirananda*, Surya Michrandi Nasution*, Marisa W. Paryasto*
Department of Computer System, Telkom University, Bandung - INDONESIA
* Corresponding author e-mail: lazuardiwp24@gmail.com, michrandy@telkomuniversity.ac.id, marisa.paryasto@telkomuniversity.ac.id

Abstract

Bitcoin is the digital currency which implements the Blockchain system an open financial accounting, The security bitcoin used key, where this key is a security and identity of Bitcoin owner. The key is use implements asymmetric cryptography digital signature scheme ECDSA (Elliptic Curve Digital Signature Algorithm) with elliptic curve point multiplication, where for the curve uses Secp256K1. Asymetric cryptogrphy generate two key ie private key and public key. Private key is a point in the curve and the public key is a coordinate (x, y) that represents the private key within the curve. This research implements key on Bitcoin system where by going through all step, it will generate private key and public key corresponding to key in Bitcoin system.

Keywords: Private Key, Public Key, Elliptic Curve Digital Signature Algorithm, Secp256K1,-

1. Introduction

In today's technological era, many sectors are changing because it is influenced by computer technology. Even the financial sector began to change because of the impact of technological developments, where banking activities have been using computerization, today the use of paper money has begun to be shifted by the use of digital money. For example, Bitcoin is currently the most widely used digital currency, in which Bitcoin is designed with the Blockchain system ie recording all transaction activities that exist on Bitcoin open to the public so it can be seen by anyone.

How the working Bitcoin system and how is security from Bitcoin, because all record transaction in spread to public. In the Bitcoin system is divided into three parts: key, address, and transaction. Key is use for security Bitcoin uses an asymetric key system, this key is also the identity of the owner, because it consists of private key and public key where each key has a different function and important in the system Bitcoin.

2. Methodology

2.1. Bitcoin

Bitcoin is an electronic money made in 2009 by Satoshi Nakamoto. Bitcoin uses a database that is distributed and spreads to the nodes of a P2P network using transaction journals, and uses cryptography to provide basic security functions, such as the bitcoin requirement can only be spent by its owner, and can never be done more than once. The design of Bitcoin allows for unauthorized (anonymous) ownership and transfer of wealth. Bitcoin can be sent via the Internet to people who have a Bitcoin address.

- Coin Bitcoin
  Bitcoin coins are defined as an electronic coin with a digital signature chain. Each owner can transfer the coins to their next owner by way of digital signature on the hash of the previous transaction and the public key of the next owner and add this to the end of the coin. The receiver verifies the signature to verify the ownership chain.
- Key Bitcoin
  The key on Blockchain Bitcoin is divided into two parts, namely the public key and private key, where the two keys are generated from the same process but different designations. Where public key will be used for the process of creating blockchain address to receive and send Bitcoin, and private key is used as digital signature in transactions.
  The use of different addresses has a positive effect, which only processes with a new public key and private key, at no cost, where the use of the same address will increase the attack

2.2 Cryptography

Cryptography (cryptography) comes from the Greek cryptós (secret) and gráphein (Writing). So, cryptography means secret writing. Cryptography is the science and art to maintain the confidentiality of the message by encoding it into a form that can no longer be understood meaning. There are four purposes of this cryptography which is also an aspect of information security that is confidentiality (keeps the content of information from anyone except who has authority), data integrity (custody of unauthorized data changes), authentication (identification and introduction of sender and recipient), and non -repudiation (prevents denial of sending any information by the sender).

Criticism is divided into two parts: Symmetric key cryptography where to perform encryption and decry using one key the same example of a caesar chiper. And another is Key-Asymmetric cryptography where to do the encryption and decryption done by different key for example ECDSA

- ECDSA
  Security key is very important because with this key someone can control, use, transfer our data. where to secure it is used Elliptic Curve Digital Signature Algorithms (ECDSA) is an asymmetric algorithm which will generate private key and public key, which algorithm is good for making random keys because using mathematical curve.
  Asymmetric Encryption is used to create keys, in order to get private key and public key. Key has a function as a digital signature. Because ECDSA is an amalgamation of Elliptic Curve Cryptography algorithm with digital signature algorithm. Where it makes this algorithm more secure than DSA algorithm.

In making the public key using Elliptic curve point multiplication process, where it exists

1. Point Addition

$$xr = \lambda^2 - xp\ xq$$

$$yr = \lambda\ (xp - xr) - yp$$

$$\lambda = \frac{Yq - Yp}{Xq - Xp}$$

2. Point doubling

$$x = \lambda^2 - 2xp$$

$$y = \lambda\ (\mathrm{xp} - \mathrm{xr})\ \text{-}\ \mathrm{Yp}$$

$$\lambda = \frac{3Xp^2 + a}{2Yp} \qquad (1)$$

2.3. Secp256K1

Secp256K1 is an elliptic curve domain parameter used as one of the standard curves, that can be used in the ECDSA algorithm scheme where this curve has the information T = (p, a, b, G, n, h) where for the curve shape is defined By equation $y^2 = x^2 + ax + b$.And the attributes of this kurba are defined by:p = Private keya & b = Values a and b on the curveG = Generation Pointn n = Range in curve

- p = FFFFFFFF FFFFFFFF FFFFFFFF FFFFFFFF FFFFFFFF FFFFFFFE FFFFFC2F= 2256 -232 -29 -28 -27 -26 -24 –1
- a = 00000000 00000000 00000000 00000000 00000000 00000000 00000000 00000000
- b = 00000000 00000000 00000000 00000000 00000000 00000000 00000000 00000007
  Base point for G That have been compressed
- G = 02 79BE667E F9DCBBAC 55A06295 CE870B07 029BFCDB 2DCE28D9 59F2815B 16F81798Base point for G That have been before compressed
- G = 04 79BE667E F9DCBBAC 55A06295 CE870B07 029BFCDB 2DCE28D9 59F2815B 16F81798 483ADA77 26A3C465 5DA4FBFC 0E1108A8 FD17B448 A6855419 9C47D08F FB10D4B8
- n = FFFFFFFF FFFFFFFF FFFFFFFF FFFFFFFE BAAEDCE6 AF48A03B BFD25E8C D0364141
- h = 01

3. System Design

Bitcoin hashavestandard to facilitate the user formaking key, address and transasksi, formaking key bitcoin use asymetric algorithm,so that will generate two key is private key and public key.

To generate a public key corresponding to the standard bitcoin is used:

- Algorithm used is ECDSA where the algorithm is asymetric algorithm so it will generate private key and public key, to generate public key useelliptic curve point multiplication for private key representation in curve.
- The curve used is Secp256K1 where this curve becomes a standard bitcoin and can not be replaced by another curve to produce a public key corresponding to the standard bitcoin.

In this section is design flowchart used specialized on key topics. This study begins by applying the creation of a key, starting with the creation of a private key and then entering into the creation of a public key in which both are designed with standard issued bitcoin.

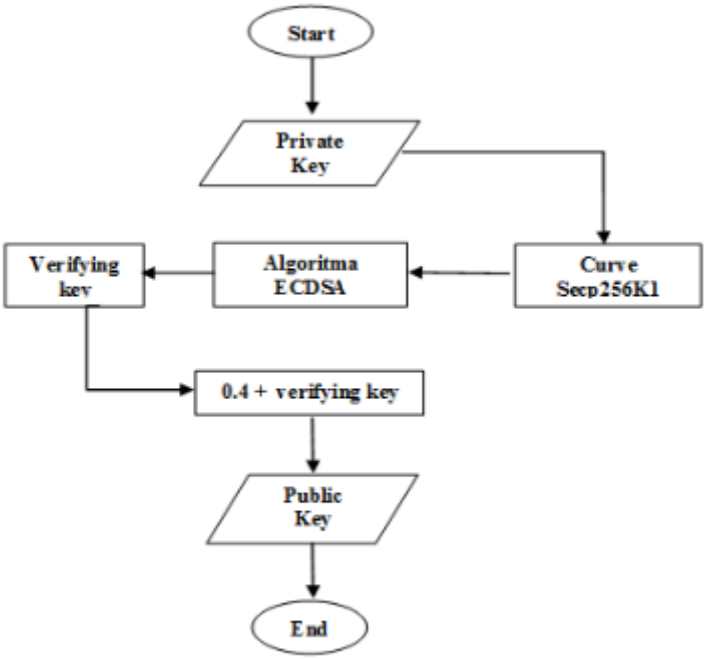

Fig. 1: Figure flowchart used specialized on key topics

Explanation:

- Private key is user input in the form of hex data.
- Private key is plotted in the Secp256k1 curve.
- Private key will be processed in ecdsa algorithm.
- From the plot process on the curve, will be generated in the form of veifying key (private key * Generation key).
- Veifying key will be added 04 at the beginning of the data, 04 itself is Bitcoin provision for public key initialization.
- The above process results into a public key.

4. Implementation and Analysis

The key on bitcoin is as a safeguard as well as the identity of the secretive bitcoin owner, in bitcoin transactions providing the raw for transfer of bitcoin.

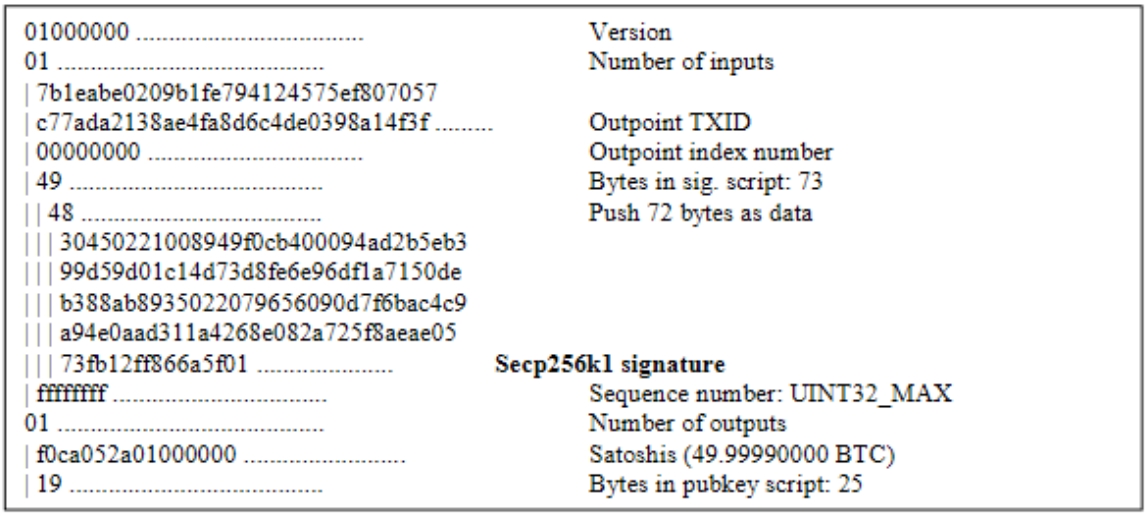

Fig. 2: Figure raw of transaction

Where the data is sent to the blockchain network to spread widely, it is seen that in the transaction process there is the use of key, both private key when making transaction where the private key will be converted into public key that will be sent entered into the transaction raw and disseminated. From this it appears that the importance of knowing the key used in bitcoin, to know the security of this key

4.1 Implementation Key

Key in bitcoin is divided into two parts: private key and public key this is because the bitcoin uses the concept of asymmetric cryptography algorithm, where to get the key through step:

4.1.1 Private Key

The private key consists of 256-bit hexadecimal characters and must meet the criteria of the Secpt256K1 curve, this is done because the private key is a point within the curve, so that the point does not cross the range within the curve and to get the private key corresponding to the standard bitcoin. A range of usable ranges that match the range of the Secpt256K1 curve:

```
N =0x1 to
N=0xFFFFFFFFFFFFFFFFFFFFFFFFFFFFFFFEBAAEDCE6AF48A03BBFD25E8CD0364140
```

Fig. 3: Figure range private key

In this research used 2 ways to generate private key that is by way of user input and generate with software, to use generated with software can use command:

```
private_key = os.urandom(32).encode("hex")
```

Fig. 4: Figure python command line for make random hex character

Implementation private key results

Table 1: Table use of manual input and software

Use	Private Key
By User	11abab5610ae3cc6b820a2c4e6f830aabbccddee40fed0198cba50221b3d5fac
Software	77acefbc10aadef45ad20abcdef1230abe34dc400febd65ae5022bb44dd60ab3

4.1.2 Public Key

The public key is the coordinate (x, y) of the private key into the Secp256K1 curve, where this curve has the equation: $y^2 = x^3 + ax + b$and the parameters T = (p , a, b, G, n):

Information :

p = Private key

a = Curve

b = Curve

G = Generation Point

n = Range curve

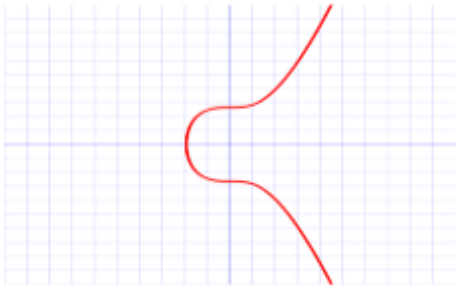

Fig. 5: Figure Curve Secp256K1 in the form$y^2 = x^3 + 0x + 7$

Public key in ECDSA is the result of multiplying private key with generation point: Public key = p * G (verifyng key)To get public key,private key we have to plot into curve by way of Elliptic curvepoint multiplication.

1. Point Addition

```
ECadd(a,b):
LamAdd = ((b[1]-a[1]) * modinv(b[0]-a[0],Pcurve)) % Pcurve
x = (LamAdd*LamAdd-a[0]-b[0]) % Pcurve
y = (LamAdd*(a[0]-x)-a[1]) % Pcurve
return (x,y)
```

Fig. 6: Figure Command point addition in python

Information :
Lam Add = λ
b [0] = Yq or Gy
a [0] = Xq or Gx
b [1] = b
a [1] = a
Pcurve = Private key
The initial step is to determine the value of LamAdd, after obtaining the value from LamAdd input the value to formula x and y to produce value (x,y)

2. Point Doubling

```
Lam = ((3*a[0]*a[0]+Acurve) * modinv((2*a[1]),Pcurve)) % Pcurve
x = (Lam*Lam-2*a[0]) % Pcurve
y = (Lam*(a[0]-x)-a[1]) % Pcurve
 return (x,y)
```

Fig. 7: Figure Command point doubling in python

Information :
a [0] = Gx
a [1] = Gy
Acurve = a
Pcurve = private key
lam = λ
The initial step is to determine the value of lam (λ), after obtaining th evalue from lam input the value to formula x and y to produce value (x,y).

to display results

```
EccMultiply(GenPoint,ScalarHex): #Double & add
    if ScalarHex == 0 or ScalarHex >= N: raise Exception("Invalid Scalar/Private Key")
    ScalarBin = str(bin(ScalarHex))[2:]
    Q=GenPoint
    for i in range (1, len(ScalarBin)):
        Q=ECdouble(Q); print "DUB", Q[0]; print
        if ScalarBin[i] == "1":
            Q=ECadd(Q,GenPoint); print "ADD", Q[0]; print
    return (Q)
```

Fig. 8: Figure Command show the result Elliptic curve point multiplication in python

Information:

ScalarHex = private key

Gen point = Generation Point

1. The first step is to ensure the private key is in accordance with the provisions of the curve where it should not be 0 and should not exceed the value of N
2. Change ScalarHex = private key to binary

3.If dcalarbin is in range 1 then do ecdouble, then print "Dub", the value of ecdouble

4.If scalarBin == 1 then do ecadd then print "ADD", the result ec add.

```
the private key:
174E1E968188807E3A2E01F6F949641776E6E2FE50BBD59FC61B1E200FC4CF80
the private key (binary) :
10541220698491683960407389552802654973678021542018299799729945808138678882176
the verifyng key :
(364526382154178364470391432893540168448522722592049320729745178592154384734 20L,
207121392619759137085732578144012330160078528622102704050012149691548511811 94L)
```

Fig. 9: Figure result Elliptic curve point multiplication

From the process of Elliptic curve point multiplication obtained verifyng key where is the coordinates (x, y) representing the private key. Bitcoin has rules in the form of a public key, where the rule is:

Public Key = Xinteger , Yinteger

Public Key Bitcoin = 04 | Xinteger | Yinteger (10)

Xinteger = 32 bytes Y integer = 32 bytes

The next step is to create a corresponding public key, is x and y must be converted with 32 bytes hexadecimal.

```
print "X convert : ";
print "%032x" % PublicKey[0] ; print
print "Y convert : ";
print "%032x" % PublicKey[1] ; print
```

Fig. 10: Figure Command for converted x,y for adjust to the bitcoin rules

Publickey [0] is X and publickey [1] represents Y where% 032x to generate 32 hexadecimal string.

```
X : 36452638215417836447039143289354016844852272259204932072974517859215438473420
X converted : 5097764ac62c32066c9291c1b884ad20df171e974d9df98921a48ce9b35768cc
Y : 20712139261975913708573257814401233016007852862210270405001214969154851181194
Y converted : 2dcaa7c771b4225155c2e76a77f884b612dbca6e52f38d245717ac1d2916128a
```

Fig. 11: Figure Result converted x,y for adjust to the bitcoin rules

After having the X and Y plots converted, the next step is to create a Public key Bitcoin where 04 (public key initialization) is added with the conversion result X and Y

```
print "04" + "%032x" % PublicKey[0] + "%032x" % PublicKey[1];
```

Fig. 12: Figure Command for make Bitcoin public key

```
Public Key :
045097764ac62c32066c9291c1b884ad20df171e974d9df98921a48ce9b35768cc2dcaa7c771b4225155c2
e76a77f884b612dbca6e52f38d245717ac1d2916128a
```

Fig. 13: Figure Result of Bitcoin public key

After going through the above process, it will generate a private key and public key in accordance with the rules imposed bitcoin.

```
Private key   :
174E1E968188807E3A2E01F6F949641776E6E2FE50BBD59FC61B1E200FC4CF80
Public key   :
045097764ac62c32066c9291c1b884ad20df171e974d9df98921a48ce9b35768cc2dcaa7c771b4225155c2
e76a77f884b612dbca6e52f38d245717ac1d2916128a
```

Fig. 14: Figure Result of Bitcoin private key and public key

The above figure is the result of a run program which displays private key and public key, where to determine whether the result of the program is in accordance with the prevailing standard, we use www.bitaddress.org as the comparison data.

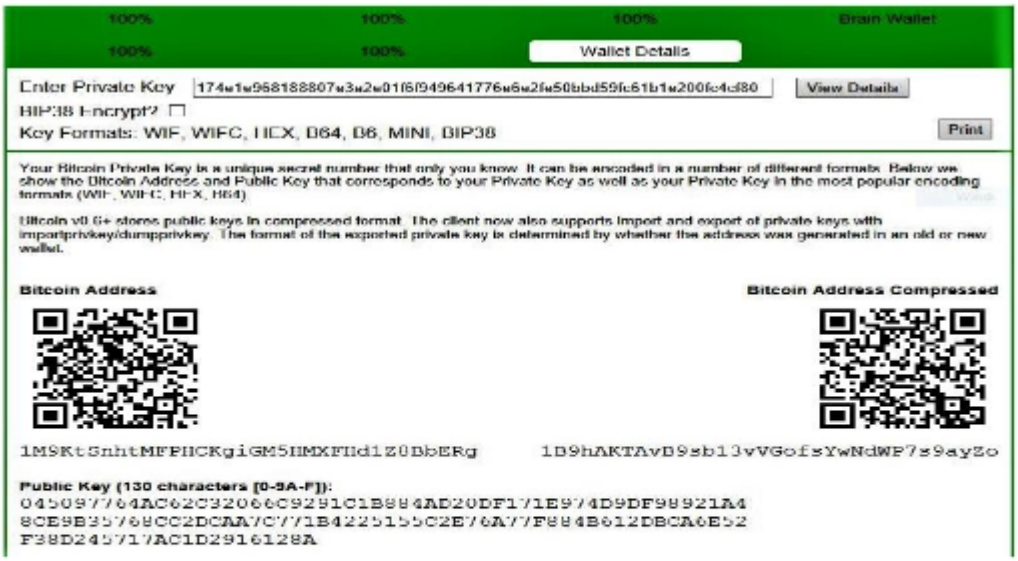

Fig. 15: Figure Result from of www.bitaddress.org

Private Key Hexadecimal Format (64 characters [0-9A-F]):
174E1E968188807E3A2E01F6F949641776E6E2FE50BBD59FC61B1E200FC4CF80
Public Key (130 characters [0-9A-F]):
045097764AC62C32066C9291C1B884AD20DF171E974D9DF98921A48CE9B35768CC2DCAA7C
771B4225155C2E76A77F884B612DBCA6E52F38D245717AC1D2916128A

Fig. 16: Figure Result from of www.bitaddress.org copy to text box

4.2 Analysis

The key in the bitcoin system is a security factor and also the identity of the bitcoin owner where the private key is the main and secret identity of the bitcoin owner and the public key as the global identity of the owner.

This private key consists of 256 bits or 64 hexadecimal. This allows the private key to be made up of many possibilities, if the private key is changed in decimal form it will generate a quinn decilion number so that there is 10^{48} probability of its inclusion which will make it more difficult to do logging.

Public key in the manufacture using curve secp256k1 where the curve has a large range, in the process of making it used Elliptic Curve Point Multiplication to determine the point of coordinates of the private key in the curve, because the public key is a combination of x and y coordinates which is the represent point of the private key.

Elliptic curve point multiplication consists of point addition and doubling point it also increases the security of this key, where the process is done until found a suitable coordinate for private key, in its application in addition program or doubling usually done more than 300 times for a private key 64 character, so to do brute force from public key to get private key really need big resource.

With a large private key range and ECDSA process with Elliptic curve point multiplication will improve the security quality of the key, if a computer can do brute force with 1 trillion guess / second cap, it will take a lot of time to determine the private key of 10^{48} possibilities.

5. Conclusion

The conclusion of this research is that key is a safety factor in bitcoin system where this key consists of two parts: private key as the main identity of bitcoin and public key where the bitcoin public key system will be used in address creation.

To create a private key enough to generate 256 bits or 64 hexadecimal characters, this is a large number, for generating a public key where using the secpt256k1 curve that has a range for a large private key, since this public key is actually the private key coordinate in the curve, where to determine the coordinates are done Elliptic curve point multiplication process, this process is also one of the key security because in the process there is a complex calculation.

Using a private key consisting of 64 hexadecimal characters and using the secp256k1 curve and the Elliptic curve point multiplication calculation will generate a private key and public key corresponding to the key blockchain bitcoin provision and corresponding to www.bitaddress.org.

6. References

Benny Roy P.N., et al, Elliptic Curve Digital Signature Algorithm (ECDSA). Institut Teknologi Bandung (ITB) at Bandung.

Danielle Drainville, 2012, An Analysis of the Bitcoin Electronic Cash System. University of Waterloo at Canada. Danny Yuxing Huang, et al, 2014, Botcoin: Monetizing Stolen Cycles. Network and Distributed System Security Symposium

Daniel R. L. Brown 2010 SEC 2: Recommended Elliptic Curve Domain Parameters Certicom Corp.

Nicolas Dorier. 2015. Programming Blockchain. Github

https://github.com/ProgrammingBlockchain/ProgrammingBlockchain

Rama Febriyan. 2015. Perbandingan Digital Signature Algorithm dan Elliptic Curve Digital Signature Algorithm.

Institut Teknologi Bandung (ITB), at Bandung.

Richard Caetano. 2015. Learning Bitcoin Embrace the new world of finance by leveraging the power of crypto-currencies using bitcoin and blockchain. PACK PUBLISHING www.it-ebooks.info

Rizqi Firmansyah ., Wahyu Suadi ., 2011, Implementasi Kriptografi dan Steganografi pada Media Gambar dengan Menggunakan Metode DES dan Region-Embed Data Density, Institut Teknologi Sepuluh Nopember at Surabaya. Satoshi Nakamoto. 2008. Bitcoin: A Peer-to-Peer Electronic Cash System. https://bitcoin.org/bitcoin.pdf Secp256k1. https://en.bitcoin.it/wiki/Secp256k1. Accessed : 18 February 2017.

Technical background of version 1 Bitcoin addresses , available at : https://en.bitcoin.it/wiki/Technical_background_of_version_1_Bitcoin_addresses . accessed on 28 April 2017. Raw Transaction Format, available at : https://bitcoin.org/en/developer-reference#raw-transaction-format , accessed on 04 April 2017.

Proceedings of the 1st Faculty of Industrial Technology International Congress
International Conference
Bandung, Indonesia, October 9-11, 2017
ISBN 978-602-53531-8-5

Object Oriented Simulation For Improving Unloading And Loading Process

Fadillah Ramadhan*, Said M. Baisa* and Arif Imran
Department of Industrial Engineering, Institut Teknologi Nasional (Itenas), Bandung - INDONESIA
* Corresponding author e-mail: f.ramadhan.email@gmail.com, said.baisa@yahoo.com

Abstract

The Unloading – loading process at Tanjung Priok port is a complex process. It still causes high dwelling time due to inaccurate quay gantry crane allocation, number of Trucks during the unloading – loading process and probabilistic elements such as Truck's speed changed, Quay Gantry Crane's speed changed and number of containers to be processed. To tackle the problem, in this paper an Object Oriented Simulation (OOS) is proposed. This method show characteristics and behavior from every class that influence the systems. Several scenarios are used. This paper illustrated the best scenario for unloading – loading container process.
Keywords: Object Oriented Simulation, Unloading-Loading, Dwelling Time, Quay Gantry Crane

1. Introduction

Shipping containers by sea transport plays an important role in the development of the world economy nowadays. The market environment in which container ports and shipping lines are operating is substantially changing. One of the main driving forces to change emerges from the globalisation process and the large-scale adoption of the container since the late 1960s according to Notteboom (2004). Sea transportation provides many benefits to companies that ship large quantities of goods and distant destinations as the costs incurred for marine transportation are less than air and land transportation although it takes longer time.

Many countries are competing to become a transit routes, temporary terminals, or countries destined for ships carrying containers because it will improve the country's economy. This will make developing countries to improve the efficiency of their existing. Tanjug Priok Port is one of the ports in Indonesia that have high intensity in serving sea transportation, many lines of import starting from the port of Tanjung Priok or export ending at the port of Tanjung Priok or just passing the port in a short time. As it have dense export activities, imports and movement of goods the port of Tanjung Priok authority must regulate the loading and unloading activities very precisely in order to obtain optimal efficiency.

Loading and unloading activities are the activities of removing containers from ships to the yard at the port and vice versa. The complexity of the loading and unloading activities and the number of linkages between the components such as the number of Quay Gantry Cranes , the number of Trucks used the total load time, and the probabilistic elements such as the speed of Quay Gantry Cranes used for loading and unloading processes are not always in similarly, the number of containers carried by each ship is not always the same amount, the speed of the truck carrying the container in the loading or unloading process is not always the same and the queue of Trucks or Quay Gantry Cranes may occur during loading or unloading process.

The complexity of loading and unloading process and the number of probabilistic elements cause the calculation of the average loading and unloading time difficult do analytically. So that the simulation is proposed in this study to determine the number of Quay Gantry Cranes and the number of Trucks in serving the loading and unloading process as according to Law (2007), the simulation model is an appropriate alternative in describing a complex system, especially when the analytic mathematical model is difficult to do.

The simulation model used is a simulation with Object Oriented Simulation (OOS) approach. An Object-Oriented Simulation models the bahivior of interacting objects over time. Object collections, called classes, encapsulate the charaterustics and functionality of common objects according to Banks (1998). OOS constructs a process method and other elements into an object that can interact with other objects. OOS has the advantage of representing

systems whose components are class and behavior in methods that are adaptable to their environment. The purpose of this simulation is to make tools that can be used to get the best scenario for unloading and loading process.

2. Object Oriented Simulation

The Object-Oriented Simulation provides a rich and lucid paradigm for building computerized models of real world phenomena. Its strength lies in its ability to represent objects and their behaviors and interaction in a cogent from that can be designed, evolved and comprehended by domain expert as well as system analysts. It allows encapsulating objects (to hide irrelevant details of their implementation) and viewing the behavior of a model at a meaningful level. It represents special relations among objects (class-subclass hierarchies) and provides "Inheritance" of attributes and behaviors along with limited taxonomic inference over these relations. It represents interactions among objects by "messages" sent between them, which provides a natural way of modeling many interactions. Despite these achievements, however, there remain several largely unexplored areas of need, requiring advances in the power and flexibility of modeling, in the representation of knowledge, in the comprehensibility, scalability and reusability of models (Rothenberg, 1989).

3. Model Development

Simulation was conducted using Visual Studio 2015, with the replication as many as 30 trials.

3.1. Assumptions

The assumptions used in this study are as follows; Simulation is only designed for the container loading / unloading process, oobservation data obtained from interviews and estimation, the size of the container is ignored, not considering the amount of Rubber Tired Gantry in the field area, as the loading process the number of containers in the field is always available, for each process of unloading and loading the number of containers processed is in the range of 100 to 150, and the distribution used is the uniform distribution.

3.2. System Identification

Unloading – loading system investigated, identification sequence as per Fig.1.

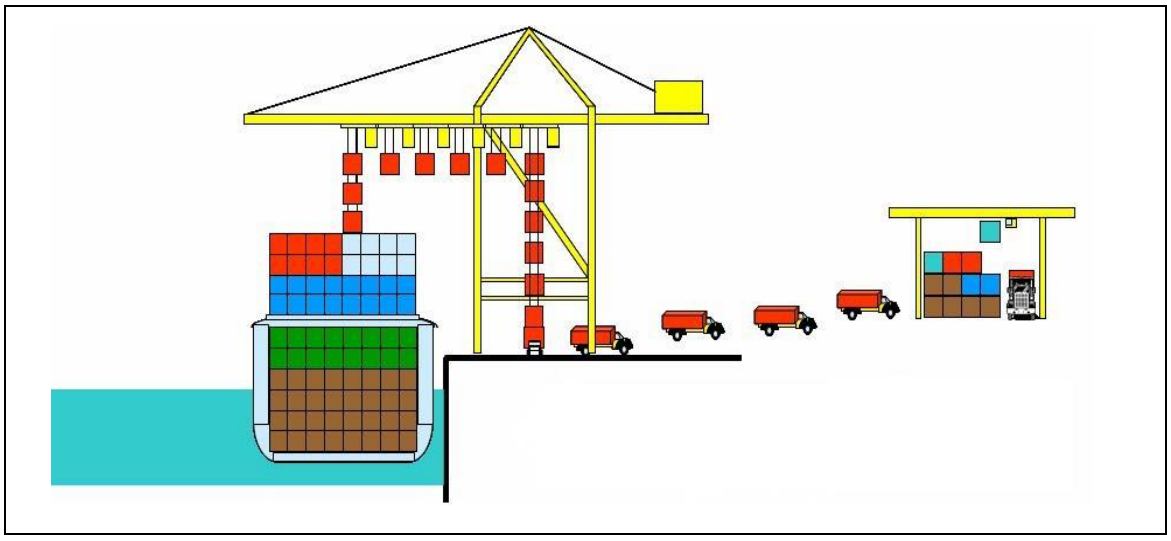

Fig. 1: Loading and Unloading Process (Suhirnoo)

As per Figure1, the unloading sequence process is the movement of a container from ship to truck by using quay gantry crane, then Trucks carry the container to the yard to and use a rubber tyred gantry to unload the container. Then, the truck goes back to Harborside. A loading process is started when Trucks carry the container from the yard using a rubber tyred gantry crane then load the container onto the ship using a quay gantry crane

.

3.3. Determination of Output Model and Variabels Model

Output modes are output generated by a model that is affected by parameter and variables. Output model in the unloading – loading process can be seen in Table 1.

Table 1: Output Model

No.	Output Model
1	Average time of unloading process
2	Average time of loading process
3	Trucks utility used during loading and unloading process
4	Quay Gantry Cranes utility used during loading and unloading process

The input variable model is affected variable that can change output model. These variables are conditions which decision maker should be taken on a system. The variables model in this unloading – loading research can be seen in Tabel 2.

Table 2: Variabels Model

No.	Variabels
1	Number of Trucks used during unloading process
2	Number of Trucks used during the loading process
3	Number of Quay Gantry Cranes used during unloading process
4	Number of Quay Gantry Cranes used during unloading process

3.4. Identification of Classes in The System

Class is an object that can take a decision and interact among agent. Interaction that happened among class will affect the overall system. The classes which are involved in the unloading – loading process such as the Ship, Quay Gantry Cranes and Trucks. The interaction is given by Figure.2.

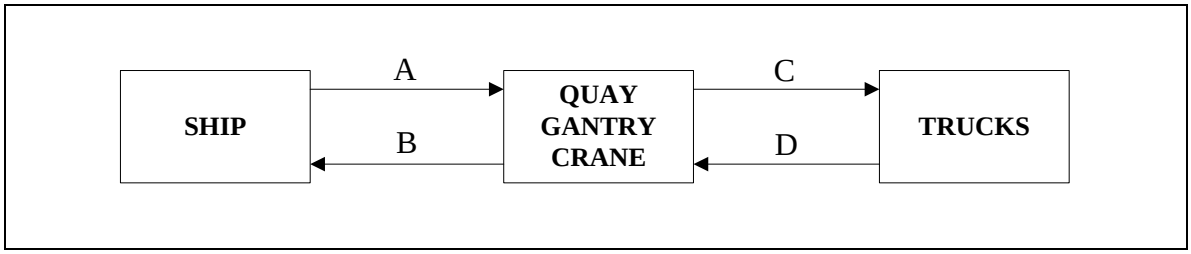

Fig. 2: Interaction Between Classes

In Figure 2, we can see that the Ship will affect Quay Gantry Cranes and Quay Gantry Cranes will affect ship (A-B), Quay Gantry Cranes will affect Trucks and vice versa (C-D).

3.5. Identification of Attributes

Attribute is characteristic that owned by the object. Attribute example owned by ship class as per Table 3.

Table 3: Ship's Attributes

No	Agent	Attribute	Remarks
1	Ship	Id	Ship identity
		Status	Ship activity (come/go)
		Maximum number of containers	Maximum number of containers that will be processed at unloading / loading
		Minimum number of containers	Minimum number of containers that will be processed at unloading / loading
		Number of containers	Number of containers that will be processed in unloading / loading
		Time of arrival	Time of arrival ship at dock
		Time of departure	Time of ship departure from the dock

3.6. Identification of Classes Behaviors

Every classes has their behaviors, behaviors are activities or habits that are routinely performed by the classes in the system and these behaviors can interact with other behaviors. Identification of classes behaviors can be seen in Table 4.

Table 4: Identification of Classes Behaviors

No.	Class	Behavior
1	Ship	The ship arrives at the port to perform the unloading process
		The ship left the port after the unloading process
		The ship arrives at the port to perform the loading process
		The ship left the port after the loading process
2	Quay Gantry Crane	Quay Gantry Crane's setup before the unloading process
		Quay Gantry Crane's setup before the loading process
		Move containers from the ship to the Trucks
		Move containers from the Trucks to the ship
3	Truck	Truck's setup before the unloading process
		Setting up Trucks before the loading process
		Trucks take container while unloading process
		Trucks take container while loading process
		Trucks back to the parking area after the unloading process is complete
		Trucks back to the parking area after the loading process is complete
		Truck waiting for Rubber Tyred Gantry operation completed during unloading process
		Truck waiting for Rubber Tyred Gantry operation completed during loading process

State diagram is a diagram showing the behavior of each class and behavioral changes that occur. State diagram of the unloading process can be seen in Fig. 3.

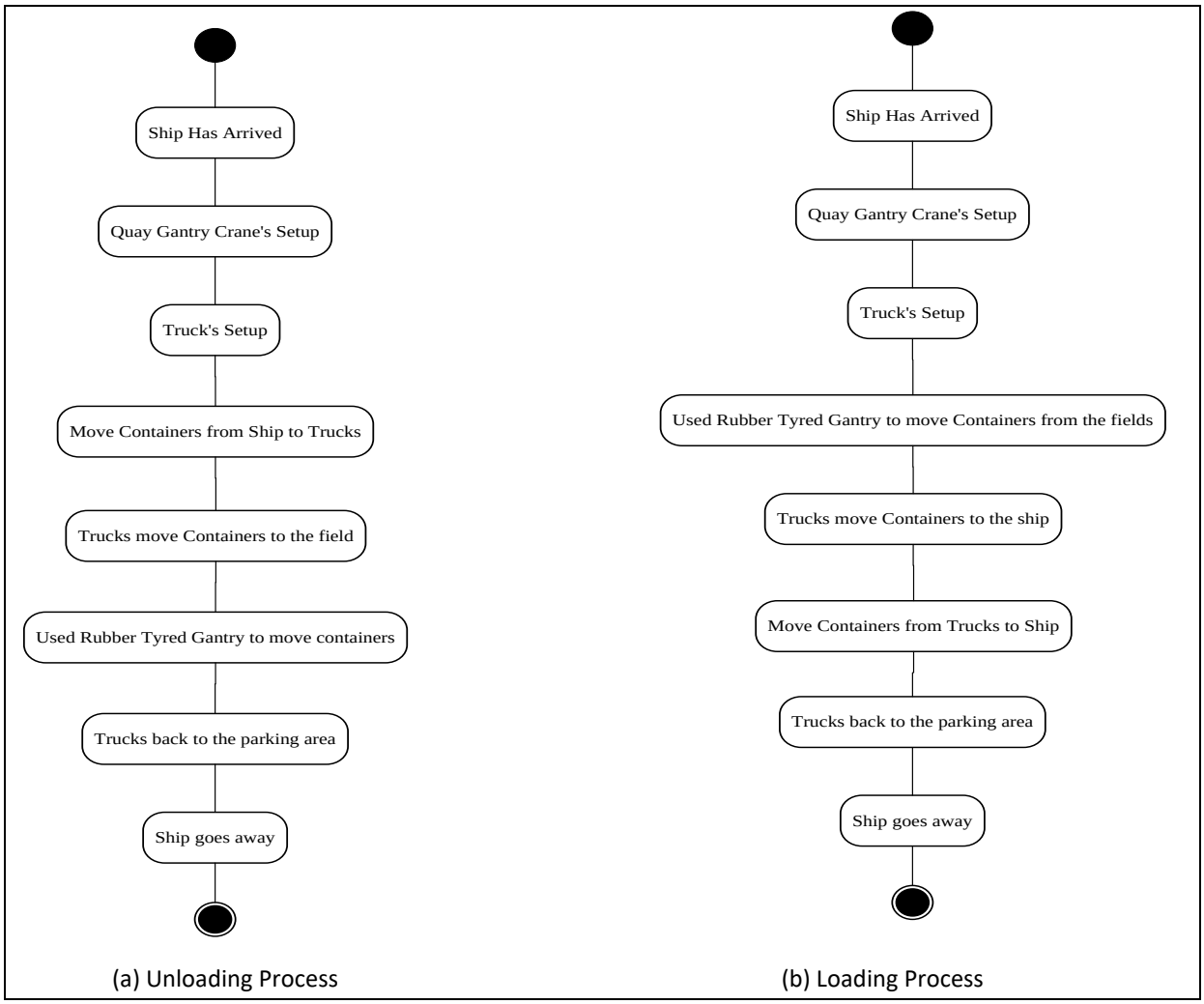

Fig. 3: State Diagram

4. Result and Discussion

Simulation is conducted by using Visual Studio 2015, with the replication as many as 30 trials. Test scenarios are done to obtain the best scenario for loading and unloading process. The result of test scenario for unloading and loading process can be seen in Table 5. and Table 6.

Table 5: Scenarios for Unloading Process

Scenario	Number of Quay Gantry Crane	Number of Trucks	Number of Ships(Units)	Average Time For Unloading Containers (minutes)	Utilization of Quay Gantry Crane (%)	Utilization of Trucks (%)
Scenario 1	1	2	2005	838	52	92
Scenario 2	2	4	3334	412	52	92
Scenario 3	2	8	4370	271	74	92
Scenario 4	3	8	4870	220	64	92
Scenario 5	3	12	5317	180	74	92

Table 6: Scenarios for Loading Process

Scenario	Number of Quay Gantry Crane	Number of Trucks	Number of Ships(Units)	Average Time For Unloading Containers (minutes)	Utilization of Quay Gantry Crane (%)	Utilization of Trucks (%)
Scenario 1	2	4	1627	1078	26	95
Scenario 2	2	8	2761	549	46	93
Scenario 3	2	12	3579	387	58	91
Scenario 4	3	9	3032	480	38	95
Scenario 5	3	12	3637	370	48	94

Table 5 shows that increasing the number of Quay Gantry Cranes used and the number of Trucks will make the average time for the loading process will be faster. The best scenario for unloading process is the scenario 5 which using 3 units Quay Gantry Cranes and 12 units Trucks with an average time of the loading process is 370 minutes from serving 3637 ships in a year. The utilization of Quay Gantry Cranes is 48% and 94% of the Trucks. The addition the number of truck should be accompanied by the addition of the number of cranes to produce faster time and higher utility.

For the unloading process the result of scenario test does not vary much with the process of loading. The best scenario for unloading process is by using 3 Quay Gantry Cranes and 12 units Trucks with average time of unloading process is 180 minutes from serving 5317 ships in a year. The utilization of Quay Gantry Crane is 74% and utilization of truck is 92%. Increasing number of Quay Gantry Cranes and the number of Trucks will make the average time for the loading process faster. Increasing the number of Quay Gantry Cranes and the number of Trucks used will not necessarily make total time became faster. If we find the case using similar number of Trucks used but different number of Quay Gantry Crane used, then we select the scenario with less Quay Gantry Cranes as more Quay Gantry Cranes will require higher cost but the average loading time generated does not very much.

Quay Gantry Cranes utility is lower when compared to the Trucks utility because the Quay Gantry Cranes and Trucks are ready to be used relatively at the same time but when the unloading process the Quay Gantry Cranes operates early after it the Quay Gantry Cranes will wait for the Trucks to operate. The Trucks operates longer than the Quay Gantry Cranes which causes the utility of the Quay Gantry Cranes to be smaller than the Trucks utility.

The Quay Gantry Cranes utility during the loading process is also smaller than the Trucks utility because the Quay Gantry Cranes and Trucks are ready in relatively the same time but the Trucks start to operate first and after that the Quay Gantry Cranes start operates that process causing incrased the waiting time for the Quay Gantry Crane and that make happen reduce the utility of the Quay Gantry Cranes.

5. Conclusion

Object Oriented Simulation is used to solve the problem of loading and unloading process and it produce: The best scenario for loading unloading process is by using 3 Quay Gantry Cranes and 12 units Trucks, the research produced a simulated model for loading unloading process by using Object Oriented Simulation, the simulated model has been designed to show the behavior of each object involved in the loading unloading process and changes in the number Quay Gantry Cranes and Trucks used in the process will affect the average time of loading and unloading process.

For future research the followings could be considered: Using truck movement animation during the loading and unloading process and consider the number of Rubber Tyred Gantry Cranes in loading and unloading proces

6. References

Banks, J., 1998. Handbook of Simulation. Georgia Institute of Technology at Atlanta, Georgia.

Law, A., 2007. Simulation Modeling and Analysis. McGrawHill. Inc.

Notteboom, T., 2004. Container Shipping and Ports: An Overview. Review of Network Economics Vol.3, Issue 2.

(b). Proses Bongkar Muat, available at: http://suhirnoo.blogspot.co.id/2012/08/sistem-operasi-petikemas.html, accessed on September 04, 2017.

(c). Rothenberg, J., 1989. Object Oriented Simulation: Where Do We Go From Here?. The RAND Corporation at Santa Monica.

(d). Sugioko, A., Nathalia, C., and Hidayat, T. P., 2014. Planning A simulation Model For Loading Unloading Containers To Decrease The Cycle Time. Proceeding 7th International Seminar on Industrial Engineering and Management. Atma Jaya University at Jakarta.

Proceedings of the 1st Faculty of Industrial Technology International Congress
International Conference
Bandung, Indonesia, October 9-11, 2017
ISBN 978-602-53531-8-5

Investigation of Classification Algorithm for Land Cover Mapping in Oil Palm Area Using Optical Remote Sensing

Anggun Tridawati* and Soni Darmawan
Department of Geodesy Engineering, Institut Teknologi Nasional (Itenas), Bandung - INDONESIA
* Corresponding author e-mail: angguntridawati.30@gmail.com

Abstract

Technological development on globalization era enable the application of remote sensing technology in access speed and accuracy for mapping land cover based on image classification. The objective on this study is to investigate the utilization of remote sensing imagery of Landsat 8 Operational Land Imager (OLI) for the classification of land cover in oil palm area. Methodology consists of collecting of Landsat 8 OLI, radiometric and geometric correction, making the Region of Interest (ROI) based on class are used in the multispectral classification process to know the land cover in the form of oil palm area, accuracy analysis, and mapping land cover classification with the highest accuracy and kappa coefficient. The algorithm used for classification of land cover types to make class are Maximum Likelihood, Minimum Distance, and Support Vector Machine (SVM) by using various bands on Landsat image and added Normalized Difference Vegetation Index (NDVI). The results in this study show that Support Vector Machine is the best Algorithm of three classification algorithms using all bands on Landsat 8 OLI image with overall accuracy of 96,21% (kappa coefficient 0,9041), Maximum Likelihood Algorithm with overall accuracy of 89,53% (kappa coefficient 0,7713), and Minimum Distance Algorithm with overall accuracy of 84,83% (kappa coefficient 0,6799).

Keywords: Support Vector Machine, Kappa Coefficient, Supervised Classification, NDVI, Landsat 8 OLI

1. Introduction

Oil palm is the world's most productive oil seed and an increasingly important agricultural product for tropical countries around the world (Butler et al., 2009). Malaysia and Indonesia fulfill 85% of Crude Palm Oil (CPO) of the world (Ministry of Agriculture, 2010). Therefore, there is an urgent need to monitor oil palm expansion in the region to provide a better estimate of smallholder plantation activities. This information is an important input to evaluate the success of development policies and the impact of these activities (I.K. Nooni, 2014). The rapidly evolving technological developments of this era of globalization allow the application of remote sensing methods in the classification of land cover in oil palm plantations. This technique is considered important and effective in monitoring land cover because of its ability to provide information of spatial diversity on the surface of the earth quickly, widely, precisely and easily (Sampurno, 2016). Oil palm mapping in tropical environments is challenging due to its landscape nature, cost of image data acquisition, and classification selection (I.K. Nooni, 2014). Remote sensing data began to be widely used to derive the information needed in environmental planning activities at local, regional, and global scales (Johannes et al., 2003 in Jensen 2005). Remote sensing has several methods developed to gain information on land cover. One widely used method is the digital multispectral classification based on statistical analysis (Hamdir, 2014). The classification of land cover or land use based on statistical pattern recognition techniques applied to remote multispectral sensing data is one of the most widely used methods in the information gathering process (Narumalani et al., 2002 in Jensen, 2005). The most common method of classification is the supervised classification method. Several algorithms in the supervised classification are Maximum Likelihood, Minimum Distance, and Support Vector Machine as done by Sampurno (2014) classification of land cover with Maximum Likelihood algorithm resulted accuracy of 99.61%. Setyowati (2015) classified land cover using Maximum likelihood algorithm to produce accuracy of 93.5%, while according to Eko (2012) Support Vector Machine algorithm is the best algorithm in classifying land cover in mangrove area with of 77.93% accuracy. However, little research has been done to map palm oil related land cover. Therefore, researchers continue to seek the best classification algorithm to further improve the accuracy of classification, especially in areas of oil palm plantations.

2. Methodology

This study is concentrated on the utilization of remote sensing technology by utilizing Landsat 8 OLI (Operational Land Imager) Satellite Image for classification of land cover in oil palm plantation area. Starting from the data collection is LANDSAT 8 OLI (Operational Land Imager) satellite imagery for the year of July 2013 and Bing Satellite imagery for December 2013. The next step is radiometric correction using MODTRAN 4 method which is the name FLAASH (Fast Line-of-sight Atmospheric Analysis of Spectral Hypercubes) available on ENVI software and geometric correction of Landsat 8 OLI imagery with Bing satellite imagery as a reference. Making Region of Interest (ROI) based on class that will be used in the classification process to know land cover in the study area in the form of oil palm, non-oil palm (settlements, road, and empty land), water, forest and cloud cover. The classification algorithm used are Maximum Likelihood, Minimum Distance, and Support Vector Machine (SVM) algorithm. Then assessment accuracy by displaying the error matrix (Confusion Matrix) for each classification algorithm. **I**n general, the methodology in this study can be seen in Figure 1.

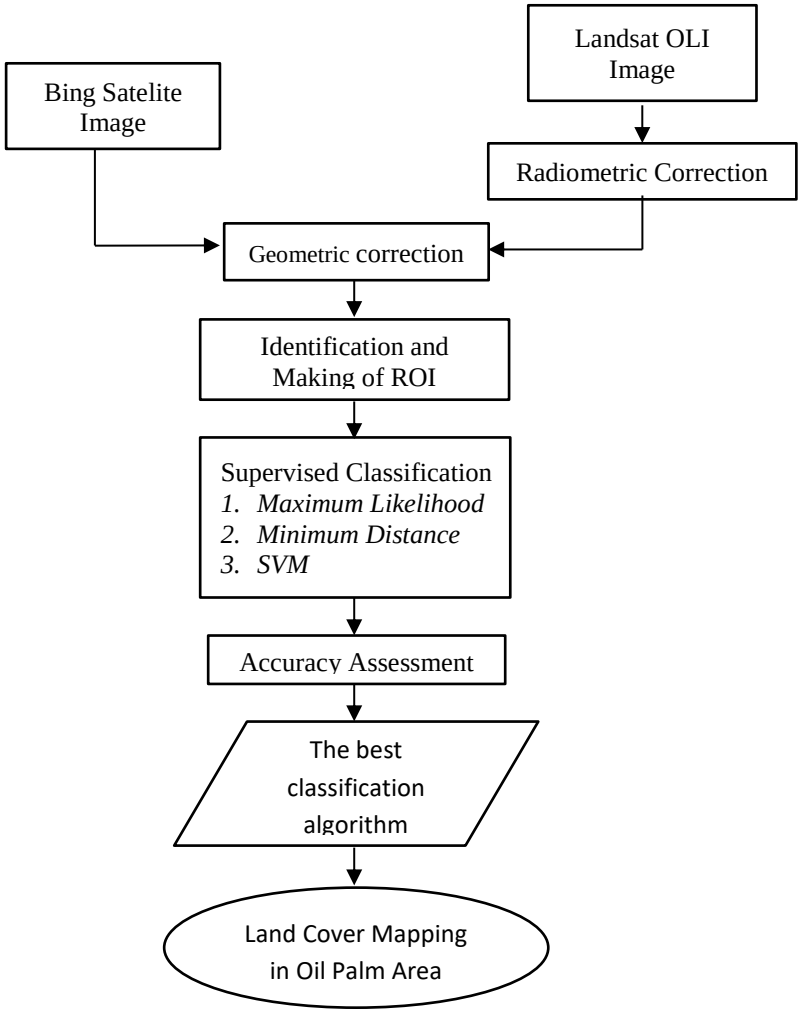

Fig. 1: Methodology on this study

2.1. Identification and Making of Region of Interest

Identification (interpretation) is done to see the difference of each class visually and then made the manufacture of ROI. This identification is done using the data from Bing satellite imagery that has a better spatial resolution of 0.6 m from Landsat 8 OLI image (30 m spatial resolution) so that the land cover is visible. For example, the appearance of oil palm trees with forests that have similarities with Bing Satellite Imagery will be seen oil palm appearance because it is planted with regular pattern. This process is done by displaying the image in a row. As in Figure 2.

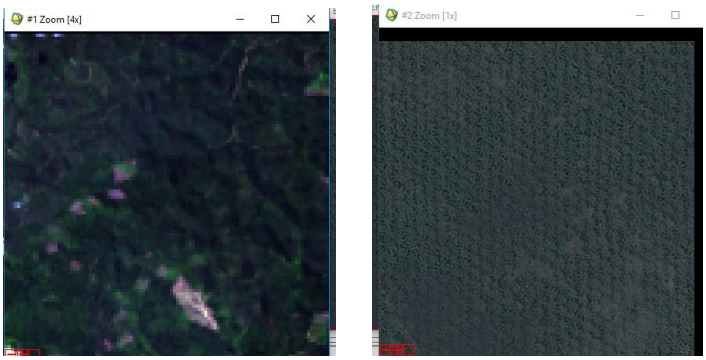

a. Landsat Satellite Image b. Bing Satellite Image

Fig. 2: Identification of Oil Palm Plantation

Oil palm plantation have patterns and textures that are different from other objects located in the area. When compared to the surrounding objects, this oil palm plantation has a pattern that is in groups and lined regularly, so that when viewed from the top has a pattern that is very orderly and neat and make the process of classification multi spectral easier. The making of Region of Interest (ROI) or grouping of pixels on each object is done to retrieve statistical information of land cover classes. The retrieval of statistical information on Landsat imagery is done by determining all sample areas of each land cover class manually with the Bing satellite imagery for each class of 3x3 pixels.

2.2 Multispectral Classification

The purpose of the classification is to produce land cover map in oil palm plantation area. The method used in this classification is the supervised classification method of Maximum Likelihood, Minimum Distance, and Support Vector Machine (SVM) algorithms using the existing bands approach on Landsat 8 OLI and added with NDVI (Normalized Difference Vegetation Index) vegetation index. Classification is based on oil palm, non-oil palm (settlements, road, and empty land), water, forest and cloud cover. The result of the multispectral classification of the three classification algorithms is the land cover map in the area of oil palm plantations.

2.2.1 Maximum Likelihood

The Maximum Likelihood algorithm will classify a pixel on a particular land cover class by calculating a probable log function (Ahmad and Quegan, 2012). Mathematically the log function formula is probably written as follows:

$$g_i(\omega) = \ln P(\omega|i) = \frac{1}{2}(\omega - m_i)^T {E_I}^{-1}(\omega - m_i) - \frac{N}{2}\ln(2\pi) - \frac{1}{2}\ln|E_i| \quad (1)$$

where $g_i(\omega) = \ln P(\omega|i)$ is a possible log function, ω is the characteristic vector of an x pixel to be classified, m_i is the average vector of the class, E_i is the covariance matrix of the class, ${E_I}^{-1}$ is the inverse of the covariance matrix and N is the number of land cover classes. This method has good performance for remote sensing, because it is suitable for the object class whose gray distribution approaches the Gaussian model (Duda, 1973).

- Result of Maximum Likelihood Algorithm

The result of this algorithm can be seen in Figure 3.

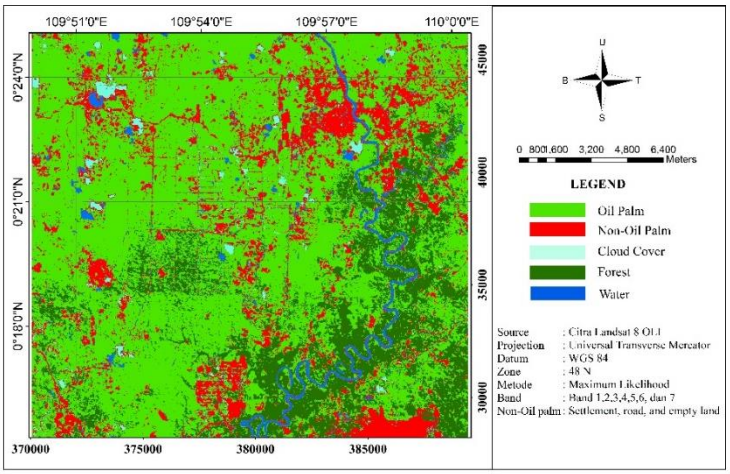

Fig. 3: Land Cover Classification Map of Maximum Likelihood

In the Gaussian Maximum Likelihood Classification method, in addition to the average variables also pay attention to the variance of the vector characteristics of objects in the class. This information is useful for knowing the distribution of each class of the measured variable.

- Accuracy Assessment

Accuracy assessment is showed by confusion matrix using kappa coefficient, that is comparing the result of classification obtained from each image with reference image. The selection of these coefficients is based on a consistency of judgment that considers the producer's accuracy and user's accuracy aspects. The kappa coefficient value has a range of 0 to +1, in the mapping process of land cover / land use an acceptable accuracy of 85%, or 0.85 (Anderson, 1976). The confusion matrix can be seen in Table 1.

Table 1: Confusion Matrix of Maximum Likelihood

Klasifikasi	Class	ROI Ground Check							
		Non-oil palm	Forest	Palm	Water	Cloud cover	Total	Product accuracy	Error omission
	Non-oil palm	270	1	41	2	0	314	85,99	14,01
	Forest	0	181	208	1	0	390	46,41	53,59
	Palm	7	7	1784	0	0	1798	99,22	0,78
	Water	2	0	3	60	0	65	92,31	7,69
	Cloud cover	0	0	7	0	90	97	92,78	7,22
	Total	279	189	2043	63	90	266	Overall accuracy	0,89572
	Product accuracy	96,77	95,77	87,32	95,24	100			
	Error omission	3,23	4,23	12,68	4,76	0		Kappa	0,7713

The result of accuracy assessment of multispectral classification with the actual condition as a whole (Overall Accuracy) is 89,53% (kappa coefficient 0,77) that indicates the process of this multispectral classification, using Maximum Likelihood algorithm can avoid interpretation error of 89.53%, so the possibility to make a mistake of only 10.47%. The accuracy is strongly influenced by the selection of samples and also the number of samples selected. For example, in the forest classification that has an accuracy of 95.77% in which of the total 189 existing samples there is 1 sample that goes into the non-oil palm class, and 7 samples into the oil palm class. This is because the similarity of form and value of Digital Number is almost the same in the oil palm and non-oil palm classes.

2.2.2 Minimum Distance

Pixel grouping is based on the shortest distance to the average vector of a class, so no unclassified pixels (John, 2012). If each pixel in the image is represented in the vector of character u, then one way to determine the membership of u is to put it into the nearest class of distance u. The distance between the u characteristic vector and the j j class pattern vector (mj) can be calculated using the Euclidean distance with the formula:

$$D_j(u) = |u - m_j| \quad (2)$$

Where j=1,2,…,M and $|a| = (a^T a)^{1/2}$ is *norm Euclidean.* The pattern vector u is assigned to the class kj if $D_J\ (u)$ is the closest distance compared to $D_p(u)$, 1< p < M, with p≠j. This method is known as a geometric classification (Hudson, 1987).

- Result of Minimum Distance Algorithm

The result of this algorithm can be seen in Figure 4.

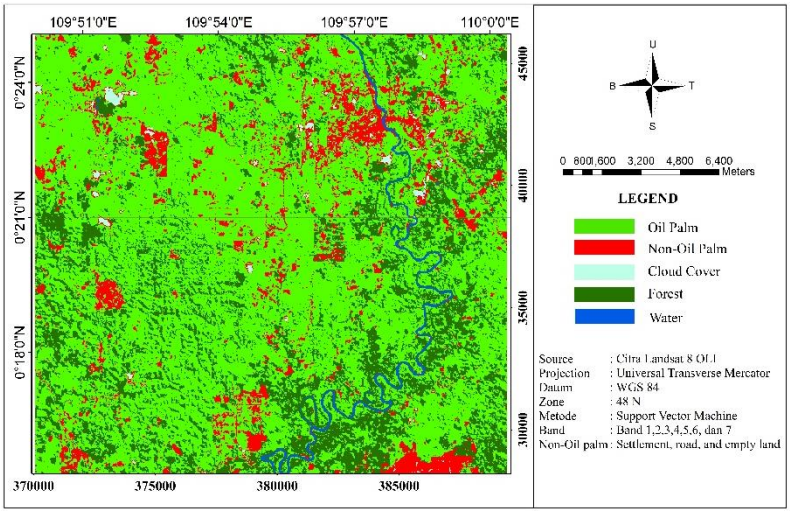

Fig. 4: Land Cover Classification Map of Minimum Distance

- Accuracy Assessment

Accuracy assessment is showed by confusion matrix using kappa coefficient, The result of accuracy assessment of multispectral classification with actual condition as a whole (Overall Accuracy) of 84.83% and Kappa coefficient shows 0.68. This indicates in this multispectral classification process, using Minimum Distance algorithm can avoid interpretation error equal to 84,83% so the possibility to make mistake only equal to 15,17%. Table of accuracy assessment can be seen in Table 2.

Table 2: Confusion Matrix of Minimum Distance

	Class	ROI Ground Check							
		Non-oil palm	Forest	Palm	Water	Cloud cover	Total	Product accuracy	Error omission
Klasifikasi	Non-oil palm	251	0	78	4	11	344	72,97	27,03
	Forest	6	177	267	3	0	453	39,07	60,93
	Palm	19	12	1698	1	0	1730	98,15	1,85
	Water	0	0	0	55	0	55	100	0
	Cloud cover	3	0	0	0	79	82	96,34	3,66
	Total	279	189	2043	63	90	2664	Overall accuracy	0,848348
	Product accuracy	89,96	93,65	83,11	87,3	87,78			
	Error omission	10,04	6,35	16,89	12,7	12,22		Kappa	0,6806

Based on table 2 in the forest classification that has an accuracy of 93.65% of which of the total 189 samples there are 12 samples entered into the palm class. This is because class retrieval with Minimum Distance algorithm is based on the closest distance, because in the study area of oil palm area there are also many forests.

2.2.3 Support Vector Machine

Support Vector Machine (SVM) is a learning system that uses hypothetical space in the form of linear functions in a high-dimensional feature space (Feature Space), trained with learning algorithms based on optimization theory by implementing learning bias derived from the theory of statistical learning (Sembiring , 2007). The main purpose of the Support Vector Machine classification is to find the best hyperplane function with the maximum hyperplane margin measurement (Muhammad, 2014) can be written with the formula:

$$f(x) = sign(\sum y_i a_i{}^0 K(X_i, X) - b^0) \quad (3)$$

Where X_i is vector of data (pixels), X_j is vector on training sample data, and y_i is kernel parameters.

- Result of Support Vector Machine

The result of this algorithm can be seen in Figure 5.

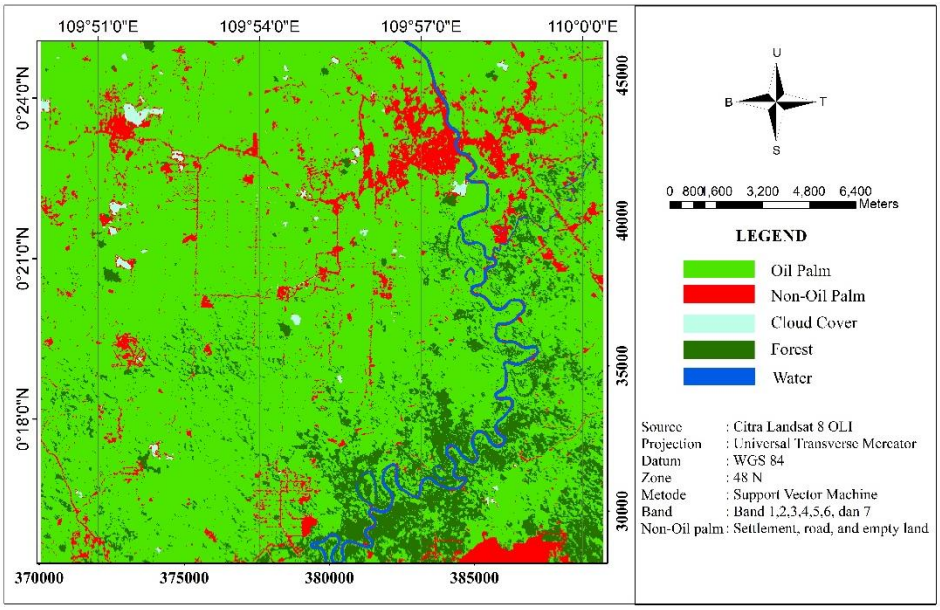

Fig. 4: Land Cover Classification Map of Support Vector Machine

- Accuracy Assessment

Accuracy assessment is showed by confusion matrix using kappa coefficient, The result of accuracy assessment of multispectral classification with the actual condition as a whole (Overall Accuracy) is 96.21% while the classification accuracy for each land cover has different percentage. Kappa shows the number 0.90. Table of accuracy assessment can be seen in Table 3.

Table 3: Confusion Matrix of Support Vector Machine

	Class	ROI Ground Check							
		Non-oil palm	Forest	Palm	Water	Cloud cover	Total	Product accuracy	Error omission
Klasifikasi	Non-oil palm	250	0	5	4	3	262	95,42	4,58
	Forest	0	176	43	3	0	222	79,28	20,72
	Palm	29	13	1995	0	1	2038	97,89	2,11
	Water	0	0	0	56	0	56	100	0
	Cloud cover	0	0	0	0	86	86	100	0
	Total	279	189	2043	63	90	2664	Overall accuracy	96,21%
	Product accuracy	89,61	93,12	97,65	88,89	95,56			
	Error omission	10,39	6,88	2,35	11,11	4,44		Kappa	0,9041

Based on the results in Table 3, the Support Vector Machine algorithm is the algorithm that produces the highest accuracy compared to the Maximum Likelihood algorithm and Minimum Distance algorithm. The kappa coefficient shows that the SVM algorithm reduces classification errors compared to Maximum Likelihood and Minimum Distance. The results of this study indicate the sensitivity of the SVM method in mapping oil palm plantations in heterogeneous environments in terms of overall accuracy, user accuracy, and product accuracy. According to Mathur (2004) the SVM classification basically takes input from the training data and predicts the input given, which outside the class forms the input by linking the training data assigned to each pixel in the image. It then operates to find the separation limit that is between the class pairs by marking each pixel as part of the class, based on the input. So the SVM algorithm classification is the most sensitive algorithm to the specified training size and the SVM algorithm has also demonstrated its potential to identify and map the distribution of oil palm in a heterogeneous environment.

2.2.2 Bands Combination Analysis

Bands used in this classification can be seen in Table 4. Based on the classification that has been done the use of all bands on Landsat 8 gives the best accuracy results.

Table 4: Combination Bands

Metode Klasifikasi	Parameter	Saluran				
		23456	234567	123456	1234567	1234567+NDVI
Maximum Likelihood	Accuracy	85,21%	87,01%	86,82%	89,53%	85,59%
	Kappa coefficient	0,6963	0,7274	0,7217	0,7713	0,7033
Minimum Distance	Accuracy	84,72%	84,61%	84,83%	84,83%	84,72%
	Kappa coefficient	0,6782	0,6772	0,6799	0,6806	0,6756
Support Vector Machine	Accuracy	94,97%	95,91%	95,35%	96,21%	95,12%
	Kappa coefficient	0,8739	0,8967	0,8828	0,9041	0,8776

The multispectral classification assumes that each object can be distinguished from other objects based on its spectral value. Based on the results of this study, the composition of the band that produces the highest accuracy is to use all bands in Landsat 8 image that are band 1,2,3,4,5,6, and 7 because more and more use of band, hence more yield more object This representation is reinforced by Danoedoro (2012) who says that the more bands used, the more accurate it is to provide accuracy.

According to Wielicki (1985), the condition of resistance can affect the overall reflectance value of an optical image. The Landsat satellite is a passive satellite that relies on the sun as an energy source. The condition of resistance will affect the amount of solar radiation that reaches the object on earth. Band 1 is a coastal / aerosol designed for aerosol monitoring closely related to band 2, visible blue. Aerosol is an airborne particle, since band 1 can be used to analyze the effect of atmospheric disturbance (aerosols), by reducing band 1 automatically the spectral information used for classification will decrease so the accuracy value will also decrease.

The NDVI value is a value for knowing the greenery of the leaves with excellent infrared wavelengths as the beginning of the division of the vegetation area. Because the optical properties of chlorophyll are so characteristic that chlorophyll absorbs the red spectrum and reflects strongly in the infrared spectrum. But whenever the addition of information is not effective because of the redundant information on multispectral bands. Such as NDVI, made from the Red and NIR bands are also used as input in the classification so that information is repeated. Therefore band bands 1,2,3,4,5,6,7 and NDVI have accuracy values smaller than band 1,2,3,4,5,6, and 7.

Classification by eliminating band 7, using bands 1,2,3,4,5,6 also has a smaller accuracy value than using all bands, because band 7 has a function can be used to detect the stress of dryness of plants and describe the burned area and fire-burning vegetation, and also sensitive to thermal radiation emitted by fire can be used to detect active fires, especially at night. Therefore, reducing band 7 gives a lower accuracy.

3. Conclusion

The classification of land cover in the oil palm plantation area of the supervised classification method of the Support Vector Machine (SVM) algorithm using all bands 1,2,3,4,5,6 and 7 on Landsat 8 OLI image is the best algorithm with overall accuracy of 96,21% (kappa coefficient 0,90) in producing land cover map in oil palm plantation area.

4. References

Ahmad A, Quegan S. 2012. Analysis of Maximum Likelihood Classification on Multispectral Data. Applied Mathematical Sciences. 129 (64):25–36.

Anderson, J. H., E., Roach J.T., & R. Wittmer. (1976). A Land Use and Land Cover Classification System for Use with Remote Sensor Data.Geological Survey Professional Paper 964. Washington: United States Government Printing Office.

Butler, R. A., L. P. Koh, and J. Ghazoul. (2009). “REDD in the Red: Palm Oil Could Undermine Carbon Payment Schemes.” Conservation Letters 2 (2): 67–73. doi:10.1111/j.1755263X.2009.00047.x.

Danoedoro, Projo. (2012). Pengantar Penginderaan Jauh Digital. Yogyakarta: ANDI Yogyakarta.

Duda, R.O., P.E. Hart. (1973). Pattern Classification and Scene Analysis, New York: Wiley

Eko, Rudi. (2012). Klasifikasi Penutupan Lahan Hutan Mangrove Di Kecamatan Buduran, Kabupaten Sidoarjo, Provinsi Jawa Timur, Dengan Citra Satelit Terrasar-X High Resolution. Skripsi Program Sarjana pada Fakultas Pertanian IPB. Bogor.

Hamdir, Ardian. (2014). Studi Perbandingan Klasifikasi Multispektral Maximum Likelihood Dan Support Vector Machine Untuk Pemetaan Penutup Lahan. Kartografi dan Pengindraan Jauh. Universitas Gajah Mada.

Hudson, William D. (1987), Digital Classification of Landsat Multispectral Scanner data – An Introduction, Research Report Natural Resources From The Michigan State University Agricultural Experiment Station East Lansing, No 483.

I.K. Nooni, A.A. Duker, I. Van Duren, L. Addae-Wireko & E.M. Osei Jnr. (2014). Support vector machine to map oil palm in a heterogeneous environment. International Journal of Remote Sensing Vol. 35, No. 13, 4778–4794.

Kementrian Pertanian. (2010). Outlook Komiditi Kelapa Sawit. Pusat dan Sistem Informasi Pertanian.

Mathur A. (2004). A relative evaluation of multiclass image classification by support vector machines. IEEE Transactions on Geoscience and Remote Sensing.

Muhammad, Teguh. (2014). Kajian Beberapa Metode Klasifikasi Citra Digital Terhadap Data Penginderaan Jauh. Fakultas Matematika Dan Ilmu Pengetahuan Alam. Institut Pertanian Bogor.

Narumalani, D.C. Rundquist, R.L. Perk, J. Schalles, K. Hutchins, dan J. Keck. (2002). Classifying and Mapping General Coral-Reef Structure Using Ikonos Data. Photogrammetric Engineering & Remote Sensing. Vol. 68, No. 12, hal: 1297-1305

Sampurno, Rizky. (2016). Klasifikasi Tutupan Lahan Menggunakan Citra Landsat 8 Operational Land Imager (Oli) Di Kabupaten Sumedang. Fakultas Teknologi Industri Pertanian, Universitas Padjadjaran

Setyowati, Heratania. (2015). Aplikasi Citra Spot-6 Berbasis Transformasi spektral Untuk Estimasi Produksi Kelapa Sawit. Kartografi dan Pengindraan Jauh Universitas Gajah Mada.

Wielicki, Bruce. (1985). Cumulus Cloud Properties Derived Using Landsat Satellite Data: Journal of Climate and Applied Meteorology vol 25 no 3.

Yohannes. (2012). Sistem Pengindraan Jauh Teknik Survey dan Pemetaan. Diktat Kuliah. Lampung: Universitas Lampung.

Proceedings of the 1st Faculty of Industrial Technology International Congress
International Conference
Bandung, Indonesia, October 9-11, 2017
ISBN 978-602-53531-8-5

Robust Indirect Adaptive Control Using RLS for DC Motor

Sabat Anwari
Department of Electrotechnic, Institut Teknologi Nasional (Itenas), Bandung - INDONESIA
Corresponding author e-mail: sabat.anwari@gmail.com

Abstract

Recently, the DC motor has been widely used in industry even though its maintenance costs are higher than the induction motor. Sometimes the conventional feedback control cannot work well to cope with the changes that vary in its dynamic system. The parameters of the dynamic system that changes with time lead to a conventional feedback control system is not able to maintain control. This is caused by circumstances which are nonlinear and receive many disturbance so that the transient response of the system to be less precise and accurate to the desired steady state conditions. To overcome these problems, this paper presents an indirect adaptive control system which can cope with the change of the dynamic DC motor system. The adaptive control scheme comprises a recursive least square (RLS) parameter identification and robust control method. A robustifying control term is added to accommodate the approximation errors and disturbance. This makes the algorithm robust to changes in the plant. Simulation results prove the effectiveness of the controller.

Keywords: DC motor, time varying, indirect adaptive control, robust control, RLS.

1. Introduction

The brushed DC motor is widely used in many variable speed drives. Open-loop operation of the motor can be unsatisfactory in some industrial applications. If the drive requires constant-speed operation under changing load torque, closed-loop control is necessary. The dynamic response of the brushed dc motor angular velocity control depends on the designed control law.

A high performance motor drive system must have good dynamic responses, although the motor parameters are time varying. The development of new technologies for dc motor control such as PID, optimal, robust, and other control laws have been proposed in many applications (Chow and Tipsuwan, 2003; Delibasi et.al., 2004; Dobra, 2002; Gurbuz, 1999; Kucukdemiral et.al., 1999; Ohm, and Oleksuk, 2002; Sevinc, 2003). Generally, these high performance control laws depend on the operation conditions. In high performance drive, adaptive control is the best control law if parameters of system to be controlled are time varying (Astrom and Wittenmark, 1995). Angular velocity control of brushed DC motor is time varying system, hence adaptive control is one of the best controller.

Adaptive control is a label assigned to a wide group of approaches, which are based on variations of the control inputs adequately to a priori unknown variations of the plant's dynamics (Craig et.al., 1987). There are two widely distinct approaches of adaptive control: direct and indirect ones (Betechuoh et.al., 2007). In direct adaptive control, the parameters defining the controller rather than describing the system itself are updated directly, while indirect adaptive control relies on on-line identification of plant parameters with an assumption that a suitable controller is implemented.

The traditional adaptive system may go unstable in the presence of small disturbances (Ioannou and Sun, 1996). We use standard gradient descent to estimate on-line the plant dynamics. The control law is synthesized based on these estimates and a robustifying control term is added to cancel out the effect of approximation errors and disturbance.

This paper proposes a high performance robust indirect adaptive control law for controlling the brushed dc motor angular velocity. This method should be able to learn about parameters changes by processing the output of system and use appropriate controller to accommodate them so it avoids the need of the knowledge the mechanical parameters of motor exactly (Astrom and Wittenmark, 1995). It is proposed the application of this technique on the mechanic part of the system.

2. Modeling

We adopt from (Kucukdemiral et.al., 1999) for the nominal first order linear model of a motor is shown in (15).

$$\frac{d\omega}{dt} + 2\,\omega = 50.3\,V_t - \frac{T_L}{19.8 \times 10^{-6}} \quad (1)$$

Since T_L is unknown, it can be included in the plant perturbation, hence transfer function of the nominal plant is

$$G_0(s) = \frac{50.3}{s+2} \quad (2)$$

The exact model and the nominal model can be related as

$$G = G_0(1+\Delta_m) \quad (3)$$

where G is exact model, G_0 is nominal model, and Δ_m is a multiplicative perturbation.

3. Indirect adaptive control

Adaptive methods seek to use on-line observations, as well as a priori information, to improve the control of system over time in response to changes and unknowns in the system and environment (Astrom and Wittenmark, 1995). Adaptive methods in control system posses several advantages, e.g., fast response, good transient response, robustness of stability, insensitivity to the matching parameters variations and external disturbances. Indirect Adaptive Control (IAC) is one of adaptive model methods.

The control system architecture is shown in Fig. 1. It can be seen that an explicit separation between identification and control is assumed. The basic idea is that a suitable controller can be designed on line if a model of the plant is estimated on line from the available input-output measurements. The scheme is termed indirect because the adaptation of the controller parameters is done in two stages: (1) on-line identification of the plant parameters; (2) on-line computation of the controller parameters based on the current identified plant model.

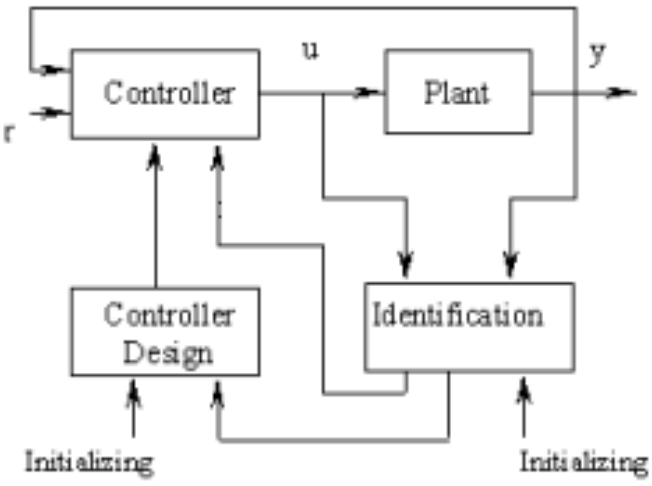

Fig. 1: The scheme of indirect adaptive control

The identification process consists of estimating the unknown parameters of the system dynamics (Ljung, 1987). The recursive least square (RLS) method has been recommended for the identification process for easy implementation and application to real systems.

Recursive least squares (RLS) methods that have been widely used with several advantages such as easy numerical solution and fast parameter convergence gives a consistent modelling accuracy over a wide range of operating conditions and is the best linear unbiased estimate (Soderstrom and Stoica, 1989; Ljung and Glad, 1994).

The discrete mathematical model of the DC motor can be described in terms of input u(t) and output y(t) with the adequate order of the coefficients A, B as:

$$Ay(t) = Bu(t-1) \tag{4}$$

where u(t) is discrete input signal, y(t) is discrete output signal, and

$$A(z^{-1}) = 1 + a_1 z^{-1} + a_2 z^{-2} + \cdots + a_n z^{-n} \tag{5}$$

$$B(z^{-1}) = b_0 + b_1 z^{-1} + b_2 z^{-2} + \cdots + b_m z^{-m} \tag{6}$$

A model of the system (4) can be presented in the form of

$$y(t) = x^T \theta \tag{7}$$

where is a vector of unknown parameters defined by

$$\theta^T = \left[-a_1, \cdots, -a_n, b_0, \cdots, -a_m\right] \tag{8}$$

and θ , vector of regression which consists of measured values of input and output

$$\begin{aligned} x^T(t) = \big[&y(t-1), \cdots, y(t-n), \\ &u(t-1), \cdots, u(t-m-1)\big] \end{aligned} \tag{9}$$

A model given with (7) presents an accurate description of the system. However, in this expression the vector of system parameters θ is not known. It is important to determine it by using available data in signal samples at system output and input. For that purpose a model of a system is supposed

$$y(t) = x^T \hat{\theta} + \hat{e}(t) \tag{10}$$

where $\hat{\theta}$ is a vector of supposed values of system parameters, and $\hat{e}(t)$ is an error in modeling at the moment t.

The vector of supposed values of the parameters, $\hat{\theta}$, should be chosen in such a way that the whole error in modeling can be minimized. From (7) and (10) it appears that

$$\hat{e}(t) = x^T(\theta - \hat{\theta}) \tag{11}$$

After the time interval of N sampling periods, a model (10) can be shown in a vector form

$$\begin{bmatrix} y(1) \\ y(2) \\ \vdots \\ y(N) \end{bmatrix} = \begin{bmatrix} \mathbf{x}^T(1) \\ \mathbf{x}^T(2) \\ \vdots \\ \mathbf{x}^T(N) \end{bmatrix} \hat{\boldsymbol{\theta}} + \begin{bmatrix} \hat{e}(1) \\ \hat{e}(2) \\ \vdots \\ \hat{e}(N) \end{bmatrix} \tag{12}$$

By choosing an adequate performance function (Robertson and Lee, 2002), based on the square prediction error:

$$J = \sum_{1}^{N} \hat{e}^2 = \hat{e}^T \hat{e} \tag{13}$$

the unknown parameters of the system are determined as a solution to:

$$\frac{\partial J}{\partial \hat{\theta}} = 0 \tag{14}$$

According to (12) and (13), the solution of the equation (14) has a form

$$\hat{\theta} = \left[x^T x\right]^{-1}\left[x^T y\right] \tag{15}$$

Sometimes, the assessment is needed to be done whenever the information is coming about input/output samples, that is, in each sampling period. The technique which is appropriate for this purpose is Recursive Least Squares Method. With this method, a supposed model from the previous sampling period $\hat{\theta}(t-1)$ is used for assessment of $\hat{y}(t)$ system output in the given sampling period. Estimated system output is compared with the real system output y(t) and on the basis of the obtained difference an error signal ε(t) is generated. Now, so called mechanism of updating, on the basis of error signal, correct values of supposed parameters of the system $\hat{\theta}(t-1)$ on $\hat{\theta}(t)$. Scheme of the recursive estimation is given in Fig. 2.

If the following symbols are introduced

$$P(t) = \left[x^T(t)x(t)\right]^{-1} \tag{16}$$

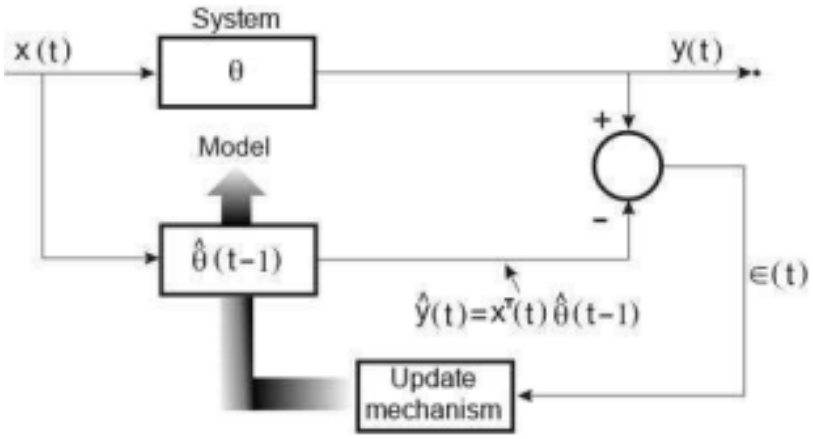

Fig. 2: Scheme of recursive least squares method

Suppose now that the DC motor parameters are identified on a a short time (eg starting). the used algorithm to identify the mechanical and electrical parameters is based on the recursive least squares:

$$\begin{aligned}
\hat{\theta}(k) &= \hat{\theta}(k-1) + L(k)\varepsilon(k) \\
\varepsilon(k) &= y(k) - \Phi^T(k)\hat{\theta}(k-1) \\
L(k) &= \frac{P(k-1)\Phi(k)}{1+\Phi^T(k)P(k-1)\Phi(k)} \\
P(k) &= P(k-1) - \frac{P(k-1)\Phi(k)\Phi^T(k)P(k-1)}{1+\Phi^T(k)P(k-1)\Phi(k)}
\end{aligned} \tag{17}$$

Accordingly, transfer function of the observed system is in the form of

$$G_p(z) = \frac{\alpha}{1-\beta z^{-1}} \tag{18}$$

Use the backward difference transformation of (18)

$$s = \frac{1-q^{-1}}{h} \tag{19}$$

The continuous parameters are found via the relations

$$\begin{pmatrix} a \\ b \end{pmatrix} = \frac{1}{h}\begin{pmatrix} 1-\alpha \\ \beta \end{pmatrix} \tag{20}$$

where h is sampling period.

The dynamic equation of a motor can be approximated by using the following first order differential equation

$$\frac{d\omega}{dt} = -a\,\omega + b\,u \tag{21}$$

where $u = V_t$.

The objective of this paper is to design a control law $u(t)$ such that, the output, $\omega(t)$, will follow a desired trajectory, $\omega_d(t)$.

Let us define the tracking error as

$$e = \omega_d - \omega \tag{22}$$

Define also an error metric as

$$\sigma = e + \lambda \int_0^t e\, d\tau \tag{23}$$

where λ is a positive scalar. Note that the choice of the metric surface, $\sigma = 0$, guarantees that the tracking error, e, is governed after such finite amount of time by the first-order differential equation $\dot{e} + \lambda e = 0$. In case of ideal error metric motion the error metric and its phase velocities should be identically zero i.e.

$$\sigma = 0 \tag{24}$$

$$\dot{\sigma} = 0 \tag{25}$$

The necessary control input can be found as

$$u = \frac{1}{b}(\dot{\omega}_d + a\,\omega + \lambda e) \tag{26}$$

Since a and b, are unknown, so we propose the use of the following control law

$$u = \frac{1}{b_m}(\dot{\omega}_d + a_m\omega + u_m + \lambda e) + u_r \tag{27}$$

where u_r is a robustifying control term. In this paper we assume that $b_m \geq 0.1$.

he robustifying control term u_r can be constructed as a function of error metric, σ, as follow

$$u_r = w\,\sigma \tag{28}$$

The weight w is adaptable that is updated during the operation. The goal is to push σ to zero in finite time. To achieve this requirement, the following Lyapunov function is selected

$$V = \frac{1}{2}\sigma^2 \tag{29}$$

The function selected is positive definite and it vanishes only when $\sigma = 0$. A global reaching condition is its time derivative be negative definite. Choosing its time derivative as

$$\dot{V} = -\gamma\sigma^2 \tag{30}$$

where, γ is a positive constant, restricts the derivative to be negative definite. Substituting (29) into (30), the following equation is obtained

$$\dot{\sigma}\sigma = -\gamma\sigma^2 \tag{31}$$

Going one step further,

$$\sigma(\dot{\sigma} + \gamma\sigma) = 0 \tag{32}$$

Hence, for the Lyapunov stability criteria to be held,

$$\dot{\sigma} + \gamma\sigma = 0 \tag{33}$$

must be satisfied for $\sigma \neq 0$. The goal is to push the function $\dot{\sigma} + \gamma\sigma$ to zero. To achieve this goal the error function

$$E = \frac{1}{2}(\dot{\sigma} + \gamma\sigma)^2 \tag{34}$$

is introduced to the error metric function and the parameters are updated accordingly.

The parameters are updated using simple gradient descent approach –in continuous form– or back propagation :

$$\dot{\theta} = -\eta\frac{\partial E}{\partial\theta} \tag{35}$$

where, η is the learning constant, generally chosen between 0 and 1. To compute the parameter updates, the derivative of the error function E w.r.t. θ should be found. Using the chain rule, the derivative can be written as

$$\frac{\partial E}{\partial\theta} = \frac{\partial E}{\partial u}\frac{\partial u}{\partial\theta} \tag{36}$$

Substituting (33) into (36) and taking the derivatives, the following equations are obtained:

$$\begin{aligned}\frac{\partial E}{\partial\theta} &= (\dot{\sigma} + \gamma\sigma)\frac{\partial(\dot{\sigma} + \gamma\sigma)}{\partial u}\frac{\partial u}{\partial\theta} \\ \frac{\partial E}{\partial\theta} &= -k(\dot{\sigma} + \gamma\sigma)\frac{\partial u}{\partial\theta}\end{aligned} \tag{37}$$

As a result, the parameters update algorithm can be stated as

$$\dot{a}_m = \eta(\dot{\sigma} + \gamma\sigma)\omega \tag{38}$$

$$\dot{b}_m = -\eta\left(\frac{\dot{\sigma} + \gamma\sigma}{b_m}\right)(\dot{\omega}_d + a_m\omega + u_m + \lambda e) \tag{39}$$

$$\dot{u}_m = \eta(\dot{\sigma} + \gamma\sigma) \tag{40}$$

$$\dot{w} = \eta(\dot{\sigma} + \gamma\sigma)\sigma \tag{41}$$

4. Simulation results

Load torque is unknown but in the simulation it is assumed as follows.

$$T_L = 19.8 \times 10^{-6}\ \text{Nm}$$

a. Assume that the values of the motor parameters are unknown

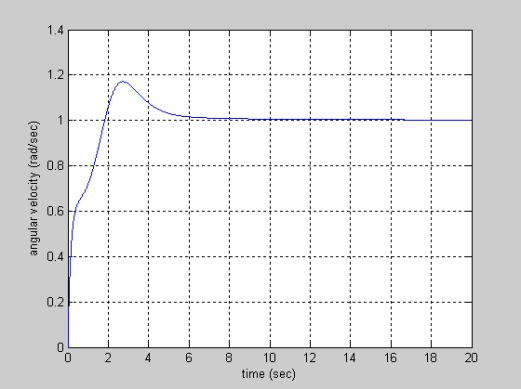

Fig. 3: Angular velocity transient response using controller with unknown parameters

b. Assume that the nominal values of the motor parameters are known

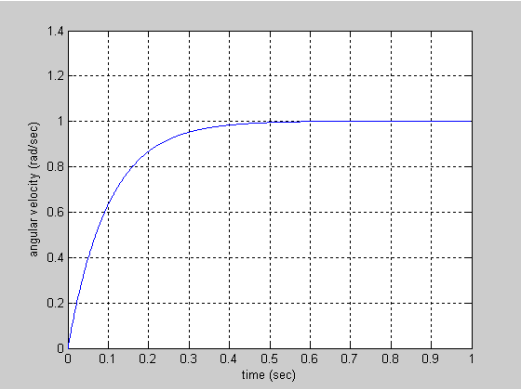

Fig. 4: Angular velocity transient response using controller with known parameters

Figure 3 shows angular velocity transient response if the motor parameters are unknown. The system is stable, but settling time is large enough, about 17 seconds. Figure **4** shows transient response after learning process to find exact parameters. Settling time is reduced, about 0.6 seconds. This facts show that control law using robust indirect adaptive control can control the angular velocity of brushed dc machine sufficiently without need to know the exact parameters. On the other hand, if the exact parameters are known then the performance of angular velocity control is better.

5. Conclusion

Actual experimentation on bulky power components can be expensive and time consuming. But simulation offers a fast and inexpensive means to learn more about these components.

The control law based on robust indirect adaptive control can control angular velocity of brushed dc motor, although the parameters of system are time varying. In order to increase the control system performance, the exact parameters are required.

The simulation and modeling of the DC motor also gave an inside look of the expected output when testing the actual DC motor. The results from the simulation were never likely to occur in real-life condition due to the response times and condition of the actual motor.

6. References

Astrom, K. J., and B. Wittenmark, 1995. Adaptive control. Massachusetts:Addison-Wesley Publishing Company.

Betechuoh, B. L., T. Marwala, and T. Tettey, 2007. Using inverse neural networks for HIV adaptive control. International Journal of Computational Intelligence Research, 3(1), 11–15,.

Chow, M. Y. and Y. Tipsuwan, 2003. Gain adaptation of networked DC motor controllers based on QOS variations. IEEE Transactions on Industrial Electronics, 50(5), 936–943.

Craig, J. J., P. Hsu, and S. S. Sastry, 1987. Adaptive control of mechanical manipulators. The Int. J. of Robotics Research, 6(2), 16–28.

Delibasi, A., T. Turker, and G. Canserver, 2004. Real time DC position control by fuzzy logic and PID controllers using labview. International IEEE Conference on Mechatronics & Robotics '04, Aachen, Germany, September, 9–15.

Dobra, P., 2002. Robust PI control for servo DC motor. International Conference on Control Applications, 1, 100–110.

Gurbuz, F., and E. Apkinar, 2002. Stability analysis of a closed loop control for a pulse width modulated DC motor drive. Turk. J. Elec. Engin., 10(3), 427–438.

Ioannou, P. A., and J. Sun, 1996. Robust Adaptive Control. New Jersey:Prentice Hall International.

Krause, P. C. , and O. Wasynczuk, 1989. Electromechanical Motion Devices. Singapore:McGraw-Hill.

Kucukdemiral, I. B., G. Cansever, and K. Gulez, 1999. Design of a dynamic and robust speed controller for a DC servo motor by using a DSP. Proc. 2nd International Conference on Mathematical and Computational Applications in Engineering, Baku, Azerbaijan, Sep. 1–3.

Ljung, L., 1987. System identification: Theory for the user. Englewood Cliffs, NJ, USA: Prentice Hall.

Ljung, L., and T. Glad, 1994. Modeling of Dynamic Systems. New Jersey: Prentice-Hall, Inc..

Ohm, D. Y., and R. J. Oleksuk, 2002. Influence of PWM schemes and commutation methods for DC and brushless motors and drives. P.E. Technology 2002 Conference, Stephens Convention Center (Rosemont, IL), Oct. 27–31.

Ong, C. M., 1998. Dynamic Simulation of Electric Machinery. New Jersey:Prentice Hall International.

Robertson D. G., and J. H. Lee, 2002. On the use of constraints in least squares estimation and control, Automatica, 38, 1113–1123.

Sevinc, A., 2003. A full adaptive observer for DC servo motors. Turk. J. Elec. Engin., 11(2), 427–438.

Soderstrom, T., and P. Stoica, 1989. System Identification. Hertfordshire: Prentice Hall International (UK) Ltd.

Proceedings of the 1st Faculty of Industrial Technology International Congress
International Conference
Bandung, Indonesia, October 9-11, 2017
ISBN 978-602-53531-8-5

Alumni Face Recognition Using Fisherface Method

Asep Nana Hermana[1,*], Irma Amelia Dewi[1], Gelar Aulia Prima Putra[2]

[1] Department of informatics, Institut Teknologi Nasional (Itenas), Bandung - INDONESIA

[2] Student Department of informatics, Institut Teknologi Nasional (Itenas), Bandung - INDONESIA

* Corresponding author e-mail: asepnana1966@gmail.com

Abstract

Face is part of the human body that became one of the uniqueness and characteristics of each individual. From time to time changes in the face will of course happen by many factors, especially age, in this case the face of alumni. Alumni is a group of people who have attended or graduated from a school or college. One of the technologies used to identify faces is facial recognition. Fisherface is one of the methods used to recognize a person's face. This study has produced a system that can help search alumni information quickly only by using face variable. Testing has been done by taking a face image using a face detector that has been inserted in the face recognition application on Android. Taken image data will be matched with the training data that has been stored in the database using the Euclidean Distance approach. The Euclidean distance between the training data and the test image data will then be calculated and searched for the lowest distance between those two. The lowest Euclidean distance means that the test image data tested has a high degree of compatibility with the training data. From the tests results can be concluded that the Fisherface method can recognize well test image data using 150 training data and 75 test image data with 100% accuracy percentage on neutral face, 80% on smiling face, 60% on face with glasses attribute, 86.66% with make-up, and 100% with sideways face.

Keywords: Face Recognition, Fisherface, Android, Euclidean Distance, Alumni

1. INTRODUCTION

1.1. Background

Difficulty to find information about alumni is still one of the problems experienced by some parties who still have business with alumni or parties who just want to find out about alumni information. Currently the way to obtain alumni information is by using the registration number of students to look for that most likely the data is not the latest data from the alumni. On the other hand, many photographs of alumni are displayed on the campus building, this could be an opportunity that can be used to search for alumni data. Therefore a system is needed that could help to obtain alumni information quickly only by using faces as the information. With the face recognition system, the search process of alumni data would be faster. Therefore, to assist in searching the alumni data, the development of facial recognition system for alumni uses Fisherface method.

1.2. Problem Identification

Based on the background of this final project proposal, it can be formulated problems that exist in this research, namely:

1. How attributes or changes in expression affect facial recognition processes.
2. How the facial recognition process with Fisherface method applied to Android-based devices.
3. How the implementation of Google Mobile Vision is used as a system to detect faces.

1.3. Aim

The purpose of this research is to apply Fisherface method to make facial recognition in order to recognize alumni on Android based mobile device.

1.4. Problem Scope

Problem scope on the research that will be implemented are:

1. Face that to be recognized is the faces of alumni of 2012 Itenas Informatics Engineering Majors.
2. The part used in face recognition is to take the whole of each pixel on a frame that has a face.
3. Frame used for facial processing only contains one face.
4. The size of the image to be used for the face recognition process is 100 x 150 pixels.

2. RESEARCH METHODOLOGY

2.1. Literature Study

Literature study in the form of reading the source of books, journals and articles about the work of facial recognition done with Fisherface method and also about the workings of applications running on Android

2.2 Data Collection Techniques

Data collection techniques by taking a photo or image that has a face, then tested with the image that has been through the process of data training so that the system can recognize the face.

2.3 Research Subjects

Research subjects in this study is the image or photo that has a face in it to examine how much the accuracy of Fisherface as face recognition method.

3. DISCUSSION

3.1. System Work Process

The development of face recognition system has two basic processes. the first one is the registration process, as the stage for entering the face image into the database as data for the training process, and the second one is the identification process, as the stage where the face recognition system is used to recognize the test face image. Figure 1 illustrates how the process performed by the system to recognize faces.

3.1.1. Workflow System

Here is an overview of how the process of facial recognition system is built. Workflow system has two basic processes, that is the registration process and identification process. The picture can be seen in figure 1..

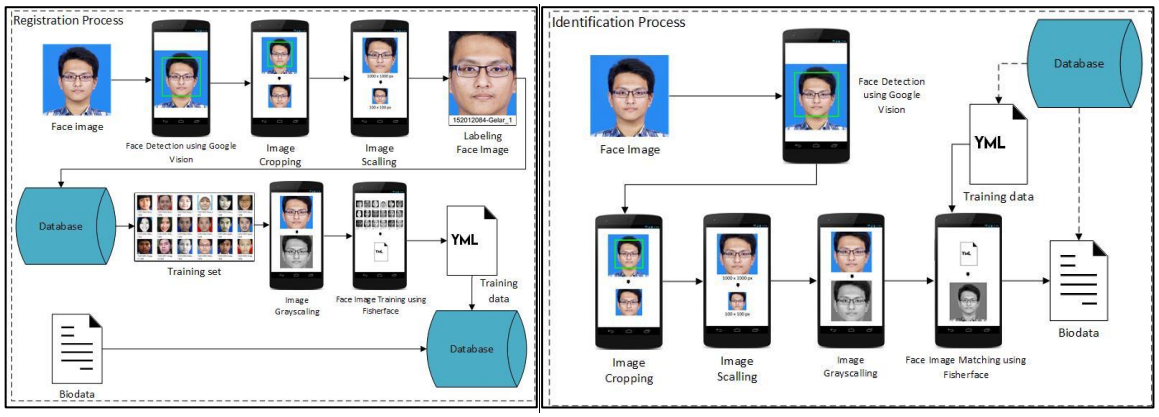

Fig. 1: Workflow system

3.1.2. Flowchart System

With the workflow used as a reference for the built system, here is an overview of each process that is done by the system as a flowchart. The system description can be seen in Figure 2 as the registration flowchart, and Figure 3 as the flowchart identification.

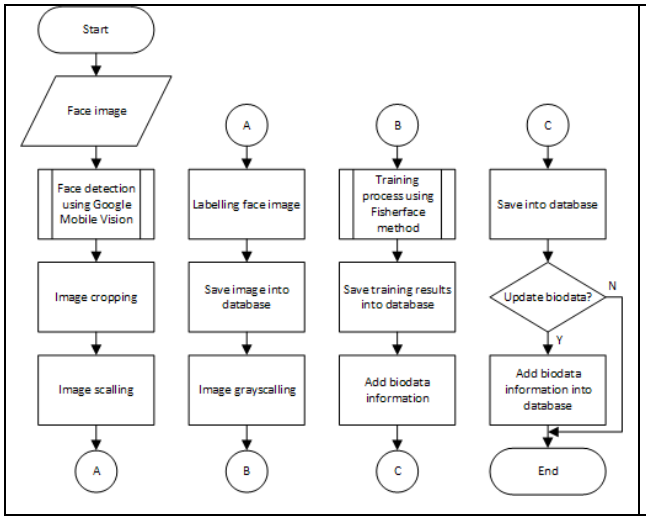

Fig. 2: Registration flowchart

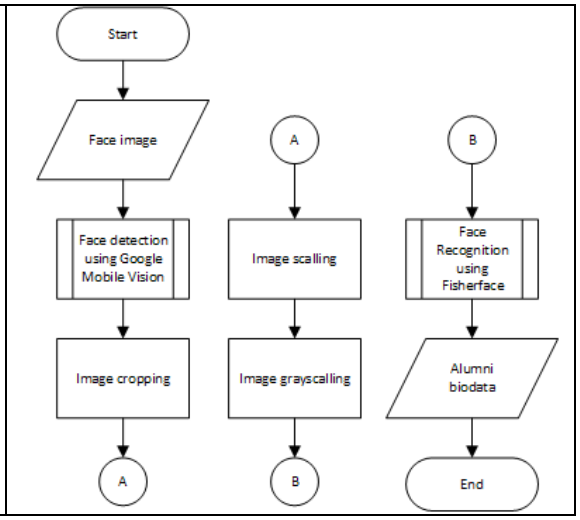

Fig. 3: Identification flowchart

3.2. Face Detection Stage

The face detection system used on systems built using face detection is owned by Google Mobile Services, that is the Vision API. This Google Mobile Vision system can detect faces that exist in an image and generate values or variables that can be used for other processes. Here is the results of the researcher how the face detection process conducted by Google Mobile Vision using flowchart in Figure 4.

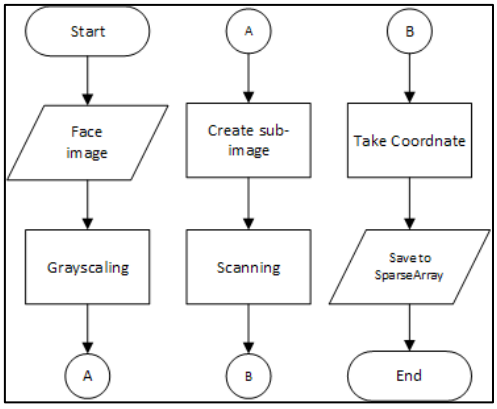

Fig. 4: Google Mobile Vision Face Detection Flowchart

3.3. Pre-Processing Stage

3.3.1. Cropping Process

This process are done so that the face image to be trained or tested will be simplified so that it can be processed by the system. As the name implies, this process of cropping or cutting the image image in accordance with the position of the detected face on the image.

This process uses 4 variables to crop the image. These variables are horizontal axis coordinate values, vertical axis coordinate values, face length values, face width values.

The value of this variable is obtained from the face detection process using Google Mobile Vision, because at the time of face detection, Google Mobile Vision will provide these values.

Suppose there are images like illustrations in figure 5, measuring 4 x 3 pixels, meaning that there is a total of 12 pixels in the image.

	0		1		2		3	
0	R	31	R	42	R	42	R	44
	G	33	G	44	G	44	G	46
	B	22	B	33	B	33	B	35
1	R	46	R	41	R	64	R	82
	G	48	G	43	G	66	G	84
	B	37	B	32	B	55	B	73
2	R	188	R	186	R	193	R	157
	G	189	G	187	G	194	G	158
	B	181	B	179	B	186	B	150

Fig. 5: Input image illustration

With the face detection system gives for example the value 0 for the horizontal axis coordinates and the value 0 for the vertical axis coordinates (coordinates (x, y) = (0,0)). From the coordinates that have been obtained, it will continue with the next process with the face detection system gives for example the value 2 for the width of the face, and the value of 2 for the face value is detected.

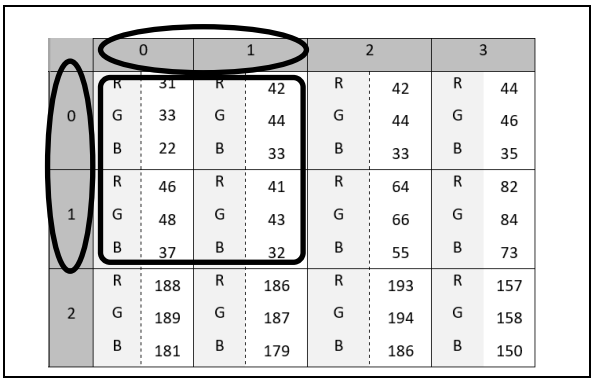

Fig. 6: Illustration of cropping area from image

Once obtained where the image coordinates and the image size, now it can be created a new image with the same size to contain the value of the old image.

	0		1	
0	R	31	R	42
	G	33	G	44
	B	22	B	33
1	R	46	R	41
	G	48	G	43
	B	37	B	32

Fig. 7: Image cropped part illustration

3.3.2. Grayscalling Process

Grayscaling process is a process whereby an image that originally has three color values, namely red, green, and blue (RGB) is converted into a single color value that can be called a gray color. Suppose there is an image input that has a 2 x 2 pixel dimension with its RGB values as follows:

Table 1: RGB values on a 2 x 2 pixel image

		y			
		0		1	
x	0	R	31	R	42
		G	33	G	44
		B	22	B	33
	1	R	46	R	41
		G	48	G	43
		B	37	B	32

Equation 1,

$$Grayscale(x,y) = \frac{R(x,y) + G(x,y) + B(x,y)}{3}$$

Explanation :

$Grayscale(x,y)$ = Grayscale value at x and y coordinate

$R(x,y)$ = Red value at x and y coordinate

$G(x,y)$ = Green value at x and y coordinate

$B(x,y)$ = Blue value at x and y coordinate

The calculation is performed on each coordinate and RGB value in the calculation is taken from the RGB value in table 1. From the calculation we have obtained grayscale value that has been rounded to be processed at the next stage. The results of the calculation of grayscale value can be seen in table 2 below.

Table 2: Grayscale value on 2 x 2 pixel image

		Y	
		0	1
x	0	29	40
	1	44	39

3.4. Facial Recognition Phase Using Fisherface Method

Phase owned by Fisherface method has two basic processes used to simplify the image form that later results from both of these processes will enter the process of finding conclusions using Euclidean Distance calculation. The process is PCA (Principal Component Analysis) and FLD (Fisher Linear Discriminant) calculations as can be seen in Figure 8, Fisherface process flowchart.

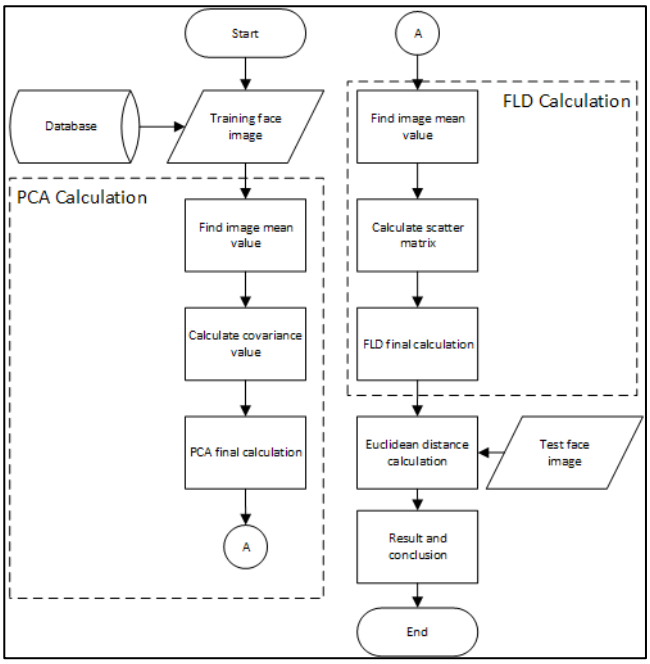

Fig. 8: Fisherface method flowchart

Here's an explanation of the picture 8:

The face image of the training included for the training process is taken from a database previously filled with facial images entered during the registration process, along with the name / label of the file.

29	44
40	39

Figure 9: First training image illustration

52	14
40	29

Figure 10: First training image illustration

After getting the facial images to be trained, then the images will be converted into flatvector, that is a one dimensional matrix. With illustration of image image 9 and picture 10 we got flatvector of each image as illustration of flatvector arrangement in figure 11.

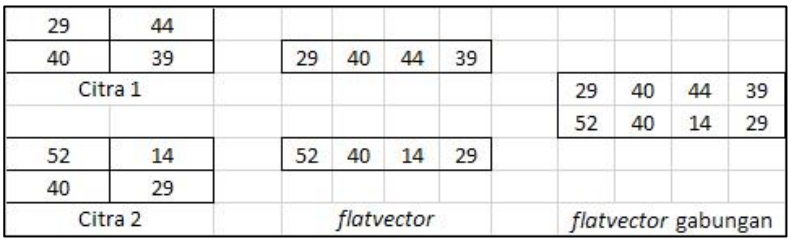

Fig. 11: flatvector arrangement

3.4.1. PCA Calculation

PCA is a technique where the processed data will undergo dimensional reduction process. But the weakness of PCA is that this calculation technique does not include labels as information from the processed data, making this PCA didn't store information from the class where the data came from. Therefore, in the Fisherface method, PCA calculation techniques will be combined with FLD calculation techniques.

After the vector of the face image is obtained, add the line to the flatvector and then divide the matrix by the number of images to obtain the average value of the image vector or its average value on each face image (average face) with equation 2.

Equation 2	Explanation:
$avg = \frac{x_1 + x_2 + x_3 + \cdots + x_n}{n}$	Avg = Average value ($x_1 + x_2 + x_3 + \cdots + x_n$) = matrix value n = amount of data

After obtaining the average value of the image, we will find the value of variance and its covariance using equation 3 and equation 4.

Equation 3	Explanation:
$var(x_i) = \sum_{i=1}^{n} \frac{(x_i - avg_{x_i})^2}{(n-1)}$	$var(x_i)$= variance value x_i= *i*-th matrix value avg_{x_i}= Average value *n* = amount of data
Equation 4 $cov(x_1, x_2) = \sum_{i=1}^{n} \frac{(x_{i1} - avg_{x_{i1}}) * (x_{i2} - avg_{x_{i2}})}{(n-1)}$	Explanation: $cov(x_1, x_2)$= Covariance value

After we get the value of variance and covariance of each image, then the value of variance and covariance is entered into equation 5 that is calculation of covariance matrix.

Equation 5	Explanation:
$Mcov = \begin{bmatrix} var(x_1) & cov(x_2, x_1) \\ cov(x_1, x_2) & var(x_2) \end{bmatrix}$	*Mcov* = Covariance Matrix value

After obtaining the covariance matrix value as in equation 5, the value of the calculation result of this covariance matrix will be recalculated to find the eigenvalues and the eigenvector value. Both of these, eigenvalues and eigenvectors, are used to obtain the component score value (PCA) using equation 6,

Equation 6	Explanation:
$\lvert Mcov - \lambda I \rvert = 0$	λI= Eigenvalue

After the eigenvector value has been obtained, the last step of the PCA calculation process is to find the value score of the component of PCA using equation 7.

Equation 7	Explanation:
$Wpca = \sum (eigenvector1 * a) + (eigenvector2 * b)$	*Wpca* = component score value *a, b* = subtraction of image vector value with the mean

After the PCA calculation is complete and the value of the component score is obtained, then the system will send the score value to the next process is the calculation of FLD.

3.4.2. FLD Calculation

FLD is one of the class specific methods, where it seeks to establish inter-class spacing between in-class scatter and intra-class scatter in order to produce good data classification. The purpose of this FLD is to reduce the dimensions of a data, but also keep the label information that shows the class or uniqueness of the data.

Find what is the average value of each image class with the following 8 equations.

Equation 8	Explanation:
$mean_{vector} = \frac{1}{n}\sum \begin{bmatrix} x1 \\ x2 \end{bmatrix}$	$mean_{vector}$= average value of each data class *n* = amount of data x1, x2 = value of each data

After obtaining the average value of each class of data, then the results of the equation 8 will be used to find the value of the difference matrix with the average of each class using equation 9.

Equation 9	Explanation:
$Si = \sum (x_{class\ i} - mean_{class\ i})^2$	*Si* = subtraction value of matrix with the mean $x_{class\ i}$ = matrix value of each class $mean_{class\ i}$= mean value of each matrix

After obtaining the value of the matrix difference with the average of each class, then the values will be processed to find the value between-class scatter and within-class scatter using equations 10 and 11.

Equation 10	Explanation:
$S_w = \sum Si$	S_w = within-class scatter value $\sum Si$ = amount of subtraction value of matrix with the mean
Equation 11	Explanation:
$S_b = (\mu 1 - \mu 2) * (\mu 1 - \mu 2)^T$	S_b = between-class scatter value $\mu 1 = mean_{class\ 1}$ $\mu 2 = mean_{class\ 2}$

If the within-class scatter and between-class scatter matrix values have been found, the scatter values as well as previously obtained PCA values will be used to find the FLD value using equation 12.

Equation 12	Explanation:
$J(w) = \frac{W_{pca} S_b w}{W_{pca} S_w w}$	*J(w)* = FLD value W_{pca} = PCA component value S_w = within-class scatter value S_b = between-class scatter value

3.4.3. Euclidean Distance

Euclidean Distance is a calculation that becomes the distance between two points. Illustration of Euclidean distance calculation will be explained as follows. Suppose that there are four face image data already stored in the database and the value is described in table 3.

Table 3: traning image data illustration

x-th person	*x*-th Pixel			
	1	2	3	4
1	5	5	4	12
2	10	4	4	3
3	4	12	7	10
4	15	5	13	12

Also note the value of the image to be tested in table 4. The value of this image that will be compared with the image of training data,

Table 4: test image data illustration

x-th person	*x*-th Pixel			
	1	2	3	4
1	6	3	7	11

With equation 13, Euclidean Distance value can be searched between test data with each training data,

Equation 13

$$d_{i,j} = \sqrt{\sum_{k=1}^{m} (x_{i,k} - j_{i,k})^2}$$

Explanation:
$d_{i,j}$ = Euclidean distance *i*-th training image, *j*-th test image
$x_{i,k}$ = *i*-th person and *k*-th pixel training image value
$j_{i,k}$ = *i*-th person and *k*-th pixel test image value

With the equation 13, we can calculate the Euclidean distance value of each training data with the test data. After each training data is calculated the distance of Euclidean it with test data and got the result, then the system will compare each result Euclidean distance and sought the lowest value which can be seen in table 5.

Table 5: each training data Euclidean distance value comparision

Number.	Euclidean Distance value	Result
$d_{1,1}$	3.8729	Has lowest value
$d_{2,1}$	9.4868	
$d_{3,1}$	9.2736	
$d_{4,1}$	11.0453	

4. TESTING

4.1. Testing Level Accuracy

Below is the result of facial recognition test using Fisherface. How to determine the success of face recognition is seen from the value of its Eucledian Distance, the smaller the value of its distance, the greater the suitability of the face. This test was conducted using 150 training data and 75 test data.

To calculate what percentage success rate of each test can be calculated by equation 15:

Equation 15

$$\frac{Sucessful\ tests}{amount\ of\ testing} * 100\%$$

Table 6: Neutral face test

Num.	Test Data	Lowest Euclidean Distance	Nearest training data	Information
1.	1st person	1537.5744	1st person	Matched
2.	2nd person	1600.8019	2nd person	Matched
3.	3rd person	926.6310	3rd person	Matched
4.	4th person	894.5393	4th person	Matched
5.	5th person	921.0817	5th person	Matched
6.	6th person	1343.0229	6th person	Matched
7.	7th person	849.1632	7th person	Matched
8.	8th person	634.4488	8th person	Matched
9.	9th person	774.6221	9th person	Matched
10.	10th person	1049.9138	10th person	Matched
11.	11th person	999.5180	11th person	Matched
12.	12th person	981.5346	12th person	Matched
13.	13th person	1283.1518	13th person	Matched
14.	14th person	846.0421	14th person	Matched
15.	15th person	1727.7218	15th person	Matched

The success rate for neutral face recognition testing is:

$$\frac{15}{15} * 100\% = 100\%$$

Table 7: Smile expression face test

Num.	Test Data	Lowest Euclidean Distance	Nearest training data	Information
1.	1st person	1628.8189	14th person	Not Matched
2.	2nd person	1366.5821	2nd person	Matched
3.	3rd person	978.8660	3rd person	Matched
4.	4th person	878.5860	4th person	Matched
5.	5th person	955.8139	5th person	Matched
6.	6th person	1430.6518	6th person	Matched
7.	7th person	972.5187	11th person	Not Matched
8.	8th person	939.7925	8th person	Matched
9.	9th person	1060.0308	9th person	Matched
10.	10th person	1191.7007	10th person	Matched
11.	11th person	1040.6404	11th person	Matched
12.	12th person	1249.6730	12th person	Matched
13.	13th person	1300.4484	11th person	Not Matched
14.	14th person	1136.6180	14th person	Matched
15.	15th person	1203.1110	15th person	Matched

The success rate for testing facial recognition of a smile expression is:

$$\frac{12}{15} * 100\% = 80\%$$

Table 8: Glasses attribute face test

Num.	Test Data	Lowest Euclidean Distance	Nearest training data	Information
1.	1st person	1675.9737	1st person	Matched
2.	2nd person	1992.5491	1st person	Not Matched
3.	3rd person	1580.6384	10th person	Not Matched

4.	4th person	1453.5284	10th person	Not Matched
5.	5th person	1390.7373	5th person	Matched
6.	6th person	1445.4361	6th person	Matched
7.	7th person	1255.4550	11th person	Not Matched
8.	8th person	1622.6678	8th person	Matched
9.	9th person	1306.5664	10th person	Not Matched
10.	10th person	1323.5438	10th person	Matched

Table 9: Glasses attribute face test (Continuation)

Num.	Test Data	Lowest Euclidean Distance	Nearest training data	Information
11.	11th person	1783.5147	11th person	Matched
12.	12th person	930.1917	12th person	Matched
13.	13th person	1621.4787	1st person	Not Matched
14.	14th person	1357.0009	14th person	Matched
15.	15th person	1032.5162	15th person	Matched

The success rate for facial recognition testing with eyeglass attributes is:

$$\frac{9}{15} * 100\% = 60\%$$

Table 10: Make-up face test

Num.	Test Data	Lowest Euclidean Distance	Nearest training data	Information
1.	1st person	1759.4565	14th person	Not Matched
2.	2nd person	1399.9398	8th person	Not Matched
3.	3rd person	1053.6622	3rd person	Matched
4.	4th person	1070.2269	4th person	Matched
5.	5th person	905.5183	5th person	Matched
6.	6th person	1240.4045	6th person	Matched
7.	7th person	908.1701	7th person	Matched
8.	8th person	1322.8184	8th person	Matched
9.	9th person	1096.1935	9th person	Matched
10.	10th person	1254.6527	10th person	Matched
11.	11th person	1042.1934	11th person	Matched
12.	12th person	1150.3180	12th person	Matched
13.	13th person	1422.5011	13th person	Matched
14.	14th person	845.5093	14th person	Matched
15.	15th person	1670.3373	15th person	Matched

The success rate for face recognition testing with make-up is:

$$\frac{13}{15} * 100\% = 86.67\%$$

Table 11: Sideway face test

Num.	Test Data	Lowest Euclidean Distance	Nearest training data	Information
1.	1st person	1168.974	1st person	Matched
2.	2nd person	321.9707	2nd person	Matched
3.	3rd person	303.772	3rd person	Matched
4.	4th person	678.7715	4th person	Matched
5.	5th person	1194.736	5th person	Matched
6.	6th person	634.7459	6th person	Matched
7.	7th person	228.9673	7th person	Matched

8.	8th person	241.6128	8th person	Matched
9.	9th person	249.9228	9th person	Matched
10.	10th person	1079.774	10th person	Matched
11.	11th person	978.3082	11th person	Matched
12.	12th person	1669.471	12th person	Matched
13.	13th person	1172.337	13th person	Matched
14.	14th person	1050.551	14th person	Matched
15.	15th person	637.6841	15th person	Matched

The success rate for sideway facial recognition testing is:

$$\frac{15}{15} * 100\% = 100\%$$

5. Conclusion

Based on the results of face recognition testing that has been done using 150 test data and 75 data of this training can be concluded the use of Fisherface method for face recognition system has 100% accuracy with neutral face, 80% with smile expression, 60% with attribute glasses, 86.66% With make-up, and 100% with a sideways face. The differences that occur in this face recognition test occur because of inadequate training data. For example if you want to recognize faces that use face attributes, training data must have image data that uses face attributes.

It can be concluded that the facial recognition system using Fisherface method is good enough to recognize faces as can be seen on the percentage of success in testing that has been done, with a record of training data that must be adequate. The more face variations that are stored in the database, the more likely it is that the face is recognizable.

6. Bibliography

Ade Bambang Kurnia. 2016. "Implementasi Pendekatan *K-Means* Dalam Menentukan Ekspresi Wajah Terhadap Suasana Hati". Bandung. Teknik Informatika. Institut Teknologi Nasional.

Deni Ramdani. 2011. "Aplikasi Perbandingan Algoritma Metode *Fisherface* Dengan Metode *Eigenface* Pada Sistem Pengenalan Pola Wajah". Bandung. Teknik Informatika. Universitas Komputer Indonesia.

Febrian Ardiyanto. 2007. "Sistem Pengenalan Wajah Berbasis Metoda *Fisherface*". Bandung. Teknik Elektro. Institut Teknologi Bandung.

Google Developers, "Detect Facial Features In Photos", https://developers.google.com/vision/android/detect-faces-tutorial, diakses (October 14, 2016).

Muhammad Boby Nicholas Argadiraksa. 2016. "Deteksi *Gender* Pada *Single Board Computer* Sebagai Kamera CCTV". Bandung. Teknik Informatika. Institut Teknologi Nasional.

Riko Arlando Saragih. 2007. "Pengenalan Wajah Menggunakan Metode *Fisherface*". Bandung. Teknik Elektro. Universitas Kristen Maranata.

Robil Widiyanto. 2013. "Analisis dan Implementasi Algoritma *Fisherface* Pada Sistem Pengenalan Wajah Untuk Keamanan *Handphone* Berbasis Android". Yogyakarta. Teknik Informatika. Universitas AMIKOM Yogyakarta.

Proceedings of the 1st Faculty of Industrial Technology International Congress
International Conference
Bandung, Indonesia, October 9-11, 2017
ISBN 978-602-53531-8-5

IMPLEMENTATION OF VIGENERE CIPHER WITH EULER KEY GENERATOR TO SECURE TEXT DOCUMENT

Mira Musrini[1,*], Budi Rahardjo[1,*] and Ramdani Krisnadi[2]

[1] Department of informatics, Institut Teknologi Nasional (Itenas), Bandung - INDONESIA

[2] Student Department of informatics, Institut Teknologi Nasional (Itenas), Bandung - INDONESIA

[*] Corresponding author e-mail: mmb0036@gmail.com, budiraharjo@itenas.ac.id

Abstract

There are times when valuable information is very vulnerable to the public. If the information is stored in a text document, in order to prevent information leakage then the text document needs to be secured. Cryptography is a science that studies character encoding, and can be used for securing text documents. In this study, the text document is secured by the vigenere algorithm where the key used is multiplied by the Euler number. The vigenere chiper algorithm with Euleur is implemented in an application built with Visual Studio. This application uses a number of 95 characters from ASCII, starting from number 32 to 126. Encryption and decryption process with vigenere chipper has been successfully done. It is expected that this research can contribute knowledge on how to secure documents.

Keywords: : cryptography, encrypt, decrypt, Vigenere Cipher, Euler

1. Introduction

Sometimes many important documents contain confidential information relating to safety, business competition and ethical considerations. In order to prevent the misuse of documents from being stollen and known to unauthorized parties, security mechanisms are required for documents. Especially information in the form of text which is an important form of digital information (Jing, 2012).

Cryptography is the science and art of changing messages or information to make it safe and immune from attack (Forouzan, 2007). Thus Cryptography is a science that can be implemented to secure documents, so that documents can only be known and accessed by authorized parties or systems .

Vigenere Cipher was chosen to be used to secure the document text in this study. This chipper was introduced first by Balise de vigenere in 1585 in 'Traicte des Chiffer', and is a poly-alphabetic chiper. This algorithm is can be easily attacked by cryptanalist using Kasiski's method (Gaines, 1956). To increase the strength of this algorithm against cryptanalist attack the key is multiplied by the Euler number. By this method a new key is generated.

The problem formulation in this research is how to apply Vigenere Cipher algorithm with key generator of Euler number to perform encryption and decryption in text document. The number of characters used is 95 of ASCII characters, from the ASCII number 32 to 126. This can be considered as scope of the study.

Penelitian ini diharapkan dapat memberikan kontribusi pada bidang pengamanan dokumen teks dan memperluas wawasan di bidang kriptografi.

2. Theory

Vigenere Chiper is symetrical chiper and considered as clasiccal cryptography. This chipper is categorized as polyapfabetic chipers. The formulation of encryption dan decryption are as follows:

Encrypt formulation for 95 characters :

$$E(p(i)) = (p(i) + k(i)) mod\ 95 \quad (1)$$

Decrypt formulation for 95 characters :

$$D(c(i)) = (c(i) - k(i)) mod\ 95 \quad (2)$$

Where :

p(i) = character in plaintext in position i

c(i) = character in chipertext in position i

k(i) = character in key in position i

Euler is a constant in mathematics and the basis of natural logarithms that have uniqueness. Euler number has infinite length (Martin, 2005). Euler number is more or less equal to 271828182845904.

3. Methodology

The key used in this Vigenere chipper has been modified, by multiplying the key with euler number. First, the selected key character was converted into decimal integer based on ASCII code, then the integer pattern of key was noted. Suppose the initial key is 23 1 15 9, then the key pattern is 2 digits 1 digit 2 digits and 1 digits.

The length of Euler number chosen is equal to length of plain text. When the number is found , multiplication between Euler and initial Key is executed . The results of the multiplication are grouped according to the pattern of the initial key.

This modification with euleur key generator may cause new encryption formulas as follows:

a. k * e = k'

b. $E(p(i)) = (p(i) + k'(i)) mod\ 95$

Where e= Euler number whose length equal to length of plaintext

k=initial key

k' =new key generated from multiplication between initial key and Euler number

The generation of new keys with Euler numbers can be explained as follows:

I. Calculate the length of plain text.

II. Convert initial key in decimal ASCII code and concatenate all integers into one number. For example if we have initial key as 14,15,7 then initial key become 14157.

III. Note the digit pattern of initial key. For example from (II), we have 14,15,7. The digit pattern is 2 digit 2 digit and 1 digit.

IV. Determine the Euler number , whose length equal the length of plain text.

V. Multiply Euler number (IV) with initial key (II). The result is in integer and grouped according to digit patterns in (III). The decimal numbers of new key is modulated by 95.

VI. All the numbers from (V) is added by 32.

VII. All the numbers result from (VI) is converted to character based on ASCII code.

Encryption with vigenere Chiper can be described as follows:

I. Rewrite the new key, and equalized length of new key to lenght of plain text. This may result as series numbers of new key and plain text.

II. Sum up new key integers with plain text integers. The result of the sum are modulated by 95.

III. The result of (b) are added by 32. After that the numbers is converted into character based on ASCII code. This is the chiper text.

Example of completed calculation of generation of new key and vigenere's encryption can be detailed as follows:

a) Suppose Plain text = "Dokumen rahasia". The lenght of plain text is 15 digit.

b) Initial key = "Ada". Decimals ASCII of initial key are 65 100 97, so k= 6510097

c) Note the digit pattern of initial key.

d) Determine the Euler number, whose length equal 10 15 digit. So, e=271828182845904.

e) Determine k'. k'=k*e= 271828182845904 X 6510097 = 1769627837660571092688. Write k according to digit pattern from b, thus k = 17,696,27,83,766,05,71,092 ,68,08 . Those numbers are modulated with 95, thus k'=17,31,27,83,6,5,71,92,68,8.

f) All of the numbers from (e) is added by 32. Thus k' = 49,63,59,115,38,37,103,124,100,40

g) the convertion of k' from (f) to character may result as k'=1 ? ; s & % g | d (. This is the new key that will be used for encryption.

h) Equalized the length of new key and length of plain text as follows:

D o k u m e n R a h a s i a

1 ? ; s &% g | d (1 ? ; s &

Since the length of new key < length of plain text, so the new key is repeated until its length is equal to length of plain text.

i) Convert plain text and new key into decimal ASCII. sum up all the numbers of new key and plain text, then results are modulated by 95. After that, the results are added to 32. Those process can be written as follows:

C1 = ((68+49) mod 95) + 32 = (117 mod 95) + 32 = 22 + 32 = 54
C2 = ((111+63) mod 95) + 32 = (174 mod 95) + 32= 79 + 32 = 111
C3 = ((107+59) mod 95) + 32) = (166 mod 95) + 32 = 71 + 32 = 103
C4 = ((117+115) mod 95) + 32 = (232 mod 95) + 32= 42 + 32 = 74
C5 = ((109+38) mod 95) + 32 = (147 mod 95) + 32= 52 + 32 = 84
C6 = ((101+37) mod 95) + 32 = (138 mod 95) + 32= 43 + 32 = 75
C7 = ((110+103) mod 95) + 32 = (213 mod 95) + 32= 23 + 32 = 55
C8 = ((32+124) mod 95) + 32 = (156 mod 95) + 32= 61 + 32 = 93
C9 = ((82+100) mod 95) + 32 = (182 mod 95) + 32= 87 + 32 = 119
C10 = ((97+40) mod 95) + 32= (137 mod 95) + 32= 42 + 32 = 74
C11 = ((104+49) mod 95) + 32= (153 mod 95) + 32= 58 + 32 = 90
C12 = ((97+63) mod 95) + 32= (160 mod 95) + 32= 65 + 32 = 97
C13 = ((115+59) mod 95) + 32 = (174 mod 95) + 32= 79 + 32 = 111
C14 = ((105+115) mod 95) + 32 = (220 mod 95) + 32= 30 + 32 = 62
C15 = ((97+38) mod 95) + 32 = (135 mod 95) + 32= 40 + 32 = 72

j. the decimal ASCII of Chipper text are: 54 111 103 74 84 75 55 93 119 74 90 97 111 62 72. The convertion those decimal numbers to ASCII code may result as 6ogJTK7]wJZao>H. So, Chipper text = 6ogJTK7]wJZao>H.

4. Implementation of Vigenere chipper with euler key generator

To illustrate a series of operations that represent an interaction between the actor and the system, the Use Case Diagram is shown as in Figure 2:

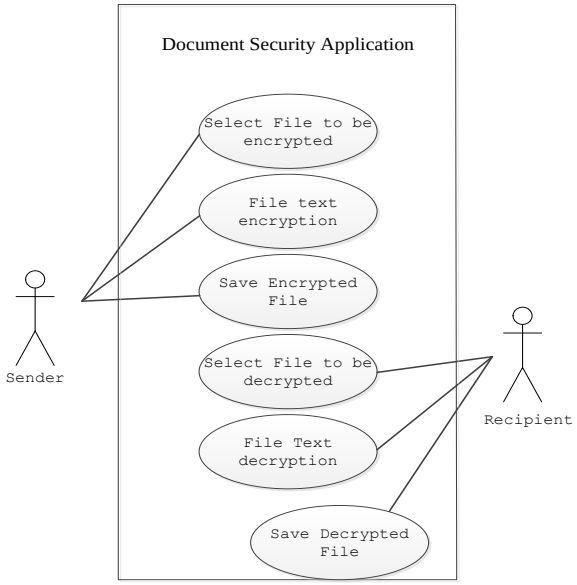

Fig. 1: Use Case Diagram

The application built with visual studio, has two functions , those are encryption file text and decryption file text. When the system is run, the menu that appears is as follows:

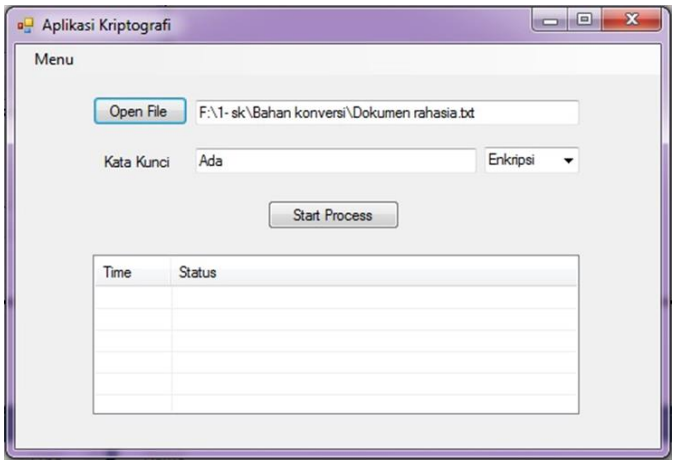

Fig. 2: Initial view of the system

File Text is chosen by clicking “open File” . Next the name of plain text file is filled in in the apeared common dialog. In this study, plain text is contain “Dokumen rahasia” , as describe in figure 3:

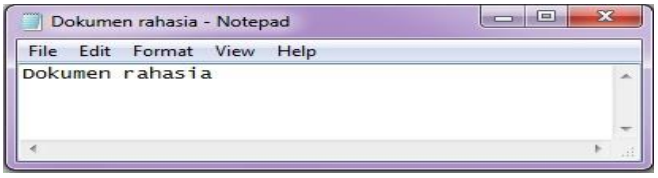

Fig. 3: Plain text document

Encryption process will be executed as “enkripsi” is chosen in the list box next to key textbox. Initial key ,”Ada”, is typed in the textbox. This application can use any key. In this case “Ada” is chosen as an example. When “Start Process” command button was clicked then encryption process is runing. The illustration of those steps can be seen in the figures 4.

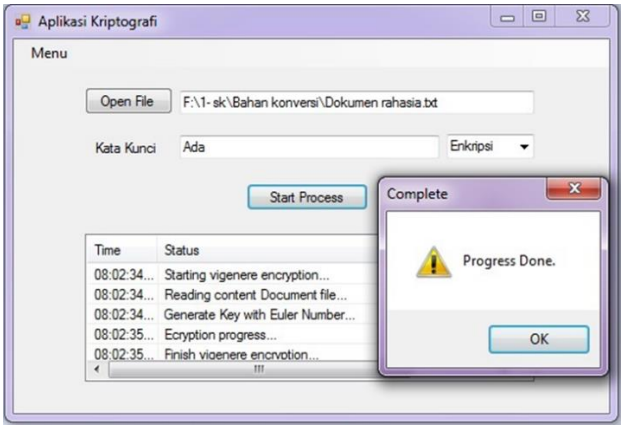

Fig. 4: Progress of encryption process

At the end of the execution, message box appears with path and chiper text file name . This is ilustrated in figure 5.

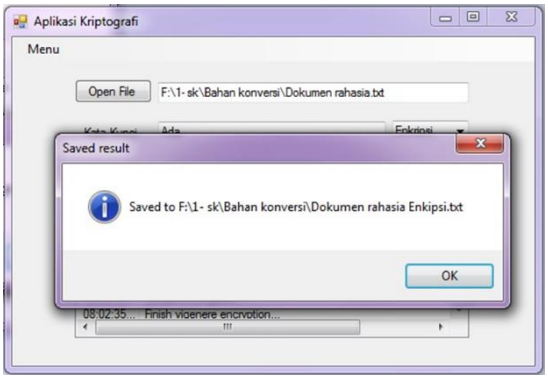

Fig. 5: notification of chipper text file at the end of encryption process

Result of encryption process can be seen in chipper text document, as ilustrated in figure 6.

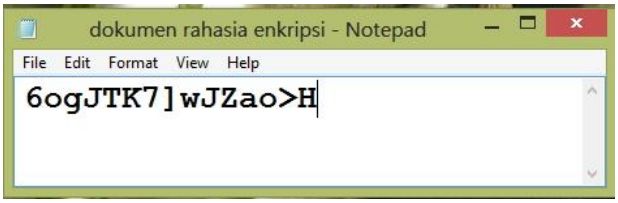

Fig. 6: Chipper text documents

5. Conclussion

1) Implementation Vigenere chiper with key generator euler to application software is succees and valid.
2) New key has very random dan very long form, due its length must equal to plain text length in text document. This circumstances may give more streghtness in algoritghm . It is expected that the algorithm is robbust against attack of cryptanalist.

6. References

Jing, Xianghe, Yu Hao, Huaping Fei, and Zhijun Li. 2012. Text Encryption Algorithm Based on Natural Language Processing. Fourth International Conference on Multimedia Information Networking and Security.2-4 Nov: 670-672.

Forouzan, B.A. and S.C. Fegan. 2007.Data Communication and Networking. 4th ed. McGraw-Hill Companies, Inc. New York.

Martin, Crossley. 2005.Essential Topology: The Euler Number.Springer. London.

Gaines, Helen Fouche.1956. Cryptanalysis. Dover. New York. Implementation of Vigenere chipper of euler key generator

Proceedings of the 1st Faculty of Industrial Technology International Congress
International Conference
Bandung, Indonesia, October 9-11, 2017
ISBN 978-602-53531-8-5

Utilization of Bottle Plastic Waste at Community Level through Gamification Method

Rio Korio Utoro
Department of Informatics, Institut Teknologi Nasional (Itenas), Bandung - INDONESIA
Corresponding author e-mail: korio.utoro@itenas.ac.id

Abstract

Based on data from the Indonesian Central Bureau of Statistics on the percentage of households by province and the treatment of waste sorting easily decayed and not easily decayed, West Java Province compared to the year 2013 suffered a setback in 2014. Based on these data, the percentage rate of un-sorted garbage increased from 69.48 % To 77.36%. If waste management, especially plastic bottle waste at the household level, can be managed in such a way, it can have a huge positive impact, especially in reducing the number of waste production that will be sent to landfill (TPA). The simplest waste management that can be done by the community is to sort out the waste that will be disposed of. Rubbish plastic bottles are separated from other household waste. Through the gamification method, people can collect points obtained from plastic bottle bins that are inserted into special machines designed for this system. The machine is placed in a place that became the center of community activities. Points collected can be exchanged for some rice. With this approach, it is hoped that people will start managing their household waste better, and the existing waste problem can be overcome.

At present the increase in the volume of plastic bottle waste in households is increasing. This is due to changes in lifestyle that are all practical, also more and more emerging mini markets that are located close to the community. With the increase in the volume of waste plastic bottles, there is a chance for garbage accumulation to occur at polling stations. Very few people in the Cigadung area, especially the poor, have the initiative to collect or separate plastic bottles from other household waste. This is because the result of collecting plastic bottles if sold is not comparable, so people just throw it away.

One of the programs owned by the Bandung City government is the welfare of the people, especially those who are economically disadvantaged. One of the efforts that have been made by the government is providing compensation, but because it is done at a certain time, residents cannot rely too much on such assistance for their daily needs. Therefore, a strategy is needed to organize welfare programs for disadvantaged people so that they can be done at any time.

BeHappyOur, adopted from the word Behavior, is a system that aims to improve people's behavior in disposing of garbage. The BeHappyOur system will be used to accommodate the needs of the poor. The BeHappyOur system is run through a garbage ATM / machine that can provide reward points with a certain amount that can be exchanged by citizens with basic necessities to the Partner. With this system, it is expected that the research partner program to improve the welfare of its citizens can run better.

Keywords: plastic bottle, waste, gamification, point system, waste management

1. Introduction

Several big cities in Indonesia are faced with problems that always recur. This can cause serious damage to the city's infrastructure. Not infrequently the damage that arises is due to negligence of the people in the city. Various disasters such as floods began to spread to various cities, but the people did not try to introspect themselves. Trash scattered everywhere is a tangible manifestation of people's lack of awareness of cleanliness. Major cities in Indonesia, especially those on the island of Java, are upgrading to Smart Cities. One city that is implementing the program is the City of Bandung. To realize the development of Smart City, one of the factors that must be

addressed is Smart Living. Smart Living is a condition where the city environment is able to provide comfort, and support survival for its people. Revitalizing infrastructure and public facilities is being carried out by the mayor of Bandung, but public awareness of cleanliness is still lacking. This is evidenced by the fact that there is still a lot of garbage scattered on the highway. The sanction of careless dumpers is not effective, because officers who are authorized to impose sanctions are not always at the scene. Therefore, a different approach is needed that can change the behavior and thinking patterns of the people so that they are more aware of environmental cleanliness. By following the current trends in society, especially the trend of technological developments, a system is needed that can use technology to embrace the community in terms of disposing of garbage.

At present the increase in the volume of plastic bottle waste in households is increasing. This is due to changes in lifestyle that are all practical, also more and more emerging mini markets that are located close to the community. With the increase in the volume of waste plastic bottles, there is a chance for garbage accumulation to occur at polling stations. Most residents, especially the less fortunate, have very few initiatives to collect or separate plastic bottle waste from other household waste. This is because the result of collecting plastic bottles if sold is not comparable, so people just throw it away.

One of the efforts that have been made is giving compensation, but because it is done at a certain time, residents cannot rely too much on the assistance for their daily needs. Therefore, a strategy is needed to organize welfare programs for disadvantaged people so that they can be done at any time.

BeHappyOur, adopted from the word Behavior, is a developed gamification system that aims to improve people's behavior in disposing of garbage. In this research activity, the BeHappyOur system will be used to accommodate the needs of the poor. The BeHappyOur system is run through a garbage machine / ATM that can issue receipts in the form of reward points with a certain amount that can be exchanged by residents with basic necessities to the Partner. With this system, it is expected that programs to improve the welfare of its citizens can be run better and more effectively.

2. Situation Analysis

Bandung have once received the title of City of Trash because the volume of garbage is very high. Based on data from the Regional Medium Term Development Plan (RPJMD), Bandung City Regulation Number 3 of 2014, it is estimated that garbage in the city of Bandung reaches around 357 tons per day.

Table 1: Results of Performance of Environmental Affairs of the Regional Government of Bandung City Period 2008-2012

No.	Aspek/Fokus/Bidang Urusan/ Indikator `Kinerja Pembangunan Daerah	Capaian Kinerja				
		2008	2009	2010	2011	2012
Lingkungan Hidup						
1	Penanganan sampah[1)]	23%	67%	70%	73%	85%
2	Cakupan pelayanan air minum2)	64,00%	66,00%	67,00%	72,00%	72,43%
3	Tempat pembuangan sampah (TPS) per satuan penduduk[2)]	77%	76%	76%	77%	76%
4	Penegakan hukum lingkungan[2)]	69,23 %	100%	100%	100%	100%

Source: LPPD AMJ Kota Bandung.

The issue of waste management in the city of Bandung, should receive special attention. The amount of garbage transported has increased significantly from 23% in 2008 to 85% in 2012, which means 15% of un-transported waste, it is estimated that 15% of this un-transported waste is managed by the community itself or dumped into rivers, land empty or on the roadside, this behavior must be changed immediately. Until 2012 Trash is transported every day as much as 1000-1100 tons or 69% of the total waste generation.

The ratio of landfill (TPS) per unit of population in the city of Bandung during the period 2008-2012 was relatively stagnant at a rate of around 76% - 77% of polling stations / population units. This shows that the capacity of TPS (m3) has increased slightly compared to the population.

Disposal of waste to Final Disposal Sites is still the main alternative for waste management in the city of Bandung, the landfill owned by the city of Bandung (TPA Jelekong, TPA Pasir Impun, TPA Cicabe) has expired and is converted into a Green Open Space; except for land after the Jelekong landfill is currently used as composting land. So that the municipal waste disposal in Bandung was diverted to the Regional Sari Mukti Landfill in Sarimukti Village, Cipatat District, West West District which would end its useful life in 2015 managed by the West Java Provincial BPSR. Considering the Sarimukti landfill will end its useful life in 2015, the Bandung city government seeks to encourage alternative waste management in another way, namely through the development of Environmentally Friendly Waste Management Technology that will be planned to process Bandung municipal waste by 700 m3 / day, the rest of Bandung City waste disposed to the Legok Nangka Regional Landfill in Garut Regency and waste management with a 3R pattern.

Based on a circular from the Mayor of Bandung Number 658.1 / SE.087-DLHK on October 3, 2018, one of which was addressed to the heads of villages throughout the city of Bandung, the mayor asked all staff to immediately form a Waste Bank at the regional apparatus / work unit / regional company to reduce waste generation. This is done because the city of Bandung does not have sufficient land for landfill (TPA), so it must dispose of garbage outside the administrative area of the city of Bandung.

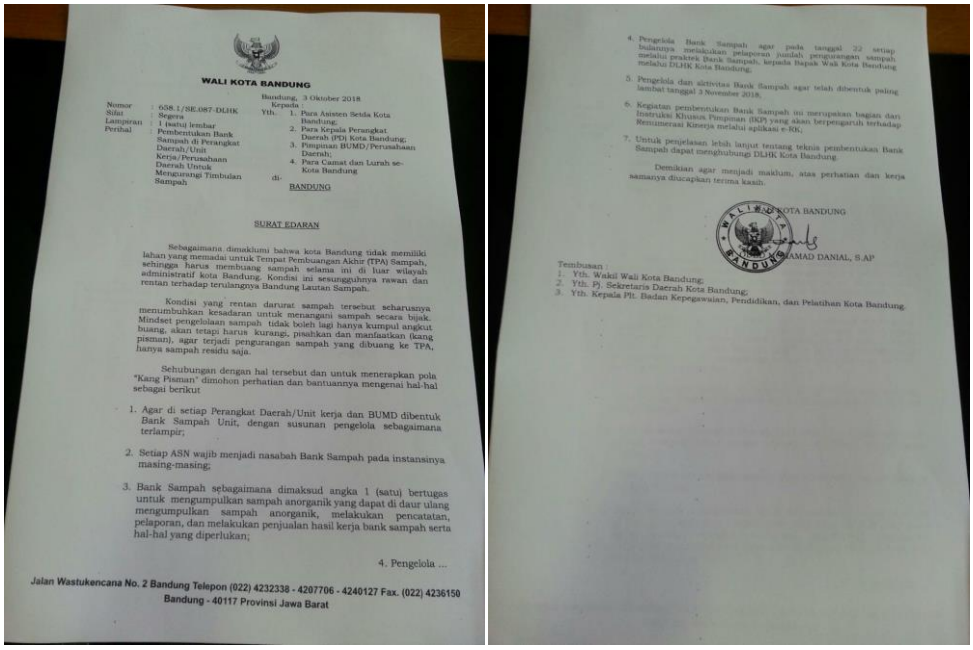

WALI KOTA BANDUNG

Bandung, 3 Oktober 2018

Nomor : 658.1/SE.087-DLHK
Sifat : Segera
Lampiran : 1 (satu) lembar
Perihal : Pembentukan Bank Sampah di Perangkat Daerah/Unit Kerja/Perusahaan Daerah Untuk Mengurangi Timbulan Sampah

Kepada :
Yth. 1. Para Asisten Setda Kota Bandung;
2. Para Kepala Perangkat Daerah (PD) Kota Bandung;
3. Pimpinan BUMD/Perusahaan Daerah;
4. Para Camat dan Lurah se-Kota Bandung

di-
BANDUNG

SURAT EDARAN

Sebagaimana dimaklumi bahwa kota Bandung tidak memiliki lahan yang memadai untuk Tempat Pembuangan Akhir (TPA) Sampah, sehingga harus membuang sampah selama ini di luar wilayah administratif kota Bandung. Kondisi ini sesungguhnya rawan dan rentan terhadap terulangnya Bandung Lautan Sampah.

Kondisi yang rentan darurat sampah tersebut seharusnya menumbuhkan kesadaran untuk menangani sampah secara bijak. Mindset penghilsaan sampah tidak boleh lagi hanya kumpul angkut buang, akan tetapi harus kurangi, pisahkan dan manfaatkan (kang pisman), agar terjadi pengurangan sampah yang dibuang ke TPA, hanya sampah residu saja.

Sehubungan dengan hal tersebut dan untuk menerapkan pola "Kang Pisman" dimohon perhatian dan bantuannya mengenai hal-hal sebagai berikut

1. Agar di setiap Perangkat Daerah/Unit kerja dan BUMD dibentuk Bank Sampah Unit, dengan susunan pengelola sebagaimana terlampir;
2. Setiap ASN wajib menjadi nasabah Bank Sampah pada instansinya masing-masing;
3. Bank Sampah sebagaimana dimaksud angka 1 (satu) bertugas untuk mengumpulkan sampah anorganik yang dapat di daur ulang mengumpulkan sampah anorganik, melakukan pencatatan, pelaporan, dan melakukan penjualan hasil kerja bank sampah serta hal-hal yang diperlukan;

4. Pengelola ...

Jalan Wastukencana No. 2 Bandung Telepon (022) 4232338 - 4207706 - 4240127 Fax. (022) 4236150
Bandung - 40117 Provinsi Jawa Barat

4. Pengelola Bank Sampah agar pada tanggal 22 setiap bulannya melakukan pelaporan jumlah pengurangan sampah melalui praktek Bank Sampah, kepada Bapak Wali Kota Bandung melalui DLHK Kota Bandung.
5. Pengelola dan aktivitas Bank Sampah agar telah dibentuk paling lambat tanggal 3 November 2018.
6. Kegiatan pembentukan Bank Sampah ini merupakan bagian dari Instruksi Khusus Pimpinan (IKP) yang akan berpengaruh terhadap Remunerasi Kinerja melalui aplikasi e-IKS;
7. Untuk penjelasan lebih lanjut tentang teknis pembentukan Bank Sampah dapat menghubungi DLHK Kota Bandung.

Demikian agar menjadi maklum, atas perhatian dan kerja samanya diucapkan terma kasih.

WALI KOTA BANDUNG

MAMAD DANIAL, S.AP

Tembusan :
1. Yth. Wakil Wali Kota Bandung;
2. Yth. Pj. Sekretaris Daerah Kota Bandung;
3. Yth. Kepala Plt. Badan Kepegawaian, Pendidikan, dan Pelatihan Kota Bandung.

Fig. 1: Circular Letter of the Mayor of Bandung regarding the establishment of a Waste Bank

One type of waste that often arises is plastic bottle waste. Plastic bottle rubbish is increasing in number because of the changing lifestyle of people who want to be more practical, so that for daily drinking needs it is not uncommon for people to prefer to buy bottled water rather than boiling water first.

Most people still do not use plastic bottle waste. The garbage is currently thrown away, even though it has a selling value even though the value is not much. A small part of the community separates plastic bottle waste from other household waste. Once collected with a certain amount and weight, it will usually be sold to plastic waste collectors.

With the presence of hygiene movements owned by Partner, waste management in the Partner area is relatively manageable, but plastic bottle waste that should be used to be a more useful economic value becomes completely untapped.

This research activity aims to change the minds of residents in terms of disposing of garbage. Through the ATM Trash tool / machine, it is expected that residents can start sorting waste by separating plastic bottle waste from other household waste. In addition, this activity is also expected to help solve the economic problems of poor people, at least for their daily needs, through the exchange of rewards points collected from the results of inserting plastic bottle garbage into the ATM Trash with a number of rice.

The output target of this activity is a gamification system, with certain development called BeHappyOur, which is expected to change the community paradigm in processing household waste, especially plastic bottles. This system will regulate plastic bottle collection activities by residents until the residents get basic food from the results of the collection of plastic bottles.

3. Implementation Methodology

Science and technology transfers carried out at each stage using the principle that every innovation that will be accepted should go through a process: Hearing, Knowing, Trying, Evaluating, Receiving, Believing, Implementing, Socializing. Through the entire process, it is hoped that innovation can be accepted by the community because the parties who convey the innovation are the government for the community. Submission of innovation to research partners is taken through stages of explanation, discussion, practice of using tools with assistance.

In general, the process of approaching the acquisition of knowledge to research Partners to run the BeHappyOur system is presented in the framework of the problem approach as follows.

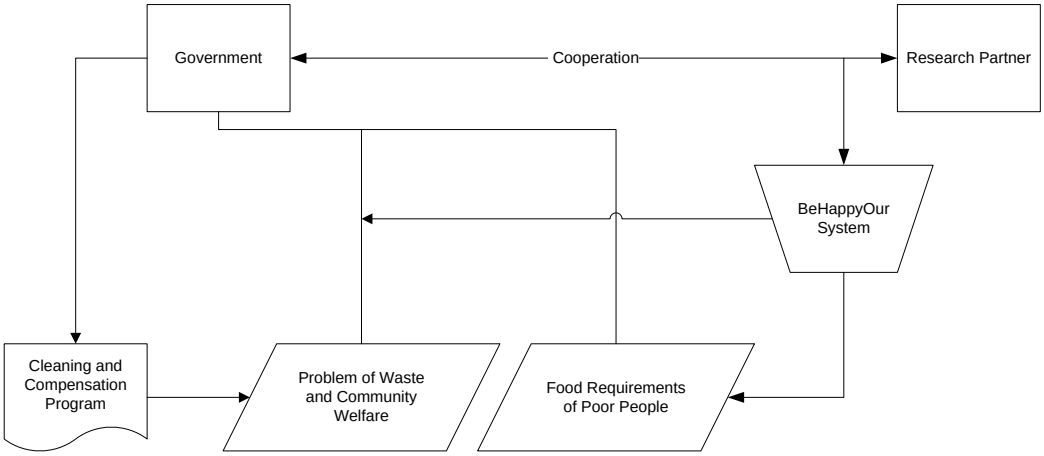

Fig. 2: Framework for Approach Problems

Based on Fig. 2. above, the government has 2 (two) main problems, namely the problem of waste and community welfare, and the food needs of the poor. To overcome the problems they have, the government implements a hygiene and compensation program for the poor. However, this is still not helpful, especially for compensation, because the program is implemented only at certain times. For the problem of food needs of the needy people who are needed daily, collaboration with research partners is carried out to supply rice, and through the BeHappyOur system, people who are less able can make a little effort to collect plastic bottle waste to be exchanged for rice through ATM machines / machines Rubbish. Thus, it is expected that the BeHappyOur system can be an alternative solution to overcome problems that are owned by the government.

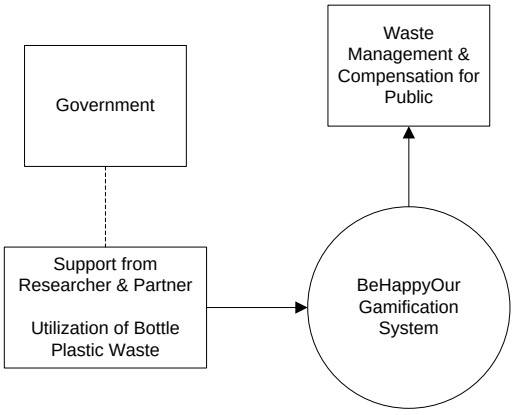

Fig. 3: Science and Technology Approach

Based on Fig. 3, above, government has been supported by researcher and partner for make some regulation about utilization of bottle plastic waste through BeHappyOur System. BeHappyOur is developed gamification system made by researcher to reduce bottle plastic waste problem in Bandung. It used game method to give some rewards to people that could manage their bottle plastic waste.

4. Conclusion

Through this research, residents can make plastic bottle waste as a source of additional sustenance, because they can exchange plastic bottles of garbage with a certain amount into a number of rice by inserting the bottle into a garbage machine / ATM device that has been provided. Waste plastic bottles that are inserted will be directly processed (pressed) by the garbage machine / ATM machine, and the processed products can be utilized by plastic bottle garbage collectors. And through the system, it is expected that the amount of plastic bottle waste can be reduced.

On the basis of existing waste problems, the solutions proposed are:

1. Implementation of the BeHappyOur system through Garbage Machine (ATM Sampah) to make the processing of plastic bottles waste interactive.
   a. This needs to be done to attract residents to sort out their household waste.
   b. Unlike the Waste Bank, the transaction process for calculating balances on garbage ATMs is done digitally.
2. Implement the gamification system on the Garbage Machine (ATM Sampah).
   a. Residents will collect points obtained when plastic bottle waste is inserted into the ATM machine.
   b. Residents can exchange a number of points with basic food provided by the government through research partners.
3. The garbage ATM system is made integrated with each other.
   This needs to be done so that the monitoring process can be carried out centrally by the government.

5. References

E. Yourdon, Modern Structured Analysis, New Jersey: Prentice Hall, 1989

Thomas Connolly, Carolyn Begg, DataBase System, “A Practical Approach to Design, Implementation, and Management”, Addision Wesley,Fourth Edition, England, 2010

RPJMD (Rencana Pembangunan Jangka Menengah Daerah Kota Bandung) 2014-2018

Proceedings of the 1st Faculty of Industrial Technology International Congress
International Conference
Bandung, Indonesia, October 9-11, 2017
ISBN 978-602-53531-8-5

Decision Support System for Bank Credit Application using Simple Additive Weighting Method

Budiraharjo[1,*], Mira Musrini[1], and Willy Edya Sukma[2]

[1] Department of informatics, Institut Teknologi Nasional (Itenas), Bandung - INDONESIA

[2] Student Department of informatics, Institut Teknologi Nasional (Itenas), Bandung - INDONESIA

[*] Corresponding author e-mail: budiraharjo@itenas.ac.id

Abstract

Decision Support System (DSS), in general, is a system that helps the decision-making process. In most applications, DSS is used to help managers in making business decisions, to improve data processing, to speed up business process, and to improve the quality and the service of banking credit approval. This paper discusses the process of building a DSS for banking credit approval using Simple Additive Weighting (SAW). SAW, which is one of the Multi-Attribute Decision Making methods, is a multicriteria decision-making technique which emphasizes the relative importance of the corresponding criterion to generate debtor's eligibility ranks to be used as the bases for banking credit grants. This study was conducted at Bank Perkreditan Rakyat Syariah (BPRS) Al-Salaam in Bandung.

Keywords: Decision Support System, Simple Additive Weighting, multicriteria decision-making, banking credit grant, eligibility rank.

1. Introduction

Banking institutions offer many monetary services; credit is one of those services. Credit is a monetary equivalent of a money or bill, subject to an agreement or an interbank borrowing and lending agreement with another party requiring the borrowing party to repay its debt after a certain period of time and with a predetermined interest amount. For the convenience of credit activities between the bank and the customer, the bank needs to assess and determine the prospective customer before coming to the decision to grant or decline credit request, this is due to the high risk of bad credits. A customer, in simpler words, should meet the criteria required by the bank before credit is granted. This situation requires banks to be able to take careful decisions in a short time considering the increasingly competitive banking business environment.

BPR Syariah (Sharia Rural Bank) is one type of banking institutions that concentrates its business in giving credits in accordance with Islamic Sharia Law. However, despite their specialization on giving banking credits, most BPR Syariahs have not utilized DSS for credit approvals. Usually approvals were made manually.

Decision Support System (DSS) is part of computer-based information systems including knowledge-based systems or knowledge management used to support decision making within an organization or company. It can also be considered as a computer system that processes data into information to take decisions from a semi-structured problem that is specific.

The problem formulation in this research is how to apply Simple Additive Weighting (SAW) method in Decision Support System in determining the rank and eligibility of prospective customers who apply for credit. The scope of this research is the criteria and the weight of criteria used by the bank. The expected results obtain from this calculation is feasibility rate of each debtor or credit applicant. The granted applicants are the ones who have the highest scores resulting from SAW calculations through a web-based application that was built as a part of this research.

The aim of this research is to build a Decision Support System application for ranking credit applicants using Simple Additive Weighting (SAW) method, while the expected outcome is an application that is capable of making quality decision in determining applicants to be granted bank credit.

2. Methodology

2.1. Decision Support System

A Decision Support System (DSS) is a computer-based information system that supports business or organizational decision-making activities. DSS helps people make decisions about problems that may be rapidly changing and not easily specified in advance. A DSS can be either fully computerized, human-powered or a combination of both. The support given by DSS can be separated into three distinct, interrelated categories: Personal Support, Group Support, and Organizational Support (Turban et. al., 2008).

The framework of Decision Support System consists of four phases:

- **Intelligence Phase**
  This first phase of the framework deals with the searching for conditions that call for decision.
- **Design Phase**
  This phase is the second step, which mostly the phase of developing and analyzing possible alternative actions of solution.
- **Choice Phase**
  In this third step, the commonly taken action is to select a course of action among those alternatives resulted in from the Design Phase.
- **Implementation Phase**
  And the final phase is to adopt the selected course of action in decision situation.

The utilization scheme of DSS in credit application process to be developed within BPR Syariah Al-Salaam Bandung's business process context can be seen as follow.

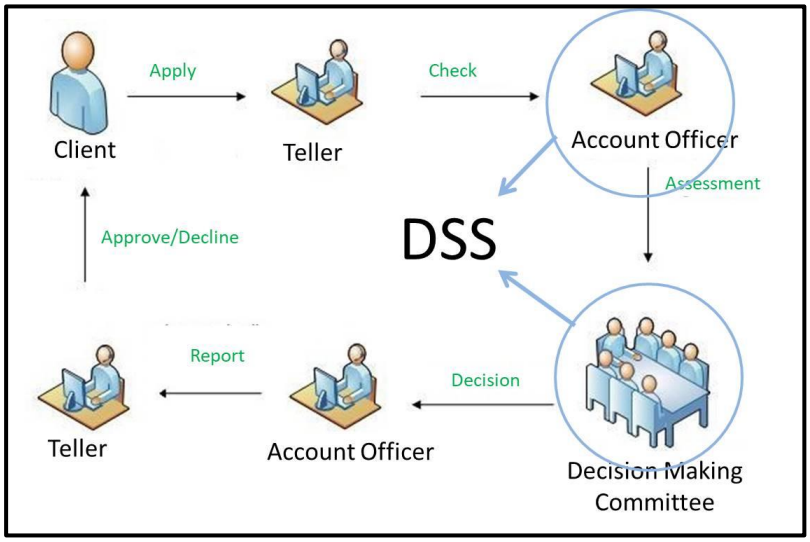

Fig. 1: DSS utilization scheme in BPR Syariah Al-Salaam's business process

2.2. Simple Additive Weighting (SAW) Method

Simple Additive Weighting Method (SAW), which is also known as weighted linear combination or scoring method, is the most popular and commonly used method of Multi Criteria Decision Making (MCDM) methods for evaluating a number of alternatives in terms of a number of decision criteria. The method is based on the weighted average. The advantage of this method is that it is a proportional linear transformation of the raw data.

The logic of the Simple Additive Weighting is to obtain a weighted sum of performance ratings of each alternative over all attributes (Roberson and Perry, 2007). The procedure is as follows:

1) Construct the criteria matrix.
2) Construct the normalized criteria matrix.
3) Weigh the normalized criteria matrix.
4) Rank the alternatives
5) Select the best alternative.

Normalization is an imperative step in Simple Additive Weighting method. There are two scenarios when normalizing criteria matrix.

The first scenario is the criteria of benefit. These criteria mean the higher numbers resulting from the normalization, the more desirable. The calculation for criteria of benefit is using the following equation.

$$r_{ij} = \frac{d_{ij}}{d_{ij}^{max}} \quad (1)$$

The second scenario is the criteria of cost. These criteria mean exactly the opposite of the criteria of benefit, i.e. the lower numbers resulting from the normalization, the more desirable. And, the normalization for criteria of cost is using equation as follows.

$$r_{ij} = \frac{d_{ij}^{min}}{d_{ij}} \quad (2)$$

where

r_{ij} : Normalized performance score

d_{ij} : Attibute score of each criterion

Max d_{ij} : Maximum score of each criterion

Min d_{ij} : Minimum score of each criterion

3. SAW Decision Making Simulation: BPR Syariah Case Study

Eligibility rank for credit approval in BPR Syariah in this phase of the process was then simulated using Simple Additive Weighting. This simulation used actual customers' data and information, and implemented the SAW procedure as discussed in the previous section.

3.1. Step 1: Construct the criteria matrix

In this phase, each criterion and its weight were determined. The criteria and their weight shown in the table below were pre-determined by BPR Syariah using its standard calculation.

Table 1: Pre-determined Criteria Matrix of BPR Syariah

C(i)	Criteria	Weight
C1	Occupation	**20%**
C2	Earnings	**25%**
C3	Collateral Value	**25%**
C4	Dependents	**10%**
C5	Home Ownership Status	**20%**

Next, a score matrix for each criterion was developed. The matrix is as seen below.

Table 2: Score Matrix guidance for each criterion

C(i)	Criteria	Score			
		1	2	3	4
C1	Occupation	Farmer/ Breeder	Private Sector Worker	Entrepreneur	State Owned Sector (BUMN) Worker
C2	Earnings	< 1,5 Million	1,5 to 3 Million	3 to 5 Million	> 5 Million
C3	Collateral Value	125 - 150 % from loan	151 - 175 % from loan	176 - 200 % from loan	> 200 % from loan
C4	Dependents	≥10	7 - 9	4 - 6	≤ 3
C5	Home Ownership Status	Rented	Mortgage	Family owned	Own house

Below is the simulation of criteria profiling using actual BPR Syariah clients' data and information.
/

Table 3: Criteria simulation using actual data samples

Alternatives (Client)		Criteria				
		Occupation	Earnings	Collateral Value	Dependents	Home Ownership Status
1	Ade Rohaya	State Worker	3 Million	180%	4	Own House
2	Devi Mulyani	Private Sector Worker	1,5 Million	125%	2	Rented
3	Dhamar Gunawan	State Worker	4 Million	175%	5	Mortgage

The next step was weighting the data from the table above using the score matrix. The result is as seen below.

Table 4: Score Matrix simulation result

Alternatives	Criteria				
	C1	C2	C3	C4	C5
A1	4	3	3	3	4
A2	2	1	1	4	1
A3	4	3	2	3	2

3.2. Step 2: Construct the normalized criteria matrix

The result from weighting each criterion in Table 4 above was then normalized using Criteria of Benefit equation. All criteria after conversion to the score matrix are benefit attributes. The Criteria of Benefit selection was due to higher scores as preference. For example, the maximum value for C1 is 4, r11 = 4/4, r21 = 2/4, and r31 = 4/4. And the result is as seen bellow.

Table 5: Normalized Criteria Matrix scores

Alternatives	Criteria				
	C1	C2	C3	C4	C5
A1	1	1	1	0.75	1
A2	0.5	0.33	0.33	1	0.25
A3	1	1	0.67	0.75	0.5

3.3. Step 3: Weigh the normalized criteria matrix

The normalized criteria matrix was then weighted using a equation as follows.

$$v_{ij} = W_{ij} * r_{ij}, \sum_{i=1}^{n} W_i = 1 \quad (3)$$

where

V_i : The score of alternatives

W_{ij} : Weigh

R_{ij} : Normalized matrix

The weighted results are as seen below.

A1= (0.2*1) + (0.25*1) + (0.25*1) + (0.1*0.75) + (0.2*1) = 0.98
A2= (0.2*0.5) + (0.25*0.33) + (0.25*0.33) + (0.1*1) + (0.2*0.25) = 0.42
A3= (0.2*1) + (0.25*1) + (0.25*0.67) + (0.1*0.75) + (0.2*0.5) = 0.79

3.4. Step 4: Rank the alternatives

The weighted scores as results from previous processes were then rank using the following equation.

$$S_i = \sum_{j=1}^{m} v_{ij}, i = 1,2,3,\ldots,n \quad (4)$$

where

S_i : Rank

V_{ij} : The score of each alternative

And the result is as follows.

Table 6: Credit applicants ranking simulation

Alternative	Client	Weighted Score	Rank
A1	Ade Rohaya	0.98	1
A3	Dhamar Gunawan	0.79	2
A2	Devi Mulyani	0.42	3

3.5. Step 5: Select the best alternatives

As depicted from Table 6 above, the applicant who has the highest score is Ade Rohaya. In the Criteria of Benefit, higher scores are more preferable that Ade Rohaya is ranked the highest, thus eligible to get credit approval

4. BPR Syariah's Decision Support System Design and Implementation

The projected BPR Syariah's Decision Support System was modeled using a simple use case diagram as seen below.

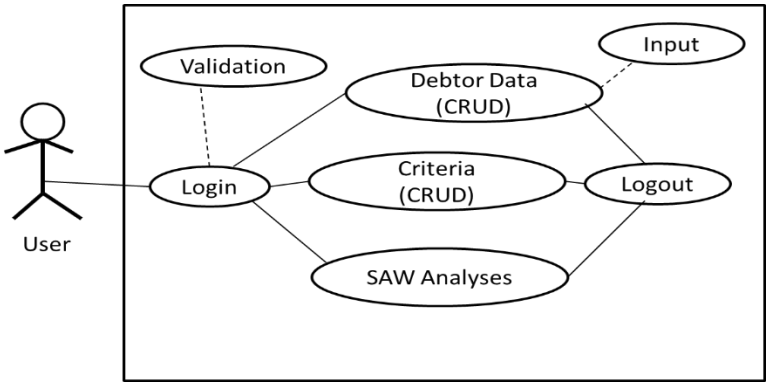

Fig. 2: BPR Syariah DSS Use Case Diagram

An implementation from the design phase was then carried out, and the most essential features from the developed DSS are as captured as follow.

Fig. 3: Login screen

Fig. 4: Home screen

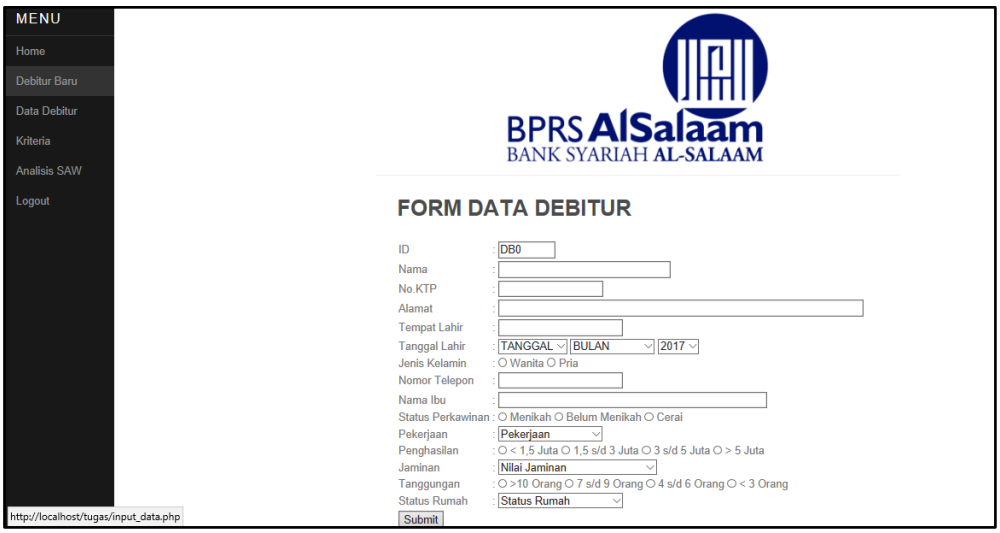

Fig. 5: Debtor application form screen

Fig. 6: SAW analyses screen

5. Conclusions

Simple Additive Weighting method (SAW), one of the most popular and widely used methods of Multi Criteria Decision Making (MCDM), has been successfully applied and simulated in the process of generating credit applicants eligibility ranks. As a follow up, a Decision Support System (DSS) was then developed incorporating the simulated SAW method to improve the business process of BPR Syariah Al-Salaam Bandung in giving its services.

6. References

Adriyendi. 2015. Multi-Attribute Decision Making Using Simple Additive Weighting and Weighted Product in Food Choice. International Journal of Information Engineering and Electronic Business, Vol. 6, pp. 8-14.

C. Ruan, and J. Yang. 2015. Hesitant Fuzzy Multi-Attribute Decision-Making Method Considering the Credibility. Journal of Computational Information Systems, Vol. 11, pp. 423-432.

Edya Sukma, Willy. 2017. Pembangunan Sistem Pendukung Keputusan Pengajuan Kredit Dengan Metode Simple Additive Weighting (SAW) (Studi Kasus : BPR Syariah). Bandung, Tugas Akhir Jurusan Teknik Informatika.

Efraim Turban; Jay E. Aronson; Ting-Peng Liang. 2008. Decision Support Systems and Intelligent Systems. New Jersey: US, Prentice Hall, Inc.

F. Burstein; C. W. Holsapple. 2008. Handbook on Decision Support Systems. Berlin: Springer Verlag.

Gachet, A. 2004. Building Model-Driven Decision Support Systems with Dicodess. Zurich, VDF.

K. S. S. Anupama, S. S. Gowri, B. P. Rao, and P. Rajesh. 2015. Application of MADM Algorithms to Network Selection. International Journal of Innovative Research in Electrical, Electronics, Instrumentation and Control Engineering, Vol. 3, Issue 6, pp. 64-67.

Kulik, C., L. Roberson and E. Perry. 2007. The Multiple-Category Problem: Category Activation and Inhibition in the Hiring Process. Acad. Manage. Rev., Vol. 32 No. 2, pp. 529-48.

L. Abdullah and C.W. R. Adawiyah. 2014. Simple Additive Weighting Methods of Multi Criteria Decision Making and Applications: A Decade Review. International Journal of Information Processing and Management, Vol. 5, No. 1, pp. 39-49.

Triantaphyllou, E. 2000. Multi-Criteria Decision Making: A Comparative Study. Dordrecht, The Netherlands: Springer.

ISBN 978-602-53531-8-5

E. * Reliability of renewable energy system; Environmental Technologies

Proceedings of the 1st Faculty of Industrial Technology International Congress
International Conference
Bandung, Indonesia, October 9-11, 2017
ISBN 978-602-53531-8-5

Reliability Analysis to Determine Mean Time between Failures (MTBF) on Machinery

Nuha Desi Anggraeni
Department of Mechanical Engineering, Institut Teknologi Nasional (Itenas), Bandung - INDONESIA
Corresponding author e-mail: nuhadesi@gmail.com

Abstract

Machinery maintenance is an activity system for maintaining, developing and maximizing all machinery facilities. To prevent damage and failure on machinery, time-based maintenance techniques are planned actions are used, but this maintenance are not effective enough to prevent failure. Thus, it is necessary to analyze machinery reliability to determine mean time between failures (MTBF). Using this method, maintenance can be done before machinery break down, which can reduce maintenance cost. This method can be perform using simple statistic as Weibull distribution, because this distribution can be used for various models of failure. Using component failures data collected at a mill, such as: explosive; broken throat-ring; lower-gate jam; plate wear; start fail; and leakage, using Weibull distribution, the result show that value of MTBF obtained from each failure as follows: broken throat-ring at 84636 hours; lower-gate jammed at 1104 hours; plate wear at 4378 hours; machine start fail at 2685 hours; and leakage at 40456 hours. Using calculation results above, maintenance should be conduct before MTBF time to keep machine work properly.

Keywords: machinery, maintenance, essential, failure, statistics

1. Introduction

In an industry, maintenance department plays an important role to support production process smoothness. Machinery maintenance is defined as the work needed to keep a machine in good condition. Maintenance can be identified into five general philosophy: a) corrective maintenance; b) preventive maintenance; c) predictive maintenance; d) zero-hours maintenance; and e) periodic maintenance. Every maintenance has the disadvantages of that each equipment needs a mix of each of these maintenance types, we cannot apply one types of maintenance to particular machinery (Bliskhe, 2000, Bossche, 1993).

Preventive maintenance mission is to maintain a level of certain service on equipment, programming the intervention of their vulnerabilities in the most opportune time. Preventive maintenance activity including partial or complete equipment inspection, overhauls of certain periods, oil change, lubrication and so on. By this method, worker can record equipment damage so that it can be known when equipment turnover or repair worn equipment before causing system failure (Narayan, 2004). It is designed to maintain and improved equipment reliability by replacing aging components before they actually fail.

Charles E. Ebeling said that, "*Reliability is defined to be the probability that component or system will perform required function for a given period of time when use understate operating condition*". Reliability is theoretically defined as the probability of success; as the frequency of failures. In this case, we can calculate reliability by using failures data obtained in the field. This data recorded every equipment failure, starting from the first time equipment is operated. Data failures hold an important role in reliability calculation.

2. Methods

A first approach would be to determine equipment criticality. Among the principal analytical tools available we find (Bloch, 1933):

- Cause-and-effect diagram
- Reliability estimating and predicting
- Failure mode and effect analysis (FMEA)
- Availability analysis

- Fault tree analysis
- Hazard analysis
- Field investigation
- Detailed design review

To support reliability-based maintenance system, it is necessary performed an analysis to determine appropriate inspection interval time. Time table mill inspection shown on fig. 1.

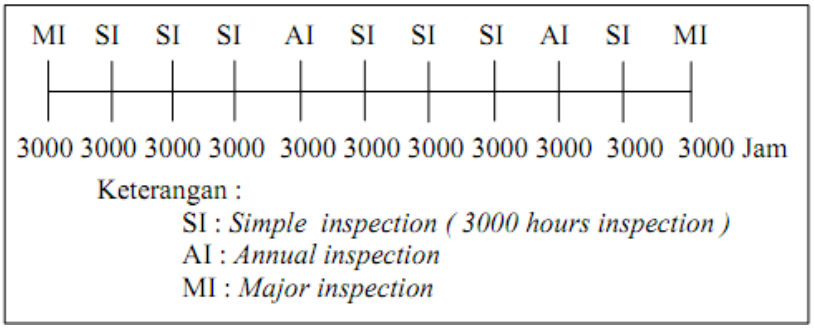

Fig. 1: Time table inspection

Mill block diagram on fig. 2 used to define the system equipment. From this diagram, essentials part of the equipment can be known and analyzed. As an example, a mill failures data describe as follows: explosive; broken throat-ring; lower-gate jam; plate wear; start fail; and leakage.

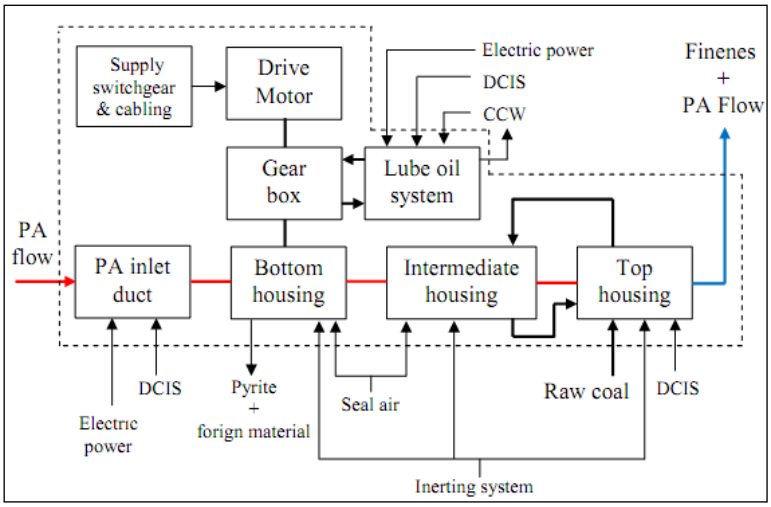

Fig. 2: Mill Block Diagram (Zulfadhli, 2010)

This failure data is analyze using Weibull distribution:

$$R(t) = \left[-\int_0^t \exp \frac{\beta}{\alpha} \left(\frac{t'}{\alpha}\right)^{\beta-1} dt' \right] = e^{-\left(\frac{t}{\alpha}\right)^{\beta}} \quad (1)$$

R (t) used to calculate reilability, with β called shape parameter which provide deep knowledge of failure proccesses behaviour. And α called scale parameter, that affect mean distribution. Weibull shape parameter explained on table 1.

Table 1: Weibull shape parameter

Value	Property
$0 < \beta < 1$	Decreasing Failure Rate (DFR)
$\beta = 1$	Constant Failure Rate (CFR), exponential distribution
$1 < \beta < 2$	Increasing Failure Rate (IFR), concave
$\beta = 2$	Rayleigh distribution (IFR)

$\beta > 2$	Increasing Failure Rate (IFR), convex
$3 \leq \beta \leq 4$	Increasing Failure Rate (IFR), approaches normal distribution, symmetrical

Failure data example show on table 2, this data only to show how to calculate the reliability.

Table 2: Leakage failure data

No	Hours fail
1	17520
2	17880
3	20496
4	22680
5	24792

Using Weibull distribution, statistic parameter of the failure show on table 3. This parameter help us to determine failure processes behavior as mention on table 1.

Table 3: Statistic parameter for failure

Failure types	Weibull Distribution			
	Shape parameter	Scale parameter	Mean	Deviation
Broken throat-ring	6.07	87497.30	81226.90	15566.10
Lower-gate jam	1.04	1577.11	1552.89	1494.67
Plate wear	6.46	4624.17	4307.44	779.15
Start fail	0.99	3836.54	3854.97	3898.36
Leakage	2.12	47639.30	42192.00	20969.50

From statistic parameter on table 3, we can calculate reliability cycles for fail component using equation 1. Reliability cycle for fail component show on table 4.

Table 4: Reliability cycles component

Failure types	Reliability Cycles (hours)				
	0.01	0.1	0.5	0.9	0.99
Broken throat-ring	117894	104426	84636	60865	40342
Lower-gate jam	8999	4175	1104	137	10
Plate wear	6005	5349	4378	3197	2160
Start fail	21257	9969	2675	343	26
Leakage	110795	76625	40456	14850	4254

3. Discussion

Normally, a system consists of a number of functional block diagrams so that the system can perform its function. Major components of the system need to be known so the system properly function. The components can be found through an analysis when and what makes the system fail. Before using reliability analysis, we must perform FMEA (Failure Mode Effects Analysis) methods to find major components and essential machine from the system. Its turn out that the mill is essential machine from the system, using qualitative analysis on existing data consider a complete data even though data are incomplete. Complete data used to calculate reliability from the system. If qualitative reliability considered incomplete, failure analysis necessary to be done on the system.

By conducting reliability analysis using Weibull distribution, for each failure, correlation coefficient value above 0.8. This indicate all failure data can be processed using Weibull distribution and instrument used on this research is valid and reliable.

From table 3, statistic parameter for failure show that on the component of failure there is an increase and decrease failure rate depends on time. It's also can be explained using bath tub curve below. By looking at the relationship between table 1, table 2 and fig. 2; it is defined that fail start consider as early failure (infant mortality) because shape parameter value between 0 and 1 was the property of (Decreasing Failure Rate) DFR (Ebeling, 1997). Lower-gate jam defined as Increasing Failure Rate (IFR) or wear out failure because value of the shape parameter is between 1 and 2. Another component failure defined as aging process because the shape parameter value above 2.

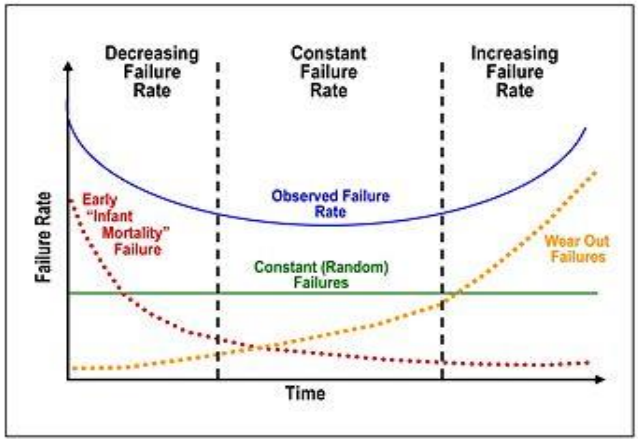

Fig. 3: Bath tub curve

Inspection time interval for maintenance can be explained on table 4. If inspection duration time is close, reliability value or success opportunities close to 100%. This mean that the system will not fail because before it becomes fail, we can prevent it. But, if the duration is to close, maintenance cost will become higher. At value 0.5, reliability can be said well, because it is average from highest and lowest value.

Fig. 4 shows that throat ring data suitable to be processed using Weibull distribution because correlation coefficient value greater than 0.8 (0.949), so the instrument used can be said valid and reliable. Shape parameter value, 6.07, indicates an increase failure rate over time, this happens when there is an aging process, or a section that tends to fail over time. If it refers to the theory, then a good value of reliability is if the value is> 0.7, when used the value of reliability of 0.5, then the mean time between failure MTBF) is 84636.5 hours.

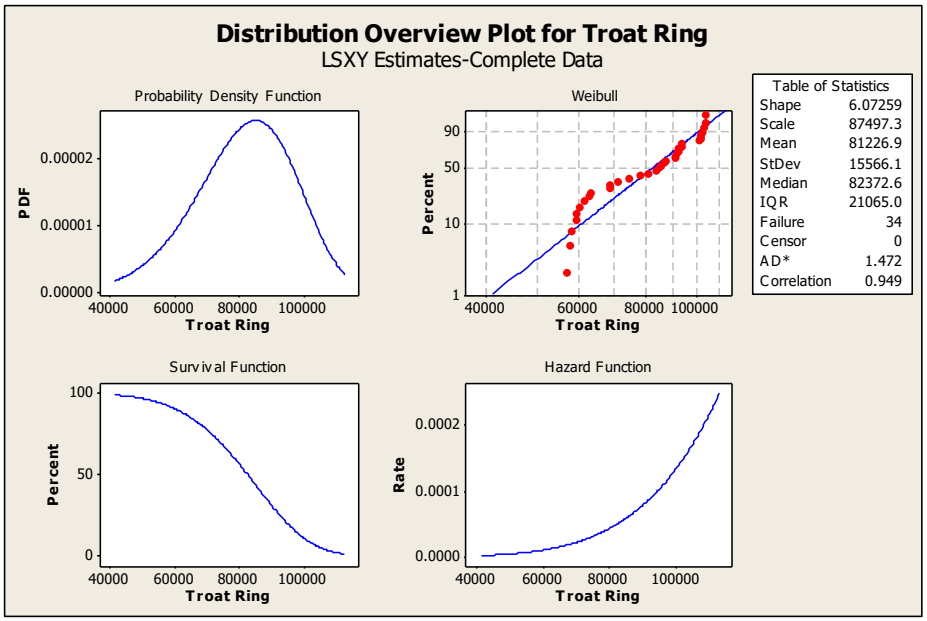

Fig. 4: Weibull distribution for throat ring

4. Conclusion

After performing reliability analysis to determine Mean Time between Failure (MTBF), it can be concluded that:

1. Reliability analysis can be done after machinery reliability assessment effort to understand effort will be used for the analysis.
2. In determining reliability, machine system has to be divided into several level, so if damage or failure occurs, source of failure can be find easily.
3. Best inspection time should be done when reliability cycles value close to 100%, this mean that the system is AGAN (As Good As New).
4. On this research reliability value 0.5 is used, because at this value failure can be prevent using correct maintenance.
5. Time inspection should be adjusted to MTBF value to prevent machinery failure.
6. The result show that value of MTBF obtained from each failure as follows: broken throat-ring at 84636 hours; lower-gate jammed at 1104 hours; plate wear at 4378 hours; machine start fail at 2685 hours; and leakage at 40456 hours.

5. References

Bloch and Geitner, 1933. An Introduction to Machinery Reliability Assessment. New York: Van Nostrand Reinhold.

Ebeling, Charles E, 1997. An Introduction to Reliability and Maintainability Engineering. McGraw-Hill International Edition.

Zulfadhli, 2010. Implementation Study of Reliability Centered Maintenance. Institut Teknologi Bandung.

Blischke, W. R., Murthy, D. N. P., 2000. Reliability Modelling, Prediction, and Optimization. John Wiley & Sons.

Bossche, A., Sherwin, D. J., 1993. The Reliability, Availability and Productiveness of System. Chapman & Hall.

Narayan, V., 2004. Effective Maintenance Management. Industrial Press

Proceedings of the 1st Faculty of Industrial Technology International Congress
International Conference
Bandung, Indonesia, October 9-11, 2017
ISBN 978-602-53531-8-5

Investigation of Land Cover Classification in Oil Palm Area Based on ALOS PALSAR 2 Image

Endyana Amin* and Soni Darmawan
Department of Geodesy Engineering, Institut Teknologi Nasional (Itenas), Bandung - INDONESIA
* Corresponding author e-mail: endyanaamin94@gmail.com

Abstract

Oil Palm is one of the most productive oil seeds in Indonesia. At present, Indonesia is the largest producer and exporter of oil palm worldwide. In general, oil palm production will be related to the age of the plant. The development of plant age will undergo physical changes in biomass and canopy density, so to identify the growth of planting age of oil palm can be used satellite image analysis from remote sensing. The objective on this study are examining techniques of image classification ALOS PALSAR 2 for land cover mapping of oil palm area. Study areas in oil palm plantations areas of Simpang Empat sub-district, Asahan Regency, North Sumatera. Methodology consisted of data collection of image ALOS PALSAR 2 and data of age of oil palm planting, the processing includes geometric correction, filtering, image cropping, making training sample using region of interest (ROI) tools, band combination, image classification for several methods like minimum distance, mahalanobis distance, maximum likelihood, and support vector machine, and then using confusion matrix for accuracy assessment. The results from this study are ALOS PALSAR 2 image classified with overall accuracy of 85.21% and coefficient kappa 0.6763 with RGB band combinations for support vector machine method as the most effective method for this research.

Keywords: remote sensing, radar image, classification, L-band, spatial distributin of age of oil palm.

1. Introduction

Oil palm is one of the most productive oil seeds and a very important commodity in agriculture in Indonesia. The production of oil palm is dominated by Indonesia and Malaysia which can produce about 85 to 90% of the world's total oil palm production. Recently, Indonesia is the largest producer and exporter of oil palm worldwide (Indonesia Investment, 2016).

Since the 1990s, oil palm plantations in expansion in the humid tropics and land under oil palm increased to 12.6 million hectares in 2010 with annual oil palm production exceeding 32 million tonnes indicating global demand for oil palm will be around 62 to 63 million tonnes by 2015 (Darmawan et al., 2016). In a long time, the world demand for oil palm shows an increasing trend with the rapidly expanding world population. Therefore, it will increase consumption of products with raw materials of oil palm (Indonesia Investment, 2016). In addition, this oil palm has many benefits for human life processed into cooking oil raw materials, butter raw materials, toothpaste raw materials, raw materials for paint, etc. (Kelapa sawit, http: //kelapasawit.ptnasa. Net / benefits-palm-palm/).

In general, oil palm production will be related to the age of the plant. Oil palm have a regular cropping pattern, because it is planted in blocks according to the year of planting. The development of plant life will undergo physical changes of biomass and canopy density, so for the provision of growth of planting age with oil palm can be done by using satellite image analysis from remote sensing data (Aswandi, 2012). Remote sensing data has been shown to play an important role in monitoring and mapping that can be used on land usage, land cover, and plantation areas (Darmawan et al., 2016).

The use of the satellite ALOS PALSAR 2 in this study because the radar image data has energy derived from the satellite itself, without the need for energy from the sun and is suitable for tropical regions such as in Indonesia. Study areas in oil palm plantations areas of of Simpang Empat sub-district, Asahan Regency, North Sumatera.

2. Methodology

The methodology consisted of data collection of ALOS PALSAR 2 and age data of oil palm, data processing including geometric correction, filtering, cropping image, making training sample using region of interest (ROI) tools, band combination, image classification by using the minimum distance method, mahalanobis distance, maximum lilkelihood, and support vector machine, to accuracy assessment using confusion matrix. In general, the methodology in this study can be seen in Figure 1.

Fig. 1: Methodology on this study

2.1. Data Collection

The data collected is include the image of ALOS PALSAR 2 Level 1.5 with 6.25 m resolution as the primary data consisting of two polarization of HH and HV. Image data acquisition on June 1 2015 obtained from Lembaga Penerbangan dan Antariksa Nasional (LAPAN) for Asahan District, North Sumatera Province. Meanwhile, data on the age of oil palm plantation in Simpang Empat sub-district, Asahan regency, North Sumatera province as secondary data calculated until 2016 also obtained from LAPAN.

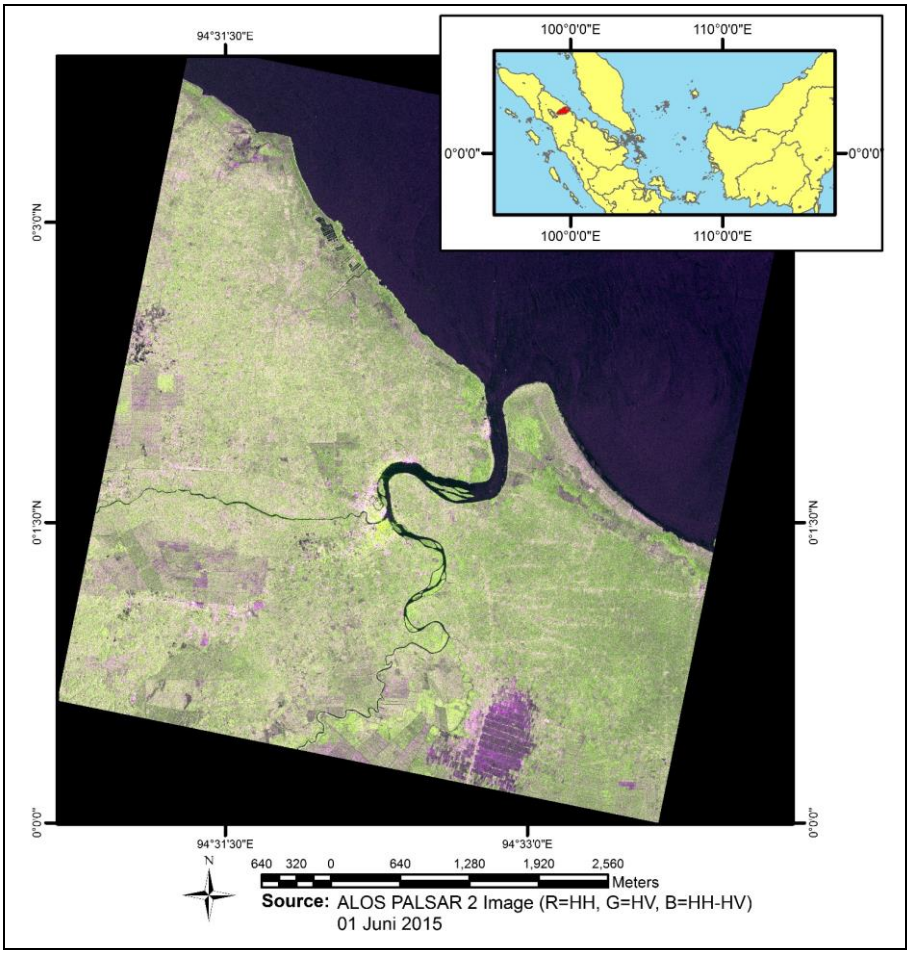

Fig. 2: Data used on study areas

2.2. Preprocessing

The image data of ALOS PALSAR 2 obtained by preprocessing for geometric correction of image, editing data of age of oil palm plant, filtering image, and cropping. After that, the process of digital image processing for making training sample to make a classification of land cover area of oil palm plantation and then accuracy assessment to determine the most effective image classification method.

- Geometric Corrections

ALOS PALSAR image 2 Level 1.5 has georeferenced that has a multi-look view and regardless of noise. In this study, checking and controlling the quality of objects in the image by making the points of Independent Control Point (ICP) as much as 15 points spread in the study area with reference used to Google Earth. The parameters used are the root mean square error (RMSE) value, if the RMSE value from the distribution of ICP points below from 1 pixel is then the result of the geometric correction of the image with the image to map method is assumed to have geometric correction systematically (Purwadhi, 2001 in Kartikasari and Sukojo, 2015).

- Editing Data of Age of Oil Palm

Editing data of age of oil palm because the data that gives information on the age of oil palm plant has a position not in accordance with the actual position, then the editing process needs to be done so that the age data of the palm oil plant is in the actual location. By improving the data position of the age of oil palm plantation, it can assist the process of image interpretation for the oil palm area.

- Filtering

The filtering process is to improve the quality of the image display and is designed to 'filter' the spectral information so as to produce a new image that has a different spectral value variation than the original image (Danoedoro, 2012). Filtering image which used in this study is the adaptive filters process, which uses filter weights that refer to the level of spots present in the image display, where the image smoothing is obtained based

on local statistical value in the filtering process (Tso and Mather 2001 in Ozdarici , 2010). Meanwhile, the type of adaptive filters used is a lee filter with size 5x5. Image filtering by lee filter type is chosen because it can be useful to smoothing the spots on the image data while maintaining the image sharpness while reducing the existing noise in the image display (Tso and Mather, 2009 in Wijaya, 2014).

- Cropping Image

Cropping is intended to make image processing for classification more effective, so the image is focused on study area which has block of age of oil palm plantation. Therefore, the study area studied is dominated by the distribution of oil palm crops.

2.3 Digital Image Processing

Digital image processing focuses on making training sample using region of interest (ROI) tools and selection of classification methods to determine an effective classification method for mapping land cover of oil palm plantation area. Meanwhile, for the band combinations, using two different combinations of HH + HV bands for the first combination and RGB band combinations consist of (R = HH, G = HV, B = HH-HV).

Region of Interest (ROI)

On this study, training sample is making by using ROI tools. This ROI tool using to create land cover classes consisting of oil palm, non-oil palm vegetation (rice fields, fields, plantations, etc.), settlements, and waters that will be used for image classification. Based on the interpretation of the image, this study area is dominated by the objects of oil palm plantation. Therefore, making training of sample are focused on samples of oil palm objects. The number of training samples can be seen in Table 1.

Table 1: Number of Training Sample

Land Cover Classes	Number of Training Sample
Oil Palm	102
Non-oil palm Vegetation	30
Settlements	30
Waters	10

- Image Classification and Accuracy Assessment

Image classification in this study using four methods, which is minimum distance, mahalanobis distance, maximum likelihood, and support vector machine. This image classification making by two band combinations, the first is HH+ HV polarization, while the second is (R = HH, G = HV, B = HH-HV). After image classification, then accuracy assessment with using confusion matrix based on the result of image classification with sample data taken by using ROI tool.

3. Conclusion

The result of image classification from image processing that has been done is the result of classification of guided image consisting of four methods, including: minimum distance, mahalanobis distance, maximum likelihood, and support vector machine. Each method involves two band combinations of HH+ HV polarization and RGB consisting of (R = HH, G = HV, B = HH-HV). From the results of classification of guided imagery and then tested the accuracy to determine the most appropriate and effective classification method for mapping the oil palm area.

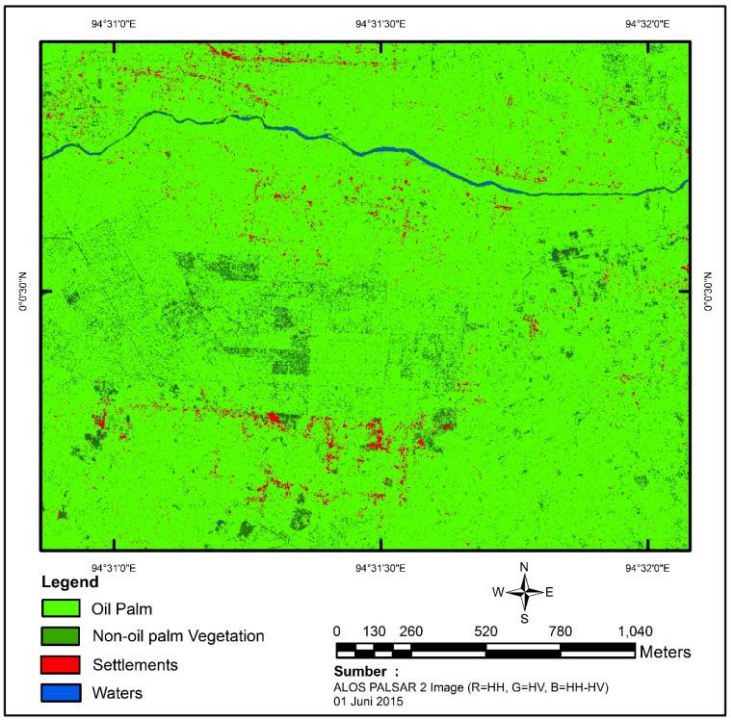

Fig. 3: Image classified using support vector machine methods (R = HH, G = HV, B = HH-HV)

After the image classification process is done for all the methods, it can be determined the most appropriate and effective classification method for mapping the oil palm plantation area based on the image of ALOS PALSAR 2 of Simpang Empat sub-district, Asahan Regency, North Sumatera Province. The parameters taken to determine the most appropriate and effective method are seen based on two main components of overall accuracy and kappa coefficient. The results of the accuracy assessment of each classification method can be seen in Table 2.

Table 2: Accuracy Assessment

Image Classification Method	Band Combinations			
	Band HH + Band HV		(R= HH, G= HV, B= HH-HV)	
	Overall Accuracy (%)	Kappa Coefficient	Overall Accuracy (%)	Kappa Coefficient
Minimum Distance	68.7686	0.4164	66.1085	0.3846
Mahalanobis Distance	73.1401	0.5004	74.6206	0.5249
Maximum Likelihood	74.5752	0.5308	77.0043	0.5682
Support Vector Machine	84.6867	0.6645	85.2112	0.6763

From that Table 2, it can be assessed that the support vector machine method is the most appropriate and effective method for mapping the oil palm plantation area based on ALOS PALSAR image 2. In addition, it can be analyzed that combination with RGB also shows that by adding band combinations, then also adds on the value of accuracy obtained. This result shows that three classification methods which is mahalanobis distance, maximum likelihood, and support vector machine produces a relatively higher accuracy when compared with band combinations that only use two polarization (HH and HV). The accuracy assessment on this study also shows that the image processing in this study is directly proportional to the research conducted by Nooni et al. (2014), which states that the support vector machine classification method is the right method for palm oil mapping and has more accuracy than the maximum likelihood method.

Based on the results of the research that has been done, it can be argued that the supervised classification for mapping of oil palm plantation land cover based on ALOS PALSAR 2 image with the Support Vector Machine (SVM) method is the most effective method among other supervised classification methods such as minimum distance, mahalanobis distance, and maximum likelihood. Using the combination of bands (R = HH, G = HV, B = HH-HV), the SVM method shsows an accuracy assesment of 85.21% and a kappa coefficient of 0.6763.

4. Acknowledgements

The authors would like to thanks to Lembaga Penerbangan dan Antariksa Nasional (LAPAN) for helping and supporting the authors to conduct this research.

5. References

Aswandi, Y. 2012. Pemanfaatan Citra Landsat 7 Untuk Estimasi Umur Tanaman Kelapa Sawit (Studi Kasus di PTPN VIII Cisalak Baru, Banten). Program Studi Manajemen Sumberdaya Lahan Institut Pertanian Bogor, Bogor.

Danoedoro, P. 2012. Pengantar Penginderaan Jauh Digital. Andi : Yogyakarta.

Darmawan, S., Takeuchi, W., Haryati, A., Najib A.M., R., and Na'aim, M. 2016. An Investigation of Age and Yield of Fresh Fruit Bunches of Oil Palm Based On ALOS PALSAR 2. University of Tokyo, Tokyo.

Indonesia Investments, Minyak Kelapa Sawit, https://indonesia investments.com/id/bisnis/komoditas/minyak-sawit/item166?

Kartikasari, A.D., and Sukojo, B.M. 2015. Analisis Persebaran Ekosistem Hutan Mangrove Menggunakan Citra Landsat-8 di Estuari Perancak Bali. Jurusan Teknik Geomatika ITS, ITS Sukolilo Surabaya.

Nooni, I.K., Duker, A.A., Duren, I.V., Wireko, L.A., and Oser Jnr, E.M. 2014. Support Vector Machine to Map Oil Palm in A Heterogeneous Environment. International Journal of Remote Sensing Vol. 35, No. 13, 4778–4794.

Ozdarici, A., and Z. Akyurek. 2010. A Comparison Of SAR Filtering Techniques On Agricultural Area Identification. Middle East Technical University, Ankara, Turkey.

PT NASA, Manfaat Kelapa Sawit, http://kelapasawit.ptnasa.net/manfaat-kelapa-sawit/

Shimada, M., Y. Kankaku, M. Watanabe, and T. Motooka. 2011. Current Status of the ALOS-2 / PALSAR-2 and the CALVAL Program. Japan Aerospace Exploration Agency (JAXA), Japan.

Wijaya. 2014. Identifikasi dan Estimasi Wilayah Interdial Menggunakan Citra Alos Palsar Data Pasang Surut dan Data DEM. Jurusan Teknik Geodesi, Universitas Gadjah Mada, Yogyakarta

ISBN 978-602-53531-8-5

F. Other topics

Proceedings of the 1st Faculty of Industrial Technology International Congress
International Conference
Bandung, Indonesia, October 9-11, 2017
ISBN 978-602-53531-8-5

Aero-hidroponic products for rural forest farming

Edi Setiadi Putra[1,*], Jamaludin[2,*]

[1] Department of Product Design, Institut Teknologi Nasional (Itenas), Bandung - INDONESIA

[2] Departement of Interior Design, Institut Teknologi Nasional (Itenas), Bandung - INDONESIA

[*] Corresponding author e-mail: jadsanaira@gmail.com ; mangjamal@gmail.com

Abstract

Today's rural farmers depend on private land, chemical fertilizers and high-cost irrigation. Farmers are less productive, because the land is getting narrower and prohibited to exploit the village forest that has become the source of village life. To improve farm productivity, agricultural systems are needed in accordance with the village environment. Through ethnographic and ergocultural studies of village farmers' behavior and rural farming patterns, as well as phenomenological studies of lifestyle changes, and the effects of modern agriculture within the village, the actual and factual description of the village situation and condition requires relevant agricultural work needs. Research on the revitalization of Tatanen Huma Sunda through aero-hydroponic science, has demonstrated the ability of aeroponic-hydroponic-aquaponic farming systems to meet the expectations of village farmers. The product design of aeroponic products for productive vegetable farming systems in forested areas (agribusiness in agroforestry) and hydro-aquaponic products for productive vegetable farming over fish ponds and home yards, is expected to be developed for village agricultural areas in Indonesia.

Keywords: ergocultural, aerohidroponic. Environment, Product Design

1. Introduction

Rural development in West Java is growing rapidly in all areas. In addition to strengthening in rural infrastructure, it also includes the attitude of the village community mentality in understanding the situation and environmental conditions.

Desa Cibeureum Kecamatan Sukamantri Kabupaten Ciamis Propinsi Jawa Barat, is one example of a village that is growing very rapidly. In agriculture, on 9 November 2006 Desa Cibeureum was declared by the Minister of Agriculture of the Republic of Indonesia as an agropolitan area marked by the inauguration of P4S (Karangsari Agricultural and Rural Training Center) as a center of agribusiness development and agroforestry activities. In the field of culture, one of Kecamatan Sukamantri special art of "bebegig" has won a parade contest at the international carnival in Rio De Jainero City of Brazil. In the social field, Desa Cibeureum has LMDH (Lembaga Desa Desa Hutan), which is very concerned about forest preservation around the village environment.

Wilderness in the village environment is essentially threatened by the development of agribusiness which requires a very wide homogeneous farmland. Some areas of deforested forest into vegetable business farmlands have a devastating impact on communities where water sources in the forests are contaminated with pesticides, resulting in widespread health disruption to villagers. In addition, the village area is also haunted by the possibility of erosion, landslide and earthquake. All villagers strongly believe in the natural balance of nature, so that if the ecosystem structure is disturbed or changed, nature will seek to reconstitute itself. The nature of the balance of nature is very influential in the life of the community in the area of forest-villages, causing high levels of public awareness in preserving this forest.

Desa Cibeureum farmers are eager to increase agricultural productivity without resorting to deforestation. Farmers need large farms to increase their productivity, but land owned generally narrows due to changes in the amount of land due to inheritance. In the village area, farmers can only work on small gardens in the yard of houses, fish ponds and rice fields in a limited area. Limited land and farm productivity demand is a common problem experienced by every smallholder farmer in forest village area. The principle of contemporary agriculture that is rampant in urban areas in various developed countries, is what is called urban farming, which is the way of modern farming by utilizing a narrow land in the yard as a hydroponic farm land that is considered very practical and productive. But the hydroponics system pioneered by the lovers of plants in several cities in Indonesia, was less developed in the general public, and tend to live only in the environment of the community of hydroponic lovers.

The principles and work systems of hydroponics, aeroponics and aquaponics introduced by urban farmers activists in various social media to Indonesian society, are basically well known to rural people, but because they are not derived from their cultural roots, village farmers are not enthusiastic about welcoming the new system. Attempts to introduce the concept of hydroponic, aeroponic and aquaponic farming in rural communities, are carried out with local cultural and policy approaches that are preserved. The principle of maintaining the ecosystem balance of forest villagers has a strong relevance to customary rules in the context of *mulasara buana* as well as the mandate of the Sundanese ancestors in preserving the natural environment.

2. Methodology

The research method used to understand the cultural roots of forest villagers is using ethnographic and phenomenological approaches. The study focuses on the philosophical and psychological aspects of their identity, so they have certain roles, functions and tasks that can be revealed, in terms of the environment in which they live. Based on geographical conditions, forest villagers residing in mountainous areas, derived from the pahuma community. Environmentally friendly people and nature lovers. The pahuma community is likely to accept the hydroponic, aquaponic, aeroponic and vertikultur farming systems that are environmentally friendly and in harmony with ecosystem situations and conditions in forests and mountains.

In analyzing the qualitative descriptive data, the effort of understanding through observation and the deepening of insight, through the process of ethnographic research methodology developed by Spradley (1985). In order to obtain comprehensive data which is a unified whole and integrated, used the method of description because the problem under study related to the concept of human behavior and human life of urban culture in the area of Bandung City. Data collection using observation techniques (field work observation) and ethnographic interviews using data collection guidelines. The ethnographic method of Spradley, as shown in the following scheme:

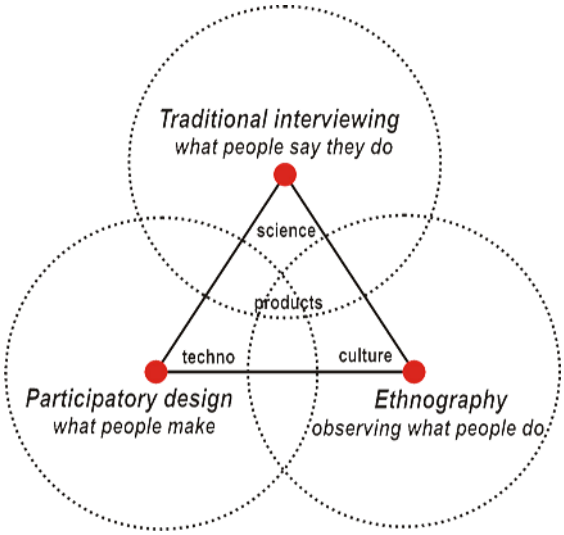

Fig. 1: The concept of ethnographic studies in the cultural sector that involves the application of science and technology (adaption of Spradley 1985)

Implementation of ethnography in the world of Product Design, is about observing the behavior of human work (observing what people do) as an influential socio-cultural point of view in design decisions. Another point of view involved in product formation is the paradigm of technology application in the form of participatory design in the form of competence in creating and producing (what people make) which is integrated with the element of science based on local wisdom, which can be absorbed through direct interview (traditional interviewing) about the fundamental capabilities possessed by a particular cultural society (what people say they do).

3. Discussion

In understanding the identity of forest village communities, a fundamental understanding of aspects relevant to the principles of natural conservation is required. This common life principle can be used to consider the hydroponic-aeroponic-aquaponic farming system as a solution to their problems.

The structure of Indonesian society according to Wertheim (1954) generally consisted of the cultivators in the inland and upland areas, the wetland farmers who settled in the watersheds, lakes and swamps, and seafaring societies (fishermen) living in the coastal areas.

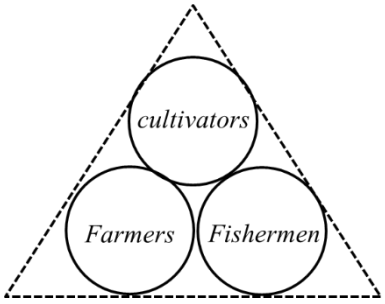

Fig. 2: The structure of Indonesian society according to Werheim (1954)

The division of the structure of Indonesian society from Werheim above shows that the societies of various ethnic groups in Indonesia, consisting of groups divided by the type of livelihood determined by the environmental conditions of the environment. Each tribe in Indonesia has the ability to adapt to its environment and gain knowledge on how to survive in its environment. These situations and conditions allow for competition or interaction between communities that make a society dominant so that it can be more developed when compared with other communities in the same tribe. This is what makes the dominant characteristic of various tribes in Indonesia.

Edi S Ekajati (2005) indicates that the Sundanese community consists of three major groups, the **pahuma** community who live in fields in the highlands and volcanic areas, **panyawah** communities living in the lowlands where there are sources of water, springs, streams, lakes and swamps, as well as **pamayang** people who live on the coast and estuaries.

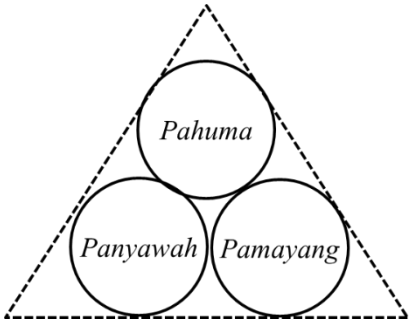

Fig. 3: Structure of Sundanese society
(source: Edi S.Ekajati 2005. Elaboration of the author)

The pahuma community lives in a highland mountainous area with a nomadic lifestyle. They are exploring in the interior of the jungle as a hunter or dipker and farming tubers and vegetables. Panyawah communities settle permanently in a fertile area that has a source of water for rice cultivation, palawija, vegetables, maintaining fish ponds and livestock. Pamayang communities living in fertile areas that have a source of water for cultivating

crops, fruits, and farms. This pamayang community has the ability to build boats and find marine fish in coastal areas. The image of the Sundanese cosmology below demonstrates the concept of trigatra in the structure of Sundanese society. Gatra pahuma (cultivators) living in the highlands or volcanic areas is a region that has a high degree as a sacred people, because it allows for a harmonious relationship between humans and the forces of nature. Pahuma serves as a guardian of nature.

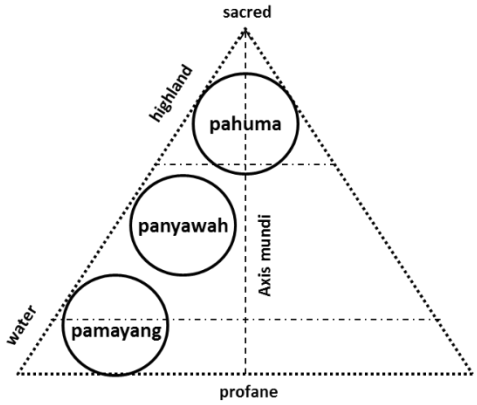

Fig 4: Overview of Sundanese Cosmology
(source: author elaboration)

The life of pahuma that has the task of preserving nature is in a sacred area called *the mandala* (sacred area). Due to its dynamic nature, pahuma is not in a permanent place. Pahuma is always moving and moving. The process of movement is often called *jarambah* or penetrated the forest up to the interior of the forest. Thus, pahuma has a lot of knowledge and unique related to the nature of the environment. Much knowledge of natural phenomena and natural guidance derived from the experience of pahuma in exploring or *ngumbara ngalalana*.

They have the ability to understand natural markers, footprints, natural forest phenomena and animal behavior in forest areas, so they can return to the village according to the rules set by their parents. They are obliged to return to the village before the sun sets. They understand very well that at night many wild animals search for prey. There is a rule that night is for animals to feed, whereas people have to rest to recover, reflect on what happens during the day, and talk to parents about things they can not yet understand.

The pahuma life in harmony with nature has placed them in a position that is highly respected by other Sundanese (panyawah and pamayang). Pahuma is considered as a sacred society, because it lives in the mandala area at the top of a hill or mountain. The towering volcanoes, a natural milestone sacred by all levels of Sundanese society, as well as by reformers who carry the message of Islam. The mountain is physically called *Giri*, whereas philosophically the *Gunung* is defined as *Guru nu Agung* (Great Teacher). Pahuma is often called *jalma gunung* or *tiyang gunung* by other people. The place of pahuma settled in calling the padukuhan.

The life of a sustainable pahuma community today is very important to be understood and appreciated, because they are able to live independently, able to harmonize with the natural environment, and never cause damage to ecosystems that impact natural disasters. Principle of life by following *pikukuh* (obedience) to *karuhun* (ancestors) for the noble task of *mulasara buana* (maintaining the universe). Pahuma society has customary rules or pukukuh karuhun which is interpreted as *patikrama*, that is *pati* (soul) and *krama* (tatakrama, procedure), which become customary law that animates all life of pahuma human being. *Tatanen Huma Sunda* (traditional procedure for Sundanese) is believed to be a source of answers to some of the difficult problems faced by villagers in forest areas, requiring farming without forest destruction or tree felling in protected and productive forest areas. Unfortunately, *Tatanen Huma Sunda* is not found in written reference form.

In cultivating fields or huma, pahuma must follow the guidance of nature. The forests that can be planted are *leuweung baladaheun* (not forest), not *leuweung larangan* (forbidden forests) or *leuweung keramat* (sacred forests). Do not disassemble the land, cut down trees and burn forest. they may only burn thorns and shrubs withered to be natural fertilizers.

Simple lifestyles, honest, patient and hard-working, are included in the *amanat buyut* and *tatakrama huma*, including: *gunung teu meunang dilebur* (mountain should not be destroyed), *lebak teu meunang diruksak* (valley should not be destroyed), *lojor teu meunang dipotong* (length should not be cut), *pondok teu meunang disambung*

(short can not be connected), *kudu ngadek sacekna* (must be printed precisely), *napas saplasna* (slash as liberally). In addition, the customary provisions in the ancient community are customary restrictions which are the guidelines and worldviews that must be run correctly. some of the surprising customary restrictions are: prohibited from altering waterways such as fish ponds or drainage, forbidden to change the shape of the land such as making a well or leveling the ground, prohibited from entering the forests to cut down trees, prohibited from using chemical technology, prohibited from planting a plantation cultivation, forbidden to keep four-legged animals such as goats and water buffalo, prohibited from arbitrary farming, forbidden to dress casually.

The forest villagers receive *the Amanat Buyut Sunda* gift of cultural roots. So as to understand why the forest should be preserved, why the water source should be maintained, why not exploit the land excessively. The offer to develop a new agricultural way that does not need to hoe the soil, do not use chemical fertilizers, does not employ livestock, does not pose a risk to the environment, is by applying a hydroponic system in the garden, aquaponic over the pond, and aeroponic in the forest.

In the beginning, the activity of cultivating plants without soil was written on Sylvia Sylvarum's book by Francis Bacon in 1627. The technique of cultivating plants using water became a very popular research. In 1699 John Woodward published a water-culture experiment with sprearmint. Jhon Woodward discovered that plants in impure sources of water actually grow better than plants that use pure water. The research of German botanist Julius Von Sach and Wilhelm Knop, in 1859 - 1865 who developed a technique of cultivation of plants without soil media, has concluded the importance of the fulfillment of mineral nutritional needs for plants, Research today is called a solution culture, regarded as a hydroponic type without media planting inert, which is a planting medium that does not contain nutrients. In 1929 William Frederick Gerickle of the University of California promoted openly about the solution culture used to produce agricultural crops. The researcher claims that hydroponics will revolutionize food crop agriculture. In 1940 Hoagland and Amon researchers from the University of California rearranged Gerickle's formula and published a book entitled Complete Guide to Soiless Gardening, which became known as hydroponics (in Greek hydro meaning water and ponos meaning power).

James S Douglas (1975) compiled a book entitled 'Hydroponics', which succeeded in transforming some vacant land in urban areas in the City of London into a fertile hydroponic farm. Some of the agricultural land that is infertile, has been successfully developed into productive hydroponic farming land in England. Bambi Turner (2012) released an online article entitled 'How Hydroponics Works', which inspires farmers in urban areas to develop hydroponic cropping systems in various ways. The concept of widespread hydroponic cultivation agriculture is static solution culture and wick system. In Indonesia static solution culture is better known as floating technique or floating raft technique, while wick sytem is known as the axis system, both of which are the simplest of all hydroponic types. Richard Stoner's (1983) study entitled aeroponic farming system, which is a hanging roots farming system, which is a system of plant roots periodically dampened with very fine nutrient solution grains. This method does not require soil media or puddles, but requires plant species that grow with a hanging roots in the air or extensive spatial growth on a regular basis. The roots of the plant moistened with a fine mist of nutrient solution can grow plants perfectly and healthy. The aeration system (wetting the roots with nutrient solution) is a major advantage of aeroponics. Researcher Anna Heiney of NASA in 2004 released an article titled 'Farming For The Future' which promotes the aeroponic system for the concept of life in the future. Some experimental plantations in outer space have proven the possibility of potential cultivation of plants in various fields or open spaces. In this concept, agriculture includes all types of planting activities that are not dependent on the existence of fertile agricultural land.

Pinus Lingga (2009) popularized hydroponics in Indonesia by publishing a manual to carry out hydroponic farming activities under the title 'Hydroponics: Farming without soil'. His experience in hydroponic farming activities inspires hydroponic farmers to try different ways to create a variety of media and hydroponic cultivation facilities, including with the use of a variety of used goods. Kunto Herwibowo and N.S Budiana (2014) developed a vegetable hydroponics system without using greenhouses for enthusiasts and crop entrepreneurs. Reno Suryani (2015) developed a hydroponics system for urban agriculture. Urban situation and conditions with narrow and expensive land, can be developed into productive hydroponic farming land.

Efforts to popularize the maintenance of plants by aerohidroponik, developing in various books, mass media and social media. The application of this system to the peasant community has never been done by other researchers, although there are many problems in rural areas related to the reduced farming facilities.

The concept of hydroponic-aquaponic applications on vacant land and fish ponds, with bamboo materials preferred by farmers rather than using pvc pipes, as well as very simple aeroponic designs with bamboo materials as tree-support constructions, more people choose, Examples of tested products:

Fig.4: Bamboo Hydroponic (source: author)

Fig.5. Bamboo Aeroponic (source: author)

4. Conclusion

Through the study of sustainable Patikrama Tatanen Huma Sunda in the area of padukuhan or Sundanese traditional countryside, obtained the picture of the importance of human understanding of the situation and the natural conditions of the environment. Just as the pahuma is obliged to mulasara buana or maintain the natural surroundings, the farmers in the forest village area have the same obligation to keep the forest ecosystem from damage and excessive exploitation.

The vision of the *mulasara buana* and the mission of *ngertakeun bumi lamba* that is firmly held by kabuyutan society, can be understood as the basis for preserving the forest, both in the category of forested forest, protected forest and prohibited forest. Utilization of forest land and fish pond as a productive vegetable garden can use the principle of huma, which is doing the process of plant maintenance without changing the structure of the environment. Not doing tree felling, excavation and ground shaking and other work that makes the earth's condition change. This principle has in common with the hydroponic principle that utilizes nutritious water flow without soil media.

Utilization of fish pond into vegetable garden can use the principle of aquaponics, where happened mutualisma process between plants and fish, through nutrient circulation from pond to medium planting vegetables which is above pond, and from plant to pond. The working principle is different from that of aquaponics in urban farming that must use electrical energy to move the water pump, in the acuponic design of this fish pond, obtained a more economical and practical way, that is utilizing the flow of water into the pool as an infinite supply of nutrients to vegetables that are above fish pond.

The principle of aeroponic work related to the supply of nutrients through the haze of nutrients absorbed by hanging plant roots can be applied to the design of aeroponic products that use the tree as a constructive part of the planting media product. In the forest every morning and evening comes a mist (fog) that provides nutritional supplements on plants that are above ground level. This principle is used to build vegetable gardens among large trees in forest areas.

The trial of the implementation of the aquaponic-hydroponic-aeroponic working principle in a landless farming system on limited landholdings shows symptoms that give rise to new enthusiasm for smallholder farmers without large farmland.

5. Acknowledgements

Thank you as much as possible to Kemenristek Dikti who is pleased to provide this research grant. Hopefully, this continuing research will give the greatest benefit to the welfare of the smallholders in the forest village area.

6. References

Adimihardja, Kusnaka. 1980. Pertanian; Mata Pencaharian Hidup Masyarakat Sunda'. Dalam Edi.S. Ekajati (ed.). Masyarakat dan Kebudayaan Sunda. Bandung: PIPR: 137-167

Agar, M. 1996. Professional Stranger: An Informal Introduction To Ethnography, (2nd ed.). Academic Press

Bambi, Turner. 2012. How Hydroponics Works. HowStuffWorks.com. Retrieved: 21-02-2016

Budiana, N.S & Fathulloh,A.S. 2015. Akuaponik: Panen Sayur Bonus Ikan. Jakarta: Penebar Swadaya.

Budiana, N.S & Kunto Herwibowo.2014. Hidroponik Sayuran. Jakarta: Penebar Swadaya

Darsa, A.Undang. 2006. Gambaran Kosmologi Sunda. Bandung: Kiblat Buku Utama

Danasamita, Saleh. Dkk.1987. Sewaka Darma Sanghyang Siksakandang Karesian Amanat Galunggung. Bandung: Proyek Penelitian dan Pengkajian Kebudayaan Sunda. Direktorat Jenderal Kebudayaan. Departemen Pendidikan Dan Kebudayaan.'

Ekajati, Edi S. 2005. Kebudayaan Sunda Suatu Pendekatan Sejarah, Jakarta: Pustaka Jaya

Fetterman. 1998. Ethnography (2nd edition). Thousand Oak CA: Sage Publicatio

G.Thiyagarajan, R.Umadevi & K. Ramesh. 2007. Hydroponics: Science Tech Entrepreneur. Ed. January 2007.

Water Technology Centre. Tamil Nadu Agricultural University. India.

Heiney, Anna. 2004. Farming For The Future. NASA .Gov. Retrieved: 20-03-2016

Jamaludin. 2010. The Aesthetic of Sundanese Tradition Design, case study: Rice Containers Design. ITB

Journal of Art and Design, ISSN 1978-3078, vol.4 No.1. 2010. 35-41.

Jamaludin.2012. Makna Simbolik Huma (ladang) di Masyarakat Baduy. Mozaik Journal of Humanism, Vol: 11/Nomor 1/2012-06, 1-8. FIB Universitas Airlangga Surabaya. ISSN: 1412-999x.

Lingga, Pinus. 2009. Hidroponik: Bercocok Tanam Tanpa Tanah. Jakarta: Penerbit Niaga Swadaya

Istiqomah, Siti. 2015. Menanam Hidroponik. Bandung: Penerbit Ganeca Exact

Saparinto, Cahyo. Liferdi L. 2016. Vertikultur Tanaman Sayur. Jakarta: Penebar Swadaya.

Skaggs, Paul. 2012. Ethnography in Product Design – Looking For Compensatory Behaviors. Journal of Management and Marketing Research. Brigham Young University.

Stoner, R. 1983. Aeroponics Versus Bed and Hydroponic Propagation. Florist Review, Vol 173 No 4477 September 22, 1983.

Suryani, Reno. 2015. *Hidroponik Budi Daya Tanaman Tanpa Tanah*. Yogyakarta: Arcitra

Proceedings of the 1st Faculty of Industrial Technology International Congress
International Conference
Bandung, Indonesia, October 9-11, 2017
ISBN 978-602-53531-8-5

Task Assessment as Learning Tools to Meet Actual Architectural Issues

Shirley Wahadamaputera*, Bambang Subekti, Theresia Pynkyawati
Department of Architecture, Institut Teknologi Nasional (Itenas), Bandung - INDONESIA
* Corresponding author e-mail: joanshirl2000@yahoo.com

Abstract

The issue of disability and Green Building often ceases only as a discourse in seminars or as a design theme for student assignment. Meanwhile, design requirements considering disability have not become a binding rule to submit in planning and construction yet, especially in public buildings design, as well as green building codes. It has to start from the awareness of the planner from the early stage through architecture education to educate the society. The studio task assessment system which contains points of assessment on meeting the standard of issues for the disabled will be an effective learning tool. Students are shaped as planners to be and responsive to the disability needs as a result. Software utilization in the learning process to test the circulation design reliability, deserves to be rewarded for high points.

Keywords: Disability, Regulation, Task Assessment, Learning Tools, software

1. Introduction

The closeness of family ties is a cultural feature of living in Indonesia. One residence can be inhabited more than one family of different ages. The system of settlements in large cities is turning to the vertical home system as a solution to the number of decent housing needs, for the middle to lower economic community. Parents in the family will someday begin to need a mobility aid to move around, alone or with the help of others. Similarly, family members with disabilities are rarely found to be entrusted to a home for disable, but they also are rarely found traveling without assistance. Thus the readiness of the circulation design on the vertical settlement system should be prepared to accommodate persons with disabilities and the elderly according to Peraturan Menteri PU no 05/PRT/M/2007.

Traveling with elderly parents, persons with disabilities in the family, pregnant women, family members during a healing period, requires the readiness of other family members. Preparation begins with finding solution to move horizontally and vertical, also the availability of toilet facilities, seating, stairs in public facilities Peraturan Menteri PU no 30/PRT/2006 pasal 1.

The design of buildings that have prepared facilities and circulation for persons with disabilities is the design of hospital buildings, considering the residents are ambulatory, bed ridden and one day care patients. Several new building designs, such as shopping centers and hotels in big cities, have complemented the design with parking facilities, toilets, elevators that are wide enough for people with disabilities and the elderly. However, the continuity of circulation between destinations within the zone of both horizontal and vertical buildings has not been considered well. The design of the ramp is still a facility that facilitates the movement of goods.

Design of a building which prepares for persons with disabilities should provide more space for vertical circulation facilities from outside the building to the inside and vice versa. Circulation between different floors also requires more space planning. A new theme in designing with a concern to disabled people and the elderly developed in 2009 (Joachim Fischer, Philipp Meuser, 2009). It was a barrier free theme in a building design, which enables disabled to move without co-assistance in both horizontal and vertical circulation, mechanical transport is required, whereby its application should begin to be considered against the green building issue.

Peraturan Menteri PU dan Perumahan Rakyat no. 02 / PRT / M / 2015 pasal 25 on Green Building that has been socialized since year 2015, regulates the selection of building objects which are classified as green buildings. Design and implementation of buildings which are classified into green buildings will be accompanied by the TABGH expert team. Socialization efforts to the community have been done through seminars and impressions on social media, still few planners apply this rule. Green building issue leave as an interesting topic in a seminar or theme in architectural education studio tasks. How should architecture education take the responsibility?

2. Literature Review

2.1. Green Building Regulation

The issue of green buildings has been regulated in Peraturan Menteri PU and Perumahan Rakyat no 02/PRT/M/2015 pasal 8, whereas for the time being 9 classes of buildings subject to the requirements of green buildings are determined based on the complexity of the functions of the building's activities and the height of the buildings. Classification according to the height of the building is regulated in other regulations PermenPU no 29 of 2006 bagian II**.** The level of imposition of green building requirements is classified into 3 levels: mandatory, recommended and voluntary according to Peraturan Menteri PU and Perumahan Rakyat no 02/PRT/M/2015 pasal 5.

2.2 Site Planning on green building design

The requirements of the Technical Planning Stage involved the requirement on site management including building orientation, site processing, contaminated land management of B3 waste, private green open space, basement tread processing, parking lot provision, outdoor or courtyard lighting system, construction of buildings above and / or underground and water and/or public facilities and provision of pedestrian paths in Peraturan Menteri PU and Perumahan Rakyat no 02/PRT/M/2015 **.** The scope of the facility's technical guidelines and accessibility regulations which should be prepared in each building design should be considered against persons with disabilities and the elderly according to Peraturan Menteri PU no 30 of 2006 pasal 1**.** Thus every building construction activity should pay attention to all technical guidelines covering the basic size of free floor space, Door, ram, stairs, elevator, stair lift, toilet, shower, sink, telephone, furniture, control equipment and equipment, and markers. Site construction should pay attention to the size of the floor, pedestrian path, parking area, ramp, signs and markers. While construction of the outdoor environment should pay attention to the technical guidance of facilities and accessibility on the floor size, pedestrian path, guiding lane, parker area, ramp, signs and markers.

Fire Protection System in building and environment is considered to the height of the building, the number of occupants, referring to the Peraturan Menteri PU no 26/ PRT/M/2008. Requirements on planning, provision and utilization of urban pedestrian infrastructure and facilities in urban areas refer to Peraturan Menteri PU no 03 / PRT/M /2014 pasal 1.

2.3. Project Based Learning Method implementation in the Architecture Studio education

Project Based Learning is a teaching method in which students gain knowledge and skills by working for an extended period of time to investigate and respond to an authentic, engaging and complex question, problem or challenge.

2.4 UNESCO-UIA Charter for Architectural Education

Objectives of architectural education according to UNESCO-UIA Charter 2011 – Seoul September 2017 for architectural education, is to meet an understanding of the relationship between people and buildings, and between buildings and their environment, and of the need to relate buildings and the spaces between them to human needs and scale.

Need of continue and contiguity circulation for disabled and aged should be fulfilled by this.

Architectural education involves the acquisition of design, knowledge and skills capabilities. Knowledge capability related to design has to meet:

• Understanding of services systems as well as systems of transportation, communication, maintenance and safety

• Understanding of the processes of technical design and the integration of structure, construction technologies and services systems into a functionally effective whole.

This means that these capabilities is to be reach as learning out comes at the end of a studio project.

3. Methods

In order to get an idea of how learning methods about facility design preparedness for people with disability is applied thoroughly in studio and response, observation on rubrics of 2 design studios and rubrics of 2 Structure and Construction responses. The rubric analysis is done by comparing the applicable regulations on person with the disabilities and the elderly and how the rating points influence the final score to get an excellent credit.

4. Study and Out comes

The study was taken on rubrics of the Architecture Department Studio of Institut Teknologi Nasional Bandung. Focused on how rubric of each studio and response contains point of assessment which meets the disabled and elderly needs of adequate circulation. Assessment task on Studio rubrics of the 5th and 6th semester and also the rubrics of the Structure and Construction Response of the 4th and 5th semester will be appropriate to this study.

Job given in 5th semester studio is a design on a 4 stories public building such as shopping mall or a dormitory, while in the 6th semester studio is a design of a public building of a long-span roof design such as indoor sport facilities or auditoriums. This type of building has to accommodate disabled activities according to Peraturan Menteri PU no 30 of 2006 pasal 1. Point of assessment in each rubric table marked with (*) symbol.

Table 1: Rubric of 5th Semester Architecture Studio

ARCHITECTURE DESIGN STUDIO IV			
Studio TASK Evaluation Sheet			
4 STOREY RETAIL BUILDING DESIGN			
Odd Semester: 2017/2018			
JOB II:			
CONCEPTS			
Mentor :			
A. CONCEPT COMPLETENESS			**40%**
1	GENERAL CONCEPT		
	·	Building definition	
2	SITE CONCEPT		
	·	Site analysis & mass ordering pattern on site	
	·	**Circulation system for vecycle and pedestrian on site ***	
3	ARCHITECTURE CONCEPT		
	·	Spacial Program & flow of activity	
	·	BCR and FAR, site area	
	·	**Zoning analysis and building circulation design ***	
	·	Facade concept and materials	
4	STRUCTURE CONCEPT		
	·	Modul of Structure	
	·	Structure system, foundation, retaining wall, beams, and roof	
	·	column, beam, floor dimensionering and stair geometry	
5	BUILDING SERVICE CONCEPT		
6	BUILDING CONTROL CONCEPT		
B. RIGHTNESS OF CONCEPT			**30%**
1	Regulation (5%)		

2	Space Requirement Program (10%)	
3	Structure (5%)	
4	Utilities (5%)	
5	Building Physics (5%)	
C. CREATIVITY		**20%**
1	Site concept (5%)	
2	Building concept (5%)	
3	Activeness in Preview (10%)	
D. TIME BOUND (Y/T*)		**10%**
P O I N T		
A : 80-100 B : 65-73 C : 50≤60 E : <41		
AB : 73≤80 BC : 60≤65 D : 40≤50		

Job given in the 4th semester on Structure and Construction response is analyzing a10 stories structure system of a rental office building or hotel, while in the 5th semester response is analyzing a long-span roof structure system of a public building.

Table 2: Rubric of 6th Semester Architecture Studio

ARCHITECTURE DESIGN STUDIO V			
Studio TASK Evaluation Sheet			
INDOOR SPORT/AUDITORIUM DESIGN			
EVEN Semester: 2016/2017			
JOB I:			
Mentor			
NO		**C R I T E R I A**	**POINT**
CONCEPT			
I. CONCEPT COMPLETENESS			**40%**
	1	Building definition	
	2	**Site analysis, and mass form ***	
	3	Mass pattern on site planning	
	4	**Vehicle and pedestrian circulation systems on site ***	
	5	Spacial program, flow of activity	
	6	Building and site regulation (BCR, FAR)	
	7	Zoning analysis + **building circulation design** *	
	8	Facade concept and material, Acoustics	
	9	Vertical & horizontal structure loading analyze	
	10	Structure Module	
	11	Structure System, foundation, wide span roof	
	12	Column, beams, floors dimensions and stairs geometry	
	13	Structure Material (column, beam, roof)	
	14	Building service concept	
	15	Building control system concept	
II. RIGHTNESS OF CONCEPT			**20%**
III. Long Span Building Design, Building Control System, Structure design, and building service concept			**10%**
IV. AESTHETIC PRESENTATION on A3 Paper Format			**10%**
V. Preview			**10%**
P O I N T			
A : 80-100 B : 65-73 C : 50≤60 E : <41			
AB : 73≤80 BC : 60≤65 D : 40≤50			

Table 3: Rubric of 4th Semester Structure and Construction

RESPONSE OF STRUCTURE AND CONSTRUCTION 3: PRESENTATION OF STRUCTURAL CONCEPT ANALYSIS			
Studio TASK Evaluation Sheet			
10 STOREY RENTAL OFFICE BUILDING DESIGN			
EVEN Semester: 2016/2017			
JOB I:			
CONCEPT			
Mentor :			
NO	**C R I T E R I A**		**POINT**
1	**ANALYSIS**		
	Structural Dimensionering Analysis		**10%**
		> Structural Aksonometry Sketches	
		> Dimensionering of Columns, Beams and foundations	
		> **Ramp geometry ***	
	- Vertical Load Analysis (gravitation)		**10%**
		> Sketch of Deformation on structures due to gravity	
		> Load distribution pattern on superstructure (upperstructure)	
		> Tension / compression mechanism on superstructure element (upperstructure)	
		> The types of joints & their effects on the shape of structural elements	
		> The force mechanism on the foundation	
	- Horizontal Load Analysis (wind)		**10%**
		> Sketches of deformation tendencies on structures due to wind load	
		> Load distribution pattern on superstructure (upperstructure)	
		> Tension / compression mechanism on superstructure element (upperstructure)	
		> Types of joints & their effects on the shape of structural elements	
		> Scetch of force mechanism on the foundation	
2	**RANCANGAN**		
	1. Floor Plan Drawing		**10%**
		> **Placement of utility equipment and shafts ***	
		> **Placement of Fire Stair ***	
	2. Elevation Drawing		**15%**
		> Building façade	
		> Material Finishing Description	
	3. Section Drawing		**20%**
		> Clarity of depiction (visible and truncated)	
		> Roof structure system and roof drain system	
		> Foundation system, tie beam, basement, drainage and floor	
	4. Main Entrance Principle Section Drawing		**25%**
		> Shows Construction Details : Roof to Foundation	

		> Shows Notation, dimension and description of material	
P O I N T			
A : 80-100 B : 65-73 C : 50≤60 E : <41			
AB : 73≤80 BC : 60≤65 D : 40≤50			

Table 4: Rubric of 5th Semester Structure and Construction

RESPONSE OF STRUCTURE AND CONSTRUCTION 4: PRESENTATION OF STRUCTURAL CONCEPT ANALYSIS			
Studio TASK Evaluation Sheet			
LONG SPAN ROOF STRUCTURE DESIGN			
Odd Semester: 2017/2018			
JOB I:			
CONCEPT			
Mentor :			
DESIGN ANALYSIS OF A LONG SPAN STRUCTURE			
NO	**C R I T E R I A**		**POINT**
1	**LITERATURE STUDY**		**10%**
		> Literature Study on Applied Long-Span Structure System	
		> Form follows function or analogy	
		> 3 D Sketches of structural aksonometry	
	Completeness and Creativity		
	Time Bound (Y/T*)		
2	**CONCEPT ANALYSIS**		**20%**
	- Vertical Load Analysis (gravitation)		
		> Sketch of Deformation on structures due to gravity	
		> Load distribution pattern on superstructure (upperstructure)	
		> Tension / compression mechanism on superstructure element (upperstructure)	
		> The types of joints & their effects on the shape of structural elements	
		> The force mechanism on the foundation	
	- Horizontal Load Analysis (wind)		
		> Sketches of deformation tendencies on structures due to wind load	
		> Load distribution pattern on superstructure (upperstructure)	
		> Tension / compression mechanism on superstructure element (upperstructure)	
		> Types of joints used & their effects on the shape of structural elements	
		> Scetch of force mechanism on the foundation	
	Completeness and Creativity		
	Time Bound (Y/T*)		
3	**DESIGN ANALYSIS**		
	1. Floor Plan Drawing		**10%**
		> Roof structure on column placement	
		> Placement of utility equipment	
	2. Elevation Drawing		**10%**
		> Building Proportion	

		> **Main Entrance Design ***	
	3. Section Drawing		**15%**
		> Height of inner space under the structure	
		> Main roofing support system	
		> Rainwater drainage system	
	4. Principle Section Drawing		**25%**
		> Roof construction and pedestal connection details	
		> Roof cover to the structure connection details	
	Completeness and Creativity		**5%**
	Time Bound (Y/T*)		**5 %**
P O I N T			
A : 80-100 B : 65-73 C : 50≤60 E : <41			
AB : 73≤80 BC : 60≤65 D : 40≤50			

Job on both studios and response session has already meets the criteria of a design project in which disabilities and aged people should be facilitate according to the Table of minimum accessible facilities on regulation Peraturan Menteri PU no 30 / PRT / 2006 Ketentuan Penutup**.**

Rubric on the Structure and Construction at the 4th semester as shown in Table 3 contains specific value on the building core design which meets the regulation on fire escape in a 10 stories public building. Although the mid-test on the Structure and Construction response is to draw a section over the main entrance, there are no points on ramps design at the entrance to facilitate the disabled and aged. There is no point to a ramp design in the floor plan, as well as toilets for the disabled.

Refers to the rubric of the 5th semester Structure and construction response as shown in Table 4, also has no specific point to a ramp design yet, although has point on entrance porch and corridor design.

The 4th and 5th semester learning outcomes of the Structure and Construction subject has to be implemented on the 5th and 6th semester Architectural Design Studio according to the designed road map of the curriculum. Meanwhile the rubric on the 5th and 6th semester of the Design Architecture studio, already have point on accessible design in the site planning as shown in Table 1 and Table 2. Although toilets for disabled and aged could easily found in almost all design floor plan, yet there is no point as a credit to this design as shown in Table 1. No wonder that this design issue being forgotten in the higher studio.

5. Conclusion

Application of green building codes to meet the need for disabled and elderly in a building design, should begin with the architecture education. The learning method of Project Based Learning applied in the Architecture Design Studio and Structure and Construction Response can act as a proper teaching medium. Tasks assessment through rubrics are prepared to give point to the green issue based on regulations which applicable to the circulation of persons with disabilities and the elderly. This will improve students respect to the building code, as well as skill in design building properly.

The studio task assessment system that contains points of assessment on meeting the standard of issues for the disabled will be an effective learning tool.

6. References

Fischer, Joachim. and Meuser, Philipp., 2009. Construction and Design Manual Accessible Architecture., DOM Publisher, Berlin, 11-13.

Peraturan Menteri PU no 30 / PRT / 2006 tentang Pedoman Teknis Fasilitas dan Aksesibilitas pada Bangunan Gedung dan Lingkungan

Peraturan Menteri PU no 29/PRT/M/2006 tentang Pedoman Persyaratan Teknis Bangunan

Peraturan Menteri PU no 05 / PRT / M / 2007 tentang Pedoman Teknis Pembangunan Rumah Susun Sederhana Bertingkat Tinggi.

Peraturan Menteri PU no 26/PRT/M/2008 tentang Persyaratan Teknis Sistem Proteksi Kebakaran Pada Bangunan Gedung Dan Lingkungan

Peraturan Menteri PU no 03 / PRT / M / 2014 tentang Pedoman Perencanaan,Penyediaan,dan Pemanfaatan Prasarana dan Sarana Jaringan Pejalan Kaki di Kawasan Perkotaan.

Peraturan Menteri PU dan Perumahan Rakyat no 02/PRT/M/2015 tentang Bangunan Gedung Hijau

UNESCO-UIA Charter 2011 – Seoul September 2017

Project Based Learning Method, available at : https://www.edutopia.org/project-based-learning, accessed on September 22, 2017.

Proceedings of the 1st Faculty of Industrial Technology International Congress
International Conference
Bandung, Indonesia, October 9-11, 2017
ISBN 978-602-53531-8-5

STUDY ON THE DEVELOPMENT OF ORNAMENTS AS THE IMPLEMENTATION CREATIVE ABILITY IN SME BASED CREATIVITY

Mohamad Arif W[1,*], Agus Rahmat M[2]

[1] Department of Product Design, Institut Teknologi Nasional (Itenas), Bandung - INDONESIA

[2] Dept. of Visual Communication Design, Institut Teknologi Nasional (Itenas), Bandung - INDONESIA

[*]Corresponding author e-mail: mawaskito@yahoo.com

Abstract

The footwear industry at this time is very rapidly growing, especially in material aspects, construction between upper and bottom, manufacturing techniques, to model variants which each have an influence in the formation of design concepts and design development of the footwear product. In the determination of design decisions relating to the model of footwear products, there are elements of design that became part of the form elements, namely color, material character, the concept of pattern pieces are also unique motifs that each provide visual reinforcement so that each product will have Different originality values.

The process of designing footwear products made in SME is often done by imitation or popularly called "ATM", ie “Amati”, “Tiru” and “Modifikasi”. Such a product development thinking pattern will not result in innovation values in the product, even such imitative habits will shape their mentality tends to be more lazy to innovate and not creative to produce new products.

One possible attempt by craftsmen to get the original and easy to do value is the use of the "stilasi" method, an attempt to discover new forms by simplifying the shape of a particular object. The process of simplifying the shape of an object is generally done on the design of traditional ornaments of the archipelago. By studying the process of creating these traditional ornaments, there will be found a basic method that can be used to develop novelty values, originality and design uniqueness in handicraft products including in footwear products. This idea development method will then be taught to the craftsmen to be able to empower their creation ability to develop the products they make.

Keywords: Creativity, decoration, stilasi, footwear industry

1. Introduction

At present, domestic industries are dealing with a globalization era that demands high competitiveness to anticipate the tightness of trade both regionally and internationally. The development of informatics technology and the existence of mutual trade agreements such as CAFTA (China Asean Free Trade Area) which started since early 2010 has made the industrial sectors in Indonesia must be ready and able to face the problems of production and trade between the limited ability of human resources, raw materials, production technology

However, the footwear sector still has promising trade opportunities as stated by the Chairman of the Indonesian Footwear Association (Aprisindo) Eddy Widjanarko, that the value of Indonesia's footwear exports has increased from US $ 3.8 billion in 2014 to US $ 4.5 billion in 2015, and in 2016 expected export of footwear Indonesia grew 11.11% to US $ 5 billion.

According to the Central Bureau of Statistics, in leather industry, leather goods and footwear are among the sectors with the fastest growth of gross domestic product in early 2016. The industrial sector grew 9.21% in the first quarter of 2016 compared to 3.98% throughout 2015.

With regard to the growth in export value of footwear products as above, it shows that footwear commodities have the opportunity to continue to be developed by creating quality products that have innovation value, unique value, novelty value so as to compete with products from countries others in the free market. The government through the Ministry of Industry (Kemenperin) continues to encourage the development of national footwear industry by creating a conducive business climate and improve its competitiveness in domestic and international markets. This is very important because the footwear industry is one of the strategic sectors of the economy because in addition to being able to provide sufficient employment, bringing large foreign exchange is also reliable as a supporter of domestic clothing readiness.

One of the innovative product development opportunities that can be done is through the development of a strategy or method of designing footwear products based on local wisdom (local genuine), which is an asset of the nation that has not been well dug as the economic potential of the community.

2. Methodology

Assessment of the creative ability possessed by small and medium industries is done through field research with qualitative descriptive method. The identification of the forms of creative activity undertaken in the industry can be traced through a review of the cultural and habitual formations that influence the development of industrial production technology itself. To explore the extent to which creative capabilities affect the activities of product development in the small industry, then the review in batik industry because it is considered to have a strong culture in terms of creative use of power in its production activities.

Observation of the creation process in the form of decoration made in the industry that produces batik Cirebonan. Cirebon batik handicraft industry historically has a process of development of various decorative creations. This is due to the influence of geographic factors Cirebon as coastal areas and social order that was built by the government in the form of a kingdom that creates two ornamental varieties of decorative palace and decorative Coastal. The main objective of the assessment of the creative process in the batik industry is to find an effective method in terms of developing new ideas related to the development of decorative designs that spearhead innovation in the batik industry.

The method of developing new ideas is expected to be implemented in small footwear industry so that the creation process in the footwear can also have the acceleration of creation as well as in the batik industry.

3. Results and Discussion

3.1. *Observation of creative activities in batik industry*

In the first observation of the creation process done in batik industry in terms of design development there are three forms of design creation activities are: imitate, modify and seek inspiration. The three design activities of decorative design become the main activities that form the culture of design development that occurs in every batik industry. However, based on a review of industry that has a high proportion of "searching for inspiration" activities, it is considered to provide a good contribution in terms of accelerating the development of innovative designs in the industry.

Inspirational search activities such as those done in Batik Komar industry aims to find novelty or innovation of its products, which has made its own distinctive advantages distinguishing Komar batik with other batik craftsmen. For example Batik Komar has created an innovation on a new product called *Shibotik*, as he revealed on the site Rumah Batik Komar (http://batik-komar.com/our-brands/shibotik/): "*Shibotik* is creative idea Batik Komar . The ultimate goal is to offer breakthroughs in applied textiles by combining cultural heritage with today's sophistication. Born with "Batik" craftsmanship for centuries in Indonesia and traditional *Shibori* dyeing techniques ". The sensitivity to discover novelty through identification and experimentation has led to innovation opportunities, one of which is gained through the experimentation of combining different cultural values.

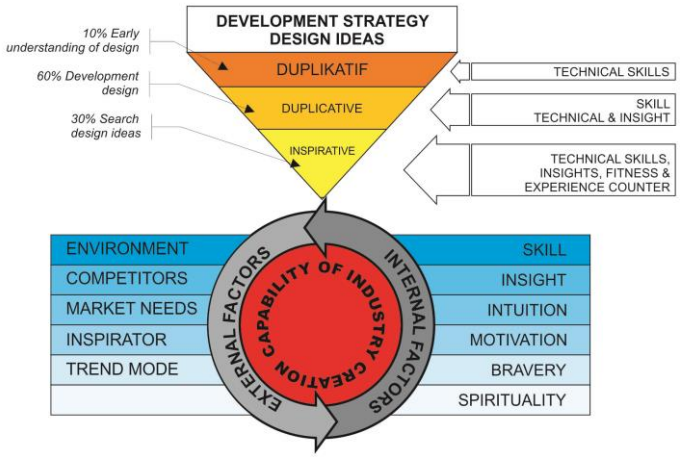

Fig 1: Scheme of implementation of creative activities at SME Batik Komar

In addition to design development activities in the form of inspiration search, productivity acceleration Batik Komar also influenced by some aspects that come from external and internal factors. External factors that influence among others: environment, competitors, market needs, inspiration and fashion trends. While the internal factors that influence the acceleration of the design creation are: skills, insight, instuisi, motivation, courage and spirituality. When compared between ikm footwear and batik ikm that made the object of research, internal and external factors are greatly affect the form of its activities. Almost all external and internal factors affecting Batik Komar also occur in other batik-batik industries, but Batik Komar has a somewhat different strategy with the occupation of Inspirator as a differentiator in the process of design development. According to Komarudin, the inspiration in question is the influence or input of people who have the depth and mastery of very good aesthetic values so as to provide certain enlightenment in relation to the discovery of new ideas of decorative designs developed. One of the inspirational figures is Sunaryo, a painter and artist.

Another aspect that is also very important by Batik Komar is the willingness and courage to experiment. Most small-medium business actors do not want to take risks to experiment with new things because they consider it counterproductive. In addition to being considered a waste of time, requires a large investment, nor have a certainty for significant success. But for Batik Komar, experimentation activities are considered the entrance to the achievement of new discovery opportunities that become its flagship.

Fig. 2: Development activities of decorative design in SME "Batik Komar"

decorative motifs applied to the fabric. Some motifs of decoration in Batik Cirebon got from various forms of inspiration, which is generally obtained due to the strong influence of the environment where the industrial society is growing. According to Irin Tambrin, batik motifs or ornaments Cirebonan style palace derived from the love of the people in the palace environment, especially on the sultan who is also as ulama (Jurnal Seni Rupa Vol. 2 No. 4 May 2002), then created the motif Batik *Keblegan, Paksi Naga Liman, Sawung Galing, Seba Dragon, Sunyaragi Park* and others. The strong influence of Islamic religion in Cirebon also influenced the style of presentation of the image done by batik craftsmen there. Irin also added that Islam that prohibits depiction of living creatures in the form of humans and animals in realistic. It has formed the technique of presenting decorative drawings on batik that leads more to geometric shapes and plant form in a simplified form.

3.2. Identify creative activities in SME of footwear

Unlike in the batik industry dominated by creative activities, in SME footwear activities that dominate is activity based on production and very little found activities related to creativity. Activities that are carried out always refers to standard Operating Procedure (SOP), whose main objective is to achieve the efficiency and effectiveness of the work. This then generates output from a typical and standardized production. Opportunity inventions novelty that should be developed in the design activities, always constrained by routine activities that do not provide opportunities to innovate. These structured activities narrow the creative development opportunities that should be owned by the business actors.

Table 1: Questionnaire results of activity type of creations in SME footwear

No	Subject	Value					Amount
1	This type of creative activity is often done	Create a New model	Make a motif on "Upper"	Combines colors & materials	Make a pattern	etc	
		6	7	16	6	1	36
		17%	19%	44%	17%	3%	

From the result of identification to 36 footwear business practitioners located around small industry center of Cibaduyut, obtained data that activities related to creativity element mostly done is effort to combine material or color (44%) in upper part. The activity is most often done to open up 2 to 3 color choices on one model. But color selection activities are often exposed to colors and materials available in material suppliers, which means that the type of color assigned often depends on the colors available only in those stores or suppliers. Due to the limited choice of colors, the most frequent action is to ask the consumer to adjust to the available colors and materials in the supplier's stores or to offer "always safe colors" such as black, tan, brown and white.

According to the results of identification, 19% of other creative activities are often done is making motifs or decorations on upper footwear. From the above data indicated that the application of decoration on shoes is not widely developed. This relates to the principle of production in the footwear SME where the resulting footwear shapes will depend on the shoelast form it possesses, the pattern cut and the judgment that the decoration does not significantly affect the attractiveness of the product. These considerations are then made the craftsmen not much change the motive of decoration, whereas the existence of decoration in essence is able to provide opportunities uniqueness of the design of the shoe itself.

Craftsmen who do the design development of decorative motifs on footwear products, obtained data that way of design development is mostly done is by modifying the existing images (61%). This is because modifying activities are still easy to do, and are considered not at risk of legal sanctions. Only a few (19%) of the respondents actually made their own decorative designs.

Table 2: Result of questionnaire of activity type of creations in SME footwear

No	Subject	Nilai					Amount
6	How to get an image form idea on the upper	Imitate	Modify	Make your own	Tell others	Ect	
		2	22	7	5	0	36
		6%	61%	19%	14%	0%	

The ability to modify objects to be used as decoration is most likely done by the craftsmen, but the obstacle faced is the ability to draw the activity of realizing the object seen or imagined onto the paper in the form of decorative pictures. Obstacles is a challenge for the craftsmen because to be able to draw required the learning process or the method of realize that is easy to learn by the craftsmen.

3.3. Application technique of decoration on upper

The shapes and techniques of decorating the footwear products vary greatly, usually depending on the type of footwear. Embroidery techniques and printing (screen printing) is usually used in sports, sneakers and casual footwear. Techniques punch (opek), hot stamp (emboss), and laser are more often used in formal and classic footwear. The most popular technique used is opek and emboss technique, because it is a technique of decorative / motif application which is relatively cheap, easy and quick to work on.

Activities that require other creative capabilities are often done is making decorative motifs / decorations above the upper (19%). Decorative manufacture above upper footwear product mostly done on footwear product of type of formal and men's women. Both types of footwear products are more often use motive designs as an attempt to provide the character and uniqueness of its products. In the survey conducted there are some popular ornamental application techniques that are done, the technique "opek" and "hot stamp" which is more often applied to men's formal shoes. For types of sports shoes and casual usually using the technique of "printing" or "embroidery". This shows the need for the presence of visual components in the form of decoration in footwear products greatly affect the visual character of the product as a whole.

Based on the same survey for the identification of application techniques of decorative motifs on upper shoes, it is found that the dominant technique used is opek/ punch technique (36%). From the results of identification, popular “opek” technique used by the footwear craftsmen because the application of this technique is considered the easiest to apply, easy to learn, can be done alone, do not demand high technology and not also demand high production costs. Another case with embroidery techniques that require high-tech machines, thus making them dependent on computerized embroidery service providers (Computerized Embroidery).

Table 3: Questionnaire results of ornamental application techniques in footwear SME

No	Subject	Value					Amount
7	Application technique image on upper	*Punch* /opek	*Printing* / sablon	*Hot stamping/ emboss*	Embroidery	Etc	
		13	8	11	3	1	36
		36%	22%	31%	8%	3%	

In addition to "opek", other ornamental application techniques are also often used is the technique of emboss / hot stamp (31%). Technique of this decorative application is also considered easy to do, cheap and can be done alone. In addition, the advantages of this technique is very possible to create images that are relatively complicated and detailed so as to provide opportunities to display more varied images. Details and variants of the design shapes generated through emboss techniques can only be matched by popular "laser" techniques.

4. Conclusions

Creative activities undertaken in SME can be grown through the establishment of ideal working conditions based on the demand for the creation of novelty. Novelty is the things that are created differently and evolve from the routine and standard activities done so far. Production and product development activities are often stuck on the condition that their productivity depends on the effectiveness and efficiency of work. So do not be surprised if many SME, especially in the footwear sector acts more as a craftmens than entrepreneurs. Craftmens are more towards performing actions of production that are similar and continuous. But entrepreneurs are always required to develop new things to answer every challenge or obstacle faced. The footwear sector needs a creative ability to develop the design quality of the products it produces, but because the systems that work in the industry are still dominated by production activities, other activities that require creative action are often ignored. Creative activities in SME footwear that allows for the most up to its ability is making designs of ornament motifs.

The ornamental making activity is considered the easiest to learn and provides novelty opportunities so as to make a differentiator from every shoe made. In addition, the difficulty in the implementation of ornament design on the upper is very easy with a variety of options in accordance with the design concepts that want to be implemented. Be creative with "opek" technique is the cheapest and easiest decorative making technique so that for craftmens who have low drawing technical ability, can be creative by making various composite form compositions to produce various designs. As for craftmens who have better technical ability, then it can make the design more complicated. Generally at this time the design development will be faster with the help of computer technology such as the technique of embroidery or laser (computerized laser cutting engraving).

Referring to the strategy undertaken in Batik Komar, then the footwear crafters are recruited to use computer technology when it wants to improve the quality and multiply the design variants. Computers can help crafters to draw an object through stylization techniques because at this time has many digital programs that are able to react a complicated object to be transformed into a simpler decorative design.

5. Acknowledgements

Thank you to the Ministry of Research, Technology and Higher Education who has provided budget assistance so that this research can be implemented. Hopefully the results of this activity can contribute to the progress of the development of small and medium sized footwear industry in Indonesia.

6. References

Meyer, F. S.,1957, *Hand Book of Ornament.* New York, N.Y. 10014, United States of America: Dover Publications, Inc.

Nadyani., 2014, Laporan Penelitian: Perancangan Sepatu Wanita Jenis Wedges Bertema Gorga dan Rumah Adat Batak Toba dengan Pendekatan Stilasi, Institut Teknologi Nasional.

Thorstensen, Thomas., 1993, Practical Leather Technology, Krieger Publishing Company, Malabar, Florida.

Yudoseputro, Wiyoso, 1983. Seni Kerajinan Indonesia, Jakarta: Depdikbud.

Soegiarty, Tity., Jernal penelitian: Dokumentasi dan Pemetaan Batik Pesisiran Daerah Sunda Sebagai sebuah

Usaha Pelestarian Budaya Bangsa.

Waskito, Arif., 2011. Laporan Penelitian: Pengembangan Desain Produk Kulit Dengan Menggunakan Teknik Cetak Sebagai Usaha Diversifikasi Produk Di Industri Kecil-Menengah Alas Kaki, Institut Teknologi Nasional.

Waskito, Arif., 2014. Laporan Penelitian: Pemanfaatan Limbah Bahan Kulit Dalam Bentuk Perca Sebagai Bahan Baku Pengembangan Desain Bergaya Mosaic Art Yang Diterapkan Pada Produk-Produk Pelengkap Interior, Institut Teknologi Nasional.

http://industri.bisnis.com/read/20160513/257/546963/ekspor-sepatu-indonesia-ke-china-melesat

https://id.pinterest.com/pin/492862752943789290/

http://saerah-bandung.blogspot.co.id/2011/03/ckr-custom-kick-rules-brass-stamp.html

http://www.stitchfx.ca/Embroidery.htmlTeknik

http://www.redtorope.com/2010/11/massively-reduce-laser-etching-time/

Proceedings of the 1st Faculty of Industrial Technology International Congress
International Conference
Bandung, Indonesia, October 9-11, 2017
ISBN 978-602-53531-8-5

EXPLORATION OF PLASTIC PVC MATERIAL FOR JEWELRY ACCESSORIES

Dedy Ismail*, Harry Indrayana
Departement of Product Design, Institut Teknologi Nasional (Itenas), Bandung, INDONESIA
* Corresponding author e-mail: dedy.sml@gmail.com

Abstract

PVC plastic material has the potential to be used as raw material for functional products, especially jewelry accessories products. The material has a characteristics, then the processing of raw materials should take into account the characteristics of its peculiarities. Through the material exploration approach, the potential can be extracted so as to produce non-conventional raw material products that have equivalence value compared to existing conventional raw materials. The exploratory approach to pvc plastic material is very appropriate for generating alternative modules in material experiments so that it can be varied in determining the potential modules in its application in jewelry accessories products. The experiments were carried out with recognition stages by giving physical treatment to bring up the initial characteristics in stages until the determination of the character of the structure on the material. The resulting products such as accessories are clear evidence that through the material exploration approach can be obtained creative opportunities for the development of products that have commercial potential, so it is expected to be utilized as an alternative in the appearance dominated by conventional materials. Through this research, the characteristic of pvc plastic material can be utilized into various jewelry products because of its uniqueness, so it can be an alternative raw material to enrich the potential of non-conventional materials of plastic materials optimally.

Keywords: Exploration, Plastic PVC, Creativity, Accessories.

1. Introduction

Understanding materials in depth is important, though not thoroughly. This is the best way in character tracing with special treatment and is applied in a design process. The perspective in terms of materials can be seen from various perspectives, depending on their interests and needs, to meet certain activities. Material can act as a 'determinant' because it is one important part of a design process, so it becomes one of the considerations in determining a design. However, the search for material characteristics can begin with the material as raw material or finished material.

PVC or polyvinyl chloride plastic material is one of the most commonly found ingredients in functional products, such as cling wrap, toys, water hoses, building pipes, plastic tablecloths, bottles and so on. With a variety of applications, in this study I restricted to take a material that has become a functional product, to be used as experimental raw materials, ie a water hose or a flexible water pipe. In addition to considering one character of the material, PVC hoses can be used as an alternative material to be used as raw materials in the process of designing functional products. This can be done in the design process by using one of the design methods of material exploration with the 'design by doing' approach.

According to Walter Gropius in the book Andry Masri (Creative lamp unique from unused materials, 2011) the approach of 'design by doing' is an approach that can be used to obtain many opportunities with the possibility of new forms of a design work. This will be applied in our research to obtain these opportunities with pvc materials and applied in one particular function as case studies, such as jewelry accessories. The design concept of jewelry accessories can elicit a considerable potential for the possible possibilities of unique forms that arise because of the physical treatment response of material exploration experiments.

2. Methodology

Beginning with an understanding of material characteristics by giving physical treatment of the material. Various kinds of physical treatment of the material, will impact physical changes or visual response in accordance with the character of the material. The variety of responses that appear in the physical treatment is in addition to being influenced by the material itself, as well as the tools used in the experiment, will have an impact on the outcome of the treatment. Even the individual who performs the process affects the response that arises as a result of the treatment with certain tools, and the treatment of sorting and selection of response results aesthetically. Because individual experience affects the object of processed material, which should be resisted to 'form' the object of processed material.

Material exploration method in the creative process to get the most optimal form of the material, which is trying to observe the visual characteristics it contains, its structural characteristics, to its dimensional characteristics, by the method of 'design by doing'. this is done because this method is very practical rely on work attitude, designing directly on the object of study to get a design work (Visual Strategy, Andry Masri, 2010). The targets resulting from this approach are to produce works that are unique and / or different from their experiments, from the impact of visual treatment of the material (response) captured visually.

Important to note also in the stages of material exploration is in the intelligence of creativity and emotion. According to Tony Buzan (Head First, 2003) in creativity intelligence, to 'dare to be different' must think in new ways to produce original, including fluency (creative ideas), flexibility, authenticity, and expanding ideas. Sometimes the condition is often neglected because it is unable to 'control themselves' in overcoming the conditions of the search process and decision-making, such as disconnecting the module used from the material response of the physical treatment at the beginning, and overly satisfied the physical treatment of the material with a limited (monotonous) sustainable. So it must be overcome by the brainstorming to optimize the required results.

3. Result and Discussion

Initial experiments in this study led to the introduction of objects with various treatments and treatments that were considered to know the characteristics of the elastic water hose, with a focus on joint experiments.

A joint experiment is a joint research conducted by a team of researchers and undergraduate students of level one and conducted on lectures at private universities Bandung, Department of Product Design, 3 Dimensional Nirmana courses. The theme used in the lecture is about basic design. From this joint experiment try to dig the material potency of each plastic processing from one of its project that is elastic water hose material.

The treatment of objects in the introduction phase experiment is not limited by the equipment in the experiment. But for the type of material is limited certain elastic water hose type. This joint study is required to conduct experiments with the treatment of elastic water hose material objects with simple tools (manual) and semi-masinal equipment. With a variety of physical treatments with different tools is expected to bring the potential with different and unique results of each individual.

Elastic water hose can be obtained in various places such as markets or material stores. With the exploration criteria of materials in each individual, it should not produce the same response or with the same module, although different treatment or otherwise. The impacts arose because these early stages, still searching and trying to produce a different response from the object under study. Without the pretensions of such treatment outcomes, any results are deemed to have potential to be developed. Experiments with the same treatment with different tools will produce different responses.

To understand the character of the material requires direct experimentation, because with a direct touch with the five senses to produce a better response. The treatment of objects continuously, indirectly can communicate well with the object that we though, and generate various responses.

Every individual has previous experience in producing a work. But when meeting with something new, what is often done is to bring the experience as a test material. The initial process in material exploration should precisely dampen the experience so as not to get stuck with the experience to generate new responses from new materials. This is not easy because it takes time to recognize and understand a character by experimenting directly and gaining new experiences from the object under study.

When the experimental results get various responses, then the development of a module to be re-processed to be made three dimensions. Processing into three dimensions requires stages in the study of structures and dimensions corresponding to the material's visual response. Three-dimensional structure can be done with various materials and varied material. Various kinds of materials available, not necessarily all can be in accordance with some modules. It takes an experiment to understand the three-dimensional structure of each module produced with the help of experience and reference library data to enrich its experimental results. The functional products used as the case in this elastic water hose exploration experiment are directed as jewelry accessories.

The exploration results of these materials with some unique forms, can be seen the possibility of the resulting bid through three-dimensional form experiments to produce aesthetic value. Design considerations are made by looking at the results of material exploration and can be compromised on functional products. The possibilities offered can be made, by making a functional product mapping tailored to the characteristics of the material. The design concept is planning the completion stage of the three dimensional form to get better visual quality and optimal by taking case study from mapping result.

Bids generated through the experimental results of elastic water hose material can present a wide range of possibilities and virtually any possible product mapping can be considered to be utilized in the refinement of a three-dimensional form. However, there should be priorities that can be considered to focus on being a case study of a functional product. Adjustment of the final three-dimensional form of experimental results should be taken into consideration in the selection of case studies to facilitate the selection of functional products.

4. Conclusions

Plastic PVC elastic water hose can be used as raw material in the process of designing a design work, especially jewelry accessories. Looking at the design aspects and approaches there are still not utilized by us, if only as the main function of the hose water. Elastic water hose is a material that has been only used as a primary function as an intermediary tool to move water from one place to a different place according to the needs of its activities. Whereas the material has enormous potential from the result of this research process with exploration approach, so the material can be utilized to be used as alternative material and applied to a design work and add value (value) of the material.

Another conclusion from this material exploration study, the material has a 'superior' and 'weak' physical characteristic. By utilizing both characters are used to generate an unexpected response. the superiority of elastic water hose plastic material is supple or flexible. While the weakness of this material is not strong with certain hot temperatures. So the two characters are used as a condition or criteria in the development of experiment. The results that appear in the physical treatment with the criteria of these two characters, produce unique and unexpected forms.

The results of this study are expected to be useful for all of us. It is not enough time to dig up such material potentials only by special treatment with a short time to get something unique and innovative. There are still many unexplored potentials of this object that have been treated only as a habit. Therefore hopefully this research can be continued and applied in the community, either develop the material that has been done research or apply research methods on different material alternatives.

7. References

Masry, Andry, 2011, Kreasi Lampu Unik dari Bahan tak Terpakai, Transmedia, Jakarta Selatan.

Masry, Andry, 2010. Strategi Visual, Bermain dengan Formalistik dan Semiotik untuk Menghasilkan Kualitas Visual dalam Desain, Jalasutra, Yogyakarta.

Buzan, Tony, 2003, Head First, 10 Cara Memanfaatkan 99% dari kehebatan otak Anda yang selama ini belum pernah Anda Gunakan, Gramedia, Jakarta.

Lawson, Bryan, 2007, Bagaimana Cara berpikir Designer – How Designer Think, Jalasutra, Yogyakarta.

Olver, Elizabeth, 2004, The Art of Jewelry Design From Idea to Reality, Page One, Hongkong.

Proceedings of the 1st Faculty of Industrial Technology International Congress
International Conference
Bandung, Indonesia, October 9-11, 2017
ISBN 978-602-53531-8-5

Invention of Glass Bottle Waste Musical Instrument

Agung Pramudya Wijaya
Department of Product Design, Institut Teknologi Nasional (Itenas), Bandung - INDONESIA
Corresponding author e-mail: pecunk@gmail.com

ABSTRACT

The performing of music arts of waste bottle sound is a contemporary music performances where all of the instruments is used where a musical alternative is the work cultivators made from waste bottle, especially glass bottles waste. This musical instruments of bottle waste that created by the tiller is a new innovation for yet never been there before. Musical instruments of bottle waste by the tiller is the findings of new research results tenants through the long process. Initially, bottle waste is a thing that is not worth, but with a touch of creativity so it have new functions and turned into works of musical instruments of high value. Process is very important from birth discovery tools music bottle waste is up to the musical performances are not separated from the application of the theory of creativity. The concept of musical performances bottle Sounds This waste is non-thematic, meaning not describe the a particular story. In general, the concept of this musical performances is exploration, the exploration of the waste bottles are made into musical instruments, exploration of musical instruments waste bottle after so, and the exploration potential of the sound of musical instruments waste bottles are then composed into a piece of music are packed in a show.

Keywords: invention, innovation, musical instruments, waste, bottle.

1. Introduction

Instrument made from glass bottle waste is a new invention in the development of experimental music, where the musical instruments produced is the result of research and experimental results conducted on the use of glass bottles waste are found in the environment around us.

The design and manufacture of musical waste glass bottles is a cultivation effort in taking a role in environmental conservation by utilizing waste, especially waste glass bottles into something more useful. With its characteristic, waste glass bottles that had been garbage or useless objects, encourage cultivators to be motivated to do a "rescue" effort by converting glass bottle waste into a series of musical instruments. Glass bottle waste has a distinctive character, both in terms of material characteristics different from other materials, as well as from the character of the form that has different shapes and sizes, and has enormous potential when given a touch of creativity. Waste glass bottles can be objects with other functions, namely objects of art that can be enjoyed visually and become a musical instrument that can be enjoyed in audio and visual in the form of a musical art performance.

Bottles are generally only as a function object that is as a container of liquid or liquid, the worker converts into objects with new functions that are more valuable (upcycle), which is an art object in the form of musical instruments that move the region from the object of entry into the arts. Based on the results of interviews and discussions with the lecturer Department of Theater; Department of Television and Film ISBI Bandung who is also a theater writer Arthur S. Nalan, said: "In the work of musical instruments made from glass bottle waste is created there is a new meaning on the bottle media used and developed, previously used only as a function bottle function but through a process of bottle creativity moving from a day to day move into the arts".

Musical instruments made from glass bottle waste can be utilized into a musical performance. Performing music art of glass bottle waste is a musical performing art that utilize a series of musical instruments made from glass bottle waste. Through a creativity-based exploration process, that is exploration of the resulting sounds, glass bottle waste can be transformed into a number of musical instruments that can produce unique and distinctive sounds.

When composed can be a work of musical composition. Prior to being a work of art of music, the creative process is first done, namely the creation of musical instruments through a process of exploration of the sounds based on the material character and the character of the bottle itself. The glass material character in this bottle will produce different sounds according to the shape and dimensions.

2. Methodology

In the design of this glass bottle music instrument, the method of creation used is:

1. Planned Method

In accordance with interviews and discussion results with a lecturer Department of Karawitan ISBI Bandung Heri Herdini, planned method that allows to be applied in the process of creation of the design work of this waste bottle is:

a. Creative Method

In the design of this bottle waste instrument, one of the methods used is the creative method, where artisans apply the creative method in making musical instruments made from waste bottles. In addition, the farmers also apply creative methods in making musical compositions that utilize musical instruments waste bottles that have been made before.

b. Exploration Method

Another method used in the design of this bottle waste instrument is the exploration method, where artisans as artists when making musical instruments made from waste bottles are exploring the media bottles themselves, whether the exploration of the character of the material, character shape, and exploration the sounds of the bottled waste. When the musical instruments of bottled waste are finished, the cultivators continue the process of exploring the sounds produced from these musical instruments into a musical instrument to perform.

c. Method of Creation

In making musical instruments from waste bottles, there is a method of creation, the method used in creating musical instruments in the form of objects.

3. Discussion

The design of musical instruments made from glass bottle waste offers a new concept in the dimensions of the art of performing music. The concept of musical performances is regarded as a show of innovative musical art because it has never existed before, by using ala-non-conventional alternative musical instruments belonging to new types of musical instruments. Almost all of the musical instruments used in this show are the results of a cultivation study designed and made solely by the cultivators, through a process of thought and a very long travel time.

This show is explorative, because all stages are done through the stages of exploration. The initial exploration phase begins by exploring the sounds of bottled waste that eventually create new musical instruments from bottled waste. These new musical instruments offer new nuances either from the way they are played or from the sounds they produce.

The next exploration stage is to explore the musical instruments of bottled waste that have been created. At this stage the exploration is to explore all possible ways to play musical instruments of waste bottles that have been created to produce new types of sounds and unique sounds that cannot be obtained from other musical instruments. After exploring the sounds of the bottled waste musical instruments, then explore the incorporation of several types of musical instrument bottles to become a musical composition that will be performed.

The design of musical instruments made from waste bottles is expected to be an inspiration, change the mindset, and can stimulate sensitivity for the wider community to be more wise in facing waste in the environment. Because basically everyone can work even with waste. If a sensitive society in treating waste, with a touch of waste creativity would be an incredible work of art.

4. References

Anggana, Rizka Dwipa, 2013. “Sampah B3 (Bahan Berbahaya dan Beracun) Rumah Tangga”. dari artikel: http://banksampahmelatibersih.blogspot.co.id/2013/sampah-b3-bahan-berbahaya-dan-beracun.html?m=1.

Duckworth, William, 1995. “Talking Music”, New York: Schirmer Books.

Poerwadarminta, W. J. S, 1976. Kamus Besar Bahasa Indonesia. Jakarta: Balai Pustaka.

Hutari, Rossana, 2011. “Kreativitas Anak”, dari artikel: http://rossanahutari.blogspot.co.id/2011/10/krativitas-anak-html.

Koentjaraningrat., 2005. “Pengantar Antropologi I”, Jakarta: Penerbit Rineka Cipta.

Rachmawati, Yeni dan Euis Kurniati., 2010. “Strategi Pengembangan Kreativitas Pada Anak”, Jakarta: Penerbit Kencana.

Triyono, Bambang, 2011. “Musik Dari Onggokan Sampah”, hal. 94, dari artikel Majalah Warisan Indonesia Vol. 1 No.4.

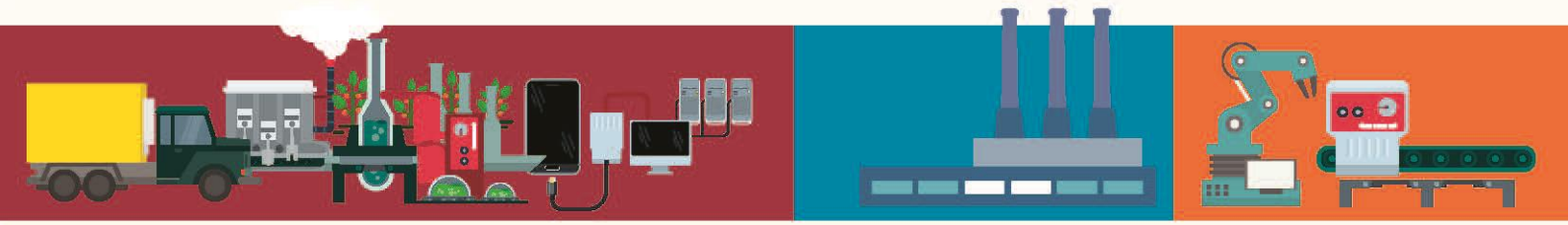

itenas
Institut Teknologi Nasional

FoITIC
Faculty of Industrial Technology International Congress

ISBN 978-602-53531-8-5

Organized by:
Faculty of Industrial Technology, Institut Teknologi Nasional (Itenas) Bandung, West Java Indonesia.
Supported by:
Institut Teknologi Nasional (Itenas) Bandung, West Java Indonesia.